Enhancing the application of field portable X-ray Fluorescence technology for the measurement of metal-contaminated soils

Marek Rouillon

BEnvSc (Hons)

Department of Environmental Sciences

Faculty of Science and Engineering

Macquarie University

Thesis presented for the degree of

Doctor of Philosophy

MACQUARIE
University
SYDNEY·AUSTRALIA

The saddest aspect of life right now is that science gathers knowledge
faster than society gathers wisdom

- Isaac Asimov

Declaration

I certify that the work in this thesis has not been submitted previously, in whole or in part, for a degree at this or any other university. Nor does it contain, to the best of my knowledge, any material published or written by another person, except where acknowledged. This thesis is comprised entirely of my own work.

Marek Rouillon

July 2017

Abstract

Field portable X-ray Fluorescence (pXRF) is utilised widely for a variety of environmental applications due to its rapid and inexpensive estimation of metal(loid) concentrations. The use of pXRF for metal-contaminated soil screening is an emerging measurement approach, however, its use for final quantitative assessments is less common, largely due to data quality concerns. This thesis evaluates the application of pXRF for the measurement of metal-contaminated soils and in turn, assesses data quality, reliability and application benefits. The thesis research applies an evidence-based approach across five inter-related papers that examine a broad spectrum of pXRF-related misconceptions. These studies cover user safety, *ex-situ* and *in-situ* analytical performance for assessment of metal-contaminated sites and related environmental investigations. The thesis is comprised of a technical assessment of pXRF and its application to investigate and understand environmental contamination problems.

The technical assessment component of the thesis is comprised of:

- the measurement of radiation dose rates from four different pXRF spectrometers to determine user pXRF-related radiation exposure
- an analytical evaluation of *ex-situ* pXRF to assess the accuracy, precision and detection limits of pXRF during the measurement of metal-contaminated soils
- an assessment of *in-situ* pXRF application for metal-contaminated site assessments to evaluate the benefits of lower cost and high volume sampling using pXRF compared to the current approach of less sampling and *ex-situ* wet chemistry analysis.

The use of pXRF for the investigation of urban metal contamination is executed using two cases studies from Sydney and Newcastle in New South Wales:

- analysis of domestic garden soils collected as part of Macquarie University's free soil metal analysis program (VegeSafe)
- assessment of inorganic and organic contaminants collected from public and private soils in a former industrial city

The outcomes of the evaluation and application of pXRF demonstrates that it is safe for users and is capable of generating accurate and inexpensive geochemical measurements of soils for a range of metal-contaminants. In addition to the five papers on pXRF, this thesis presents three additional case studies examining contemporary and legacy metal contamination hazards in other mining and urban centres across Australia. Collectively, these research studies demonstrate that both legacy and contemporary environmental contamination by toxic metal(loid)s remains a hazard and a potential risk of harm to Australian residents.

Acknowledgements

Sometimes it only takes one moment, for everything to change.

Towards the end of my undergraduate career, I faced a looming fail grade on a group research project. Only given a handful of days to amend the semester long report, I willingly re-wrote the entire report and earned a pass grade on behalf of six students. That small taste of confidence compelled me into an Honours project where I learned new analytical techniques and the art of scientific writing. The rest is history.

For this I give my sincere thanks to my Honours and PhD supervisor Mark Taylor for giving me that second chance all those years ago. Your guidance and continuous support has made this journey both possible and memorable. You have taught me how to write efficiently, think critically and design research projects.

I give my whole hearted thanks to my Honours and PhD co-supervisor Damian Gore, for his mentorship and motivation from my early days in undergraduate studies, through Honours and into PhD research. Learning XRF was just the beginning. You challenged me, let me make mistakes, and showed me the wonders of trusting the laboratory process.

Damian and Mark, you both have undeniably shaped me into the scientist I am today. I could not ask for two better mentors during my PhD journey.

Many thanks go to Sam Habib, Andrew Taylor, and Jake Jarvinen from Olympus Australia for their tremendous support and expertise on all matters of pXRF. I always enjoyed discussing my research with you every time I visit. Thanks to Andrew Evans, Shiva Prasad and Richard Coghlan from the National Measurement Institute for their research advice, feedback and excellent laboratory experience. My days at NMI were few, yet imperative in my understanding of industry.

Thank you to the hundreds of Australian gardeners that I met during my involvement in the VegeSafe program. Your enthusiasm in urban gardening and eagerness to learn about environmental issues was inspiring and was the motivational catalyst for one of my papers.

Special thanks goes to our research team, Paul Harvey, Louise Kristensen and Chenyin Dong for their assistance in both the field and lab work, in the various projects we've all undertaken. I am equally as thankful for having the opportunity to assist you all during your PhD journeys

Table of Contents

Acronyms and abbreviations

AAS	Atomic Absorption Spectrometry
Ag	Silver
ANOVA	Analysis of Variance
As	Arsenic
Cd	Cadmium
CI	Confidence Interval
Cr	Chromium
CRM	Certified Reference Materials
Cu	Copper
Fe	Iron
g/cm^3	Grams per cubic centimetre
GC	Gas Chromatography
ha	Hectares
HCl	Hydrochloric acid
$HClO_4$	Perchloric acid
HF	Hydrofluoric acid
Hg	Mercury
HIL	Health Investigation Level
HNO^3	Nitric acid
ICP–AES	Inductively Coupled Plasma Atomic Emission Spectrometry
ICP–MS	Inductively Coupled Plasma Mass Spectrometry
kV	Kilovolt
LGA	Local Government Area
mg/kg	Milligrams per kilogram
MMT	Methylcyclopentadienyl Manganese Tricarbonyl
Mn	Manganese
mSv	Milli Sievert
MXFLR	Maximum Likelihood Functional Linear Relationship
NATA	National Association of Testing Authorities
NEPM	National Environment Protection Measure 1999
Ni	Nickel
NIST	National Institute of Standards and Technology
NRC	National Research Council of Canada
NSW EPA	New South Wales Environment Protection Authority
Pb	Lead
pXRF	Field portable X-ray Fluorescence
QAQC	Quality Assurance Quality Control
r^2	Coefficient of Variation/Goodness of Fit
RP	Relative Proximity
RPD	Relative Percent Difference
RSD	Relative Standard Deviation
s_{anal}	Analytical standard deviation
SEM	Scanning Electron Microscopy
$s_{geochem}$	Geochemical standard deviation
SiO_2	Silicon dioxide
SOP	Standard of Operating Procedure
Sr	Strontium
s_{samp}	Sampling standard deivation
Sv	Sievert
Ti	Titanium
U_{anal}	Analytical uncertainty
UCL	Upper Confidence Limit
U_{meas}	Measurement uncertainty
U_{samp}	Sampling uncertainty
US EPA	United States Environmental Protection Agency
wt %	Weight percent
XRF	X-ray Fluorescence
Zn	Zinc
µg/dL	Micrograms per decilitre
$µg/m^2$	Micrograms per square metre
µm	Micrometres
µSv	Micro Sievert (unit of ionizing radiation dose)
µSv/h	Micro Sieverts per hour

Thesis structure

This thesis is structured into six chapters. The eight research papers and two communication articles within this thesis are presented in Chapter Two, Three, Four, Five and Appendix A. Chapter Two identifies the risk of radiation dispersion around field portable X-ray Fluorescence (pXRF) spectrometers during the measurement of a range of materials. Chapter Three evaluates the analytical capabilities of a pXRF spectrometer for the *ex-situ* measurement of metal-contaminated soils and compares the data against accredited laboratory techniques. Chapter Four discusses the advantages of integrating *in-situ* pXRF to enhance the confidence of decision making in metal contaminated site assessments. Chapter Five presents two pXRF application case studies that demonstrate the accurate and cost-efficient use of pXRF for metal contamination investigations. Appendix A includes three metal contamination studies that evaluate the efficacy of abatement and washing strategies used to reduce contemporary and legacy metal exposures in three metal-contaminated cities of Australia. These three research papers were designed, written and published during my PhD candidature and are included to complement the main research chapters in this thesis.

Author contribution to publications

Chapter 2: Radiation safety assessment

Paper One: Rouillon, M. (80 %), Kristensen, L.J. (7 %), Gore, D.B. (13 %) 2015. Handheld X-ray Fluorescence Spectrometers: Radiation Exposure Risks of Matrix-Specific Measurement Scenarios. Applied Spectroscopy 69(7), 815-822.

This study was developed by Rouillon and Gore. All authors were involved in laboratory experiments and data interpretation. Writing was performed by Rouillon. Editing and reviewing were conducted by all authors.

Chapter 3: Analytical evaluation of pXRF

Paper Two: Rouillon, M. (85 %) and Taylor, M.P. (15 %) 2016. Can field portable X-ray Fluorescence (pXRF) produce high quality data for application in environmental contamination research? Environmental Pollution 214, 255-264.

This paper was developed by Rouillon and Taylor. Laboratory analyses and writing was performed by Rouillon. Editing and reviewing were conducted by Rouillon and Taylor.

Chapter 4: *In-situ* pXRF assessment

Paper Three: Rouillon, M. (80 %), Taylor, M.P. (10 %), Dong, C. (10 %) 2017. Reducing risk and increasing confidence of decision making at a lower cost: Infield pXRF assessment of metal contaminated sites. Environmental Pollution 229, 780-789.

This study was designed by Rouillon. Fieldwork and laboratory analyses were conducted by Rouillon and Dong. Writing was performed by Rouillon. All authors were involved in editing and reviewing the paper.

Chapter 5: pXRF application case studies

Paper Four: Rouillon, M. (75 %), Harvey, P.J. (10 %), Kristensen, L.J. (3 %), George, S.G. (2 %), Taylor, M.P (10 %) 2017. VegeSafe: A community science program measuring soil-metal contamination, evaluating risk and providing advice for safe gardening. Environmental Pollution 222, 557-566.

This paper was designed by Rouillon and Taylor. All authors were involved in the VegeSafe program. Sample collection and laboratory work were conducted by Rouillon, Harvey and

Kristensen. Writing was performed by Rouillon. Editing and reviewing were conducted by all authors.

Article One: Rouillon, M. (75 %), Kristensen, L (1 %), Taylor, M.P. (20 %), Harvey, P.J. (2 %), George, S.G. (2 %) 2017. Elevated lead levels in Sydney backyards: here's what you can do. The Conversation. January 17, 2017. <www.theconversation.com/elevated-lead-levels-in-sydney-back-yards-heres-what-you-can-do-68499>

This article was written by Rouillon and Taylor based on the findings in **Paper Four**. Editing and reviewing were conducted by Rouillon and Taylor.

Paper Five: Harvey, P.J. (55 %), **Rouillon, M. (20 %)**, Dong, C. (5 %), Ettler, V. (5 %), Handley, H.K. (2 %), Taylor, M.P (5 %), Tyson, E. (2 %), Tennant, P. (2 %), Telfer, V. (2 %), Trinh, R. (2 %) 2017. Geochemical sources, forms and phases of soil contamination in an industrial city. Science of the Total Environment 584-585, 505-514.

This study was designed by Harvey, Rouillon and Taylor. Fieldwork was conducted by Harvey, Rouillon, Dong, Tyson, Tennant, Telfer and Trinh over many trips to Newcastle. Laboratory analyses were conducted by Harvey, Rouillon, Dong and Ettler. Writing was performed by Harvey and Rouillon. Editing and reviewing were conducted by all authors.

Appendix A

Paper Six: Taylor, M.P. (35 %), Mould, S.A. (35 %), Kristensen, L.J. (20 %), **Rouillon, M. (10 %)** 2014. Environmental arsenic, cadmium and lead dust emissions from metal mine operations: Implications for environmental management, monitoring and human health. Environmental Research 135, 296-303.

This study was designed by Taylor. Fieldwork was conducted by all four authors. Writing was completed by Taylor and Mould. Editing and reviewing were performed by all authors.

Article Two: Taylor, M.P. (40 %), Kristensen, L.J. (25 %), **Rouillon, M. (15 %)**, Mould, S.A. (20 %) 2014. Toxic playgrounds. Broken Hill kids exposed to poisonous dust. The Conversation. October 16, 2014. <https://theconversation.com/toxic-playgrounds-broken-hill-kids-exposed-to-poisonous-dust-32325>

This article was written by Taylor, Kristensen, Rouillon and Mould based on the findings of **Paper Six**. Editing and reviewing were conducted by all authors.

Paper Seven: Taylor, M.P. (35 %), Zahran, S. (25 %), Kristensen, L. (25 %), **Rouillon, M. (15 %)** 2015. Evaluating the efficacy of playground washing to reduce environmental metal exposures. Environmental Pollution 202, 112-119.

This paper was developed by Taylor as a follow up to a previous study. Fieldwork was conducted by Kristensen and Rouillon. Laboratory analysis was conducted by Kristensen. Statistical analysis was completed by Zahran. Writing was completed by Taylor, Zahran and Kristensen. All authors assisted in editing and reviewing the paper.

Paper Eight: Harvey, P.J. (48 %), Taylor, M.P. (15 %), Kristensen, L.J. (15 %), Grant-Vest, S. (3 %), **Rouillon, M. (15 %)**, Wu, L. (2 %), Handley, H.K. (2 %) 2016. Evaluation and assessment of the efficacy of an abatement strategy in a former lead smelter community, Boolaroo, Australia. Environmental Geochemistry and Health 38, 941-954.

This paper was designed by Harvey and Taylor. Fieldwork was conducted by Harvey, Taylor, Kristensen, Grant-Vest and Rouillon. Laboratory analyses were conducted by Harvey and Wu. Writing was completed by Harvey and Grant-Vest, and was further contributed to by Taylor, Kristensen and Rouillon. Editing and reviewing was performed by all authors.

Chapter One: Introduction

1.1 Field portable X-ray Fluorescence (pXRF) technology

X-ray Fluorescence (XRF) is a non-destructive, elemental analysis technique capable of measuring a variety of materials (Cesareo et al. 1998; Brouwer 2003). The XRF technique is based on the principle that individual atoms emit characteristic X-ray photons when excited by an energy source. The detection of element-specific photons emitted from a sample enables both qualitative element identification and estimation of elemental abundance (Brouwer 2003). More specifically, the excitation of an atom ejects an inner shell electron, creating an inner shell vacancy. The inner shell vacancy is filled by an outer shell electron to return the atom to a ground state (Weindorf et al. 2014a). This process releases photons with energies equivalent to the difference between the two shells, and are characteristic to each electron shell transition of each element (Kalnicky and Singhvi 2001). The detection of these fluorescent photons are compared against similar energy intensities from the measurement of reference materials, allowing for the elemental quantification of unknown samples.

The mathematical relationship between the fluorescence of atoms and their atomic number was first discovered by Moseley in 1913 (Jenkins 2012). Development of more sensitive photon detectors were necessary to make XRF viable, which did not occur until the 1940s, and by the 1950s the first commercial XRF spectrometers were available (Jenkins 1988). The advancement and miniaturisation of XRF components in the 1970s and 1980s led to smaller, multi-piece instruments with early generation microprocessors (Bosco 2013). However, it was not until 1994 that the first handheld XRF spectrometer (Figure 1.1a) was commercially available for lead (Pb) paint and soil testing (OENHP 2002). These early field portable XRF (pXRF) instruments used radioactive isotopes as energy sources (e.g. cadmium 109 and americium 241), which were susceptible to energy fading and quickly became a business liability in terms of safe disposal (Bosco 2013).
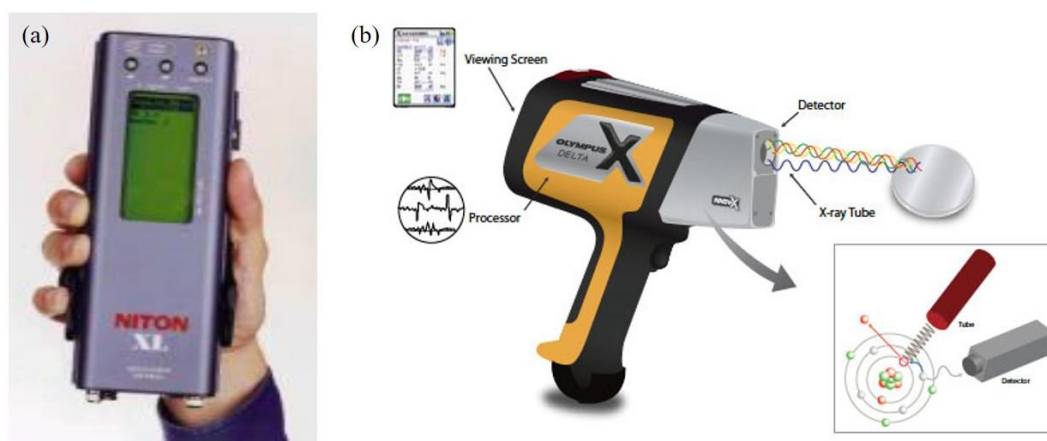
Figure 1.1: (a) The first handheld XRF spectrometer, Niton XL-309 and (b) an overview of a new generation field portable XRF spectrometer, Olympus DELTA Premium XRF Analyser (OENHP 2002; Olympus 2017).

Less than 10 years later, the development of miniaturized X-ray tubes provided an alternative energy source for safer and more reliable excitation of atoms (Weindorf et al. 2014a). The ensuing miniaturization of internal components lead the way for new generation, ergonomic pXRF spectrometers such as the Olympus DELTA Premium XRF Analyser (Figure 1.1b). Since the launch of X-ray tube powered pXRF spectrometers in 2002, an array of manufacturers have designed their own pXRFs in an effort to provide a superior, user-friendly technology to emerging markets. Additional pXRF accessories such as battery charging stands and integrated geographic information system (GIS) devices enable users to operate the spectrometers efficiently for a variety of pXRF applications (e.g. Niton XL3t Series – Thermo Fisher Scientific 2012).

1.2   Environmental applications of pXRF

Field portable XRF has been broadly employed for a variety of industries including alloy identification, archaeology, biology, forensics, mineral exploration, mining, pharmaceutical and for the screening of consumer products for toxic metals (West et al. 2013; Weindorf et al. 2014a). Its use for environmental investigations for the measurement of soils, sediments, woods, paints, water and air filters is well established.

1.2.1   Soils (trace metals)

Numerous studies have evaluated and applied pXRF for the rapid estimation of toxic metal and metalloids (hereafter referred to as metals), such as arsenic (As) and Pb, in soils. Parsons et al. (2013) evaluated both *in-situ* and *ex-situ* (off-site) pXRF measurements of trace (<40 mg/kg) concentrations of As and found quantitative measurements were possible, even with minimal soil preparation. Haffert and Craw (2009) investigated the spatial extent of As contamination in the soils of a former arsenopyrite smelting area in New Zealand using pXRF. An area of 3.25 ha was identified to contain As concentrations in excess of the commercial/industrial recommended guideline of 500 mg/kg. Argyraki et al. (1997) evaluated *in-situ* pXRF measurements of Pb at a former Pb smelting site in Derbyshire, UK. They found that when pXRF data were corrected for moisture and surface roughness, there was little analytical bias between *in-situ* pXRF and the comparative method of Inductively Coupled Plasma Atomic Emission Spectrometry (ICP–AES). Moreover, Chou et al. (2010) measured both soil As and Pb concentrations by pXRF to rapidly generate an updated geochemical map of the greater New Orleans area, post Hurricane Katrina.

Comparisons of pXRF measurements against established wet chemistry analytical techniques such as Flame Atomic Absorption (FAA) and ICP–AES are common to evaluate pXRF

performance. Clark et al. (1999) measured 21 soil samples from the copper (Cu) smelting region of Poland by *in-situ* and *ex-situ* pXRF, FAA and laboratory XRF. They assessed the effect of particle size on comparability between pXRF and laboratory methods of FAA and XRF and found slightly stronger agreement between the techniques with smaller particle size. By contrast, Kilbride et al. (2006) found particle size had no significant impact on pXRF analysis when comparing both dual isotopes and X-ray tube powered pXRFs to ICP–AES analysis. In contrast, Vanhoof et al. (2004) demonstrated significant improvements to pXRF comparisons with ICP–AES data after limited sample preparation, which included drying and grinding samples. Overall, the published literature contains a wide range of analytical evaluations of pXRF data quality, largely due to the different levels of data quality that are considered acceptable (See Chapter Three).

Field portable XRF is a lower cost option for geochemical surveys in areas where access to laboratory analysis is difficult, such as remote parts of South America or Africa for example. Higueras et al. (2012) explored the potential for rapid pXRF soil screening at abandoned mine sites and concluded that pXRF should become the 'equipment of choice' for environmental monitoring in developing countries, due to its reliability and affordability when compared to laboratories. Similarly, Loredo et al. (2008) used pXRF to screen a former mine site in Spain and found high concentrations of As (mean As = 549 mg/kg), among other metals posing a threat to the surrounding environment. Another mining area in Spain was investigated by Peinado et al. (2010). Their study concluded that pXRF provided sufficient preliminary spatial data to guide future mobility and bio-availability assessments of soil As at the site. Pure Earth, a non-for-profit, pollution clean-up organisation uses pXRF screening at used Pb-acid battery sites in low income countries to identify priority clean up scenarios (Ericson et al. 2016).

Mapping pXRF data with GIS enables users to produce detailed spatial distribution maps of contaminants at a given site. For instance, Carr et al. (2008) mapped Cu, zinc (Zn), As and Pb concentrations in the soils of a recreational park in Ireland. Some of the spatial data was presented as a three-dimensional map to assist non-experts, such as local government representatives, to better understand the distribution and severity of the Pb contamination (Figure 1.2). Radu et al. (2013) also mapped soil pXRF data at two sites in Ireland and identified the most likely Pb sources using GIS and geostatistical analysis. A similar study was conducted by Ran et al. (2014) where *in-situ* soil pXRF data from the Yangtze Delta area in China were mapped to determine the areas with greater environmental risk. The study also used a combination of multivariate analysis and geostatistics to determine the major sources of metals (i.e. anthropogenic or lithogenic). Weindorf et al. (2012) investigated the environmental quality of sugarcane fields using a combination of *in-situ* pXRF, principal component analysis and

ordinary kriging for GIS modelling. Further studies by Weindorf et al. (2013) and Paulette et al. (2015) mapped a range of soil metals in former mining and smelting areas of Romania, and used GIS to interpolate the proportion of area that exceeds the action limits for metals.

Studies into the errors associated with both field and laboratory pXRF measurements have also been explored. Taylor et al. (2005) assessed the soil metal heterogeneity of two sites by pXRF and X-ray Microprobe and found that the spatial heterogeneity of metals were influenced by the source of contamination. A study by Ramsey and Boon (2012) demonstrated that despite higher measurement uncertainties (*in-situ* pXRF – 154 % vs. lab pXRF – 110 %), As measurements made *in-situ* can be more 'fit for purpose' than their *ex-situ* equivalents due to lower overall costs. This is largely because both *in-situ* and *ex-situ* measurements are usually limited by uncertainties related to sampling rather than analysis (sampling contributed >93 % of the measurement variance for both *in-situ* and lab measurements). A complementary study by Boon and Ramsey (2012) demonstrated the issue of sampling limitation using two case studies that measured soil As and total petroleum hydrocarbons by pXRF and UV Fluorescence, respectively.
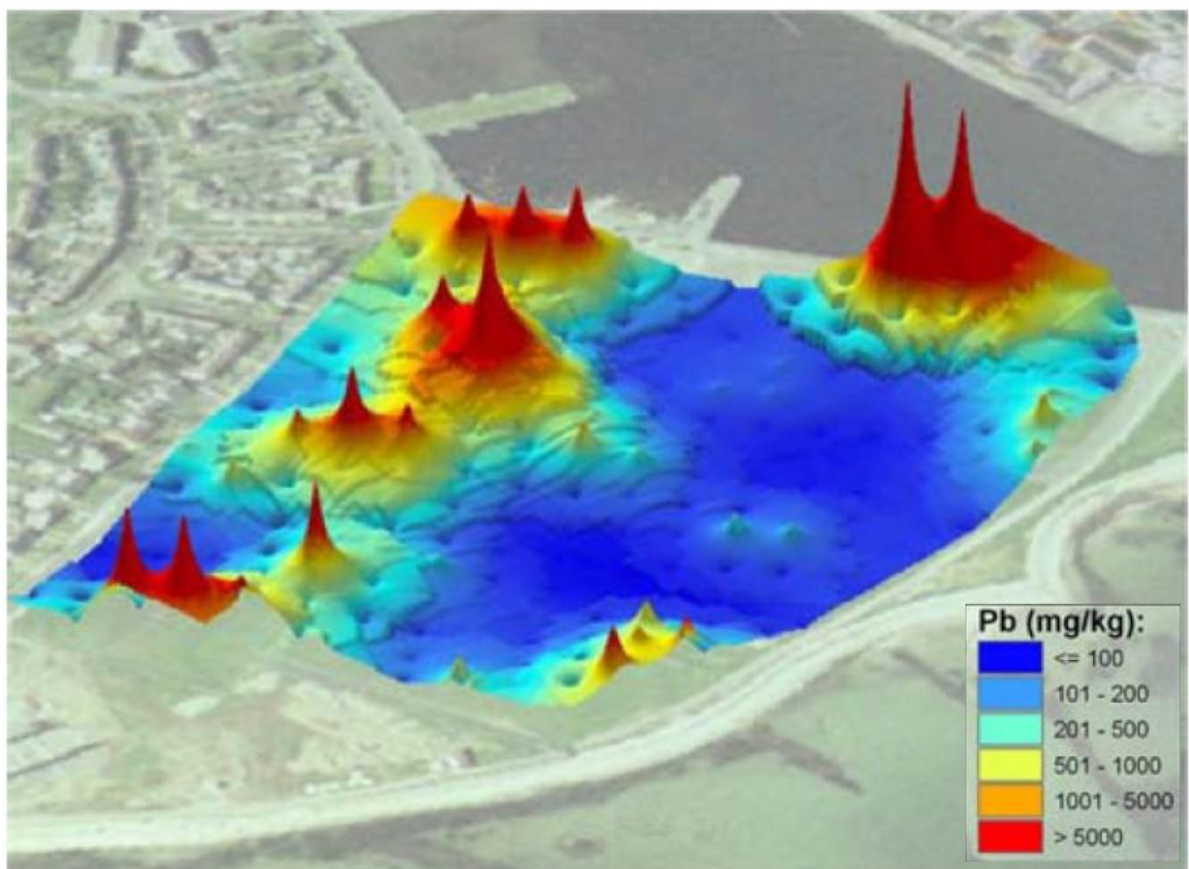
Figure 1.2: A three-dimensional estimation of Pb concentrations in soils of a recreational park in Galway City, Ireland (Source: Carr et al. 2008).

1.2.2 Soils (major elements) and sediments

Field portable XRF has also been used classify soils through the measurement of major elements such as calcium, titanium (Ti) and iron (Fe). Stockmann et al. (2016) utilised pXRF to verify the primary parent materials of soils and to identify the main pedogenic processes occurring at three different soil profiles in New South Wales (NSW), Australia. They found that *in-situ* pXRF provided good agreement ($r^2 = 0.81$) with *ex-situ* pXRF (air-dried and ground samples) for the Desilication index (ratio of silica to resistant oxides). Zhu et al. (2011) estimated the clay content and texture of surface and subsurface soils using *in-situ* pXRF elemental composition ratios and laboratory measurements. The measurement of agriculturally important elements by pXRF was further demonstrated by McLaren et al. (2012) through measurement comparisons with certified reference materials (CRMs), ICP–AES, benchtop XRF and neutron activation analysis. Despite the wide range of regression gradients between pXRF and the reference techniques (m = 0.06 (Mg) to 80.1 (Pb)), relationships between pXRF and the reference techniques were generally strong ($r^2 = 0.70$ (Cu) to 0.99 (Fe)). Similarly, Piercey and Devine (2014) assessed the analytical performance of pXRF in the measurement of lithogenic materials such as drill core samples. Their *ex-situ* pXRF evaluation determined that pXRF cannot be used as an alternative to high quality laboratory measurement techniques such as fusion ICP–AES and Inductively Coupled Plasma Mass Spectrometry (ICP–MS), yet can provide 'fit for purpose' data. It is important to point out that Piercey and Devine (2014) acknowledge their single point calibration method for pXRF was inferior when compared to using multiple calibration points per element, which could have been obtained by expanding their CRM suite.

Shand and Wendler (2014) studied the influence of organic content on pXRF measurements and determined that user-specific calibrations were required to measure accurately organic-rich soils. Moisture content (%) is also known to influence the accuracy of pXRF measurements. By comparing four different moisture content conditions (in-situ, dried soil at 105 °C, 40 % moisture content and saturated soil), Sahraoui and Hachicha (2017) revealed that a linear relationship exists between in-situ, dried soil and 40 % moisture content conditions, yet saturated soil generated the most inaccurate measurements. This is consistent with Weindorf et al. (2014b), who found significant underestimation of pXRF measurements where soil moisture content exceeded 40 %. Yet, the impact of soil moisture can also be corrected for. In this regard, Bastos et al. (2012) proposed a pXRF correction method for soil moisture using low-energy background.

Sediments can also be measured by pXRF, provided the moisture content of the samples are known. Metal contamination of estuarine sediments from the Derwent estuary in Hobart, Australia were investigated by Gregory et al. (2013). The samples were dried then measured by pXRF as loose material through polyethylene bags, and were validated by frequent measurement of a sludge reference material. Stallard et al. (1995) utilised pXRF to measure the metal content of oceanic sediments in the San Diego Bay, USA. They evaluated wet sediment samples against dried samples and found good pXRF performance in the rapid measurement of freshly collected wet samples. Lastly, in their study of saturated contaminated sediments, Lemiere et al. (2014) demonstrated that using a filter-press to uniformly lower the water content in sediments is sufficient to accurately categorise sediments based on their metal content.

1.2.3 Treated wood and Pb-based paint

The addition of toxic metals to domestic products, such as chromated copper arsenate (CCA) treated wood and Pb-based paints, have led to the widespread contamination of these metals in the environment. Block et al. (2007) evaluated the performance of pXRF in the measurement of CCA treated wood, and found a high correlation between pXRF and atomic absorption spectrometry (AAS) ($r^2 = 0.97$) in the measurement of As in wood. Mielke et al. (2010) measured 132 wood samples from children play areas using pXRF in metropolitan New Orleans, USA. They found a strong association between soil and wood As concentrations using pXRF, with more than one-third of playgrounds containing CCA treated wood. Non-destructive XRF measurements of Pb in household paints have been used for over 40 years to rapidly and inexpensively identify the risks of Pb exposure for that household. Reece et al. (1972) measured the Pb content of households where children presented elevated blood Pb levels using an early generation on-site XRF and found exterior painted surfaces had greater Pb concentrations than interior surfaces. Further, Ashley et al. (1998) demonstrated *in-situ* pXRF measurement of Pb-based paint, and compared this screening method to other on-site and *ex-situ* measurement techniques such as anodic stripping voltammetry and AAS.

1.2.4 Dust wipes and air filters

Field portable XRF can also provide real-time screening data for surface dust accumulation and air filters in workplaces. Dost (1996) assessed the on-site application of pXRF for the measurement of surface wipes, air filters and powders in a workplace environment. The study found pXRF to be a cost-effective and rapid approach for the measurement of toxic metals such as As, cadmium (Cd) and Pb. Morley et al. (1999) collected 65 air filters used to monitor air Pb concentrations at a bridge blasting abatement project. They used pXRF to provide near real-time data for workplace conditions and validated the findings with a strong correlation ($r^2 =$

0.985) against a reference method (Graphite furnace atomic absorption). Bartley et al. (2007) also measured Pb concentrations from air filters at workplaces where Pb is used or where Pb is a by-product. They found no statistically significant difference between on-site pXRF measurements and the reference laboratory based method of analysis, validating its use for routine testing. Lawryk et al. (2009) also assessed pXRF measurements of air filters in the workplace, yet expanded their investigations to other metals such as manganese (Mn), chromium (Cr), and Zn, and determined pXRF metal estimations useful for the assessment of worker inhalation exposure.

1.3 Advantages and disadvantages of pXRF

Field portable XRF has several unique and appealing advantages over other laboratory analysis techniques, which have been covered extensively in the literature (Kalnicky and Singhvi 2001; Weindorf et al. 2014a; Horta et al. 2015). For the measurement of metal-contaminated soils, these advantages are listed below:

➢ Wide elemental coverage (magnesium to uranium) and concentration range (low mg/kg to 100 wt % quantification)

➢ Small instrument size and lightweight build (~2 kg) enables easy operation and transport (Olympus 2016)

➢ Rapid *in-situ* measurement of soils allows for higher sampling resolution at metal-contaminated sites

➢ Measurements conducted *in-situ* provides information on the spatial distribution of contaminants and the degree of soil heterogeneity without disturbing sampling location (Argyraki et al. 1997)

➢ *In-situ* measurements do not require removal of soils for sampling, and lowers costs of sample transport and storage (Weindorf et al. 2014a)

➢ Real-time data generation can guide further judgemental sampling to identify the extent of contamination hot spots (Kalnicky and Singhvi 2001)

➢ Non-destructive pXRF measurements provide excellent analytical precision and enables data comparison of the 'same sample' with other measurement techniques

➢ Low cost of operation and relatively low cost of ownership (when compared to other measurement techniques)

➢ Limits of detection for environmentally important metals such as As, Cd and Pb are usually lower than national and international soil metal guidelines

However, every analytical technique also has limitations associated with their use. The disadvantages of pXRF measurement of metal-contaminated soils are provided below:

➢ Limits of detection vary across elements due to physical and chemical interferences, and are usually higher than laboratory techniques (Horta et al. 2015)

➢ Physical matrix effects (variation in physical character of sample) can impact pXRF measurements

➢ Measurement of elements with low atomic numbers (i.e. sodium and below) is currently not possible

➢ Users are typically less experienced when compared to operators of laboratory instruments

➢ In-field operation training is limited

➢ Difficult to apply quality control measures on *in-situ* measurements due to clear disparity between reference materials and surface soil samples

➢ Moisture content of soils can impact pXRF measurement of lighter metals (Bastos et al. 2012)

Many of these limitations related to soil analysis can be addressed by undertaking light sample preparation or calibrations. Understanding the dominant matrix composition of a sample, and applying a calibration specific for that matrix mitigates measurement inaccuracies (See Chapter Three). The low moisture content of soils from arid environments have negligible influence on pXRF measurements, while soils containing >30 % moisture can be dried prior to measurement to increase accuracy (Weindorf et al. 2014a). The measurement of elements with atomic numbers lower than magnesium is less relevant for environmental applications, and more relevant for mineral exploration and mining applications. Contaminants of concern such as Cr, Zn and Pb, and metals specific to the *Resource Conservation Recovery Act* (RCRA) such as As, Cd and silver (Ag) are all quantifiable by pXRF (US EPA 2017). Understanding the strengths and weaknesses of any analytical technique is fundamental for effective application in its desired field. Unfortunately, these limitations have largely deterred pXRF implementation in the environmental industry (other than for screening), particularly in Australia, where assessments of potentially contaminated soils are carried out by sending samples to accredited laboratories for analysis.

1.4 Current approach to sampling and analysis

The estimation of metal concentrations in contaminated soil by the contaminated land industry is typically assessed by sampling and wet chemistry analyses such as ICP–AES or ICP–MS.

Soil sampling protocols, such as Australian Standards 4482.1 (Standards Australia 2005), provide information related to the sampling design, collection of samples and quality assurance procedures for environmental professionals (Standards Australia 2005). General sampling practices consist of the removal of foreign objects and debris from the sampling location and collection of the upper 0–2 cm of soil down to 2 m in depth (varies based on investigation objectives) using a trowel into a labelled, metal-free bag or jar for laboratory analysis. The number of samples collected is usually guided by the minimum sampling requirements set by the sampling protocol, or by the relevant state regulatory authority (e.g. NSW EPA 1995). Due to the costs associated with laboratory analysis, the number of samples used to characterise a site is generally kept to a minimum, unless there is evidence to suggest more samples are required for characterisation. The minimum requirements for quality assurance reporting, according to Australian Standard 4482.1 (2005) are one field and laboratory duplicate for every 20 samples to assess the variation in sampling and analysis. Finally, a chain and custody form is completed to transfer the samples to a commercial laboratory for wet chemistry analysis.

When coupled with acid digests that target labile elements (e.g. aqua regia), these analytical techniques measure the total acid-extractable metal concentrations of soils and dusts, and provides an estimate of the maximum metal availability to plants (Vercoutere et al. 1995; Chen and Lena 2001). For environmental investigations, there is usually little need to measure residual metal concentrations bound on and within silicate matrices as they are deemed environmentally unimportant when compared to weak acid metal extraction (Niskavaara et al. 1997). While there are no specific Australian legislative requirements for a consistent acid extraction process for environmental investigations, ICP–MS analysis after aqua regia metal extraction has become commonplace. Wet chemistry extracts can also be used to determine Pb isotope compositions of samples, which assist in identifying the origin of metal contaminants in the environment. This is particularly useful for investigations where multiple contaminant sources may be present, and where a multiple weight of evidence approach may be required to identify a polluter.

Like many countries around the world, Australia has a long history of mining and smelting activities that have left a legacy of metal contamination in the environment (Kristensen et al. 2017). Communities living near metal industries (e.g. mining operations) are more likely to be exposed to metal contaminant hazards than those who live far away from them (Dong and Taylor 2017). Hence, to better understand metal contaminant hazards in these communities, three studies were conducted using the conventional approach of sampling and wet chemistry analysis and are presented in Appendix A. **Paper Six** investigates soil and dust metal accumulation in playgrounds of Broken Hill, a mining city in western NSW with >100 years of

Zn/Ag/Pb mining (Kristensen and Taylor 2016). **Paper Seven** evaluates the efficacy of a playground washing regime in Port Pirie, a regional city in South Australia where >120 years of Pb smelting has contaminated the surrounding city (Taylor et al. 2013). Lastly, **Paper Eight** assesses a Pb abatement strategy designed to reduce metal contamination hazards from historical smelter emissions and the distribution of Pb-rich slag material (Morrison and Gulson 2007) at Boolaroo, a small suburb 140 km north of Sydney.

These three studies measure metal concentrations in surface soils, vacuum dust, surface dust, and hand wipes using aqua regia acid digestion and ICP–MS analysis at the National Measurement Institute (NMI). Samples were measured by a National Association of Testing Authorities (NATA) accredited method, which allowed for greater focus towards the study findings rather than the measurement method and approach. In addition to acid extractable metal concentrations, these studies also utilise Pb isotope compositions and bio-accessible Pb concentrations to support the primary findings of **Papers Six** and **Eight** respectively. **Paper Six** also uses Pb isotope compositions to establish the source of the Pb-rich dust on the playground nearest to the mining operation (PG3) was indistinguishable, within analytical precision, to the established isotope composition of the local Broken Hill orebody (Figure 1.3). This isotope composition evidence identified the local mining operation as the primary source of metals in playground dusts, and assisted in advocating for stronger measures to protect the community from Pb hazards (ABC 2015). **Paper Eight** used bio-accessible Pb concentrations (mean = 92 % bio-accessibility) in vacuum dusts to demonstrate a clear Pb hazard remains in the residential homes of Boolaroo, post Pb abatement. These complementary analyses were able to be measured on the same analytical instrument as the acid extractable metal concentrations (Perkin Elmer Elan DRC II ICP–MS), demonstrating one of many advantages associated with *ex-situ* sampling and wet chemistry analysis.
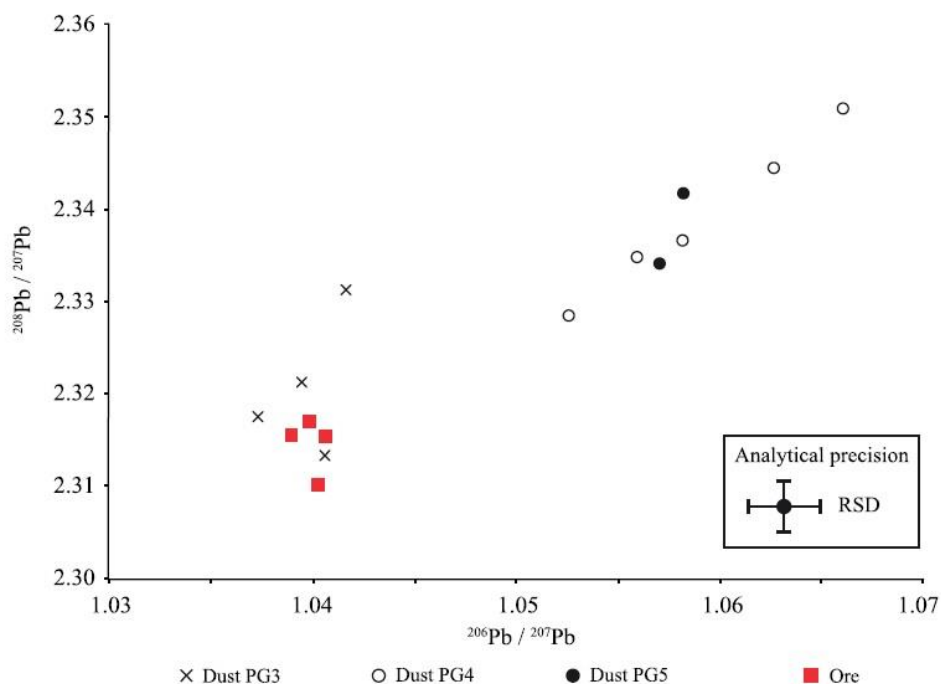
Figure 1.3: Stable Pb isotope ratios for dust Pb at the playground closest to the active mining operations were similar to values published for Broken Hill ore body Pb (Cooper et al. 1969; Gulson and Mizon 1979; Chiaradia et al. 1997; Townsend et al. 1998) (Source: Taylor et al. 2014).

1.5 Shortfalls to the current approach

Despite generating consistent and robust environmental data, the current approach of sampling and wet chemistry analysis also has a number of drawbacks. Wet chemistry analyses have an associated cost attached to each individual measurement that can prove costly when a large number of samples are submitted for metal quantification. For NATA-accredited analyses, measurement of eight metals by commercial laboratories can typically range between AU$14-28 per sample, while government laboratories may charge in excess of AU$50 per sample. If a full suite of elements is desired, commercial laboratories usually charge AU$17–56 per sample, while government laboratories can offer a full elemental suite for AU$130 per sample. These measurement costs often exclude additional laboratory expenses such as administration fees (~AU$25–30 per sample batch), waste disposal fees (~AU$1 per sample), drying fees (~AU$1.50 per sample) and sample homogenisation fees (~AU$6.50 per sample). The relatively high costs associated with off-site laboratory analyses can impact the number of samples collected (Boon and Ramsey 2012), and consequently may impact the investigation outcome. Turnaround times for commercial laboratory analyses (~7–10 days) can also prolong the completion of an investigation, particularly if the data indicates that a second visit to the field site is required to collect more samples. Most commercial laboratories do offer optional express turnaround times for clients who require rapid data analysis, and can range from 3 day reporting (~12.5 % total surcharge) to same day analysis (~100 % total surcharge).

Commercial laboratories assure their clients that their accredited laboratory methods achieve a specified level of data quality. For the measurements of soil and dust samples in **Papers Six**, **Seven** and **Eight**, the acceptable recovery of the NATA-accredited laboratory method was 75–120 %, while the acceptable relative percent difference (RPD, i.e. measurement repeatability) was <44 % for concentrations >5 times the limit of reporting (NMI 2015). Accredited laboratory methods are not always matrix-specific, yet can be aimed at certain sample groups such as air filters or soils. One of the lesser known limitations of accredited laboratory methods is that the estimates of analytical precision and bias are routinely conducted on in-house reference materials (fine grained and homogenous) that are substantially different to the submitted field samples (wet, coarse grained, heterogeneous) (See Section 3.3) (Boon and Ramsey 2012). Despite the quantitative assurances that accredited laboratory methods provide accurate metal quantification of field samples, the majority (>90 %) of error in measurements are usually derived from the sampling process. The estimation of sampling error in environmental investigations does incur extra costs, and are usually approximated using the minimal requirements set by the sampling protocol. Paradoxically, the majority of investigation costs are directed towards the laboratory analysis, not the field sampling where the greatest errors lie (Ramsey and Boon 2012).

The ability to send one sample to a laboratory and have it simultaneously measured by a range of different analytical methods is powerful, yet can also be slow and costly for environmental investigations. Most of the limitations presented above can potentially be addressed using a rapid, cost-effective, on-site measurement alternative such as pXRF, provided the data is fit for purpose for its intended use.

1.6   Aims

While the acceptance and application of pXRF is well established in other disciplines such as mineral exploration and mining, the use of pXRF in environmental investigations for final quantitative assessment is less common and is not included as a method of choice even in the recent 2013 revision of the *National Environment Protection (Assessment of Site Contamination) Measure 1999*. The specific reason(s) for the limited willingness of organisations to use pXRF is unclear, however it is likely due to a combination of the technology's current disadvantages and the fact that pXRF has a strong reputation as a screening device, rather than an analytical tool. Many pXRF users lack analytical experience, and when poor comparisons are achieved using established *ex-situ* laboratory techniques, the fault is typically directed towards the instrument, not the user. Therefore, it is vital to independently and accurately evaluate the analytical capabilities of pXRF technology to

enhance future environmental investigations of metal-contaminated soils. This thesis evaluates the validity of both *in-situ* and *ex-situ* pXRF measurements of metal-contaminated soil to address the evidence gap associated with pXRF analysis of environmental contaminants in soils.

The primary aims of this thesis, presented through the studies in the following chapters include:

➢ Quantification and assessment of the radiation exposure risk from pXRF spectrometers during the measurement of a range of materials.

➢ Evaluation of the analytical performance of *ex-situ* pXRF in the measurement of certified reference materials and metal-contaminated soil samples.

➢ Evaluation of the potential integration of *in-situ* pXRF for metal-contaminated site assessments.

➢ Assessment of pXRF application using case studies that investigate the distribution and source of soil metal contaminants in two urban centres.

Through these four overarching aims, the objective is to develop a more advanced understanding of pXRF safety, analytical performance and its efficacy for its application to assess metal-contaminated soils. Examination of measurement variables, comparisons with established analytical wet chemistry techniques and opportunities for environmental applications are explored. The aims of this thesis support each other to create a holistic evaluation of pXRF for the measurement of metal-contaminated soils. A secondary aim of this thesis is to investigate contemporary and legacy metal contamination hazards using pXRF and wet chemistry analysis.

1.7   Materials and methods

The aims of this thesis have been achieved using a variety of measurement techniques to assess the accuracy and precision of pXRF measurements, and to holistically investigate the sources and forms of contaminants in urban centres. Due to the uncertain stance of pXRF from both research and industry professionals, a multiple lines of evidence approach was used to provide a complete set of information regarding user safety, analytical quality and pXRF applicability when measuring metal-contaminated soils. Details of the methods and materials used for each study in this thesis are provided within each study publication.

With the exception of **Paper One**, which compares the radiation dispersion from three competing pXRF manufacturers, **Papers Two**, **Three**, **Four** and **Five** were completed using an Olympus Premium Innov-X XRF Analyser. It is relevant to note that while Olympus Australia provided financial, technical and instrument support for this thesis, they did not design or conduct any part of the research or writing of articles. While there are clear differences in manufacturer hardware arrangements and software, this thesis utilised one pXRF spectrometer to address the aims presented above. A range of certified reference materials and metal-contaminated soil samples were used to assess pXRF performance in **Papers Two**, **Three**, **Four** and **Five**. Analytical indicators were applied to quantify the precision and accuracy of pXRF measurements. These included elemental recoveries (%), relative proximity (RP), relative standard deviation (RSD), US EPA data quality guidelines (US EPA 1998), linear regression statistics and point by point graphs. Comparisons with established wet chemistry analytical methods (ICP–AES and ICP–MS) from both research and commercial laboratories were conducted with each sample set to provide external validation values for pXRF measurements.

In order to address the aims of **Papers Four**, **Five**, **Six**, **Seven** and **Eight,** pXRF was used as part of a multiple lines of evidence approach alongside other analytical techniques, to delineate the sources and causes of metal contamination in each of the locations examined. Metal contamination investigations used a variety of environmental samples to evaluate contaminant hazards in the environment, including; surface and subsurface soils, surface dust, hand dust, vacuum dust and waste slag material. Bio-accessible metal concentrations provided insight of the absorption of metals in the human digestion tract during exposure. Organic contaminants such as polycyclic aromatic hydrocarbons (PAHs) were also measured to corroborate inorganic metal concentrations for the assessment of contaminated soil. Lead isotope compositions were used to estimate the source contribution from likely causes of metal contamination in the environment such as ore processing and leaded petrol emissions. X-ray Diffraction and Scanning Electron Microscopy data complemented Pb isotope data to strengthen the identification of metal sources in the environment. In **Paper Four**, sample metadata was used to estimate source contributions to soil Pb contamination where Pb isotopes could not differentiate between similar source signatures (e.g. Pb-based paints and leaded petrol emissions). The wide range of materials and methods used in this thesis enabled a comprehensive investigation of pXRF user safety, analytical performance and potential for environmental application for the measurement of metal-contaminated soils.

1.8 References

Argyraki, A., Ramsey, M.H., Potts, P.J. 1997. Evaluation of Portable X-ray Fluorescence Instrumentation for in situ Measurements of Lead on Contaminated Land. Analyst 122, 743-749.

Ashley, K., Hunter, M., Tait, L.H., Dozier, J., Seaman, J.L., Berry, P.F. 1998. Field investigation of on-site techniques for the measurement of lead in paint films. Field analytical chemistry and technology 2(1), 39-50.

Australian Broadcasting Corporation (ABC). 2015. Lead clean up begins at Broken Hill playgrounds. <http://www.abc.net.au/news/2015-05-27/lead-clean-up-begins-at-broken-hill-playgrounds/6500416> (accessed 21 April 2017).

Bastos, R.O., Melquiades, F.E., Biasi, G.E.V. 2012. Correction for the effect of soil moisture on in situ XRF analysis using low-energy background. X-ray Spectrometry 41, 304-307.

Block, C.N., Shibata, T., Solo-Gabriele, H.M., Townsend, T.G. 2007. Use of handheld X-ray fluorescence spectrometry units for identification of arsenic in treated wood. Environmental Pollution 148, 627-633.

Boon, K.A., Ramsey, M.H. 2012. Judging the fitness of on-site measurements by their uncertainty, including contribution from sampling. Science of the Total Environment 419, 196-207.

Bosco, G.L. 2013. Development and application of portable, hand-held X-ray fluorescence spectrometers. James L. Waters Symposium 2012 Report. Trends in Analytical Chemistry 45, 121-134.

Brouwer, P., 2003. Theory of XRF - Getting acquainted with the principles. PANalytical B.V., The Netherlands.

Carr, R., Zhang, C., Moles, N., Harder, M. 2008. Identification and mapping of heavy metal pollution in soils of a sports ground in Galway City, Ireland, using a portable XRF analyser and GIS. Environmental Geochemistry and Health 30, 45-52.

Cesareo, R., Castellano, A., Cuevas, A.M. 1998. Energy dispersive X-ray fluorescence analysis of thin and intermediate environmental samples. X-ray spectrometry 27(4), 257-264.

Chiaradia, M., Chenhall, B.E., Depers, A.M., Gulson, B.L., Jones, B.G. 1997. Identification of historical lead sources in roof dusts and recent lake sediments from an industrialized area: indications from lead isotopes. Science of the Total Environment 205, 107–128.

Chen, M., Lena, Q.M. 2001. Comparison of three aqua regia digestion methods for twenty Florida soils. Soil Science Society of America Journal 65, 491–499.

Chou, J., Elbers, D., Clement, G., Bursavich, B., Tian, T., Zhang, W., Yang, K. 2010. In situ monitoring (field screening) and assessment of lead and arsenic contaminants in the greater New Orleans area using a portable x-ray fluorescence analyser. Journal of Environmental Monitoring 12, 1722–1729.

Clark, S., Menrath, W., Chen, M., Roda, S., Succop, P. 1999. Use of a field portable X-ray fluorescence analyzer to determine the concentration of lead and other metals in soils. Annals of Agricultural and Environmental Medicine 6, 27-32.

Cooper, J.A., Reynolds, P.H., Richards, J.R. 1969. Double-spike calibration of the Broken Hill standard lead. Earth and Planetary Science Letters 6, 467–478.

Dong, C. Taylor, M.P. 2017. Applying geochemical signatures of atmospheric dust to distinguish current mine emissions from legacy sources. Atmospheric Environment 161, 82-89.

Dost, A.A. 1996. Monitoring surface and airborne inorganic contamination in the workplace by a field portable x-ray fluorescence spectrometer. Annals of Occupational Hygiene 40, 589–610.

Ericson, B., Landrigan, P., Taylor, M.P., Frostad, J., Caravanos, J., Keith, J., Fuller, R. 2016. The Global Burden of Lead Toxicity Attributable to Informal Used Lead-Acid Battery (ULAB) Sites. Annals of Global Health 82(5), 686-699.

Gregory, D., Meffre, S., Large, R.R. 2013. Mineralogy of metal contaminated estuarine sediments, Derwent estuary, Hobart, Australia: Implications for metal mobility. Australian Journal of Earth Sciences 60, 589-603.

Gulson, B.L., Mizon, K.J. 1979. Lead isotopes as a tool for gossan assessment in base metal exploration. Journal of Geochemical Exploration 11, 299–320.

Haffert, L., Craw, D. 2009. Field quantification and characterization of extreme arsenic concentrations at a historic mine processing site, Waiuta, New Zealand. New Zealand Journal of Geology and Geophysics 52, 261–272.

Higueras, P., Oyarzun, R., Iraizoz, J.M., Lorenzo, S., Esbri, J.M., Martinez-Coronado, A. 2012. Low-cost geochemical surveys for environmental studies in developing countries: Testing a field portable XRF instrument under quasi-realistic conditions, Journal of Geochemical Exploration 113, 3-12.

Horta, A., Malone, B., Stockmann, U., Minasny, B., Bishop, T.F.A., McBratney, A.B., Pallasser, R., Pozza, L. 2015. Potential of integrated field spectroscopy and spatial analysis for enhanced assessment of soil contamination: A prospective review. Geoderma 241-242, 180-209.

Jenkins, R. 1988. X-ray Fluorescence Spectrometry. John Wiley & Sons, Inc, Hoboken, NJ, USA.

Jenkins, R. 2012. History and Development of X-ray Fluorescence Spectrometry, in X-ray Fluorescence Spectrometry 152, 2nd Ed., John Wiley & Sons, Inc., Hoboken, NJ, USA.

Kalnicky, D.J., Singhvi, R. 2001. Field portable XRF analysis of environmental samples. Journal of Hazardous Materials 83, 93-122.

Kilbride, C., Poole, J., Hutchings, T.R., 2006. A comparison of Cu, As, Cd, Zn, Fe, Ni and Mn determined by acid extraction/ICP-OES and ex-situ field portable X-ray fluorescence analyses. Environmental Pollution 143, 16-23.

Kristensen, L.J. Taylor, M.P. 2016. Unravelling a 'miner's myth' that environmental contamination in mining towns is naturally occurring. Environmental Geochemistry and Health 38(4), 1015-1027.

Kristensen, L.J., Taylor, M.P., Flegal, A.R. 2017. An odyssey of environmental pollution: The rise, fall and remobilisation of industrial lead in Australia. Applied Geochemistry 83, 3-13.

Lawryk, N.J., Febg, H.A., Chen, B.T. 2009. Laboratory evaluation of a field-portable sealed source X-ray fluorescence spectrometer for determination of metals in air filter samples. Journal of Occupational and Environmental Hygiene 6, 433–445.

Lemiere, B., Laperche, V., Haouche, L., Auger, P. 2014. Portable XRF and wet materials: application to dredged contaminated sediments from waterways. Geochemistry: Exploration, Environment, Analysis 14, 257-264.

Loredo, J., Álvarez, R., Ordòñez, A., Bros, T. 2008. Mineralogy and geochemistry of the Texeo Cu–Co mine site (NW Spain): screening tools for environmental assessment. Environmental Geology 55, 1299–1310.

McLaren, T.I., Guppy, C.N., Tighe, M.K., Forster, N., Grave, P., Lisle, L.M., Bennett, J.W. 2012. Rapid, Nondestructive Total Elemental Analysis of Vertisols using Portable X-ray Fluorescence. Nutrient Management & Soils & Plant Analysis. Soil Science Society of America Journal 76, 1436-1445.

Melquiades, F.L., Appoloni, C.R. 2004. Application of XRF and field portable XRF for environmental analysis. Journal of Radioanalytical and Nuclear Chemistry 262(2), 533-541.

Mielke, H.W., Gonzales, C.R., Cahn, E., Brumfield, J., Powell, E.T., Mielke, P.W. 2010. Soil arsenic surveys of New Orleans: localized hazards in children's play areas. Environmental Geochemistry and Health 32, 431–440.

Morley, J.C., Clark, C.S., Deddens, J.A., Ashley, K., Roda, S. 1999. Evaluation of a portable X-ray fluorescence instrument for the determination of lead in workplace air samples. Applied Occupational and Environmental Hygiene 14, 306-316.

Morrison, A. L., & Gulson, B. L. 2007. Preliminary findings of chemistry and bio-accessibility in base metal smelter slags. Science of the Total Environment 382, 30–42.

National Measurement Institute (NMI). 2015. Method NT2.49: Determination of Acid Extractable Elements in Soils, Sediments, Sludges and Solid Waste. Inorganics Section. 1-32.

New South Wales Environment Protection Authority (NSW EPA), 1995. Sampling Design Guidelines. Contaminated Sites. <http://www.epa.nsw.gov.au/resources/clm/95059sampgdlne.pdf> (accessed 02 March 2017).

Niskavaara, H., Reimann, C., Chekushin, V., Kashulina, G. 1997. Seasonal variability of total and easily leachable element contents in topsoils (0–5 cm) from eight catchments in the European arctic (Finland, Norway, and Russia). Environmental Pollution 96, 261–274.

Olympus. 2016. Vanta Specifications. Handheld X-ray Fluorescence. 1-2. <http://www.olympus-ims.com/en/vanta/> (accessed 11 April 2017).

Olympus. 2017. Delta Alloys and Metals Handheld XRF Analyzer. XRF and XRF Analysers. <http://www.olympus-ims.com/en/delta-premium/> (accessed 12 April 2017).

Operating Engineers National Hazmat Program (OENHP). 2002. Technology Safety Data Sheet. Niton XL-309 (Lead Paint Analyser). Version A. 1-7.

Parsons, C., Grabulosa, E.M., Pili, E., Floor, G.H., Roman-Ross, G., Charlet, L. 2013. Quantification of trace arsenic in soils by field-portable X-ray fluorescence spectrometry:

Considerations for sample preparation and measurement conditions. Journal of Hazardous Materials 262, 1213-1222.

Paulette, L., Man, T., Weindorf, D.C., Person, T. 2015. Rapid assessment of soil and contaminant variability via portable X-ray fluorescence spectroscopy: Copsa Mica Romania. Geoderma 243-244, 130-140.

Peinado, F.M., Ruano, S.M., Gonzalez, M.G.B., Molina, C.E. 2010. A rapid field procedure for screening trace elements in polluted soil using portable X-ray fluorescence (PXRF). Geoderma 190, 76-82.

Piercey, S.J., Devine, M.C. 2014. Analysis of powdered reference materials and known samples with a benchtop, field portable X-ray fluorescence (pXRF) spectrometer: evaluation of performance and potential applications for exploration lithogeochemistry. Geochemistry: Exploration, Environment, Analysis 14, 139-148.

Radu, T., Gallagher, S., Byrne, B., Harris, P., Coveney, S., McCarron, S., McCarthy, T., Diamond, D. 2013. Portable X-ray Fluorescence as a Rapid Technique for Surveying Elemental Distributions in Soil. Spectroscopy Letters: An International Journal for Rapid Communication 46(7), 516-526.

Ramsey, M.H., Boon, K.A. 2012. Can in-situ geochemical measurements be more fit-for-purpose than those made ex-situ? Applied Geochemistry 27, 969-976.

Ran, J., Wang, D., Wang, C., Zhang, G., Yao, L. 2014. Using portable X-ray fluorescence spectrometry and GIS to assess environmental risk and identify sources of trace metals in soils of peri-urban areas in the Yangtze Delta region, China. Environmental Science: Processes & Impacts 16, 1870-1877.

Reece, R.M., Reed, A.J., Clark, C.S., Angoff, R.C., Casey, K.R., Challop, R.S., McCabe, E. 1972. Elevated blood lead and the in situ analysis of wall paint by –ray fluorescence. The American Journal of Diseases of children 24, 500-502.

Sahraoui, H., Hachicha, M. 2017. Effect of soil moisture on trace elements concentrations using portable X-ray Fluorescence Spectrometer. Journal of Fundamental and Applied Sciences 9(1), 468-484.

Shand, C.A., Wendler, R., 2014. Portable X-ray fluorescence analysis of mineral and organic soils and the influence of organic matter. Journal of Geochemical Exploration 143, 31-42.

Stallard, M.O., Apitz, S.E., Dooley, C.A. 1995. X-ray fluorescence spectrometry for field analysis of metals in marine sediments. Marine Pollution Bulletin 31(4-12), 297-305.

Standards Australia (AS 4482.1). 2005. Guide to the investigation and sampling of sites with potentially contaminated soil Non-volatile and semi-volatile compounds. Standards Australia. 1-59.

Stockmann, U., Cattle, S.R., Minasny, B., McBratney, A.B. 2016. Utilising portable X-ray fluorescence spectrometry for in-field investigation of pedogenesis. Catena 139, 220-231.

Taylor, M.P., Camenzuli, D., Kristensen, L.J., Forbes, M., Zahran, S. 2013. Environmental lead exposure risks associated with children's outdoor playgrounds. Environmental Pollution 178, 447–454.

Taylor, P.D., Ramsey, M.H., Potts, P.J. 2005. Spatial contaminant heterogeneity: quantification with scale of measurement at contrasting sites. Journal of Environmental Monitoring 7, 1364-1370.

Thermo Fisher Scientific. 2012. Thermo Fisher Scientific Embeds GPS Functionality in all Niton XL3t Series XRF Analyzers. <http://news.thermofisher.com/press-release/thermo-scientific/thermo-fisher-scientific-embeds-gps-functionality-all-niton-xl3t-ser> (accessed 09 June 2017).

Townsend, A.T., Yu, Z., McGoldrick, P., Hutton, J.A. 1998. Precise lead isotope ratios in Australian galena samples by high resolution inductively coupled plasma mass spectrometry. Journal of Analytical Atomic Spectrometry 13, 809–813.

United States Environmental Protection Agency (US EPA), 1998. Environmental Technology Verification Report, Field Portable X-ray Fluorescence Analyzer. Metorex X-MET 920-P. <http://nepis.epa.gov/Adobe/PDF/30003LR0.pdf> (accessed 25 June 2015).

United States Environmental Protection Agency (US EPA). 2017. Resource Conservation and Recovery Act (RCRA) Laws and Regulations. <https://www.epa.gov/rcra> (accessed 11 April 2017).

Vanhoof, C., Corthouts, V., Tirez, K. 2004. Energy-dispersive X-ray fluorescence systems as analytical tool for assessment of contaminated soils. Journal of Environmental Monitoring 6, 344-350.

Vercoutere, K. Fortunati, U., Muntau, H., Griepink, B., Maier, E.A. 1995. The certified reference materials CRM 142 R light sandy soil, CRM 143 R sewage sludge amended soil and CRM 145 R sewage sludge for quality control in monitoring environmental and soil pollution. Fresenius Journal of Analytical Chemistry 352, 197-202.

Weindorf, D.C., Zhu, Y., Chakraborty, S., Bakr, N., Huang, B. 2012. Use of portable X-ray fluorescence spectrometry for environmental quality assessment of peri-urban agriculture. Environmental Monitoring and Assessment 184, 217-227.

Weindorf, D.C., Paulette, L., Man, T. 2013. In-situ assessment of metal contamination via portable X-ray fluorescence spectroscopy: Zlatna, Romania. Environmental Pollution 182, 92-100.

Weindorf, D.C., Bakr, N., Zhu, Y. 2014a. Chapter One: Advances in Portable X-ray Fluorescence (PXRF) for Environmental, Pedological, and Agronomic Applications. Advances in Agronomy 128, 1-45.

Weindorf, D.C., Bakr, N., Zhu, Y., McWhirt, A., Ping, C.L., Michaelson, G., Nelson, C., Shook, K., Nuss, S. 2014b. Influence of Ice on Soil elemental Characterization via Portable X-ray Fluorescence Spectrometry. Pedsphere 24(1), 1-12.

West, M., Ellis, A., Potts, P.J., Streli, C., Vanhoof, C., Wegrzynek, D., Wobauschek, P. 2013. 2013 Atomic spectrometry update – A review of advances in X-ray fluorescence spectrometry. Journal of Analtical Atomic Spectrometry 28, 1544-1590.

Zhu, Y. Weindorf, D.C., Zhang, W. 2011. Characterising soils using a portable X-ray fluorescence spectrometer: 1. Soil texture. Geoderma 167-168, 167-177.

Chapter Two: Radiation safety assessment

2.1 Prologue

Note: the term handheld XRF (HHXRF) was used in this chapter over pXRF.

Operation of handheld XRF spectrometers requires users to obtain a radiation user licence from the relevant state protection authority (NSW EPA 2017) and be trained by a manufacturer's representative, or by attending a radiation safety course. Training content typically covers X-ray sources, XRF hardware and basic radiation safety principles, such as do not hold the measurement object in your hand during operation. These courses, however, do not provide sufficient detail on the variation of radiation dispersion from materials of differing densities, nor third dimensional dose rates around spectrometers. For example, radiation profiles found in the user guides from two of Australia's leading handheld XRF distributors (Olympus and Bruker), are shown in Figure 2.1 and 2.2 respectively. Handheld XRF applications vary across a range of disciplines, and subsequently results in a range of matrices being measured. The absence of radiation safety information around specific handheld XRF applications was the catalyst for the study presented in Section 2.2.

This chapter presents the first detailed evaluation of radiation dispersion around handheld XRF spectrometers during the measurement of a range of materials. Understanding the radiation intensity and scattering direction from materials, as well as directly from the spectrometer, is vital for user confidence and safety, particularly as the technology continues to grow into new markets that are likely to comprise of inexperienced users. This paper addresses this safety knowledge gap and contributes to this thesis by identifying variables (such as instrument snout design and angle of scattering back to the user) that influence the radiation exposure of a user. This study also calculates the effective body radiation dose received during a hypothesised yearly handheld XRF operation scenario, and compares it against common radiation exposure sources such as medical imaging and natural background radiation.
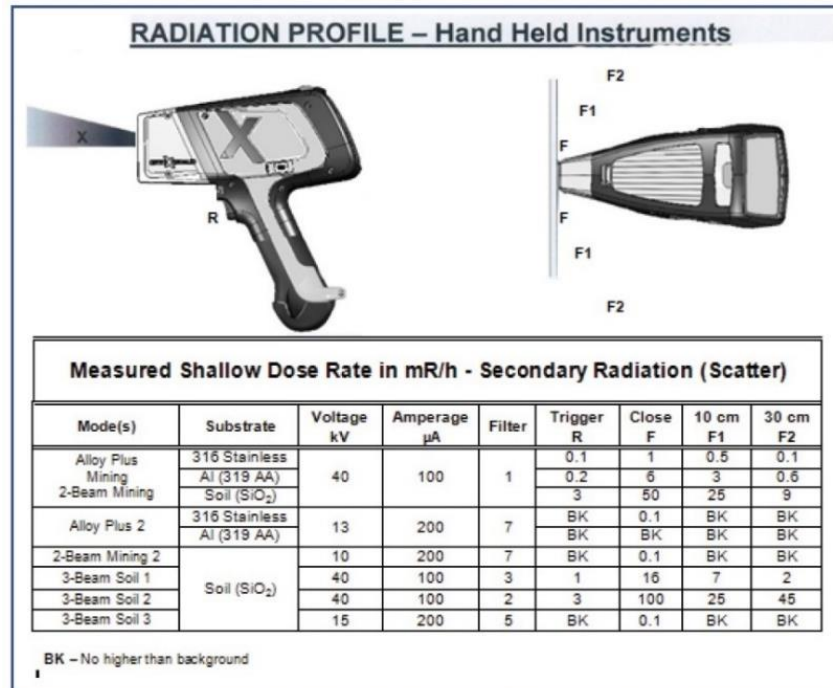
Figure 2.1: Radiation profile over different variables for the Innov-X (now owned by Olympus Ltd Pty) DELTA XRF spectrometer (Innov-X Systems 2010).

Figure 2.2: Radiation profile during the measurement of a '*sufficiently thick sample*' using two different beams for a Bruker Tracer SD XRF spectrometer (Bruker Elemental 2010).

2.2 Paper One

Publication

Handheld X-ray Fluorescence Spectrometers: Radiation Exposure Risks of Matrix-Specific Measurement Scenarios

---

Abstract: This study investigates X-ray intensity and dispersion around handheld X-ray Fluorescence (XRF) instruments during the measurement of a range of sample matrices to establish radiation exposure risk during operation. Four handheld XRF instruments representing three manufacturers were used on four smooth, flat-lying materials of contrasting matrix composition. Dose rates were measured at 10, 20, 30 and 40 cm intervals every 30° around the instrument at 0 and 45° from the horizontal, as well as vertically from the instrument screen. The analysis of polyethylene recorded dose rates 156 times higher (on average) than steel measurements and 34 times higher than both quartz sand and quartz sandstone. A worst-case exposure scenario was assumed where a user analyses a polyethylene material at arm's reach for one hour each working day for one year. This scenario resulted in an effective body dose of 73.5 μSv, equivalent to three to four chest X-rays (20 μSv) a year, twenty times lower than the average annual background radiation exposure in Australia and well below the annual exposure limit of 1 mSv for non-radiation workers. This study finds the advantages of using handheld XRF spectrometers far outweighs the risk of low radiation exposure linked to X-ray scattering from samples.

Keywords: Radiation, X-Ray Fluorescence, XRF, Handheld XRF, Exposure risk, Matrix, Scattering, Dose rates.

Paper One of this thesis has been removed due to copyright reasons

2.3 Improper HHXRF practice

In order to develop our understanding of commonly applied handheld XRF practices, this paper was presented as a poster at two analytical X-ray conferences in 2014 (Australian X-ray Analytical Association and Denver X-ray conference) prior to formal peer review and publication (Figure 2.3). Delegates at the conference shared their stories of handheld XRF operation from a range of industries. One example took place in a museum, where a research assistant was measuring hundreds of wooden artefacts from Australia. The spectrometer was orientated upwards with the measurement window pointing to the ceiling and each artefact was balanced on top of the instrument snout. Due to the large size of some of the artefacts, shielding (e.g. a test stand) was not used to mitigate radiation dispersion. Other safety concerns raised included the fact that the handheld XRF set up was only 1–2 meters from the desk of another research assistant, who was unaware of the radiation hazard behind her.
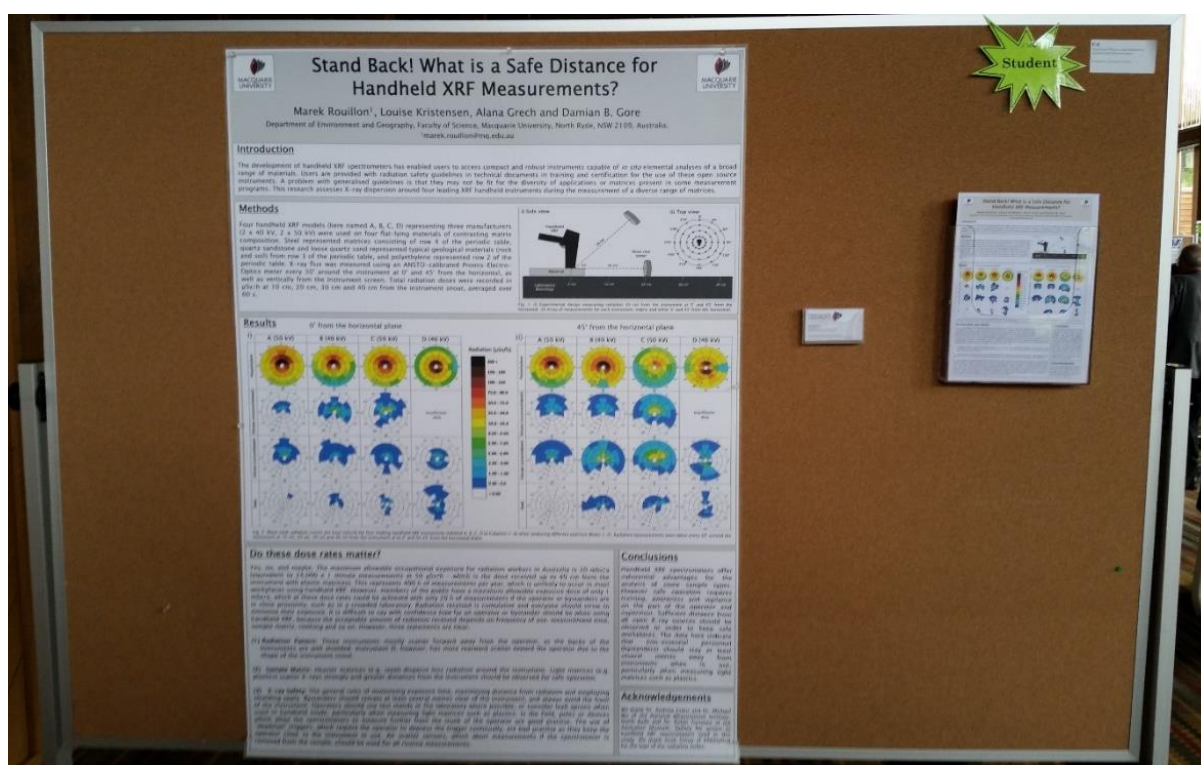
Figure 2.3: Presentation of radiation scattering from materials during handheld XRF operation at the Denver X-ray Conference in Big Sky, Montana, USA.

These stories were later confirmed through a series of photographs from an Australian museum demonstrating pXRF operation. The investigators are shown balancing artefacts on the instrument snout, with no shielding at close proximity to the operator (Figure 2.4). The photographs show measurement of (a) a basalt axe head from Australia and (b) stone tools from China, using the same pXRF instrument as Model D in **Paper One**. The stone tools shown in panel (b) are quite small and easily could have been measured within a shielding cap, yet there is no evidence of a shielding cup or plate being used in the photograph. Unfortunately such

practice is not uncommon. Despite users being trained to understand radiation hazards associated from handheld XRF use, there remains a persistent ignorance of basic radiation safety principles, such as the ALARA principle (as low as reasonably achievable), to minimise exposures where possible (NRC 2014). Handheld XRF radiation safety may be most relevant for archaeological research, as large proportions of artefacts contain rough, uneven surfaces that are measured without shielding.

Figure 2.4: HHXRF measurement of (a) a basalt axe head and (b) stone tool artefacts in museums. Source: Australian Museum (2009) and University of Sydney (2014).

The measurement of soils presents less radiation risk to the user for a number of reasons. Soils can be prepared to present a flat surface for measurement, minimising radiation dispersion between the spectrometer and the target sample. The use of optional accessories such as an extension pole or a soil foot assists in ergonomic and hands-free *in-situ* testing (Olympus 2017), while maximising the distance between user and instrument during operation. *Ex-situ* soil measurements can be carried out using a test stand, where shielding and interlock protocols prevent X-ray generation if the stand is open. The use of these optional accessories (extension pole, soil foot and test stands) were utilised where possible during each study in this thesis.

Yet, it is worth noting that handheld XRF operators in the mining, exploration and environmental fields also measure soil samples through plastic zip-lock bags (e.g. Peinado et al. 2010). While this was not a scenario investigated in **Paper One**, the presence of a thin layer of polyethylene between the handheld XRF and the soil sample would theoretically increase the radiation exposure dose to the user. Further work is required to determine the radiation exposure of polyethylene-bound soil sample measurements to a handheld XRF user.

2.4 References

Australian Museum. 2009. Image: Peter Grave using pXRF.
    <https://australianmuseum.net.au/image/peter-grave-using-pxrf> (accessed 16 April 2017).

Bruker Elemental. 2010. X-Ray Radiation Safety. Manual for Operator Training.
    030.0011.01.0. 1-57.

Innov-X Systems. 2010. User Manual. Delta [TM] Family: Handheld XRF Analyzers. Revision
    June 2010.

National Regulatory Commission (NRC). 2014. ALARA. Subpart A-20. 1003. <
    https://www.nrc.gov/reading-rm/basic-ref/glossary/alara.html> (accessed 20 February
    2017).

New South Wales Environment Protection Authority (NSW EPA). 2017. Radiation user
    license – criteria. Managing radiation in NSW.
    <http://www.epa.nsw.gov.au/radiation/licensing/licensingcriteria.htm#analytical>
    (accessed 27 April 2017).

Olympus. 2017. The DELTA professional. Olympus. <http://www.olympus-ims.com/en/xrf-
    xrd/delta-handheld/delta-prof/> (accessed 20 February 2017).

Peinado, F.M., Ruano, S.M., Gonzalez, M.G.B., Molina, C.E. 2010. A rapid field procedure for
    screening trace elements in polluted soil using portable X-ray fluorescence (PXRF).
    Geoderma 190, 76-82.

University of Sydney. 2014. Image: pXRF analysis in China.
    <https://australianmuseum.net.au/image/pxrf-analysis-in-china> (accessed 16 April 2017).

Chapter Three: Analytical evaluation of pXRF

3.1   Prologue

Understanding the importance of measurement variables such as sample preparation and presentation, and the use of matrix-specific calibrations are essential for achieving consistent and accurate pXRF data (Willis and Duncan 2008). While this information is well known for many benchtop XRF users, pXRF users are often provided little analytical training prior to operation. It is mandatory that users undergo radiation safety training prior to instrument operation, as mentioned in Chapter Two (Liddle 2012). However, analytical pXRF training is optionally accessed through external workshops, typically by XRF consultants, some manufacturers or at conferences at an additional cost. Moreover, the well-known screening use of pXRF has largely underemphasized and incorrectly informed users with regard to its analytical capabilities (Kenna et al. 2010).

This chapter presents a comprehensive evaluation of the analytical capabilities of a new generation pXRF for the measurement of metal-contaminated soils. The following research study addresses knowledge gaps in the pXRF user field:

(a) to provide limited advice and effective communication of XRF basic protocols to enable inexperienced pXRF users to achieve accurate and reliable soil metal measurements

(b) to evaluate the analytical performance of a pXRF spectrometer when instrument, sample and measurement variables were optimized.

In the study presented below, the accuracy of pXRF measurements were compared against soil CRM values, commercial ICP–AES and research grade ICP–MS measurements. This study contributes to the second aim of this thesis in that it demonstrates that pXRF can generate high quality research data, equivalent to (and at times better than) commercial ICP–AES measurement data, which along with ICP–MS, are typically the analytical instrument of choice for commercial environmental investigations. Lastly, the economic rationale of pXRF analysis as an alternative to traditional wet chemistry analyses is examined. The issue of analytical costs is paramount in many studies as funding is typically the limiting factor for the number of sample measurements in an investigation. As detailed in Chapter Four, the number of samples in a study has a critical impact on the confidence of the mean values and the range of values associated with the 95 % confidence interval, which is often applied to determine the next steps in contaminated site assessments.

3.2 Paper Two

Publication

Can field portable X-ray fluorescence (pXRF) produce high quality data for application in environmental contamination research?

_____

Abstract: This research evaluates the analytical capabilities of a field portable X-ray fluorescence spectrometer (pXRF) for the measurement of contaminated soil samples using a matrix-matched calibration. The calibrated pXRF generated exceptional data quality from the measurement of ten soil reference materials. Elemental recoveries improved for all 11 elements post-calibration with reduced measurement variation and detection limits in most cases. Measurement repeatability of reference values ranged between 0.2–10 % relative standard deviation, while the majority (82 %) of reference recoveries were between 90–110 %. Definitive data quality, the highest of the US EPA's three level quality ranking, was achieved for 15 of 19 elemental datasets. Measurement comparability against inductively coupled plasma atomic emission spectroscopy (ICP–AES) values was excellent for most elements (e.g, r^2 0.999 for Mn and Pb, r^2 >0.995 for Cu, Zn and Cd). Parallel measurement of reference materials revealed ICP–AES and ICP–MS measured Ti and Cr poorly when compared to pXRF. Individual recoveries of soil reference materials by both ICP–AES and pXRF showed that pXRF was equivalent to or better than ICP–AES values for all but two elements (Ni, As). This study demonstrates pXRF as a suitable alternative to ICP–AES analysis in the measurement of Ti, Cr, Mn, Fe, Cu, Zn, Sr, Cd, and Pb in metal-contaminated soils. Where funds are limited, pXRF provides a low-cost, high quality solution to increasing sample density for a more complete geochemical investigation.

Keywords: Field portable X-ray fluorescence spectrometry, pXRF, ICP–AES, evaluation, data quality.

Can field portable X-ray fluorescence (pXRF) produce high quality data for application in environmental contamination research? ☆

Marek Rouillon [*], Mark P. Taylor

Department of Environmental Sciences, Faculty of Science and Engineering, Macquarie University, Sydney, NSW 2109, Australia

ABSTRACT

This research evaluates the analytical capabilities of a field portable X-ray fluorescence spectrometer (pXRF) for the measurement of contaminated soil samples using a matrix-matched calibration. The calibrated pXRF generated exceptional data quality from the measurement of ten soil reference materials. Elemental recoveries improved for all 11 elements post-calibration with reduced measurement variation and detection limits in most cases. Measurement repeatability of reference values ranged between 0.2 and 10% relative standard deviation, while the majority (82%) of reference recoveries were between 90 and 110%. Definitive data quality, the highest of the US EPA's three level quality ranking, was achieved for 15 of 19 elemental datasets. Measurement comparability against inductively coupled plasma atomic emission spectrometry (ICP-AES) values was excellent for most elements (e.g, r^2 0.999 for Mn and Pb, $r^2 > 0.995$ for Cu, Zn and Cd). Parallel measurement of reference materials revealed ICP-AES and ICP-MS measured Ti and Cr poorly when compared to pXRF. Individual recoveries of soil reference materials by both ICP-AES and pXRF showed that pXRF was equivalent to or better than ICP-AES values for all but two elements (Ni, As). This study demonstrates pXRF as a suitable alternative to ICP-AES analysis in the measurement of Ti, Cr, Mn, Fe, Cu, Zn, Sr, Cd, and Pb in metal-contaminated soils. Where funds are limited, pXRF provides a low-cost, high quality solution to increasing sample density for a more complete geochemical investigation.

© 2016 Elsevier Ltd. All rights reserved.

Abbreviations

CRM	certified reference material
ICP-AES	inductively coupled plasma atomic emission spectrometry
ICP-MS	inductively coupled plasma mass spectrometry
mg/kg	milligrams per kilogram
MXFLR	maximum likelihood functional linear relationship
NIST	National Institute of Standards and Technology
NRC	National Research Council of Canada
pXRF	field portable X-ray fluorescence spectrometer
r^2	coefficient of variation/goodness of fit
RP	relative proximity
RSD	relative standard deviation

1. Introduction

Field portable X-ray fluorescence spectrometers (pXRF) have improved dramatically in the last 10 years due to the miniaturization of components such as the X-ray tube, development of advanced silicon drift detectors, and improvements in quantification algorithms (Hall et al., 2014; Hou et al., 2004; Radu et al., 2013; Shand and Wendler, 2014; Weindorf et al., 2014). These instruments have the potential to provide rapid, cost-effective, non-destructive alternatives to traditional expensive and time-consuming wet chemistry analysis in environmental monitoring and screening (Argyraki et al., 1997; Potts and West, 2008; Schneider et al., 1999). Their implementation in geochemical research (Clark et al., 1999; Wu et al., 2012) and as *in situ* screening tools for contaminated land monitoring is well documented (CLEA, 2002; Radu et al., 2013; Shefsky, 1999; Vanhoof et al., 2004; Weindorf et al., 2013) however, data from pXRF are typically supported by a secondary analysis technique (US EPA, 2004).

The acceptance of pXRF as a suitable future alternative to traditional laboratory analyses such as benchtop X-ray fluorescence

---

spectrometry (XRF), atomic absorption spectrometry (AAS), inductively coupled plasma atomic emission spectrometry (ICP-AES), and inductively coupled plasma mass spectrometry (ICP-MS) is mixed due to varying pXRF evaluations. In order to optimize data quality, pXRF users should develop their own calibrations specific to the material they intend to measure (Hall et al., 2014; Kenna et al., 2011; Piercey and Devine, 2014), yet some pXRF evaluations are carried out using 'out of the box' factory settings, and subsequently achieve sub-optimal results. Hall et al. (2014) broadly investigated the analytical performance of five pXRFs in the measurement of 41 powdered certified reference materials (CRMs) using default factory settings. Comparability with reference values were largely affected by the wide range of matrices present in the CRM suite, resulting in generally poor agreement with reference values. The authors acknowledged that the wide array of matrices made it impractical to modify calibrations for the study, which reduced the analytical performance of the pXRF instruments.

In contrast, the pXRF evaluation carried out by Kenna et al. (2011) measured both reference materials and Hudson River sediments using an Innov-X Alpha series 4000 pXRF. The instrument was externally calibrated using soil, sediment and shale CRMs and consequently produced high quality data for a range of elements. Kenna et al. (2011) concluded that when calibrated, pXRF is comparable to traditional laboratory analysis of Hudson River sediments. There are many reasons that may contribute to inconsistencies across pXRF performance evaluations such as the rapid advancement of pXRF technology in recent years (Radu et al., 2013; Shand and Wendler, 2014), selection and preparation quality of samples, selection of pXRF instrument and application of user-defined calibrations (Kenna et al., 2011). These variables should be optimized when evaluating an analytical instrument to provide the best possible opportunity to assess its analytical capabilities. This study optimizes these instrument, sample, and measurement variables through a detailed methodological approach, and evaluates the performance of a pXRF in the measurement of reference materials and contaminated soil samples after employing a matrix-specific calibration.

2. Experimental design

2.1. Instrument and calibrations

An Olympus Delta Premium XRF Analyzer fitted with a 50 kV, 4 W Ta anode X-ray tube and a silicon drift detector was used in this study. The recommended operational procedures set by the manufacturer were followed throughout this study, including: daily measurements of an energy calibration check, measurements of a silicate (SiO_2) blank, and measurements of National Institute of Standards and Technology (NIST) reference materials every 20–25 samples to monitor instrument performance. The pXRF instrument was operated in a shielded test stand to eliminate radiation exposure associated with extensive pXRF use (Rouillon et al., 2015).

In addition to evaluating the manufacturer's factory settings, a matrix matched calibration was developed for the measurement of contaminated soils. This calibration was achieved by adjusting elemental user factors and offsets (slopes and intercepts) after repeated measurements of up to 10 reference materials all comprised of the same silicate-based soil matrix (Supplementary Table A). This calibration strategy was repeated three times using a different combination of reference materials including a range of samples with lower elemental concentrations. The three calibrations were then combined into a final calibration by selecting the user factors and offsets that achieved the best elemental recoveries for each element.

2.2. Reference materials

Ten CRMs with similar matrix composition were selected for this study (Supplementary Table A). This study only evaluated certified and reference values, rather than all elemental values reported within a sample. The CRMs comprised soils (n = 5) and sediments (n = 5) from NIST and the National Research Council of Canada (NRC). Reference materials covered the range of elemental concentrations in typical contaminated and non-contaminated soils for Ti, Cr, Mn, Fe, Ni, Cu, Zn, As, Sr, Cd, and Pb. The CRMs were thoroughly mixed in their bottles by shaking prior to packing in 35 mm open ended PANalytical XRF cups held using 3.6 μm Chemplex Mylar X-ray film.

2.3. Contaminated soil samples

Seventy five metal contaminated soil samples were analyzed to further evaluate the performance of the pXRF. Six soil samples were collected from Boolaroo, a small town north of Sydney contaminated by the emissions of a Zn/Pb smelter operating until 2003 (Harvey et al., 2015). Six soil samples were collected from Broken Hill, a mining city in western New South Wales contaminated by more than 100 years of Zn/Pb ore extraction (Dong et al., 2015). Eleven estuarine samples were collected from Leichhardt River adjacent to Mt. Isa Mines, one of Australia's largest atmospheric polluters of metals (Taylor and Hudson-Edwards, 2008). Lastly, 52 soil samples contaminated by the historic use of leaded petrol and lead-based paints were collected from Sydney (VegeSafe, 2015).

In order to minimize measurement uncertainty, samples were subject to the same preparation steps as the CRM suite. This ensures a consistent particle size between the CRMs and samples throughout the study, an important parameter in XRF analysis (Willis and Duncan, 2008). Samples were air dried at 40 °C for 72 h to replicate natural drying on hot days and to prevent the loss of volatile elements such as As. Soil aggregates were crushed using an agate mortar and pestle and sieved through a 2 mm stainless steel sieve to remove gravel and organic debris. The <2 mm fraction was ground using a Retsch MM 301 Mixer Mill so that >95% of the sample would pass through a 74 μm sieve. This was confirmed by monitoring the particle size distribution of the samples using a Malvern Mastersizer 2000 particle size analyzer. All equipment was cleaned between samples with ethanol and KimWipes. Approximately 10 g of <74 μm soil sample was packed in 35 mm open ended PANalytical XRF cups using 3.6 μm Chemplex Mylar X-ray film. Samples were homogenized within their metal free bags by turning the bags over for 3 min each prior to packing in XRF cups.

2.4. Analysis of sample suite

Soil samples and CRMs were placed on the measurement window and measured five times at 60 s per measurement condition (180 s total measurement) using the proprietary soil mode. To monitor sample homogeneity from preparation, three soil samples were prepared in triplicate into three XRF cups and were assessed via their relative standard deviation (RSD). No reference values exist for the contaminated soil samples, so the pXRF analyzed fractions were also measured for their 'near total' metal concentrations using ICP-AES. Soil samples were measured first by pXRF, then the sample within the XRF cup was sent for ICP-AES analysis. This was intended to minimize any sample mis-representation from within a larger sample, and directly compare pXRF metal concentrations against ICP-AES (Shefsky, 1999).

2.5. Inductively coupled plasma atomic emission spectrometry

In many environmental investigations, trace metal concentrations are measured using ICP-AES or ICP-MS after a HNO_3/HCl acid digestion. This measurement technique provides 'total acid extractable' metal concentrations which in some environmental investigations may be more appropriate than 'total metal' concentrations (Kilbride et al., 2006; Schneider et al., 1999). However, to accurately compare against 'total metal' pXRF measurements, a strong acid digestion was required to extract as close to 100% of elements as possible. Hence, 75 soil samples and six CRMs were digested in perchloric ($HClO_4$), nitric (HNO_3), hydrofluoric (HF) and hydrochloric (HCl) acids and analyzed using a Varian 725-ES ICP-AES at a commercial laboratory. Six CRMs (NIST 1944, 2586, 2587, 2709a, RM 8704, NRC PACS-2) were measured simultaneously because their silicate matrices and trace metal concentrations were similar to the 'experimental' soil samples. This has a further benefit of enabling comparison of the elemental recoveries between the two measurement techniques. Recovery rates of the CRMs by ICP-AES are in Supplementary Table B. Three procedural laboratory blanks returned mean concentrations of <0.5 mg/kg for Cd, <1 mg/kg for Cr and Sr, <2 mg/kg for Ni, Cu, Zn and Pb, <5 mg/kg for Mn

and As, and <0.01 wt% for Ti and Fe. Mean duplicate analyses returned a RSD of 3.7%.

To validate the ICP-AES measurements of trace metals, five soil samples and three soil CRMs were also analyzed at a research laboratory by an Aglient 7700x ICP-MS after a two-step acid digestion (HF/HNO_3 then HNO_3/HCl acids). Although ICP-MS can achieve lower detection limits than ICP-AES, the comparison of elevated metal concentrations in contaminated soil would rarely approach detection limits of either instrument so comparison of the data from these instruments is reasonable. Measurements of soil samples and recoveries of CRMs by ICP-MS were largely comparable to those achieved by ICP-AES (Supplementary Table C). To reflect the characteristic data quality returned by commercial laboratories, neither ICP-AES nor ICP-MS methods were altered from normal practices for the measurement of soil samples.

2.6. Evaluation of data quality

Field portable XRF measurements were plotted against CRM and ICP-AES values for comparison. The Maximum Likelihood Functional Linear Relationship (MXFLR) method (Ripley and Thompson, 1987) was used to compare pXRF measurements and CRM values as it incorporates individual errors on each x and y variable (Hall et al., 2011, 2014). Deming regression was used in the comparison between pXRF and ICP-AES values as it incorporates errors on both x and y axes assuming the RSD is similar across the measurement range. From these graphs, the slope (m), intercept (b) and goodness of fit (r^2) were used to assess the accuracy of the instruments calibration in conjunction with individual recovery (%) and mean relative proximity (RP). Recovery was calculated as ((pXRF value/reference value) × 100), RP as (absolute (100 − recovery value)) and the RSD as ((standard deviation/mean) × 100).

In most cases, a CRM trace metal concentration was high (e.g. NIST 2710a, Zn 4180 mg/kg) which subsequently expanded the plot and clustered lower values. These high values were removed in an additional set of 'trimmed' graphs to emphasize the linear relationship at lower concentrations where pXRF measurement uncertainty is known to increase. Detection limit was calculated as three times the standard deviation of a sample mean where the element is 3–10 times the expected detection limit, while precision

Table 1
US EPA criteria for establishing data quality (US EPA, 1998).

Data quality level	Statistical requirement
Definitive	$r^2 = 0.85–1.0$. Relative standard deviation (RSD) ≤10%. Inferential statistics must indicate the two datasets are statistically similar (at the 5% level) i.e. relationship $y = x$ accepted.
Quantitative screening	$r^2 = 0.70–1.0$. Relative standard deviation (RSD) < 20%. Inferential statistics indicate the two data sets are statistically different i.e. relationship $y = mx$ or $y = mx + c$ accepted.
Qualitative screening	$r^2 < 0.70$. Relative standard deviation (RSD) > 20%. Inferential statistics indicate two data sets are statistically different.

Table 2
Mean RP and RSD for reference materials pre- and post-calibration displayed to 2 significant figures. Detection limits are displayed to one decimal place. **Bold** values represent improved absolute RP and RSD post-calibration.

Element	Calibration detection limit (mg/kg)	CRM values		Mean accuracy RP (%)		Mean precision RSD (%)	
		Min (mg/kg)	Max (mg/kg)	Factory	Calibration	Factory	Calibration
Ti	[a]	3110	6550	4.1	**3.1**	0.46	0.58
Cr	7.7	23	301	33	**8.1**	5.1	**3.0**
Cr (<150 mg/kg)	7.7	23	130	35	**6.4**	6.2	**3.5**
Mn	9.1	229	2140	3.8	**3.2**	0.84	**0.80**
Mn (<1200 mg/kg)	9.1	229	1000	3.6	**2.7**	0.90	**0.87**
Fe[b]	[a]	2.81%	5.16%	5.9	**4.2**	0.30	**0.21**
Ni	10.1	8	85	130	**40**	5.1	8.8
Ni (>10 mg/kg)	10.1	22	85	63	**11**	4.6	**8.2**
Cu	4.0	18.5	3420	29	**15**	5.4	**2.4**
Cu (<500 mg/kg)	4.0	18.5	380	34	**18**	6.1	**2.6**
Zn	5.1	103	4180	9.8	**5.4**	1.1	**0.82**
Zn (<1000 mg/kg)	5.1	103	656	11	**5.8**	1.1	**0.90**
As	3.4	8.7	1540	15	**12**	8.0	**7.3**
As (<120 mg/kg)	3.4	8.7	107	16	**14**	8.9	**8.1**
Sr	2.7	84.1	276	6.2	**3.9**	0.99	**0.86**
Cd	2.2	2.71	54.1	48	**7.2**	5.8	8.6
Cd (<20 mg/kg)	2.2	2.71	12.3	48	**7.8**	6.8	10.0
Pb	3.0	17.3	5520	9.7	**3.4**	2.0	**1.8**
Pb (<500 mg/kg)	3.0	17.3	432	13	**4.6**	2.7	**2.5**

[a] Detection limits were not calculated for Ti and Fe as no CRM values between 3 and 10 times the expected manufacturer detection limit were present in the CRM suite.
[b] Fe CRM values are displayed in wt%.

was determined by the RSD of the five measurements used for determining each measurement mean. To further compare pXRF measurements to both reference and ICP-AES values, pXRF data were benchmarked against three data quality levels established by the United States Environmental Protection Agency (US EPA, 1998). The RSD, goodness of fit (r^2), slope and intercept values were used to determine which data quality threshold was achieved per element (Table 1).

3. Results & discussion

3.1. Impact of a matrix-matched calibration

Performance of the soil matrix calibration was first evaluated against factory settings through repeated measurements of the ten CRMs. Relative proximity improved for all 11 elements post-calibration, most notably in the trimmed datasets given the soil matrix calibration focused on lower concentrations. Significant RP improvements can be seen for Cr (<150 mg/kg) from 35% to 6.4%, Cd from 48% to 7.2% and Pb (<500 mg/kg) from 13% to 4.6% (Table 2). Relative proximity demonstrates the proportional difference from the reference value and provides no information on the distribution of pXRF recoveries nor the direction of the rotational bias. Hence, in conjunction with RP, accuracy was assessed using individual CRM recoveries against elemental concentrations for both calibration strategies (Fig. 1).

Fig. 1 demonstrates significant improvement in pXRF measurements post-calibration. The number of recovery points outside the 80–120% recovery band decreased from 28% (n = 96) under the factory settings to 4% when measured with the soil matrix calibration. Of the recovery points still outside the 80–120% recovery band after matrix calibration, three points improved post-calibration, while one point was only detected post-calibration (Supplementary Table D). Factory settings performed well for
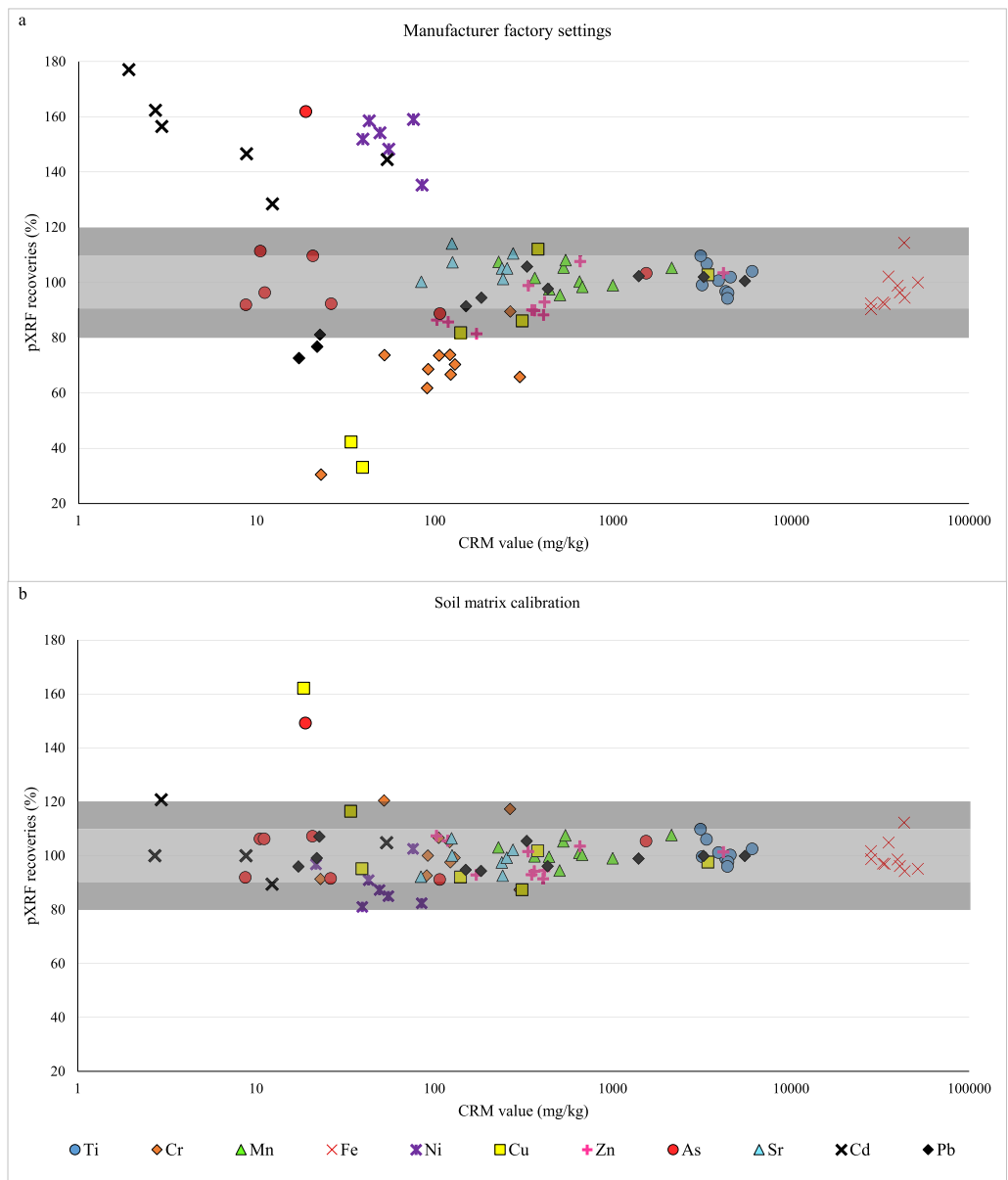

Fig. 1. Comparison of a) factory settings and b) soil matrix calibrations for individual elemental recoveries of CRMs. pXRF recovery for NIST 2710a Ni value of 8.0 mg/kg not shown for factory (675%) and soil matrix calibrations (338%).

elemental concentrations >400 mg/kg, with elemental recoveries from 88 to 114%. At lower concentrations the majority of recovery points outside the 80—120% band were Cr, Ni and Cd measurements. These elements required stronger slope and intercept correction to transform pXRF measurements closer to 100% recovery. Examples of both ideal and poor regression slopes using the factory settings are in Supplementary Figures A and B, for Mn and Cr, respectively. Minimal calibration improvement was required for Mn as recoveries by the factory settings ranged from 95.5 to 108% (Supplementary Table D), which produced ideal slope and r² values of 1.011 and 0.998 respectively (Supplementary Figure A).

Mean CRM recovery for Cr (<150 mg/kg) under the factory settings was 67.4% (Supplementary Table D), indicating a negative rotational bias in the regression that generated a slope of 0.775 (Supplementary Figure B). The r² values for Cr pre- and post-calibration were consistent at 0.976 and 0.975, respectively, suggesting a simple correction of slope and intercept values was necessary to achieve more accurate CRM recoveries (Supplementary Figure B). Calibration improved regression slope from 0.775 to 0.983, intercept value from −6.5 to 5.6 mg/kg, mean RP from 35% to 6.4% and RSD from 6.2% to 3.5% (Table 2). Examples of significant improvement in CRM recovery post-calibration is evident for Cr in the measurement of NIST 2587 (68.6% to 100%), NIST 2709a (70.3% to 99.2%) and NRC BCSS-1 (66.7% to 97.6%)

(Supplementary Table D). Strong rotational bias also influenced Ni and Cd measurements and were similarly corrected to improve CRM recoveries and regression slopes closer to the target of 1.

Precision improved post-calibration for all elements except for Ti, Ni, and Cd (Table 2). The precision of measurements under the factory settings ranged from 0.3 to 8.9% RSD, well below the ≤10% RSD criteria for definitive data quality set by the US EPA (Table 1), which prioritizes the improvement of CRM recoveries over repeatability. Detection limits also decreased for all elements post-calibration except for Cr, Zn, and Pb.

3.2. pXRF measurement of certified reference materials

Performance of the soil matrix calibration was evaluated further by examining the elemental detection limits, measurement repeatability and accuracy of pXRF measurements. Individual pXRF measurements, measurement repeatability and recoveries of each CRM are in Supplementary Table E for all 11 elements. A summary of the pXRF measurement performance for each element is in Supplementary Table F.

3.2.1. Elemental detection limits
Calculated detection limits were near to or lower than the suggested manufacturers' detection limits for nine of the eleven
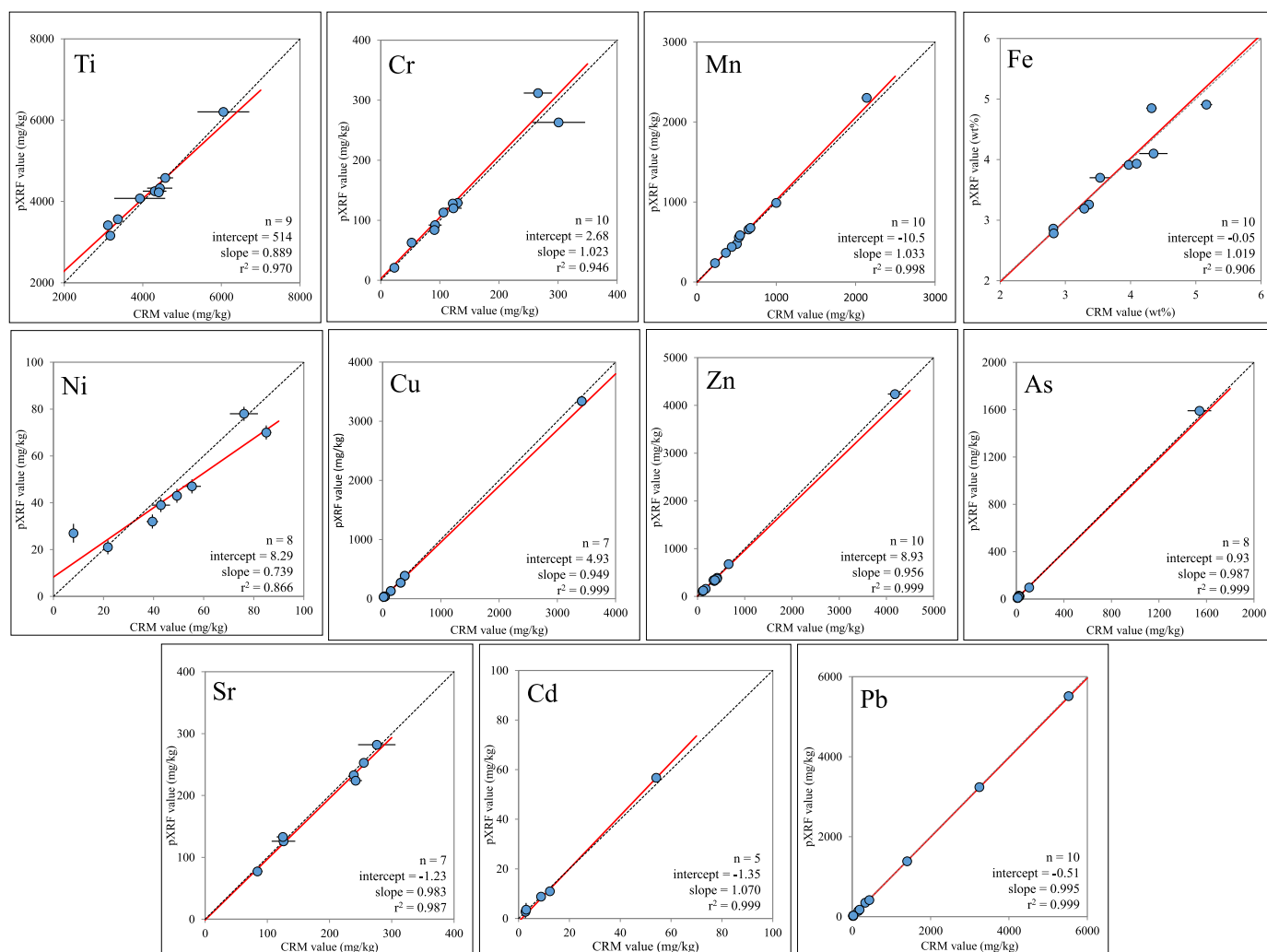
**Fig. 2.** Regression of pXRF measurements against CRM values for untrimmed datasets. MXFLR relationship (solid red line) and 100% recovery (dashed black line) are shown in each plot. Error bars represent upper and lower limits for each CRM value in the x-axis, and pXRF ± values in the y-axis. (For interpretation of the references to color in this figure legend, the reader is referred to the web version of this article.)

elements. Minimum CRM concentrations for Ti and Fe were 3110 mg/kg and 2.8 wt% respectively, and were not low enough to calculate their respective detection limits. The selection of a pXRF instrument with a Ta X-ray tube has excellent potential to detect Cd at low concentrations using the Cd K-shell emissions, however can suffer from spectral interferences from Ta tube L-shell emissions near the K-shell lines of Ni and Cu. If measuring Cd at low concentrations is not of interest to the pXRF user, then the selection of a Rh or Ag anode X-ray tube can improve the measurements of Ni and Cu at low concentrations.

3.2.2. Precision

Measurement repeatability by pXRF was excellent for the majority of elements with the mean RSD ranging from 0.21% for Fe to 10.0% for Cd (Table 2). Exceptional repeat measurements were observed for Ti, Cr, Mn, Fe, Cu, Zn, Sr, and Pb, especially in higher concentrations (Supplementary Table E). Removal of high elemental concentrations in the trimmed datasets generated slightly higher RSD values than untrimmed datasets (Table 2). The least precise repeat measurements occurred at low concentrations of Ni, As, and Cd. For example the measurement of As in PACS-2 (measured 21, 23, 24, 26, 27 mg/kg; certified 24 mg/kg) resulted in a RSD of 9.6% (Supplementary Table E). Regardless, the majority of higher RSD values were observed in concentrations lower than what would be anticipated in metal-contaminated soils.

3.2.3. Accuracy

Accuracy of pXRF measurements was assessed using CRM recoveries, mean RP, and graphical comparison against reference values using MXFLR regression. Elemental recoveries were excellent for the calibrated pXRF data with 82% of measurements within the 90—110% recovery band and 96% inside the 80—120% band (Fig. 1, Supplementary Table D). Similar to RSD, recoveries and RP can also become magnified at lower elemental concentrations, and were observed in the four cases outside the 80—120% recovery band. The mean recoveries of ten CRMs were Ti 101%, Cr 102%, Mn

102%, Fe 100%, Ni 89%, Cu 108%, Zn 99%, As 106%, Sr 99%, Cd 103%, and Pb 99% (Supplementary Table D). Measurements of Ni were slightly underestimated, while Cu and As were slightly overestimated, particularly at low concentrations.

Mean RP was slightly higher for the trimmed datasets due to better pXRF determination at elevated concentrations within the calibration and also due to the proportional nature of RP at lower concentrations. It was for this reason that CRM recoveries and RP were not viewed independently without acknowledging the concentrations of each measurement. Most of the trimmed datasets presented remove a highly concentrated CRM value. However, the trimmed dataset for Ni removes a low CRM value of 8.0 mg/kg (NIST 2710a) as the value was below the detection limit of 10 mg/kg (Table 2).

The relationship between pXRF measurements and CRM values were plotted for untrimmed and trimmed datasets in Figs. 2 and 3 respectively. Table 3 lists the statistical outcomes of MXFLR regression to satisfy the criteria required to categorize the level of data quality established per element (US EPA, 1998). Excellent agreement between pXRF and CRM values was demonstrated through the high r^2 values which ranged from 0.866 to 0.999 for the untrimmed datasets and 0.906—0.996 for the trimmed datasets (Figs. 2 and 3). In some cases the combination of a highly concentrated value and the clustering of low concentration values create an artificially high r^2 of 0.999 (e.g. Cu, Zn, and As; Fig. 2). Intercept values for untrimmed and trimmed datasets were generally very close to 0, ranging from −10.5 to 14.5 for every element except Ti (Table 3). The lowest reference value for Ti was 3110 mg/kg and consequently was not low enough to refine the lower end of the regression (Table 3). Slope values were excellent with the majority of elemental datasets (14 of 19) generating slope values between 0.90 and 1.10 (Table 3).

3.2.4. Data quality

Goodness of fit, mean RSD, and inferential statistics of both slope and intercept values were used to categorize the quality of
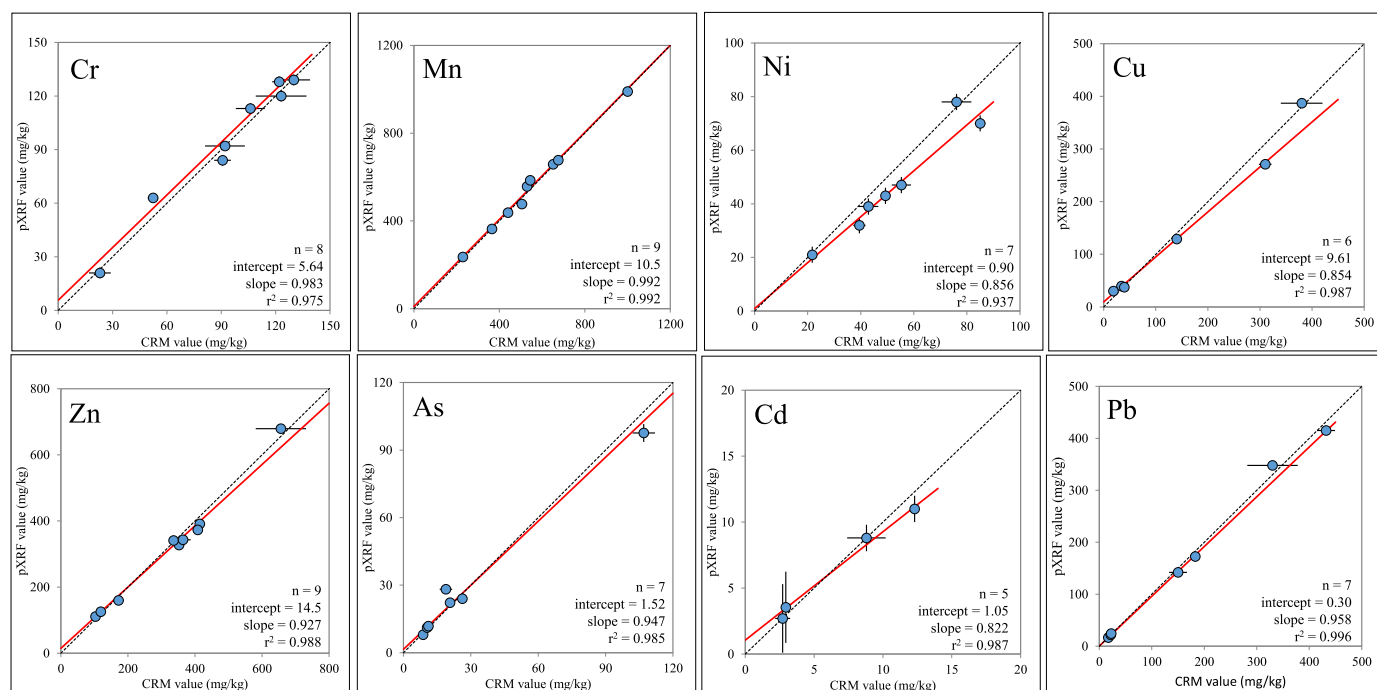

Fig. 3. Regression of pXRF measurements against CRM values for trimmed. MXFLR relationship (solid red line) and 100% recovery (dashed black line) are shown in each plot. Error bars represent upper and lower limits for each CRM value in the x-axis, and pXRF ± values in the y-axis. (For interpretation of the references to color in this figure legend, the reader is referred to the web version of this article.)

Table 3
MXFLR regression data of pXRF measurements against CRM values. r^2 and slope values are rounded to 3 decimal places, RSD is displayed to 2 significant figures, and intercept and 95% confidence intervals are displayed to 3 significant figures.

Element	n	r^2	RSD	Slope	Slope 95% CI	Intercept	Intercept 95% CI	Data quality[a]
Ti	9	0.970	0.58	0.889	(0.711, 1.06)	514	(−99.7, 1130)	Definitive
Cr	10	0.946	3.0	1.023	(0.896, 1.15)	2.68	(−8.79, 14.2)	Definitive
Cr (<150 mg/kg)	8	0.975	3.5	0.983	(0.833, 1.13)	5.64	(−7.34, 18.6)	Definitive
Mn	10	0.998	0.80	1.033	(0.977, 1.09)	−10.5	(−44.7, 23.7)	Definitive
Mn (<1200 mg/kg)	9	0.992	0.87	0.992	(0.923, 1.06)	10.5	(−29.3, 50.3)	Definitive
Fe (wt%)	10	0.906	0.20	1.019	(0.953, 1.08)	−0.05	(−0.264, 0.164)	Definitive
Ni	8	0.866	8.8	0.739	(0.605, 0.873)	8.29	(1.37, 15.2)	Quantitative
Ni (>10 mg/kg)	7	0.937	8.2	0.856	(0.683, 1.03)	0.90	(−8.39, 10.2)	Definitive
Cu	7	0.999	2.4	0.949	(0.916, 0.982)	4.93	(1.22, 8.64)	Quantitative
Cu (<500 mg/kg)	6	0.987	2.6	0.854	(0.784, 0.924)	9.61	(4.71, 14.5)	Quantitative
Zn	10	0.999	0.82	0.956	(0.909, 1.01)	8.93	(−2.75, 20.6)	Definitive
Zn (<1000 mg/kg)	9	0.988	0.90	0.927	(0.871, 0.983)	14.5	(1.35, 27.6)	Quantitative
As	8	0.999	7.3	0.987	(0.882, 1.09)	0.93	(−1.13, 2.99)	Definitive
As (<120 mg/kg)	7	0.985	8.1	0.947	(0.803, 1.09)	1.52	(−1.03, 4.06)	Definitive
Sr	7	0.987	0.86	0.983	(0.854, 1.11)	−1.23	(−28.0, 25.5)	Definitive
Cd	5	0.999	8.6	1.070	(0.965, 1.17)	−1.35	(−4.63, 1.93)	Definitive
Cd (<20 mg/kg)	4	0.987	10	0.822	(−0.141, 1.78)	1.05	(−8.95, 11.1)	Definitive
Pb	10	0.999	1.8	0.995	(0.984, 1.01)	−0.51	(−2.29, 1.27)	Definitive
Pb (<500 mg/kg)	7	0.996	2.5	0.958	(0.883, 1.03)	0.30	(−2.22, 2.82)	Definitive

[a] Data quality levels are defined by US EPA (1998).

data produced by the pXRF (Table 3). Fifteen of the nineteen elemental datasets returned definitive data quality (Tables 2 and 4), capable of generating reportable standalone data (US EPA, 1998). These elements include Ti, Cr, Mn, Fe, Ni (>10 mg/kg), Zn, As, Sr, Cd and Pb (Table 3). Nickel, Cu, and Zn (<1000 mg/kg) did not satisfy the $y = x$ relationship model as the 95% confidence limits did not contain the target values of 1 and 0 for slope and intercept values respectively. They did satisfy the next data quality level of quantitative screening (Table 1). Unlike definitive data, quantitative screening data requires that at least 10% of the data be confirmed using analytical methods capable of generating definitive level data, such as ICP-AES or ICP-MS (US EPA, 1998).

The data quality established in this study is specific to this pXRF instrument, the measurement of powdered soil CRMs and the concentration ranges per element. Yet more importantly, demonstrates the analytical performance of new generation pXRFs in the measurement of contaminated soils. Variation in analytical performance between different pXRF instruments is well established (Hall et al., 2014), and is almost expected given the wide range of X-ray tubes, detectors, and software available, hence the need for individual calibration of each pXRF instrument.

Table 4
Mean recovery and RP by pXRF and ICP-AES in the measurement of six soil CRMs. Verdict based on the difference between mean RP of six CRMs as an indicator of performance.

Element	Mean pXRF recovery (%)	Mean ICP-AES recovery (%)	Mean pXRF RP (%)	Mean ICP-AES RP (%)	Difference of mean RP (ICP-AES − pXRF)	pXRF verdict against ICP-AES
Ti	101.7	88.0	2.6	12.0	+9.4	Better
Cr	100.1	83.0	5.5	17.0	+11.5	Better
Mn	101.7	95.4	3.4	5.4	+2.0	Equivalent
Fe	99.0	94.1	3.1	5.9	+2.9	Better
Ni	87.8	92.3	13.2	7.8	−5.4	Worse
Cu	105.6	90.2	11.9	9.8	−2.1	Equivalent
Zn	100.0	99.4	5.4	3.8	−1.6	Equivalent
As	109.1	101.3	15.7	8.6	−7.1	Worse
Sr	98.2	101.2	2.5	2.3	−0.2	Equivalent
Cd	106.9	95.1	6.9	4.9	−2.0	Equivalent
Pb	97.8	95.1	3.6	5.6	+2.0	Equivalent

3.3. pXRF comparability against ICP-AES

Measurements of 75 soil samples using pXRF and ICP-AES are in Supplementary Table G, with detailed summaries of elemental measurements in Supplementary Table H. Elemental relationships between pXRF and ICP-AES measurements were plotted using Deming regression as untrimmed (Fig. 4) and trimmed (Fig. 5) datasets to assess comparability at lower concentration ranges. Performance of ICP-AES was also assessed by the parallel measurement of six CRMs by comparing the mean recovery and RP against those achieved by pXRF (Table 4, Supplementary Table B). Homogeneity of the contaminated soil samples was ensured through triplicate analyses of three samples returning RSD of 0.8% for Pb to 8.2% for As.

3.3.1. Elements determined better by pXRF (Ti, Cr, Fe)

Measurement of six CRMs demonstrated excellent elemental determination by pXRF and revealed significant underestimation of Ti, Cr, and Fe by ICP-AES. Mean CRM recoveries by ICP-AES were 88.0% (Ti), 83.0% (Cr) and 94.1% (Fe), while recoveries by pXRF were 101.7% (Ti), 100.1% (Cr) and 99.0% (Fe) (Table 4, Supplementary Table B). The discrepancy between pXRF and ICP-AES measurements were also observed in the ICP-AES regression for these three elements (Fig. 4). Almost every sample plotted above the 100% recovery line suggesting the underestimation of Ti, Cr, and Fe by ICP-AES was not isolated to the measurement of CRMs but was also apparent in the soil samples (Supplementary Table G). Incomplete sample digestion was the most probable cause of under-reporting, however instrument inaccuracies may also contribute to these inferior recoveries. While sample decomposition included HF in addition to $HClO_4$, HNO_3, and HCl acids, a longer and stronger acid digestion may be required to fully extract these elements that may be trapped within refractory matrices. Excellent CRM recoveries, RP, regression against CRM values and as a result, definitive level data quality suggests that pXRF determined Ti, Cr, and Fe more accurately than ICP-AES. Consequently, data quality criteria were not applied to the 75 pXRF measurements due to abundant, and at times, inferior CRM recoveries by ICP-AES (Table 4, Supplementary Table B).
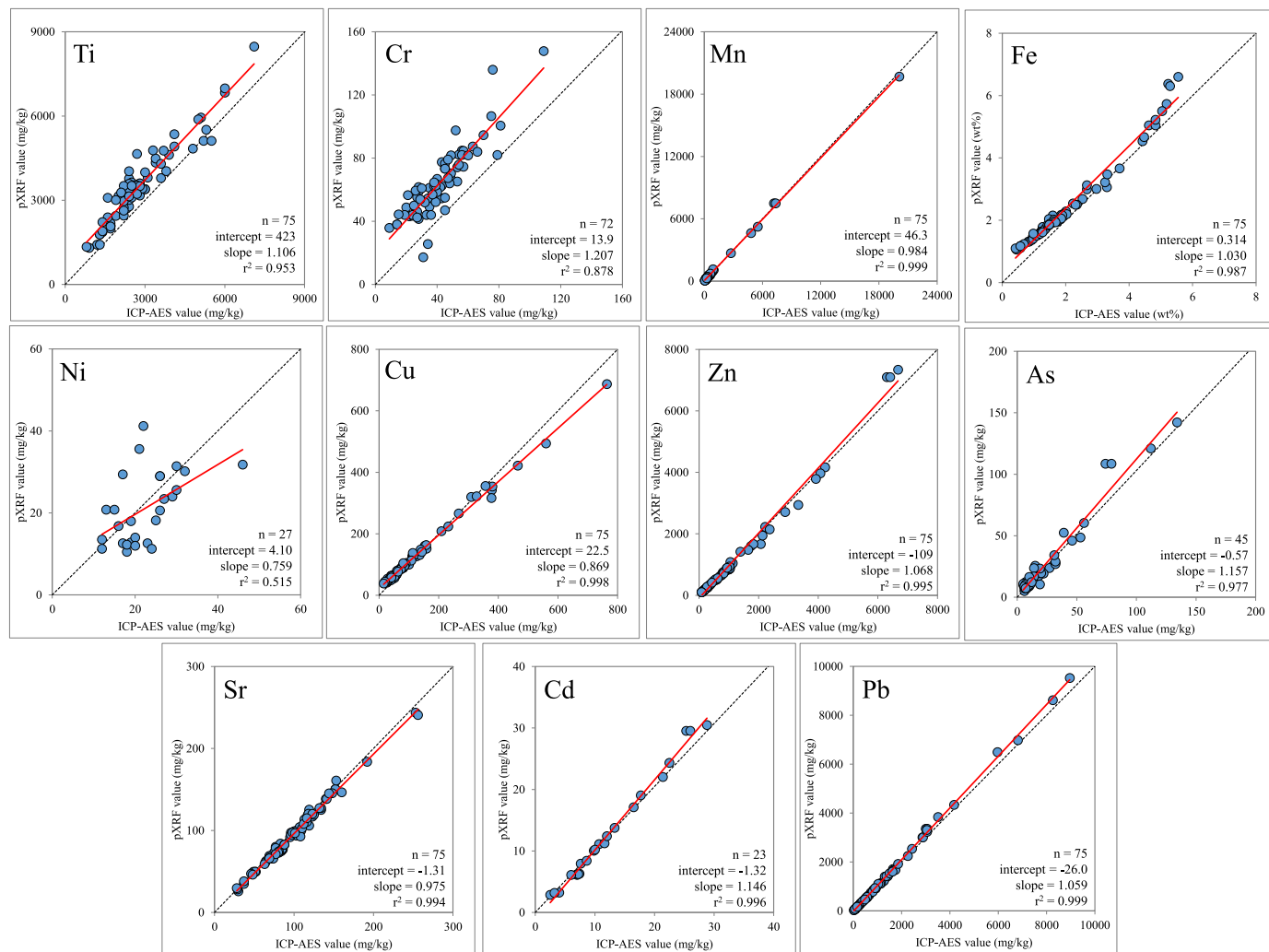
Fig. 4. Regression of pXRF measurements against ICP-AES analysis for untrimmed datasets. Deming relationship (solid red line) and 100% recovery (dashed black line) are shown in each plot. (For interpretation of the references to color in this figure legend, the reader is referred to the web version of this article.)
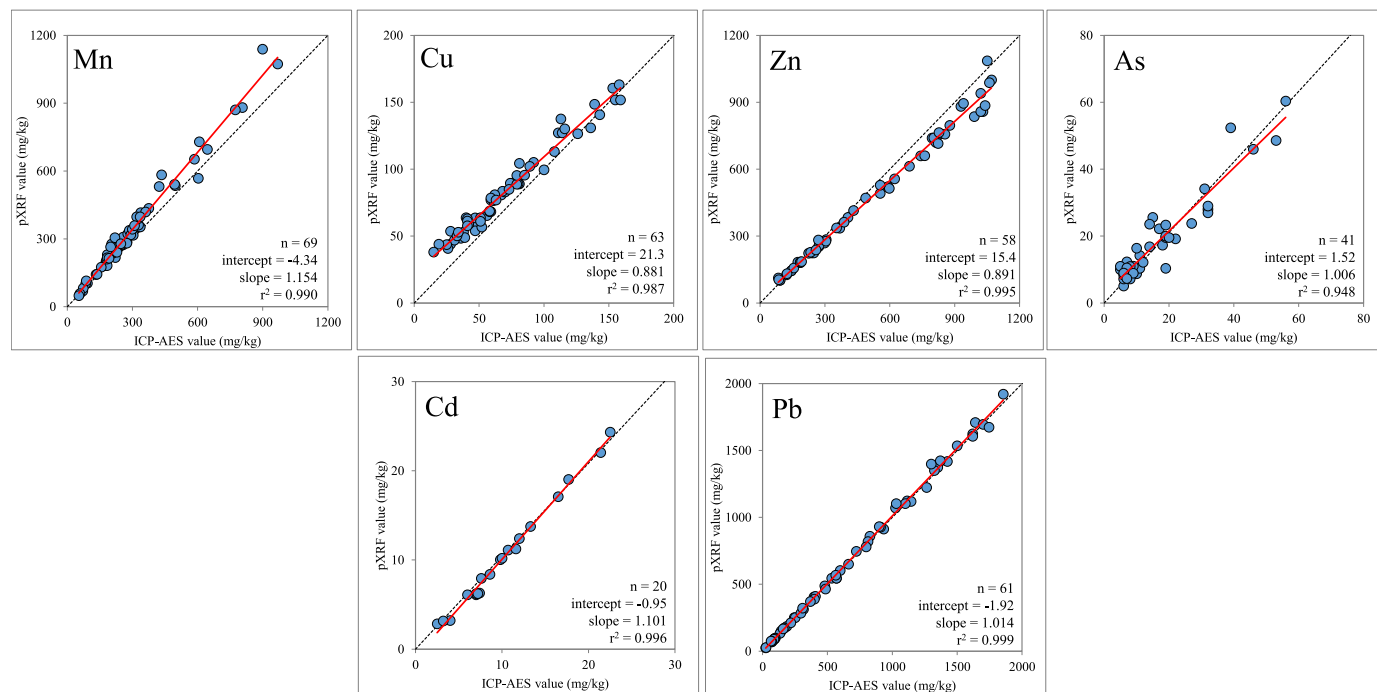

Fig. 5. Regression of pXRF measurements against ICP-AES analysis for trimmed datasets. Deming relationship (solid red line) and 100% recovery (dashed black line) are shown in each plot. (For interpretation of the references to color in this figure legend, the reader is referred to the web version of this article.)

3.3.2. Excellent pXRF comparability against ICP-AES (Mn, Cu, Zn, As, Sr, Cd, Pb)

High r^2 values of >0.9 were achieved for 15 of 17 elemental datasets, demonstrating excellent correlation between the techniques. Exceptional agreements ($r^2 > 0.99$) were evident in the untrimmed and trimmed plots of Mn, Cu, Zn, Sr, Cd, and Pb (Figs. 4 and 5). Slope values ranged from 0.869 to 1.157, however intercept values were typically further from 0 than those achieved in the regression against the CRMs. The increased spread of measurements within a larger concentration range allowed improved understanding of pXRF performance where CRM values were limited. For example, excellent regression and distribution of 61 data points were observed in the Pb (<2000 mg/kg) plot generating ideal r^2, slope and intercept values of 0.999, 1.014, and −1.92 respectively (Fig. 5).

Excellent agreement of Mn, Cu, Zn, As, Sr, Cd, and Pb measurements was supported through comparable CRM recoveries. Mean recoveries of CRM measurements by ICP-AES were typically slightly lower than those achieved by pXRF (Table 4, Supplementary Table B). In the three cases where the mean RP achieved by pXRF was elevated (Ni, Cu, As), the same increase was observed in ICP-AES measurements, indicating both techniques encountered difficulties in the measurement of Ni, Cu, and As. Through the comparisons of mean recoveries, RP, and excellent regression against ICP-AES values, pXRF was equivalent to ICP-AES in the measurement of Mn, Cu, Zn, Sr, Cd, and Pb. Arsenic was better determined by ICP-AES (Table 4), however increasing the concentration range (8.7—26 mg/kg) of the six CRMs would improve the recoveries achieved by pXRF.

3.3.3. Poor pXRF comparability against ICP-AES (Ni)

Given the limited concentration range of pXRF measurements for Ni and the selection of a pXRF fitted with a Ta anode X-ray tube, it was not unexpected that Ni was not well determined compared to the other elements assessed. Only 27 of the 75 contaminated soil samples were above the pXRF detection limit of 10 mg/kg, generating an r^2 of 0.515 and a slope value of 0.759 (Fig. 4). However, both techniques performed poorly in the measurement of the six CRMs. Mean CRM recovery by pXRF and ICP-AES were 87.8% and 92.3%, while mean RP were 13.2% and 7.8% respectively (Table 4). The comparability of Ni measurements would have improved with the measurement of samples with Ni concentrations >50 mg/kg. To optimize the measurement of Ni by pXRF, an instrument fitted with either a Rh or Ag anode X-ray tube would likely produce more accurate data.

3.4. Implications of pXRF and ICP-AES comparisons

One of the main advantages of pXRF spectrometry is the portable nature of the instrument, low cost of purchase and ownership enabling users to generate real-time, quantitative information, inexpensively in the field (Potts and West, 2008; Radu et al., 2013; Schneider et al., 1999; Weindorf et al., 2014). A variety of studies have investigated the effectiveness of *in situ* pXRF in generating reliable measurements on soil Pb concentrations (Argyraki et al., 1997; Bernick et al., 1995a, 1995b; Clark et al., 1999; Shefsky, 1999), yet users continue to encounter problems with sample heterogeneity, grain size and matrix effects, moisture content and surface roughness. This study minimized these common sample inconsistencies through sample preparation, homogenization and analysis of samples in packed XRF cups. In doing so, the analytical performance of the pXRF was optimized, enabling more accurate comparison against ICP-AES and ICP-MS measurements.

Separate assessment would be required to confirm equivalent performance on pXRFs other than the Olympus spectrometer used here. Given the typical application of pXRFs in the field, additional research is required to determine if a field method, capable of generating data quality sufficient for standalone pXRF reporting of contaminated soils, can be achieved.

Wet chemistry techniques such as ICP-AES and ICP-MS are used widely for accurate reporting of elemental values in the mining, geological, and environmental industries. However, all measurement techniques contain measurement variation due to sample representation, sample collection, preparation and analytical error (Shefsky, 1999). The majority of accredited wet chemistry methods report data within ±20% of the elemental recoveries of certified or reference values (e.g. NMI, 2016), and at times assure their clients that the data is usually accurate to ±10% error. This study found that in the measurement of soil CRMs, the proportion of reported values within ±10% error was significantly greater for pXRF (86%) than ICP-AES (68%) and ICP-MS (53%) (Supplementary Tables B and C), however more reference materials would be required to effectively compare these elemental recoveries. Consequently, the criteria used to establish data quality levels were not applied to the pXRF vs ICP-AES elemental datasets as the errors introduced by ICP-AES measurements would misleadingly degrade calculated data quality levels for the pXRF.

Reasons for the differences in elemental recoveries between the different analytical instruments cannot be established unequivocally. Although samples were homogenized for pXRF analysis in line with the original preparation of the CRMs, it is possible that sample heterogeneity may have resulted in different elemental values returned between the analytical techniques. This study attempted to minimize such differences by ensuring the same samples were analyzed first by pXRF and subsequently by ICP-AES and ICP-MS. However, it must be noted that pXRF measurements require 5—10 g of sample and subsequent ICP-AES and ICP-MS used a sub-sample of ~0.5 g for analysis.

Notwithstanding these unknowns, there are clear benefits of using pXRF. The ease of its use enables operators to generate matrix specific calibrations to optimize measurements. Further, soils are not required to be subject to additional treatments prior to analysis in the same way as ICP-AES or ICP-MS analysis requires digestion, which has the potential to introduce further variability in the elemental recoveries. Other advantages of pXRF relate to analysis costs. For example, where project costs are limited but there are adequate human resources for sample preparation and substantive sample numbers are required, which is typically the case for research-based exploratory investigations within universities, pXRF is a reliable low-cost option. By contrast, while laboratory ICP-AES or ICP-MS costs could limit site interpretation, the advantage is 'consumer confidence'. Elemental analyses are carried out by NATA accredited laboratories for contaminated land assessments, councils and EPAs and often require independent analysis, which is subsequently interpreted by an environmental scientist. Hence, the use and application of the different techniques depends on the needs and purpose of the end user. For example, if a metal-contaminated site required a high sample density investigation to provide accurate characterization, pXRF has demonstrable capacity to generate data that is equivalent to ICP-AES analysis at a fraction of the cost. However, if the site had metal concentrations approaching the detection limits of the pXRF, which is often not relevant for contaminated site investigations, another measurement technique would be required. In summary, the data produced in this study suggests that while caution should be applied when comparing data acquired from different measurement techniques,

pXRF is capable of generating comparable data to that returned by an accredited commercial laboratory.

4. Conclusions

Field portable XRF is capable of generating reliable, high quality elemental concentration data for metal-contaminated soils. A matrix matched calibration markedly enhanced the analytical performance of the pXRF instrument with improved elemental recoveries, lower measurement variation, and lower detection limits. Repeated measurements of ten CRMs generated definitive data quality, capable of standalone reporting for Ti, Cr, Mn, Fe, Ni (>10 mg/kg), Zn, As, Sr, Cd, and Pb while quantitative screening data quality was achieved for Ni, Cu, and Zn (<1200 mg/kg) datasets. Measurement of 75 contaminated soil samples by pXRF demonstrated excellent agreement with ICP-AES data. Parallel measurement of six CRMs by pXRF and ICP-AES revealed that pXRF was equivalent to, or better than, ICP-AES data for Ti, Cr, Mn, Fe, Cu, Zn, Sr, Cd, and Pb measurements.

This study validates pXRF as a suitable alternative to ICP-AES for a range of elements in the measurement of metal-contaminated soils. These outcomes can be achieved with appropriate sample handling, preparation, and instrument calibration, producing data that are equivalent or better than ICP-AES. However, caution is advised when comparing pXRF data to ICP-AES or ICP-MS data as inconsistent (and at times inferior) elemental recoveries were present in the solution-based analytical methods, demonstrating that with proper sample preparation pXRF can be equivalent to, or better than these methods.

Acknowledgements

Appendix A. Supplementary data

Supplementary data related to this article can be found at http://dx.doi.org/10.1016/j.envpol.2016.03.055.

References

Argyraki, A., Ramsey, M., Potts, P.J., 1997. Evaluation of portable X-ray fluorescence instrumentation for in situ measurements of lead on contaminated land. Analyst 122, 743–749.

Bernick, M.B., Kalnicky, D., Prince, G., Singhvi, R., 1995a. Results of field-portable X-ray fluorescence analysis of metal contaminants in soil and sediment. J. Hazard. Mater. 43, 101–110.

Bernick, M.B., Getty, D., Prince, G., Sprenger, M., 1995b. Statistical evaluation of field portable X-ray fluorescence soil preparation methods. J. Hazard. Mater. 43, 111–116.

Clark, S., Menrath, W., Chen, M., Roda, S., Succop, P., 1999. Use of a field portable X-ray fluorescence analyzer to determine the concentration of lead and other metals in soils. Annu. Agric. Environ. Med. 6, 27–32.

Contaminated Land Exposure Assessment Model (CLEA), 2002. Technical Basis and Algorithms. Department for Environment, Food and Rural Affairs. Environmental Agency, Bristol.

Dong, C., Taylor, M.P., Kristensen, L.J., Zahran, S., 2015. Environmental contamination in an Australian mining community and potential influences on early childhood health and behavioural outcomes. Environ. Pollut. 207, 345–356.

Hall, G., Buchar, A., Bonham-Carter, G., 2011. CAMIRO Project 10E01, Phase 1, Quality Control Assessment of Portable XRF Analysers: Development of Standard Operating Procedures, Performance on Variable Media and Recommended Uses. Canadian Mining Industry Research Organization (CAMIRO) exploration division (accessed 25 07 15). https://www.appliedgeochemists.org/index.php/publications/other-publications/2-uncategorised/106-portable-xrf-for-the-exploration-and-mining-industry.

Hall, G.E., Bonham-Carter, G.F., Buchar, A., 2014. Evaluation of portable X-ray fluorescence (pXRF) in exploration mining: phase 1, control reference materials. Geochem. Explor., Environ. Anal. 14, 99–123.

Harvey, P.J., Taylor, M.P., Kristensen, L.J., Grant-Vest, S., Rouillon, M., Wu, L., Handley, H.K., 2015. Evaluation and assessment of the efficacy of an abatement strategy in a former lead smelter community, Boolaroo, Australia. Environ. Geochem. Health 1–14.

Hou, X., He, Y., Jones, B.T., 2004. Recent advances in portable X-ray fluorescence spectrometry. Appl. Spectrosc. 39, 1–24.

Kenna, T.C., Nitsche, F.O., Herron, M.M., Mailloux, B.J., Peteet, D., Sritrairat, S., Sands, E., Baumgarten, J., 2011. Evaluation and calibration of a Field Portable X-Ray Fluorescence spectrometer for quantitative analysis of siliciclastic soils and sediments. J. Anal. At. Spectrom. 26, 395–405.

Kilbride, C., Poole, J., Hutchings, T.R., 2006. A comparison of Cu, As, Cd, Zn, Fe, Ni and Mn determined by acid extraction/ICP-OES and ex situ field portable X-ray fluorescence analyses. Environ. Pollut. 143, 16–23.

National Measurement Institute (NMI), 2016. Inorganics Quality Manual – Method Number NT2.49: Determination of Total Acid Extractable Metals in Soil Using Inductively Coupled Plasma Mass Spectrometry and Inductively Coupled Plasma Atomic Emission Spectrometry.

Piercey, S.J., Devine, M.C., 2014. Analysis of powdered reference materials and known samples with a benchtop, field portable X-ray fluorescence (pXRF) spectrometer: evaluation of performance and potential applications for exploration lithogeochemistry. Geochem. Explor., Environ. Anal. 14, 139–148.

Potts, P.J., West, M., 2008. Portable X-Ray Fluorescence Spectrometry: Capabilities for in Situ Analysis. RSC Publishing, London, UK.

Radu, T., Gallagher, S., Byrne, B., Harris, P., Coveney, S., McCaron, S., McCarthy, T., Diamond, D., 2013. Portable X-ray fluorescence as a rapid technique for surveying elemental distributions in soil. Spectrosc. Lett. 46 (7), 516–526.

Ripley, B.D., Thompson, M., 1987. Regression techniques for the detection of analytical bias. Analyst 112, 377–383.

Rouillon, M., Kristensen, L., Gore, D.B., 2015. Handheld X-ray fluorescence spectrometers: radiation exposure risks of matrix-specific measurement scenarios. Appl. Spectrosc. 69 (7), 815–822.

Schneider, J.F., Johnson, D., Stoll, N., Thurow, K., 1999. Portable X-ray fluorescence spectrometry characterization of arsenic contamination in soil at a German military site. J. Field Anal. Chem. 4, 12–17.

Shand, C.A., Wendler, R., 2014. Portable X-ray fluorescence analysis of mineral and organic soils and the influence of organic matter. J. Geochem. Explor. 143, 31–42.

Shefsky, S., 1999. Comparing Field Portable X-Ray Fluorescence (XRF) to Laboratory Analysis of Heavy Metals in Soil. International Symposium of Field Screening Methods for Hazardous Wastes and Toxic Chemicals (Las Vegas, Nevada, USA).

Taylor, M.P., Hudson-Edwards, K.A., 2008. The dispersal and storage of sediment associated metals in an arid river system: the Leichhardt River, Mount Isa, Queensland, Australia. Environ. Pollut. 152, 193–204.

United States Environmental Protection Agency (US EPA), 1998. Environmental Technology Verification Report, Field Portable X-ray Fluorescence Analyzer. Metorex X-MET 920-P (accessed 25 07 15). http://nepis.epa.gov/Adobe/PDF/30003LR0.pdf.

United States Environmental Protection Agency (US EPA), 2004. Method 6200-Field Portable X-ray Fluorescence Spectrometry for the Determination of Elemental Concentrations in Soil and Sediment, pp. 1–32 (accessed 27 08 15). http://www3.epa.gov/epawaste/hazard/testmethods/sw846/pdfs/6200.pdf.

Vanhoof, C., Corthouts, V., Tirez, K., 2004. Energy-dispersive X-ray fluorescence systems as analytical tool for assessment of contaminated soils. J. Environ. Monit. 6, 344–350.

VegeSafe, 2015. Latest Findings. VegeSafe (accessed 21 05 15). http://research.science.mq.edu.au/vegesafe/.

Weindorf, D.C., Bakr, N., Zhu, Y., 2014. Advances in portable X-ray fluorescence (PXRF) for environmental, pedological, and agronomic applications. Adv. Agron. 128, 1–45.

Weindorf, D.C., Paulette, L., Man, T., 2013. In-situ assessment of metal contamination via portable X-ray fluorescence spectroscopy: Zlatna, Romania. Environ. Pollut. 182, 92–100.

Willis, J.P., Duncan, A.R., 2008. Understanding XRF Spectrometry, Volume 1 Basic Concepts and Instrumentation. PANalytical B.V, The Netherlands.

Wu, C., Tsai, H., Yang, K., Wen, K., 2012. How reliable is X-ray fluorescence (XRF) measurement for different metals in soil contamination? Environ. Forensics 13, 110–121.

3.3   Calibrated pXRF vs. ICP–AES and ICP–MS

When samples are sent to a laboratory for analysis, a quality assurance and control (QAQC) report is returned to the client with metal concentration estimates, highlighting the precision and accuracy of the analytical technique. In-house reference materials are often used to calculate these values, which are selected to match closely the material sent in by the client, when possible. Unfortunately, not all materials sent in for analysis are of a similar matrix and composition to a laboratory's in-house standards used for QAQC reporting, and subsequently may mislead actual precision and accuracy estimates. To test this theory, elemental recoveries from QAQC reports were compared to recoveries from three soil CRMs submitted for commercial ICP–AES and research grade ICP–MS measurements. Relative proximities (RP) were used to compare the mean distance away from 100 % elemental recoveries and are displayed in Table 3.1. Elemental recoveries from the three soil CRMs are presented in Figure 3.1 for all three measurement techniques.

Table 3.1: Mean relative proximity (mean absolute distance away from 100 % recovery) comparison between QAQC reported in-house reference materials, and soil CRMs submitted for both commercial ICP–AES and research grade ICP–MS.

	In-house reference materials	Soil CRMs
pXRF		6.0 %
Commercial ICP–AES	6.4 %	8.1 %
Research grade ICP–MS	7.7 %	11 %
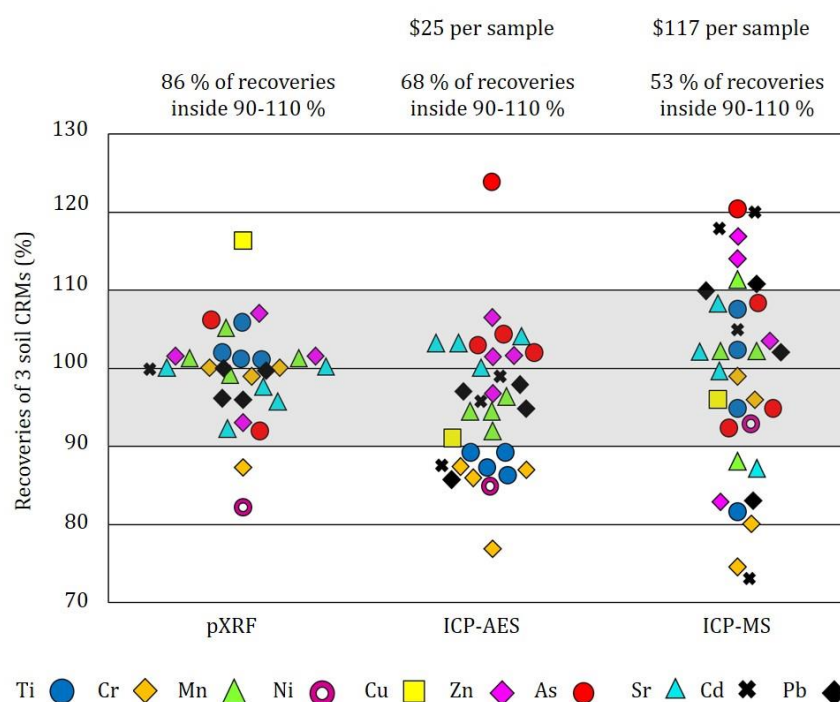
Figure 3.1: Comparison of CRM recoveries (%) by pXRF, ICP–AES and ICP–MS for the measurement of three soil CRMs (NIST 2586, 2587, 2709a).

As anticipated, slightly higher mean RP (%) were achieved in the measurement of soil CRMs than the measurement of in-house reference materials for both ICP–AES and ICP–MS techniques (Table 3.1). This may be due to the regular measurement of in-house reference materials, and/or possibly due to a mismatch in the composition or matrix of samples. Field portable XRF was specifically calibrated for the silicate-based soil matrix being measured, while both wet chemistry methods used a general standard operating procedure (SOP) that measured metal contents in soil. However, further measurements of both in-house reference materials and matrix-specific CRMs are required to definitively comment on such disparity.

Figure 3.1 shows the greatest spread of CRM recoveries for ICP–MS measurements, despite being the most expensive analysis at \$117 per sample. A common misconception in environmental analyses is that cheaper analytical tests generate more inaccurate measurements. Interestingly, the percentage of elemental recoveries within a 90–110 % recovery range increased with cheaper analytical methods, with 86 % of elemental recoveries falling in this ideal ±10 % band for pXRF. This study's comparison of established wet chemistry methods and *ex-situ* pXRF analysis has revealed two important points.

(a) ICP–AES and ICP–MS recoveries were overall slightly less accurate when compared to the matrix-calibrated pXRF, yet remained largely inside their NATA-accredited accuracy confines of 75–120 % recovery.

(b) The generation of high quality data by pXRF was specific for the measurement of a particular matrix which it was calibrated for.

The level of pXRF data quality achieved in this study suggest a similar form of accreditation may be possible for *ex-situ* pXRF measurements for a specified matrix, when certain sample preparation criteria are met. Further work is required to determine the maximum possible number of elements eligible for such accreditation, as this study investigated 11 elements (Ti, Cr, Mn, Fe, nickel (Ni), Cu, Zn, As, strontium, Cd and Pb). The high accuracy of *ex-situ* pXRF measurements has clear potential to offer users a low cost alternative to wet chemistry analyses for the determination of metal concentrations in soils. To establish the full analytical potential of these instruments for other environmental mediums (e.g. dust, plants and water), similar in-depth investigations using matrix-specific calibrations, CRM values and NATA-accredited laboratory methods should be conducted. Nonetheless, *ex-situ* pXRF measurements do not fully utilise the technology's two most powerful advantages of *in-situ* application and rapid contaminant evaluation. Hence, *in-situ* pXRF is assessed for the measurement of metal-contaminated soils in Chapter Four.

3.4 References

Kenna, T.C., Nitsche, F.O., Herron, M.M., Mailloux, B.J., Peteet, D., Sritrairat, S., Sands, E., Baumgarten, J. 2011. Evaluation and calibration of a Field Portable X-Ray Fluorescence spectrometer for quantitative analysis of siliciclastic soils and sediments. Journal of Analytical Atomic Spectrometry 26, 395-405.

Liddle, S.A. 2012. Guidance on the Safe Use of Handheld XRF Analysers. The Society for Radiological Protection. Darlington, Devon, UK.

Willis, J.P., Duncan, A.R. 2008. Understanding XRF Spectrometry, Volume 1 Basic Concepts and Instrumentation. PANalytical B.V. The Netherlands.

Chapter Four: *In-situ* pXRF assessment

4.1 Prologue

In-situ pXRF has been widely categorized as a useful screening and survey tool for the detection of metal contamination in soils, largely due to its inexpensive and rapid operation (Argyraki et al. 1997; Vanhoof et al. 2004). Numerous *in-situ* pXRF evaluations and applications are published in the literature using a variety of pXRF instruments, elements and measurement approaches. These evaluations have examined the applicability of pXRF for rapid metal-contaminated site assessments with and without quantifying the accuracy and precision of *in-situ* pXRF measurements. For example, an application study by Carr et al. (2008) investigated heavy metal concentrations in the soils of a sports field in Ireland. The study concluded pXRF was effective at mapping contamination when combined with GPS technology, yet there was no mention, calculation or validation of instrument accuracy nor precision when taking *in-situ* measurements. Some *in-situ* pXRF studies have reported mean recovery rates from the measurement of powdered CRMs (e.g. Peinado et al. 2010; Higueras et al. 2012; Paulette et al. 2015), however these recoveries are not likely to be representative of wet, unprepared field pXRF measurements and consequently such studies fail to address the resounding data quality concern that limits wider uptake of pXRF. Weindorf et al. (2012) used both CRM recoveries and wet chemistry validation for assessing the accuracy of their *in-situ* pXRF measurements, providing a more robust evaluation of *in-situ* pXRF performance. Such variability across publications hinders any consensus of the applicability of *in-situ* pXRF for non-screening purposes. It is possible that this uncertainty has deterred policy makers and environmental industries in Australia in uptaking *in-situ* pXRF technology for the assessment of metal-contaminated sites. It is also likely that incorrect attempts at quantifying *in-situ* pXRF accuracy and applicability have misled attitudes towards its usefulness for site assessments.

There will always remain a quantifiable risk associated with decision making associated with environmental data, including assessment of metal-contaminated sites, regardless of the analytical technique used. For instance, it is well known that the primary contributor to measurement uncertainty, and subsequently the uncertainty of decision making, does not originate from the analytical technique, but rather the uncertainties related to sampling and site representativeness (Vanhoof et al. 2004; Boon and Ramsey 2012). Reducing this risk is critical for any investigation, company or regulator to avoid false positive or false negative decisions. Reducing risk of making an incorrect assessment is usually achieved by increasing the number of samples taken at a site, thereby increasing the confidence interval around the mean values derived. The relatively low cost of *in-situ* pXRF measurements, when compared to the current approach of *ex-situ* sampling and wet chemistry analysis, enables users to increase the number

of measurements taken at a site, without drastically increasing costs. This issue is examined in this chapters research study.

This study was split into five sections to address the various components of an *in-situ* pXRF site assessment. This paper contributes to this thesis by examining some of the limitations associated with *in-situ* pXRF use including *in-situ* pXRF accuracy, the estimation of uncertainties of individual measurements, and presenting clear and concise solutions to these limitations. This study also discusses the current approach to site reporting and the potential benefits of integrating estimated measurement uncertainties into the primary findings of site characterisation.

4.2   Paper Three

Publication

Reducing risk and increasing confidence of decision making at a lower cost: *In-situ* pXRF assessment of metal-contaminated sites

Abstract: This study evaluates the *in-situ* use of field portable X-ray Fluorescence (pXRF) for metal-contaminated site assessments, and assesses the advantages of increased sampling to reduce risk, and increase confidence of decision making at a lower cost. Five metal-contaminated sites were assessed using both *in-situ* pXRF and *ex-situ* inductively coupled plasma mass spectrometry (ICP–MS) analyses at various sampling resolutions. Twenty second *in-situ* pXRF measurements were corrected using a subset of parallel ICP–MS measurements taken at each site. Field and analytical duplicates revealed sampling as the major contributor (>95 % variation) to measurement uncertainties. This study shows that increased sampling led to several benefits including more representative site characterisation, higher soil-metal mapping resolution, reduced uncertainty around the site mean, and reduced sampling uncertainty. Real time pXRF data enabled efficient, on-site decision making for further judgemental sampling, without the need to return to the site. Additionally, *in-situ* pXRF was more cost effective than the current approach of *ex-situ* sampling and ICP–MS analysis, even with higher sampling at each site. Lastly, a probabilistic site assessment approach was applied to demonstrate the advantages of integrating estimated measurement uncertainties into site reporting.

Reducing risk and increasing confidence of decision making at a lower cost: *In-situ* pXRF assessment of metal-contaminated sites.☆

Marek Rouillon [a, *], Mark P. Taylor [a, b], Chenyin Dong [a]

[a] *Department of Environmental Sciences, Faculty of Science and Engineering, Macquarie University, Sydney, NSW 2109, Australia*
[b] *The Energy and Environmental Contaminants Research Centre, Department of Environmental Sciences, Faculty of Science and Engineering, Macquarie University, Sydney, NSW 2109, Australia*

ARTICLE INFO

ABSTRACT

This study evaluates the *in-situ* use of field portable X-ray Fluorescence (pXRF) for metal-contaminated site assessments, and assesses the advantages of increased sampling to reduce risk, and increase confidence of decision making at a lower cost. Five metal-contaminated sites were assessed using both *in-situ* pXRF and *ex-situ* inductively coupled plasma mass spectrometry (ICP–MS) analyses at various sampling resolutions. Twenty second *in-situ* pXRF measurements of Mn, Zn and Pb were corrected using a subset of parallel ICP–MS measurements taken at each site. Field and analytical duplicates revealed sampling as the major contributor (>95% variation) to measurement uncertainties. This study shows that increased sampling led to several benefits including more representative site characterisation, higher soil-metal mapping resolution, reduced uncertainty around the site mean, and reduced sampling uncertainty. Real time pXRF data enabled efficient, on-site decision making for further judgemental sampling, without the need to return to the site. Additionally, *in-situ* pXRF was more cost effective than the current approach of *ex-situ* sampling and ICP–MS analysis, even with higher sampling at each site. Lastly, a probabilistic site assessment approach was applied to demonstrate the advantages of integrating estimated measurement uncertainties into site reporting.

© 2017 Elsevier Ltd. All rights reserved.

1. Introduction

Land contamination is a ubiquitous, worldwide problem resulting from various industrial activities such as chemical manufacturing, mining, and metal refining (Bastos et al., 2012; Vacca et al., 2012). Metal and metalloid contaminants (hereafter referred to as metals) often accumulate in high concentrations in soils, posing potential health risks to humans and biota if left unmanaged (Boon and Ramsey, 2010). Government bodies limit the maximum acceptable concentration of contaminants in soils for the land's current or intended use, in an effort to minimise risks associated with exposure (Brevik, 2013). For instance in New South Wales (NSW), Australia, contaminated sites are overseen and regulated, in part, by the state Environment Protection Authority (NSW EPA, 2015). If contamination is observed or suspected, there is a duty to report by the polluter or land owner to the NSW EPA

under Section 60 of the *Contaminated Land Management Act 1997* (NSW), when certain notification triggers are met. For both on-site and off-site soil contamination, two notification triggers exist that target the site and samples, specifically (NSW EPA, 2015):

(1) "The 95% upper confidence limit on the arithmetic average concentration of a contaminant in or on soil is equal to or above the Health Investigation Level and/or Health Screening Level for that contaminant for the current or approved use of the respective on-site land …"

(2) "The concentration of a contaminant in an individual soil sample is equal to or more than 250% of the Health Investigation Level and/or Health Screening Level for that contaminant for the current or approved use of the respective on-site land … and a person has been or foreseeably will be exposed to the contaminant or a by-product of the contaminant."

Similar notification triggers are used worldwide, with contamination being typically assessed using *ex-situ* sampling and wet chemistry analyses such as Inductively Coupled Plasma Mass

Spectrometry (ICP—MS) (e.g. US EPA, 2002). Soil metal contamination is characteristically heterogeneous and may require many samples to adequately characterise a site. For example, the 95% upper confidence limit (UCL) used in notification trigger 1, is influenced strongly by the number of samples taken to calculate the mean. Calculation of the UCL with fewer samples decreases the confidence in accurately locating the mean due to an increased confidence interval (CI) (Boon and Ramsey, 2010). Inversely, an increased number of samples is likely to increase the confidence in locating the mean by decreasing the CI. Infield sampling is typically constrained due to the cost of individual analyses charged by commercial laboratories (Ramsey and Boon, 2012).

The use of *in-situ* measurement techniques for soil metals, such as field portable X-ray Fluorescence (pXRF), have been increasingly applied as screening tools for the presence of trace metals due to their rapid, simple and inexpensive operation (e.g. Argyraki et al., 1997; Bernick et al., 1995; Boon and Ramsey, 2012; Carr et al., 2008; Clark et al., 1999; Higueras et al., 2012; Horta et al., 2015; Kalnicky and Singhvi, 2001; Parsons et al., 2013; Paulette et al., 2015; Peinado et al., 2010; Radu et al., 2013; Ran et al., 2014; Taylor et al., 2004, 2005; Vanhoof et al., 2004; Weindorf et al., 2013). *In-situ* pXRF for assessing contaminated sites has some advantages over *ex-situ* laboratory analyses including the low cost of ownership and operation and instantaneous on-site estimates of metals (Ramsey and Boon, 2012; Weindorf et al., 2014). The ability to guide field-based decision making, such as identification of contaminant hot spots and delineation of contaminant zones at low cost is indispensable for ensuring representative assessments of metal-contaminated sites (Melquiades and Appoloni, 2004). However, the difficulties of deriving analytical quality control on field samples, higher pXRF detection limits and limited training of operators when compared to *ex-situ* laboratory techniques are also well known (Peinado et al., 2010). The mismatch between field samples (unprepared, heterogeneous surface soils) and reference materials (dried, homogenous powders) makes quantification of analytical bias challenging (Boon and Ramsey, 2012). Moreover, the widespread screening use of pXRF (e.g. Restriction of Hazardous Materials, Bosco, 2013) have largely underplayed and inappropriately informed users in regards to its analytical capabilities.

Measurement techniques are most effectively employed when their advantages are fully utilised and the drawbacks are mitigated where possible. With this in mind, this study evaluates the potential integration of *in-situ* pXRF for the assessment of metal-contaminated sites. Hence, the aims of this paper are therefore to:

1. Assess the reliability of *in-situ* pXRF data compared to *ex-situ* commercial ICP—MS analysis.
2. Determine error contributions from sampling and analysis towards measurement uncertainty.
3. Evaluate the advantages of increased sampling using *in-situ* pXRF and its impact on decision making.
4. Estimate the overall costs involved for *in-situ* and *ex-situ* measurement approaches.
5. Demonstrate the advantages of integrating measurement uncertainty into site reporting.

2. Methods

2.1. Site selection and sampling design

Five metal-contaminated sites of varying sizes and land uses in NSW, Australia, were selected for this study (Table 1). Sites 1 and 3 were located near a former zinc/lead (Zn/Pb) smelter, whose surrounding suburbs were subject to decades of slag material distribution and metal-rich atmospheric depositions (Batley, 1992; Harvey et al., 2016; Morrison and Gulson, 2007). Site 2 was located at a primary school in inner city Sydney, where seven-decades of leaded petrol emissions, coupled to the use of Pb-based paint since the 19th century have contaminated the surrounding environment (Kristensen, 2015; Rouillon et al., 2017). Sites 4 and 5 were located in a mining city where >100 years of Zn/Pb mining and early smelting have contaminated city soils with Zn— and Pb—rich emissions (Dong et al., 2015; Kristensen and Taylor, 2016).

All five sites were measured systematically in a grid pattern using the minimum recommended resolution for both the current regulatory approach of *ex-situ* sampling and ICP—MS analysis (NSW EPA, 1995) and a proposed *in-situ* pXRF measurement approach (Table 1). Similar analytical and statistical approaches to metal-contaminated site assessments exist around the world, yet for the purpose of this comparative study, the current regulatory practice of sampling and off-site laboratory measurements, set by the NEPM (2013) and the NSW EPA (1995), are compared against an *in-situ* pXRF method. A pilot study was conducted at a small (0.04 ha), geochemically heterogeneous site and determined 30 samples as a reliable and robust minimum for estimating a site mean (cf. Student, 1908) (Supplementary Fig. 1). An increased sampling resolution was used for *in-situ* pXRF measurements to assess the benefits of increased sampling at metal-contaminated sites. After the measurement of surface soil contamination using a systematic assessment approach (pXRF Phase 1), a second phase of measurements was undertaken halfway between targets of interest (e.g. where sample concentration > guideline) and adjacent samples (pXRF Phase 2). This second phase (judgemental sampling) utilised the advantages of real-time pXRF data which assisted in identifying hot spots without the need to return to the site.

2.2. In-situ pXRF measurement approach

Sites were measured *in-situ* at the minimum resolution specified in Table 1, using an Olympus Delta Premium XRF Analyser fitted

Table 1
Minimum sampling resolution for the current regulatory approach (NSW EPA, 1995) and proposed *in-situ* pXRF approach per given site size. *The number of samples taken at Site 4 was 36 for ICP–MS and 46 for pXRF Phase 1.

Site number	Land use type	Size (ha)	Current minimum samples (ICP–MS)	Proposed minimum samples for *in-situ* pXRF (pXRF Phase 1)	Systematic + judgemental sampling for *in-situ* pXRF (pXRF Phase 1 + 2)
1	Empty house lot	0.1	6	30	64
2	School grounds	0.6	15	30	76
3	Recreational park	1.0	21	30	61
4	Sports field	2.2	*35	*45	83
5	Recreational park	2.8	40	50	90

with a 50 kV, 4 W Ta anode X-ray tube and a silicon drift detector. Measurement targets were pre-determined and marked with flags. Grasses and debris were removed where necessary to expose the surface soil layer, which was compacted prior to pXRF analysis. The pXRF measurement window was cleaned with KimWipes between samples to mitigate cross contamination. Samples were measured for 20 s on Beam II (40 kV) using the proprietary soil mode for manganese (Mn), Zn, and Pb concentrations. Despite being measured most accurately on Beam III (15 kV), Mn was included in this assessment to ascertain if elements can be measured accurately on other X-ray beams that are not intended for its measurement. The pXRF was protracted from the operator via an extension pole to minimise radiation exposure associated with pXRF operation (Rouillon et al., 2015) and to provide ergonomic *in-situ* measurements.

Recommended operational procedures were followed (cf. Rouillon and Taylor, 2016), including daily measurements of an energy calibration check, measurements of a silicate (SiO_2) blank and National Institute of Standards and Technology certified reference materials (CRMs: NIST 2709a, 2710a, 2711a) throughout the measurement process. Instrument detection limits for Mn, Zn and Pb measurements were 9.1, 5.1 and 3.0 mg/kg respectively, while the mean relative standard deviation for these elements were 0.8, 0.8 and 1.8% (Rouillon and Taylor, 2016). Mean pXRF recoveries were 102% (Mn), 99% (Zn) and 99% (Pb) for *ex-situ* measurements, however these are not likely to be representative of *in-situ* measurements. Hence, the analytical bias of *in-situ* pXRF measurements were corrected using ICP–MS analysis (Section 2.5).

2.3. ICP–MS analysis

Sites were sampled and measured by ICP–MS at the minimum resolution specified in Table 1. Surface soils were collected at 0–2 cm depth and analysed for total acid extractable metal concentrations at the National Measurement Institute at North Ryde, Australia. Approximately 0.5 g of sample was digested in 3 mL of 10 M HCL and 3 mL of 16 M HNO_3, and measured using an Agilent 7900 ICP–MS for Mn, Zn and Pb concentrations (NMI, 2014). Six procedural blanks returned concentrations <0.5 mg/kg for all elements. Laboratory control spikes were 99%, 105% and 102%, while matrix control spikes were 93–106%, 97–112% and 83–116% for Mn, Zn and Pb respectively. Duplicate analyses were 0–39% (Mn), 0.1–27% (Zn) and 0.1–18% (Pb).

2.4. Sampling, analytical and measurement uncertainty

The simplest and most cost efficient method for estimating sampling and analytical precision, and ultimately measurement uncertainty is using a balanced duplicate method (Supplementary Fig. 2) (Ramsey et al., 1992, 2002). Ten to 15% (n ≥ 3) of samples

from each site were randomly selected for duplicate sampling and analysis for both *in-situ* pXRF and ICP–MS measurement approaches. Duplicate samples (S1, S2) were taken at 10% of the mean grid spacing distance between targets at 90° orientation from each other. Duplicate analyses (A1, A2) were conducted for each duplicate sample. The variation between sample duplicates demonstrates sampling ambiguity, including small scale heterogeneity of the sample and precisely locating the sample target. The variation between analyses of the same sample duplicate provides variation of the analytical process and technique. To estimate individual contributions to variance and uncertainty, duplicates data were analysed using robust analysis of variance (RANOVA). Robust ANOVA was selected over standard ANOVA to down-weigh the effect of outliers in the frequency distribution, and provide more reliable estimates of variances (Ramsey and Ellison, 2007). Calculation of measurement uncertainty via RANOVA is further explained and demonstrated in Boon and Ramsey (2010). Analytical bias was not included in variance estimates given the disparity between soil reference materials (dry/small particles) and the field sample (wet/varying particle size).

2.5. In-situ pXRF data correction

To correct for analytical bias and moisture content, parallel measurements of both *in-situ* pXRF and ICP–MS were conducted at the same sample targets (T) used for duplicate analyses at each site. This form of pXRF data adjustment has previously been applied in *in-situ* vs. *ex-situ* measurement comparisons (e.g. Ramsey and Boon, 2012). The sample was first measured by pXRF, then sampled directly under the measurement window location by inserting a 35 mm open ended XRF cup 2 cm into the soil. This was done to ensure the sample measured by *in-situ* pXRF was as close to the 'same' sample measured by ICP–MS as possible. Prior to pXRF data correction, ICP–MS data was converted from 'dry weight' to 'as received' basis using moisture content (%) estimated by the commercial laboratory (Supplementary Table 1). A Deming regression was used to plot both measurement techniques with pXRF placed on the x–axis, and ICP–MS on the y–axis. Rotational (slope, m) and translational (intercept, b) bias were corrected for *in-situ* pXRF data by solving for 'y' in 'y = mx + b'.

3. Results and discussion

3.1. Corrected in-situ pXRF data

Calculating *in-situ* pXRF analytical bias using CRMs is not recommended due to the clear disparity between the quality of field sample (wet, coarse, heterogeneous soil) and CRMs (dry, fine and homogeneous soil). Hence, 20 s *in-situ* pXRF measurements were corrected at each site using ICP–MS data, provided the relationship
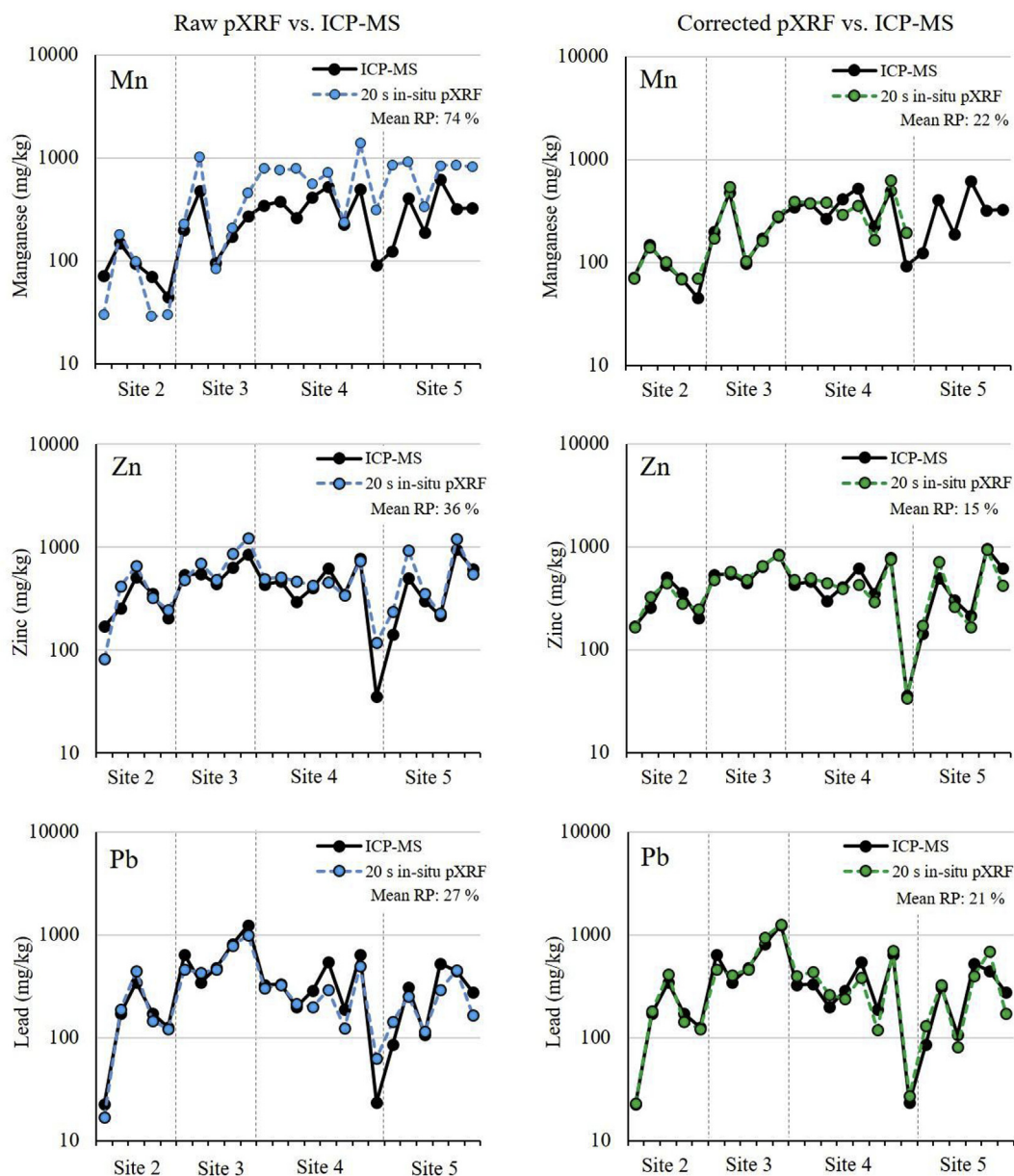
Fig. 1. Point by point graphs of 20 s *in-situ* pXRF measurements against ICP—MS data at four metal-contaminated at Sites 2—5. Impact of *in-situ* pXRF data adjustment using ICP—MS data is demonstrated between pre- and post-correction rows. Relative proximity (RP) gives an indication of pXRF inaccuracy when compared to a reference value (ICP—MS data) and is calculated by RP = (absolute (100—recovery value).

between pXRF and ICP—MS measurements were systematic (Regression plots are provided in Supplementary Fig. 3). The moisture content of soil samples were estimated by the commercial laboratory prior to ICP—MS analysis and are presented alongside pre- and post-correction pXRF data in Supplementary Table 1. Sites 2—5 were comprised largely of a single soil matrix, and achieved strong correlations between the two measurement techniques (Fig. 1). Due to the presence of multiple matrices at Site 1 (silicate based soils and glassy black slag particles), *in-situ* pXRF did not generate a systematic relationship with ICP—MS data, and were not corrected. The low number of data correction samples at this site (n = 5), combined with the marked small—scale heterogeneity of each sample are likely contributors to the weak correlation. Despite efforts of sampling for ICP—MS analysis from directly under the pXRF measurement window, the issue of mis-representation when comparing measurements from different techniques remained.

Samples sent for ICP—MS analysis were not homogenised in the field, nor homogenised prior to measurement by the commercial laboratory to reflect standard commercial practice. Homogenisation of these samples would have likely improved comparisons between the analytical techniques.

Relative proximity (RP = absolute (100—(pXRF value/ICP—MS value))) is a useful indicator of inaccuracy as it demonstrates the proportional difference away from the reference value (Rouillon and Taylor, 2016). After pXRF data correction, the mean RP improved from 74% to 22% for Mn (Sites 2—4), 36%—15% for Zn and from 27% to 21% for Pb measurements (Fig. 1). *In-situ* pXRF Mn measurements were not corrected at Site 5 due to poor, non-systematic correlation with ICP—MS measurements ($r^2 = 0.153$). The large improvement in Mn RP at Sites 2—4 is likely due to its measurement on a non-primary X-ray beam (40 kV instead of 15 kV). The poor correlation between raw pXRF and ICP—MS for Mn

concentrations suggest *in-situ* pXRF measurement using a primary X-ray beam is required to guide judgemental sampling. Raw pXRF measurements of Zn and Pb were not markedly different from ICP−MS values for the majority of samples, justifying their use to guide judgemental sampling. Using ICP−MS data as reference values, mean *in-situ* pXRF recoveries were 109% (Mn), 101% (Zn) and 103% (Pb) across Sites 2−5, validating the use of *in-situ* pXRF when the data is corrected with laboratory analyses. Moreover, 20 s *in-situ* pXRF measurements enabled the inclusion of numerous additional inexpensive on-site measurements.

3.2. Sampling and analysis in measurement uncertainty

Contributions towards measurement uncertainty (U_{meas}) were estimated using RANOVA analysis (Supplementary Table 2). Variance between field duplicate sets (s_{samp}) reveal soil heterogeneity at sample locations, and the contaminant concentration range that a user may encounter when attempting to locate the sample. Variance between analytical sets (s_{anal}) reveals the imprecision of repeat measurements for a specific analytical method. *In-situ* pXRF duplicate analyses were typically more precise than the ICP−MS method across the five sites, largely because ICP−MS analytical duplicates were split prior to sample digestion, rather than at the end of the sample preparation process. Estimated sampling and analytical contributions towards site measurement uncertainties are summarised in Table 2. High sample and site heterogeneity at Site 1 contributed to large measurement uncertainties for all three contaminants assessed. Sampling uncertainty contributed more than 99% of the total measurement uncertainty at Site 1, highlighting the need for an increased sampling resolution at heterogeneous sites (Table 2). Theoretically, increasing the sampling resolution by a factor of n will reduce the sampling uncertainty by $1-(1/\sqrt{n})$ (Gy, 1979). However in practice this was not always achieved, *in-situ* pXRF measurements (n = 30) were five times the sampling resolution of *ex-situ* ICP−MS measurements (n = 6) for Site 1, yet uncertainties still remained high. Probable explanations include the contaminant distribution was not uniformly heterogeneous across the site and/or because *in-situ* pXRF duplicate sampling occurred at more heterogeneous areas.

Sampling (U_{samp}) was the primary contributor to measurement uncertainty at the other four sites, regardless of measurement approach (Table 2). Despite the application of consistent duplicate sampling approaches, estimated measurement uncertainties varied

considerably between the two techniques (e.g. U_{meas} for Site 5 Pb: ICP−MS−31.6%, pXRF−103%). Duplicate sampling was not systematically distributed across each site, but were selected randomly prior to visiting each site. Given the heterogeneity of soil contamination at the sites, it is possible that this could have skewed uncertainty estimates, particularly where by chance, selected samples were grouped in an unrepresentative area of the site. Further, the low number of duplicate samples (10−15%, n ≥ 3) used for estimating measurement uncertainty at each site may not have been sufficient. Boon and Ramsey (2010, 2012) used a minimum of eight duplicate samples for estimating measurement uncertainty, however such a protocol was difficult to apply when the minimum regulatory sampling requirement for a 0.1 ha site is only six samples (NSW EPA, 1995).

3.3. Advantages of increased sampling

Increased site sampling has several benefits including: generation of more representative site data, a better understanding of contaminant distribution, reducing the probability of missing contaminant hot spots, increased confidence of site mean reporting, and a reduction in sampling uncertainty (Gy, 1979) (Fig. 2). Increased sampling was undertaken using *in-situ* pXRF to assess these benefits and its impact on site decision-making. For example, soil Pb concentrations at Site 2 are compared using the minimum sampling resolution specified in Table 1 for both measurement approaches (i.e. a 0.6 ha area with 15 samples for ICP−MS as per the NSW EPA (1995) guideline vs. 30 pXRF samples) (Fig. 3). Both measurement approaches generated similar soil Pb maps, with higher soil Pb concentrations found towards the south-west (SW) side of the site (Fig. 3). Increased sampling by *in-situ* pXRF identified the same proportion (20%) of samples over the relevant health investigation level (HIL) of 300 mg/kg as the ICP−MS approach, but at twice the resolution, increasing the confidence that this was a true estimate. Real-time pXRF data enabled efficient judgemental sampling around samples with soil Pb concentrations >300 mg/kg (Fig. 3). These additional data were critical for revealing the extent of higher Pb concentrations towards the SW edge of the site. *In-situ* pXRF has the clear benefits of enabling the investigator to make informed decisions with respect to the need for additional judgemental sampling, without the need to return to the site, potentially saving both time and costs when compared to *ex-situ* sampling approaches.

Table 2
Summary of sampling, analytical and measurement uncertainties (%) of soil Mn, Zn and Pb concentrations at five metal-contaminated sites. Both *ex-situ* ICP−MS and *in-situ* pXRF measurement approaches are presented. Values in **bold** represent >95% variance contribution towards measurement uncertainties. Values with an asterisk (*) represent uncorrected *in-situ* pXRF data.

		ICP−MS				pXRF		
		Sampling	Analysis	Measurement		Sampling	Analysis	Measurement
Mn	Site 1	**221**	16.4	222	Site 1	***248**	*8.4	*249
	Site 2	15.4	11.4	19.2	Site 2	19.3	5.1	20.0
	Site 3	6.5	14.1	15.5	Site 3	49.6	16.7	52.3
	Site 4	51.4	17.3	54.2	Site 4	**63.0**	8.9	63.6
	Site 5	42.3	13.0	44.3	Site 5	*54.3	*15.9	*56.6
Zn	Site 1	**221**	9.4	221	Site 1	***190**	*5.6	*190
	Site 2	2.3	**8.4**	8.7	Site 2	**36.1**	4.1	36.3
	Site 3	15.1	8.4	17.3	Site 3	19.6	6.1	20.5
	Site 4	**51.4**	9.7	52.3	Site 4	53.8	16.8	56.4
	Site 5	**65.9**	11.1	66.8	Site 5	**59.0**	10.1	59.8
Pb	Site 1	**178**	9.7	179	Site 1	***190**	*5.4	*190
	Site 2	**65.0**	13.1	66.3	Site 2	**102**	2.9	102
	Site 3	21.6	14.4	25.9	Site 3	72.1	22.2	75.4
	Site 4	66.1	17.1	68.3	Site 4	**58.3**	5.8	58.6
	Site 5	28.4	13.7	31.6	Site 5	**102**	10.5	103
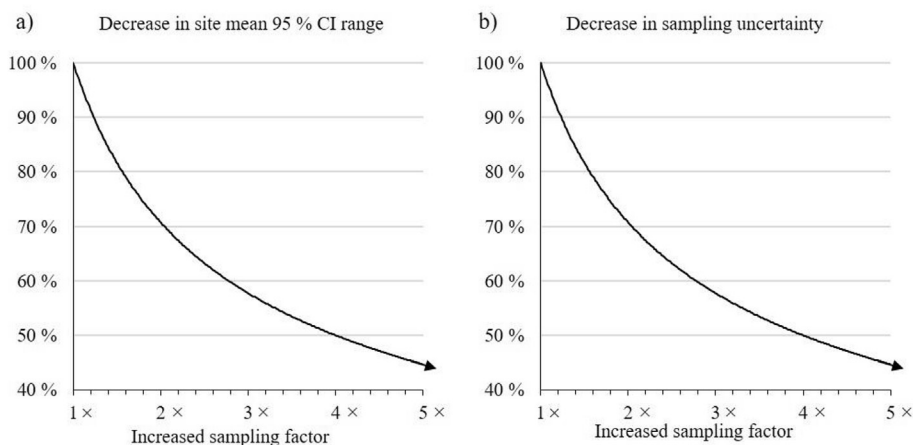
Fig. 2. Impact of increased sampling on both the a) 95% confidence interval around a site mean, and b) sampling uncertainty. Assuming site mean and standard deviation remain constant, an increase in sampling by a factor of 3 (i.e. from 20 to 60 samples) reduces the confidence interval range and sampling uncertainty by $1-(1/\sqrt{3}) = 42\%$. Reduction of sampling uncertainty from increased sampling was adapted from Gy (1979).
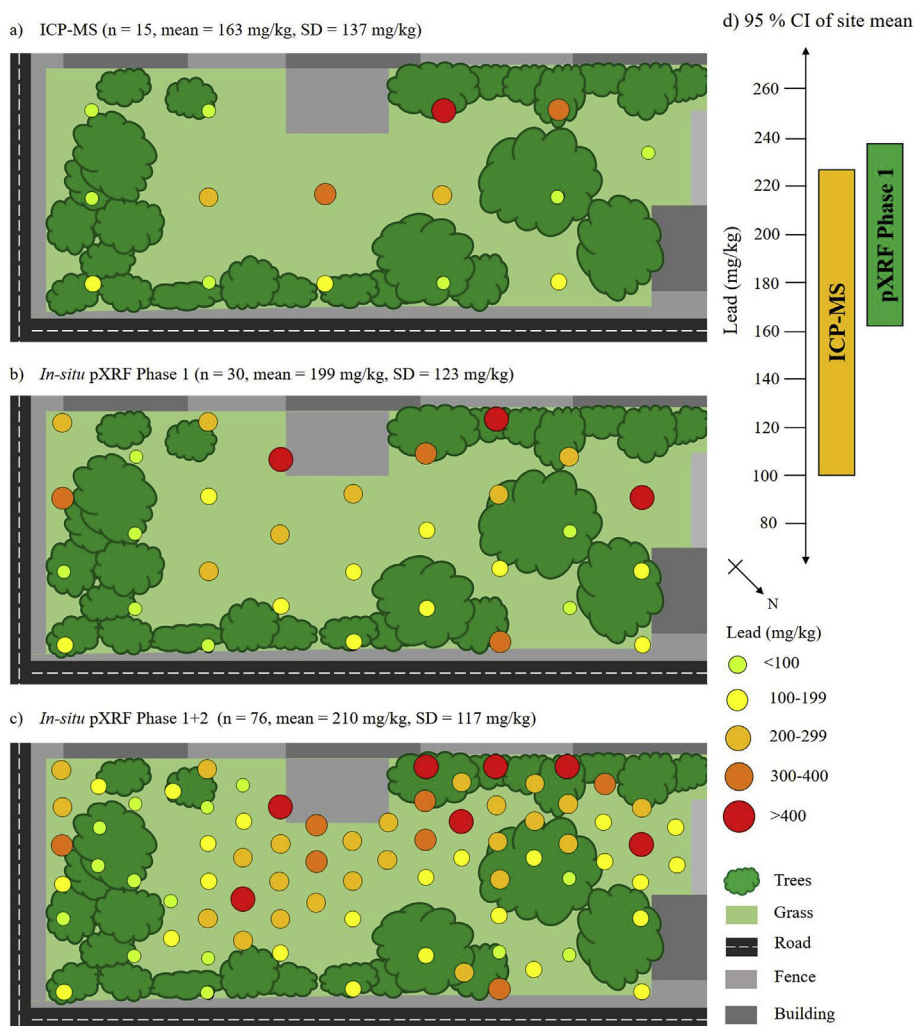
Fig. 3. Systematic spatial distribution of soil lead concentrations at Site 2 for a) ICP–MS measurements (n = 15) and b) *in-situ* pXRF Phase 1 measurements (n = 30). c) Real time pXRF data (Phase 1 + 2) enabled efficient judgemental sampling directly after *in-situ* pXRF Phase 1. d) Uncertainty (95% CI) on the site mean is compared for ICP–MS and *in-situ* pXRF Phase 1 measurement approaches.

In NSW the duty to notify contamination under the *Contaminated Land Management Act 1997* (NSW), is required where the upper confidence limit (95% CI) of a site mean is equal to, or exceeds the relevant HIL for the respective land use (NSW EPA, 2015). The 95% CI of a site mean is calculated using four variables: mean, student's t statistic, standard deviation and the number of samples:

$$CI = \mu \pm t \, (\sigma / \sqrt{n})$$

where CI = confidence interval, μ = arithmetic mean, t = student's t statistic (level of significance and n−1 degrees of freedom), σ = standard deviation and n = number of samples. For sites with a coefficient of variation >1.2, refer to Procedure G of NSW EPA (1995). Coefficient of variation is the ratio of the standard deviation against the mean, and is calculated as CV = (σ/μ) × 100.

Assuming the mean and standard deviation of a site remain constant, increasing the number of samples by a factor of n should theoretically reduce the 95% CI range by $1 - (1/\sqrt{n})$. To demonstrate this, the minimum sampling resolution for ICP−MS (n = 15) and *in-situ* pXRF (n = 30) approaches are compared at Site 2 (Fig. 3). Sampling was increased by a factor of two, hence the anticipated decrease in site mean CI range was $1 - (1/\sqrt{2}) = 29\%$. The mean CI range of ICP−MS and *in-situ* pXRF approaches were 124 mg/kg and 77 mg/kg Pb, respectively, resulting in a decrease of the site CI range by 38% (Fig. 3). The two measurement approaches resulted in similar UCL values of 225 mg/kg (ICP−MS) and 238 mg/kg (pXRF), both less than the soil Pb HIL guideline of 300 mg/kg. The second notification trigger (an individual soil sample being equal to or greater than 250% of the relevant HIL guideline) was also not met, with maximum Pb concentrations of 472 mg/kg and 493 mg/kg for ICP−MS and pXRF approaches respectively, meaning that in this case, neither approach was sufficient to trigger the duty to report.

Calculation of the UCL with low sample numbers expands the 95% confidence interval, and may erroneously extend the UCL above a HIL guideline. Subsequently, this may lead to a false positive i.e. a decision that the site should undergo further investigation (NEPM, 2013) and/or remediation. Misclassification of sites is more likely to occur where site assessments rely on small sample numbers because they fail to accurately represent the real site mean. Thus, small sample numbers can result in higher sampling uncertainty and consequently, a reduced confidence end-users may have in reporting the site mean (Fig. 2). Alternatively, site assessments with high sample numbers reduce sample uncertainty and consequently reduce the likelihood of site misclassification due to increased confidence in reporting a site mean. For example, a 50% reduction in sampling uncertainty and site mean confidence range requires a four-fold increase in sampling resolution (Fig. 2). This can prove costly using the current approach of *ex-situ* sampling and wet-chemistry analyses because a large percentage of costs relates to laboratory fees. Yet ultimately, improvements to site characterisation do not relate to the selection of analytical technique (ICP−MS or pXRF), but rather is primarily impacted by the number of samples collected.

3.4. Cost effectiveness of in-situ pXRF site assessments

Increased sampling involves extra costs regardless of the analytical technique due to field labour and analytical costs. Yet, unlike wet chemistry analyses, *in-situ* pXRF has practically no analytical costs in terms of instrument operation or field consumables. The primary costs of *in-situ* pXRF relate to field labour and analysis of a subset of samples by a commercial laboratory using ICP−MS. The total costs involved for both *in-situ* pXRF and *ex-situ* sampling and ICP−MS analysis for the minimum sampling (Table 1)

of metal-contaminated sites were estimated using assumptions of individual costs (Fig. 4). Variables include field labour (AU$150/hour), commercial ICP−MS analysis (AU$22.60/sample), time between samples and for *ex-situ* soil sampling (45 s/sample), time for *in-situ* pXRF measurements (20 s/sample), time and costs for parallel sampling for *in-situ* pXRF data correction and ownership of an environmental pXRF unit (AU$83/site). Field portable XRF ownership cost (AU$40,000) was split over the mean lifetime of a pXRF (7 years), under the assumption that it is utilised for a site assessment twice every working week. Total cost estimations do not include duplicate sampling and analysis, which would vary based on the number of duplicates taken.

In-situ pXRF assessment of metal-contaminated sites were more cost-efficient, even with increased sampling, than the current approach of *ex-situ* sampling and ICP−MS analysis (Fig. 4). Sampling resolution of both systematic and judgemental *in-situ* pXRF phases were greater than the minimum sampling requirements for the ICP−MS approach (Table 1), and subsequently generated more information per site. This explains why *in-situ* pXRF Phase 1 (n = 30) and 1 + 2 (n = 64) at the smallest site (Site 1) were more expensive than the ICP−MS approach (n = 6). Both measurement approaches are compared for soil Zn concentrations and overall costs at Site 4 (Fig. 4, Supplementary Fig. 4). Real-time *in-situ* pXRF data identified slightly higher metal concentrations at the oval border, which guided further same-day judgemental sampling towards street corners. When compared to *ex-situ* sampling and ICP−MS analysis, *in-situ* pXRF provided more than twice (2.3 times) as many site measurements for Site 4 at approximately half the cost (AU$466 vs. AU$880) (Fig. 4).

It is also possible to utilise the savings accrued using a pXRF for site assessment costs towards reducing uncertainties. For example, for the same cost as the ICP−MS approach at Site 4 (AU$880), the application of *in-situ* pXRF will enable systematic assessment at >4.5 times the resolution (165 vs. 36 samples), reducing both sampling and site mean uncertainty by >50% (Fig. 2). This is important as sampling typically contributes the greatest error towards measurement uncertainty (see Section 3.2). Through
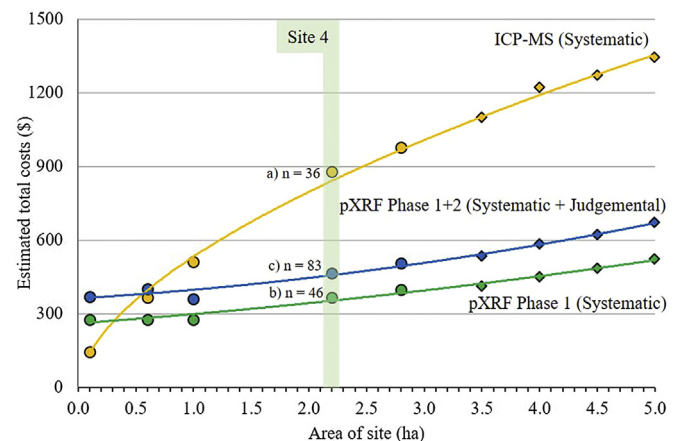
Fig. 4. Estimated total costs for the characterisation of metal-contaminated sites at the minimum sampling resolution for ICP−MS and *in-situ* pXRF. Cost assumptions include: labour call out rate = $150/hour, *in-situ* pXRF measurement = 20 s, pXRF ownership cost = $83/assessment, time between samples = 45 s, commercial laboratory eight element analysis = $22.60/sample. The cost of duplicate sampling to establish measurement uncertainty was not included given that this would vary according to the number of duplicate samples being taken. Circles are estimated costs from the five-metal contaminated sites in this study, while diamonds are projected costs for sites larger than 3 ha. The number of samples used to characterise Zn concentrations at Site 4 are shown for a) the ICP−MS approach (n = 36), b) pXRF Phase 1 (n = 46), and c) pXRF Phase 1 + 2 (n = 83).

increased sampling achieved by applying a cheaper, but ultimately equally reliable analytical technique, large measurement uncertainties associated with field heterogeneity can be more adequately addressed.

3.5. Shift towards probabilistic classification of sites

The current approach of metal-contaminated site characterisation compares soil metal concentrations to the relevant HIL guidelines (NSW EPA, 2015), under the notion that individual measurements are correct. Every measurement is incorrect to some extent due to uncertainty contributions from both field sampling and analysis (Boon and Ramsey, 2010). In cases where field and analytical duplicates are taken, measurement variation is typically presented separately from the primary findings in a Quality Assurance/Quality Control section. Given the typically heterogeneous nature of metal-contaminated sites, this variation should ideally be presented as a part of the primary findings to reduce the risk of site misclassification.

Integration of measurement uncertainty into site reporting, also known as probabilistic classification, was first suggested by Ramsey and Argyraki (1997). Probabilistic classification includes the estimated measurement uncertainty (%) of a site and places it around each sample concentration, enabling the investigator to report with 95% confidence that a sample falls within a concentration range (Boon and Ramsey, 2010). This concentration range (C) is then compared to the relevant guideline (G), and placed in one of four categories:

- Definitely under guideline − Probability of C > G (<2.5%)
- Possibly over guideline − Probability of C > G (2.5—50%)
- Probably over guideline − Probability of C > G (50—97.5%)
- Definitely over guideline − Probability of C > G (>97.5%)

To illustrate this probabilistic approach, soil Pb concentrations from Site 4 were plotted in increasing order with and without the estimated measurement uncertainty of 58.6% (Fig. 5). A deterministic (non-uncertainty) approach identified 72% of samples below the HIL guideline of 600 mg/kg Pb for public open spaces such as sporting fields (NEPM, 2013). The application of a probabilistic approach identifies uncertainties around each measurement and classifies samples based on the probability they exceed the guideline value. Only 47% of samples had measurement uncertainty ranges below the guideline, which signifies to the investigator a >97.5% probability these samples do not exceed the guideline (Fig. 5). Comparatively, a larger proportion of samples exceeded the guideline using the current approach (28%) than a probabilistic approach (5%), due to the exclusion of field and analytical variation. Clearly, this might lead to a false positive scenario, i.e. a decision that determines a site is contaminated to the extent that it warrants remediation.

Reducing the risk of both site and sample misclassification is perhaps the most important advantage of a probabilistic approach (Boon and Ramsey, 2010). Conversely, it also increases the proportion of samples that are 'possibly' or 'probably' over a guideline. This knowledge gap can be addressed through increased sampling to reduce the estimated measurement uncertainty of a site, which would in turn reduce the uncertainty range around each sample. The confidence level of reporting (i.e. 90, 95 or 99%) and classification categories (e.g. definitely over guideline) can also be modified for specific data quality objectives. Nevertheless, probabilistic reporting of metal-contaminated sites demonstrates that the investigator understands the true variation of measurements at a site, and can tailor their findings accordingly. This enables investigators to make more robust decisions by lowering the risk of site misclassification.

4. Potential limitations of *in-situ* pXRF

1) This study evaluated *in-situ* pXRF measurements directly on wet, unprepared soils. Moisture content can impact the accuracy of pXRF measurements, particularly on elements with low
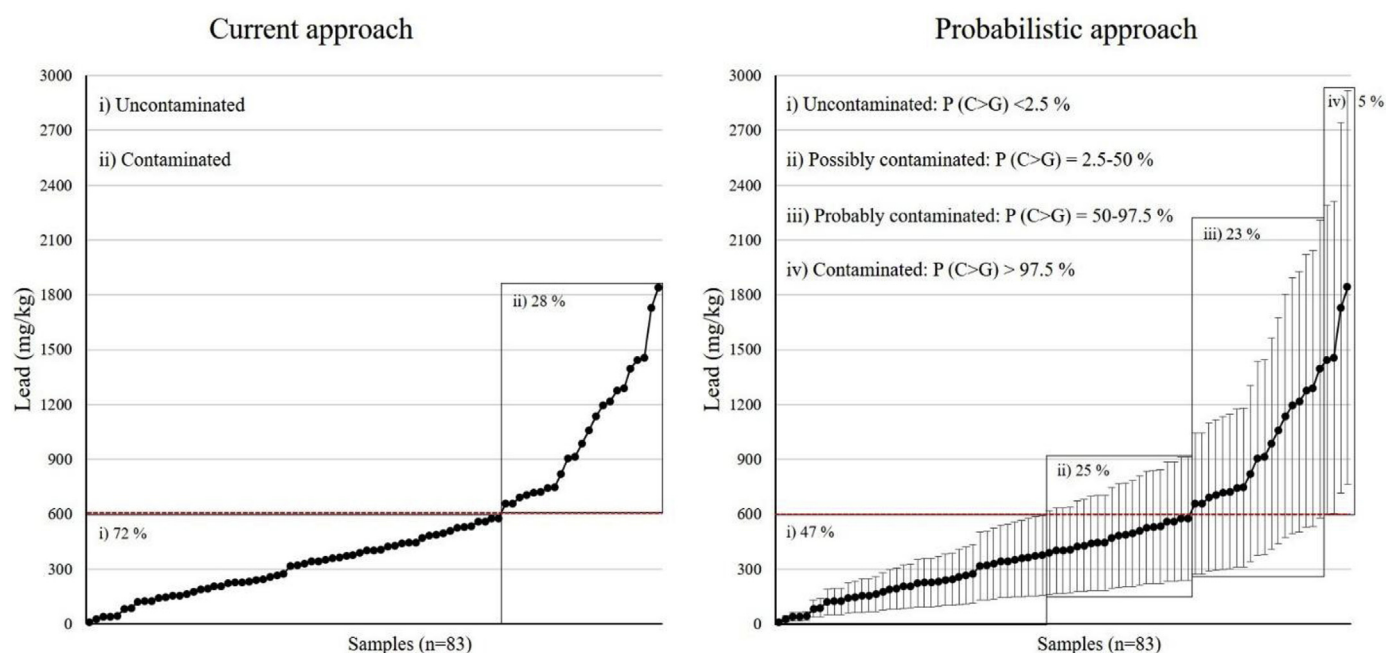
Fig. 5. Comparison between the current approach and probabilistic *in-situ* pXRF approach to metal-contaminated soil classification for Pb concentrations at Site 4. Measurement uncertainty was estimated to be 58.6% (Table 2), and represents the error bars around each sample. The Australian health investigation level (HIL−C) for sports fields is 600 mg/kg for Pb and is represented by the dotted red line. P = Probability of, C = concentration of sample, G = guideline.

atomic numbers (Bastos et al., 2012). Estimated moisture content (%) was used from the subset of ICP−MS measurements at each site to adjust the wet chemistry data to an 'as received' basis (Weindorf et al., 2012). This was done to compare and correct accurately for any analytical bias between the two measurement techniques, and to represent actual exposures that could potentially be experienced by an organism (Ramsey and Boon, 2012).

2) Environmental investigations measure surface and subsurface soils to ascertain the distribution of contaminants across a site and down the soil profile. This study did not investigate subsurface soil metal concentrations, yet measurements of auger soils could be expedited using similar *in-situ* pXRF protocols. Although further research is required to ascertain if *in-situ* pXRF can be applied to subsurface soils, there is no clear technical barrier for that to not be the case.

3) *In-situ* pXRF data at Site 1 did not correlate strongly with ICP−MS data due to the presence of multiple matrices in the soil (silicate based soils and glassy black slag particles). As a result, these samples were subject to light sample preparation steps, including drying and gently crushing using a mortar and pestle, and were re-measured by pXRF through a polyethylene bag. As expected, correlation with ICP−MS data improved significantly (Supplementary Figures 3 and 5) suggesting some sample preparation may be required when multiple matrices are present on site.

4) An important limitation of the application of *in-situ* pXRF is that it can only be addressing inorganic contamination. By comparison, *ex-situ* analysis of soils allows for samples to be split and subject to a variety of metal and non-metal contaminants such as hydrocarbons, organics and persistent chemicals, which are also common co-contaminants at sites. It is possible that future developments to pXRF may be capable of non-metal contaminant screening via add-on accessories. For example, *in-situ* soil screening of total petroleum hydrocarbons (CSIRO, 2012) and asbestos (Thermo Scientific, 2011) exist, however these are measured using separate analysers.

5. Conclusions and recommendations

In-situ pXRF was demonstrated to be a powerful and cost effective tool for metal-contaminated site assessments when complemented with ICP−MS data. Twenty second *in-situ* pXRF measurements were corrected using parallel ICP−MS data, allowing for accurate, rapid and inexpensive high resolution sampling. Field and analytical duplicates revealed sampling as the primary contributor to high measurement uncertainties, regardless of analytical technique. Increased sampling generated more representative site data, higher resolution contaminant mapping, increased confidence in reporting site means and decreased uncertainty related to sampling. Real time pXRF data also has the clear benefit over *ex-situ* ICP−MS analysis by enabling effective judgemental sampling for detecting contaminant hot spots. The *in-situ* pXRF assessment method proposed here was also usually more cost efficient than the current approach of *ex-situ* sampling and ICP−MS analysis, despite increased sampling by pXRF. Finally, integrating measurement uncertainty into site reporting data can lower the risk of site misclassification.

Every analytical technique have advantages and disadvantages associated with their application. This study targeted the advantages of *in-situ* pXRF, while simultaneously addressing the shortfalls of its use. Understanding the analytical capabilities and limitations of *in-situ* pXRF allowed for effective and reliable assessment of metal-contaminated sites. However, further work is

required to demonstrate if other environmentally significant contaminants (e.g. nickel, arsenic and mercury) can be assessed using the methods described in this paper. The proposed *in-situ* pXRF method is a cost-effective alternative to wet chemistry analysis, capable of lowering misclassification risks and generating higher confidence in site data when compared to the data from the current regulatory practice in NSW, Australia. Supplementing slower and more expensive analytical methods (ICP−MS) with a rapid and cheaper analytical technique (pXRF) should be considered for metal-contaminated site assessments in other regulatory jurisdictions in Australia and around the world. This is particularly relevant where high soil metal heterogeneity requires the use of many samples for site characterisation.

Appendix A. Supplementary data

Supplementary data related to this article can be found at http://dx.doi.org/10.1016/j.envpol.2017.06.020.

References

Argyraki, A., Ramsey, M.H., Potts, P.J., 1997. Evaluation of portable x-ray fluorescence instrumentation for in situ measurements of lead on contaminated land. Analyst 122, 743–749.

Bastos, R.O., Melquiades, F.L., Biasi, G.E., 2012. Correction for the effect of soil moisture on in situ XRF analysis using low-energy background. X-ray Spectrom. 41, 304–307.

Batley, G., 1992. Investigation report CET/LHIR077. Leachability of lead and other trace metals from lead-zinc smelter slag. Commonw. Sci. Industrial Res. Organ. Div. Coal Energy Technol. Centre Adv. Anal. Chem. 1–10.

Bernick, M.D., Kalnicky, D.J., Prince, G., Singhvi, R., 1995. Results of field-portable X-ray fluorescence analysis of metal contaminants in soil and sediment. J. Hazard. Mater. 43, 101–110.

Boon, K.A., Ramsey, M.H., 2010. Uncertainty of measurement or of mean value for the reliable classification of contaminated land. Sci. Total Environ. 409, 423–429.

Boon, K.A., Ramsey, M.H., 2012. Judging the fitness of on-site measurements by their uncertainty, including contribution from sampling. Sci. Total Environ. 419, 196–207.

Bosco, G.L., 2013. James L. Waters Symposium 2012 Report. Development and application of portable, hand-held X-ray fluorescence spectrometers. Trends Anal. Chem. 45, 121–134.

Brevik, E.C., 2013. Soils and human health: an overview. In: Brevik, E.C., Burgess, L.C. (Eds.), Soils and Human Health. CRC Press, Boca Raton, pp. 59–82.

Carr, R., Zhang, C., Moles, N., Harder, M., 2008. Identification and mapping of heavy metal pollution in soils of a sports ground in Galway City, Ireland, using a portable XRF analyser and GIS. Environ. Geochem. Health 30, 45–52.

Clark, S., Menrath, W., Chen, M., Roda, S., Succop, P., 1999. Use of a field portable X-ray fluorescence analyzer to determine the concentration of led and other metals in soil samples. Ann. Agric. Environ. Med. 6, 27–32.

Commonwealth Scientific and Industrial Research Organisation (CSIRO), 2012. Portable Device Detects Soil Contamination. News. Ziltek. http://www.ziltek.com.au/pdf/CSIRO%20News%20Release%20-%20Portable%20device%20detects%20soil%20contamination.pdf (accessed 21 March 2017).

Dong, C., Taylor, M.P., Kristensen, L.J., Zahran, S., 2015. Environmental contamination in an Australian mining community and potential influences on early childhood health and behavioural outcomes. Environ. Pollut. 207, 345–356.

Gy, P., 1979. Sampling of Particulate Materials − Theory and Practice. Elsevier, Amsterdam, pp. 1–450.

Harvey, P.J., Taylor, M.P., Kristensen, L.J., Grant-Vest, S., Rouillon, M., Wu, L., Handley, H.K., 2016. Evaluation and assessment of the efficacy of an abatement strategy in a former lead smelter community, Boolaroo, Australia. Environ. Geochem. Health 38 (4), 941–954.

Higueras, P., Oyarzun, R., Iraizoz, J.M., Lorenzo, S., Esbri, J.M., Martinez-Coronado, A., 2012. Low-cost geochemical surveys for environmental studies in developing countries: testing a field portable XRF instrument under quasi-realistic conditions. J. Geochem. Explor. 113, 3—12.

Horta, A., Malone, B., Stockmann, U., Minasny, B., Bishop, T.F.A., McBratney, A.B., Pallasser, R., Pozza, L., 2015. Potential integrated field spectroscopy and spatial analysis for enhanced assessment of soil contamination: a prospective review. Geoderma 241—242, 180—209.

Kalnicky, D.J., Singhvi, R., 2001. Field portable XRF analysis of environmental samples. J. Hazard. Mater. 93—122.

Kristensen, L., 2015. Quantification of atmospheric lead emissions from 70 years of leaded petrol consumption in Australia. Atmos. Environ. 111, 195—201.

Kristensen, L.J., Taylor, M.P., 2016. Unravelling a 'miner's myth' that environmental contamination in mining towns is naturally occurring. Environ. Geochem. Health 38 (4), 1015—1027.

Melquiades, F.L., Appoloni, C.R., 2004. Application of XRF and field portable XRF for environmental analysis. J. Radioanalytical Nucl. Chem. 262 (2), 533—541.

Morrison, A.L., Gulson, B.L., 2007. Preliminary findings of chemistry and bio-accessibility in base metal smelter slags. Sci. Total Environ. 382, 30—42.

National Measurement Institute (NMI), 2014. Method NT2.49: Determination of Acid Extractable Elements in Soils, Sediments, Sludges and Solid Waste. Inorganic Section. National Measurement Institute, Sydney.

National Environmental Protection Measure (NEPM), 2013. Schedule B1: Guideline on Investigation for Soil and Groundwater, p. 57. Available at: http://www.scew.gov.au/system/files/resources/93ae0e77-e697-e494-656f-afaaf9fb4277/files/schedule-b1-guideline-investigation-levels-soil-and-groundwater-sep10.pdf (accessed 29 January 2017).

New South Wales Environmental Protection Authority (NSW EPA), 1995. Sampling Design Guidelines. Contaminated Sites. http://www.epa.nsw.gov.au/resources/clm/95059sampgdlne.pdf (accessed 02 March 2017).

New South Wales Environmental Protection Authority (NSW EPA), 2015. Guidelines on the Duty to Report Contamination under the Contaminated Land Management Act 1997. http://www.epa.nsw.gov.au/resources/clm/150164-report-land-contamination-guidelines.pdf (accessed 04 March 2017).

Parsons, C., Grabulosa, E.M., Pili, E., Floor, G.H., Roman-Ross, G., Charlet, L., 2013. Quantification of trace arsenic in soils by field-portable X-ray fluorescence spectrometry: considerations for sample preparation and measurement conditions. J. Hazard. Mater. 262, 1213—1222.

Paulette, L., Man, T., Weindorf, D.C., Person, T., 2015. Rapid assessment of soil and contaminant variability via portable X-ray fluorescence spectroscopy: copsa Mica Romania. Geoderma 243—244, 130—140.

Peinado, F.M., Ruano, S.M., Gonzalez, M.G.B., Molina, C.E., 2010. A rapid field procedure for screening trace elements in polluted soil using portable X-ray fluorescence (PXRF). Geoderma 190, 76—82.

Radu, T., Gallagher, S., Byrne, B., Harris, P., Coveney, S., McCarron, S., McCarthy, T., Diamond, D., 2013. Portable x-ray fluorescence as a rapid technique for surveying elemental distributions in soil. Spectrosc. Lett. Int. J. Rapid Commun. 46 (7), 516—526.

Ramsey, M.H., Argyraki, A., 1997. Estimation of measurement uncertainty from field sampling: implications for the classification of contaminated land. Sci. Total Environ. 198, 243—257.

Ramsey, M.H., Boon, K.A., 2012. Can *in situ* geochemical measurements be more fit-for-purpose than those made *ex situ*? Appl. Geochem. 27, 969—976.

Eurachem, Eurolab, Citac, Nordtest, AMC Guide. In: Ramsey, M.H., Ellison, S.L.R. (Eds.), 2007. Measurement Uncertainty Arising from Sampling: a Guide to Methods and Approaches, ISBN 978 0 948926 26 6, pp. 1—103.

Ramsey, M.H., Thompson, M., Hale, M., 1992. Objective evaluation of precision requirements for geochemical analysis using robust analysis of variance. J. Geochem. Explor. 44, 23—36.

Ramsey, M.H., Taylor, P.D., Lee, J., 2002. Optimized contaminated land investigation at minimum overall cost to achieve fitness-for-purpose. J. Environ. Monit. 4, 809—814.

Ran, J., Wang, D., Wang, C., Zhang, G., Yao, L., 2014. Using portable X-ray fluorescence spectrometry and GIS to assess environmental risk and identify sources of trace metals in soils of peri-urban areas in the Yangtze Delta region, China. Environ. Sci. Process. Impacts 16, 1870—1877.

Rouillon, M., Taylor, M.P., 2016. Can field portable X-ray Fluorescence (pXRF) produce high quality data for application in environmental contamination research? Environ. Pollut. 214, 255—264.

Rouillon, M., Kristensen, L.J., Gore, D.B., 2015. Handheld x-ray fluorescence spectrometers: radiation exposure risks of matrix-specific measurement scenarios. Appl. Spectrosc. 69 (7), 815—822.

Rouillon, M., Harvey, P., Kristensen, L., George, S., Taylor, M.P., 2017. VegeSafe: a community science program measuring soil-metal contamination, evaluating risk and providing advice for safe gardening. Environ. Pollut. 222, 557—566.

Student, 1908. Probable error of a correlation coefficient. Biometrika 6 (2—3), 302—310.

Taylor, P.D., Ramsey, M.H., Potts, P.J., 2004. Balancing measurement uncertainty against financial benefits: comparison of in situ and ex situ analysis of contaminated land. Environ. Sci. Technol. 38, 6824—6831.

Taylor, P.D., Ramsey, M.H., Potts, P.J., 2005. Spatial contaminant heterogeneity: quantification with scale of measurement at contrasting sites. J. Environ. Monit. 7, 1364—1370.

Thermo Scientific, 2011. Thermo Scientific MicroPHAZIR AS, Handheld Asbestos Analyzer. Product Specification. https://www.thermofisher.com.au/Uploads/file/Environmental-Industrial/Environmental-Monitoring-Safety/Industrial-Hygiene-Instruments/MicroPhazir-Asbestos-Analyser-TFS.pdf (accessed 21 March 2017).

United States Environmental Protection Agency (US EPA), 2002. Calculating Upper Confidence Limits for Exposure Point Concentrations at Hazardous Waste Sites. United States Environmental Protection Agency, Washington, D.C, pp. 1—32.

Vacca, A., Bianco, M.R., Murolo, M., Violante, P., 2012. Heavy metals in contaminated soils of the Rio Sitzerri floodplain (Sardinia, Italy): characterisation and impact of pedodiversity. Land Degrad. Dev. 23, 350—364.

Vanhoof, C., Corthouts, V., Tirez, K., 2004. Energy-dispersive X-ray fluorescence systems as analytical tool for assessment of contaminated soils. J. Environ. Monit. 6, 344—350.

Weindorf, D.C., Zhu, Y., Chakraborty, S., Bakr, N., Huang, B., 2012. Use of portable X-ray fluorescence spectrometry for environmental quality assessment of peri-urban agriculture. Environ. Monit. Assess. 184, 217—227.

Weindorf, D.C., Paulette, L., Man, T., 2013. In-situ assessment of metal contamination via portable X-ray fluorescence spectroscopy: zlatna, Romania. Environ. Pollut. 182, 92—100.

Weindorf, D.C., Bakr, N., Zhu, Y., 2014. Chapter one: advances in portable x-ray fluorescence (pXRF) for environmental, pedological, and agronomic applications. Adv. Agron. 128, 1—45.

4.3   Limitations of Experimental Design

This study was designed and completed using a limited financial budget, of which the majority of funds were assigned to commercial ICP–MS analyses of field samples and duplicates for comparison with *in-situ* pXRF. This subsequently limited numerous variables within this study that made themselves apparent during the writing of this manuscript. For instance, the original strategy was to evaluate five elements (Mn, Cu, Zn, As, and Pb), however due to the cost of selecting elements for ICP–MS reporting, only three elements (Mn, Zn, and Pb) were possible.

Secondly, the number of duplicate targets at each site was limited to 10–15 % (n > 3) of the total number of samples taken to estimate the site mean. A minimum of three targets were selected as 10–15 % of the minimum sampling resolution for the current regulatory approach for Site 1 (n = 6) was $0.15 \times 6 = 0.9$ targets. Even at Site 3 (1.0 ha), the number of targets used to estimate measurement uncertainty was $0.15 \times 21 \sim 3$ targets. Ideally, the estimation of measurement uncertainty for each approach should have been performed using at least eight sample targets for each measurement approach, as per Boon and Ramsey (2010; 2012). This ultimately would have provided superior estimates of measurement uncertainty at each site, and most likely lowered the disparities of sampling uncertainty between the two measurement approaches.

Thirdly, the number of ICP–MS measurements used to correct *in-situ* pXRF data at each site were limited. Establishing a correction curve at each site using a limited number of data points was sub-optimal because fewer points meant that individual data points have a stronger influence on the regression curve. A minimum of five data points were used for *in-situ* pXRF correction at Sites 1, 2 and 3, with up to eight data points used at Sites 4 and 5. Also, samples used for data correction were randomly pre-determined prior to visiting the site. *In-situ* pXRF correction would have benefitted from: (a) increasing the number of data points used and (b) selecting sample points to cover the wide concentration range for each element observed at the site.

Fourthly, the benefits of a greater sampling density is not unique to pXRF, instead pXRF was selected over ICP-MS to demonstrate these advantages due to its low measurement cost, allowing for greater sampling densities to be achieved. Further, it may have been useful to compare the costs of each measurement method when sampling densities were identical, however, the aim of **Paper Three** was to demonstrate the potential for increased sampling densities (and its subsequent advantages) when utilising an inexpensive, field measurement method.

There were also some limitations not associated with site costs. The selection of the five contaminated sites were based on site access at the time and were largely Pb-contaminated. A wider range of metal-contaminated sites could have ultimately been more useful in demonstrating *in-situ* pXRF application more broadly. Additionally, in this study, sample locations were pre-determined using both aerial imagery and reference markers (trees, fences, etc.). Field portable XRF instruments can come equipped with built-in global positioning system (GPS) within the instrument, allowing the collection of both the chemistry and geo-location of each *in-situ* measurement (e.g. Niton XL3t Series – Thermo Fisher Scientific 2012). This can guide field users to specific co-ordinates for grid measurements, once the area of the site has been established.

It is also now possible to wirelessly send collected pXRF data to a laptop running a geographic information system program in real-time to further expedite the decision making process (Olympus 2017). This would ultimately assist field users in interpreting contaminant distribution at a site and guide further judgemental sampling, saving both time and money. As pXRF technology continues to improve in areas of hardware, software and additional accessories, the attractiveness of *in-situ* pXRF for metal-contaminated site assessments will undoubtedly draw more interest from environmental industries, provided studies (such as this one) practically demonstrate the advantages in a communicable manner.

4.4 References

Argyraki, A., Ramsey, M.H., Potts, P.J. 1997. Evaluation of Portable X-ray Fluorescence Instrumentation for in situ Measurements of Lead on Contaminated Land. Analyst 122, 743-749.

Boon, K.A., Ramsey, M.H. 2010. Uncertainty of measurement or of mean value for the reliable classification of contaminated land. Science of the Total Environment 409, 423-429.

Boon, K.A., Ramsey, M.H. 2012. Judging the fitness of on-site measurements by their uncertainty, including contribution from sampling. Science of the Total Environment 419, 196-207.

Carr, R., Zhang, C., Moles, N., Harder, M. 2008. Identification and mapping of heavy metal pollution in soils of a sports ground in Galway City, Ireland, using a portable XRF analyser and GIS. Environmental Geochemistry and Health 30, 45-52.

Higueras, P., Oyarzun, R., Iraizoz, J.M., Lorenzo, S., Esbri, J.M., Martinez-Coronado, A. 2012. Low-cost geochemical surveys for environmental studies in developing countries: Testing a field portable XRF instrument under quasi-realistic conditions, Journal of Geochemical Exploration 113, 3-12.

Olympus. 2017. XRF and XRD Anlayzers, Vanta. <http://www.olympus-ims.com/en/vanta/#!cms[tab]=%2Fvanta%2Foverview> (accessed 23 March 2017).

Paulette, L., Man, T., Weindorf, D.C., Person, T. 2015. Rapid assessment of soil and contaminant variability via portable X-ray fluorescence spectroscopy: Copsa Mica Romania. Geoderma 243-244, 130-140.

Peinado, F.M., Ruano, S.M., Gonzalez, M.G.B., Molina, C.E. 2010. A rapid field procedure for screening trace elements in polluted soil using portable X-ray fluorescence (PXRF). Geoderma 190, 76-82.

Thermo Fisher Scientific. 2012. Thermo Fisher Scientific Embeds GPS Functionality in all Niton XL3t Series XRF Analyzers. <http://news.thermofisher.com/press-release/thermo-scientific/thermo-fisher-scientific-embeds-gps-functionality-all-niton-xl3t-ser> (accessed 09 June 2017).

Vanhoof, C., Corthouts, V., Tirez, K. 2004. Energy-dispersive X-ray fluorescence systems as analytical tool for assessment of contaminated soils. Journal of Environmental Monitoring 6, 344-350.

Weindorf, D.C., Zhu, Y., Chakraborty, S., Bakr, N., Huang, B. 2012. Use of portable X-ray fluorescence spectrometry for environmental quality assessment of peri-urban agriculture. Environmental Monitoring and Assessment 184, 217-227.

Chapter Five: pXRF application case studies

5.1   Prologue

There are a range of pXRF applications currently employed within the environmental sector, including measurement of major (Weindorf et al. 2014) and trace elements in soils (Parsons et al. 2013), CCA treated wood in playgrounds (Block et al. 2007) and air filters used in the workplace (Morley et al. 1999). These applications utilise the advantages of pXRF, provided the data are fit-for-purpose for the objectives they intend to answer. For example, the study by Morley et al. (1999) evaluated the performance of pXRF in the measurement of Pb in workplace air filters by comparing it to a more expensive and time-consuming analytical technique (Graphite Furnace AA). They found that pXRF can be used for the rapid, on-site determination of Pb exposure, which could be communicated directly to workers. The method was inaccurate by 16.4 % when compared to the reference technique, however the data generated by pXRF was sufficient in identifying Pb exposure hazards in a timely manner, and subsequently was fit-for-purpose.

Not every pXRF application requires impeccable precision and accuracy constraints if the application objectives are intended to 'guide' decisions rather than report absolute metal concentrations (e.g. LEWG 2016, pp. 24–25). The ability of pXRF to provide immediate estimates of metal contaminants is powerful for any environmental application, especially when coupled with effectively cost-free measurements. Field portable XRF could ultimately be implemented to benefit non-scientists, or non-pXRF users in screening for metal contaminants that would otherwise remain unknown due to analytical costs from commercial laboratories, and the lack of data interpretation. This in turn assists in bridging the knowledge gap between scientists and the community by making science interactive, accessible and affordable.

Lubchenco (1998) proposed a new social contract for science, in order to assist the dissemination of knowledge from science to the wider audience in a fast-paced and dynamic world. Contemporary scientists should seek to: (a) address the most urgent needs of society, in proportion to their importance; (b) communicate their knowledge and understanding widely in order to inform decisions of individuals and institutions; and (c) exercise good judgment, wisdom, and humility. Hence, in an effort to inform and educate the community with regards to metal contaminants that may be present at residential properties, environmental science staff and PhD researchers at Macquarie University launched a citizen-science program called VegeSafe (VegeSafe 2017).

5.2　The VegeSafe program

The recent rise of urban agriculture in Sydney, and Australia more broadly, has seen many inner city families begin to grow food in their backyards (Wise 2014), yet most gardeners are largely unaware of the metal contamination hazards that may exist in urban soils. The VegeSafe program was established to inform the Australian public about potential metal contaminants in their garden soils. The community focused program offers free soil metal screening for residential and community garden soils to assist gardeners to better understand the hazards of metal contamination in an urban environment. The VegeSafe program started at the Macquarie University Open Day event in September 2013. One week prior to launch, VegeSafe issued a media release (Macquarie University Newsroom 2013) in the hope of broadcasting the event more widely. Interviews on both Sydney radio (ABC 702) and print and online media (Sydney Morning Herald 2013) assisted in informing gardeners on how and where to participate. The overwhelming response received on Open Day saw more than 160 soil samples screened by pXRF, with further samples being submitted in the following weeks. The success of the Open Day event indicated that there was a clear demand for publicly accessible soil metal screening. This presented itself as an excellent opportunity to engage and inform the community on matters of environmental health, while simultaneously accessing a large number of soil samples from understudied private spaces.

Over the following months, VegeSafe visited and screened soils from primary schools, community gardens and domestic gardens across Sydney, with more enquiries for soil metal screening arriving each day. To meet the growing local demand, VegeSafe invited participants to mail their samples directly to the University, and eventually were receiving samples from interstate. A University-based website (see: research.science.mq.edu.au/vegesafe) and a social media webpage were established (see: www.facebook.com/MQVegeSafe) to assist community participation in the program. These webpages provide both detailed soil sampling instructions (Appendix E, Figure E1) and participant metadata and consent forms (Appendix E, Figure E2) that participants need to complete. Sampling instructions guide participants through the sampling protocol, with information on where to sample soils, as well as matching the labelled bagged samples to their metadata/consent form. Consent was requested from participants to allow the submitted samples to be used for research purposes. Metadata information was requested to develop a better understanding of variables that might be influencing soil metal contamination. These include the address of the residential property, approximate age of the property, primary construction material of the property, if the residence external walls are painted, and the localities of individual soil samples with respect to the participants property.

Soil samples (with their attached forms) are sent to Macquarie University to be screened for eight metal(loid)s including As, Cd, Cr, Cu, Mn, Ni, Pb and Zn using pXRF. Screening consists of 60 second pXRF measurement directly on the soil sample, without any sample preparation or treatment. Metal estimates are then inputted into an online database with participant metadata, and a formal report is generated. The report (Appendix E, Figure E8) includes soil metal concentrations, a table of relevant and international soil metal guidelines and links to advice about 'what to do next' if their soils contain elevated concentrations of metals. These reports are then emailed back to the participant, so that they can make informed decisions on how to best manage contaminated soil, completing the VegeSafe process cycle (Figure 5.1).
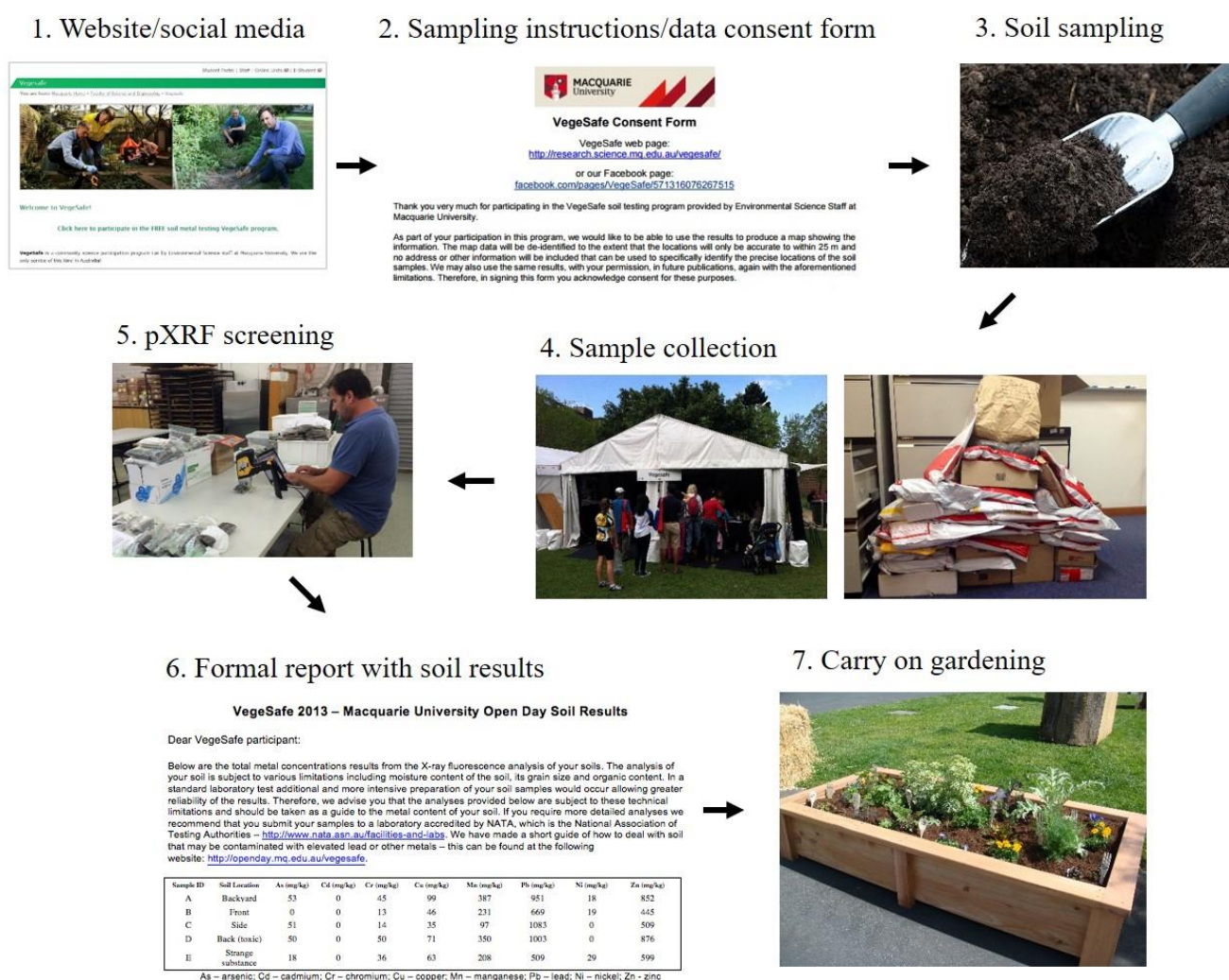
Figure 5.1: Participation in the VegeSafe program. Full sampling instructions, data consent form and report can be found in Appendix E.

In order to provide soil metal screening to the community in a timely fashion, samples were rapidly screened with the knowledge that the data generated are a 'guide' to the metal concentrations of a sample. A number of analytical limitations are acknowledged in the formal report provided to each participant (Appendix E, Figure E8) which states:

"The analysis of your soil is subject to various limitations including moisture content of the soil, its grain size and organic content. In a standard laboratory test additional and more intensive preparation of your soil samples would occur allowing greater reliability of the results. Therefore, we advise you that the analyses provided below are subject to these technical limitations and should be taken as a guide to the metal content of your soil."

The report also provides links to NATA-accredited laboratories which can provide more detailed analyses at a cost, should the participant desire further testing. We found that for most participants, the screening quality data generated by pXRF was sufficient to guide the management of potentially contaminated soil. However, there were also limitations associated with participant sampling. Despite providing clear sampling instructions, some participants submitted a minute quantity of soil (~1–5 g), while some physically delivered five potato sacks (~15 kg each) of soil for analysis. There were also cases of participants submitting leaves, plant roots, sand, water, and compost materials for analysis. Nevertheless, the majority (>95 %) of participants did follow the soil sampling instructions which enabled a fairly consistent collection of soil samples from homes.

Since its launch, VegeSafe has provided free soil metal tests to over 1,500 Australian homes and community gardens, resulting in over 6,500 individual soil metal tests. It is the largest program of its kind in Australia. The collection of thousands of soil samples from across Australia enabled unprecedented and efficient access to an understudied private residential soil environment. Inviting the community to sample on behalf of the researchers also empowers gardeners, as they are now directly involved in the soil metal screening method.

Preliminary pXRF screening data of Sydney revealed markedly high Pb concentrations in home garden soils. Soil Pb concentrations were typically greatest towards the older suburbs located in the Inner West, and inner city areas, and generally decreased with distance from the city area (Figure 5.2). Yet, despite collection of hundreds of samples from the greater Sydney area, the quality of the screening data remained a concern, particularly if the overall results be publicly reported. Hence, in order to confidently and accurately report the findings of the programs data, a higher data quality level was sought. A selection of VegeSafe collected samples were chosen for sample preparation and analysis by pXRF. The measurement of these samples were validated using both CRMs and wet chemistry analyses, and are reported in **Paper Four**.

This chapter showcases two pXRF application case studies that enhance our understanding of soil metal concentrations and distribution across two Australian cities. **Paper Four** investigates

metal contamination of Sydney residential garden soils, including soils from front yards, drip lines (adjacent to house walls), back yards and food-growing vegetable gardens. This study utilised VegeSafe metadata to estimate the relative source contributions from Pb-based paint and leaded petrol, and identifies households most at risk from Pb hazards. Lastly, several recommendations are proposed to mitigate Pb hazards in the community, such as policy improvements around the improper removal of Pb-based paint. This paper contributes to this thesis by utilising pXRF to accurately and inexpensively measure metal contaminated soils in urban areas.
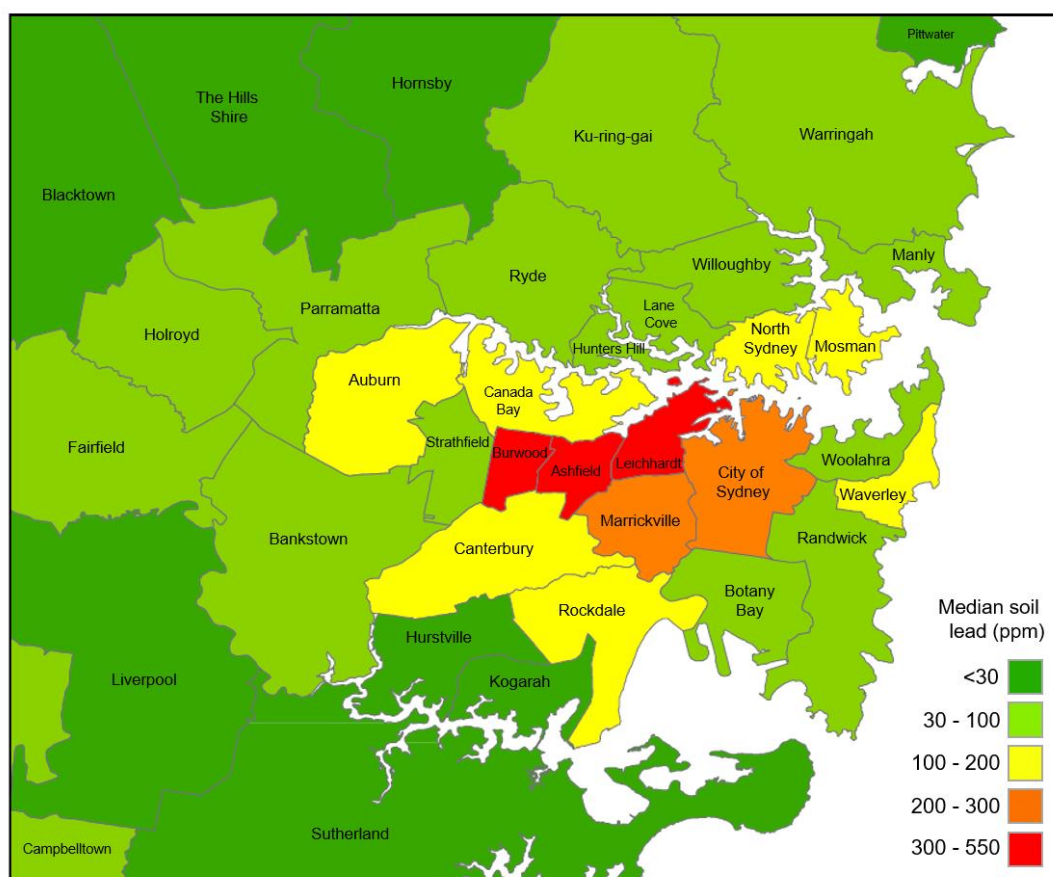
Figure 5.2: Median soil Pb concentrations per local government area of Sydney, using pXRF screening quality data (Source: Rory Williams, Department of Environmental Sciences, Macquarie University).

In addition to **Paper Four**, a science communication article of the study findings was published on the online platform of *The Conversation* (**Article One**). This article summarised the research in **Paper Four** using lay terminology and enabled intelligent public discussion on the prevalence and importance of environmental health. The VegeSafe program always intended to provide more information to the community so that they could make informed decisions towards safe urban gardening. Published science articles are rarely accessible to the public due to the high costs of journal subscriptions and/or individual article costs (AU$35.95 for **Paper**

Four), hence *The Conversation* science article removes this financial and knowledge barrier between researchers and the community.

Paper Five examines both inorganic and organic contaminants in public (e.g. street verges and parks) and private space soils in Newcastle, a former industrial city north of Sydney. This paper uses a combination of multiple analytical techniques including pXRF, ICP–MS (bio-accessibility and Pb-isotope compositions), X-ray Diffraction, Scanning Election Microscopy and Gas Chromatography to holistically assess the potential hazards posed by soil contaminants. Additionally, this paper utilised pXRF to measure the metal content of vertical soil profiles to identify the extent of waste material historically distributed across the city.

5.3 Paper Four

Publication

VegeSafe: A community science program measuring soil-metal contamination, evaluating risk and providing advice for safe gardening

Abstract: The extent of metal contamination in Sydney residential garden soils was evaluated using data collected during a three-year Macquarie University community science program called VegeSafe. Despite knowledge of industrial and urban contamination amongst scientists, the general public remains under-informed about the potential risks of exposure from legacy contaminants in their home garden environment. The community was offered free soil metal screening, allowing access to soil samples for research purposes. Participants followed specific soil sampling instructions and posted samples to the University for analysis with a field portable X-ray Fluorescence (pXRF) spectrometer. Over the three-year study period, >5200 soil samples, primarily from vegetable gardens, were collected from >1200 Australian homes.

As anticipated, the primary soil metal of concern was lead; mean concentrations were 413 mg/kg (front yard), 707 mg/kg (drip line), 226 mg/kg (back yard) and 301 mg/kg (vegetable garden). The Australian soil lead guideline of 300 mg/kg for residential gardens was exceeded at 40 % of Sydney homes, while concentrations >1000 mg/kg were identified at 15 % of homes. The incidence of highest soil lead contamination was greatest in the inner city area with concentrations declining towards background values of 20–30 mg/kg at 30–40 km distance from the city. Community engagement with VegeSafe participants has resulted in useful outcomes: dissemination of knowledge related to contamination legacies and health risks; owners building raised beds containing uncontaminated soil and in numerous cases, owners replacing all of their contaminated soil.

Keywords: Lead, Soil contamination, Sydney, Urban gardens, X-ray fluorescence spectrometry

Invited paper

VegeSafe: A community science program measuring soil-metal contamination, evaluating risk and providing advice for safe gardening☆

Marek Rouillon [a, *], Paul J. Harvey [b], Louise J. Kristensen [a, c], Steven G. George [a], Mark P. Taylor [a, *]

[a] Department of Environmental Sciences, Faculty of Science and Engineering, Macquarie University, Sydney, NSW 2109, Australia
[b] Department of Earth and Planetary Sciences, Faculty of Science and Engineering, Macquarie University, Sydney, NSW 2109, Australia
[c] Department of Chemistry and Biochemistry, University of California, San Diego, La Jolla, CA 92093, USA

ABSTRACT

The extent of metal contamination in Sydney residential garden soils was evaluated using data collected during a three-year Macquarie University community science program called VegeSafe. Despite knowledge of industrial and urban contamination amongst scientists, the general public remains under-informed about the potential risks of exposure from legacy contaminants in their home garden environment. The community was offered free soil metal screening, allowing access to soil samples for research purposes. Participants followed specific soil sampling instructions and posted samples to the University for analysis with a field portable X-ray Fluorescence (pXRF) spectrometer. Over the three-year study period, >5200 soil samples, primarily from vegetable gardens, were collected from >1200 Australian homes.

As anticipated, the primary soil metal of concern was lead; mean concentrations were 413 mg/kg (front yard), 707 mg/kg (drip line), 226 mg/kg (back yard) and 301 mg/kg (vegetable garden). The Australian soil lead guideline of 300 mg/kg for residential gardens was exceeded at 40% of Sydney homes, while concentrations >1000 mg/kg were identified at 15% of homes. The incidence of highest soil lead contamination was greatest in the inner city area with concentrations declining towards background values of 20—30 mg/kg at 30—40 km distance from the city. Community engagement with VegeSafe participants has resulted in useful outcomes: dissemination of knowledge related to contamination legacies and health risks; owners building raised beds containing uncontaminated soil and in numerous cases, owners replacing all of their contaminated soil.

© 2016 Elsevier Ltd. All rights reserved.

1. Introduction

Urban agriculture in the form of city farms, community gardens and verge gardens, are rapidly growing in popularity in many cities across the world (Alaimo et al., 2008; Keisling and Manning, 2010; Bugdalski et al., 2013; Mitchell et al., 2014; City of Sydney, 2016; City of West Hollywood, 2016). While the motives for urban agriculture may be diverse, the social and mental health benefits of urban green spaces and community involvement are well established (Alaimo et al., 2008; Wise, 2014). In Australia, 89% of the population live in cities (World Bank, 2013), with almost half (48%) of all households in metropolitan areas growing some form of edible produce (Wise, 2014). A recent Australian survey by Wise (2014) found most food gardens are located in either front or back yards (74%), 13% of participants grow food on street verges, 12% on balconies or in container gardens and only 1% from community gardens. In Sydney, food gardens are often located in older, heavily urbanized suburbs and are harvested from both above ground, and in ground vegetable plots.

Urban soils are notorious sinks for lead (Pb) and other metal and metalloid (hereafter referred to as metal) contaminants as a result of industrial and historic traffic emissions, waste incineration and application of paint containing Pb (hereafter referred to as Pb paint)

(Birmili et al., 2006; Szolnoki et al., 2013; Laidlaw et al., 2014; Kristensen, 2015). In Sydney alone, approximately 34,000—41,000 tonnes of Pb were emitted from the tailpipes of motor vehicles in the metropolitan area during 70 years of leaded fuel use (Kristensen, 2015). Widespread application of Pb paint (1—50 wt% Pb) on houses built pre-1970 was common with the majority of houses built during this period being painted with Pb paint at some point (NSW EPA, 2016a).

Metal contamination in residential garden soils is well documented. Contaminated garden soils are a global problem: Canada (Hendershot and Turmel, 2007), Denmark (Warming et al., 2015), France (Douay et al., 2013), Hungary (Szolnoki et al., 2013), Italy (Ferri et al., 2015) and the United States (Finster et al., 2004; Clark et al., 2008; Cheng et al., 2011; Mitchell et al., 2014; Filippelli et al., 2015). Despite a range of industrial metals being present in garden soils (Birmili et al., 2006; Szolnoki et al., 2013), Pb is typically the metal of most concern due to its toxicity, persistence and abundance in the urban environment (Lanphear et al., 1998; Mielke et al., 1999). To address this pervasive issue, screening programs, such as the New York State Department of Health soil screening and outreach program (New York State Department of Health, 2016), have been set up to raise awareness of soil Pb contamination within communities.

Widespread environmental Pb contamination has been previously documented in Sydney and its suburbs (Laidlaw and Taylor, 2011). A study by Fett et al. (1992) measured garden soils at 18 inner Sydney residential properties (hereafter referred to as homes) and found soil Pb concentrations up to 5400 mg/kg, with a median of 1944 mg/kg. A further study by Olszowy et al. (1995) showed that soils with the greatest mean (379 mg/kg) and median Pb (225 mg/kg) concentrations were from older Sydney suburbs with higher traffic density. The lowest soil Pb concentrations were from newer Sydney suburbs with lower traffic density. In the inner-Sydney suburb of Glebe, Markus and McBratney (1996) analyzed 219 soil samples from home gardens, parks, and nature strips and found 50% of soil samples exceeded the Australian residential Pb guideline of 300 mg/kg. Recent studies of urban soils by Snowdon and Birch (2004) and Birch et al. (2011) identified median soil Pb of 203 mg/kg (n − 374) in the Sydney Iron Cove catchment and 150 mg/kg (n − 491) in Port Jackson (Sydney harbour) estuary catchment, respectively. In contrast, studies that specifically investigate vegetable garden soil contamination in Australian homes are scarce. Kachenko and Singh (2006) measured metals in food-growing soils and vegetables from 24 sites within the Sydney basin, and despitelow soil metal concentrations (Pb 2.8—198 mg/kg), 32% of vegetables exceeded the allowable Pb levels set by the Australian and New Zealand Food Authority, respectively.

Previous studies in Sydney have often focused in publicly accessible areas (e.g. street verges, open spaces and parks), mainly due to the difficulties of accessing a large number of private properties for a suitable sample size. Metals found in public open spaces may not be representative of contamination at homes where different sources and soil practices exist (Mielke et al., 1983; Schwarz et al., 2012). Deterioration of Pb paint from old buildings (Gulson et al., 1995; NSW EPA, 2016a) along with the domestic use of pesticides (Kessler, 2013; Szolnoki et al., 2013) are sources of copper (Cu), zinc (Zn), and arsenic (As) contamination in domestic gardens.

1.1. Public access to soil metal screening via the VegeSafe program

To assist urban gardeners in Sydney and Australia more broadly to understand their soil environment, we initiated a free soil metal screening program called VegeSafe in 2013 (VegeSafe, 2015) to delineate, evaluate, and advise about potential risks arising from metal contamination (ABC, 2014, 2015). This community focused program provides free soil metal screening to participants using field portable X-ray Fluorescence (pXRF). The program provides participants with a formal report on their soil metal results and advice about 'what to do next' in the event of soils containing elevated concentrations of metals (VegeSafe, 2015). Participants provide a signed consent form with their samples permitting the use of their de-identified data in research. Similar programs, such as the Safe Urban Gardening Initiative in Indianapolis, USA, have been successful in engaging urban gardeners to better understand metal contamination in an urban setting (Filippelli et al., 2015). As of September 2016, VegeSafe has provided >5200 free soil metal tests to >1200 homes and community gardens across Australia, representing unprecedented access to the otherwise largely inaccessible private soil environment of Australia. The program aims to encourage participants to grow their own food in the knowledge that their soils contain metals below what are considered to be acceptable thresholds for gardening. Hence, this study investigates soil metal concentrations at Sydney homes using data obtained through the VegeSafe program. Discussion of Pb sources in the urban environment is also presented.

2. Methods

2.1. Sample collection and preparation

Samples were collected by VegeSafe participants from up to four areas around their homes including; front yards, drip lines (adjacent to houses), back yards (non-food growing soil) and vegetable gardens (food growing soil). Participants followed a sampling protocol that involved sampling soil at 0—2 cm depth and placing into labelled zip-lock plastic bags (Supplementary Fig. 1). Participants completed consent forms (Supplementary Fig. 2) and also provided metadata including sample location, age of house and presence of exterior painted surfaces. Samples were received via mail parcels to the University or at one of various VegeSafe events across Sydney (VegeSafe, 2015). For this study, 410 soil samples were selected from 203 homes within a pre-defined area consisting of 22 local government areas (LGAs) of Sydney (Fig. 1). The study area was determined using soil metal results from previous studies in public areas (e.g. Olszowy et al., 1995; Birch et al., 2011) as well as from the VegeSafe program to focus on homes most likely impacted by metal contamination. Twenty six reference samples were collected from eight semi-rural properties outside of this study area to represent soil concentrations in what were estimated to be areas largely unaffected by metal contamination (Fig. 1).

Samples were air dried at 40 °C for 72 h, crushed using a mortar and pestle and sieved through a 2 mm stainless steel sieve to remove coarse debris before passing through a 500 μm sieve. Composite sample preparation was carried out when multiple samples of the same type (i.e. 3 vegetable garden samples) were collected from the same home. Equipment was cleaned between samples with ethanol and KimWipes. Samples were thoroughly mixed by turning the sample bags over for 180 s each prior to packing in XRF cups. Approximately 10 g of <500 μm soil sample were packed in 35 mm open ended PANalytical XRF cups using 3.6 μm Chemplex Mylar Thin-Film for analysis.

2.2. Field portable X-ray Fluorescence (pXRF) analysis

An Olympus Premium Innov-X XRF Analyser fitted with a 50 kV, 4 W Ta anode X-ray tube and a silicon drift detector was used for the measurement of Mn (manganese), Cu, Zn, As and Pb concentrations in soils. Operational procedures followed throughout this study included: daily measurements of an energy calibration check,

Local Government Area

1. Parramatta	12. Burwood
2. Ryde	13. Ashfield
3. Willoughby	14. Leichhardt
4. Manly	15. Sydney
5. Auburn	16. Woollahra
6. Canada Bay	17. Waverley
7. Hunters Hill	18. Canterbury
8. Lane Cove	19. Marrickville
9. North Sydney	20. Rockdale
10. Mosman	21. Botany Bay
11. Strathfield	22. Randwick
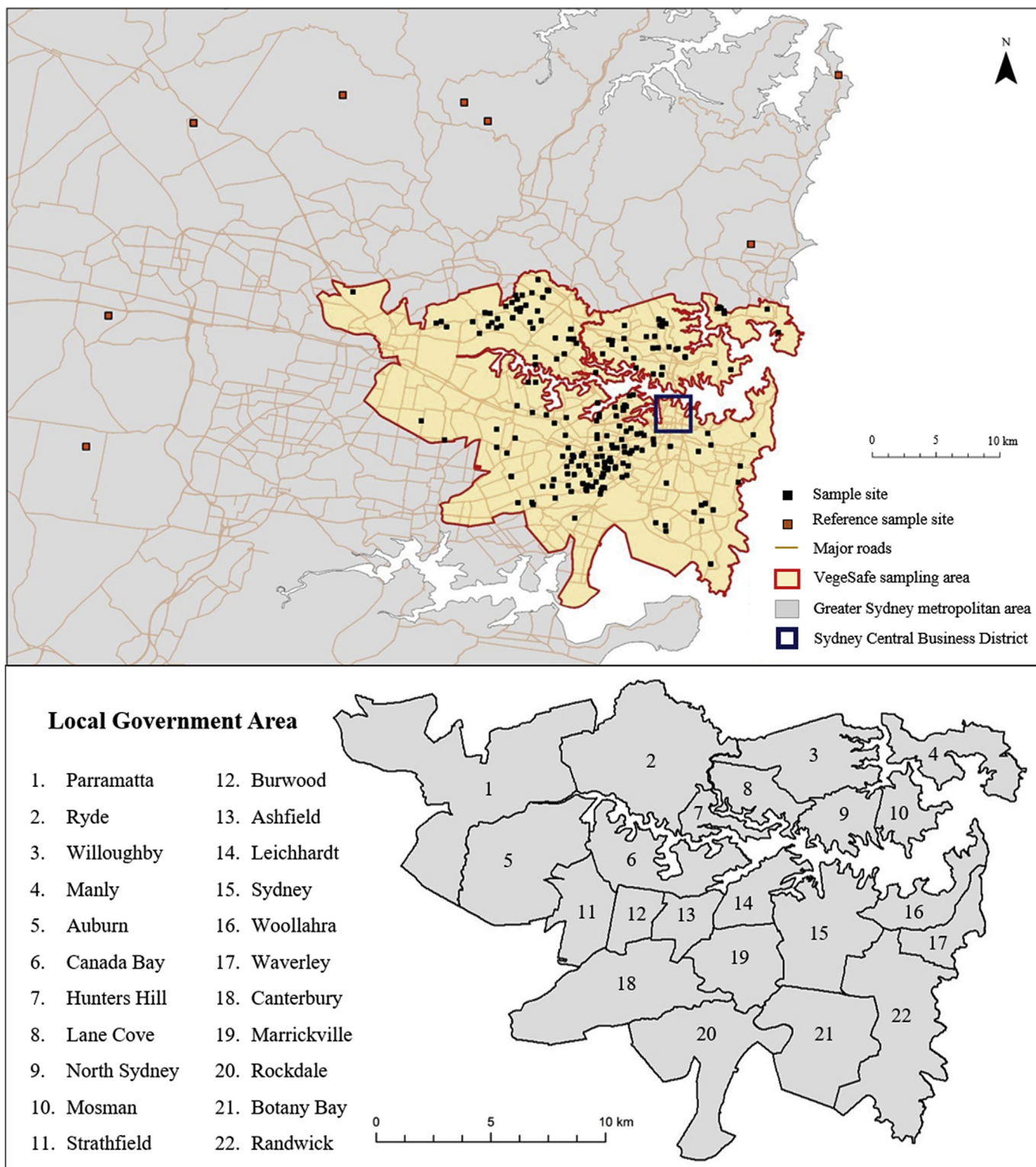
Fig. 1. Sample site locations of 203 homes within the sampling area of 22 Local Government Areas. Eight reference homes are also displayed towards the outer Sydney metropolitan area. Note: this image was generated prior to New South Wales council amalgamation in 2016 (Local Government New South Wales, 2016).

measurements of a silicate (SiO_2) blank at the beginning and end of daily sample analysis to ensure no instrument contamination had occurred, and measurement of National Institute of Standards and Technology certified reference materials (CRMs: NIST 2586, 2587, 2709a, 2710a, 2711a) every 20−25 samples to monitor instrument performance. Soil samples and CRMs were measured at 60 s per X-ray beam (180 s total measurement time) using the proprietary soil mode. A matrix matched calibration was applied to the pXRF using the method defined in Rouillon and Taylor (2016) to optimize analytical performance for metal-contaminated silicate-based soils.

Table 1
Summary of detection limits, precision and accuracy achieved by pXRF. CRM values and instrument detection limits are displayed as mg/kg. Relative standard deviation of ten CRMs[a] and ten <500 μm soil samples[b]. Recovery was calculated as (pXRF value/reference value × 100), relative proximity as (absolute (100 − recovery value)) and the relative standard deviation as (standard deviation/mean × 100).

	Mn	Cu	Zn	As	Pb
Minimum CRM value	229	19	103	9	17
Maximum CRM value	2140	3420	4180	1540	5520
Instrument detection limits	9	4	5	3	3
Analytical precision[a]	0.8%	2.4%	0.8%	7.3%	1.8%
Analytical precision[b]	1.0%	2.8%	0.7%	9.4%	0.8%
Sample homogeneity	5%	4%	4%	18%	4%
Recovery	102%	108%	99%	106%	99%
Relative proximity	3%	8%	5%	12%	3%

The pXRF instrument was operated in a shielded test stand to eliminate radiation exposure associated with extensive pXRF use (Rouillon et al., 2015).

2.3. Quality assurance and quality control

Ten CRMs of similar compositional matrix and trace element concentration were selected to assess the quality of pXRF measurements (cf. Rouillon and Taylor, 2016). The CRMs were mixed thoroughly in their bottles by shaking prior to packing in 35 mm open ended PANalytical XRF cups using 3.6 μm Chemplex Mylar Thin-Film. Instrument detection limits, analytical precision, sample homogeneity, mean recoveries and relative proximity (RP) of each element are provided in Table 1. Analytical precision was determined from the relative standard deviation (RSD) calculated from the five measurements that used for determining each measurement mean. Sample homogeneity was measured through triplicate preparation and analysis of ten soil samples. An additional validation step for the pXRF analytical data was obtained by processing 49 soil samples in a four acid sample decomposition ($HClO_4$, HNO_3, HF and HCl acid) and analysed using a Varian 725-ES inductively coupled plasma atomic emission spectrometer (ICP-AES) for their 'near total' metal concentrations (ALS, 2009). Three procedural laboratory blanks returned mean concentrations of <2 mg/kg for Cu, Zn and Pb and <5 mg/kg for Mn and As. Excellent agreement between pXRF data with CRM (r^2 0.999) and ICP-AES data (r^2 0.999) demonstrates pXRF was a robust alternative to ICP-AES for the measurement of metals in soils (Supplementary Fig. 3; Rouillon and Taylor, 2016).

3. Results and discussion

3.1. Soil metal concentrations

Soil metal data for Sydney soils are presented in Table 2. Soil concentrations were benchmarked against reference values determined from control sites at outer Sydney homes (Fig. 1) and the Australian health investigation level for residential soils (HIL-A) (NEPM, 2013). The mean Mn concentration within the sampling area (306 mg/kg) was not significantly different (p > 0.05) to the reference mean (360 mg/kg) despite the brief use of methylcyclopentadienyl manganese tricarbonyl (MMT) as an additive in Pb replacement petrol (2001−2004) during the phasing out of leaded petrol (Australian Government, 2005; Cohen et al., 2005). These findings are consistent with work by Bhuie and Roy (2001) who found no significant increase in soil Mn away from highways, despite 25 years of MMT use in Canada. Similarly, Gulson et al. (2014) found no significant relationships between traffic proximity and Mn concentrations in soil. The maximum Mn concentration of 1040 mg/kg was well below the Australian HIL-A guideline of 3000 mg/kg (Table 2) and subsequently was not investigated further.

Concentrations of Cu, Zn and As were significantly greater (p < 0.001) than reference values. This is not unexpected given the widespread use of Cu, Zn and As in a range of industrial products including pesticides (Szolnoki et al., 2013), paints (Gulson et al., 1995; NSW EPA, 2016a), and motor-vehicles (Wuana and Okiemen, 2011). The maximum concentration of Cu (717 mg/kg) and Zn (2880 mg/kg) did not approach the Australian HIL-A guideline of 7000 and 8000 mg/kg, respectively. By contrast, several homes had soil As concentrations near the Australian guideline value of 100 mg/kg. While no samples exceeded the HIL-A guideline for As, the data demonstrates that almost half (46%) would exceed the more conservative Canadian soil guideline of 12 mg/kg (CCME, 2013). Even though none of the metal concentrations other than Pb exceeded the Australian HIL-A guideline, this does not preclude potential adverse health effects from exposure to these contaminants at lower levels (Aelion et al., 2009).

The mean Pb concentration within the study area was 415 mg/kg, considerably greater than the reference mean of 33 mg/kg measured in outer Sydney soils, and the mean geogenic Pb concentration (<30 mg/kg) established in the literature (Olszowy et al., 1995; Kachenko and Singh, 2006; Wu et al., 2016). Maximum soil Pb concentrations were 2460 mg/kg (front yard), 6490 mg/kg (drip line), 1810 mg/kg (back yard), and 3080 mg/kg (vegetable garden) (Table 2). Forty percent of homes within the study area contain soil in excess of the Australian HIL-A guideline of 300 mg/kg for Pb in one or more garden areas; 21% exceeded this value in two or more garden areas. Soil Pb concentrations >1000 mg/kg were identified at 30 of 203 (15%) Sydney homes.

3.2. Spatial distribution of Pb (home scale)

Soil metal concentrations varied significantly across homes. Median soil Cu, Zn, As and Pb concentrations were greatest at drip line locations and typically decreased towards the other three garden locations sampled (Table 2). Median soil Pb concentrations were 174 mg/kg in front yards, 345 mg/kg in drip lines, 126 mg/kg in back yards and 135 mg/kg in vegetable gardens. This trend of increasing soil Pb concentrations towards building structures is consistent with previous studies. Mielke et al. (1983) found soil Pb concentrations greatest adjacent to buildings in inner city Baltimore, USA, attributing it to airborne leaded petrol emissions. Similarly, Schwarz et al. (2012) demonstrated a near exponential increase in soil Pb concentrations towards buildings in their study of 61 homes in Baltimore. These studies suggested two primary contributors to the high soil Pb concentrations found adjacent to buildings: 1) buildings provide a surface for airborne Pb particles to adhere to and ultimately deposit on to adjacent soil and 2) deteriorating Pb paint. The data from this study demonstrates a similar trend for soil Zn concentrations, and to a lesser extent Cu and As, suggesting these metals have been deposited in a similar manner around homes. Surprisingly, vegetable gardens had slightly higher Zn and Pb concentrations than back yard soils, despite typically being located furthest from houses in Australia. Industrial sources of Zn include traffic emissions, paint, and galvanized coated roofing, gutters and stormwater pipes. The presence of existing vertical structures (e.g. fences and trees) along the boundaries of homes can enhance the deposition of atmospherically sourced metals (Mielke et al., 1983; Schwarz et al., 2012). This may be more relevant for older homes where long-standing fences or trees have retained undisturbed soil for many years. Urban gardeners who grow vegetables in plots beneath the drip lines of their house, are likely to be

Table 2
Soil Mn, Cu, Zn, As and Pb concentrations (mg/kg) from front yard, drip line, back yard and vegetable garden areas. Values are displayed up to 3 significant figures.

	Mn	Cu	Zn	As	Pb		Mn	Cu	Zn	As	Pb
Front yard						**Drip line**					
Number detected	92	92	92	92	92	Number detected	97	97	97	91	97
Minimum	85	36	72	3	32	Minimum	83	32	50	2	15
10th percentile	154	43	113	6	47	10th percentile	155	46	154	6	58
25th percentile	209	51	174	7	69	25th percentile	183	56	242	9	163
Median (50%)	291	67	262	10	174	Median (50%)	266	77	472	15	345
75th percentile	403	90	439	24	542	75th percentile	340	120	739	26	752
90th percentile	482	121	793	31	1190	90th percentile	425	149	1080	41	1480
Maximum	1040	413	1240	76	2460	Maximum	743	233	2880	97	6490
Aus soil guideline[a]	3000	7000	8000	100	300	Aus soil guideline[a]	3000	7000	8000	100	300
% > guideline[a]	–	–	–	–	32%	% > guideline[a]	–	–	–	–	57%
Mean	317	80	349	16	413	Mean	282	90	574	21	707
Reference mean	301	46	142	6	31	Reference mean	397	54	178	10	35
Back yard						**Vegetable garden**					
Number detected	80	80	80	79	80	Number detected	141	141	141	140	141
Minimum	81	29	64	3	22	Minimum	91	33	50	3	14
10th percentile	151	42	110	5	36	10th percentile	174	48	129	5	34
25th percentile	203	49	152	6	48	25th percentile	224	59	196	7	60
Median (50%)	274	68	238	11	126	Median (50%)	304	73	284	10	135
75th percentile	369	98	418	17	339	75th percentile	383	96	469	18	334
90th percentile	452	129	777	24	705	90th percentile	480	132	736	32	745
Maximum	686	646	1790	55	1810	Maximum	813	717	2020	92	3080
Aus soil guideline[a]	3000	7000	8000	100	300	Aus soil guideline[a]	3000	7000	8000	100	300
% > guideline[a]	–	–	–	–	24%	% > guideline[a]	–	–	–	–	26%
Mean	299	89	367	14	266	Mean	319	88	387	15	301
Reference mean	297	41	101	7	29	Reference mean	412	55	163	7	36

[a] Australian health investigation level for soils under category residential A – garden/accessible soil (home grown produce <10% fruit and vegetable intake (no poultry), also includes childcare centres, preschools and primary schools) (NEPM, 2013).

doing so in contaminated soils; 57% of drip line samples exceeded the Australian HIL-A guideline for soil Pb of 300 mg/kg.

3.3. Spatial distribution of Pb (city scale)

Spatial distribution of soil Pb data are displayed in Fig. 2, while soil Mn, Cu, Zn and As data are provided in Supplementary Figures 4-7 respectively. The greatest soil Pb concentrations were located to the west and south-west of the Sydney central business district in an area known as the Inner West (Fig. 2). This area is dominated by old medium-high density housing and high traffic roads, which has been contaminated by the widespread historic use of leaded petrol and paints (Markus and McBratney, 1996; Laidlaw and Taylor, 2011). Low soil Pb (<99 mg/kg) concentrations were found predominately towards the outer parts of the study area, demonstrating a trend of decreasing soil Pb concentrations away from the older, inner areas of Sydney (Fig. 2). However, low soil Pb concentrations were also observed throughout inner Sydney, most likely a result of clean soil introduction, particularly for the planting of vegetable gardens.

The majority of high soil Pb concentrations were located within three LGAs: City of Sydney, Leichhardt Municipal Council and Marrickville Council (Figs. 1 and 2). Mean soil Pb concentrations in these council areas were 883 mg/kg, 960 mg/kg and 689 mg/kg respectively. A significant proportion (74%) of homes within these LGAs contain soil Pb in excess of the Australian guideline; one third of these homes recorded >1000 mg/kg Pb in one or more garden samples. There are >150,000 houses within the boundaries of the City of Sydney, Leichhardt and Marrickville LGAs (ABS, 2011), and although this study examines 161 samples from 74 homes in these areas, the consistency of the results reveals a concerning pattern of environmental Pb contamination. Homes within these LGAs are some of the first built during the central Sydney expansion

between 1788 and 1917 (Kelly, 1987). As a result they have a higher proportion of Pb paint surfaces, which are known to correlate strongly with high soil Pb concentrations (Mielke, 1999; Schwarz et al., 2012).

3.4. House age, and contribution of leaded petrol and paint to soil Pb

Leaded paint and petrol are the two most dominant sources of Pb in the residential environment of Sydney over the last century (Markus and McBratney, 1996; Laidlaw and Taylor, 2011), with minor contributions from former and present industries. In Australia, Pb paint contained up to 50 wt% Pb during its early use and was incrementally reduced to 1.0 wt% and 0.1 wt% Pb by 1970 and 1997, respectively (Australian Government, 2014). Following the reduction of Pb in paint, houses were painted with titanium- or zinc-based paints. The median age of homes within the study area is 80 years, while the median age of reference homes is 30 years. The increase of soil Pb concentrations due to the age of house and prevalence of Pb paint have been documented previously (e.g. Sutton et al., 1995; Jacobs et al., 2002; Schwarz et al., 2012). There is an absence of research, however, examining the relationship between age of house, soil Pb concentrations and the presence or absence of exterior painted surfaces, especially in Australia.

Painted homes have greater median soil Pb concentrations (366 mg/kg) than non-painted homes (130 mg/kg). Consequently, painted homes have a higher proportion of soil exceeding the HIL-A guideline of 300 mg/kg (60% for painted versus 19% for non-painted). Soil Pb concentrations increase with age of house for both painted and non-painted homes, but at different rates (Fig. 3). Soil Pb concentrations at non-painted homes gradually increase at an average rate of 22 mg/kg per decade until median concentrations plateau at 226 mg/kg for homes built pre-1914. In contrast,
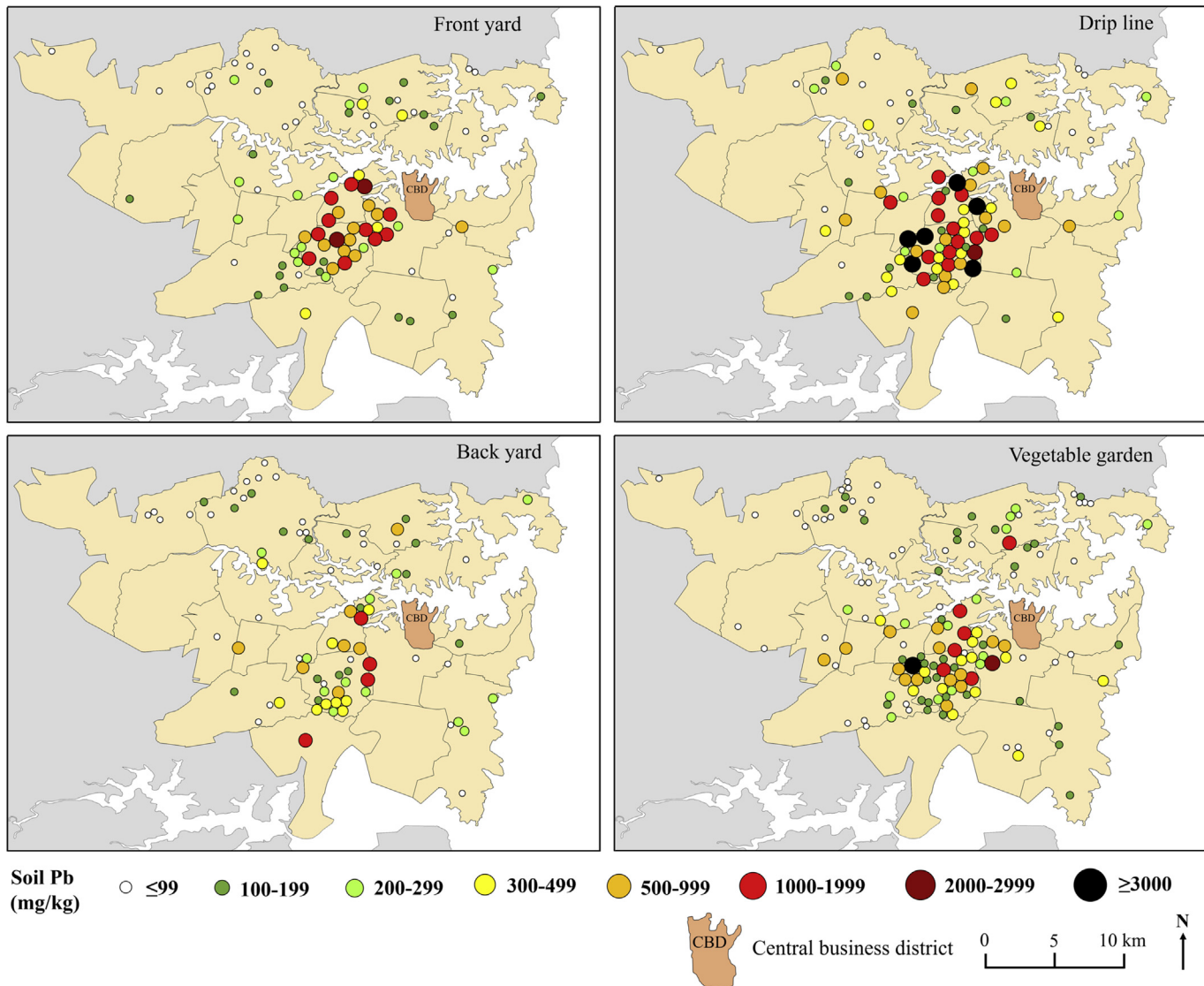
Fig. 2. Soil Pb concentrations of front yard (n = 92), drip line (n = 97), back yard (n = 80) and vegetable gardens (n = 141) areas in Sydney homes, Australia. Distributions of soil Mn, Cu, Zn and As data are provided in Supplementary Figures 4-7, respectively.

median soil Pb concentrations at painted homes increase by an average of 76 mg/kg per decade from 45 mg/kg for post-1975 homes to 806 mg/kg for homes built pre-1895 (Fig. 3). Soil from older painted homes are more likely to exceed the 300 mg/kg soil guideline than younger painted homes; 85% of painted homes built between 1895 and 1914 had one or more soil samples in excess of this guideline compared to 43% of painted homes built between 1955 and 1975. The withdrawal of Pb from paints can be seen in Fig. 3. Comparable median soil Pb concentrations at painted (45 mg/kg) and non-painted (50 mg/kg) homes built after 1970 suggests the additional Pb loading from Pb paints has been eradicated in modern homes.

Source apportionment in environmental investigations is typically estimated using elemental isotopic ratios (e.g. Gulson et al., 1995; Kristensen et al., 2015). However for this study, we estimate the contributions of three main Pb sources using metadata collected as part of the VegeSafe program. Source contributions to soil Pb are estimated using median soil Pb data from non-painted and painted homes applying the assumption that soil from non-painted homes is comprised of geogenic Pb (conservative

estimate of 30 mg/kg for the Sydney Basin, see Wu et al., 2016) and leaded petrol emissions. Soil from painted homes are assumed to have similar contributions with an additional input from Pb paint. The temporal shifts in Pb contribution from these three Pb sources for soils at painted homes over the last 120 years are estimated in Fig. 3. According to the data, the dominant source of soil Pb for older painted homes is Pb paint, most likely a function of its early use, combined with a longer time period for deterioration of painted surfaces and deposition into adjacent soil. However, improper removal of these paints by blasting, sanding and scraping can expedite generation of Pb rich dust particles that have been demonstrated to contaminate nearby homes (Gulson et al., 1995; Jacobs et al., 2003). This could explain why a few non-painted homes had abnormally high soil Pb concentrations; for example a 70 year old double brick (unpainted exterior) Marrickville home had soil Pb up to 3220 mg/kg. Marrickville is an suburb of Sydney where 'do it yourself' renovations of old homes are increasingly common, with approximately 320 development applications for alterations and additions each year (New South Wales Department of Environment and Planning, 2015).
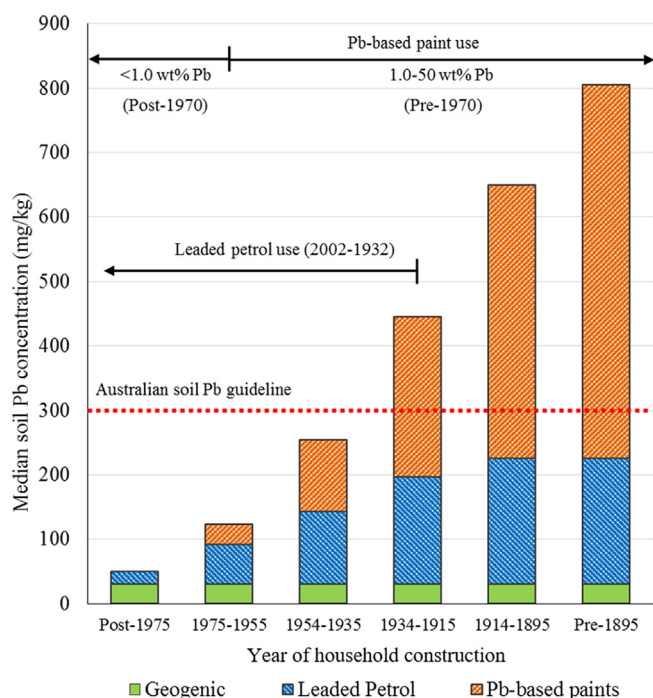
Fig. 3. Estimated Pb contributions from geogenic, leaded petrol emissions and Pb paint sources to median soil Pb concentrations of painted Sydney homes based on household construction era. The Australian health investigation level (HIL-A) for soil Pb is 300 mg/kg and is displayed as the red dashed line (NEPM, 2013). (For interpretation of the references to colour in this figure legend, the reader is referred to the web version of this article.)

The lowering of Pb concentration in both petrol emissions and Pb paint, and the eventual removal of both products is reflected by estimated decreased anthropogenic contributions to soil Pb at newer homes (Fig. 3). These findings are further supported by Wu et al. (2016), who showed that anthropogenic Pb isotopic signatures shifted to more geogenic signatures in lichens (used as environmental proxies) during the phasing out of leaded petrol in the Sydney basin.

There are estimated over 3.5 million homes in Australia built pre-1971 (Berry et al., 1994), the majority of which were likely coated with Pb paint at some stage. The impact of Pb paint is further demonstrated by the difference in median soil Pb concentrations between painted and non-painted homes across the four garden areas in Fig. 4. The distribution of soil Pb around homes (Fig. 4) is broadly consistent with cross sectional schematics presented in Olszowy et al. (1995) and Mielke (1999). However, this study demonstrates a marked shift of median soil Pb concentrations from non-painted to painted homes built pre-1970 (Fig. 4), supporting the estimated Pb loading from paints in Fig. 3.

3.5. Public health implications

Soil, including that used for edible produce, forms part of the exposure pathway for Pb absorption (Paustenbach et al., 1997; Hunt et al., 2006; Spliethoff et al., 2016). In Australia, exposure risks are assessed using the formal environmental health risk assessment system (Enhealth, 2012). In addressing the risk, strategies to eliminate hazardous exposures before they occur (i.e. primary prevention) could be supported with this and other relevant datasets (e.g. Birch et al., 2011; Laidlaw and Taylor, 2011; Gulson et al., 2014). Lanphear et al. (2005) and Lanphear (2015) identified two relevant salient facts about primary prevention: (1) the

effects of Pb toxicity has its greatest relative impacts at <10 μg/dL of blood Pb and (2) the majority of population IQ points are lost from Pb exposure below the current United States and Australian acceptable maximum blood Pb level of 5 μg/dL. The data show that soil from painted pre-1970 homes have higher Pb concentrations than non-painted pre-1970 homes, likely due to the additional loading from Pb paints (Figs. 3 and 4). Many pre-1970 Sydney homes still contain paint with up to 50 wt% Pb on exterior walls, fences, eves, doors and window frames. As a result, these homes still have the potential to further contaminate the surrounding environment through the deterioration or improper removal of these paints. Over time, deterioration or deliberate removal of Pb paint increases remobilization into soils and household dusts.

This risk is evidenced by Australian blood Pb notification data which identify the primary causes of non-occupational Pb exposures are associated with Pb paints. For instance, in 2003, 78% of Queensland notifiable blood Pb cases (>15 μg/dL) were attributed to Pb paint. Childrens (0–4 years of age) blood Pb concentrations ranged 15–49 μg/dL (median 26 μg/dL) (Queensland Health, 2003). Indeed, more than half (55%) of all non-occupational Pb exposures in Queensland between 2000 and 2011 were related or directly attributed to Pb paints (Queensland Health, 2011). The equivalent Pb exposure data for New South Wales (NSW) was obtained from NSW Health. The dataset could not be used because it contained incomplete entries on blood Pb exposures cases. Blood Pb assessment of Sydney residents primarily occurs as a result of individuals requesting a blood Pb test (unlike Australian mining and smelting communities where there is ongoing testing of children under 5 years of age – e.g. Taylor et al., 2011, 2014). As a result, any such data from cities is likely to represent only a fraction of actual Pb exposure cases in Australia (Taylor et al., 2012).

To demonstrate the importance of lead-safe paint removal, Jacobs et al. (2003) presented a case study from New Orleans, USA, where the improper, uncontained sanding of Pb paint from the exterior walls of a house led to the death of a Labrador retriever (blood Pb 177 μg/dL), lead poisoning of three children who were immediately hospitalized and over US$195,000 in Pb contamination cleanup costs. The professional painting contractors did not determine the Pb content of the painted walls prior to sanding and did not use lead-safe practices during the 6 week renovation (Jacobs et al., 2003). As a result of such cases, the United States Environmental Protection Agency (US EPA) introduced the 'Renovation, Repair and Painting' rule where contractors involved in the renovation, repair or painting projects, that disturb Pb paint from homes built pre-1978, must be certified and follow explicit work
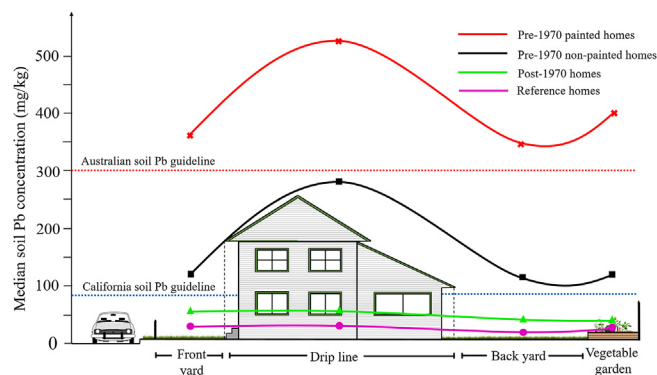
Fig. 4. Cross section schematic of a typical inner Sydney residential home with median soil Pb concentrations for painted pre-1970 homes, non-painted pre-1970 homes, post-1970 homes and reference homes. The vegetable garden is displayed at the rear of the back yard, as this was the case for the majority of homes.

practices to prevent further Pb contamination and exposure (HUD, 2016a). The rule also states that all contractors must provide Pb hazard information pamphlets (see US EPA, 2013) to all pre-1978 homes where children (0–6 years) live. In addition, the United States introduced the 'Lead Disclosure' rule in 1996 where the seller or lessor of a house built pre-1978 must disclose any known information regarding Pb paint or Pb hazards before the sale or lease of the property (HUD, 2016b). Non-compliance of either rule can result in fines issued by the US EPA (e.g. Harrington, 2012). These legislative instruments were implemented to prevent further Pb contamination and exposures associated with high-risk housing coated with Pb paint. Unfortunately in Australia, there are no legislations in place remotely similar to the 'Lead Disclosure' or 'Renovation, Repair and Painting' rules implemented in the United States. This is despite knowledge of the widespread use of up to 50 wt% Pb in paints until 1970 and the high proportion of Pb paint-related blood Pb cases in children (Queensland Health, 2011).

This study identified 40% of Sydney homes and >70% of inner city homes contain soil in excess of the Australian HIL-A guideline for Pb. However, amendments to relevant policies are unlikely to occur without further evidence of existing sources (e.g. Pb paint) directly causing numerous elevated blood Pb cases in urban communities. The true number of elevated blood Pb cases in Sydney and other major cities are likely to be much greater than the available data indicates. Applying Pb exposure rates (>5 μg/dL) in children in the United States, Taylor et al. (2012) estimated approximately 100,000 Australian children aged 0–4 years may have blood Pb concentrations in excess of the current national intervention guideline of 5 μg/dL. Such an estimation is certainly plausible given the high soil Pb concentrations found at Sydney homes. A systematic blood Pb survey of children living in high-risk areas, such as inner city suburbs with high soil Pb concentrations, would be a more accurate representation of current Pb exposures. The only national Australian blood Pb survey was in 1995 (Donovan, 1996). Available resources should be focused on informing the community on Pb paint hazards, as was recommended by Gulson et al. (2014).

3.6. How can residents become further informed about possible lead contamination at home?

As part of the VegeSafe program, each participant receives a formal report with their soil metal results, a table of relevant Australian soil metal guidelines to benchmark results and further information on the best ways to mitigate soil metal contamination (Supplementary Fig. 8). Typical advice varies between participants depending on the severity of soil Pb contamination in their yards, however some common guidance is given in most cases. For example, if Pb concentrations exceed the 300 mg/kg guideline in non-food growing soil, such as the front yard or drip line locations, VegeSafe recommends maintaining year-round coverage of lawn or mulch to minimize potential dust generation. However, if the 300 mg/kg guideline is exceeded in food growing soil, such as a vegetable garden, we recommend replacing the existing soil with new, uncontaminated soil or simply relocating the food growing to an above ground vegetable plot.

The information and advice VegeSafe provides to the community supports the NSW EPA fact sheets on Pb safety (NSW EPA, 2016b), which have been distributed to major hardware stores, childcare centers, and home and renovation shows across NSW. However, further outreach is required to distribute such information directly to residents living in areas with high soil Pb contamination. In this regard, it is recommended that local councils should become more involved in circulating such information. VegeSafe participants also have recommended the program to neighbours, family and friends, particularly those living in high-risk areas such

as the inner city. Such endorsements promote discussion of environmental health throughout communities, resulting in the public becoming better informed about how to mitigate sources of metal contamination in gardens. This assists the public in utilizing their urban space more safely, hence VegeSafe's motto '*carry on gardening*'.

3.7. Limitations

While we are confident our sampling instructions were detailed and repeatable, we acknowledge our sample collection method could not guarantee consistent sampling between participants. The VegeSafe program collected soil from participating homes across Sydney and subsequently did not produce a systematic coverage of the entire city. Additionally, VegeSafe participants were not required to submit soil samples from every garden area, rather we suggested that participants sample from the following four locations: front yards, drip lines, back yards and vegetable gardens. We acknowledge that obtaining samples from every garden area per home would have improved the consistency of the sample collection method.

Typically, Pb source apportionment is carried out using Pb isotopic composition ratios (e.g. Chiaradia et al., 1997). However, we estimated source contributions to soil Pb loading using metadata provided by each VegeSafe participant. We acknowledge there are limitations of this approach, such as the generalization of painted houses to contain Pb paint if constructed prior to 1970. However, the overall results from this study correspond to the timing of the withdrawal of Pb from paint and petrol providing support for, and confidence in our conclusions.

4. Conclusions and recommendations

This study found soil Pb concentrations in excess of the Australian health guideline of 300 mg/kg at 40% of Sydney homes. Fifteen percent of sampled homes contain soil Pb >1000 mg/kg. Soil metal concentrations were typically greatest at drip line locations around homes in the inner city, with concentrations decreasing with distance away from the city center. Median soil Pb concentrations at painted homes were significantly greater than non-painted homes of a similar age (Fig. 3), demonstrating a significant contribution to soil Pb loading from Pb paint. The removal of leaded petrol and the reduction in Pb concentration in exterior paints (to <0.1 wt%) are also reflected within our dataset, demonstrating the efficacy of eliminating such products from use. Unfortunately, Pb paint is still present on countless homes in Australia and has the potential to further contaminate the home environment through deterioration and its improper removal.

The VegeSafe program has provided >5200 free soil metal tests to Australian residents and subsequently has re-focused the community's attitude towards environmental contamination, largely because their properties have been directly impacted. Our data demonstrates Pb paint is a major source of Pb contamination around Sydney homes, particularly in the inner city. Young families are increasingly moving into older homes that often require renovation, and frequently are not informed on Pb paint hazards. We recommend further effort is required by local councils and regulatory bodies to adequately inform families living in Pb prone areas of the dangers of soil contamination and Pb paint hazards in the home environment. Additionally, this study demonstrated the effectiveness of crowd sourced sample collection of private residential soils through a community science program and should be replicated in other major cities around the world. Adaptation of this citizen science approach could also be applied to other environmental investigations of traditional and emerging contaminants.

Acknowledgements

Appendix A. Supplementary data

Supplementary data related to this article can be found at http://dx.doi.org/10.1016/j.envpol.2016.11.024.

References

Aelion, C.M., Davis, H.T., McDermott, S., Lawson, A.B., 2009. Soil metal concentrations and toxicity: associations with distances to industrial facilities and implications for human health. Sci. Total Environ. 407, 2216–2223.

Alaimo, K., Packnett, E., Miles, R.A., Kruger, D.J., 2008. Fruit and vegetable intake among urban community gardeners. J. Nutr. Educ. Behav. 40, 94–101.

Australian Broadcasting Corporation (ABC), 2014. Growing Veggies Safely in Your Backyard: Avoiding the 'legacy of Our Industrial Activities'. ABC News. Available at: http://www.abc.net.au/news/2014-08-29/growing-safe-veggies-in-your-sydney-backyard/5705016, 6 June 2016.

Australian Broadcasting Corporation (ABC), 2015. Fact Sheet: Safe Soil. Gardening Australia. Available at: http://www.abc.net.au/gardening/stories/s4197011.htm, 6 June 2016.

Australian Bureau of Statistics (ABS), 2011. Quickstats. Data & Analysis. Available at: http://www.abs.gov.au/, 11 April 2016.

Australian Government, Department of the Environment, 2014. Lead in House Paint. Available at: http://www.environment.gov.au/protection/chemicals-management/lead/lead-in-house-paint, 29 January 2016.

Australian Government, Department of Industry, Tourism, Resources, 2005. Canberra ACT. Petrol – Frequently Asked Questions. Available at: http://www.industry.gov.au/content, 29 January 2016.

Australian Laboratory Systems (ALS), 2009. Geochemical Procedure ME-ICP61 - Trace level methods using conventional ICP-AES analysis, pp. 1–2. Available at: www.alsglobal.com, 29 January 2016.

Berry, M., Garrad, J., Greene, D., Crooks, M.L., 1994. Reducing Lead Exposure in Australia. Commonwealth Department of Human Services and Health, Canberra.

Bhuie, A.K., Roy, D.N., 2001. Deposition of Mn from Automotive Combustion of Methylcyclopentadienyl Manganese Tricarbonyl beside the Major Highways in the Greater Toronto Area, Canada. Air & Waste Manag. Assoc. 51, 1288–1301.

Birch, G.F., Vanderhayden, M., Olmos, M., 2011. The nature and distributions of metals in soils of the Sydney estuary catchment, Australia. Water Air & Soil Pollut. 216, 581–604.

Birmili, W., Allen, A.G., Bary, F., Harrison, R.M., 2006. Trace metal concentrations and water solubility in size-fractionated atmospheric particles and influences of road traffic. Environ. Sci. Technol. 40 (1), 1144–1153.

Bugdalski, L., Lemke, L.D., McElmurry, S.P., 2013. Spatial variation of soil lead in an urban community garden: implications for risk-based sampling. Risk Anal. 34, 17–27.

Canadian Council of Ministers of the Environment (CCME), 2013. Canadian Environmental Quality Guidelines. Chemicals. Available at: http://www.ccme.ca/en/resources/canadian_environmental_quality_guidelines/, 29 January 2016.

Cheng, Z., Lee, L., Dayan, S., Grinshtein, M., Shaw, R., 2011. Speciation of heavy metals in garden soils: evidences from selective and sequential chemical leaching. J. soils sediments 11, 628–638.

Chiaradia, M., Chenhall, B.E., Depers, A.M., Gulson, B.L., Jones, B.G., 1997. Identification of historical lead sources in roof dusts and recent lake sediments from an industrialized area: indications from lead isotopes. Sci. Total Environ. 205, 107–128.

City of West Hollywood, 2016. Edible Parkway Gardening, pp. 1–2. Available at: www.weho.org, 1 February 2016.

City of Sydney, 2016. Our City Farm Plan: a Place to Grow and Engage in Arming, Learning and Community Building in the Heart of Sydney. Sydney 2030, pp. 1–43. Available at: http://www.cityofsydney.nsw.gov.au/, 14 March 2016.

Clark, H.F., Hausladen, D.M., Brabander, D.J., 2008. Urban gardens: lead exposure, recontamination mechanisms, and implications for remediation design. Environ. Res. 107, 312–319.

Cohen, D.D., Gulson, B.L., Davis, J.M., Stelcer, E., Garton, D., Hawas, O., Taylor, A., 2005. Fine-particle Mn and other metals linked to the introduction of MMT into gasoline in Sydney, Australia: Results of a natural experiment. Atmos. Environ. 39, 6885–6896.

Donovan, J., 1996. Lead in Australian Children. Report on the National Survey of Lead in Children. Australian Institute of Health and Welfare, Canberra, pp. 1–124. Available at: http://www.abc.net.au/radionational/linkableblob/3988162/data/lead-in-children-data.pdf, 9 September 2016.

Douay, F., Pelfrène, A., Planque, J., Fourrier, H., Richard, A., Roussel, H., Girondelot, B., 2013. Assessment of potential health risk for inhabitants living near a former lead smelter. Part 1: metal concentrations in soils, agricultural crops, and homegrown vegetables. Environ. Monit. Assess. 185, 3665–3680.

Enhealth, 2012. Environmental Health Risk Assessment: Guidelines for Assessing Human Health Risks from Environmental Hazards. Available at: http://www.eh.org.au/documents/item/916, 2 November 2016.

Ferri, R., Hashim, D., Smith, D.R., Guazzetti, S., Donna, F., Ferretti, E., Curatolo, M., Moneta, C., Beone, G.M., Lucchini, R.G., 2015. Metal contamination of home garden soils and cultivated vegetables in the province of Brescia, Italy: Implications for human exposure. Sci. Total Environ. 518–519, 507–517.

Fett, M.J., Mira, M., Smith, J., Alperstein, G., Causer, J., Brokenshire, T., Gulson, B., Cannata, S., 1992. Community prevalence survey of children's blood lead levels and environmental lead contamination in inner Sydney. Med. J. Aust. 157 (7), 441–445.

Filippelli, G.M., Risch, M., Laidlaw, M.A.S., Nichols, D.E., Crewe, J., 2015. Geochemical legacies and the future health of cities: A tale of two neurotoxins in urban soils. Elem. Sci. fo Anthropocene 3. http://dx.doi.org/10.12952/journal.elementa.000059.

Finster, M.E., Gray, K.A., Binns, H.J., 2004. Lead levels of edibles grown in contaminated residential soils: a field survey. Sci. Total Environ. 320, 245–257.

Gulson, B.L., Davis, J.J., Bawden-Smith, J., 1995. Paint as a source of recontamination of houses in urban environments and its role in maintaining elevated blood leads in children. Sci. Total Environ. 164, 221–235.

Gulson, B., Mizon, K., Taylor, A., Korsch, M., Davis, M.J., Louie, H., Wu, M., Gomez, L., Antin, L., 2014. Pathways of Pb and Mn observed in a 5-year longitudinal investigation in young children and environmental measures from an urban setting. Environ. Pollut. 191, 38–49.

Harrington, E., 2012. EPA Levies $40,000+ Fines on Landlords Who Fail to Provide 'EPA-approved' Pamphlets to Tenants. Available at: http://www.cnsnews.com/news/article/epa-levies-40000-fines-landlords-who-fail-provide-epa-approved-pamphlets-tenants, 31 October 2016.

Hendershot, W., Turmel, P., 2007. Is food grown in urban gardens safe? Integr. Environ. Assess. Manag. 3, 463–464.

United States Department of Housing and Urban Development (HUD), 2016a. The renovation, repair and painting rule. Healthy Homes and Lead Hazard Control. Available at: http://portal.hud.gov/hudportal/HUD?src=/program_offices/healthy_homes/training/rrp/rrp, 1 June 2016.

United States Department of Housing and Urban Development (HUD), 2016b. The lead disclosure rule. Healthy Homes and Lead Hazard Control. Available at: http://portal.hud.gov/hudportal/HUD?src=/program_offices/healthy_homes/enforcement/disclosure, 2 June 2016.

Hunt, A., Johnson, D.L., Griffith, D.A., 2006. Mass transfer of soil indoors by track-in on footwear. Sci. Total Environ. 370 (2–3), 360–371.

Jacobs, D.E., Clickner, R.P., Zhou, J.Y., Viet, S.M., Marker, D.A., Rogers, J.W., Zeldin, D.C., Broene, P., Friedman, W., 2002. The Prevalence of Lead-Based Paint Hazards in U.S. Housing. Environ. Health Perspect. 110 (10), 599–606.

Jacobs, D.E., Mielke, H., Pavur, N., 2003. The High Cost of Improper Removal of Lead-Based Paint from Housing: A Case Report. Environ. Health Perspect. 111 (2), 185–186.

Kachenko, A.G., Singh, B., 2006. Heavy metal contamination in vegetables grown in urban and metal smelter contaminated sites in Australia. Water, Air, Soil Pollut. 169, 101–123.

Keisling, F., Manning, C., 2010. How green is your thumb? Environmental gardening identity and ecological gardening practices. J. Environ. Psychol. 30 (3), 315–327.

Kelly, M., 1987. Sydney City of Suburbs. New South Wales University Press, Kensington, NSW, Australia, p. 213.

Kessler, R., 2013. Urban gardening: Managing the Risks of Contaminated Soil. Environ. Health Perspect. 121 (11–12), 327–333.

Kristensen, L., Taylor, M.P., Morrison, A.L., 2015. Lead and zinc dust depositions from ore trains characterized using lead isotopic compositions. Environ. Sci. Process. Impacts 17 (3), 631–637.

Kristensen, L., 2015. Quantification of atmospheric lead emissions from 70 years of leaded petrol consumption in Australia. Atmos. Environ. 111, 195–201.

Laidlaw, M.A.S., Taylor, M.P., 2011. Review: Potential for childhood lead poisoning in the inner cities of Australia due to exposure to lead in soil dust. Environ. Pollut. 159, 1–9.

Laidlaw, M.A.S., Zahran, S., Pingitore, N., Clague, J., Devlin, G., Taylor, M.P., 2014. Identification of lead sources in residential environments: Sydney, Australia. Environ. Pollut. 184, 238–246.

Lanphear, B.P., 2015. The Impact of Toxins on the Developing Brain. Annu. Rev. Public Health 36, 211–230.

Lanphear, B.P., Homung, R., Khoury, J., Yolton, K., Baghurst, P., Bellinger, D.C., Canfield, R.L., Dietrich, K.N., Bornschein, R., Greene, T., Rothenberg, S.J., Needleman, H.L., Schnaas, L., Wasserman, G., Graziano, J., Roberts, R., 2005. Low-Level Environmental Lead Exposure and Children's Intellectual Function: An International Pooled Analysis. Environ. Health Perspect. 113 (7), 894–899.

Lanphear, B.P., Matte, T., Rogers, J., Clickner, R., Dietz, B., Bornschein, R., Succop, P., Mahaffey, K., Dixon, S., Galke, W., Rabinowitz, M., Farfel, M., Rohde, C., Schwartz, J., Ashley, P., Jacobs, D., 1998. The contribution of lead-contaminated house dust and residential soil to children's blood lead levels: a pooled analysis of 12 epidemiological studies. Environ. Res. 79, 51–68.

Local Government New South Wales, 2016. Reform – Fit for the Future. Available at: http://www.lgnsw.org.au/key-initiatives/reform-fit-for-the-future, 9 September 2016.

Markus, J.A., McBratney, A.B., 1996. An urban soil study: heavy metals in Glebe, Australia. Aust. J. Soil Res. 34, 453–465.

Mielke, H.W., Anderson, J.C., Berry, K.J., Mielke, P.W., Chaney, R.L., Leech, M., 1983. Lead Concentrations in Inner-City Soils As a Factor in the Child Lead Problem. Am. J. Public Health 73 (12), 1366–1369.

Mielke, H.W., 1999. Lead in the Inner Cities. Am. Sci. 87, 62–73.

Mielke, H.W., Gonzales, C.R., Smith, M.K., Mielke, P.W., 1999. The urban environment and children's health: soils as an integrator of lead, zinc, and cadmium in New Orleans, Louisiana, USA. Environ. Res. 81, 117–129.

Mitchell, R.G., Spliethoff, H.M., Ribaudo, L.N., Lopp, D.M., Shayer, H.A., Marquez-Bravo, L.G., Lambert, V.T., Ferenz, G.S., Russell-Anelli, J.M., Stone, E.B., McBride, M.B., 2014. Lead (Pb) and other metals in New York community garden soils: Factors influence contaminant distributions. Environ. Pollut. 187, 162–169.

National Environmental Protection Measure (NEPM), 2013. Schedule B1: Guideline on Investigation for Soil and Groundwater, p. 57. Available at: http://www.scew.gov.au/system/files/resources/93ae0e77-e697-e494-656f-afaaf9fb4277/files/schedule-b1-guideline-investigation-levels-soil-and-groundwater-sep10.pdf, 29 January 2016.

New South Wales Department of Environment & Planning, 2015. ePlanning, Data Reports. New South Wales Government. Available at: http://datareporting.planning.nsw.gov.au/ldpm-download-data, 16 May 2016.

New South Wales Environmental Protection Agency (NSW EPA), 2016a. Fact Sheet: Old Lead Paint. Available at: http://www.epa.nsw.gov.au/resources/pesticides/lead-old-paint-fact-sheet-150700.pdf, 21 March 2016.

New South Wales Environmental Protection Agency (NSW EPA), 2016b. Lead safety. The NSW EPA Lead Fact Sheet Series 2016. Available at: http://www.epa.nsw.gov.au/pesticides/lead-safety.htm, 8 August 2016.

New York State Department of Health, 2016. Soil Screening & Outreach Events. Department of Health, New York State. Available at: http://www.health.ny.gov/environmental/outdoors/garden/soil_screening.htm, 22 August 2016.

Olszowy, H., Torr, P., Imray, P., 1995. Trace element concentrations in soils from rural and urban areas of Australia. Dep. Hum. Serv. Health 4, 1–88.

Paustenbach, D.J., Finley, B.L., Long, T.F., 1997. The critical role of house dust in understanding the hazards posed by contaminated soils. Int. J. Toxicol. 16, 339–362.

Queensland Health, 2003. Blood Lead Notifications in Queensland 2003. Queensland Government, pp. 1–8. Available at: https://www.health.qld.gov.au/ph/documents/ehu/31751.pdf, 25 April 2016.

Queensland Health, 2011. Non-Occupational Blood Lead Notifications in Queensland 2011. Queensland Government, pp. 1–6. Available at: https://www.health.qld.gov.au/ph/documents/ehu/bl-notif-2011.pdf, 4 April 2016.

Rouillon, M., Taylor, M.P., 2016. Can field portable X-ray fluorescence (pXRF) produce high quality data for application in environmental contamination research? Environ. Pollut. 214, 255–264.

Rouillon, M., Kristensen, L., Gore, D.B., 2015. Handheld X-ray fluorescence spectrometers: radiation exposure risks of matrix-specific measurement scenarios. Appl. Spectrosc. 69 (7), 815–822.

Schwarz, K., Pickett, S.T.A., Lathrop, R.G., Weathers, K.C., Pouyat, R.V., Cadenasso, M.L., 2012. The effects of the urban built environment on the spatial distribution of lead in residential soils. Environ. Pollut. 163, 32–39.

Spliethoff, H.M., Mitchell, R.G., Shayler, H., Marquez-Bravo, L.G., Russell-Anelli, J., Ferenz, G., McBride, M., 2016. Estimated lead (Pb) exposures for a population of urban community gardeners. Environ. Geochem. Health 38 (4), 955–971.

Snowdon, R., Birch, G.F., 2004. The nature and distribution of copper, lead, and zinc in soils of a highly urbanized sub-catchment (Iron Cove) of Port Jackson, Sydney. Aust. J. Soil Res. 42, 329–338.

Sutton, P.M., Athanasoulis, M., Flessel, P., Guirguis, G., Haan, M., Schlag, R., Goldman, L.R., 1995. Lead Levels in the Household Environment of Children in Three High-Risk Communities in California. Environ. Res. 68, 45–57.

Szolnoki, Zs, Farsang, A., Puskas, I., 2013. Cumulative impacts of human activities on urban garden soils: origin and accumulation of metals. Environ. Pollut. 177, 106–115.

Taylor, M.P., Schniering, C.A., Lanphear, B.P., Jones, A.L., 2011. Lessons Learned on Lead Poisoning in Children: One-hundred years on from Turner's Declaration. J. Pediatr. Child Health 47 (12), 849–856.

Taylor, M.P., Winder, C., Lanphear, B.P., 2014. Australia's leading public health body delays action on the revision of the public health goal for blood lead exposures. Environ. Int. 70, 113–117.

Taylor, M.P., Winder, C., Lanphear, B.P., 2012. Eliminating childhood lead toxicity in Australia: a call to lower the intervention level. Med. J. Aust. 197 (9), 493.

United States Environmental Protection Agency (US EPA), 2013. Protect Your Family from Lead in Your Home, p. 16. Available at: https://www.epa.gov/sites/production/files/201309/documents/lead_in_your_home_brochure_book_color_508.pdf, 2 June 2016.

VegeSafe, 2015. Welcome to VegeSafe. Available at: http://research.science.mq.edu.au/vegesafe/, 29 January 2016.

Warming, M., Hansen, M.G., Holm, P.E., Magid, J., Hansen, T.H., Trapp, S., 2015. Does intake of trace elements through urban gardening in Copenhagen pose a risk to human health? Environ. Pollut. 202, 17–23.

Wise, P., 2014. Grow Your Own. The Potential Value and Impacts of Residential and Community Food Gardening. Policy Brief No. 59. March 2014. ISSN 1836–9014. Available at: http://www.tai.org.au/sites/defualt/files/PB%2059%20Grow%20Your%20Own.pdf, 21 March 2016.

World Bank, 2013. Urban Population (% of Total). Available at: http://data.worldbank.org/indicator/SP.URB.TOTL.IN.ZS, 21 March 2016.

Wuana, A., Okiemen, F.E., 2011. Heavy metals in contaminated soils: A review of sources, chemistry, risks and best available strategies for remediation. ISRN Ecol. 402647, 1–20.

Wu, L., Taylor, M.P., Handley, H.K., Wu, M., 2016. Australian atmospheric lead deposition reconstructed using lead concentrations and isotopic compositions of archival lichen and fungi. Environ. Pollut. 208, 678–687.

5.4   Article One

The Conversation

Elevated lead levels in Sydney back yards: here's what you can do

_____

Rouillon, M., Kristensen, L. Taylor, M.P., Harvey, P.J., George, S.G.

January 17, 2017 6.05am AEDT

Figure 5.3: Marek Rouillon and Professor Mark Taylor testing garden soils using pXRF.

In our recent study we found that 40 % of 203 Sydney homes we sampled contain lead in garden soil above the Australian health guideline of 300 milligrams per kilogram (mg/kg). This presents a hazard because soil lead can adhere to or get absorbed into edible plants. An additional pathway of exposure occurs when contaminated soil dust enters homes and is accidentally ingested. Lead is a potent neurotoxin that affects childhood development.

Urban agriculture and VegeSafe

Urban agriculture is becoming more popular across Australia. Almost half (48 %) of all households in metropolitan areas are now growing some form of edible produce. Most lead contamination is a result of the historical use of lead petrol and lead-based paint (now phased out) and previous industrial emissions. Scientists and regulators are well aware of these legacy issues, but the general public remains under-informed about the potential risks. To help urban gardeners assess contamination risks associated with their garden soils, we started the community science initiative VegeSafe in 2013. This program offers free soil metal screening to participants. Each participant receives a formal report on their soil metal results and advice

about what to do next if soils contain elevated concentrations of metals. We have provided 5,500 free soil metal tests to over 1,300 homes and community gardens (Australia-wide), the largest program and study of its kind in Australia.

What did we find?

As well as the 40 % of Sydney gardens containing soil above the 300 mg/kg Australian health guideline, approximately one in seven homes had soils lead levels greater than 1,000 mg/kg. Soil metal concentrations were typically greatest around drip lines. Soil lead concentrations were greatest in the City of Sydney and former local government areas of Leichhardt Municipal Council and Marrickville Council, which had mean soil lead concentrations of 883 mg/kg, 960 mg/kg and 689 mg/kg, respectively.
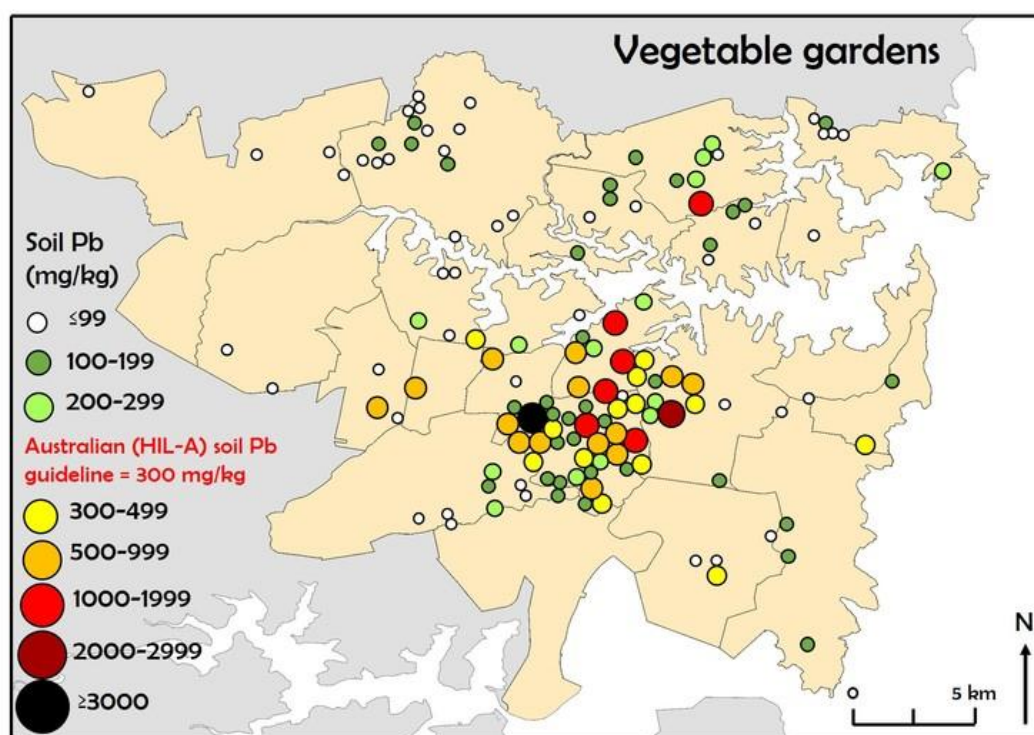
Figure 5.4: Soil lead concentrations of vegetable garden soils from 141 Sydney homes. Map represents one of four areas around homes (front yard, drip line, back yard and vegetable garden) in this study.

Homes with painted exteriors built before 1970 were more likely to have soils contaminated with lead. The highest levels are at homes 80 years or older. This is likely to have been caused by lead-rich paint, which contained up to 50 % lead prior to 1970. Lead in paint was reduced to less than 1,000 mg/kg (0.1 %) by 1997. We observed the environmental benefit of the withdrawal of lead from paints and leaded petrol (removed in 2002) in our study. Garden soils at newer homes contain the least lead. Soil lead concentrations decrease with distance from Sydney's city centre, where there are more old homes and greater density of traffic and industry.

Public health

Lead exposure is especially detrimental for children because their neurological and skeletal systems are developing. Adults are also adversely affected, with studies showing increased blood pressure and hypertension associated with sub-clinical exposures. Toxicological evidence also shows that exposure reduces semen quality and extends the time to pregnancy. In short, lead is detrimental to all human systems and exposures should be avoided or minimised at all times.

Our study demonstrates lead contamination in garden soils is greater at painted homes than non-painted homes. Many pre-1970 Australian homes still contain paint with up to 50 % lead on exterior walls, fences, eves, doors and window frames. The main risk of exposure arises when lead-based paint deteriorates or is removed improperly. Indeed, many home renovators unwittingly expose themselves and others due to a lack of knowledge of lead hazards.
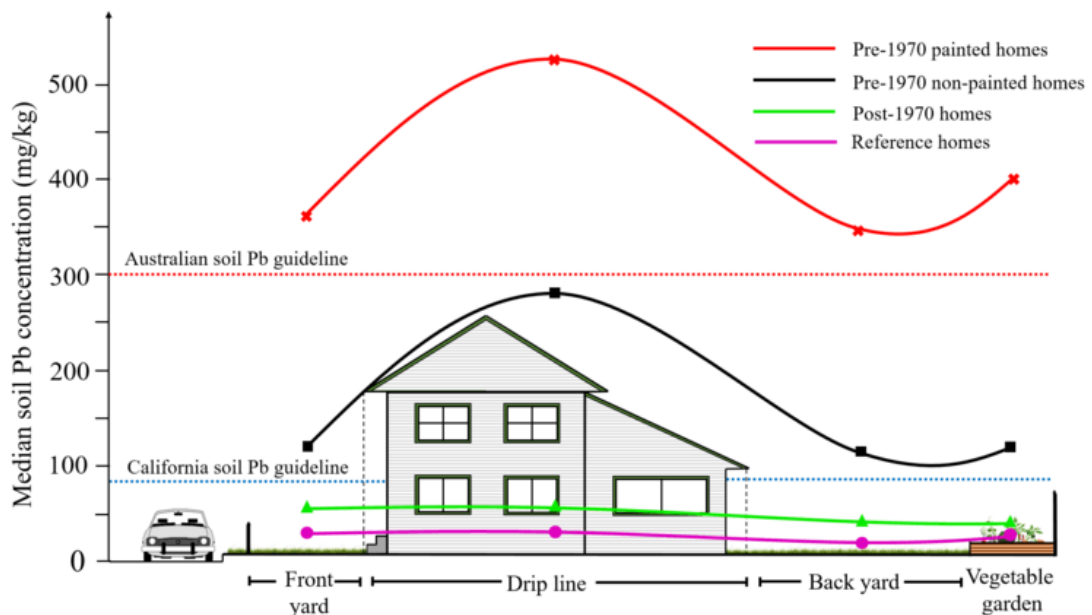
Figure 5.5: Cross-section schematic of a typical inner-Sydney residential home with median soil Pb (lead) concentrations for painted pre-1970 homes, non-painted pre-1970 homes, post-1970 homes and reference homes. The vegetable garden is displayed at the rear of the back yard, as this was the case for the majority of homes.

Reducing exposure

The United States Environmental Protection Agency introduced legislation specifically targeting houses with lead paint to prevent contamination and to minimise avoidable lead exposures. Unfortunately this regulatory gap has not been filled in Australia. Despite the widespread historic use of lead-based paints and the high proportion of exposure related to it, our data reveals a concerning legacy of soil lead contamination in older suburbs. We recommend that people residing at or planning to purchase or renovate homes built before 1970

should get their soils and paint tested for lead. Using a qualified lead-abatement decorator in older homes would also help prevent exposure. Where parents and homeowners think they may have caused exposure, their GPs can provide a blood lead test. Reducing even low-level exposures is critical, as demonstrated by Bruce Lanphear's "prevention paradox" (see the image below). The graphic illustrates that the most IQ points across a population are lost from low-level lead exposures.

Figure 5.6: Paints containing lead are no longer used in Australia, but remain on countless homes.
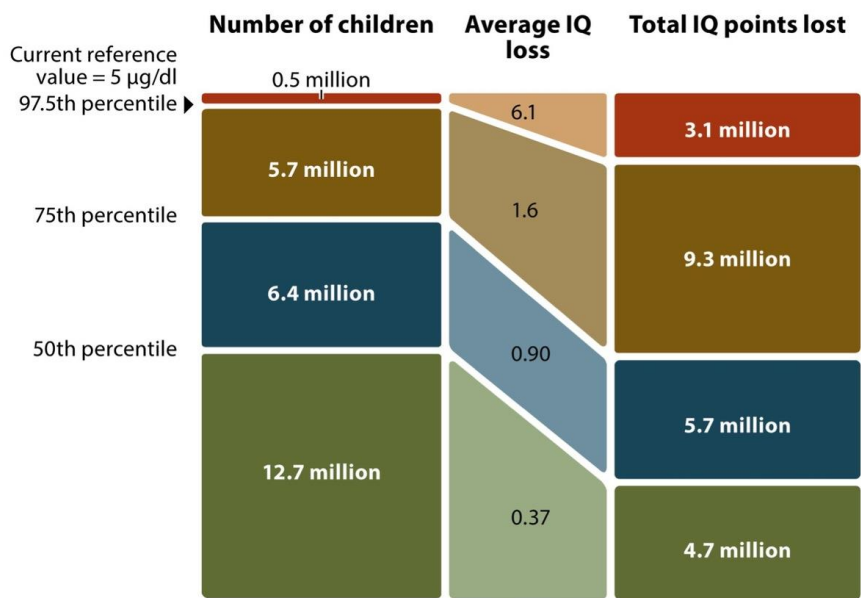
Lanphear BP. 2015.
Annu. Rev. Public Health. 36:211–30

Figure 5.7: Bruce Lanphear's prevention paradox. The majority of IQ points lost to lead exposure occurs in children who have low-to-moderate exposure to lead. Adapted from Reference (Lanphear 2015).

What can gardeners do?

Where non-food-growing soils exceed the Australian soil metal guidelines, we recommend maintaining year-round cover of lawn or mulch to minimise dust generation. Where metal guidelines are exceeded in food-growing soils, we recommend either replacing existing soil with new, uncontaminated soil, or relocating the food garden to an above-ground vegetable plot (again with new soil). In this way, gardeners can exercise our motto, which is to carry on gardening knowing their soils are clean.

5.5   Outcomes of Paper Four and Article One

One of the main objectives behind publication of **Paper Four** and **Article One**, was to disseminate the study findings in a communicable manner to as many Australian gardeners as possible. A second media release (Macquarie University Newsroom 2017) summarising the main findings of study was distributed to major media outlets on the same day that **Article One** was published. **Article One** (*The Conversation*) drew more than 7,000 online readers in the first week and was further distributed through social and professional media channels more than 700 times (Figure 5.8). Public engagement with the article revealed most readers agree that further policy improvements are necessary to prevent the improper removal, or power sanding, of Pb-based paints from the exteriors of homes.
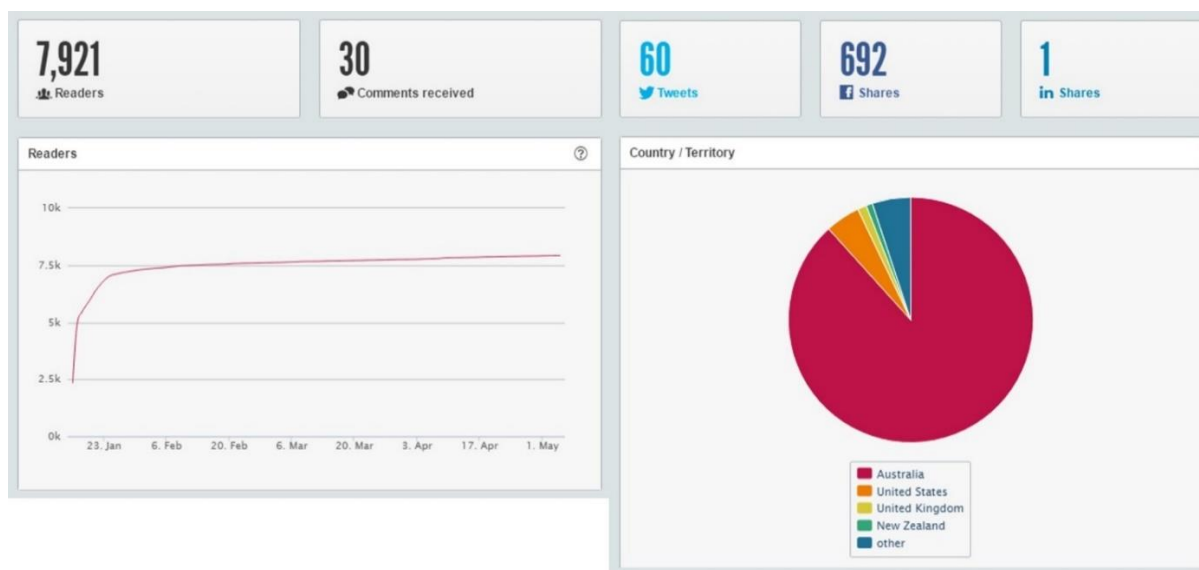
Figure 5.8: Approximate reach statistics for Article One in *The Conversation* as of May 6, 2017.

Over the following days after the media release, VegeSafe was interviewed by numerous forms of media including national and local radio (ABC Sydney, ABC Adelaide, 2SER Radio, 89.3 FM and 3BA FM), national and local TV news programs (Channel 7 News and broadcast from 15 local news networks), state and local newspapers (The Sun Herald, Sydney Morning Herald, The Daily Telegraph, Inner West Courier, The West Australian, The Northern Daily Leader and WA Today), online news platforms (Sydney Morning Herald, News.com and ABC Online) and local magazine outlets (Central Sydney Magazine and Il Globo magazine). The most wide-reaching broadcasting platform was Channel 7 News, with an estimated 453,000 viewers tuning in to watch the 90 second segment. Yet, despite the authors best efforts to explain the findings to journalists using appropriate terminology such as '*elevated soil Pb concentrations*' and '*adverse health impacts*', the study findings quickly became sensationalised in the hopes of attracting more readers and viewership. Fear provoking titles such as "*The Sydney suburbs with*

the most poisonous soil" (Figure 5.9) and "*Is your garden soil toxic*?" are common practice when studies covering contamination are reported. However, some articles were communicated truthfully, without deliberate over exaggeration. For instance, an editorial piece in the Sydney Morning Herald (2017) titled: "*Get the lead out, in every sense*" praised the program and study findings stating:

> "*Macquarie University is to be commended for offering a soil testing service for those worried about what they might be feeding their family in their attempts at self-sufficiency.*"
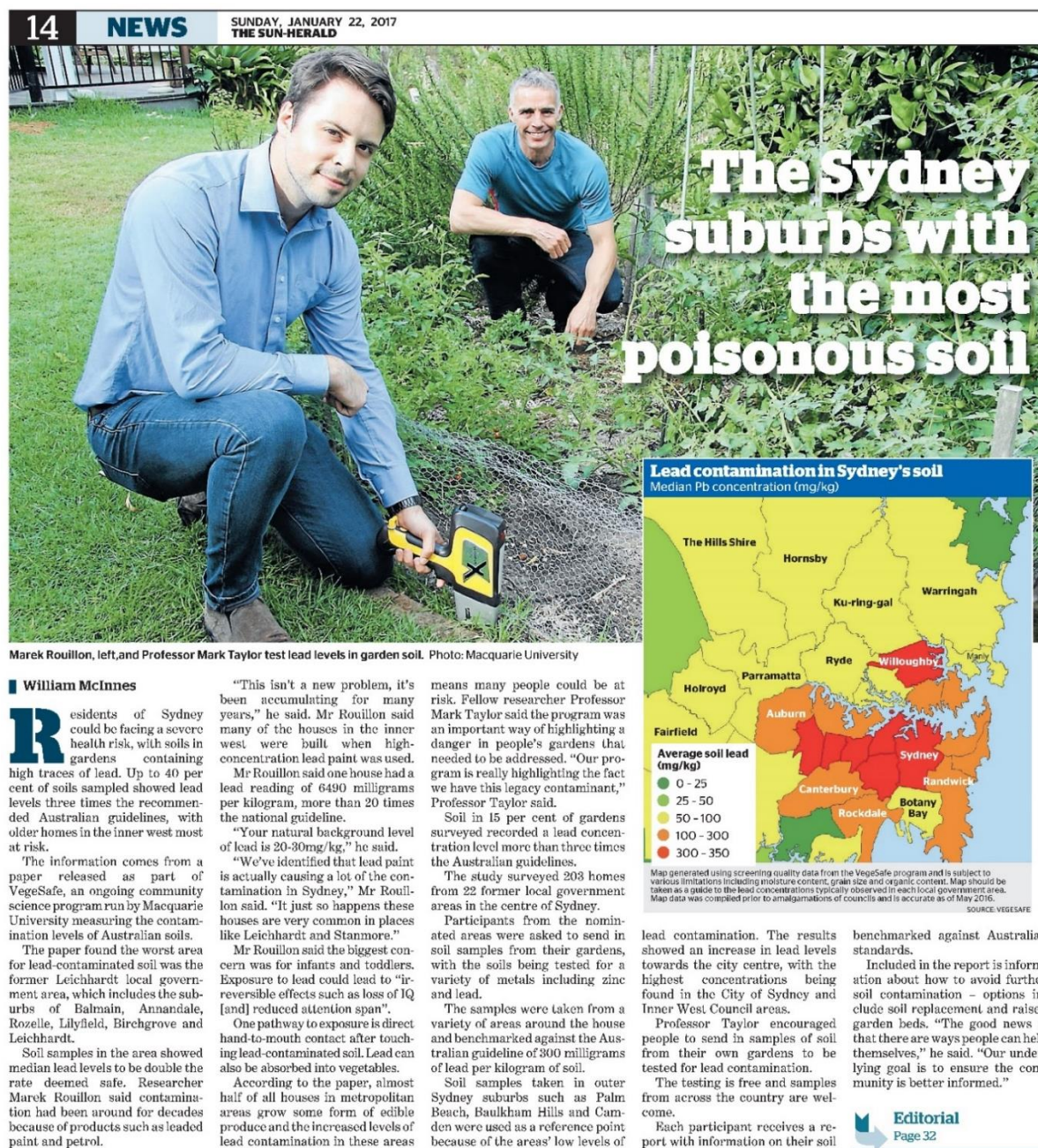
Figure 5.9: The Sun Herald coverage of the study findings on January 22, 2017.

The media coverage re-energized public discussion on environmental health topics such as the historical use of Pb in products, and potential Pb hazards around homes. This has always been

a core focus for the program, to give people the confidence to '*carry on gardening*' in the knowledge that their soils are metal free, as is the produce from their gardens (VegeSafe 2017). Following the coverage, VegeSafe received hundreds of samples from around the country for further soil metal screening.

Not long after, VegeSafe was invited to discuss the study findings with both the New South Wales Environment Protection Authority (NSW EPA) and NSW Public Health. The meeting was a success, with all three parties recognising the importance of further community education of Pb hazards, in addition to government resources such as the Pb fact sheet series by the NSW EPA (2016). The Pb fact sheet series includes information on old Pb paint, renovations of old homes, and Pb in ceiling dust, and is available in multiple languages online. This information is publicly available on the NSW EPA website. Yet far too often, residents remain unaware of potential Pb hazards and their associated health risks because they have not previously seen the information, nor do they know it exists. **Paper Four** acknowledged that while this information exists, further outreach is required by state and local governments to distribute these educational materials directly to residents living in areas with high soil Pb concentrations, such as the Inner West and inner city areas.

The findings of **Paper Four**, and the VegeSafe program more broadly, were later the subject of a series questions asked in the legislative assembly of State (NSW) Parliament on February 16th, 2017. Independent member for Sydney, Alex Greenwich asked five questions to the Ministers of Environment, Heritage and Local Government regarding what current/future action the government has/will take towards Pb safety (Parliament of NSW 2017). Responses were given on March 23rd, 2017, and are provided below:

Q1. What proactive action does the Government take to inform the community about potential lead problems apart from information on the Environment Protection Agency website?
"In addition to Environment Protection Authority's (EPA) Lead Safety website, the Government has developed a number of initiatives that deal with lead contamination."

Q2. What steps have been taken since the VegeSafe program research was released in January 2017?
"The EPA has undertaken a preliminary technical review of the report. This preliminary review found the size fraction of the household soils selected for lead analysis was not consistent with the size fraction recommended by the National Environmental Protection (Assessment of Site Contamination) Measure. Despite this limitation, the EPA acknowledges that the aim of the

VegeSafe program was to raise community awareness about the potential risks of growing vegetables in urban soils, and that the advice provided to the community about their vegetable garden soils was consistent with widely accepted practices."

Q3. What action has the Government taken to inform and update:

    a. **Parents of children at greater risk of impacts;**

    b. **People with edible food gardens;**

    c. **Homeowners renovating where lead-based paint and lead dust could be uncovered?**

"This information can be found at http://www.epa.nsw.gov.au/pesticides/lead-safety.htm"

Q4. What action has the Government taken to review/update current lead pollution guidelines or advice?

"This is a matter for the Australian Government Environmental Health Standing Committee."

Q5. What further action will the Government take to address potential risks from lead pollution in soils across inner Sydney?

"The EPA is proactively engaged with NSW Health and local councils to ensure it remains informed of any issues associated with community level adverse health outcomes and any contamination issues that may require notification to the EPA."

Some of the responses were not entirely pertinent to the question being asked (i.e. Q2 and Q5), while some were more adequately addressed (i.e. Q1). Yet, perhaps the most relevant question towards the outcomes from **Paper Four** was Question Two. Unfortunately, the response did not provide any information regarding steps that have been taken since the research was released (i.e. the question asked), but instead subtly disregarded the study findings because the particle size chosen for pXRF analysis was not consistent with the size fraction recommended by the National Environmental Protection Measure (NEPC 2013). Upon review of the NEPM (NEPC 2013), we found that the methods used in **Paper Four** were consistent with the recommended guidelines, and that the wrong advice was given to the Minister for Environment from the NSW EPA. Section 4.2.4.3 of the NEPM (NEPC 2013) covers sieving preparation for dry analysis and states:

> *"Unless impracticable or not recommended for a specific method, the sample portion for analysis should be of a size to pass a 2.0 mm aperture sieve. This may be achieved by grinding, if appropriate… If another particle size is chosen, this should be consistently used within an analysis regime and reported with analytical results"* (NEPC 2013, pp. 17).

Soil samples used in **Paper Four** passed through a 2 mm stainless steel sieve before passing through a 500 μm sieve (Rouillon et al. 2017). It is unfortunate that the NSW EPA erroneously reviewed **Paper Four**, as the objectives of this publication were to investigate Pb hazards present in residential backyards and to inform previously unaware gardeners of the metal contamination at their homes. Both of these matters should be of greater interest to the NSW EPA and local councils most impacted by soil Pb contamination, as it promotes two of the key objectives in the *Protection of the Environment Operations Act 1997,* which states (pp. 2):

The objects of this act are as follows:
- *(a) To provide increased opportunities for public involvement and participant in environmental pollution,*
- *(b) To ensure that the community has access to relevant and meaningful information about pollution.*

Coincidentally, an article by Central Sydney Magazine (2017) revealed that when asked about soil Pb contamination in backyards, the relevant government bodies of City of Sydney, NSW EPA and NSW Health were quick to pass the responsibility rather than addressing the issue:

"Mr Rouillon called on regulatory bodies and the City of Sydney to take responsibility for increasing the public's awareness of the issue and to take proactive steps to provide free soil testing – analysis which can be prohibitively expensive."

"A City spokesman would not answer when asked whether residents were at risk, stating that "the monitoring and management of lead levels in soil is largely the responsibility of the EPA (Environment Protection Agency)" but that the City considered land contamination when determining development applications. An EPA spokeswoman said NSW Health was the best contact regarding blood tests, precautions and health risks, that the local council had frameworks for development on sites potentially contaminated and that the EPA's core focus was raising awareness of historical lead contamination so people could take precautions to avoid exposure" (Central Sydney Magazine 2017).

Article One was republished in the June 2017 issue of *Chemistry in Australia*, a magazine for and about chemical science professionals. Shortly after its re-publication, the editor advised us that an opinion piece (letter to the editor) has been submitted for publication by an environmental auditor in response to our article (Appendix E, Excerpt 1). The auditor's remarks largely questioned our inclusion and application of the HIL guidelines in **Article One**. It was apparent that the auditor did not understand the purpose of this research, nor did the auditor

read the original scientific article of **Paper Four**, which was the basis of **Article One**. While the comments presented may be factually correct for other scenarios, for example contaminated site assessments presented in **Paper Three**, they are not relevant for residents who seek useful information and guidance on the state of their garden soils. Moreover, not one of the Australia's contaminated land auditors have reached out to provide meaningful and practical advice to the broader public on this issue, which is of clear interest to the community.

Yet, despite the questionable criticism of particle sizes and the use of HIL values, **Paper Four**, **Article One** and their related media coverage re-focused the communities' attention towards environmental contamination. Ongoing participation in the VegeSafe program demonstrates that a large proportion of the community does care about soil contamination, particularly because they can access soil metal screening that is specific to their property. VegeSafe directly engages with the community and regularly visits community gardens, schools, and community and gardening festivals to further educate the public on environmental health and Pb hazards around the home. Moreover, the VegeSafe program demonstrates that the soil screening service was not only effective at identifying soil metal contamination, but was conducted at minimal cost, running largely from participant donations. Given that there is a demonstrable need for VegeSafe, the NSW EPA could consider adopting a similar program, or at the very least consider supporting the University-based screening service given that both the NSW EPA and VegeSafe have similar goals of educating the community on Pb hazards.

It is important to note that the samples in **Paper Four**, **Article One** and their subsequent media articles were collected on a participation basis via the VegeSafe program, and consequently were not collected systematically across the Sydney basin. This is one of the limitations of using a citizen science approach to collect many samples from hard to access environments (private residences). A greater participation interest was evident from suburbs in the Inner West and from areas where vegetable gardening was common, which was likely to have skewed summarised soil metal data from across the entire sampling area. Hence, the use of phrases such as "*40 % of Sydney homes*" may not have been entirely representative of the city-wide contamination picture, due to the distribution of sampling locations used in the study.

5.6 Cost estimations of pXRF application in Paper Four

Analysis costs often control the data resolution of a study, and thereby the confidence that one can attach to any findings, particularly when projects have limited financial resources such as University-based research. Consequently, the sampling resolution of a study can become impacted, which is much more critical in the geochemical-heterogeneous urban environment.

This may be more relevant at the household scale where decision-making for owners is more use-specific and critical (Figure 5.5) (Schwarz et al. 2012). If researchers are limited by funding, but have lower constraints on the time available for a project, pXRF offers a low cost, reliable alternative for the measurement of metal-contaminated soils (Rouillon and Taylor 2016).

Paper Four utilized *ex-situ* pXRF to inexpensively measure the metal content of Sydney garden soils. The estimated cost of all consumables used for the pXRF measurement of 436 soil samples was AU$445 (Figure 5.10). An Olympus pXRF analyzer can be rented for one week at approximately AU$2000, while a further AU$1650 ($30/hr) is required for a research assistant to complete sample preparation over 6–7 days. Hence, the total analytical costs involved in measuring 436 soil samples by pXRF range between AU$445 and AU$4095 depending on the use of a research assistant and access to a pXRF, and would take approximately 2–3 weeks to complete.
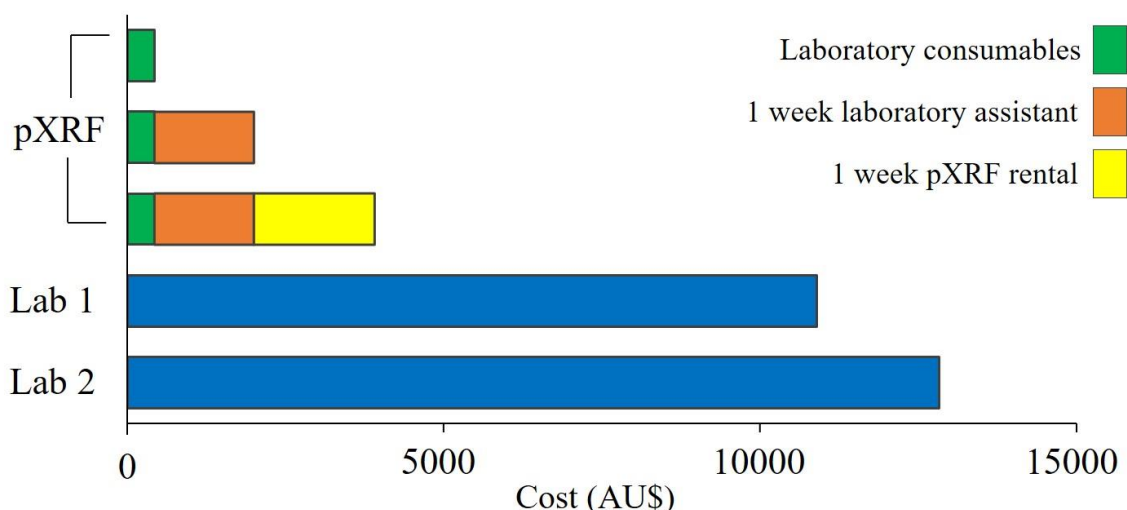
Figure 5.10: Cost comparison between pXRF and NATA-accredited ICP–AES analyses from two different laboratories for the measurement of 436 soil samples.

By contrast, analysis of the same 436 samples by NATA-accredited ICP–AES methods at commercial laboratories ranged between AU$11,430 and AU$26,720 for Mn, Cu, Zn, As and Pb concentrations, and typically takes between 1–2 weeks (Figure 5.10). Excellent agreement between pXRF with both CRM and ICP–AES data demonstrates that pXRF is a viable analytical alternative to traditional wet chemistry techniques for the measurement of metal-contaminated soils (Rouillon and Taylor 2016). While there are limitations to such a comparison, such as metal concentrations approaching pXRF detection limits (Willis and Duncan, 2008), there are also clear cost benefits when certain sample and concentration criteria

are met. Thorough and consistent sample preparation methods ensured robust, repeatable and accurate sample analysis using the pXRF despite not grinding samples to <74 µm to match the grain size presented by CRMs used in the matrix calibration (Rouillon and Taylor 2016). The lower costs of pXRF operation for environmental investigations enables users to increase the sample density of a study and re-direct valuable funds for more complicated analyses such as organics or Pb isotope analysis, as was the case for **Paper Five**.

5.7 Paper Five

Publication

Geochemical sources, forms and phases of soil contamination in an industrial city

Abstract: This study examines current soil contamination in an Australian industrial city, Newcastle. Public (roadside verges and parks) and private (homes) surface soils (n= 170) contained metal(loid)s elevated above their respective Australian Health Investigation Levels (HIL). Lead (Pb), the most common contaminant in the city, exceeds the HIL for residential soils (HIL-A, 300 mg/kg) in 88 % of private soils (median: 1140 mg/kg). In-vitro Pb bio-accessibility analysis of selected soils (n = 11) using simulated gastric fluid showed a high affinity for Pb solubilisation (maximum Pb concentration: 5190 mg/kg, equating to 45 % Pb bio-accessibility). Highly soluble Pb-laden Fe- and Mn-oxides likely contribute to the bio-accessibility of the Pb. Public and private space surface soils contain substantially less radiogenic Pb (range: $^{208}Pb/^{207}Pb$: 2.345–2.411, $^{206}Pb/^{207}Pb$: 1.068–1.312) than local background soil ($^{208}Pb/^{207}Pb$: 2.489, $^{206}Pb/^{207}Pb$: 1.198), indicating anthropogenic contamination from the less radiogenic Broken Hill type Pb ores ($^{208}Pb/^{207}Pb$: 2.319, $^{206}Pb/^{207}Pb$: 1.044). Source apportionment using Pb isotopic ratio quantification and soil mineralogy indicate the city's historic copper and steel industries contributed the majority of the soil contaminants through atmospheric deposition and use of slag waste as fill material. High-temperature silicates and oxides combined with rounded particles in the soil are characteristic of smelter dust emissions. Additionally, a preliminary investigation of polycyclic aromatic hydrocarbons in soils, sometimes associated with ferrous metal smelting, coal processing or burning of fossil fuels, shows that these too pose a health exposure risk (calculated in comparison to benzo(a)pyrene: n = 12, max: 13.5 mg/kg, HIL: 3 mg/kg).

Keywords: Soil, Metal(loids), Lead isotopes, Bio-accessibility, Mineralogy of metal-bearing particles, Newcastle

Geochemical sources, forms and phases of soil contamination in an industrial city

P.J. Harvey [a,*], M. Rouillon [b], C. Dong [b], V. Ettler [c], H.K. Handley [a], M.P. Taylor [b], E. Tyson [b], P. Tennant [b], V. Telfer [b], R. Trinh [b]

[a] Department of Earth and Planetary Sciences, Faculty of Science and Engineering, Macquarie University, Sydney, NSW 2109, Australia
[b] Department of Environmental Sciences, Faculty of Science and Engineering, Macquarie University, Sydney, NSW 2109, Australia
[c] Institute of Geochemistry, Mineralogy and Mineral Resources, Faculty of Science, Charles University, Albertov 6, Prague 2 128 43, Czech Republic

HIGHLIGHTS

- Ferrous and non-ferrous metal smelting have caused an environmental contamination legacy in the city environment.
- Children exposed to the soils in the city are vulnerable to metal(loid) and polycyclic aromatic hydrocarbon exposure.
- Human health exposure risks should be considered when repurposing industrial cities for changing land-uses.

GRAPHICAL ABSTRACT

ABSTRACT

This study examines current soil contamination in an Australian industrial city, Newcastle. Public (roadside verges and parks) and private (homes) surface soils (n = 170) contained metal(loid)s elevated above their respective Australian Health Investigation Levels (HIL). Lead (Pb), the most common contaminant in the city, exceeds the HIL for residential soils (HIL-A, 300 mg/kg) in 88% of private soils (median: 1140 mg/kg). In-vitro Pb bio-accessibility analysis of selected soils (n = 11) using simulated gastric fluid showed a high affinity for Pb solubilisation (maximum Pb concentration: 5190 mg/kg, equating to 45% Pb bio-accessibility). Highly soluble Pb-laden Fe- and Mn-oxides likely contribute to the bio-accessibility of the Pb. Public and private space surface soils contain substantially less radiogenic Pb (range: $^{208}Pb/^{207}Pb$: 2.345–2.411, $^{206}Pb/^{207}Pb$: 1.068–1.312) than local background soil ($^{208}Pb/^{207}Pb$: 2.489, $^{206}Pb/^{207}Pb$: 1.198), indicating anthropogenic contamination from the less radiogenic Broken Hill type Pb ores ($^{208}Pb/^{207}Pb$: 2.319, $^{206}Pb/^{207}Pb$: 1.044). Source apportionment using Pb isotopic ratio quantification and soil mineralogy indicate the city's historic copper and steel industries contributed the majority of the soil contaminants through atmospheric deposition and use of slag waste as fill material. High-temperature silicates and oxides combined with rounded particles in the soil are characteristic of smelter dust emissions. Additionally, a preliminary investigation of polycyclic aromatic hydrocarbons in soils, sometimes associated with ferrous metal smelting, coal processing or burning of fossil fuels, shows that these too pose a health exposure risk (calculated in comparison to benzo(a)pyrene: n = 12, max: 13.5 mg/kg, HIL: 3 mg/kg).

© 2017 Elsevier B.V. All rights reserved.

1. Introduction

Urban environmental contamination is an issue common to industrial cities throughout the world (Filippelli et al., 2015). Historically, employees would live close to their work, resulting in dense urban

* Corresponding author.
E-mail address: paul.harvey@mq.edu.au (P.J. Harvey).

development around industrial operations. Due to the proximity of industrial operations to urban environments there is the potential for adverse impacts on human health arising from industrial emissions (Csavina et al., 2012; Dong et al., 2015; Ettler et al., 2009; Gulson et al., 1994; Gulson et al., 2004; Gulson et al., 2009; Morrison, 2003; Taylor et al., 2010; Taylor et al., 2013; Taylor et al., 2014a; Taylor et al., 2014b).

By 2050, the majority of the global population is expected to transition from rural to urban-metropolitan living, increasing the risk associated with contaminated urban lands (United Nations (UN), 2015). The resulting environmental contamination burden from industrial cities is demonstrated in Detroit, USA, which has been considered one of the most contaminated cities in the USA (Lougheed, 2014). Sulfur dioxide, heavy metals, hydrocarbons and other organic contaminants that were emitted to the atmosphere during the city's automobile manufacturing era, accumulated in the urban soil environment and have been subsequently linked to a range of health impacts including
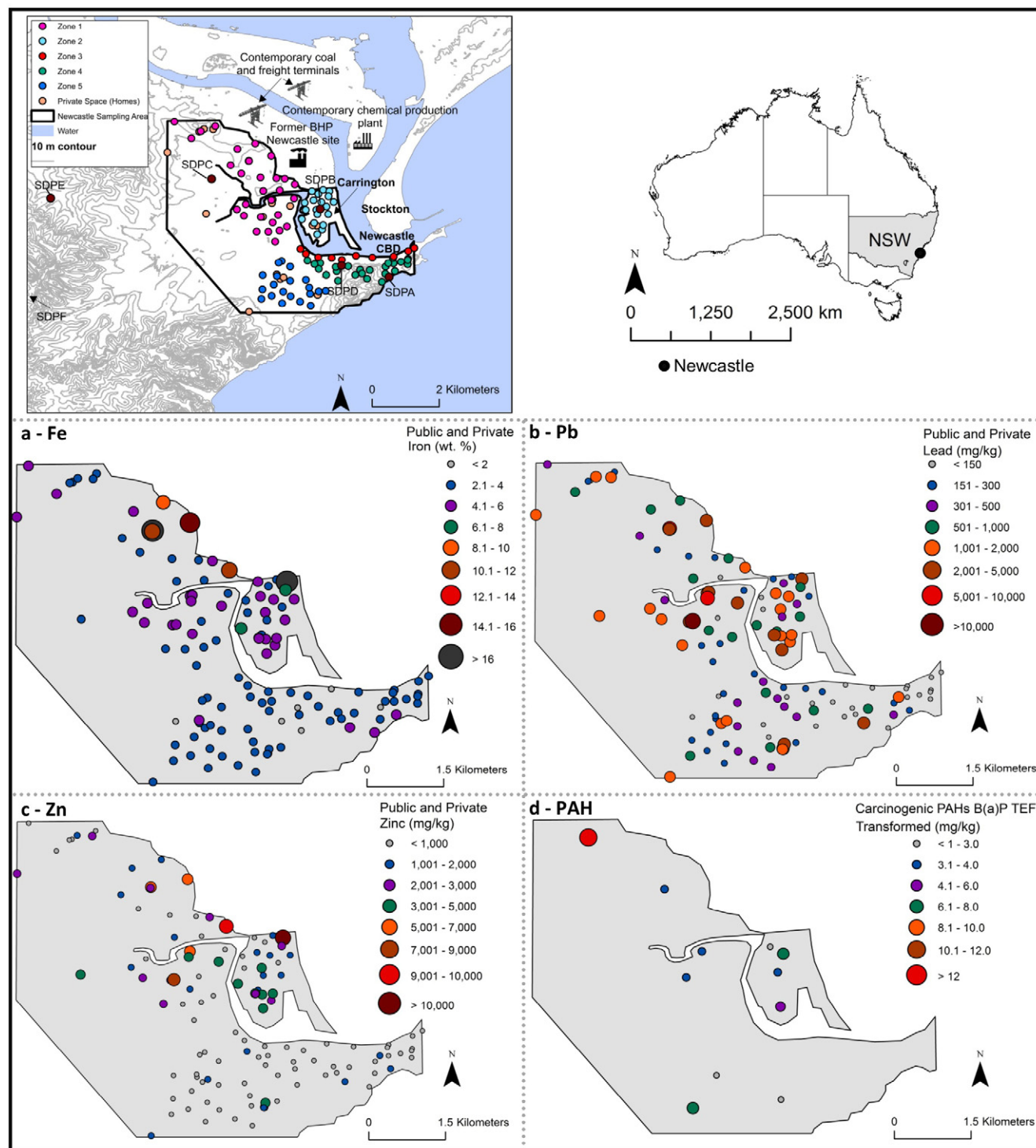
Fig. 1. Soil analyte concentrations within Newcastle (Australia) (panel a - iron, b - lead, c - zinc, d - TEF transformed PAHs). Sites marked SDP- are soil depth profiles.

chronic respiratory diseases and mental disabilities, particularly in infants and young adults (Canfield et al., 2003; Dong et al., 2015; Lougheed, 2014; Taylor et al., 2016). Although Detroit battles legacy environmental contamination issues, modern industrial processes can also contribute to the environmental contamination burden. More recently, the rapid and spontaneous expansion of China's manufacturing and industrial economy has resulted in an overlap of land-use with urban-residential areas. The emissions generated from industrial processes have been linked to substantial carcinogenic health effects in the city of Beijing (Chen et al., 2015). In order to address this problem, a better understanding of environmental contamination and the impacts on population health in urban-industrial environments is required.

This study investigates an Australian industrial city, Newcastle, and the risk of exposure associated with environmental contaminants in the soils of the city. Newcastle, approximately 200 km north of Sydney (Fig. 1), was historically a manufacturing-based city. However, the city has recently become a regional population center, with an economy moving towards services, arts and tourism (Newcastle City Council (NCC), 2013, 2015). Large-scale industrial operations began in the mid 1800's with the Wallaroo Copper Company smelter (1868 to 1892) processing annually ~1300 tonnes of low grade Wallaroo Mine (South Australia) copper ore (NCC, 1997; SMH, 1871a; SMH, 1871b; The Mercury, 1867). During that time, a number of other operations were also established, including the Waratah Coal Company (SMH, 1871b), the English and Australian Copper Company (EACC) smelter in 1867 (SM, 1872) and the Sulphide Corporation Pb smelter at nearby Boolaroo in 1897 (Dames and Moore, 1994). The port and shipping facilities of Newcastle quickly became strategic industrial infrastructure as Pb sulfide ore was shipped through the Port of Newcastle to Boolaroo (NMH, 1902; Quorn Mercury, 1900a). In 1907 the Melbourne and Great Northern Smelter also joined the Cu smelting operations at Newcastle (MDM, 1907; SCT & WA, 1907). The Broken Hill Proprietary (BHP) Newcastle Steel Mill and subsidiaries were the industrial focus of Newcastle from 1915 until their closure in 1999 (Parliament of New South Wales, 1999). At peak operation, the facilities employed ~12,000 people (BHP Co. LTD, 1949; Parliament of New South Wales, 1999). The BHP operation became an industrial giant with the addition of, and partnership with, two other large scale manufacturers of steel products (BHP Co. LTD, 1949; NS, 1925; Parliament of New South Wales, 1999). Today, coal and freight shipping terminals and an ammonium nitrate facility dominate the industrial activities of the city.

Despite the industrial heritage of Newcastle, there has been no publicly accessible wide-scale geochemical assessment of soils in the city area. This study investigates soil metal(loid)s and polycyclic aromatic hydrocarbons (PAHs) to help close this knowledge gap and highlight potential environmental contamination risks associated with living in an industrial city.

2. Methods

2.1. Soil sampling

2.1.1. Soil metal(loid) concentrations

Newcastle city was divided into five sampling areas (Fig. 1) to reflect the dominant land use types covering open spaces, retail and industrial (Zone 1), residential (Zone 2), rehabilitated industrial land along the foreshore now used for high density residential (Zone 3), Central Business District (CBD) (Zone 4) and low to medium density residential (Zone 5). Soils collected in public spaces (n = 103) were sampled from roadside verges, parklands and other accessible locations. Soils collected from private spaces (n = 67 from 23 homes) were obtained through the Macquarie University VegeSafe soil metal testing program (Rouillon et al., 2016), where Newcastle community members submitted samples for analysis. Samples were also received from outside of the specified target area but were included here to provide additional detail to the investigation. Public space samples were collected at the surface (0–2 cm)

in accordance with the standard methods (Taylor et al., 2010). A number of control sites (n = 6) with pits dug to a defined depth of 40 cm irrespective of soil horizons were sampled throughout the city to determine local background soil concentrations.

2.1.2. Slag deposits

A slag waste deposit was identified outcropping on a beach adjacent to a children's playground in Stockton (Fig. 1). Large chunks of a black glass-like slag and a ferrous slag material were collected using a rock hammer to separate them from the consolidated mass. This deposit has been documented in the local media as one of many civil works sites in the city where BHP-derived material was used as stabilization fill (NMH, 1948a; NMH, 1948b; NMH, 1949a; NMH, 1949b; NS, 1926; NS, 1948).

2.1.3. Soil polycyclic aromatic hydrocarbon concentrations

Coal, ferrous metal smelting and fossil fuels present significant sources of environmental PAH contamination (Albuquerque et al., 2016; Odabasi et al., 2010; Yang et al., 2016). To further compliment the metal(loid) analysis, a preliminary investigation of soil PAH concentrations was conducted. Soil samples for PAH analysis were collected from 12 locations around the city (Fig. 1d). Soils were collected in clean glass bottles with a Teflon lid and stored at <4 °C until analysis.

2.2. Laboratory analysis

2.2.1. Soil metal(loid) concentrations

Soil samples (n = 170) were oven dried at 40 °C for 72 h, then sieved to <180 μm. This fraction was selected for analysis because the research evidence shows that finer soil fractions are susceptible to re-suspension and subsequent ingestion or inhalation (Horowitz, 1991; Youn et al., 2016). Approximately 10 g of the <180 μm sample was packed in 35 mm open ended PANalytical XRF cups using 3.6 μm Chemplex Mylar X-ray film for analysis. An Olympus Delta Premium XRF Analyzer (pXRF) fitted with a 50 kV, 4 W Ta anode X-ray tube and a silicon drift detector was used for the measurement of Ti, Cr, Mn, Fe, Cu, Zn, As, Cd and Pb concentrations in surface and subsurface soils. Analysis was conducted at Macquarie University. Recommended operational procedures were followed, including: daily measurements of an energy calibration check, measurements of a silicate (SiO₂) blank at the beginning and end of analysis to ensure no instrument contamination had occurred, and measurements of NIST certified reference materials (CRMs) conducted every 25 samples to monitor instrument performance (Table 1). Soil samples and CRMs were placed on the measurement window and analyzed using the proprietary soil mode at 60 s per measurement condition (180 s total measurement). A matrix-matched calibration was applied to optimize the pXRF in the measurement of metal-contaminated silicate-based soils (Rouillon and Taylor, 2016).

Instrument detection limits, analytical precision, sample homogeneity and recoveries of each element are presented in Table 1. Analytical precision was determined by the relative standard deviation (RSD) of

Table 1
Summary of the limits of detection, analytical precision, sample homogeneity and recoveries for pXRF.

	Ti	Cr	Mn	Fe	Cu	Zn	As	Cd	Pb
pXRF									
Limit of detection	[c]	8	9	[c]	4	5	3	2	3
Analytical precision[a] (%)	<1	3	<1	<1	2	<1	7	9	2
Analytical precision[b] (%)	<1	1	<1	<1	1	<1	7	12	<1
Sample homogeneity (%)	2	5	1	<1	2	<1	7	10	1
Mean CRM recovery (%)	101	102	102	100	108	99	106	103	99

[a] Relative standard deviation of reference material suite.
[b] Relative standard deviation of soil samples.
[c] Limits of reporting were not calculated for Ti and Fe as no CRM values between 3 and 10 times the expected manufacturer detection limit were present in the CRM suite.

samples (n = 18) analyzed in triplicate (Table 1), while soil (n = 7) homogeneity (RSD) was measured by triplicate preparation and analysis.

2.2.2. In-vitro Pb bio-accessibility

Spatially diverse soil samples with a range of total Pb concentrations (n = 12) were digested using the US EPA (2012) method for in-vitro Pb bio-accessibility on the <180 μm soil fraction (Horowitz, 1991; Youn et al., 2016). Soil (~1 g) was digested in 100 ml 0.4 M glycine in de-ionized water adjusted to pH 1.5 using hydrochloric acid (HCl, Reagent Grade, Sigma Aldrich) and analyzed for total Pb on the National Measurement Institute's (North Ryde, Sydney) Agilent 7900 ICP-MS, with a limit of detection (LOR) of 0.5 mg/kg. All blanks were <0.5 mg/kg and laboratory control spikes were between 90 and 130%. Relative percent difference for replicate analysis (n = 2) was <20%. Sample duplicate analysis (n = 1) had an RSD < 20%.

2.2.3. Soil Pb isotopic compositions

To understand potential sources of soil metal contaminants, Pb isotopic compositions were determined for soils with a range of concentrations and locations, slag samples and reference ore specimens (Broken Hill and Wallaroo mine galena) (n = 18). Broken Hill galena was used as an end-member due to its prolific use in commercial and industrial commodities (Gulson et al., 2004). Wallaroo galena was used as a reference specimen as the copper ore processed at the Wallaroo Copper Company smelter was often co-associated with galena deposits as impurities in the host orebody. Samples were extracted using an aqua regia (HNO$_3$/HCl) digestion to mobilize the labile Pb bound to the soil matrix (Ayuso et al., 2013; Civitillo et al., 2016; Das et al., 2016; Gallego et al., 2016). Following digestion, the samples was centrifuged and the supernatant filtered using a 0.45 μm Minisart syringe filter. Soils were analyzed on an Agilent 7900 ICP-MS at the National Measurement Institute following the method and instrument conditions detailed previously in Kristensen and Taylor (2016). Measurement values were collected for ^{202}Hg, ^{204}Pb, ^{206}Pb, ^{207}Pb and ^{208}Pb and then corrected for variation based on blank values and the effect of ^{202}Hg on ^{204}Pb. Samples were bracketed during analysis with NIST 981 SRM (certified values: ^{206}Pb/^{204}Pb: 16.94, ^{206}Pb/^{207}Pb: 1.09, ^{208}Pb/^{207}Pb: 2.37). This method for Pb isotope ratio quantification reports ^{204}Pb/^{206}Pb: 0.0590 ± 0.0005, ^{207}Pb/^{206}Pb: 0.915 ± 0.004 and ^{208}Pb/^{206}Pb: 2.168 ± 0.009 as a maximum uncertainty for NIST 981 (Kristensen et al., 2016).

2.2.4. Soil mineralogy

To explore the mineralogy of contaminants in public and private soils (n = 9), heavy mineral separation was conducted on the <180 μm sieved fraction for soils from a range of metal(loid) concentrations and locations around the city, following established methods (Ettler et al., 2016).

The phase composition of the samples (n = 9) was assessed by X-ray powder diffraction analysis (XRPD) using a PANalytical X'Pert Pro diffractometer with an X'Celerator detector (PANalytical, the Netherlands) (analytical conditions: CuKα radiation at 40 kV and 30 mA, 2theta range 2–80°, step 0.02°, counting time 150 s per step). The XRPD pattern was analyzed using X'Pert HighScore Plus 3.0 software coupled to the Crystallography Open Database (COD) (Gražulis et al., 2012). Relative abundances of phases were estimated from XRPD patterns using the relative intensity ratio (RIR) method.

Heavy mineral fractions, prepared as polished sections, were examined under a Leica DM LP polarizing microscope (Leica, Germany) followed by an automated scanning electron microscope (TIMA 3LM, TESCAN Integrated Mineral Analyzer, Czech Republic) operating at 25 keV using a 'dot-mapping' mode method (dot spacing of 2 μm). The integrated images were then used to identify metal(loid)-bearing particles and their distribution.

Particles, from two representative samples from private land with the highest metal(loid) content, were examined using a scanning electron microscope (SEM; TESCAN VEGA3 XM, Czech Republic operating at 20 kV) equipped with an energy dispersion spectrometer (EDS; Quantax 200 X-Flash 5010, Bruker, Germany).

2.2.5. Soil polycyclic aromatic hydrocarbon concentrations

Approximately 1 g of the <180 μm fraction was mixed with anhydrous sodium sulfate (Na$_2$O$_4$S, Reagent Grade, Sigma Aldrich). The sample was then extracted in 1:1 dichloromethane (CH$_2$Cl$_2$, Reagent Grade, Sigma Aldrich) and acetone (C$_3$H$_6$O, Reagent Grade, Sigma Aldrich) and then concentrated prior to analysis on an Agilent 5975 gas chromatography mass selective detector (GC-MSD) at the National Measurement Institute, North Ryde. The instrument was operated in selected ion monitoring mode for 15 PAHs (naphthalene, acenaphthylene, acenaphthene, fluorene, phenanthrene, anthracene, fluoranthene, pyrene, benz(a)anthracene, chrysene, benzo(b)&(k)fluoranthene, benzo(a)pyrene, indeno(1,2,3-cd)pyrene, dibenzo(a,h)anthracene and benzo(g,h,i)perylene). All PAHs have a LOR of 0.5 mg/kg except for

Table 2
Newcastle city (Australia) soil element concentrations (mg/kg) (pXRF derived) for public spaces in addition to median soil element concentrations for each sampling zone. Complete dataset is presented in Supplementary data 2.

	Ti	Cr	Mn	Fe[a]	Cu	Zn	As	Cd	Pb
Private spaces									
n detected	67	67	67	67	67	67	67	11	67
Minimum	2520	54	120	1.31	44	140	8	3	42
25th percentile	4090	96	600	2.38	130	740	21	4	570
Median	5180	128	790	3.36	180	1190	35	5	1140
75th percentile	6210	179	1240	4.50	300	2070	63	6	1770
Maximum	12,200	2400	3600	16.0	1040	8570	283	9	1.16[a]
Mean	5160	190	1020	4.00	252	1690	56	5	1630
NEPM (2013) HIL-A	No value	100 (VI)	3000	No value	7000	8000	100	20	300
n > guideline	–	[b]	2	–	0	1	8	0	59
% > guideline	–	[b]	4%	–	0	2%	12%	0	88%
Public spaces									
n detected	103	100	100	103	103	103	103	13	103
Minimum	1670	38	180	1.36	34	96	5	3	14
25th percentile	3870	76	600	2.43	70	270	12	4	120
Median	4660	92	920	3.00	110	550	22	6	280
75th percentile	5390	140	1540	4.11	240	1230	44	11	617
Maximum	14,760	710	4490	17.1	1170	1.2[a]	380	16	4650
Mean	4850	120	1230	3.67	180	1120	37	7	550
NEPM (2013) HIL-A	No value	100 (VI)	3000	No value	7000	8000	100	20	300
n > guideline	–	[b]	8	–	0	2	5	0	45
% > guideline	–	[b]	8%	–	0%	2%	5%	0%	44%
Median per zone (public spaces)									
Zone 1 (n = 29)	4650	140	1450	3.99%	170	980	34	6	500
Zone 2 (n = 19)	5130	140	1810	4.34%	330	1860	44	6	900
Zone 3 (n = 10)	4490	85	750	2.75%	100	340	12	<LOD	170
Zone 4 (n = 25)	5120	92	670	2.65%	74	270	15	3	130
Zone 5 (n = 20)	4240	77	730	2.56%	78	410	16	<LOD	230

– Cannot be calculated due to the absence of a NEPM (2013) HIL.
[a] Concertation presented as wt%.
[b] Indicates that the soil NEPM (2013) HIL is based on element species rather than total concentration, this analysis was not conducted in this study and cannot be calculated. LOD indicates analytical limit of detection.

Table 3
Soil toxicity equivalence factor (TEF) transformed PAH concentrations for Newcastle city (Australia) surface soil samples.

Sample	x co-ordinate	y co-ordinate	TEF PAH 1	TEF PAH 2	TEF PAH 3	TEF PAH 4	TEF PAH 5	TEF PAH 6	TEF PAH 7	$\sum$ TEF PAH
Zone 5 S1	151.765942	-32.935172	0.08	0.0068	0.14	1.0	0.0061	***	0.0076	1.2
Zone 5 S4	151.751481	-32.936583	0.35	0.035	0.69	5.2	0.029	0.57	0.034	**6.9**
Zone 5 S5	151.755347	-32.931136	0.15	0.015	0.31	2.2	0.014	***	0.016	2.7
Zone 2 S1	151.765858	-32.91974	0.24	0.021	0.45	3.3	0.02	***	0.024	**4.1**
Zone 2 S2	151.765405	-32.914048	0.20	0.020	0.42	2.7	0.019	***	0.022	**3.4**
Zone 2 S2**	151.765405	-32.914048	0.23	0.022	0.45	3.2	0.020	***	0.024	**3.9**
Zone 2 S3	151.764169	-32.909803	0.061	0.006	0.15	0.96	0.0072	***	0.0089	1.2
Zone 2 S4	151.766314	-32.910977	0.40	0.038	0.73	5.4	0.031	0.70	0.035	**7.3**
Zone 1 S5	151.746816	-32.900268	0.20	0.020	0.44	2.9	0.020	***	0.025	**3.6**
Zone 1 S2	151.750378	-32.914897	0.18	0.020	0.43	2.8	0.018	***	0.020	**3.5**
Zone 1 S4	151.752958	-32.910561	0.17	0.018	0.37	2.7	0.016	***	0.020	**3.3**
Zone 1 S7	151.734307	-32.891691	0.73	0.075	1.4	9.8	0.061	1.4	0.076	**13.5**

TEF PAH: 1 - Benz(*a*)anthracene, 2 – Chrysene, 3 - Benzo(*b*)&(*k*)fluoranthene, 4 - Benzo(*a*)pyrene, 5 - Indeno(1,2,3-*cd*)pyrene, 6 - Dibenzo(*a,h*)anthracene, 7 - Benzo(*g,h,i*)perylene.
All concentrations in mg/kg.
Concentrations in bold exceed the NEPM (2013) HIL for TEF transformed PAH (3 mg/kg).
Cells denoted with *** cannot be calculated as the non-transformed data was <LOR.
Sample marked with ** is a field duplicate.

benzo(*b*)&(*k*)fluoranthene which has an LOR of 1 mg/kg. Laboratory blanks contained <LOR for each analyte and laboratory control spikes were 94–130% for all analytes.

2.3. Data analysis

Inorganic elemental concentrations were benchmarked against Australian Health Investigation Levels for residential soils (HIL-A) (NEPM, 2013, Table 2). The NEPM (2013) identifies eight carcinogenic PAHs categories (reported here as seven PAHs categories as benzo(*b*)&(*k*)fluoranthene were not separated in the analysis method): benz(*a*)anthracene, chrysene, benzo(*b*)&(*k*)fluoranthene, benzo(*a*)pyrene, indeno(1,2,3-*cd*)pyrene, dibenzo(*a,h*)anthracene and benzo(*g,h,i*)perylene). The toxicity of these eight PAHs are weighted using a toxicity equivalence factor (TEF) relative to the most toxic PAH benzo(*a*)pyrene, the HIL for the sum of these weighted PAHs is 3 mg/kg (Table 3).

3. Results and discussion

3.1. Soil metal(loid) concentrations

Newcastle was divided into five soil sampling zones to characterize different land uses across the city (Fig. 1). Within these zones, public and private space surface soils were analyzed. A summary of surface soil metal(loid) concentrations is presented in Fig. 1 and Table 2, with the complete data set provided in Supplementary data.

Public space surface soils – The greatest concentrations of Fe, Pb and Zn were detected in the Zone 1 and Zone 2 sampling areas (Fig. 1, Table 2). Soil Fe concentrations were >17 wt% in soils of the Zone 2 sampling area (Fig. 1, Table 2). Soil Pb concentrations were detected at a maximum of 4650 mg/kg (median: 280 mg/kg, n = 103) with the greatest median Pb concentrations in Zone 2 (median: 900 mg/kg, n = 19) followed by Zone 1 (median: 500 mg/kg, n = 29). Zinc concentrations were detected at a maximum of 1.2 wt% in Zone 1 (Fig. 1). The Zone 2 sampling area had the greatest median concentration of soil Zn (1860 mg/kg) (Fig. 1, Table 2). All elements of interest (Table 2), except Ti, had the highest median concentration in Zones 1 and 2. Titanium (n = 103; median: 4830 mg/kg; max: 14,760 mg/kg) is predominantly a geogenic element and had no clear spatial concentration pattern, however, concentration spikes were detected across the city.

Private (residential) space surface soils – Surface soil samples collected from private gardens were markedly more contaminated than those in public spaces (Table 2). Soil Fe was detected with a maximum of 16 wt% in Zone 1 with a median across all sample zones of 3.36 wt% (n = 67). Soil Pb was detected up to a maximum concentration of 1.16 wt% (Zone 1, Fig. 1) (median: 1140 mg/kg, n = 67). The maximum

Zn concentration detected (8570 mg/kg) was in Zone 1 (Fig. 1; Table 2). Private soils contained a median Zn concentration of 1190 mg/kg. Over 90% of homes exceeded the 300 mg/kg Australian soil Pb HIL-A (NEPM, 2013), with As, Mn and Zn exceeding their respective HIL-A values at 30%, 9% and 4% of homes (Table 2). Soil samples were not collected from private spaces in Zone 3 and 4 where high-density housing and ground surface cover limited access to soil.

Soil metal(loid) concentrations from depth profiles in Newcastle are presented in Fig. 2 and in Supplementary data 1. Subsurface soils collected from depth profiles within the urban areas (profiles a–d, Fig. 1) showed that metal(loid) concentrations did not necessarily decrease with depth (Fig. 2, panels a–d). Soil metal(loid) concentrations remain at ~100 mg/kg for Mn, Pb and Zn at 30 cm in depth profile a, while all other depth profiles (b–c, Fig. 2) have concentrations > 100 mg/kg for all metal(loid)s. Soil depth profile b had Pb concentrations > HIL-A of 300 mg/kg (NEPM, 2013); until >10 cm depth. Soil depth profile c showed an increase in soil metal(loid) concentration to depth, with Mn concentrations (1430 mg/kg) at 30 cm depth double surface values (700 mg/kg) (Fig. 2). Soil Pb concentrations in profile 3 also remained above the HIL-A (300 mg/kg; NEPM, 2013) at 30 cm depth. Other metal(loid)s not presented in Fig. 2, but reported in Supplementary data 1, show that concentrations also increase with depth (e.g. Fe: 2.29 wt% at surface; 3.79 wt% at 30 cm depth) implying that profile c likely occupies a brownfield site now repurposed as a parkland. By contrast two additional soil depth profiles from remnant bushland (Figs. 1 and 2, e–f) showed a clear decrease in metal(loid) concentrations with depth. These data are comparable to uncontaminated soil concentrations at depth from similar studies of industrial cities (e.g. Rouillon et al., 2013, Mn: ~100 mg/kg; Pb: <5 mg/kg; Zn: ~30 mg/kg). The data show that surface soil metal(loid)s from Newcastle have been enriched significantly by anthropogenic sources.

3.2. Potential source(s) of inorganic soil contaminants

It is well documented that Cu smelter waste, and more recently, steel smelter waste was used prolifically around the Newcastle city area as landfill and stabilization material (NMH, 1948a; NMH, 1948b; NMH, 1949b; NS, 1926; NMH, 1925; SA, 1951; SMH, 1948; The Australasian, 1905; TNC, 1950). Much of this material may have contained Broken Hill Pb ore due to the movement of this ore through the Newcastle Ports from BHP to the Sulphide Company smelter (later the Pasminco Cockle Creek Smelter) at Boolaroo (Petersburg Times, 1901; PPR, 1904; Quorn Mercury, 1900). The Sulphide Company also contributed large volumes of smelter waste for capital works (Gulson et al., 2004; Morrison, 2003; Morrison and Gulson, 2007; Morrison et al., 2016).
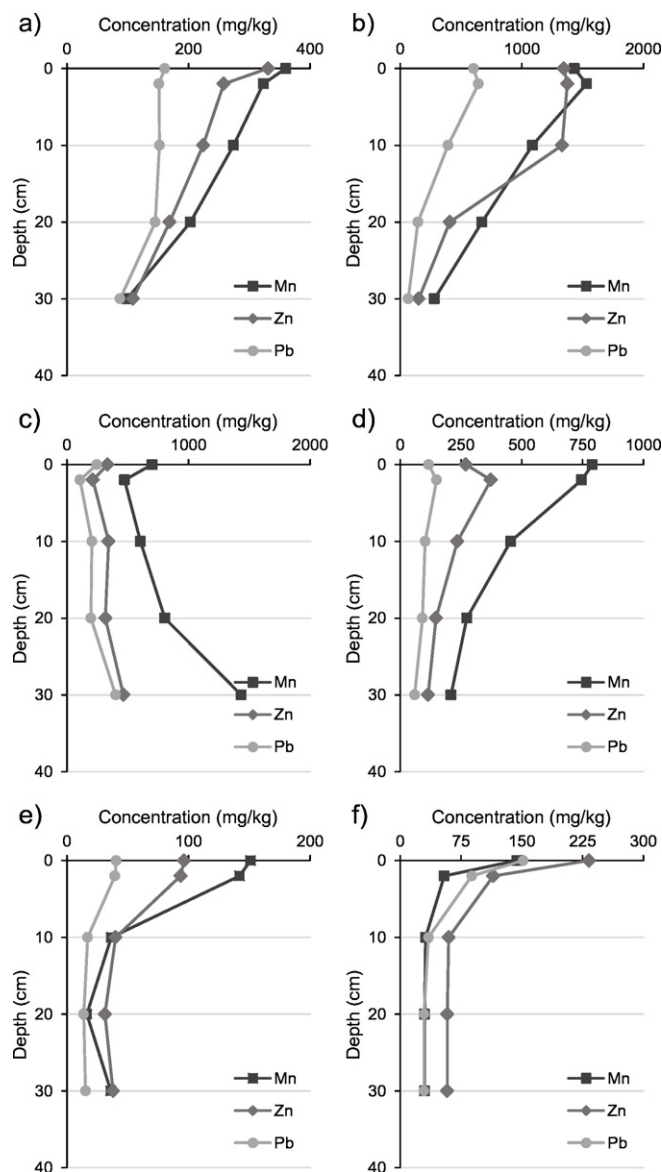
Fig. 2. Soil depth profiles from urban areas (a–d) and remnant bushland (e–f) in Newcastle city (Australia) displaying Mn, Pb and Zn soil concentrations. Complete data and site locations are provided in Supplementary data 1.

This study's bulk mineralogical investigation of soils showed that high-temperature silicates (clinopyroxenes, olivines and glass) typically originating from smelting industry, as well as smelter-derived oxides (spinels) were present in the majority of the samples (Supplementary data 4). All the samples contained geogenic/pedogenic heavy minerals such as zircon, Ti-, Fe- and Al-bearing oxides in addition to traces of quartz and other geogenic minerals. No metal(loid)-bearing phases were detected by XRPD indicating that contaminants are bound in trace phases in the soil materials (Supplementary data 4).

Fe and Mn oxides were the most common metal-bearing phases in soils, with Fe oxides containing high Pb levels (up to 27.3 wt% PbO) (Fig. 3b, c, e, f). The occurrence of smelter-derived slag-like particles, possibly windblown from slag dumps (Fig. 3a, c, e, f, i) and rounded particles characteristic of quenched melt droplets from the smelter emissions (Fig. 3b) implies they are derived from smelting emissions. Metal-bearing droplets in slag particles corresponded to Cu sulfides; slag silicates and glass also containing Cu and Zn are characteristic of Cu smelting waste materials (Ettler et al., 2009; Ettler et al., 2016). By contrast, mine-derived sulfides (commonly identified with weathering

rims) were relatively rare in the studied soils (Fig. 3d). Lead phosphates (Fig. 3f, h, i), arsenates (Fig. 3f) and sulfates (Fig. 3h) were common. Some of these form solid solutions (mimetite – pyromorphite; Fig. 3h) or are associated to similar phases (anglesite – barite) (Fig. 3h). Given that these phases are relatively insoluble, the Pb release from these compounds in aqueous environments would be minimal. Rare particles of Sn oxides were also observed (Fig. 3f) with weathering rims enriched in metal(loids) including Pb, Sb and Zn. Interestingly, metals (mainly Pb and Zn) were bound in Fe and Mn oxides formed as weathering products on particles (e.g. Fig. 3b, c), indicating contaminants can be absorbed from surrounding soil during the formation of secondary Fe-Mn oxides.

Lead isotopic compositions were used in this study to delineate potential contaminant sources. The Pb isotopic compositions of soils and reference samples (galena and slag) are presented in Fig. 4 and Supplementary data 3. Surface soils from public and private spaces (n = 8) have similar loosely clustered Pb isotopic compositions (range: $^{208}Pb/^{207}Pb$: 2.345–2.411, $^{206}Pb/^{207}Pb$: 1.068–1.312). Lead isotopic compositions of soils collected from depth profiles (n = 3) within the urban area (profiles b, c, d; Fig. 1) fall within the range of Pb isotopic compositions of surface soils in public and private spaces (range: $^{208}Pb/^{207}Pb$: 2.370–2.406, $^{206}Pb/^{207}Pb$: 1.093–1.234). Lead isotopic compositions from soil collected from the depth profile in the remnant bushland (profile e; Fig. 1; n = 1) are more radiogenic and outside of the range of urban surface soils ($^{208}Pb/^{207}Pb$: 2.489, $^{206}Pb/^{207}Pb$: 1.198) (Fig. 4, Supplementary data 3). Lead isotopic compositions for the two slag samples reveal divergent Pb isotopic compositions. A black glassy material similar to non-ferrous smelter slag as identified in other studies (Morrison and Gulson, 2007; Piatak et al., 2015) was less radiogenic than surface soils ($^{208}Pb/^{207}Pb$: 2.319, $^{206}Pb/^{207}Pb$: 1.044) (Fig. 4, Supplementary data 3). A second slag deposit that was more similar to ferrous smelter slag as identified in other studies (Piatak et al., 2015) contained more radiogenic Pb than surface and depth profile soils ($^{208}Pb/^{207}Pb$: 2.543, $^{206}Pb/^{207}Pb$: 1.318) (Fig. 4, Supplementary data 3). The Wallaroo Mine copper ore that was smelted at the site prior to Newcastle BHP was co-associated with galena Pb ore ($^{208}Pb/^{207}Pb$: 2.640, $^{206}Pb/^{207}Pb$: 1.477), which has more radiogenic Pb isotopic compositions compared to bushland depth profile soil ($^{208}Pb/^{207}Pb$: 2.489, $^{206}Pb/^{207}Pb$: 1.198) and slag (Fig. 4, Supplementary data 3). Consequently, we used Wallaroo galena Pb isotopic compositions as an end-member for source apportionment analysis. Although the Pb bearing Cu ore associated with the Wallaroo Mine was smelted in large volumes during the early industrial era of Newcastle it appears to have had little influence on soil Pb isotopic compositions (Fig. 4, Supplementary data 3). The other Pb isotopic composition end-member used is the less radiogenic Broken Hill ore ($^{208}Pb/^{207}Pb$: 2.319, $^{206}Pb/^{207}Pb$: 1.044) (Fig. 4, Supplementary data 3).

The Pb isotopic compositions (Fig. 4, Supplementary data 3) showed an enrichment of public and private space soils (Fig. 4) by the distinct Broken Hill Pb isotope signature ($^{208}Pb/^{207}Pb$: 2.319, $^{206}Pb/^{207}Pb$: 1.044). Enrichment of public and private soils less radiogenic Pb sources suggests an introduction of Broken Hill type ore bearing material (e.g. black glassy slag waste and fill material) into the Newcastle city environment. Leaded petrol and paint are also potential contributors to Pb in the surface soils of the urban environment (Datko-Williams et al., 2014; Kristensen, 2015; Laidlaw et al., 2012; Mielke et al., 1983; Mielke and Reagan, 1998; Mitchell et al., 2014; Zahran et al., 2013). The Pb isotopic ratios of the soils derived from ICP-MS do not allow discrimination between these tightly clustered sources (Fig. 4). However, despite this limitation, the data show clearly that Pb sources match closely the Broken Hill ore signature in urban soils.

3.3. Soil polycyclic aromatic hydrocarbon concentrations

Soil PAH concentrations are presented in Fig. 1 and Supplementary data 2. Soil samples (n = 12) contained 12 of the 15 target PAH
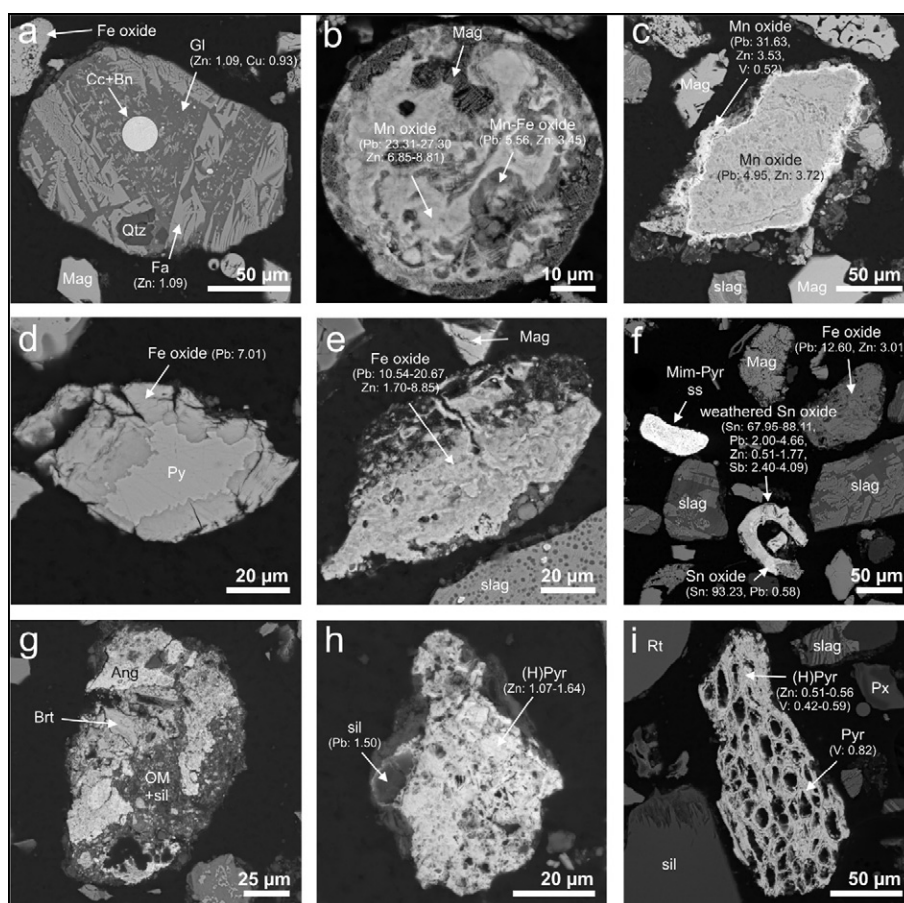
Fig. 3. Scanning electron micrographs in back-scattered electrons (BSE) of representative metal(loid)-bearing particles from two samples (PRS3D and PRS4C) from Newcastle city soils (Australia). Complete data available in Supplementary data 4. a) Smelter slag particle composed of Fe-olivine (fayalite), metal-bearing glass and symplectitic inclusions of chalcocite and bornite (PRS3D); b) Slag-like particle originating probably from smelter dust emissions composed of magnetite sub-micrometric dendrites and newly-formed Mn- and Mn-Fe oxides resulting from alteration process in soil (PRS4C); c) Mn oxide particle particularly rich in metals associated with slag particles and magnetite grains (PRS3D); d) Weathered pyrite grain with Fe-oxide rim (PRS3D); e) Metal-bearing Fe oxide associated with slag and magnetite particles (PRS3D); f) Mimetite-pyromorphite solid solution (ss) associated to weathered Sn-oxide and Fe-oxides particles, slag and magnetite grains (PRS3D); g) Complex intergrowth of barite and anglesite with organic matter and unidentified silicate material (PRS3D); h) (hydroxyl)pyromorphite grain associate with unidentified Pb-bearing silicate (probably slag glass) (PRS3D); i) Sponge-like particle composed of hydroxylpyromorphite and pyromorphite associated to rutile and smelter-derived silicates (slag) (PRS4C). The metal(loid) concentrations obtained by EDS are expressed in wt% of oxides. Abbreviations: Ang – anglesite (PbSO$_4$), Bn – bornite (Cu$_5$FeS$_4$), Brt – barite (BaSO$_4$), Cc – chalcocite (Cu$_2$S), Fa – fayalite (Fe$_2$SiO$_4$), Gl – glass (slag), (H)Pyr – hydroxypyromorphite (Pb$_5$(PO$_4$)$_3$OH), Mag – magnetite (Fe$_3$O$_4$), Mim - mimetite (Pb$_5$(AsO$_4$)$_3$Cl), OM – organic matter; Px – pyroxene ((Ca,Fe,Mg)$_2$Si$_2$O$_6$), Py – pyrite (FeS$_2$), Pyr – pyromorphite (Pb$_5$(PO$_4$)$_3$Cl), Qtz – quartz (SiO$_2$), Sil – unidentified silicate; Rt – rutile (TiO$_2$).
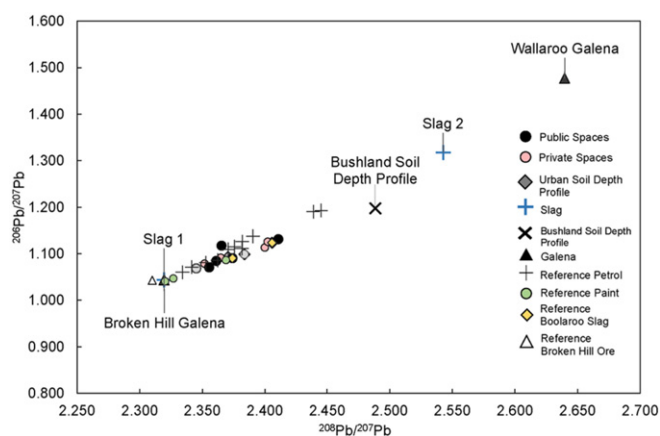
Fig. 4. Lead isotopic compositions of Newcastle city (Australia) soils and slag and galena from Broken Hill and Wallaroo Mines analyzed in this study. Standard deviation from repeat analysis (10 analyses) of one sample: ^{208}Pb/^{207}Pb: 0.004, ^{206}Pb/^{207}Pb: 0.004. Comparison is made to reference Pb isotopic compositions from the nearby Sulphide Corporation's Boolaroo smelter slag (Gulson et al., 2004), Broken Hill ore galena (Gulson, 1984), petrol and paint values (Gulson et al., 1982; Laidlaw et al., 2014).

compounds (Supplementary data 2). The carcinogenic compound benzo(a)pyrene was detected in all samples with the maximum concentration in Zone 1 (9.8 mg/kg; Fig. 1). Nine samples exceeded the Australian HIL-A guideline (3 mg/kg) for benzo(a)pyrene TEF transformed PAHs (Table 3, Fig. 1, max - 13.5 mg/kg). The maximum TEF transformed PAH concentration (13.5 mg/kg) was detected in Zone 1 sampling area.

3.4. Potential health impacts of soil contamination

Soils in Newcastle are contaminated by a range of metal(loid)s and PAHs. While there is strong evidence to link the soil metal(loid) concentrations to the legacy industrial activities of the city, the source of PAHs in Newcastle is unclear. Steel manufacturing (Khaparde et al., 2016; Song et al., 2015; Yang et al., 2002), coal transport (Huang et al., 2013; Wang et al., 2016), and incomplete combustion of motor vehicle emissions (Jedrychowski et al., 2015; Perer et al., 2006) are known to contribute PAHs to the soil environment. Regardless of the source, recent studies have demonstrated a link between pre-natal and early life exposure to PAHs (Huang et al., 2013) and a range of cancers (Lemieux et al., 2015; Mordukhovich et al., 2016; Perer et al., 2006; Zhang et al., 2016).

Exposure to PAHs in the Newcastle soil environment, combined with the metal(loid) contaminants is likely to generate a significant burden of disease.

Blood Pb (and other metals) analysis of the Newcastle population would be one determinant of exposure to contaminated soils in Newcastle. Unfortunately, no such data exists. Given the paucity of blood Pb (and other metals) data, surrogate indicators are used here to predict the potential health impacts of Pb contaminated soils in the city. Our in-vitro bio-accessibility analysis (n = 11) shows that the Pb found in soils would be subject to absorption following ingestion of soils from the study area (Table 4). This is not surprising given that the Pb-bearing Fe- and Mn-oxides identified in Fig. 3b and c are known to be susceptible to dissolution under acidic conditions. Moreover, the in-vitro bio-accessible Pb concentrations indicate a potential burden of disease associated with Newcastle's soil Pb concentrations, which could be better quantified with a childhood blood Pb survey in Newcastle city linked to participant's home soil and dust metal analysis.

3.5. Managing environmental contaminants in Newcastle city

Some information is available to landowners about the potential risk of environmental contamination in Newcastle, but it is not extensive and it is often site specific. In addition to sites being listed on the NSW Environment Protection Authority's (NSW EPA) list of notified contaminated sites (NSW EPA, 2016) some properties in Carrington have a certificate issued under section 149 of the *Environmental Planning and Assessment Act 1979* (NSW) advising purchasers:

> Land history information indicates that the subject land may be within an area which was once low lying and may have been filled. Limited investigation indicates that the filling material may contain ballast and industrial slag which contains some heavy metals including lead. The Council does not hold information which allows it to say whether or not the subject land contains such filling material and purchasers should make their own enquiries in this respect. If the land does contain such filling material this should be taken into account in the use and the development of the property. Soil sampling and remediation may be required for the further development of the land.

To address the absence of site-specific contamination information, soil metal screening programs such as VegeSafe (Rouillon et al., 2016) could be employed across the city to help inform homeowners of extant soil metal(loid) contamination on their property and the potential associated risks. Such information can be used by homeowners to initiate mitigation strategies, including: engagement of professional trained contractors to remediate soils where appropriate; using raised garden beds for food growing; removing and replacing soils in areas regularly visited by children and pets.

3.6. Industry, smelting and development in global urban cities - environmental implications

This study demonstrates the extensive environmental contamination legacy that can be created by a long history of manufacturing, processing and smelting along with inappropriate waste disposal in urban environments. In 2011, it was estimated that around 30% of the global feedstock for ferrous ore processing was discarded generating ~550 million tons of waste slag (Van Oss, 2011). The waste material produced from manufacturing industries, typically rich in a range of environmental contaminants, is often discarded haphazardly in the environment, leading to problematic brownfield sites, requiring costly environmental clean-up (Gallego et al., 2016).

4. Conclusions

This study details a significant potential health risk associated with environmental metal(loid) and PAH contamination of soils in the industrial city of Newcastle, Australia. Surface soils collected from public (roadside verges and parks) and private (homes) spaces (n = 170) show that a range of metal(loid)s are present in the soils above their relevant Australian Health Investigation Level (HIL) concentrations. Lead was the most common contaminant detected in the city soils with a median concentration of 1140 mg/kg in private space soils. Deep soil metal(loid) concentrations across the city were also elevated indicating contamination was laterally and vertically pervasive. In-vitro bio-accessibility analysis of Pb in soils (maximum Pb concentration: 5190 mg/kg; 45% Pb bio-accessibility) revealed these were readily available to the gastric system. Soil Pb isotopic compositions (range: $^{208}Pb/^{207}Pb$: 2.345–2.411, $^{206}Pb/^{207}Pb$: 1.068–1.312) show that the anthropogenic contamination was sourced from a low radiogenic source, with a Broken Hill type Pb orebody ($^{208}Pb/^{207}Pb$: 2.319, $^{206}Pb/^{207}Pb$: 1.044) being the most likely origin. Examination of soil mineralogy, particularly the rounded quenched droplet particles extracted during heavy mineral separation (Fig. 3), indicates that Pb and soil metal(loid) contaminants are derived predominantly from smelter emissions and industrial waste slag. An additional burden of contamination in the city soils comes from elevated levels of PAH compounds, typically associated with coal, ferrous metal smelting and fossil fuels, with 75% of samples (n = 12) analyzed exceeding the Australian HIL-A guideline for benzo(*a*)pyrene TEF transformed PAHs.

Source assessment of the environmental contamination indicates that historic and legacy Cu and steel smelting industries in the city have contributed substantially to the contamination of soils. This study highlights the health risks faced by communities residing in industrial locations and demonstrates the 'need to know' so that individuals can protect themselves from unnecessary and potentially toxic exposures.

Acknowledgements

Table 4
In-vitro bio-accessible soil Pb concentrations.

Sample	In-vitro bio-accessible Pb (mg/kg)	Total Pb (mg/kg)	% bio-accessible[a]
PRS10B	5000	7640	65
PRS7A	732	2830	26
PRS3D	1670	3420	49
Zone 1 S7	1730	1550	112
Zone 2 S17	1410	2770	51
PRS8C	282	1060	27
Zone 1 S20	972	2060	47
Zone 1 S9	607	4650	13
PRS4C	5190	11,570	45
Zone 2 S4	1350	2550	53
Zone 2 S4[b]	1340	2550	52
NIST2586 (500 mg/kg)	156		31
BLK	<0.5		-
CAL-24 (10 ppm)	10		-

NIST2586 is a Pb paint contaminated soil used to assess the extraction efficiency of the in-vitro bio-accessibility method.
BLK = analysis blank.
CAL-24 = 10 ppm 12-element standard reference material used during IPC-MS analysis.
- not applicable.
[a] Calculated from pXRF total.
[b] Denotes field duplicate sample.

Appendix A. Supplementary data

Supplementary data to this article can be found online at http://dx.doi.org/10.1016/j.scitotenv.2017.01.053.

References

Albuquerque, M., Coutinho, M., Borrego, C., 2016. Long-term monitoring and seasonal analysis of polycyclic aromatic hyrdocarbons (PAHs) measured over a decade in the ambient air of Porto, Portugal. Sci. Total Environ. 543, 439–448.

Ayuso, R.A., Foley, N.K., Seal II, R.R., Bove, M., Civitillo, D., Cosenza, A., Grezzi, G., 2013. Lead isotope evidence for metal dispersal at the Callahan Cu–Zn–Pb mine: Goose Pond tidal estuary, Maine, USA. J. Geochem. Explor. 126, 1–22.

BHP Co. LTD, 1949. Progress: Outlining the Main Factors in the Establishment and Growth of the Newcastle Steel Works, and Giving Details of the Operations Required in Iron and Steel Manufacture. The Broken Hill Co. LTD, Melbourne.

Canfield, R.L., Henderson, C.R., Cory-Slechta, D.A., Cox, C., Jusko, T.A., Lanphear, B.P., 2003. Intellectual impairment in children with blood lead concentrations below 10 μg per deciliter. N. Engl. J. Med. 348, 1517–1526.

Chen, H., Teng, Y., Lu, S., Wang, Y., Wang, J., 2015. Contamination features and health risk of soil heavy metals in China. Sci. Total Environ. 512, 143–153.

Civitillo, D., Ayuso, R.A., Lima, A., Albanese, S., Esposito, A., Cannatelli, C., De Vivo, B., 2016. Potentially harmful elements and lead isotopes distribution in a heavily anthropized suburban area: the Casoria case study (Italy). Environ. Earth Sci. 75, 1325.

Csavina, J., Field, J., Taylor, M.P., Gao, S., Landázuri, A., Betterton, E.A., Saez, A.E., 2012. A review on the importance of metals and metalloids in atmospheric dust and aerosol from mining operations. Sci. Total Environ. 433, 58–73.

Dames and Moore, 1994. Review and Summary of Available Data Soil Lead Distribution around Boolaroo Smelter for Pasminco Metals – Sulphide PTY LTD. Dames and Moore.

Das, A., Krishna, K., Kumar, R., Das, A., Sengupta, S., Ghosh, J.G., 2016. Tracing lead contamination in foods in the city of Kolkata, India. Environ. Sci. Pollut. Res. 23, 22454–22466.

Datko-Williams, L., Wilkie, A., Richmond-Bryant, J., 2014. Analysis of U.S. soil lead (Pb) studies from 1970 to 2012. Sci. Total Environ. 468, 854–863.

Dong, C., Taylor, M.P., Kristensen, L.J., Zahran, S., 2015. Environmental contamination in an Australian mining community and potential influences on early childhood health and behavioural outcomes. Environ. Pollut. 207, 345–356.

Ettler, V., Johan, Z., Kříbek, B., Šebek, O., Mihaljevič, M., 2009. Mineralogy and environmental stability of slags from the Tsumeb smelter, Namibia. Appl. Geochem. 24, 1–15.

Ettler, V., Johan, Z., Kříbek, B., Veselovský, F., Mihaljevič, M., Vaněk, A., Penížek, V., Majer, V., Sracek, O., Mapani, B., Kamona, F., Nyambe, I., 2016. Composition and fate of mine- and smelter-derived particles in soils of humid subtropical and hot semi-arid areas. Sci. Total Environ. 563, 329–339.

Filippelli, G.M., Risch, M., Laidlaw, M.A., Nichols, D.E., Crewe, J., 2015. Geochemical legacies and the future health of cities: a tale of two neurotoxins in urban soils. Elementa 3, 59.

Gallego, J.R., Rodríguez-Valdés, E., Esquinas, N., Fernández-Braña, A., Afif, E., 2016. Insights into a 20-ha multi-contaminated brownfield megasite: an environmental forensics approach. Sci. Total Environ. 563, 683–692.

Gražulis, S., Daškevič, A., Merkys, A., Chateigner, D., Lutterotti, L., Quirós, M., Serebryanaya, N.R., Moeck, P., Downs, R.T., Le Bail, A., 2012. Crystallography Open Database (COD): an open-access collection of crystal structures and platform for world-wide collaboration. Nucleic Acids Res. 40, D420–D427.

Gulson, B.L., 1984. Uranium-lead and lead-lead investigations of minerals from the Broken Hill lodes and mine sequence rocks. Econ. Geol. 79, 476–490.

Gulson, B.L., Mizon, K.J., Korsch, M.J., 1982. Fingerprinting the source of lead in Sydney air using lead isotopes. Publication of Commonwealth Scientific & Indus Res Org, Australia.

Gulson, B.L., Mizon, K.J., Law, A.J., Korsch, M.J., Davis, J.J., Howarth, D., 1994. Source and pathways of lead in humans from the Broken Hill mining community; an alternative use of exploration methods. Econ. Geol. 89, 889–908.

Gulson, B.L., Mizon, K.J., Davis, J.D., Palmer, J.M., Vimpani, G., 2004. Identification of sources of lead in children in a primary zinc-lead smelter environment. Environ. Health Perspect. 112, 52–60.

Gulson, B., Korsch, M., Matisons, M., Douglas, C., Gillam, L., McLaughlin, V., 2009. Wind-blown lead carbonate as the main source of lead in blood of children from a seaside community: an example of local birds as "canaries in the mine". Environ. Health Perspect. 117, 148–154.

Horowitz, A.J., 1991. A primer on sediment-trace element chemistry. second ed. Lewis, Chelsea, Michigan.

Huang, H.B., Chen, G.W., Wang, C.J., Lin, Y.Y., Liou, S.H., Wang, S.K., 2013. Exposure to heavy metals and polycyclic aromatic hydrocarbons and DNA damage in Taiwanese traffic conductors. Cancer Epidemiol. Biomark. Prev. 22, 102–108.

Jedrychowski, W.A., Perera, F.P., Maugeri, U., Majewska, R., Mroz, E., Flak, E., Camann, D., Sowa, A., Jacek, R., 2015. Long term effects of prenatal and postnatal airborne PAH exposures on ventilatory lung function of non-asthmatic preadolescent children. Prospective birth cohort study in Krakow. Sci. Total Environ. 502, 502–509.

Khaparde, V.V., Bhanarkar, A.D., Majumdar, D., Rao, C.V.C., 2016. Characterization of polycyclic aromatic hydrocarbons in fugitive PM10 emissions from an integrated iron and steel plant. Sci. Total Environ. 562, 155–163.

Kristensen, L.J., 2015. Quantification of atmospheric lead emissions from 70 years of leaded petrol consumption in Australia. Atmos. Environ. 111, 195–201.

Kristensen, L.J., Taylor, M.P., 2016. Unravelling a 'miner's myth' that environmental contamination in mining towns is naturally occurring. Environ. Geochem. Health 38, 1015–1027.

Kristensen, L.J., Taylor, M.P., Evans, A.J., 2016. Reply to Gulson's comments on 'tracing changes in atmospheric sources of lead contamination using lead isotopic compositions in australian red wine'. Chemosphere 165, 579–584.

Laidlaw, M.A.S., Zahran, S., Mielke, H.W., Taylor, M.P., Filippelli, G.M., 2012. Re-suspension of lead contaminated urban soil as a dominant source of atmospheric lead in Birmingham, Chicago, Detroit and Pittsburgh, USA. Atmos. Environ. 49, 302–310.

Laidlaw, M.A.S., Zahran, S., Pingitore, N., Clague, J., Devlin, G., Taylor, M.P., 2014. Identification of lead sources in residential environments: Sydney Australia. Environ. Pollut. 184, 238–246.

Lemieux, C.L., Long, A.S., Lambert, I.B., Lundstedt, S., Tysklind, M., White, P.A., 2015. Cancer risk assessment of polycyclic aromatic hydrocarbon contaminated soils determined using bioassay-derived levels of benzo[a]pyrene equivalents. Environ. Sci. Technol. 49, 1797–1805.

Lougheed, T., 2014. Arising from the ashes? Environmental health in Detroit. Environ. Health Perspect. 122, A324–A331.

MDM, 1907. Our Newcastle Letter. Maitland Daily Mercury Tuesday 23 July 1907. Available at:. http://trove.nla.gov.au/newspaper/article/124428751 (accessed 09 January 2017).

Mielke, H.W., Reagan, P.L., 1998. Soil is an important pathway of human lead exposure. Environ. Health Perspect. 106, 217–229.

Mielke, H.W., Anderson, J.C., Berry, K.J., Mielke, P.W., Chaney, R.L., Leech, M., 1983. Lead concentrations in inner-city soils as a factor in the child lead problem. Am. J. Public Health 73, 1366–1369.

Mitchell, R.G., Spliethoff, H.M., Ribaudo, L.N., Lopp, D.M., Shayler, H.A., Marquez-Bravo, L.G., Lambert, V.T., Ferenz, G.S., Russell-Anelli, J.M., Stone, E.B., McBride, M.B., 2014. Lead (Pb) and other metals in New York City community garden soils: factors influencing contaminant distributions. Environ. Pollut. 187, 162–169.

Mordukhovich, I., Beyea, J., Herring, A.H., Hatch, M., Stellman, S.D., Teitelbaum, S.L., Richardson, D.B., Millikan, R.C., Engel, L.S., Shantakumar, S., Steck, S.E., Neugut, A.I., Rossner, P., Santella, R.M., Gammon, M.D., 2016. Polymorphisms in DNA repair genes, traffic-related polycyclic aromatic hydrocarbon exposure and breast cancer incidence. Int. J. Cancer 139, 310–321.

Morrison, A.L., 2003. An assessment of the effectiveness of lead pollution reduction strategies in North Lake Macquarie, NSW, Australia. Sci. Total Environ. 303, 125–138.

Morrison, A.L., Gulson, B.L., 2007. Preliminary findings of chemistry and bioaccessibility in base metal smelter slags. Sci. Total Environ. 382, 30–42.

Morrison, A.L., Swierczek, Z., Gulson, B.L., 2016. Visualisation and quantification of heavy metal accessibility in smelter slags: the influence of morphology on availability. Environ. Pollut. 210, 271–281.

National Environment Protection Measure (NEPM), 2013. National Environment Protection Measure 1999 Schedule B1. Federal Register of Legislative Instruments, Australia.

Newcastle City Council (NCC), 1997. Information sheet industrial filling used in Carrington. Newcastle City Council. Available at:. http://www.newcastle.nsw.gov.au/getattachment/Business/Regulations/Health-safety/Contaminated-Land/Carrington_contaminated_land.pdf.aspx?lang=en-AU (accessed 09 January 2017).

Newcastle City Council (NCC), 2013. Newcastle 2030: Our Vision for a Smart, Liveable and Sustainable City – Newcastle Community Strategic Plan (Revised 2013). The City of Newcastle. Available at:. http://www.newcastle.nsw.gov.au/Council/Our-Responsibilities/Newcastle-2030-Vision-Strategic-Plan (accessed 09 January 2017).

Newcastle City Council (NCC), 2015. Local Planning Strategy - Background Report. The City of Newcastle. Available at:. http://www.newcastle.nsw.gov.au/Newcastle/media/Documents/Strategies,%20Plans%20and%20Policies/Strategies/Local-Planning-Strategy-Background-Report-2015.pdf (accessed 09 January 2017).

NMH, 1902. Sulphide Corporation a Prosperous Year. Solution of a Great Problem. Newcastle Morning Herald Saturday 22 February 1902. Available at:. http://nla.gov.au/nla.news-article135339351 (accessed 09 January 2017).

NMH, 1925. Carrington Council Meeting. Newcastle Morning Herald and Miners' Advocate (Thursday 30 July 1925. Available at: http://trove.nla.gov.au/newspaper/article/137830721?searchTerm=carrington%20council%20meeting&searchLimits=dateFrom=1925-01-01|||dateTo=1925-12-31 accessed 09 January 2017).

NMH, 1948a. Slag Ruins Beach, Says Club Captain. Newcastle Morning Herald Friday 20 August 1948. Available at:. http://nla.gov.au/nla.news-article140356359 (accessed 09 January 2017).

NMH, 1948b. Council Dumped 800 Tons Slag. Newcastle Morning Herald Monday 21 June 1948. Available at:. http://nla.gov.au/nla.news-article134334745 (accessed 09 January 2017).

NMH, 1949a. Rapid Slag Dumping at Stockton. Newcastle Morning Herald Thursday 24 March 1949. Available at:. http://trove.nla.gov.au/newspaper/article/134339600? searchTerm=Rapid%20Slag%20Dumping%20at%20Stockton&searchLimits= (assessed 09 January 2017).

NMH, 1949b. Dumps Scoured for Stone to Fight Erosion. Newcastle Morning Herald and Miners' Advocate Tuesday 5 April 1949. Available at:. http://trove.nla.gov.au/ newspaper/article/134343452?searchTerm=Dumps%20scoured%20for%20stone% 20to%20fight%20erosion&searchLimits= (accessed 09 January 2017).

NS, 1925. Faith and Courage in Newcastle Industries. Newcastle Sun Tuesday 3 November 1925. Available at:. http://trove.nla.gov.au/newspaper/article/163367941? searchTerm=Faith%20and%20Courage%20in%20Newcastle% 20Industries&searchLimits= (accessed 09 January 2017).

NS, 1926. Slag for Road, Stockton Council's Decision, Fullerton Rd Work. Newcastle Sun Wednesday 10 February 1926. Available at:. http://trove.nla.gov.au/newspaper/ article/163396050?searchTerm=Slag%20for%20Road%20Stockton%20Council%E2% 80%99s%20Decision&searchLimits= (accessed 09 January 2017).

NS, 1948. B.H.P. Gift Slag Being Dumped At Stockton. Newcastle Sun Friday 30 July 1948. Available at:. http://nla.gov.au/nla.news-article158263500 (accessed 09 January 2017).

NSW EPA, 2016. List of NSW Contaminated Sites Notified to EPA. (Available at). http:// www.epa.nsw.gov.au/clm/publiclist.htm (accessed 04 January 2017).

Odabasi, M., Bayram, A., Elbir, T., Seyfioglu, R., Dumanoglu, Y., Ornektekin, S., 2010. Investigation of soil concentrations of persistent organic pollutants, trace elements, and anions due to iron-steel plant emissions in an industrial region in Turkey. Water Air Soil Pollut. 213, 375–388.

Parliament of New South Wales, 1999. BHP Newcastle Steelworks Closure. Legislative Assembly Hansard 22 September 1999. Available at:. http://23.101.218.132/prod/web/ common.nsf/V3HHBDay?open&key=19990922 (accessed 09 January 2017).

Perer, A.F.P., Rauh, V., Whyatt, R.M., Tsai, W.-Y., Tang, D., Diaz, D., Hoepner, L., Barr, D., Tu, Y.-H., Camann, D., Kinney, P., 2006. Effect of prenatal exposure to airborne polycyclic aromatic hydrocarbons on neurodevelopment in the first 3 years of life among inner-city children. Environ. Health Perspect. 114, 1287–1292.

Petersburg Times, 1901. Port Pirie Shipping Departures October 27. Petersburg Times Friday 4 October 1901. Available at:. http://trove.nla.gov.au/newspaper/article/ 124969874?searchTerm=Port%20Pirie%20Shipping%20Departures&searchLimits= (accessed 09 January 2017).

Piatak, N.M., Parsons, M.B., Seal II, R.R., 2015. Characteristics and environmental aspects of slag: a review. Appl. Geochem. 57, 236–266.

PPR, 1904. Sailed Shipping Report 5th July. Port Pirie Recorder and North Western Mail (Wednesday 6 July 1904. Available at: http://trove.nla.gov.au/newspaper/article/ 95260908?searchTerm=Shipping%20Port%20Pirie&searchLimits=l- decade=190|||l-year=1904|||l-month=7 accessed 09 January 2017).

Quorn Mercury, 1900a. Port Pirie Shipping Departures. Quorn Mercury Friday 2 November 1900. Available at:. http://nla.gov.au/nla.news-article213625784 (accessed 09 January 2017).

Rouillon, M., Taylor, M.P., 2016. Can field portable X-ray fluorescence (pXRF) produce high quality data for application in environmental contamination research? Environ. Pollut. 214, 255–264.

Rouillon, M., Gore, D.B., Taylor, M.P., 2013. The nature and distribution of Cu, Zn, Hg, and Pb in urban soils of a regional city: Lithgow, Australia. Appl. Geochem. 36, 83–91.

Rouillon, M., Harvey, P.J., Kristense, L.J., George, S.G., Taylor, M.P., 2016. VegeSafe: A community science program measuring soil-metal contamination, evaluating risk and providing advice for safe gardening. Environ. Pollut. http://dx.doi.org/10.1016/j. envpol.2016.11.024.

SA, 1951. Railway Laws Under Fire – Road Slag Delivery. Singleton Argus Friday 22 June 1951. Available at:. http://trove.nla.gov.au/newspaper/article/82758348? searchTerm=Railway%20Laws%20Under%20Fire&searchLimits= (accessed 09 January 2017).

SCT&WA, 1907. Newcastle. South Coast Times and Wollongong Argus Saturday 27 April 1907. Available at:. http://trove.nla.gov.au/newspaper/article/141921919? searchTerm=Melbourne%20and%20Great%20Northern% 20Newcastle&searchLimits= (accessed 09 January 2017).

SM, 1872. Opening of the English and Australian Copper Company's Works New Lambton Newcastle. Sydney Mail and New South Wales Advertiser Saturday 22 June 1872. Available at:. http://trove.nla.gov.au/newspaper/article/13259327 (accessed 09 January 2017).

SMH, 1871a. Hunter River Copper Works: Port Waratah. Sydney Morning Herald Thursday 14 September 1871. Available at:. http://trove.nla.gov.au/newspaper/article/ 18757249 (accessed 09 January 2017).

SMH, 1871b. Copper Smelting Works at Waratah. Sydney Morning Herald Friday 6 October 1871. Available at:. http://trove.nla.gov.au/newspaper/article/13246089 (accessed 09 January 2017).

SMH, 1948. Newcastle Seeks McGirr's Aid. Sydney Morning Herald Tuesday 20 July 1948. Available at:. http://trove.nla.gov.au/newspaper/article/18078411?searchTerm= Newcastle%20Seeks%20McGirr%E2%80%99s%20Aid&searchLimits= (accessed 09 January 2017).

Song, N., Ma, J., Yu, Y., Yang, Z., Li, Y., 2015. New observations on PAH pollution in old heavy industry cities in northeastern China. Environ. Pollut. 205, 415–423.

Taylor, M.P., Mackay, A.K., Hudson-Edwards, K.A., Holz, E., 2010. Soil Cd, Cu, Pb and Zn contaminants around Mount Isa City, Queensland, Australia: potential sources and risks to human health. Appl. Geochem. 25, 841–855.

Taylor, M.P., Camenzuli, D., Kristensen, L.J., Forbes, M., Zahran, S., 2013. Environmental lead exposure risks associated with children's outdoor playgrounds. Environ. Pollut. 178, 447–454.

Taylor, M.P., Davies, P.J., Kristensen, L.J., Csavina, J.L., 2014a. Licenced to pollute but not to poison: the ineffectiveness of regulatory authorities at protecting public health from atmospheric arsenic, lead and other contaminants resulting from mining and smelting operations. Aeolian Res. 14, 35–52.

Taylor, M.P., Mould, S.A., Kristensen, L.J., Rouillon, M., 2014b. Environmental arsenic, cadmium and lead dust emissions from metal mine operations: implications for environmental management, monitoring and human health. Environ. Res. 135, 296–303.

Taylor, M.P., Forbes, M.K., Opeskin, B., Parr, N., Lanphear, B.P., 2016. The relationship between atmospheric lead emissions and aggressive crime: an ecological study. Environ. Health 15, 23.

The Australasian, 1905. Broken Hill Proprietary Company Manufacturing of Spelter Works at Newcastle. The Australasian Saturday 22 April 1905. Available at:. http://trove.nla. gov.au/newspaper/article/139804665?searchTerm=Broken%20Hill%20Proprietary% 20Company%20Manufacturing%20of%20Spelter%20Works%20at% 20Newcastle&searchLimits= (accessed 09 January 2017).

The Mercury, 1867. Hunter River Copper Works. The Mercury Thursday 12 September 1867. Available at:. http://trove.nla.gov.au/newspaper/article/8847971 (accessed 09 January 2017).

TNC, 1950. Bitumening of Highway by April. The Northern Champion Wednesday 15 February 1950. Available at:. http://trove.nla.gov.au/newspaper/article/162461085? searchTerm=Bitumening%20of%20Highway%20by%20April&searchLimits= (accessed 09 January 2017).

United Nations (UN), 2015. World Urbanization Prospects: The 2014 Revision (ST/ESA/ SER.A/366). Department of Economic and Social Affairs, Population Division Available at:. https://esa.un.org/unpd/wup/Publications/Files/WUP2014-Report.pdf (accessed 9 January 2017).

United States Environmental Protection Authority (US EPA), 2012,. Standard Operating Procedure for an In-vitro Bio-accessibility Assay for Lead in Soil.

Van Oss, H.G., 2011. Slag, Iron and Steel: U.S. Geological Survey, Minerals Yearbook. vol. 1 pp. 69.1–69.9.

Wang, X., Thai, P.K., Li, Y., Li, Q., Wainwright, D., Hawker, D.W., Mueller, J.F., 2016. Changes in atmospheric concentrations of polycyclic aromatic hydrocarbons and polychlorinated biphenyls between the 1990s and 2010s in an Australian city and the role of bushfires as a source. Environ. Pollut. 213, 223–231.

Yang, H.-H., Lai, S.-O., Hsieh, L.-T., Hsueh, H.-J., Chi, T.-W., 2002. Profiles of PAH emission from steel and iron industries. Chemosphere 48, 1061–1074.

Yang, J., Yu, F., Yu, Y., Zhang, J., Wang, R., Srinivasulu, M., Vasenev, V., 2016. Characterization, source apportionement, and risk assessment of polycyclic aromatic hydrocarbons in urban soil in Nanjing, China. J. Soils Sediments http://dx.doi.org/10.1007/ s11368-016-1585-0.

Youn, J.-S., Csavina, J., Rine, K.P., Shingler, T., Taylor, M.P., Sáez, A.E., Betterton, E.A., Sorooshian, A., 2016. Hygroscopic properties and respiratory system deposition behavior of particulate matter emitted by mining and smelting operations. Environ. Sci. Technol. 50, 11706–11713.

Zahran, S., Mielke, H.W., McElmurry, S.P., Filippelli, G.M., Laidlaw, M.A.S., Taylor, M.P., 2013. Determining the relative importance of soil sample locations to predict risk of child lead exposure. Environ. Int. 60, 7–14.

Zhang, J., Wang, P., Li, J., Mendola, P., Sherman, S., Ying, Q., 2016. Estimating population exposure to ambient polycyclic aromatic hydrocarbon in the United States – part II: source apportionment and cancer risk assessment. Environ. Int. 97, 163–170.

5.8 References

Block, C.N., Shibata, T., Solo-Gabriele, H.M., Townsend, T.G. 2007. Use of handheld X-ray fluorescence spectrometry units for identification of arsenic in treated wood. Environmental Pollution 148, 627-633.

Central Sydney Magazine. 2017. Soiled: Researchers find backyard lead levels in the city are THREE times the safe limit. Heather McNab. 25 January 2017. Page 9.

Lead Expert Working Group (LEWG). 2016. Lead Expert Working Group Report on Managing Residual Lead Contamination in North Lake Macquarie. Report prepared for the NSW Environment Protection Authority. December 2016. 1-118.

Lubchenco, J. 1998. Entering the Century of the Environment: A New Social Contract for Science. Science 279, 491-497.

Macquarie University Newsroom. 2013. Is your garden putting your health at risk? Free test for soil metal contamination at open day 2013. Newsroom. <http://www.mq.edu.au/newsroom/2013/09/07/is-your-garden-putting-your-health-at-risk-free-test-for-soil-metal-contamination-at-open-day-2013/> (accessed 27 March 2017).

Macquarie University Newsroom. 2017. VegeSafe community program tracks urban soil environmental pollution. Newsroom. <http://www.mq.edu.au/newsroom/2017/01/17/vegesafe-community-program-tracks-urban-soil-environmental-pollution/> (accessed 29 March 2017).

Morley, J.C., Clark, C.S., Deddens, J.A., Ashley, K., Roda, S. 1999. Evaluation of a portable X-ray fluorescence instrument for the determination of lead in workplace air samples. Applied Occupational and Environmental Hygiene 14, 306–316.

New South Wales Environment Protection Authority (NSW EPA). 2016. <Lead Safety. http://www.epa.nsw.gov.au/pesticides/lead-safety.htm> (accessed 02 April 2017).

Parliament of New South Wales. 2017. 4788- Lead Pollution. Legislative Assembly, House Papers. <https://www.parliament.nsw.gov.au/la/papers/pages/qanda-tracking-details.aspx?pk=234655> (accessed 02 April 2017).

Parsons, C., Grabulosa, E.M., Pili, E., Floor, G.H., Roman-Ross, G., Charlet, L. 2013. Quantification of trace arsenic in soils by field-portable X-ray fluorescence spectrometry: Considerations for sample preparation and measurement conditions. Journal of Hazardous Materials 262, 1213-1222.

Rouillon, M., Harvey, P., Kristensen, L., George, S., Taylor, M.P. 2017. VegeSafe: a community science program measuring soil-metal contamination, evaluating risk and providing advice for safe gardening. Environmental Pollution 222, 557-566.

Rouillon, M., Taylor, M.P. 2016. Can field portable X-ray fluorescence (pXRF) produce high quality data for application in environmental contamination research? Environmental Pollution 214, 255-264.

Shefsky, S. 1999. Comparing Field Portable X-Ray Fluorescence (XRF) To Laboratory Analysis of Heavy Metals in Soil. International Symposium of Field Screening Methods for Hazardous Wastes and Toxic Chemicals. Las Vegas, Nevada, USA.

Sydney Morning Herald. 2013. Lead threat to children from home veggie gardens. NSW News. <http://www.smh.com.au/nsw/lead-threat-to-children-from-home-veggie-patches-20130906-2tan9.html> (accessed 27 March 2017).

Sydney Morning Herald. 2017. Get the lead out in every sense. Editorials. <http://www.smh.com.au/comment/smh-editorial/get-the-lead-out-in-every-sense-20170119-gtv54r.html> (accessed 02 April 2017).

VegeSafe. 2017. What is VegeSafe? Macquarie University. <https://research.science.mq.edu.au/vegesafe/what-is-vegesafe/> (accessed 31 March 2017).

Weindorf, D.C., Bakr, N., Ahu, Y. 2014. Advances in Portable X-ray Fluorescence (pXRF) for environmental, pedological, and agronomic applications. Advances in Agronomy 126, 1-45.

Willis, J.P., Duncan, A.R. 2008. Understanding XRF Spectrometry, Volume 1 Basic Concepts and Instrumentation. PANalytical B.V, The Netherlands.

Wise, P. 2014. Grow Your Own. The Potential Value and Impacts of Residential and Community Food Gardening. Policy Brief No. 59. March 2014. ISSN 1836-9014. <http://www.tai.org.au/sites/defualt/files/PB%2059%20Grow%20Your%20Own.pdf> (accessed 21 March 2016).

Chapter Six: Synthesis of research

6.1 Summary of thesis work

The primary aim of this thesis was to investigate and enhance the environmental application of pXRF for the measurement of metal-contaminated soils. In order to achieve this, this thesis used evidence-based data to evaluate a broad spectrum of pXRF-related misconceptions including user safety (**Paper One**), *ex-situ* analytical performance (**Paper Two**), *in-situ* application potential for metal-contaminated site assessments (**Paper Three**), and its application for environmental investigations (**Papers Four** and **Five**). Furthermore, a secondary aim of this thesis was to investigate contemporary (**Papers Six** and **Seven**) and legacy (**Papers Four**, **Five** and **Eight**) metal contamination hazards using pXRF and wet chemistry analysis. In addition, an underpinning research aim was to communicate science effectively to the public, in an attempt to bridge the gap between science and the community. This was achieved through the development of a citizen-science program (VegeSafe) and a series of online science communication articles (**Articles One** and **Two**). Overall, the studies completed fulfil the aims of this thesis and contribute to a more comprehensive understanding of pXRF application for the measurement of metal-contaminated soils. Consequently, the evidence shows that pXRF can be used for the safe, accurate and inexpensive quantification of metal contaminants in soils, and is demonstrated through the following papers.

Paper One provides the first independent examination of pXRF radiation hazards and benchmarks the exposure risks of pXRF operation to more common radiation exposures. This study found that pXRF radiation hazards are dependent on a number of variables including measurement times, sample density, design of spectrometer snout and position around spectrometers (Rouillon et al. 2015). Despite the low radiation intensities detected from pXRF spectrometers, the advantages associated with pXRF far outweigh the low risks associated with radiation exposure from X-ray scattering. The hypothesised exposure scenario of pXRF soil measurements for one hour each working day resulted in markedly less radiation exposure per year (<3 µSv) than natural potassium–40 in the body (390 µSv) (Rouillon et al. 2015). The comparison against common radiation exposures (e.g. Dental X-ray, mean background radiation, etc.) was key to demonstrating that pXRF is a safe technology when used appropriately. This finding was able to then be communicated effectively to industry members.

Paper Two presents a detailed assessment of pXRF analytical performance for the *ex-situ* measurement of metal-contaminated soils. Measurement variables such as sample preparation and matrix-specific calibrations were optimised to provide the best possible opportunity to assess the analytical capabilities of pXRF. Field portable XRF measurements were benchmarked against CRM values, commercial ICP–AES measurements, research-grade

ICP–MS measurements, and US EPA (1998) data quality criteria. This study found that pXRF is capable of generating high quality measurement data that is equivalent to, and at times better than, commercial ICP–AES measurements. These findings are consistent with previous pXRF evaluations (Kilbride et al. 2006; Kenna et al. 2010; Parsons et al. 2013). Importantly, this study differs in that it is one of the first studies to utilise a broad range of comparative measures for the assessment of *ex-situ* pXRF measurements.

Paper Three demonstrates the advantages of integrating *in-situ* pXRF technology with the current *National Environment Protection (Assessment of Site Contamination) Measure 1999* (NEPM) approach of sampling and off-site laboratory measurements for the assessment of metal-contaminated sites (NEPC 2013). Five research aims were addressed individually to holistically evaluate *in-situ* pXRF application including the correction of *in-situ* pXRF data using ICP–MS measurements and quantification of field- and analysis-based uncertainties for site assessments. This study found that the combined use of *in-situ* pXRF with a small subset of ICP–MS measurements can produce superior and more cost-effective site information when compared to the current approach of merely using off-site laboratory measurements. Increased sampling by pXRF led to numerous benefits including the generation of more representative mapping and site data, greater confidence for reporting site means, a reduction of uncertainties related to site means and sampling and lower site misclassification risks. This research study validates the combined use of *in-situ* pXRF with ICP–MS measurements as a solution to enhancing data quality at metal-contaminated sites characterised by contaminant heterogeneity.

Paper Four investigates metal contamination of Sydney residential garden soils using samples collected through Macquarie University's VegeSafe program. This study found a significant proportion of sampled Sydney homes (40 %) contain soil Pb concentrations over the Australian health investigation level (HIL–A) of 300 mg/kg, while Pb concentrations >1000 mg/kg were identified at 15 % of sampled homes (NEPC 2013). Median soil Pb concentrations of painted homes (366 mg/kg) were considerably greater than non-painted homes (103 mg/kg), demonstrating a significant contribution from Pb-based paints to soil Pb (Rouillon et al. 2017a). The use of *ex-situ* pXRF for this research was also demonstrated to be particularly cost effective (AU\$445−4095) when compared to the current approach of wet chemistry analysis (AU\$11,430−26,720). The main findings of this research were made available for public discussion as **Article One**, and were widely covered in numerous forms of media (newspapers, radio, TV), state parliament question time, meetings with relevant environment authorities and local gardening groups.

Paper Five assesses organic and inorganic contaminant concentrations across the former industrial city of Newcastle. This study examined soil samples from public and private spaces and subsurface soil pits using a variety of measurement techniques, including: pXRF for metal concentrations, ICP–MS for Pb-bioavailability and Pb isotope compositions, XRD and SEM for mineralogy, and Gas Chromatography (GC) for organic contaminants. The study identified that soil metal contaminants (Mn, Zn and Pb) were largely the result of smelter emissions and waste used for fill from the former Newcastle (NSW) Cu smelting and steel industries, respectively. The use of pXRF, a relatively inexpensive method for soil metal quantification allowed for the available budget to be spent on more expensive laboratory measurements such as Pb isotope analysis and GC.

Papers One to **Five** holistically address the primary aims of this thesis by examining the validity of both *in-situ* and *ex-situ* pXRF measurements. These studies address the knowledge gap that have until now largely precluded its more widespread environmental use. **Papers Four** to **Eight** explore contemporary and legacy metal contamination hazards in Australia and their impacts on public health, and are discussed below.

6.2 Metal contamination in Australia

Ore extraction and smelting of metal products have been well documented as important contributors of metal contamination in Australia in areas such as Boolaroo (Morrison 2003; **Paper Eight** – Harvey et al. 2015), Broken Hill (Boreland et al. 2002; **Paper Six** – Taylor et al. 2014a; Dong et al. 2015), Esperance (Gulson et al. 2009), Mount Isa (Taylor et al. 2010; Mackay et al. 2013), Port Kembla (Chiaradia et al. 1997; Martley et al. 2004) and Port Pirie (Cartwright et al. 1976; Taylor et al. 2013, **Paper Seven** – Taylor et al. 2015). Some of these small cities have since ceased smelting operations leaving a legacy of environmental contamination from the by-products of smelter fallout and slag re-use as land fill, while other cities continue to extract and refine metal-rich ores. These metal operations have, and in some cases continue to contribute to contemporary metal contamination hazards in the form of metal-rich dusts and soils (Kristensen et al. 2017).

Unfortunately, the safeguard of human health in these communities is typically of secondary priority when compared to ensuring the continual operation of these metal industries for sustained and increased economic growth (Taylor et al. 2014b). Despite the monitoring of industrial emissions, there is often an impediment of establishing if elevated metal concentrations in soils or dusts are the result of an industry, or if they are occur naturally in the environment (Kristensen and Taylor 2016). A multiple lines of argument approach is typically

required to ascertain the origin of metal contamination hazards. These can involve depth pit sampling to estimate surface metal enrichment, comparison of elemental isotope compositions against ore body signatures, elemental ratio signatures, spatial and temporal monitoring of dust metal accumulation and statistical tests around a suspected source of contamination (e.g. Gulson et al. 1995; Taylor et al. 2010; Kristensen and Taylor 2016; Harvey et al. 2017).

Metal contamination in Australia is not solely limited to mining and smelting communities. Contamination is also ubiquitous in urban centres due to the historical use of Pb products such as leaded petrol and Pb-based paints (Noller and Smythe 1974; Mielke et al. 1983; Birch et al. 2011). Every large urban city across the world has been impacted to some extent by the extensive use of Pb products (e.g. Christchurch, N.Z. – Ashrafzadeh et al. 2017; Detroit, U.S.A – Bugdalski et al. 2013; Rome, Italy – Calace et al. 2012). However, since the reduction and removal of Pb from these products, there remains a common fallacy that 'because they are no longer sold, the issue of metal contamination in no longer present'. Metals such as Pb can remain in soils for up to 700 years after deposition (Semlali et al. 2004) and may become concentrated close to vertical structures, presenting greater localised hazards (Mielke et al. 1999; Schwarz et al. 2012).

Hence, to better protect communities from metal exposures arising from metal-contamination hazards, investigations must be able to evaluate the distribution and concentration of metal contaminants in environments where exposure is likely. **Papers Six** and **Seven** investigate *ongoing* temporal and spatial metal-rich dust accumulation on public playgrounds in Broken Hill and Port Pirie, respectively. In contrast, **Papers Four**, **Five** and **Eight** examine *legacy* metal contamination hazards in the form of elevated soil and dust metals in Sydney, Newcastle and Boolaroo, respectively.

6.2.1 Contemporary hazards

The cities of Broken Hill and Port Pirie were built upon large-scale mining and metal refining operations that have operated for over 120 years (Solomon 1988). Both cities have had a long history of elevated childhood blood Pb exposures, with recent estimates of 21 % and 23 % of children (<5 years) exceeding the former blood Pb level of 10 µg/dL in Broken Hill and Port Pirie, respectively (Taylor et al. 2014c). In order to understand the hazards that contribute to elevated blood Pb cases, it is important to assess the environments where children are active, both inside and outside of their homes. One of these areas of exposure are publicly accessible outdoor playgrounds that are approximately evenly distributed across both cities, to enable

equitable access for young families. These environments became the focus for **Papers Six** and **Seven**.

By simulating child's play on public playgrounds in Broken Hill, **Paper Six** used pre- and post-play hand wipes to evaluate the risk a child has of metal exposure from playing. This study found the greatest metal exposure occurred at the playground closest to the active mining operation, with Pb isotope compositions of the accumulated dust to be indistinguishable from the local ore body. On average, post-play hand wipes had 72 times more Pb content than pre-play hand wipes (Taylor et al. 2014a). Temporal sampling revealed that recontamination of playgrounds occurred within 24 hours of sampling, indicating that any future playground washing regimes may not be entirely effective. The frequent recontamination of playgrounds suggest that nearby residences, schools and parks are likely to be also affected by the ongoing emissions, depositions and remobilisation of metal-rich dust, which further increases the risk of metal exposure for children in Broken Hill.

Outcomes of this study were later publicly broadcasted in an online article in *The Conversation* (**Article Two**). When asked about a solution to playground contamination in Broken Hill, a NSW Health spokesman said "*the Broken Hill community had long been aware of the concerns and should continue with abatement measures, including ensuring children wash their hands after play.*" (ABC 2014). Measures to reduce metal exposure in Broken Hill have partially been redirected towards the residents themselves (Figure 6.1), despite evidence showing that the local mining operations are a major source of metal-rich dust in Broken Hill (Dong and Taylor 2017).

Figure 6.1: A Broken Hill Council sign on children's playground equipment (Daily Telegraph 2015).

Nevertheless, this study, along with other environmental health studies and monitoring programs have led to the allocation of more than $13 million of funding from the NSW Government to address Pb contamination in Broken Hill (Humphries 2015). In addition, the NSW EPA allocated an extra $225,000 of funding from the Environmental Trust (Speakman 2015) for measures to address Pb contamination at playgrounds, an outcome directly due to the research from **Paper Six**. Further, a pollution reduction program was issued to Perilya (the active mining operation) by the NSW EPA to reduce dust emissions (NSW EPA 2016a). These results are excellent news for the residents of Broken Hill, who require further assistance from local and state health authorities to minimise childhood Pb exposure.

Taylor et al. (2013) first conducted the hand wipe study in the Zn/Pb smelter city of Port Pirie. This work was followed by the regular washing of playgrounds by the local council. The effectiveness of playground washing in reducing metal exposure was not specifically evaluated and consequently was the subject of investigation in 2015. **Paper Seven** evaluated the proficiency of the playground washing regime in Port Pirie, and found that despite the new program of playground washing, post-play hand wipes still exceeded a relevant health guideline of 800 $\mu g/m^2$ for Pb. The washing of playgrounds reduced post-play hand wipe Pb accumulation by 56 % when compared to post-play hand wipes on non-wash days (Taylor et al. 2015). Yet, the benefits of washing were limited by rapid recontamination of playgrounds, with Pb loadings increasing by ~5 % every hour after washing (Figure 6.2). Similar to **Paper Six**, this study found that dust Pb loadings were greater closer to the suspected contamination source, and that playground washing only provides a short-term reduction of metal loading, due to continuous Pb emissions from the Port Pirie smelter.

The two playground studies conducted in Port Pirie have had a significant impact on the washing regime of the playgrounds in the city. Prior to the first playground study in 2011 (i.e. Taylor et al. 2013), only one playground in Port Pirie was regularly washed (pers. comm. D. Farquhar 2011). Once the first study was completed, the findings were provided to South Australia Health and Port Pirie Council ahead of publication and the washing regime increased to 22 washes per week across nine playgrounds, and one kindergarten playground (Taylor et al. 2015). After online publication of the first study, Nyrstar (smelter company) and Port Pirie Regional Council increased the washing regime to 49 washes per week. Following the online publication of the second study (**Paper Seven**), washes across Port Pirie were increased to a total of 81, with 61 washes across 16 public playgrounds, and 20 washes across nine child care centres, primary schools and kindergarten playgrounds (TLAP 2015). The success of these studies in advocating for stronger protective measures to combat contemporary metal-rich

hazards provides a much needed short term solution for Port Pirie. Yet, the regular washing of playgrounds is not an efficient and viable long-term solution if metal-rich smelter emissions continue to blanket the city in metal-rich dust. A further, more impactful response to the evidence produced by the Port Pire research, is that the cause of both historical and contemporary lead emissions, the Nyrstar smelter, has determined to upgrade their facilities at a cost of >$500 million to reduce Pb emissions to the city (ABC 2015). Additionally, the company has promised $35 million over ten years to implement a Pb abatement program in the city to reduce children's blood Pb levels and their exposure sources within the community (Port Pirie Transformation not dated)

Figure 6.2: Dust accumulation on hands after 20 minutes of simulated play on children's playground equipment in Port Pirie, South Australia (ABC 2013).

Neither **Paper Six** nor **Seven** utilised pXRF to monitor playground dust, soil or hand wipe metal concentrations, yet this does not preclude its application in this field. Dost (1996) used pXRF to measure metal (e.g. As, Cd and Pb) concentrations on indoor surface wipes, while Gorce and Roff (2016) measured surface wipes by pXRF to screen workplace surfaces rapidly for Pb exposure. Applying a similar principle to outdoor surface wipes could prove useful if regular monitoring of playground and outdoor dust metal concentrations are required.

6.2.2   Legacy hazards

Pb-based paints

Historic metal contamination of urban centres and former metal industry cities has left a legacy of soil contamination hazards in residential areas. **Paper Four** identified elevated Pb contamination in the garden soils of Sydney residences, largely the product of the historical use and application of leaded petrol and Pb-based paints, respectively (Noller and Smythe 1974;

124

Mielke et al. 1983; Birch et al. 2011). Addressing existing soil Pb contamination is challenging, particularly when the contamination of potentially thousands of Sydney homes is downgraded as '*diffuse urban pollution'* and consequently is largely exempt from the NSW EPA's duty to report (see Section 6.3.3). However, given that urban Pb contamination is sourced partially from Pb-based paint, there remains a practical opportunity to address further Pb exposure from Pb-based paints that may still remain on >3.5 million Australian homes built pre-1971 (Berry et al. 1994).

First, the relative contribution of soil Pb from Pb-based paints must be estimated in order to justify targeting its regulation. This was attempted initially using Pb isotope compositions on co-located soil and paint samples (from the same home), by comparing them against reference geogenic and air filter signatures (Figure 6.3). Relative contribution estimates via Pb isotopes were unable to discriminate between sources primarily due to both leaded petrol and Pb-based paint products were made using the same Broken Hill Pb ore (Gulson et al. 1995), resulting in overlapping compositions (Figure 6.3). Lead isotope compositions are generally successful at delineating Pb contributions estimates from samples with distinctly different Pb isotope signatures (e.g. Figure 4 – **Paper Five**). However, the superimposition of Pb isotope compositions from leaded petrol (via air filters), Pb-based paints and garden soils compelled the authors of **Paper Four** to estimate the relative Pb contributions using another method.
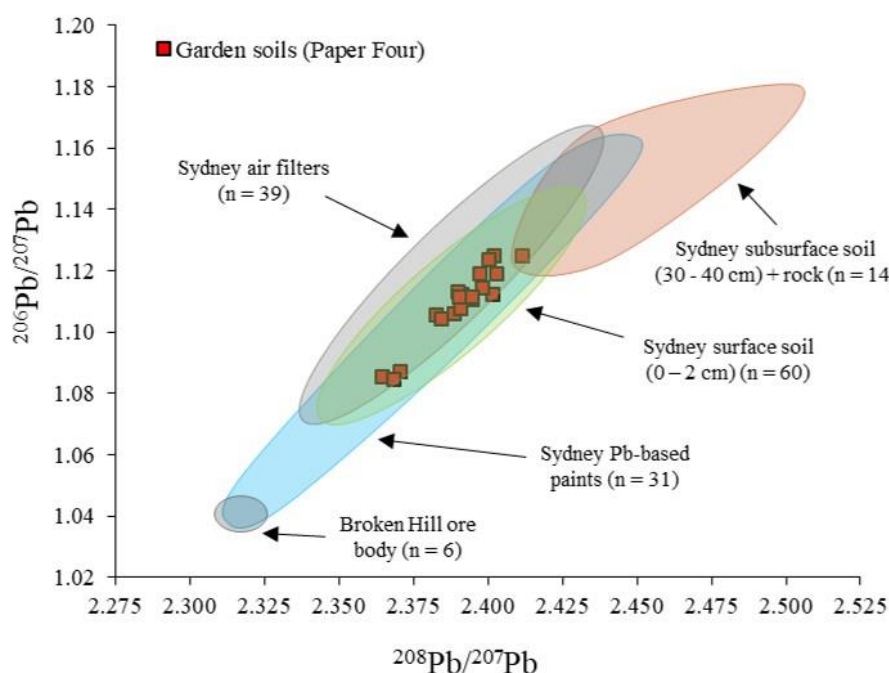
Figure 6.3: Lead isotope compositions (^{208}Pb/^{207}Pb / ^{206}Pb/^{207}Pb) of Sydney garden soils from **Paper Four** compared against documented Sydney air filter compositions and Pb-based paint samples. The shaded areas represent characteristic signatures for; red – Sydney subsurface soils and rocks (Wu et al. 2016), green – Sydney surface soils (Laidlaw et al. 2014; Wu et al. 2016; Zhou et al. Under Review), blue – Sydney Pb-based paints (Laidlaw et al. 2014), light grey – Sydney air filters (Kristensen et al. 2017), and Broken Hill ore (Cooper et al. 1969).

The collection of VegeSafe metadata in **Paper Four** allowed for simple attributes of the contribution from Pb-based paints under the assumption that soil Pb from non-painted homes was primarily sourced from leaded petrol and geogenic Pb (Rouillon et al. 2017a). These estimations are supported by: (1) the temporal phasing out of Pb products when plotted against median soil Pb concentrations of different house age groups (Figure 6.4); (2) the observed temporal shift in soil Pb to more geogenic signatures during the phasing out of Pb products in Sydney (Wu et al. 2016); and (3) the agreement in this study to other similar cross sectional schematics of Pb contamination around homes with and without Pb-based paints by Olszowy et al. (1995) and Mielke (1999).
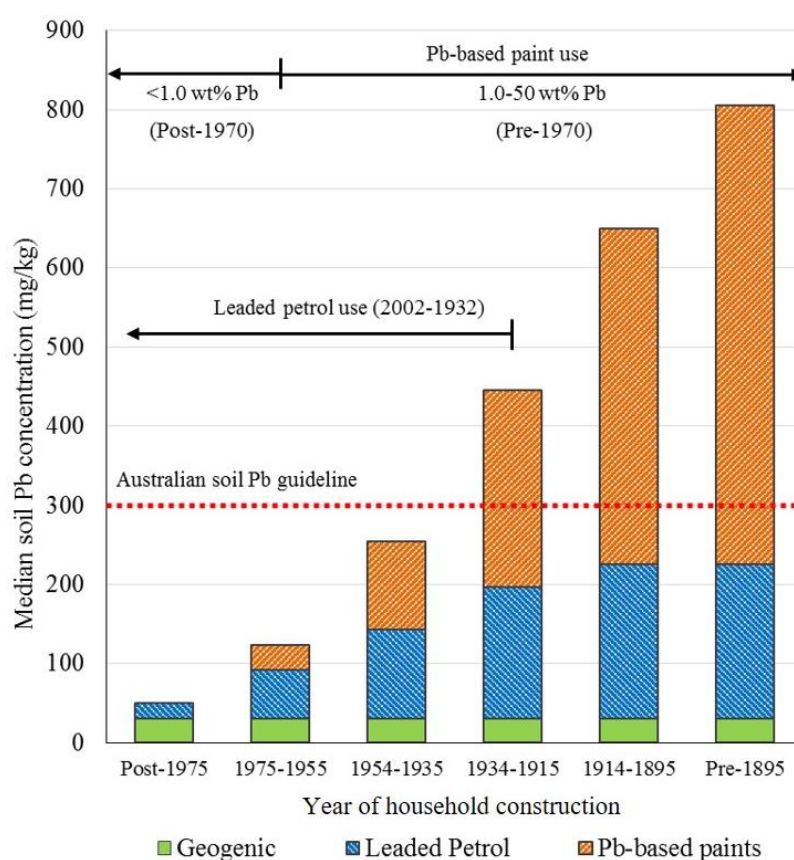
Figure 6.4: Estimated Pb contributions from geogenic, leaded petrol emissions and Pb paint sources to median soil Pb concentrations of painted Sydney homes based on household construction era. The Australian health investigation level (HIL-A) for soil Pb is 300 mg/kg and is displayed as the red dashed line (NEPC 2013). Source: Figure 3 – Rouillon et al. 2017a.

Paper Four identified that Pb-based paint was the dominant source of Pb in the garden soils of older homes in Sydney and discusses the potential health implications of Pb-based paint contamination. At present, the primary way residents in NSW can become informed of Pb hazards are through limited online educational materials that are made available to the public by the NSW EPA (2016) and NSW Health (2016a). These fact sheets contain a brief introduction of Pb, the potential sources of Pb around homes, and the best ways to mitigate Pb exposure. However, only when a child has already been Pb exposed, and the parent/s have taken

their child for a blood Pb test, does a local public health unit become informed of the Pb exposure, and even then, some Pb exposure cases do not warrant a physical assessment of the home environment (Table 6.1 – NSW Health 2016b). For example, a Sydney family were recently alarmed to discover their 2 year old daughter had elevated blood Pb levels, yet there was no follow up assessment of the home by the local public health unit, only a letter in the mail arrived (Daily Telegraph 2017).

Table 6.1: Response protocol for single elevated blood Pb concentration notification in non-endemic areas. The protocol outline below is for new notifications. If the notification relates to follow up from a previous notified blood Pb concentration within the last 12 months, the Public Health Unit response can be modified according to the circumstances of the case (Adapted from NSW Health 2016b).

Level	Blood Pb concentration	Age	Public Health Unit response
1	≥5 but <10 µg/dL	<5	• **Information:** Consult treating doctor. Standard letter to case's parent/guardian and NSW Health's factsheet 'Lead exposure in children' • **Risk management:** If requested by the doctor or the family offer counselling, on risk reduction/contact management to case parents/guardians. • **Blood tests:** Household members may need to be tested particularly young children and pregnant women.
		≥5	• **Information:** Refer to Level 1, <5 years of age. • **Risk management:** Not routine. At the discretion of the Public Health Unit. • **Blood tests:** Refer to Level 1, <5 years of age.
2	≥10 but <25 µg/dL	<5	• **Information:** Refer to Level 1, <5 years of age. • **Risk management:** Offer counselling/home risk assessment to case's parents/guardians as appropriate. • **Blood tests:** Refer to Level 1, <5 years of age + Retest blood Pb concentration after 6 months or earlier if clinically indicated.
		≥5	• **Information:** Consult treating doctor. Standard letter to case. • If non occupational exposure provide Pb factsheet on risk identification and management to requesting doctor or case as appropriate. • **Work related exposures**: Suggest case or treating doctor advice patient to discuss blood Pb concentration with employer in the case of occupational exposure. Inform SafeWork in case of cluster of cases. • **Risk management:** Offer counselling/home risk assessment to case as appropriate. • **Blood tests:** Refer to Level 1, <5 years of age.
3	≥25 but <45µg/dL	<5	• Same as Level 2, plus: • **Environmental assessment:** Conduct preliminary environmental assessment, including home visit, exposure pathways and sampling if source not obvious. • **Expert advice:** Seek expert advice from clinical toxicologist for future blood Pb concentration retesting
		≥5	• Same as Level 2, plus: • **Environmental assessment:** Refer to Level 3, <5 years of age. • **Work related exposures**: Strongly suggest case or treating doctor consult SafeWork NSW for further advice on occupational exposure, if appropriate.
4	≥45µg/dL	All ages	• Same as Level 3, plus: • **Medical treatment:** If blood Pb concentration ≥45 µg/dL in a child ensure treating doctor is aware of result when received as blood Pb concentrations at these levels may require urgent medical treatment (chelation). • **Medical treatment:** If blood Pb concentration ≥70 µg/dL requesting doctor is aware of the result as blood Pb concentrations at these levels in an adult may require urgent medical treatment (including chelation).

Presently, there are no preventative measures in place to avert childhood Pb exposures from Pb-based paints in NSW other than online educational materials and limited leaflet distribution at some hardware stores, childcare centres and home and renovation shows. It is unclear what proportion of Sydney residents have accessed these materials, or even know if they exist. Providing such information directly to residents living in areas with a higher risk of Pb contamination, or residents living in older housing through letter drops, should be of greater priority to environment authorities to prevent future Pb exposures. Unfortunately, environmental health authorities in NSW appear to be content with an arrangement that 'reacts' to the notification of childhood Pb exposure cases, rather than one that 'prevents' them. It is also unclear how many childhood Pb exposure cases in NSW, and Australia, go unnoticed as Pb exposure symptoms are not distinctly obvious to parents, and it is usually up to the child's doctor to request a blood Pb test, should they suspect Pb exposure. Applying childhood Pb exposure rates from the United States, Taylor et al. (2012) concluded approximately 100,000 Australian children (0–4 years) may have blood Pb concentrations in excess of 5 µg/dL. A similar estimation is proposed by the Children's Hospital at Westmead (2014) who approximate >75,000 Australian children (0–4 years) have elevated blood Pb concentrations.

Introducing preventative measures, such as Pb policies similar to the Renovation, Repair and Painting (RRP) rule and the Lead Disclosure rule used in the United States (US HUD 2016), could be considered by the NSW EPA and NSW Health, which would reverse the current passive approach towards urban metal contamination (see Section 6.3.3). These preventative measures could be implemented using inexpensive, real-time pXRF data, used in a monitoring capacity similar to the Broken Hill Environmental Lead Program (BHELP) as described in **Example Three** of Section 6.4.1. Further, the NSW EPA could start a Pb paint program where residents living in housing built pre-1970 have access to a free service which provides Pb-based paint screening using pXRF, particularly as pXRF measurements are practically cost-free.

Paper Five examined metal contamination in the private and public soils of a former industrial city, after more than 100 years of Cu smelting, shipping of ore and steel manufacturing (NCC 1997; Parliament of New South Wales 1999). The study found high soil Pb concentrations that would readily be absorbed following soil ingestion (mean in-vitro bio-accessibility soil Pb = 46 %) in ex-industrial areas of the city (Harvey et al. 2017). The use of Pb isotope compositions and SEM suggested Newcastle's former Cu and steel industries contributed the majority of soil contaminants from the use of slag waste material as fill, and the atmospheric deposition of metal-rich particles. As mentioned for **Paper Four** above, identifying the source and distribution of metal contamination hazards provides an opportunity to address the

contamination practically. This study suggests that some residents may have unknowingly purchased land with metal-rich waste fill, a result of no disclosure about the lands history from the previous owner, and the lack of information attached to Section 149 certificates (see Section 6.3.2).

The findings of **Paper Five** were later the focus of an article by the Newcastle Herald (2017a) with an online poll revealing the majority (78 %) of Newcastle residents are concerned about potential legacy Pb hazards in their backyard. The article was written using colourful language on a topic that already concerned local residents. For instance, the first sentence states "*LARGE parts of Newcastle remain drenched in a toxic cocktail of heavy metals and cancer-causing hydrocarbons that rained down for decades during the city's industrial heyday*" (Newcastle Herald 2017a). Unsurprisingly, this article became the focus of an opinion letter written by an occupational hygienist that was published the following month (Newcastle Herald 2017b). The letter criticized the journalists' emotive wording, the lack of science in the article, and the disparity between the findings of **Paper Five**, and a 1995 study he was a co-author on that measured soil Pb concentrations in parks and playgrounds of Newcastle. These public remarks were later addressed in a formal reply to the Newcastle Herald (2017c).

Smelter emissions

A common misconception regarding metal contamination, is that if there is no longer an active source of contamination (i.e. an active smelter), the problem goes away. The Zn/Pb smelter of Boolaroo closed in 2003 after more than 100 years of intermittent operation, which resulted in elevated blood Pb levels of children in the surrounding suburbs, and left a legacy of Pb contamination across the surrounding area (Gulson et al. 2004). To lower the risk of metal exposure, Pasminco, the smelter company, and the NSW EPA developed a Lead Abatement Strategy (LAS) as a practical solution to manage smelter-related soil Pb contamination. The LAS used a combination of adding soil to cover existing soil contamination, and excavation of soils where Pb concentrations exceeded 2500 mg/kg Pb, or 1500 mg/kg Pb for shady spots with low grass cover (Harvey et al. 2016). However, the efficacy of abatement was never assessed. **Paper Eight** investigated the effect of the LAS on Pb concentrations in both private and public soils in the area. The study found no significant difference in soil Pb concentrations for properties pre- and post-abatement. Measurement of household vaccum dust revealed highly bio-accessible Pb (median 90 %) remains as a potential exposure pathway. The LAS did not include non-residential properties such as schools and playgrounds (median Pb = 920 mg/kg), sport fields (median Pb = 1280 mg/kg) and open spaces (median Pb = 620 mg/kg) for abatement, which are areas where children may also be exposed to Pb hazards. In fact, Sites 1

(median Pb = 2900 mg/kg) and 3 (median Pb = 460 mg/kg) from **Paper Three** were located within the LAS, and were sampled post-abatement.

Paper Eight revealed three concerning facts about the LAS in Boolaroo:

    (a) The LAS was ineffective at abating soil Pb concentrations at residential properties

    (b) The LAS did not address significant Pb hazards that remain in both public and private spaces

    (c) There were no plans to assess the efficacy of the LAS post-abatement (Harvey et al. 2016).

The LAS was originally developed to "*reduce the current potential exposure for residents of the nominated properties that could arise from previous lead dust deposition such that the exposure levels from lead dust deposition after the LAS has been completed are within acceptable limits during everyday living*" (Zines 2007). This objective specifically excluded smelter-related slag material (54–80 % bioavailable Pb), which was widely distributed to many residential properties in the surrounding area as backyard and landscaping fill (Morrison and Gulson 2007; Morrison et al. 2016).

The study findings and the uncovering of major oversights in the handling of the LAS were provided to the NSW EPA prior to publication in late 2014. The NSW EPA determined that a lead expert working group (LEWG) needed to be established to evaluate the effectiveness of the LAS, and to resolve other Pb contamination issues arising from the Pasminco smelter in Boolaroo (NSW EPA 2015a). This group was likely formed largely in response to public pressure arising from the 'Toxic truth' series, a special investigation into the ineffectiveness of the LAS, Pb pollution in Boolaroo and surrounding suburbs, and the legacy of contamination left by Pasminco (Newcastle Herald 2017b). The first instalment of Toxic truth was a 17 page story that increased public awareness and concern within the local and surrounding community (LEWG 2016). The investigation continued to approximately 100 online and print articles from November 2014 to June 2015 (Newcastle Herald 2017d). One of the online articles featured a publicly accessible, and interactive map of soil and dust Pb concentrations based on the data in **Paper Eight** (Figure 6.5), which drew further interest from the public and environment authorities. The unveiling of soil Pb concentrations in popular community areas, such as Speers Point Park (4990 mg/kg Pb) raised concerns by the public, particularly as the comparative benchmark soil Pb guideline is merely 600 mg/kg (Figure 6.5).
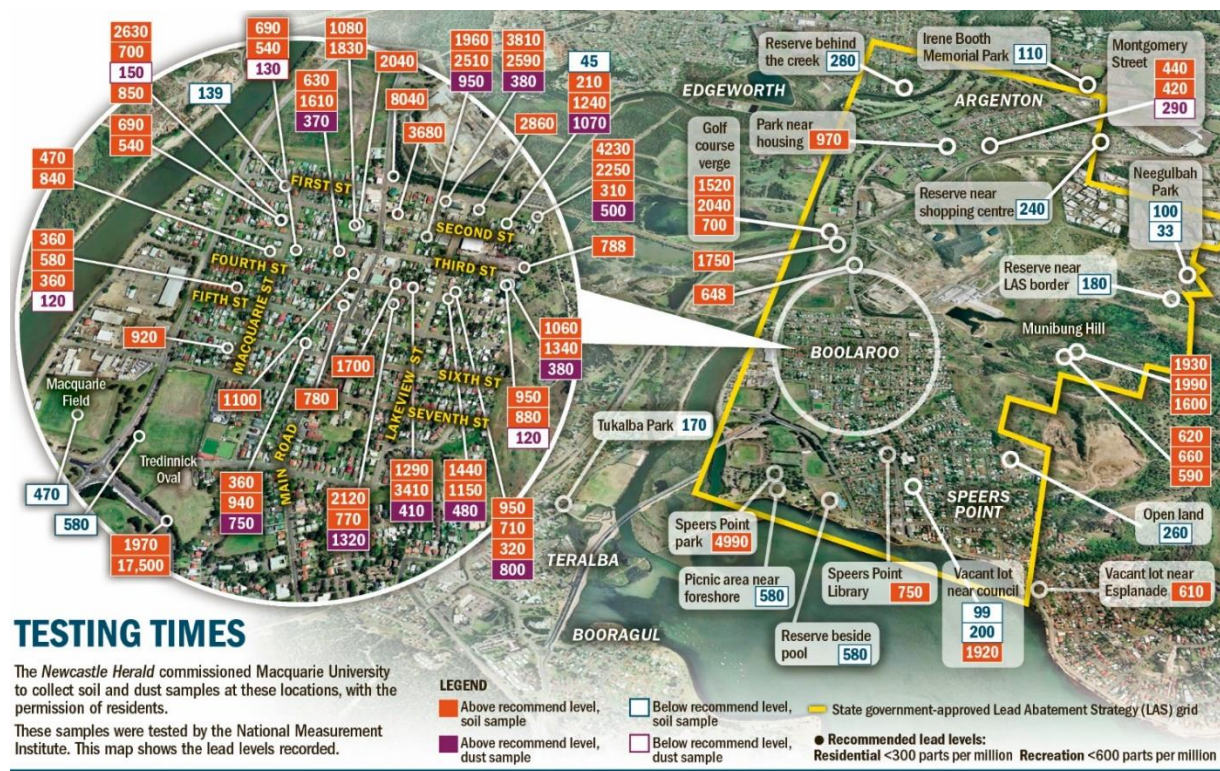
Figure 6.5: Newcastle Herald map of elevated soil Pb concentrations found by Environmental Scientists from Macquarie University across the suburbs of Argenton, Boolaroo and Speers Point. This figure was published as part of the Newcastle Herald Toxic Truth special investigation in 2014 (Newcastle Herald 2014).

Pasminco was required to use the HILs as site criteria for the remediation of the smelter site in 2007, meaning where soil metals exceed the HILs, excavation of soil was to occur until soil metal concentrations were below HIL values (LEWG 2016). Yet bizarrely, the LAS for residents had a specific abatement criteria that did not require the excavation of soil until Pb concentrations reached 2500 mg/kg, or 1500 mg/kg if in a shady spot with low grass cover (Harvey et al. 2016). It is unclear why the abatement of residential properties by the LAS allowed for considerably weaker environmental protection than during the remediation of the smelter site itself. If the smelter remediation site criteria of 300 mg/kg of Pb for residential areas was deemed appropriate for a non-occupied site, it raised the simple question of equality: why wasn't the same criteria used for the residential properties of Boolaroo (and surrounding suburbs), particularly as these properties were contaminated by the smelter company? **Example One** in Section 6.4.1 introduces the use of pXRF to guide the Pasminco smelter remediation. The use of pXRF for environmental investigations in Australia is not fully recommended by the NEPM (NEPC 2013), and is further discussed in Section 6.3.1.

6.3 Current policy surrounding pXRF application

6.3.1 Contaminated site assessments

Contaminated site assessments in Australia are guided by field and laboratory approaches described in the NEPM (NEPC 2013). The NEPM was formed to provide a nationally consistent approach for the assessment of site contamination, ensuring systematic assessment practices are conducted by all members of the environmental industry (NEPC 2013). Volume 1 of the NEPM highlights the key principles of the measure that should be observed, including information on data collection and chemical analyses. Section 13 of Volume 1 states that chemical analyses should be measured using approved standard methods performed at laboratories that are NATA-accredited for the analysis of the relevant environmental medium (NEPC 2013). It also states that field analytical methods should only be performed by appropriately skilled personnel using approved standard methods. The use of field-based testing methods are described in further detail in Section 7.4 of Schedule B2 of the NEPM (NEPC 2013), which states:

"A variety of field screening techniques may be used to provide immediate (real-time) information about the concentration and distribution of contaminants on contaminated sites. These tests, by their very nature, are less rigorous and reliable than analytical tests conducted in a laboratory, however, they provide cheaper and quicker results to guide the design of further sampling strategies for site assessment.

Their use as the sole source of analytical data in the assessment of potentially contaminated sites is inappropriate as they may give falsely high or low results."

While these statements are cautiously true when comparing the analytical quality of an individual *in-situ* measurement against a NATA-accredited laboratory measurement, it does not acknowledge that analytical measurements, by their very nature, are limited by the sampling that precedes it. As demonstrated in **Paper Three**, irrespective of the analytical technique, the sampling process contributes the greatest error towards the overall assessment of metal-contaminated sites. Increased sampling using the quicker, cheaper *in-situ* pXRF technique reduces errors associated with sampling caused by site heterogeneity. Using the approach detailed in **Paper Three**, the pXRF generates more informative site assessment data than the current NEPM approach, which relies on less sampling and ICP–AES or ICP–MS analysis. The issue of 'less reliable' tests using field based techniques are discussed further for pXRF in Section 7.4.4 of Schedule B2 of the NEPM (NEPC 2013):

"X-ray fluorescence (XRF) is a rapid screening tool that can be used to measure metal concentrations in soil. Performance is dependent on the metal, the soil matrix and soil moisture content. Although a range of heavy metals can be simultaneously detected, there are potential interferences that influence the method accuracy and precision. The US EPA has developed a methodology to guide XRF analysis (US EPA 2007).

The advantages of XRF include real-time results, when used in scanning mode on surface soil, or near real-time results when deeper samples are collected and analysed in the field. The usefulness for specific site-characterisation purposes can be evaluated by comparison of results from split samples analysed by field XRF with laboratory results over a range of analyte concentrations."

The section includes various limitations associated with *in-situ* pXRF, yet does not provide advice or steps on how to address them, other than to refer to US EPA method 6200 (US EPA 2007). If the drawbacks of a field technique can be sufficiently addressed, the advantages of real-time, rapid and low cost measurements can be realised and harnessed for superior site assessments. Similarly, this was demonstrated in **Paper Three**, where a small subset (5–10 %) of NATA-accredited ICP–MS measurements were used to establish correction factors for *in-situ* pXRF measurements for each site. It is worth noting that soil metal assessments by ICP–AES or ICP–MS analysis are not without its own limitations when compared against robust pXRF data (see Section 3.3). Correction of *in-situ* pXRF data enabled the measurement of many more samples on-site, reducing the risk of sample and site misclassification, without the financial constraints associated with off-site laboratory measurements.

In-situ pXRF measurements are not designed to 'replace' or be the 'sole source' of analytical data for contaminated site assessments, but rather can be used to assist in addressing a range of limitations associated with the current NEPM approach. **Paper Three** provides the foundations for the development of a field-based site method that utilises *in-situ* pXRF coupled with a subset of laboratory based validation measurements. Similar site investigation methods have been published as detailed standard operating procedures (SOPs) that are actively applied by the environmental industry such as AS 4482.1 – 'Guide to the investigation and sampling of sites with potentially contaminated soil: Non-volatile and semi-volatile compounds' (Standards Australia 2005) and AS 4874 – 'Guide to the investigation of potentially contaminated soil and deposited dust as a source of lead available to humans' (Standards Australia 2000).

6.3.2 Duty to report and section 149 certificates

The examination of residential soils in **Papers Four** and **Five** found a large proportion of homes in Sydney (40 %) and Newcastle (>90 %) had soil Pb concentrations greater than the HIL–A guideline of 300 mg/kg for residential soils (NEPC 2013). In fact, numerous homes in both cities were found to contain Pb concentrations at over 10 times the HIL–A guideline (NEPC 2013), with maximum soil Pb concentrations of 6490 mg/kg (Sydney) and 11,600 mg/kg (Newcastle). Despite the clear hazards associated with high soil Pb contamination in residential properties (Pausetenbach et al. 1997; Hunt et al. 2006; Spliethoff et al. 2016), it is unlikely that any investigation, reporting or remediation of these properties will occur, due to exemptions in the current regulatory policy.

In NSW, *the Contaminated Land Management (CLM) Act 1997* was established to provide a process for the investigation and remediation of contaminated land. As discussed in **Paper Three**, where contamination is observed or suspected, there is a duty to report by the polluter or land owner to the NSW EPA under section 60 of the *CLM Act 1997*. There are, however, various scenarios not intended to be captured by the duty to report, including '*widespread diffuse urban pollution that is not attributed to a specific industrial, commercial or agricultural activity*' (NSW EPA 2015b, pp. 10). Soil Pb contamination in urban centres are characteristically considered as '*diffuse urban pollution*' and consequently do not warrant any further investigation. Subsequently, there is no requirement for the reporting of leaded petrol- or Pb-based paint-contaminated public or private land, even when the NEPM HIL–A guidelines are exceeded by 10 times or more. For instance, a purchaser may not be aware of actual or potential contaminated land they are about to acquire. However, as per the guidelines of the duty to report, if the same contamination were to occur as a result of a '*specific industrial, commercial or agricultural activity*', it is likely that the contamination would be reported to the NSW EPA (2015b), as per section 60 of the *CLM Act 1997*.

Section 149 certificates under the *Environmental Planning and Assessment Act 1979* (NSW) can be sought for any land within council boundaries, and can include information regarding the potential or reported contamination of land. These certificates may enable the purchaser of land an opportunity to determine if the land was previously contaminated, or if the land is likely contaminated due to its location or history. Some local councils in NSW utilise section 149 certificates to retain information on contaminated land within council areas. However, at present, such practice is not mandatory, nor consistent across NSW (Taylor and Cosenza 2016). As noted in the recent review of the NSW EPA's management of contaminated sites, the inclusion of land contamination information in section 149 certificates only occurs if certain

criteria are met in the council's policy on contaminated land (Taylor and Cosenza 2016). Local councils are able to develop their own contaminated land policies, and subsequently their own criteria to determine if land contamination information should be included in section 149 certificates, without input or approval from the NSW EPA. Hence, one of the recommendations of the NSW EPA review is to ensure local councils develop uniform and approved council policies for land contamination and criteria for section 149 certificates, so that purchasers can be adequately and equally informed on land contamination information prior to land acquisition (Taylor and Cosenza 2016).

6.3.3   Addressing diffuse urban pollution with pXRF

The NSW EPA regulates contaminated land primarily using a 'polluter pays' principle, meaning that when contamination has occurred as a result of an individual or organisation's actions or negligence, the NSW EPA can use its powers under the *CLM Act 1997* to require *'the assessment and remediation of sites where contamination is significant enough to warrant regulation'* (NSW EPA 2015b). However, a shortfall of this approach exists where an organisation who have contaminated land no longer exists, or the contamination has occurred as a result of '*diffuse urban pollution'*. These scenarios prove difficult for the NSW EPA, who do not have the resources to manage contamination issues on their own without a polluter (or in some situations, the taxpayer) to finance the operation of assessment and clean-up. However, just because of the absence of individuals or organisations responsible for the widespread contamination of urban soils identified in **Paper Four** (and to a lesser extent **Five**), is not an adequate reason that the contamination should remain exempted from environmental regulation.

The NSW EPA strives to *'protect the environment by regulating activities that could have an impact on the health of the NSW environment and its people'* (NSW EPA 2013).Yet, the exempted '*diffuse urban pollution*' is ironically perhaps most relevant for residents living in urban centres, particularly when such information on land contamination is withheld from residents to avoid '*unnecessarily blighting that land and causing undue concern*' (SMH 2017). Exposure to contaminated soil is most likely to occur within the boundaries of residential properties, where residents spend the most time renovating, entertaining and gardening. Further, residential properties can become significantly contaminated due to small-scale spatial factors such as the accumulation of '*diffuse urban pollution*' alongside building structures (Mielke et al. 1983; Schwarz et al. 2012) and the presence, or improper removal of deteriorating Pb-based paints (Gulson et al. 1995; NSW EPA 2016b). Kristensen (2015) estimated that between 34,000–41,000 tonnes of Pb were emitted from the tailpipes of motor vehicles in

Sydney during the period of leaded petrol emissions (1932–2002). Further, it is possible that a greater amount of Pb was used in Pb-based paints (up to 50 wt % concentration prior to 1970) on >3.5 million Australia houses built pre-1971 (Berry et al. 1994), however this has yet to be estimated.

To estimate the impact of '*diffuse urban pollution*' on children's blood Pb concentrations in Sydney, Laidlaw et al. (2017) used 341 surface soil Pb concentrations using both observed (34 %) and recommended (50 %) Pb bio-availability estimates and modelled the outcomes using the US EPA IEUBK (Integrated Exposure Uptake Biokinetic) model. Their study estimated that 5.6 % of Sydney children aged 24 months could potentially have blood Pb concentrations greater than the National Health and Medical Research Council (NHMRC) reference level of 5 ug/dL (Figure 6.6a). The Laidlaw et al. (2017) study's prediction of blood Pb concentrations is conservative at best, as samples were collected from a variety of land uses including commercial, residential, park lands, road verges, government and institutional spaces. Soil Pb concentrations from these areas were considerably lower than those from private residences in **Paper Four** (Figure 6.6b), where the greatest exposure to soils exist for a toddler. This suggests that the percentage of children with blood Pb concentrations greater than 5 µg/dL may in reality be higher than predicted by Laidlaw et al. 2017. It is relevant to note that Laidlaw et al. (2017) systematically sampled across metropolitan Sydney at a resolution of one sample per 1 km^2, while soil samples measured in **Paper Four** were collected non-systematically, on a participation basis via the VegeSafe program, and would likely be only representative of exposures in the home environment.

As demonstrated in **Paper Four**, soil Pb contamination at residential properties can be heterogeneous in its distribution and concentration, and may require numerous measurements to adequately characterise a site. The use of a rapid, on-site measurement technique, such as pXRF, could assist in addressing the information gap of contamination at residential properties by providing inexpensive, screening quality information for section 149 certificates. Risk-based categorisation of land contamination (e.g. low, medium and high risk) could simplify information for potential owners and can guide further laboratory analyses, should they be required (see Ericson et al. 2016). This inexpensive measurement option should ideally be used in council areas where soil Pb contamination is known to be prevalent, and can supplement section 149 certificates in instances where there is no previous information on land contamination.

	IEUBK predicted blood Pb concentrations (Laidlaw et al. 2017)	(b) Comparison of soil Pb statistics between Sydney studies

(b) Comparison of soil Pb statistics between Sydney studies

	Laidlaw et al. (2017)	Rouillon et al. (2017)
Mean	**133**	**415**
Minimum	5	14
25th Percentile	30	71
Median	**61**	**189**
75th Percentile	130	468
90th Percentile	260	1050
Maximum	9400	6490
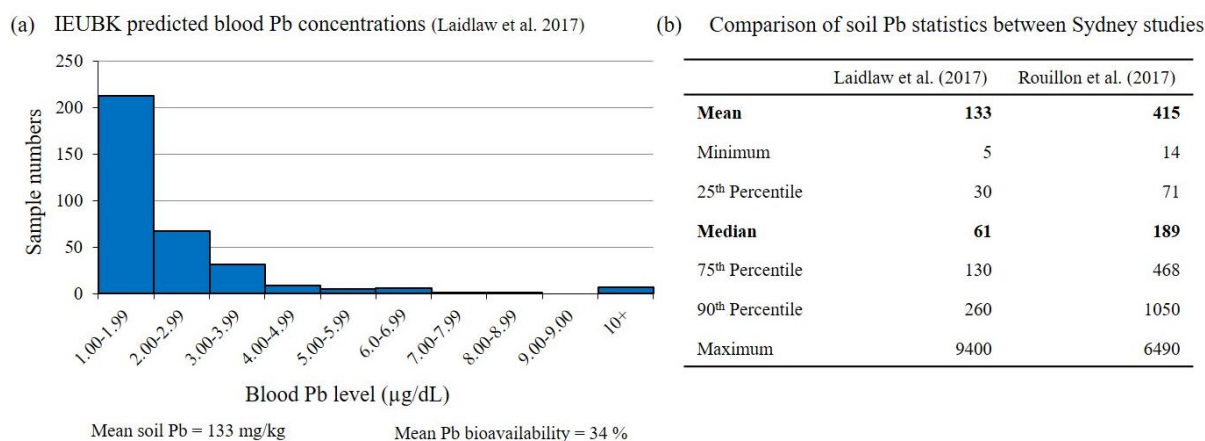
Figure 6.6: (a) Predicted blood Pb concentrations of 24 month old children living in metropolitan Sydney using the IEUBK model and the observed 34 % Pb bioavailability (from Laidlaw et al. 2017). (b) Comparison of soil Pb statistics between the study of modelled blood Pb concentrations (Laidlaw et al. 2017) and **Paper Four** (Rouillon et al. 2017a).

It is not clear why '*diffuse urban pollution*' has been largely exempted from NSW environmental regulation, as there is no published justification for its exemption. However, the absence of '*a specific industrial, commercial or agricultural activity*' leading to such contamination and the sheer costs involved in addressing '*diffuse urban pollution*' at potentially tens of thousands of residential properties is likely to have contributed to its exclusion. As noted by Taylor and Cosenza (2016), there are financial obstacles preventing the NSW EPA from accessing funds for new environmental matters:

'*Support for unforeseen matters requires either drawing on pre-allocated resources from existing programs resulting in a reduced operational activity in those areas or seeking additional treasury support. The absence of a separate, recurrent budget to resource the NSW EPA's response to significant unforeseen contamination events could limit its capacity to address contamination and protect human health.*' (Taylor and Cosenza 2016, pp. 163)

This further supports the case for using a cost-efficient soil metal assessment protocol for potentially contaminated sites that can provide fit-for-purpose information in situations where funding is restricted. Interestingly, pXRF has already been trialled briefly by both government and industries primarily as a screening tool, and is covered in the following section.

6.4   National and international pXRF uptake

6.4.1   Industry examples

The application of pXRF for the measurement of metal-contaminated soils in Australia is limited, largely due to its cautionary restriction from the NEPM (NEPC 2013) and the lack of reputable field-based pXRF protocols available for metal-contaminated soil analysis. There are

however emerging examples of industry utilising *in-situ* pXRF screening as the part of their investigation of metal contaminants in soils. The array of examples below exhibit the current state of environmental pXRF application in Australia, with both sound (**Examples One** to **Four**) and poor (**Example Five**) pXRF operation and interpretation of pXRF data.

Example One: Smelter remediation

In 2001, after more than 100 years of intermittent operation, Pasminco notified the NSW EPA that their Cockle Creek Smelter site was significantly contaminated with metals (LEWG 2016). The smelter site closed in 2003 and remediation began in 2007, which consisted of excavation and relocation of contaminated material into an on-site containment cell. To determine the depth of soil excavation, *in-situ* pXRF was applied as an initial assessment, but was not used for validation sampling (LEWG 2016). Where *in-situ* pXRF indicated the concentrations of metals were above the site criteria (e.g. Pb – 300 mg/kg for future residential areas), further excavation of the soil was performed.

Example Two: Screening for Pb tailings

Towards the end of 130 years of discontinuous Pb mining in Northampton, Western Australia, Pb tailings were distributed around town for use in driveways, garden beds and outbuildings (NLTP 2013). The remainder of the Pb tailings were sealed in an on-site contaminant cell, however numerous residential properties remained contaminated with Pb tailings. In 2010, Aurora Environmental (consultant) was appointed to assess the Pb contamination using *in-situ* pXRF (Gillam, L. no date). Properties were prioritised into low, medium and high risk of containing Pb tailings based on the pXRF and laboratory validation data (NTLP 2013). Validation sampling was conducted based on initial pXRF readings. For instance, all pXRF measurements around the HIL–A guideline of 300 mg/kg for Pb (i.e. 200–400 mg/kg) were also measured by an off-site laboratory, while 1–5 % and 5 % of measurements <200 mg/kg and >400 mg/kg were also validated by laboratory measurements, respectively. Both pXRF and laboratory data were displayed using aerial imagery at each residential property (Figure 6.7).

Example Three: Environmental monitoring

In 2015, the NSW Government assigned $13 million to help address the issue of Pb contamination and exposure in Broken Hill, after more than 130 years of continuous Zn/Ag/Pb mining (Solomon 1988). With some of the new funding, the Broken Hill Environmental Lead Program (BHELP) Steering Committee purchased a pXRF to assist in monitoring homes where children present elevated blood Pb concentrations (BHELP 2016). The pXRF is used to generate immediate estimates of Pb in soils, dust and paint samples, reducing the time for

decision-making and expediting the reduction of Pb exposure in homes. Five percent of all pXRF measurements are validated by off-site laboratory measurements, and early comparisons between the two measurement techniques reveals that the decisions made on-site by pXRF do not differ to those made using laboratory data (pers. Comm. BHELP 2016). This allows for rapid data generation by pXRF, and reduces the costs associated with long term environmental monitoring of homes. In the first 6 months of use, 85 properties have been assessed using pXRF, with 679 soil and 125 paint samples tested (BHELP 2016). The estimated cost savings of using pXRF over more-expensive laboratory measurements are approximately $250,000 over the lifetime of the BHELP.

PIN: XXXX

PROPERTY INFORMATION

Street Address: XXXXXX   Owner: XXXXXXXX

Occupier: XXXXXX/none   Consent Obtained: Y/N

CONTACT DETAILS: name, phone, email

Property Type/Use: residential/commercial (eg mechanic)/recreation/education/reserve/ others

Special Conditions or Notes: XXXXXX

INTERVIEW

Conducted By: XXXXXXX   Person Interviewed: owner or occupier

Interview Date/Method: XXXXX/in person, phone, email

INSPECTION

Conducted By: XXXXXXX   Date: planned for XXXXX or completed on XXXXX

Tailings Observed: Y/N/Possibly

Location(s) of Tailings: around shed base and driveway only

RESULTS

XRF Locations	XRF Results (ppm)	Soil Sample Locations	Analytical Results (mg/kg)
XRF-1	220	-	-
XRF-2	50	-	-
XRF-3	1200	SS1	1225
XRF-4	625	SS2	580

❌ XRF only   ❌ XRF and analytical soil sample

Figure 6.7: Example of pXRF screening and laboratory measurement report at a residential property in Northampton, Western Australia (Gillam, L. no date).

Example Four: Mercury (Hg) contaminated Defence site

Environment Resources Management Australia (consultant) was commissioned by the Australian Defence Industries to remediate Hg-contaminated soil after years of wastewater discharge from propellant manufacturing at their industrial site in Mulwala, NSW (ERM Australia 2004). An early generation pXRF was used (See Figure 1.1) to screen soils for Hg contamination by categorising soil into one of four waste classifications (A: <50 mg/kg Hg, B: 50–75 mg/kg Hg, C: 75–250 mg/kg Hg, D: >250 mg/kg Hg). Excavation of soil continued until all pXRF Hg measurements were <50 mg/kg (Figure 6.8a) and a further 0.5 metres of soil was

removed, both laterally and vertically (ERM Australia 2004). Prior to remediation, ERM compared pXRF and off-site laboratory Hg measurements and established a relationship existed between the two measurement techniques, and therefore could be used to guide laboratory validation sampling after excavation (Figure 6.8b). Soil Hg concentrations by pXRF ranged from 6–3000 mg/kg (n=595), which were removed until validation laboratory sampling returned <1 mg/kg Hg.
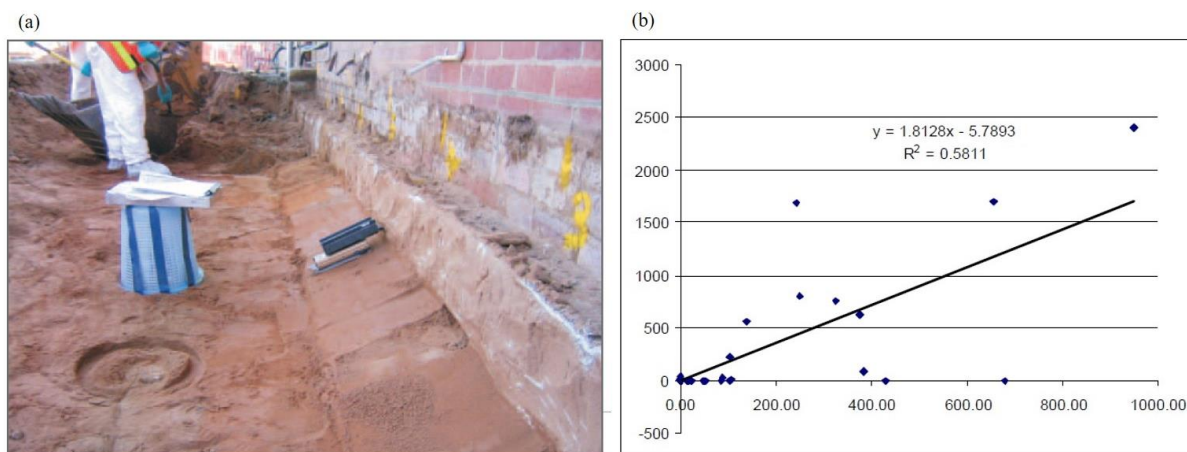
Figure 6.8: (a) Field portable XRF measurement of Hg contaminated soil and (b) reported comparison between pXRF and laboratory data for Hg measurements (ERM Australia 2004).

Example Five: Pb-contamination from a large water pipe

In 2011, the Hunter Water Corporation commissioned Sinclair Knight Merz (consultant) to investigate Pb contamination in the soils surrounding a large water pipe that was sealed with Pb joints (SKM 2012). To assess the severity and extent of Pb contamination from the pipe, *in-situ* pXRF was utilised on soil along adjacent to the pipeline, perpendicularly from the pipe and at an adjacent property. Field portable XRF measurements of Pb (n=199) were validated against 24 off-site laboratory measurements using RPD (relative percentage difference), with a variance of up to 50 % RPD deemed acceptable (SKM 2012). The mean soil Pb concentration of *in-situ* pXRF measurements near the water pipe was 1264 mg/kg (range 5–32,557 mg/kg), and was 80 mg/kg (5–999 mg/kg) for measurements in the adjacent property (SKM 2012). The findings from this assessment were semi-consistent with Harvey et al. (2015), who found greater Pb concentrations in soils directly under the pipeline (mean 6460 mg/kg) as a result of deteriorated Pb solder in the joints of the pipeline.

6.4.2   Effective and poor industry pXRF practice

Effective pXRF practice

These industry examples of *in-situ* pXRF application utilise the spectrometers main strengths of inexpensive, increased on-site sampling, and rapid, real-time data generation. All five examples used pXRF as a guide to determine the concentration of soil metals present, with

validation from a subset of off-site laboratory data. This should be mandatory when utilising *in-situ* pXRF measurements as there are many field and analytical variables that contribute to the estimation of metals (see **Paper Three**). **Example Two** used the NEPM HIL–A guideline of 300 mg/kg for Pb as the site criteria for classification, and therefore ensured all measurements near the guideline (200–400 mg/kg) were co-measured by an off-site laboratory, while a smaller proportion (≤5 %) were validated for Pb concentrations <200 mg/kg and >400 mg/kg. This is good practice to ensure *in-situ* pXRF measurements close to the NEPM guideline being applied are indeed correct. Metal-contaminated soils are often highly heterogeneous in contaminant distribution, as a single analytical measurement could potentially be considerably different to a measurement from a sample right next to it (see **Paper Three**). **Example Four** used composite measurements (the practice of conducting many measurements at the one sample location and using the mean) to mitigate soil heterogeneity. However, it is unclear from the investigation report how many pXRF measurements constituted an averaged measurement. Lastly, pXRF data in **Examples One**, **Two** and **Four** enabled real-time, on-site decision-making for further soil excavation or waste classification. These industry examples demonstrated some understanding of effective pXRF use and the mitigation of limitations associated with *in-situ* pXRF measurements. However, a number of shortfalls were observed, primarily in the investigation reports of **Examples Four** and **Five**, which are discussed below.

Poor pXRF practice

The main drawbacks of pXRF application in these industry practices were (a) the lack of pXRF measurement correction using off-site laboratory validation measurements, and (b) the lack of field and sampling QAQC to establish the uncertainty around measurements. Measurement validation is useful for demonstrating the difference between screening quality *in*-situ pXRF and NATA-accredited laboratory data. However, if a consistent under- or over-reporting trend of pXRF metal concentrations is observed, correction of *in-situ* pXRF data can be attempted to align pXRF measurements to those provided by a NATA-accredited laboratory method. For instance, **Example Five** repeatedly stated that the wet field condition hampered pXRF measurements of Pb, and as a result there were large discrepancies between pXRF and laboratory data. This limitation could have been addressed using the data correction method presented in **Paper Three**. This pXRF data correction procedure assumes the laboratory method is truly accurate and provides a total (or near-total) digestion for true comparison against pXRF measurements (see Section 3.3).

The reporting of laboratory focused QAQC components such as laboratory duplicates, matrix spike recoveries and method blanks are common practice in investigation reports, yet the lack

of field and sampling based QAQC in these investigation reports is concerning, but not surprising. Volume 3: Site Characterisation guidelines of the NEPM (NEPC 2013) does not require the collection of field duplicates, nor the estimation of uncertainties related to sampling or soil heterogeneity. Section 19.10 of Volume 3 of the NEPM (NEPC 2013) lists a checklist of field QAQC components required for assessment reports but does not include the collection of field duplicates, see below (pp. 123):

19.10   Quality assurance and quality control checklist

Field quality assurance and quality control

- ➢ details of sampling team
- ➢ decontamination procedures carried out between sampling events
- ➢ field logs for samples collected — including time, location, initials of sampler, duplicate locations, duplicate type, chemical analyses to be performed, site observations and weather conditions
- ➢ chain-of-custody fully identifying (for each sample) the sampler, nature of the sample, collection date, analyses to be performed, sample preservation method, departure time from the site and dispatch courier(s)
- ➢ sample splitting techniques
- ➢ statement of duplicate frequency (for intra-laboratory and inter-laboratory duplicate samples and duplicate sample results)
- ➢ field blank results
- ➢ background sample results
- ➢ rinsate sample results
- ➢ laboratory-prepared trip spike results for volatile analytes
- ➢ trip blank results
- ➢ field instrument calibrations (when used)

Paper Three identified large uncertainties associated with sampling and site heterogeneity (>95 % of total measurement variability), and recommended that these variables, at the very minimum, should be quantified to demonstrate sampling uncertainties. The omission of such information in assessment reports is not only widespread, but is detrimental to environmental companies, because they fail to estimate the risk involved in site characterisation. *In-situ* pXRF can offer additional measurements for field duplicates at very little extra cost to the investigator, which ultimately improves assessment reports by demonstrating an understanding of site and sample variability.

There were also an array of discrepancies related to pXRF data interpretation observed in the industry examples. The correlation of pXRF vs. laboratory data for Hg measurements in **Example Four** was not only weakly correlated ($r^2 = 0.5811$), but had no indication of which axis was pXRF or the laboratory data. Further, the regression equation of $y = 1.8128x – 5.7893$ indicated one measurement technique was reporting measurements on average >1.8 times greater than the other technique (Figure 6.8b). **Examples Four** and **Five** assumed that all non-detect pXRF measurements (i.e. <LOD) were 0 mg/kg. This is misleading as when used *in-situ*, pXRF has higher limits of detection than those calculated using dry, fine grained homogenous powders (see **Paper Three**). The assessment report of **Example Five** stated that a relative percent difference (RPD) of 50 % between pXRF and laboratory data was deemed acceptable for their investigation. Not only was this allowance level precariously high, numerous RPD values were incorrectly calculated in the report (SKM 2012). Comparison between the two measurement techniques were never going to be useful for this investigation as samples for the laboratory measurements were collected at 0–10 cm in depth (SKM 2012), while *in-situ* pXRF measures approximately <1 cm in depth. Finally, despite repeatedly stating the wet field conditions impacted pXRF measurements, there was no quantification or even estimation of field moisture content, which could have been used with the laboratory measurements to correct pXRF measurements for moisture content.

It is clear from the examples listed above that the majority of environmental pXRF operators are somewhat inexperienced, particularly in *in-situ* pXRF application, data interpretation, field QAQC, and laboratory validation sampling. The sampling requirements to representatively compare two measurement techniques needs to be conducted carefully, using methods similar to those described in **Paper Three**. When one samples is measured by two techniques, high soil heterogeneity can impact sample representativeness, and can result in the measurement of two different soil samples. Every effort must be made to ensure the sample measured by the laboratory is as similar as the sample measured previously by pXRF (see **Paper Two**).

6.4.3   Teaching and community pXRF initiatives

Field portable XRF has also been extensively used to engage both high school and university level students in learning about soil metal contamination and environmental health (Gore et al. 2014). The ability to generate rapid data for immediate discussion with students on geochemical trends in the environment is powerful. At Macquarie University, pXRF has been used by the Department of Environmental Sciences to generate real-world data for students to use in assessments, and to provide an introduction towards developing a scientific investigation (Gore et al. 2014). For instance, high school students from Broken Hill spent a day working alongside

undergraduate students and staff from Macquarie University to investigate soil metal contamination near railways tracks using pXRF for field information and screening. This work, which was published a year later using ICP–MS and Pb isotope compositions (Kristensen et al. 2015), determined that the transport of ore out of Broken Hill in uncovered train wagons was the primary contributor to high soil metal concentrations adjacent to railway tracks. In other examples, pXRF was used as the main analytical tool in identifying geochemical trends across residential areas for 3rd year Macquarie University Environmental Science students. As part of their capstone Environment subject, students are required to conduct a research style project in identifying or addressing an environmental issue. The access to, and low operation cost of *ex-situ* pXRF enabled multiple student groups to develop a sampling plan (Figure 6.9), collect samples in the field, prepare them for pXRF analysis, and with the assistance of staff, analyse the samples for their metal content in the safety of a test stand. These projects have been conducted at well-known metal-contaminated areas of NSW including Port Kembla (Figure 6.9), Broken Hill, Boolaroo and Newcastle, which later formed the basis of **Paper Five**.
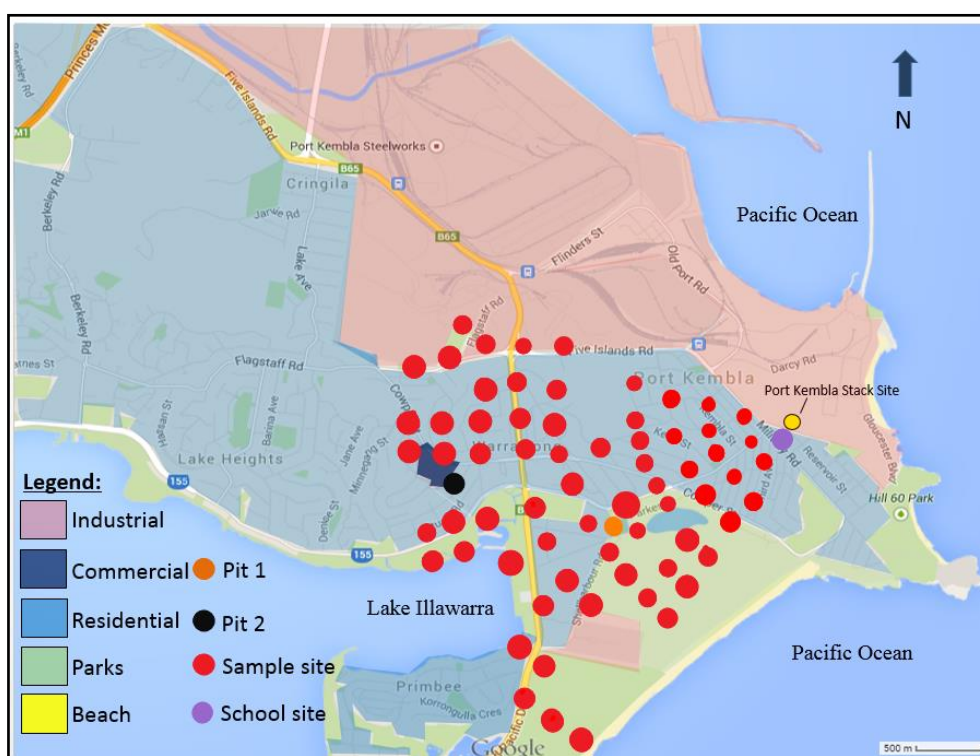
Figure 6.9: Sampling plan map generated by undergraduate students for a study that investigates soil metal contamination from the suspected contamination point source in Port Kembla, NSW (Jones et al. 2015).

In order to better understand soil sampling methods and analysis, Environmental Science students at Macquarie University were invited to participate in the VegeSafe program. Students collected soil from their properties using the VegeSafe soil sampling instructions (Appendix E) for analysis by pXRF, before discussing factors that may influence soil metal concentrations and the analysis itself. These examples introduce students to a new analytical technique and

teach students the fundamental components of a successful science investigation including experimental design, collection, preparation and analysis of samples, QAQC, report writing and critical thinking (Gore et al. 2014).

In addition to the VegeSafe program (Chapter Five), pXRF has also been used successfully as the primary screening tool for soil metal contamination abroad. Professor Gabriel Filippelli from Indiana University-Purdue University, Indianapolis, USA, has led a program similar to VegeSafe that offers free soil metal screening with pXRF and advice to the residents of Indiana (IUPUI 2010). Professor Filippelli's 'Garden Safe, Garden Well' program has been well received by the local community, who strive to become more self-sustained by growing food at home (IUPUI 2012). In New York State, several agencies have collaborated to provide the community with free soil metal screening and advice to better help people to understand urban soils (CWMI 2010). Similar to VegeSafe, this service to the community has also been utilised for scientific research with numerous publications arising from the large sample collection (e.g. Mitchell et al. 2014; Spliethoff et al. 2014; 2016). Further, the EMPACT (Environmental Monitoring for Public Access & Community Tracking) 'Lead Safe Yard Project' was introduced in Boston, Massachusetts, in 1998 to investigate and combat childhood Pb exposures from elevated soil Pb in residential areas (EMPACT 2001). The use of pXRF was central to the success of this project, as it was able to provide residents with on-site, real-time information about the potential Pb contamination of their yards, at no cost to the home owners. The investigators use the mean soil Pb concentration for a given area of a yard and classify them into one of four categories (Table 6.2), which correspond to a recommended interim action (EMPACT 2001).

Table 6.2: Actions recommended for different soil Pb concentrations by the EMPACT (2001) Pb-safe yard project.

EMPACT Pb-safe yard project	
Soil Pb concentration*	**Recommended interim action**
>5000 mg/kg (very high)	If soil removal or permanent barriers are not possible: • Install semi-permanent barrier, such as a wood-framed dripbox filled with gravel or mulch • Relocate gardens – unsafe for all types of gardening
2000-5000 mg/kg (high)	• Relocate gardens – unsafe for all types of gardening • Relocate children's play area, pet area, and picnic area, if possible. If not, install wood platform or wood-framed raised play and picnic area filled with woodchips • Install path of walking stones for high-traffic areas • Seed and fertilize grassy areas, or cover with mulch or woodchips if not suitable for grass
400-2000 mg/kg (moderately high)	• Install raised-bed garden and supplement with clean topsoil • Install wood-framed raised play and picnic area filled with woodchips • Install path of walking stones for high-traffic areas • Seed and fertilize grassy areas, or cover with mulch or woodchips if not suitable for grass
<400 mg/kg (urban background)	• No treatment necessary

*Based on *in-situ* pXRF analysis of surface soils (typically 15 to 25 samples per yard) and Pb concentration mapping of the entire yard to include areas of special concern (play areas, gardens, outside eating areas, pet runs, etc.)

These community-focused environmental programs in the United States have paved the way for similar soil screening programs in other countries, largely due to a sound understanding of urban metal contamination in urban cities, access to government funding sources, and experience using early generation pXRF spectrometers. The expansion of publicly accessible soil screening programs in developing countries should be considered by their relevant health authorities, particularly in areas where Pb contamination is prevalent and areas where home-grown food consumption is part of a regular diet. Lastly, Pure Earth, a non-for-profit organisation based in New York, USA, use pXRF extensively to rapidly identify (and later clean up) pollution issues in low- and middle-income countries such as Armenia, Ghana, Nigeria, Vietnam and Uruguay (Pure Earth 2014).

6.5   Evaluation of pXRF for metal-contaminated soils

The promise of a rapid and inexpensive geochemical technique that can be used in the field to guide judgemental sampling for environmental assessments is enticing, particularly where investigators lack site history information. Field portable XRF can deliver these unique advantages to supplement environmental assessments, however there are also well-known challenges that have deterred many environmental users from utilising pXRF. After several discussions with environmental consultants and state regulators in Australia, it appears the drawbacks of most concern are the potential for radiation exposure, pXRF measurement inaccuracy, the impact of moisture content on pXRF measurements (i.e. semi- or fully-saturated soils) and the shallow depth of soil measurement. These concerns are reasonable, and certainty not unexpected as the current responsibility of potential users would increase from merely sampling soils and sending them away for wet chemistry analysis, to understanding and applying an analytical technique in the field. Similar to other measurement techniques, the data acquired from pXRF is subject to many variables, including the sample itself, spectrometer arrangement and calibration, the measurement process and field conditions. Under certain circumstances, these variables can also be optimised, to generate accurate and cost-effective environmental data. If new pXRF users better understood these variables, they are more likely to achieve the fit-for-purpose data they envisioned when acquiring a pXRF. These common concerns surrounding pXRF can be easily abated, and are discussed below.

6.5.1   Addressing non-pXRF user concerns

The concern of pXRF radiation exposure was addressed in **Paper One**, which reveals that while there are measurable radiation doses associated with pXRF measurements, the estimated exposure dose is negligible. The hypothetical scenario used in **Paper One** is conservative at best, as radiation dose measurements were made at arm's length and not at the distance a typical

user would be using *in-situ* pXRF, nor for *ex-situ* pXRF measurements within the confines of a radiation shielding test stand. It is understandable that new pXRF users are cautious towards utilising an open radiation source spectrometer. However, when these 'measurable' exposures are benchmarked against common everyday exposures (Table 6.3), it is clear that the benefits of pXRF far outweigh the negligible radiation exposure when used appropriately.

Table 6.3: Effective body doses from common sources of radiation exposure (Public Health England 2011; ARPANSA 2012; American Cancer Society 2013).

Typical radiation exposure	Effective whole body dose
Yearly exposure of the hypothetical scenario when analyzing quartz sandstone, loose quartz sand or steel materials	**<3 µSv**
Dental X-ray	5 µSv
Average background radiation per day (varies)	5-10 µSv
Anterior-Posterior Chest X-ray	20 µSv
Five hour airplane flight (varies with latitude and altitude)	40-60 µSv
Yearly exposure of the hypothetical scenario when analyzing polyethylene	**73.5 µSv**
Yearly dose from natural potassium in the body	390 µSv
Mammogram	400 µSv
Maximum allowable exposure for non-radiation workers in Australia and the USA per year	1 mSv
Computed Tomography (CT) - Head	2 mSv
Worldwide average background radiation per year	2.4 mSv
Computed Tomography (CT) - Chest	7 mSv
Computed Tomography (CT) - Abdomen	10 mSv
Maximum allowable occupational exposure for radiation workers in Australia per year	20 mSv
Maximum allowable occupational exposure for radiation workers in the USA per year	50 mSv
Level at which changes in blood cells can be readily observed	100 mSv
Dose limit for US radiation workers in life-saving operations	250 mSv
Acute radiation effects including nausea and a reduction in white blood cell count	1 Sv
Severe radiation poisoning, in some cases fatal	2 Sv
Usually fatal radiation poisoning, survival possible with immediate treatment	4 Sv
Fatal dose, with or without treatment	8 Sv

*Study results in the context of common radiation exposure dosages in bold.

The accuracy of pXRF measurements is perhaps the most common question amongst non-pXRF users. Paradoxically, it is also perhaps the most difficult to quantify correctly. Similar to laboratory-based analytical instruments that are operated by a trained laboratory team, the success of accurate pXRF measurements largely depends on the user and their decisions before, during and after the measurements. Prior to measurement, the user must consider which elements and what concentration range they seek, if these elements have any known chemical or spectral interferences, and what sample preparation steps are required (if any) to accurately measure these elements given the field conditions. During the measurement, the user must decide which calibration to use, which X-ray beams to measure from, what is the measurement period and how they will estimate accuracy (i.e. CRMs or an external reference method). After the measurement, the user must contemplate what is the acceptable accuracy range for their data quality objectives, how they will present both precision and accuracy estimates, and if they need to correct the pXRF data. Understanding these variables and their influence on the measurement of specific elements is where most pXRF users fall short, and where the greatest

development needs to occur (see Section 6.5.3). Further, the estimation of pXRF accuracy itself has its own challenges, particularly when taking *in-situ* pXRF measurements and validating them with laboratory wet chemistry analysis (see **Paper Three**).

Presently, environmental investigators are able to sample soils from a range of field conditions (dry, semi-saturated and/or fully saturated soils). Commercial laboratories can then estimate the proportion of total solids (%) in these samples by drying subsamples and converting the data from 'wet weight' or 'as submitted' to 'dry weight' analysis. In contrast, *in-situ* pXRF directly measures the metal content of soils with varying amounts of moisture saturation. High soil moisture can reduce the intensity of fluorescent X-ray signals back to the detector (Bastos et al. 2012), which can impact all aspects (precision, detection limits and accuracy) of pXRF measurements (Ge et al. 2005). Therefore, it is vital for *in-situ* pXRF users to mitigate the influence of soil moisture, particularly for saturated soils where the greatest loss of signal occurs (Sahraoui and Hachicha 2017). Hence, **Paper Three** presents a novel *in-situ* pXRF measurement method for various degrees of soil moisture content (1–69 %; Appendix D Supplementary Table 1) using the subset of validation wet chemistry data. Other methods of moisture correction for pXRF are presented by Ge et al. (2005), Bastos et al. (2012) and Sahraoui and Hachicha (2017).

According to the NEPM (NEPC 2013) and Australian Standard 4482.1 (Standards Australia 2005), surface soils should be sampled for wet chemistry analyses at 0–100 mm or 0–150 mm depth, unless there is evidence of a thin superficial layer of contamination. On the other hand, *in-situ* pXRF measurements measure the uppermost (<10 mm) soil layer due to the superficial penetration and fluorescence of X-ray photons. The validation of *in-situ* pXRF measurements against samples collected at 0–100 mm or 0–150 mm is likely to be poor as the two techniques measure different soil depths, and consequently different samples. In order to compare both measurement methods accurately, they must be sampled from the sample location, at the same depth, as closely as reasonably possible. However, if the site criteria require pXRF measurement of surface soils at a greater depth (i.e. 0–150 mm), or from subsurface soils, then some light sample preparation could be implemented before measurement in a pXRF cup fitted with Mylar film or through a polyethylene bag (e.g. US EPA 2015).

6.5.2   Holistic pXRF evaluation

This thesis presents five research papers (**Papers One** to **Five**) that contribute to an all-inclusive evaluation of pXRF and its environmental application for the measurement of metal-contaminated soils. This thesis finds pXRF as a safe and effective geochemical tool, that when

used correctly disperses minimal, but measurable radiation intensities as a result of X-ray scattering from samples (Rouillon et al. 2015). If soils undergo simple sample preparation steps (i.e. drying, sieving, crushing and homogenising), *ex-situ* pXRF is capable of generating accurate and inexpensive measurements for a range of metals that rival the quality of measurements produced by commercial wet chemistry analysis (Rouillon and Taylor 2016). Yet, when used *in-situ*, pXRF can offer multiple advantages over off-site analysis methods including the inexpensive high density characterisation of sites and the generation of real-time data to guide judgemental sampling (Rouillon et al. 2017b). Further, pXRF can help identify soil metal contamination issues in urban centres by generating rapid, inexpensive screening data for the community, so they can make informed decisions about gardening in urban spaces (Harvey et al. 2017; Rouillon et al. 2017a).

This thesis has demonstrated that pXRF is capable of generating safe, accurate, and inexpensive geochemical measurements of soils for a range of metal-contamination investigations. Yet, this thesis has also identified a variety of factors that adversely impact the safety and accuracy of pXRF measurements. In order to consistently achieve effective pXRF data, pXRF users should understand the many variables that can contribute to both successful and unsuccessful, *in-situ* and *ex-situ* measurement programs. The assurance of 'out of the box' quality performance by pXRF manufacturers may mislead potential new users to believe they simply need to 'point and analyse' for accurate measurements. While on the other hand, the widespread screening use of pXRF may inappropriately inform users that high quality data is unattainable.

6.5.3   Development of pXRF users and methods

Given the numerous variables associated with environmental pXRF application, and the potential to generate high quality data both *ex-situ* (**Paper Two**) and *in-situ* (**Paper Three**), it is apparent that the greatest limiting factor for accurate pXRF measurements is the user and their understanding of pXRF-related variables. As discussed in Section 3.1, pXRF users are not required to undertake analytical training when acquiring a pXRF, but may choose to participate in pXRF workshops at an additional cost. These workshops present a great deal of information usually in a short period of time, yet ultimately lack practical modules and hands-on training, which would undoubtedly be useful for new users. This is in vast contrast to the operators of wet chemistry spectrometers at commercial laboratories, who are trained to operate off stringent SOPs that can also become NATA-accredited methods. Commercial laboratories are able to frequently provide accurate measurement data to their clients largely for three reasons; (1) they can mitigate the influence of numerous sample and analytical variables in a controlled environment, (2) they can ensure the same sample preparation and measurement practices are

carried out via explicit SOPs from their well-trained personnel, and (3) they undertake regular inter-laboratory proficiency assessments (e.g. NMI 2014).

The lack of a reputable, and publicly accessible pXRF method for the measurement of metal-contaminated soils likely hinders the development of pXRF users. Without a sound understanding of XRF theory and the variables relating to sample preparation and/or calibrations, new pXRF users require some form of guidance. The US EPA 6200 method (US EPA 2007) provides some introductory information for pXRF users, particularly for those without analytical training, yet lacks direction for users who want to follow specific methods. In these cases, the development of pXRF SOPs are required so that users can simply follow directions to consistently generate accurate, fit-for-purpose data. These SOPs could be specific for particular elements, matrices, field conditions and/or investigation types (preliminary or detailed), yet could also be designed to empower users to make decisions based on their desired data quality outcomes (see Figure 6.10). These decision-based methods could assist new pXRF users to understand the importance of sample preparation steps, and its impact on pXRF data quality. Further, the method could also guide users through the post-measurement process, which may include *in-situ* pXRF data correction, presentation of precision and accuracy estimates in reporting and interpretation of data.

If environmental users had access to detailed, yet fool-proof pXRF methods that can achieve a specific level of data quality, it is likely that the advantages of pXRF would be utilized by the environmental industry more confidently. Reputable pXRF methods could also be implemented in environmental regulatory legislation such as the NEPM (NEPC 2013) or NSW EPA sampling guidelines (NSW EPA 1995) as an alternative or supplementary method to the characterisation of metal-contaminated sites. These methods should ideally be applicable to all pXRF spectrometers, provided they meet some form of minimum requirement for both hardware and software components, given that new pXRF units are often regularly released by manufacturers.
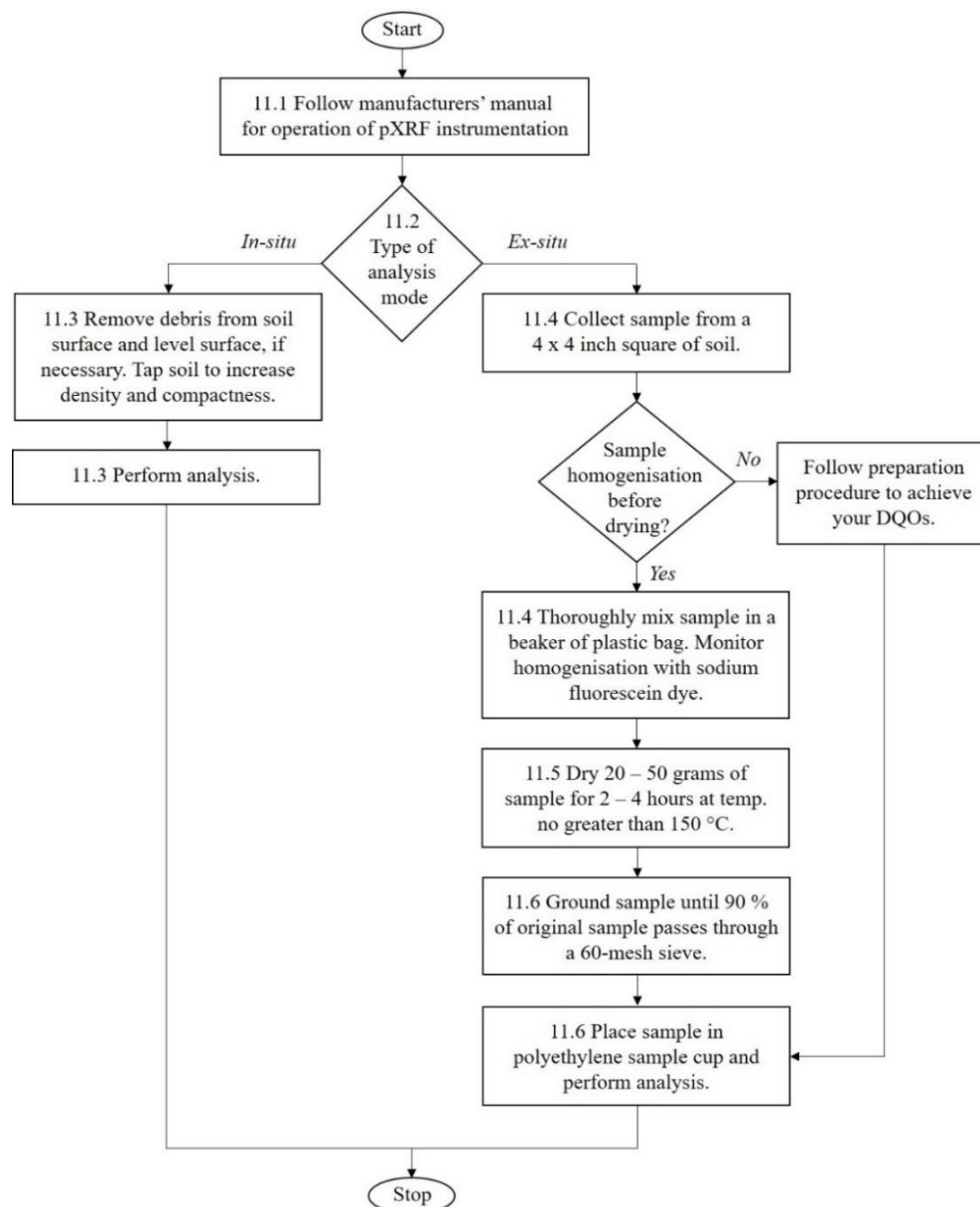
Figure 6.10: Summary of guidance by US EPA pXRF method 6200 – Field portable X-ray fluorescence spectrometry for the determination of elemental concentrations in soil and sediment. (US EPA 2007).

6.6   Future direction for pXRF

Field portable XRF technology has markedly improved in recent years due to the miniaturisation of internal components, detectors and X-ray tubes, and the development of user interfaces, pXRF software, and ergonomic exterior designs (Weindorf et al. 2014a). Newly improved flagship spectrometers are released frequently by major pXRF manufacturers, which bring improved software features and superior hardware when compared to its predecessors. For instance, the pXRF used in **Papers One** to **Five** was an Olympus DELTA Premium XRF Analyzer. This spectrometer, while capable of achieving accurate and cost-effective data for environmental contamination investigations, had no internal GPS system, cooling fan, WiFi connectivity and was not dust or water resistant (Olympus IMS 2014). In late 2016, Olympus released the new Vanta XRF Analyzer that addressed all of the above drawbacks, and also

improved the internal electronics, enhancing the durability of the spectrometer (Olympus IMS 2017).

The rapid improvement of pXRF technology can lead to numerous benefits for environmental users, particularly the capacity for faster, more precise and higher accuracy data. Firstly, higher X-ray counts per second in new pXRF spectrometers leads to greater analytical precision, which means lower measurement times for users. This can reduce labour costs for pXRF users, particularly in the field where many *in-situ* measurements are required. Secondly, geo-referenced pXRF data can be sent to a computer via WiFi for real-time integration into third party geographic information systems software. This can accelerate decisions for further judgemental sampling or supplement preliminary characterisation of sites, which can lower the overall costs associated with metal-contaminated site assessments. Thirdly, integrated GPS can guide users to pre-determined locations in the field for measurements, eliminating the need for a separate GPS unit or map of the site. Finally, the simplification and customisation of the user interface can tailor to the needs of users and their specific applications. These are a few examples of new features and improvements that have recently been implemented in pXRF spectrometers.

As noted in **Paper Three**, *in-situ* pXRF is limited by the fact it can only measure metal contaminants. In contrast, the current practice of sampling and off-site measurements allow for the wide coverage of inorganic, hydrocarbon, organic and persistent chemical contaminants that often co-exist at contaminated sites. Future developments to pXRF may enable users to simultaneously screen for non-metal contaminants via optional add-on accessories. Such technology certainly exists in the form of portable screening tools by Ziltek (CSIRO 2012) and Thermo Scientific (2001), yet these are measured by separate analysers. By applying a similar *in-situ* measurement approach to **Paper Three**, it may be possible that future pXRF site assessments could address a greater range of contaminants simultaneously.

6.7   Conclusions

This thesis has examined and evaluated the environmental application of pXRF for the measurement of metal contaminated soils against the current standard practice of sampling and wet chemistry analysis. The research presented in this thesis investigates multiple, yet interrelated, facets related to pXRF safety, analytical performance and *in-situ* and *ex-situ* application. This thesis has determined that pXRF is not only capable of generating high quality data, but that it should also be widely employed as the primary tool for metal contaminated site assessments, with supplementary wet chemistry validation. The numerous advantages of *in-situ*

and *ex-situ* pXRF, and the strategies used to mitigate disadvantages, have been addressed so that users can efficiently, accurately and safely utilise pXRF technology for their assessments of metal-contaminated soils.

This thesis has also examined contemporary and legacy metal contamination hazards in both mining and urban centres of Australia using pXRF and wet chemistry analyses. The studies presented in this thesis demonstrate that metal contamination hazards continue to plague communities from both current smelting and mining emissions, the historical use of Pb products (*inter alia* other toxic contaminants) and the distribution of waste materials. Investigation of these hazards have enhanced dust mitigation strategies in Broken Hill and Port Pirie, stimulated reassessment of the abatement of legacy smelter-related hazards in Boolaroo, and informed public discussion around environmental health and safe urban gardening in Sydney, Newcastle and beyond.

The studies in this thesis add to the international body of research on pXRF analytical evaluations and application for environmental assessments conducted since the mid-1990s. Moreover, this thesis provides an updated appraisal of pXRF, using the latest technology to ascertain its efficacy for environmental investigations. By assessing and addressing a diverse range of pXRF-related misconceptions related to safety and analytical data quality, this thesis provides a contemporary, holistic and more complete understanding of pXRF and its application towards environmental investigations. This enhanced understanding of pXRF facilitates further discussion with environmental users and regulators, so that informed decisions surrounding its use can be attained.

The research in this thesis has challenged the current perception that pXRF produces unreliable and inferior data compared to the current standard approach using wet chemistry analysis. These studies have demonstrated that when used correctly, pXRF can provide high quality data for the measurement of metal-contaminated soils, and should be utilised in conjunction with wet chemistry analyses to combat challenges during site characterisation, including high metal heterogeneity and unguided judgemental sampling. Additionally, this thesis has showcased a practical and cost-effective, community-focused pXRF application in VegeSafe, that has assisted thousands of urban gardeners in understanding potential metal(loid) hazards to help them utilise their backyard space safely for self-sustainability.

The emerging use of pXRF screening by the Australian environmental industry is promising, particularly where it has been used effectively. However, its omission from the NEPM (NEPC

2013) and the absence of established field-based pXRF methods in Australia have largely deterred users from harnessing the benefits associated with pXRF. The studies in this thesis contribute to the scientific body of evidence necessary to validate the rapid and inexpensive implementation of pXRF for environmental contamination research and metal-contaminated site investigations.

6.8   References

American Cancer Society. 2013. General Questions and Comments on Radiation Risk: Find Support and Treatment. <http://www.cancer.org/treatment/understandingyourdiagnosis/> (accessed 17 June 2014).

Ashrafzadeh, S., Lehto, N.J., Oddy, G., McLaren, R.G., Kang, L., Dickinson, N.M., Welsch, J., Robinson, B.H. 2017. Heavy metals in suburban gardens and the implications of land-use change following a major earthquake. Applied Geochemistry. In Press, Corrected Proof. http://dx.doi.org/10.1016/j.apgeochem.2017.04.009

Australian Broadcasting Corporation (ABC). 2013. Lead checks made on playground equipment at Port Pirie. <http://www.abc.net.au/news/2013-07-25/lead-checks-on-playground-equipment/4842862> (accessed 08 June 2017).

Australian Broadcasting Corporation (ABC). 2014. Broken Hill children affected by contaminated playgrounds, researchers say. <http://www.abc.net.au/news/2014-10-16/contaminated-playgrounds-a-danger-to-broken-hill-kids-research/5817244> (accessed 08 June 2017).

Australian Broadcasting Corporation (ABC). 2015. Nyrstar Smelter $500m redevelopment secures Port Pirie future, SA Premier says during first visit. <http://www.abc.net.au/news/2015-06-24/sa-premier-tours-redeveloped-nyrstar/6570520> (accessed 11 June 2017).

Australian Radiation Protection and Nuclear Safety Agency (ARPANSA). 2012. Assessment of the Impact on Australia from the Fukushima Dai-ichi Nuclear Power Plant Accident. Technical Report Series No. 162. <https://www.arpansa.gov.au/sites/g/files/net3086/f/legacy/pubs/technicalreports/tr162.pdf> (accessed 12 May 2014).

Bastos, R.O., Melquiades, F.L., Biasi, G.E. 2012. Correction for the effect of soil moisture on in situ XRF analysis using low-energy background. X-ray Spectrometry 41, 304-307.

Berry, M., Garrad, J., Greene, D., Crooks, M.L. 1994. Reducing Lead Exposure in Australia. Commonwealth Department of Human Services and Health, Canberra.

Birch, G.F., Vanderhayden, M., Olmos, M. 2011. The nature and distribution of metals in soils of the Sydney estuary catchment, Australia. Water, Air & Soil Pollution 216, 581-604.

Boreland, F., Lyle, D.M., Wlodarczyk, J., Balding, W.A., Reddan, S. 2002. Lead dust in broken hill homes: a potential hazard for young children? Australian and New Zealand Journal of Public Health 26, 203-207.

Bugdalski, L., Lemke, L.D., McElmurry, S.P. 2013. Spatial variation of soil lead in an urban community garden: Implications for risk-based sampling. Risk Analysis 34(1), 17-27.

Calace, N., Caliandro, L., Petronio, B.M., Pietrantonio, M., Pietroletti, M., Trancalini, V. 2012. Distribution of Pb, Cu, Ni and Zn in urban soils in Rome city (Italy): effect of vehicles. Environmental Chemistry 9, 69-76.

Cartwright, B., Merry, R.H., Tiller, K.G. 1976. Heavy metal contamination of soils around a lead smelter at Port Pirie, South Australia. Australian Journal of Soil Research 15, 69-81.

Chiaradia, M., Chenhall, B.E., Depers, A.M., Gulson, B.L., Jones, B.G. 1997. Identification of historical lead sources in roof dusts and recent lake sediments from an industrialized area: indications from lead isotopes. Science of the Total Environment 205, 107-128.

Commonwealth Scientific and Industrial Research Organisation (CSIRO). 2012. Portable Device Detects Soil Contamination. News. Ziltek <http://www.ziltek.com.au/pdf/CSIRO%20News%20Release%20-%20Portable%20device%20detects%20soil%20contamination.pdf> (accessed 21 March 2017).

Cooper, J.A., Reynolds, P.H., Richards, J.R. 1969. Double-spike calibration of the Broken Hill standard lead. Earth and Planetary Science Letters 6, 467–478.

Daily Telegraph. 2015. Broken Hill: Children face danger in lead-laced city. <http://www.dailytelegraph.com.au/news/nsw/broken-hill-children-face-danger-in-leadlaced-city/news-story/8879d077e56a20005c8a184449dcc18d?nk=402742947320cca7d2642628aff9930a-1497145475> (accessed 08 June 2017).

Daily Telegraph. 2017. A Sydney family were left in shock to discover their child had contracted lead poisoning. Inner West Courier Inner West. June 13 2017. <http://www.dailytelegraph.com.au/newslocal/inner-west/a-sydney-family-were-left-in-shock-to-discover-their-child-had-contracted-lead-poisoning/news-story/df29102c01360a2d4d4bf14f357df204?nk=402742947320cca7d2642628aff9930a-1497360746> (accessed 14 June 2017).

Dong, C., Taylor, M.P., Kristensen, L.J., Zahran, S. 2015. Environmental contamination in an Australian mining community and potential influences on early childhood health and behavioural outcomes. Environmental Pollution 207, 345-356.

Dong, C. Taylor, M.P. 2017. Applying geochemical signatures of atmospheric dust to distinguish current mine emissions from legacy sources. Atmospheric Environment 161, 82-89.

Dost, A.A. 1996. Monitoring surface and airborne inorganic contamination in the workplace by a field portable x-ray fluorescence spectrometer. Annals of Occupational Hygiene 40, 589–610.

Environmental Monitoring for Public Access & Community Tracking (EMPACT). 2001. Lead Safe Yards. Developing and Implementing a Monitoring, Assessment, and Outreach Program for Your Community. US EPA. 1-152.

Environmental Resources Management (ERM) Australia. 2004. Contamination, Validation and Verification of Mercury Impacted Soil – ADI Mulwala. August 2004. <http://www.defence.gov.au/id/_Master/docs/Mulwala/MecuryImpactedSoil.pdf> (accessed 19 May 2017).

Ericson, B., Landrigan, P., Taylor, M.P., Frostad, J., Caravanos, J., Keith, J., Fuller, R. 2016. The Global Burden of Lead Toxicity Attributable to Informal Used Lead-Acid Battery (ULAB) Sites. Annals of Global Health 82(5), 686-699.

Farquhar, D. 2011. *Personal Communication. Port Pirie Council.*

Ge, L., Lai, W., Lin, Y. 2005. Influence of and correction for moisture in rocks, soils and sediments on in situ XRF analysis. X-ray Spectrometry 34, 28–34.

Gillam, L. No date. Northampton Lead (Pb) – A 'Heavy' Legacy. Public Health and Clinical Services. Department of Health. Government of Western Australia. 1-25. <https://www.ehawa.org.au/documents/item/674> (accessed 19 May 2017).

Gorce, J.P., Roff, M. 2016. Immediate screening of lead exposure in the workplace using portable X-ray fluorescence. Journal of Occupational Environmental Hygiene 13(2), 102-111.

Gore, D.B., Taylor, M.P., Pritchard, R.G., Fryirs, K.A. 2014. On-site teaching with XRF and XRD: training the next generation of analytical X-ray professionals. Powder Diffraction 29, S8-S14.

Gulson, B.L., Davis, J.J., Bawden-Smith, J. 1995. Paint as a source of recontamination of houses in urban environments and its role in maintaining elevated blood leads in children. Science of the Total Environment 164, 221-235.

Gulson, B., Korsch, M., Matisons, M., Douglas, C., Gillam, L., McLaughlin, V. 2009. Windblown lead carbonate as the main source of lead in blood of children from a seaside community: an example of local birds as "canaries in the mine". Environmental Health Perspectives. 117, 148-154.

Gulson, B. L., Mizon, K. J., Davis, J. D., Palmer, J. M.,Vimpani, G. 2004. Identification of sources of lead in children in a primary zinc–lead smelter environment. Environmental Health Perspectives 112, 52–60.

Harvey, P.J., Rouillon, M., Dong, C., Ettler, V., Handley, H.K., Taylor, M.P, Tyson, E., Tennant, P., Telfer, V., Trinh, R. 2017. Geochemical sources, forms and phases of soil contamination in an industrial city. Science of the Total Environment 584-585, 505-514.

Harvey, P.J., Taylor, M.P., Handley, H.K. 2015. Widespread Environmental Contamination Hazards in Agricultural Soils from the Use of Lead Joints in Above Ground Large-Scale Water Supply Pipelines. Water, Air and Soil Pollution 226(6), 1-9.

Harvey, P.J., Taylor, M.P., Kristensen, L.J., Grant-Vest, S., Rouillon, M., Wu, L., Handley, H.K. 2016. Evaluation and assessment of the efficacy of an abatement strategy in a former lead smelter community, Boolaroo, Australia. Environmental Geochemistry and Health 38, 941-954.

Humphries, K. 2015. Media Release: NSW Government commit more than $13 million to reduce lead levels in Broken Hill. <http://www.epa.nsw.gov.au/resources/MinMedia/EPAMin150213.pdf> (accessed 08 June 2017).

Hunt, A., Johnson, D.L., Griffith, D.A. 2006. Mass transfer of soil indoors by track-in on footwear. Science of the Total Environment 370(2-3), 360-371.

Indiana University-Purdue University Indianapolis (IUPUI). 2010. Urban gardeners Beware: Is There Lead in Your Soil and Food? Department of Earth Sciences. < http://earthsciences.iupui.edu/news/urban-gardeners-beware-there-lead-your-soil-and-food> (accessed 23 May 2017).

Indiana University-Purdue University Indianapolis (IUPUI). 2012. Garden Safe Garden Well. Centre for Urban Health. 1-27.

Jones, E., Lavas, E., McKinnon, C. Thanki, K. 2015. Port Kembla Soil Contamination Investigation. Investigation of Heavy Metal Contamination of Soils In Port Kembla. Environmental Science Undergraduate Research Project. Macquarie University. 1-41.

Kenna, T.C., Nitsche, F.O., Herron, M.M., Mailloux, B.J., Peteet, D., Sritrairat, S., Sands, E., Baumgarten, J. 2011. Evaluation and calibration of a Field Portable X-Ray Fluorescence spectrometer for quantitative analysis of siliciclastic soils and sediments. Journal of Analytical Atomic Spectrometry 26, 395-405.

Kilbride, C., Poole, J., Hutchings, T.R. 2006. A comparison of Cu, Pb, As, Cd, Zn, Fe, Ni and Mn determined by acid extraction/ICP-OES and ex situ field portable X-ray fluorescence analyses. Environmental Pollution 143, 16-23.

Kristensen, L. 2015. Quantification of atmospheric lead emissions from 70 years of leaded petrol consumption in Australia. Atmospheric Environment 111, 195-201.

Kristensen, L.J., Taylor, M.P. 2016. Unravelling a 'miner's myth' that environmental contamination in mining towns is naturally occurring. Environmental Geochemistry and Health 38(4), 1015-1027.

Kristensen, L.J., Taylor M.P., Flegal, A.R. 2017. An odyssey of environmental pollution: The rise, fall and remobilisation of industrial lead in Australia. Applied Geochemistry 83, 3-13.

Kristensen, L.J., Taylor, M.P., Morrison, A.L. 2015. Lead and zinc dust depositions from ore trains characterised using lead isotopic compositions. Environmental Science: Processes & Impacts 17, 631-637.

Laidlaw, M.A.S., Mohmmad, S.M., Gulson, B.L., Taylor, M.P., Kristensen, L.J., Birch, G. 2017. Estimates of potential childhood lead exposure from contaminated soil using the US EPA IEUBK Model in Sydney, Australia. Environmental Research 156, 781-790.

Laidlaw, M.A.S., Zahran, S., Pingitore, N., Clague, J., Devlin, G., Taylor, M.P. 2014. Identification of lead sources in residential environments: Sydney, Australia. Environmental Pollution 184, 238-246.

Lead Expert Working Group (LEWG). 2016. Lead Expert Working Group Report on Managing Residual Lead Contamination in North Lake Macquarie. Report Prepared for the NSW Environment Protection Authority. December 2016. <http://www.epa.nsw.gov.au/resources/Lead/lead-expert-working-group-report.pdf> (accessed 18 May 2017).

Mackay, A.K., Taylor, M.P., Munksgaard, N.C., Hudson-Edwards, K.A., Burn-Nunes, L. 2013. Identification of environmental lead sources and pathways in a mining and smelting town: Mount Isa, Australia. Environmental Pollution 180, 304-311.

Martley, E., Gulson, B.L., Pfeifer, H.R. 2004. Metal concentrations in soils around the copper smelter and surrounding industrial complex of Port Kembla, NSW, Australia. Science of the Total Environment 325, 113-127.

Mielke, H.W. 1999. Lead in the Inner Cities. American Scientist 87, 62-73.

Mielke, H.W., Anderson, J.C., Berry, K.J., Mielke, P.W., Chaney, R.L., Leech, M. 1983. Lead Concentrations in Inner-City Soils As a Factor in the Child Lead Problem. American Journal of Public Health 73(12), 1366-1369.

Mitchell, R.G., Spliethoff, H.M., Ribaudo, L.N., Lopp, D.M., Shayer, H.A., Marquez-Bravo, L.G., Lambert, V.T., Ferenz, G.S., Russell-Anelli, J.M., Stone, E.B., McBride, M.B. 2014. Lead (Pb) and other metals in New York community garden soils: Factors influence contaminant distributions. Environmental Pollution 187, 162-169.

Morrison, A.L. 2003. An assessment of the effectiveness of lead pollution reduction strategies in North Lake Macquarie, NSW, Australia. Science of the Total Environment 303, 125-138.

Morrison, A. L., Gulson, B. L. 2007. Preliminary findings of chemistry and bio-accessibility in base metal smelter slags. Science of the Total Environment 382, 30–42.

Morrison, A.L., Swierczek, Z., Gulson, B.L. 2016. Visualisation and quantification of heavy metal accessibility in smelter slags: The influence of morphology on availability. Environmental Pollution 210, 271-281.

National Environment Protection Council (NEPC). 2013. National Environment Protection (Assessment of Site Contamination) Measure 1999. <http://www.nepc.gov.au/nepms/assessment-site-contamination> (accessed 03 May 2017).

National Measurement Institute. 2014. Interlaboratory Comparison. RGM 14-01. Raw Natural Gas. 1-41. <http://www.measurement.gov.au/Publications/ProficiencyStudyReports/Documents/RGM14-01.pdf> (accessed 06 July 2017).

Newcastle City Council (NCC). 1997. Information sheet industrial filling used in Carrington. Newcastle City Council. <http://www.newcastle.nsw.gov.au/getattachment/Business/Regulations/Health-safety/Contaminated-Land/Carrington_contaminated_land.pdf.aspx?lang=en-AU> (accessed 09 January 2017).

Newcastle Herald. 2014. Toxic Truth: Taxpayers to pay for clean-up. <http://www.theherald.com.au/story/2714126/taxpayers-to-pay-for-clean-up/> (accessed 09 June 2017).

Newcastle Herald. 2017a. Newcastle put on lead alert following contamination study. Newcastle Herald. <http://www.theherald.com.au/story/4415392/newcastle-put-on-lead-alert/> (accessed 13 June 2017).

Newcastle Herald. 2017b. Toxic truth. A Newcastle Herald Investigation. <http://www.theherald.com.au/news/toxic-truth/> (accessed 12 June 2017).

Newcastle Herald. 2017c. Opinion – Reply to criticism of soil pollution research. <http://www.theherald.com.au/story/4580152/reply-to-criticism-of-soil-pollution-research/> (accessed 04 June 2017).

Newcastle Herald. 2017d. Toxic truth archive. <http://www.theherald.com.au/story/2711882/toxic-truth-archive/?cs=305> (accessed 12 June 2017).

New South Wales Environment Protection Authority (NSW EPA). 1995. Sampling Design Guidelines. Contaminated Sites. <http://www.epa.nsw.gov.au/resources/clm/95059sampgdlne.pdf> (accessed 02 March 2017).

New South Wales Environment Protection Authority (NSW EPA). 2013. Protecting your environment. <http://www.epa.nsw.gov.au/protectingyourenvironment.htm> (accessed 16 May 2017).

New South Wales Environment Protection Authority (NSW EPA). 2015a. Lead expert working group—lead exposure management for the suburbs surrounding the former Pasminco lead smelter. <http://www.epa.nsw.gov.au/MediaInformation/lead-expertworking-group.htm> (accessed 12 June 2017).

New South Wales Environment Protection Authority (NSW EPA). 2015b. Guidelines on the Duty to Report Contamination under the Contaminated Land Management Act 1997. <http://www.epa.nsw.gov.au/resources/clm/150164-report-land-contamination-guidelines.pdf> (accessed 04 March 2017).

New South Wales Environment Protection Agency (NSW EPA). 2016a. Licence Variation. Environmental Protection Licence. 1-28. <http://www.epa.nsw.gov.au/prpoeoapp/ViewPOEONotice.aspx?DOCID=-1&SYSUID=1&LICID=1545186> (accessed 04 June 2017).

New South Wales Environment Protection Agency (NSW EPA). 2016b. Fact Sheet: Old Lead Paint. <http://www.epa.nsw.gov.au/resources/pesticides/lead-old-paint-fact-sheet-150700.pdf> (accessed 15 March 2016).

New South Wales Health (NSW Health). 2016a. Lead exposure in children. <http://www.health.nsw.gov.au/environment/factsheets/Pages/lead-exposure-children.aspx> (accessed 12 June 2017).

New South Wales Health (NSW Health). 2016b. Lead in blood control guideline. <http://www.health.nsw.gov.au/Infectious/controlguideline/Pages/lead.aspx> (accessed 12 June 2017).

Noller, B.N., Smythe, L.E. 1974. Distribution of lead in vegetation bordering roads in the Sydney metropolitan area. Search 5, 108-110.

Northampton Lead Tailings Project (NLTP). 2013. Final minutes of steering committee meeting. 13 September 2013. 1-21.

Olszowy, H., Torr, P., Imray, P. 1995. Trace element concentrations in soils from rural and urban areas of Australia. Department of Human Services and Health, South Australian Health Commission 4, 1-88.

Olympus Inspections and Maintenance Systems (IMS). 2014. DELTA Premium. Handheld XRF Analyzer Specifications. 1-2. <https://www.olympus-ims.com/en/delta-premium/#!cms[tab]=%2Fdelta-premium%2Fresources> (accessed 26 June 2017).

Olympus Inspections and Maintenance Systems (IMS). 2017. Vanta. Rugged. Revolutionary. Productive. 1-2. <https://www.olympus-ims.com/en/vanta/#!cms[tab]=%2Fvanta%2Fresources> (accessed 26 June 2017).

Parliament of New South Wales, 1999. BHP Newcastle Steelworks Closure. Legislative Assembly Hansard 22 September 1999.

<http://23.101.218.132/prod/web/common.nsf/V3HHBDay?open&key=19990922> (accessed 09 January 2017).

Parsons, C., Grabulosa, E.M., Pili, E., Floor, G.H., Roman-Ross, G., Charlet, L. 2013. Quantification of trace arsenic in soils by field-portable X-ray fluorescence spectrometry: Considerations for sample preparation and measurement conditions. Journal of Hazardous Materials 262, 1213-1222.

Paustenbach, D.J., Finley, B.L., Long, T.F. 1997. The critical role of house dust in understanding the hazards posed by contaminated soils. International Journal of Toxicology 16, 339-362.

Port Pirie Transformation. No date. The community – Delivering a sustainable future. <http://www.portpirietransformation.com/index.php/community> (accessed 03 July 2017).

Public Health England. 2011. Ionising Radiation: Dose Comparisons. <https://www.gov.uk/government/publications/ionising-radiation-dose-comparisons/ionising-radiation-dose-comparisons> (accessed 02 August 2014).

Pure Earth. 2014. Tools of the Trade: The XRF Finds Toxic Hotspots in 30 Seconds. <www.pureearth.org/tag/xrf/> (accessed 06 July 2017).

Rouillon, M., Taylor, M.P., Dong, C. 2017b. Reducing risk and increasing confidence of decision making at a lower cost: *In-situ* pXRF assessment of metal-contaminated sites. Environmental Pollution. In Press, Corrected Proof. http://dx.doi.org/10.1016/j.envpol.2017.06.020

Rouillon, M., Harvey, P.J., Kristensen, L.J., George, S.G., Taylor, M.P. 2017a. VegeSafe: A community science program measuring soil-metal contamination, evaluating risk and providing advice for safe gardening. Environmental Pollution 222, 557-566.

Rouillon, M., Kristensen, L.J., Gore, D.B. 2015. Handheld X-ray Fluorescence Spectrometers: Radiation Exposure Risks of Matrix-Specific Measurement Scenarios. Applied Spectroscopy 69(7), 815-822.

Rouillon, M. Taylor, M.P. 2016. Can field portable X-ray fluorescence (pXRF) produce high quality data for application in environmental contamination research? Environmental Pollution 214, 255-264.

Sahraoui, H., Hachicha. M. 2017. Effect of soil moisture on trace elements concentrations using portable x-ray fluorescence spectrometer. Journal of Fundamental and Applied Sciences 9(1), 468-484.

Schwarz, K., Pickett, S.T.A., Lathrop, R.G., Weathers, K.C., Pouyat, R.V., Cadenasso, M.L. 2012. The effects of the urban built environment on the spatial distribution of lead in residential soils. Environmental Pollution 163, 32-39.

Semlali, R.M., Dessogne, J.B., Monna, F., Bolte, J., Azimi, S., Denaix, L. 2004. Modeling lead input and output in soils using lead isotopic geochemistry. Environmental Science & Technology 38, 1513-1521.

Sinclair Knight Merz (SKM). 2012. Lead Investigation – Chicester Trunk Gravity Main Corridor and Pisani Property, Woodberry. Investigation Report commissioned by Hunter Water Corporation. Sinclair Knight Merz, St Leonards. 1-59.

Solomon, R.J. 1988.The richest lode: Broken Hill 1883–1988. Hale & Iremonger, Sydney, NSW.

Speakman, M. 2015. Media release: work underway to reduce lead in Broken Hill playgrounds. <http://www.epa.nsw.gov.au/resources/MinMedia/EPAMinMedia15052601.pdf> (accessed 11 June 2017).

Splietoff, H.M., Mitchell, R., Ribaudo, L.N., Taylor, O., Shayler, H.A., Greene, V., Oglesby, D. 2014. Lead in New York City community garden chicken eggs: influential factors and health implications. Environmental Geochemistry and Health 36(4), 633-649.

Spliethoff, H.M., Mitchell, R.G., Shayler, H., Marquez-Bravo, L.G., Russell-Anelli, J., Ferenz, G., McBride, M. 2016. Estimated lead (Pb) exposures for a population of urban community gardeners. Environmental Geochemistry and Health 38(4), 955-971.

Standards Australia. 2000. AS 4874-2000. Guide to the investigation of potentially contaminated soil and deposited dust as a source of lead available to humans. <https://infostore.saiglobal.com/en-au/Standards/AS-4874-2000-318623/> (accessed 03 May 2017).

Standards Australia. 2005. AS 4482.1-2005. Guide to the investigation and sampling of sites with potentially contaminated soil Non-volatile and semi-volatile compounds. <https://infostore.saiglobal.com/store/details.aspx?ProductID=315364> (accessed 03 May 2017).

Sydney Morning Herald (SMH). 2017. EPA keeps contamination hidden to protect property prices. <http://www.smh.com.au/nsw/epa-keeps-contamination-hidden-to-protect-property-prices-20170526-gwe2mb.html> (accessed 06 July 2017).

Targeted Lead Abatement Program (TLAP). 2015. Updated Port Pirie Playground Cleaning Schedule – March 20th, 2015. <http://tlap.com.au/news/118-updated-playground-cleaning-schedule-march-20th-2015> (accessed 11 June 2017).

Taylor, M.P. 2016. *Personal communication: Broken Hill Environmental Lead Program (BHELP).*

Taylor, M.P., Camenzuli, D., Kristensen, L.J., Forbes, M., Zahran, S. 2013. Environmental lead exposure risks associated with children's outdoor playgrounds. Environmental Pollution 178, 447-454.

Taylor, M.P., Cosenza, I.J. 2016. Review of the New South Wales Environment Protection Authority's Management of Contaminated Sites. Macquarie University, NSW, Australia. ISBN:978-1-74138-444-4

Taylor, M.P., Davies, P.J., Kristensen, L.J., Csavina, J.L. 2014b. Licenced to pollute but not to poison: the ineffectiveness of regulatory authorities at protecting public health from atmospheric arsenic, lead and other contaminants resulting from mining and smelting operations. Aeolian Research 14, 35-52.

Taylor, M.P., Mackay, A.K., Hudson-Edwards, K.A., Holz, E. 2010. Soil Cd, Cu, Pb and Zn contaminants around Mount Isa city, Queensland, Australia: potential sources and risks to human health. Applied Geochemistry 25, 841-855.

Taylor, M.P., Mould, S.A., Kristensen, L.J., Rouillon, M. 2014a. Environmental arsenic, cadmium and lead dust emissions from metal mine operations: implications for

environmental management, monitoring and human health. Environmental Research 135, 296-303.

Taylor, M.P., Winder, C., Lanphear, B.P. 2012. Eliminating childhood lead toxicity in Australia: a call to lower the intervention level. Medical Journal of Australia 197(9), 493.

Taylor, M.P., Winder, C., Lanphear, B.P. 2014c. Australia's leading public health body delays action on the revision of the public health goal for blood lead exposures. Environmental International 70, 113-117.

Taylor, M.P., Zahran, S., Kristensen, L., Rouillon, M. 2015. Evaluating the efficacy of playground washing to reduce environmental metal exposures. Environmental Pollution 202, 112-119.

The Children's Hospital at Westmead. 2014. Lead. Fact Sheet. 1-2. <https://www.schn.health.nsw.gov.au/files/factsheets/lead-en.pdf> (accessed 05 July 2017).

Thermo Scientific. 2011. Thermo Scientific MicroPHAZIR AS, Handheld Asbestos Analyzer. Product Specification. <https://www.thermofisher.com.au/Uploads/file/Environmental-Industrial/Environmental-Monitoring-Safety/Industrial-Hygiene-Instruments/MicroPhazir-Asbestos-Analyser-TFS.pdf> (accessed 21 March 2017).

United States Environmental Protection Agency (US EPA). 1998. Environmental Technology Verification Report, Field Portable X-ray Fluorescence Analyzer. Metorex X-MET 920-P. <http://nepis.epa.gov/Adobe/PDF/30003LR0.pdf> (accessed 25 July 2015).

United States Environmental Protection Agency (US EPA). 2007. Method 6200: Field Portable X-Ray Fluorescence Spectrometry for the determination of elemental concentrations in soil and sediment. SW-846. Revision 0. February 2007. <https://www.epa.gov/sites/production/files/2015-12/documents/6200.pdf> (accessed 04 May 2017).

United States Environmental Protection Agency (US EPA). 2015. SESD Operating Procedure. SESDPROC-107-R3. 1-11. <https://www.epa.gov/sites/production/files/2016-01/documents/field_xrf_measurement107_af.r3.pdf> (accessed 24 June 2017).

United States Department of Housing and Urban Development (US HUD). 2016. The renovation, repair and painting rule. Healthy Homes and Lead Hazard Control. <http://portal.hud.gov/hudportal/HUD?src¼/program_offices/healthy_homes/training/rrp/rrp> (accessed 12 June 2017).

Weindorf, D.C., Bakr, N., Zhu, Y. 2014. Chapter One: Advances in Portable X-ray Fluorescence (PXRF) for Environmental, Pedological, and Agronomic Applications. Advances in Agronomy 128, 1-45.

Wu, L. Taylor, M.P., Handley, H.K., Wu, M. 2016. Australian atmospheric lead deposition reconstructed using lead concentrations and isotopic compositions of archival lichen and fungi. Environmental Pollution 208, 678-687.

Zhou, X., Taylor, M.P., Davies, P.J. Under Review. Natural and industrial sources of trace contaminants in Australian native bees. Environmental Pollution.

Zines, D. 2007. Lead abatement strategy implementation documentation. Prepared by Fitzwaller Group for Ferrier Hodgson, Pasminco Cockle Creek Smelter Administrator. <http://www.pasminco.com.au/files/20110414133639936.pdf> (accessed 12 June 2017).

Appendix

Appendix A

Environmental contamination studies often investigate the hazards or risks posed by contaminant concentrations or forms to humans and biota. Some investigations sample soils to estimate hazards when compared against relevant guidelines such as the NEPM (2013). Further, soil is easily accessible and has well established sampling and measurement criteria used for quantification. Other studies estimate the risk of metal exposure from dust loadings, as dust metal has a stronger correlation with blood metal concentrations than soil metals (Gulson et al. 2006). Metal-rich dust can accumulates on surfaces at different rates, and can be collected using a variety of methods. Three localities (Broken Hill – **Paper Six**, Port Pirie – **Paper Seven**, and Boolaroo – **Paper Eight**) were investigated to better understand the hazards and risks posed to residents from metal contaminants in a variety of ways. Despite the soil and dust samples not being primarily measured using pXRF, these studies form part of this thesis in regards to a more holistic understanding of metal exposures from current and legacy contamination sources.

Paper Six

Publication

Environmental arsenic, cadmium and lead dust emissions from metal mine operations: Implications for environmental management, monitoring and human health

Abstract: Although blood lead values in children are predominantly falling globally, there are locations where lead exposure remains a persistent problem. One such location is Broken Hill, Australia, where the percentage of blood lead values >10 μg/dL in children aged 1–4 years has risen from 12.6 % (2010), to 13 % (2011) to 21 % (2012). The purpose of this study was to determine the extent of metal contamination in places accessible to children. This study examines contemporary exposure risks from arsenic, cadmium, lead, silver and zinc in surface soil and dust, and in pre- and post-play hand wipes at six playgrounds across Broken Hill over a 5-day period in September 2013. Soil lead (mean 2,450 mg/kg) and zinc (mean 3,710 mg/kg) were the most elevated metals in playgrounds. Surface dust lead concentrations were consistently elevated (mean 27,500 μg/m^2) with the highest lead in surface dust (59,900 μg/m^2) and post-play hand wipes (60,900 μg/m^2) recorded close to existing mining operations. Surface and post-play hand wipe dust values exceeded national guidelines for lead and international benchmarks for arsenic, cadmium and lead. Lead isotopic compositions (^{206}Pb/^{207}Pb, ^{208}Pb/^{207}Pb) of surface dust wipes from the playgrounds revealed the source of lead contamination to be indistinct from the local Broken Hill ore body. The data suggest frequent, cumulative and ongoing mine-derived dust metal contamination poses a serious risk of harm to children.

Keywords: Lead, Arsenic, Cadmium, Dust Deposition, Health

CrossMark

Environmental arsenic, cadmium and lead dust emissions from metal mine operations: Implications for environmental management, monitoring and human health

Mark Patrick Taylor *, Simon Anthony Mould, Louise Jane Kristensen, Marek Rouillon

Environmental Science, Department of Environment and Geography, Faculty of Science, Macquarie University, Sydney, NSW 2109, Australia

ARTICLE INFO

ABSTRACT

Although blood lead values in children are predominantly falling globally, there are locations where lead exposure remains a persistent problem. One such location is Broken Hill, Australia, where the percentage of blood lead values $> 10\ \mu g/dL$ in children aged 1–4 years has risen from 12.6% (2010), to 13% (2011) to 21% (2012). The purpose of this study was to determine the extent of metal contamination in places accessible to children. This study examines contemporary exposure risks from arsenic, cadmium, lead, silver and zinc in surface soil and dust, and in pre- and post-play hand wipes at six playgrounds across Broken Hill over a 5-day period in September 2013. Soil lead (mean 2,450 mg/kg) and zinc (mean 3,710 mg/kg) were the most elevated metals in playgrounds. Surface dust lead concentrations were consistently elevated (mean $27,500\ \mu g/m^2$) with the highest lead in surface dust ($59,900\ \mu g/m^2$) and post-play hand wipes ($60,900\ \mu g/m^2$) recorded close to existing mining operations. Surface and post-play hand wipe dust values exceeded national guidelines for lead and international benchmarks for arsenic, cadmium and lead. Lead isotopic compositions ($^{206}Pb/^{207}Pb$, $^{208}Pb/^{207}Pb$) of surface dust wipes from the playgrounds revealed the source of lead contamination to be indistinct from the local Broken Hill ore body. The data suggest frequent, cumulative and ongoing mine-derived dust metal contamination poses a serious risk of harm to children.

© 2014 Elsevier Inc. All rights reserved.

1. Introduction

This study examines metal and metalloid concentrations (arsenic (As), cadmium (Cd), lead (Pb), silver (Ag) and zinc (Zn)) in contemporary soils and dusts in Australia's oldest lead-zinc mining city of Broken Hill. The adverse health risks to humans from metal and metalloid exposure are serious and well known. Childhood Pb exposure causes irreversible damage to neurological functions due to its toxicity (National Toxicology Program (NTP) 2012; Needleman, 2004; Taylor et al., 2012; 2014b). Children are at higher risk of environmental metal poisoning than adults due to their small body size, earlier stage of development, and because of their tendency to engage in hand-to-mouth behaviour (Kranz et al., 2004; Simon et al., 2007; Viverette et al., 1996). Environmental sources and pathways of exposure are important areas of study for risk mitigation. Research focused on household exposures has identified sources of Pb in metal mining and smelting communities as being dominated by ore body and smelted metals

along with lesser contributions from a combination of lead-based paints and leaded petrol residues. Lead dust in houses and surrounding soils are important exposure pathways (Gulson et al., 1994, 1995, 1996; Mackay et al., 2013; Soto-Jiménez and Flegal, 2011; Taylor et al., 2010). Recent research in the smelting community of Port Pirie, South Australia, identified playground use as a potential source of metal exposure (Taylor et al., 2013). Similarly, Viverette et al. (1996) found in their day care centre hand Pb study that outdoor sources of contamination can be more important for childhood Pb exposure than indoor sources.

Broken Hill in far western New South Wales (NSW; Fig. 1) was established around one of the world's largest silver-lead-zinc deposits, which has been mined continuously since its discovery in 1883 (Solomon, 1988). Smelting was also carried out in the city during the early years of ore extraction, but ceased in 1898 (Woodward, 1965), with the majority of the ore being transferred to Port Pirie for smelting until recently when the bulk has been sent to overseas for processing. The waste from 130 years of mining dominates the city's landscape, with the old gossan extrusion being replaced by covered slagheaps in the centre of the city. Mining operations in the city of Broken Hill continue

---

* Corresponding author. Fax: +61 2 9850 8420.
E-mail address: mark.taylor@mq.edu.au (M.P. Taylor).
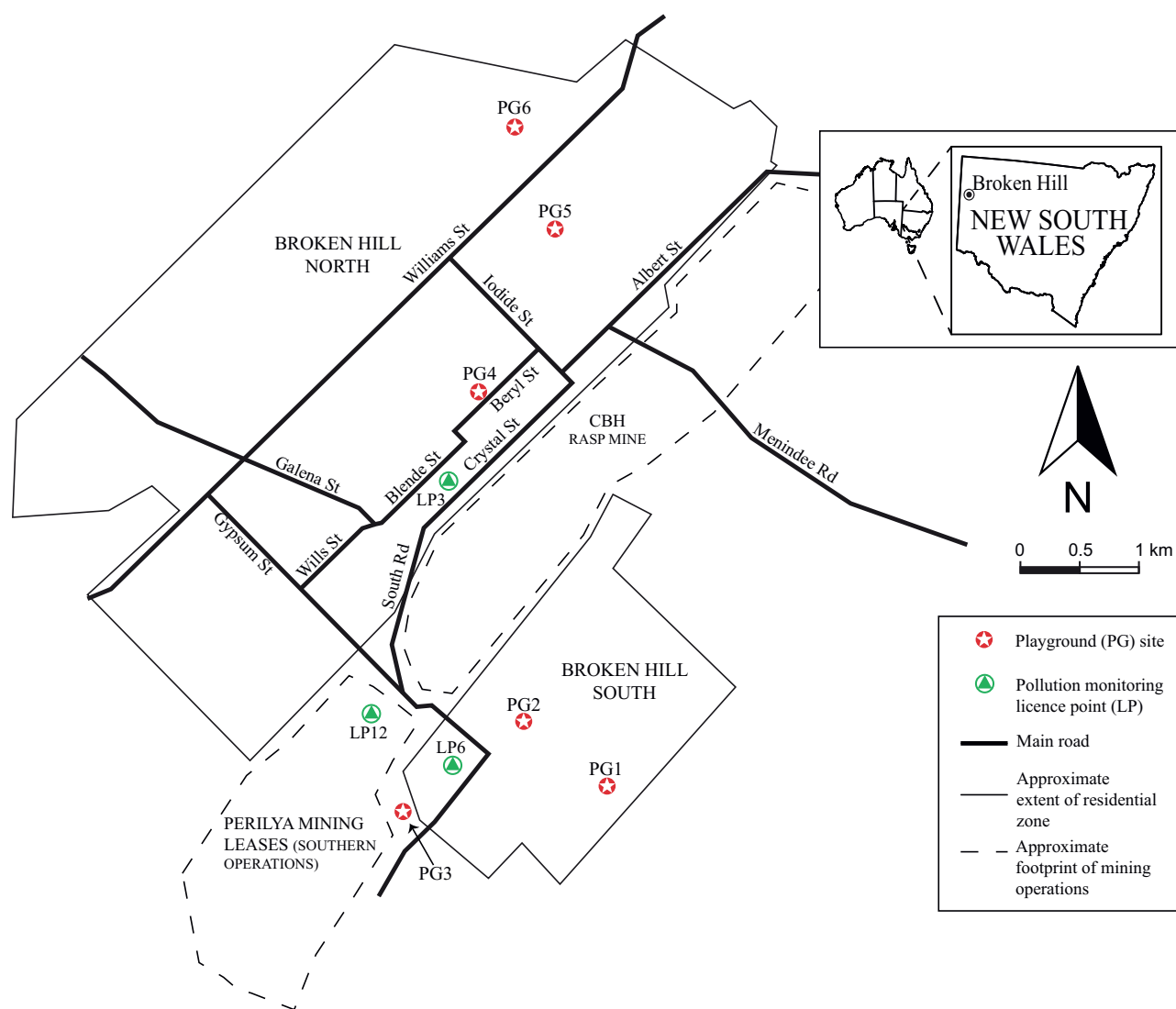
Fig. 1. Map of Broken Hill showing playground sites sampled, locations of contemporary mining activity, and pollution monitoring sites referred to herein.

underground in the central area of the line of lode (CBH, Rasp Mine, Fig. 1) and also to the south (Perilya mining leases, Fig. 1). Although mineral extraction at both sites is now entirely underground, processing and transport of the ore occurs at the surface. Industry monitoring data from CBH Resources Ltd. (2014) and Perilya Broken Hill Ltd. (2014) show that Pb-rich dust emissions and deposition continue to impact the surrounding environment, although the full impact of operations on the urban environment are difficult to ascertain as there are limited dust deposition monitoring sites in the city (measuring total dust or Pb in dust as $\mu g/m^2$). There are no NSW Environmental Protection Authority monitoring sites for dust, dust Pb or lead-in-air or other metals in Broken Hill, despite other similar mining and smelting impacted locations such as Mount Isa and Port Pirie having independent monitoring in their city environments (Taylor et al., 2014a). National Pollutant Inventory (NPI) data show that Perilya Broken Hill mines (North and South) emitted an estimated 26,000 kg Pb, 58,000 kg Zn, 670 kg As and 240 kg Cd to the atmosphere during 2012–2013 (National Pollutant Inventory (NPI) 2014b). CBH Resources (Broken Hill Operations Pty. Ltd.), emitted an estimated 97 kg Pb and 150 kg Zn to the atmosphere over the same period (National Pollutant Inventory (NPI) 2014a) in 2012-2013.

Unlike most locations in Australia, blood Pb levels have been rising in recent years in Broken Hill (Taylor et al., 2014b). For

example, the geometric mean blood Pb of children aged 1-4 years has risen from 4.8 µg/dL in 2011 to 5.4 µg/dL in 2012 (Lesjak et al., 2013). Further, the proportion of children over the current national goal of 10 µg/dL (which is currently under review, (Taylor et al., 2014b)) has also increased in recent years from 12.6% (2010), to 13% (2011) to 21% (2012) (Lesjak et al., 2013). Therefore in the context of rising blood lead levels, the purpose of this study is to evaluate contemporary metal exposure risks in soils and dusts across Broken Hill city and to determine the likely sources as well as possible mitigation strategies, where necessary.

2. Methods

2.1. Field sampling

Six playgrounds distributed across Broken Hill (Fig. 1) were sampled daily over a 5-day period between 16th to 20th September 2013. Playgrounds 1 (Duff St. Park; PG1), 2 (Patton Park; PG2) and 3 (Zinc Lakes; PG3) were located south of the ore body. Playgrounds 4 (Sturt Park; PG4), 5 (Queen Elizabeth Park; PG5) and 6 (Broken Hill Regional Aquatic Centre; PG6) were located north of the ore body. A minimum of two surface soil samples were taken from each of the six playgrounds ($n=14$) at a depth of 0–2 cm in accordance with AS 4874-2000 (Standards Australia, 2000). Soil samples were collected using a plastic trowel that was wiped clean each time prior to sampling using KimWipes™ and deionised water. Before sampling commenced, the trowel was passed through soils immediately adjacent to the

sample site to remove any possible effects associated with the previous sample site (c.f. Taylor and Hudson-Edwards, 2008). Bulk soil samples were collected in sealed polyethylene ziplock bags and sent for analysis at the National Measurement Institute (NMI), Sydney.

Dust wipes were used to measure the daily deposition of dust on horizontal surfaces in playgrounds. A single horizontal surface was chosen for each playground and re-sampled once per day for five days ($n=30$). Sample areas were marked out and measured, allowing all results to be standardised to a concentration expressed in $\mu g/m^2$. The wiped surface areas are provided in Supplementary Table S1. The surfaces selected for sampling were free from paint and exposed to the atmosphere but were in discrete locations such that they were unlikely to be disturbed by playground users. The dust wipes used were the Lead Wipe™ and were collected using the method described in ASTM E 1728-03 (American Society for Testing and Materials, 2003). Dust wipes were collected at approximately the same time (9am) each sample day.

Playground sampling involved 'simulated play' to measure metal loadings that children might be exposed to during interaction with the playgrounds (see the approach used in Taylor et al., 2013). Each day, the same researcher 'played' on the play equipment at the allocated site for 10 min (1 researcher for each of the 6 playgrounds sampled over the five days), mimicking the exploratory behaviour of a child. Adult researchers undertook the child-simulated play rather than actual children to provide reliability and consistency of method. The researchers' hands were cleaned thoroughly with dust wipes prior to play and following play ($n=30$ paired samples) using the method employed by Taylor et al. (2013). Pre- and post-play wipes were analysed separately for metals and compared to measure the effect of contact with the play equipment. Hand surface area was calculated for each play participant using DuBois and DuBois (1916) and then converted to $\mu g/m^2$ to allow comparison between each of the playgrounds over the 5-day period.

2.2. Laboratory analysis

Soil samples and dust wipes were analysed by NMI for As, Ag, Cd, Pb and Zn. Soil samples were sieved to < 2 mm prior to digestion. Soil samples (0.5 g) were digested in a 1:1 ratio of nitric acid and hydrochloric acid (Evans, 2012). Dust wipes were digested in a 3:1 ratio of aqua regia (Evans, 2013). Soil samples and dust wipes were measured for their metal concentrations using a Varian 730-ES ICP-OES and Perkin Elmer Elan DRC II ICP-MS. Reagent blanks, dust wipe blanks, duplicates, matrix spike and reference material AGAL-10 (Hawkesbury River Sediment) were also analysed to verify sample data quality.

Lead isotopic compositions of selected samples ($n=11$) were determined using a PerkinElmer Elan DRC IIS ICP-MS after optimising sample concentrations. Analyses were conducted with concentration-matched measurements of NIST SRM 981 bracketing each sample, which were used to correct for isotopic mass fractionation.

2.3. Laboratory Quality Assurance / Quality Control

Soil blanks returned < 0.5 mg/kg for all metals. Duplicate analysis returned relative percent differences (RPD) $< 13\%$ for all elements. Recovery rates were measured using certified reference material AGAL-10 and sample matrix spiking. Recovery rates were 98–120% for the certified reference material and 93-99% for the matrix spikes. Dust wipe blanks returned $< 0.1\ \mu g$/wipe for As and Zn and $< 0.05\ \mu g$/wipe for Cd, Pb and Ag, all of which were below the laboratory limit of reporting. Recovery rates were 94-98% for AGAL-10 and 85-103% for matrix spikes. Analytical precision (RSD) for lead isotopic compositions was 0.14%, 0.10% and 0.20% for $^{206}Pb/^{207}Pb$, $^{208}Pb/^{207}Pb$ and $^{206}Pb/^{204}Pb$ respectively.

2.4. Statistical analysis

Wilcoxon signed-rank tests for hand wipe data were performed using the VassarStats web-based application developed by Lowry (2014). Regression analysis was used to assess the relationship between surface Pb loadings and those recovered on post-play hand wipes. Values were calculated using the Minitab

version 16.2.4 software package. Data were Log-transformed to satisfy normality assumptions.

3. Results

3.1. Surface dust metal

Daily data measured from the playground surface dust wipes show that deposition of fine Pb-rich particles across Broken Hill was a daily occurrence over the 5-day study period. Playground 3 showed consistently higher dust Pb loadings than all other playgrounds (Table 1). Australian Standard AS 4361.2-1998 (Standards Australia, 1998) provides an outdoor dust Pb limit of 8,000 $\mu g/m^2$, which was exceeded at Playground 3 on all days and at Playground 5 on two days. We also applied the Government of Western Australia (2007) clean up goal of 400 $\mu g/m^2$ for surfaces accessible to children to our data as a benchmark because of its specific reference to children. Table 1 shows the specific days and corresponding locations where the Government of Western Australia cleanup goal was exceeded. The cleanup goal was exceeded on all days at Playgrounds 3 and 5, and at Playground 1 on 4 of the 5 sample days. Supplementary Table S1 shows metal loadings on surfaces for each playground on Day 1 as an indication of 'typical' loadings on surfaces not regularly cleaned, with subsequent sample days 2–4 showing the daily (24-hour) rate of deposition. There is no Australian standard for dust As, Cd or Pb deposition rates. However, the German TA Luft (2002) standard sets maximum acceptable daily dust loading values for As (4 $\mu g/m^2$/day), Cd (2 $\mu g/m^2$/day) and Pb (100 $\mu g/m^2$/day). The same standards are used as trigger values with respect to the environmental monitoring and assessment of the Mount Isa Mines operations (Taylor et al., 2014a; Supplementary Table 1). Playgrounds 2 and 3 exceeded this limit for As and Playgrounds 1, 2 and 3 exceeded the Cd benchmark. All playgrounds except Playground 6 exceeded the TA Luft (2002) value for dust Pb deposition. Rainfall of 1.2 mm very early on Day 1 of sampling (Bureau of Meteorology, 2014a) could have contributed to reducing the metal loading measured on this day. Rainfall of 6.8 mm was also recorded on 13th September, three days prior to Day 1 (Bureau of Meteorology, 2014a). We note also that sampling was undertaken at a particularly windy time of year, with mean 3 pm wind speeds being typically higher in September compared to the rest of the year at Patton Street (51-year record) (Bureau of Meteorology, 2014b).

3.2. Soil metal

Soil Pb concentrations in three playgrounds (Playgrounds 1–3) exceeded the National Environmental Protection Measure (NEPM, 2013) Health Investigation Level (HIL) soil Pb guidelines (600 mg/kg) for land categorised as Recreational C, public open space. Mean concentrations of all metals in the < 2 mm fraction were highest at Playground 3 (Fig. 2). Playgrounds 1–4 exceeded the HIL soil Pb value (300 mg/kg) for land categorised as Residential A (including

Table 1
Summary of daily surface dust Pb loadings for each playground to three significant figures. Values in bold exceed the Government of Western Australia (2007) cleanup goal of 400 $\mu g/m^2$.

Playground	Day 1 ($\mu g/m^2$)	Day 2 ($\mu g/m^2$)	Day 3 ($\mu g/m^2$)	Day 4 ($\mu g/m^2$)	Day 5 ($\mu g/m^2$)
1	**942**	**628**	**507**	**411**	362
2	333	**467**	389	**767**	267
3	**59,900**	**35,600**	**15,500**	**16,400**	**9,960**
4	**633**	**733**	211	167	100
5	**8,440**	**6,560**	**4,220**	**8,780**	**6,890**
6	**418**	102	173	84.4	37.8
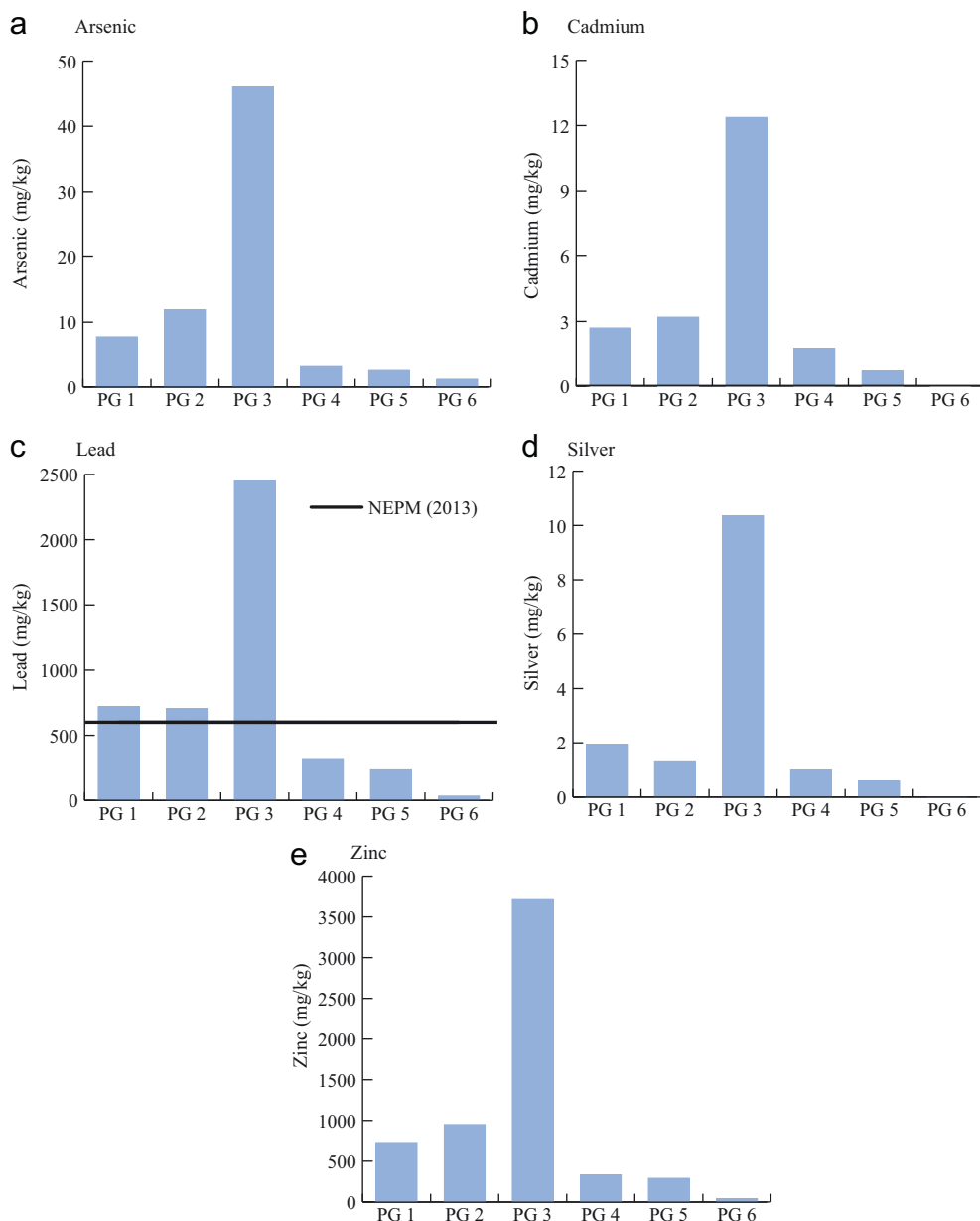
Fig. 2. Mean metal concentrations in soils at each playground. Playgrounds 1, 2 and 3 exceeded Pb concentrations for recreational zones according to NEPM (2013) soil guidelines. The NEPM (2013) soil guideline is shown only for Pb because playground soils did not exceed the guideline values for As, Cd, Ag or Zn.

childcare centres, kindergartens, preschools and primary schools and their integral playgrounds), which is considered to be more appropriate standard for our study given that young children use these facilities.

No other soil metals exceeded the NEPM (2013) guidelines. Total extractable metal concentrations of As, Ag, Cd, Pb and Zn, for all soil samples can be found in Supplementary Table S2. Other international organisations provide more conservative guidelines for metals in soil than Australia. California, Canada and the US EPA set soil Pb guidelines at 80 mg/kg, 140 mg/kg and 400 mg/kg respectively, while soil As guidelines are 0.07 mg/kg, 12 mg/kg and 0.61 mg/kg, respectively (California Environmental Protection Agency (CEPA), 2005; Canadian Conference of Medical Education (CCME), 2013; United States Environmental Protection Agency (EPA), 2013). The Norwegian soil guidelines specifically refer to soil used in children's playgrounds for As, Cd, Pb and Zn of 8 mg/kg, 1.5 mg/kg, 60 mg/kg and 200 mg/kg, respectively (Norwegian Pollution Control Authority (NPCA), 2009). The data

in Fig. 2 show clearly that these playground-specific values were exceeded in nearly all of the playgrounds in the south part of Broken Hill (PG1 – PG3) compared to the playgrounds in the north of the city (PG4 – PG6), which have much lower soil metal concentrations.

3.3. Pre- and post-play hand wipe metal loadings

Pb loadings on hands increased significantly on post-play wipes at all playgrounds (Fig. 3; Supplementary Table S3), indicating the availability of contaminated dust to children using play equipment. The mean increase in Pb on post-play hand wipes across all playgrounds was 72 times higher than pre-play loadings. The maximum post-play loading measured was 60,900 $\mu g/m^2$ (more than 150 times the Government of Western Australia cleanup goal of 400 $\mu g/m^2$). A Wilcoxon signed-rank test showed that the increase in metal loading on hands after play was significant (95% confidence) for As ($p = 0.001$), Cd ($p = < 0.0001$), Pb ($p = < 0.0001$),
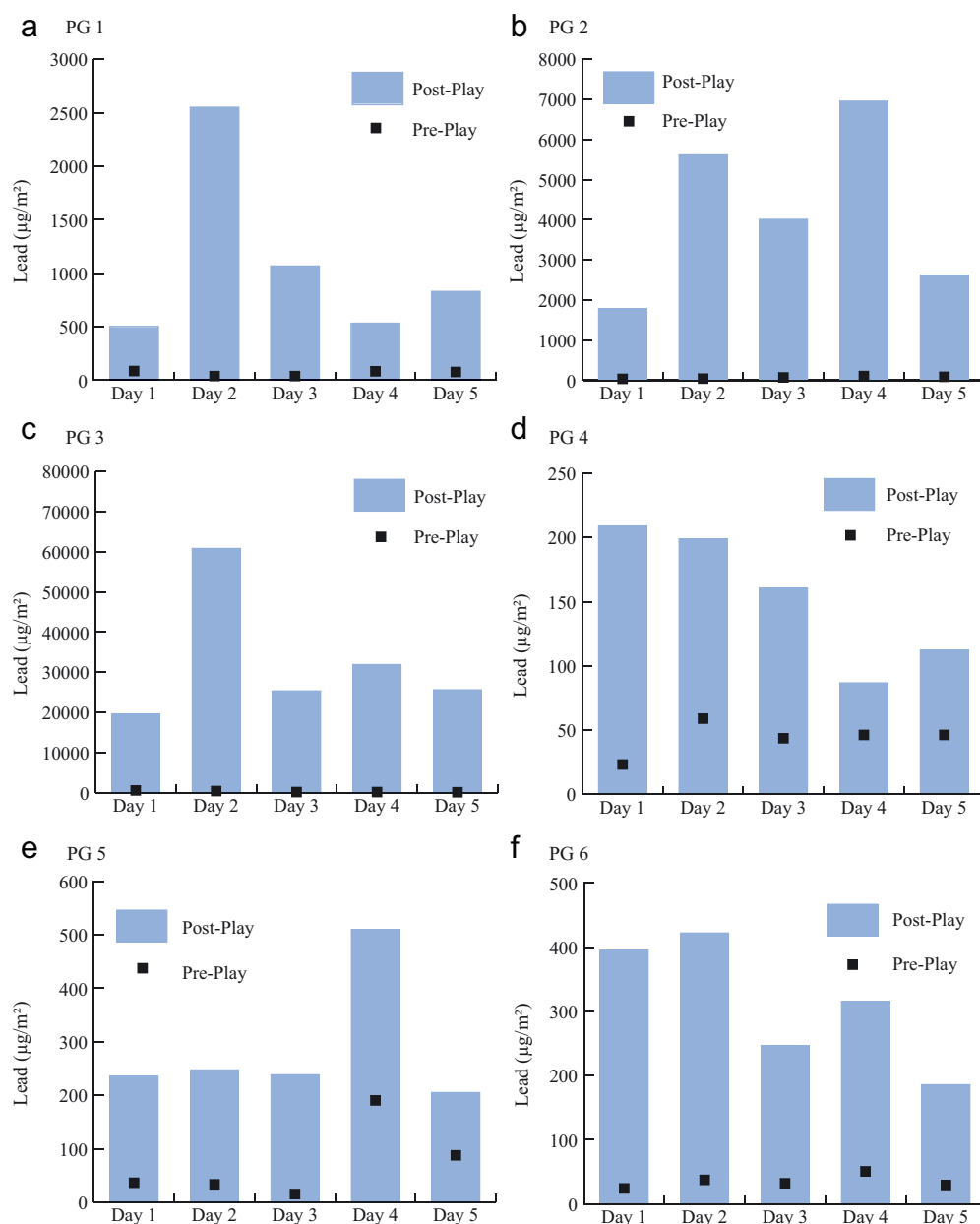
Fig. 3. Lead loadings on hands pre- and post-play for each of the six playgrounds sampled. Post-play hand wipes had significantly higher loadings than pre-play for As, Cd, Pb and Zn (see Supplementary Table S3).

and Zn ($p= < 0.0001$). No significant increase was found for Ag ($p=0.221$).

Pearson correlation analysis showed a significant, positive relationship between surface dust metals and those recovered in post-play hand wipes (As $−p= < 0.0001$; Ag $−p= < 0.0001$; Cd $−p= < 0.0001$; Pb $−p= < 0.0001$; Zn $−p=0.007$), demonstrating the importance of atmospheric deposition of fine metal rich dusts in contributing to the total playground exposure risks.

3.4. Lead isotopic analysis

Lead isotopic compositions ($^{206}Pb/^{207}Pb$, $^{208}Pb/^{207}Pb$) for dust samples from Playgrounds 3–5 (Supplementary Table S4) were compared to those of the Broken Hill ore body values published previously (Chiaradia et al., 1997; Cooper et al., 1969; Gulson and Mizon 1979; Townsend et al., 1998). Dust wipes from Playground 3 are indistinguishable, within analytical precisions, from the ore body isotopic composition (Fig. 4). Lead isotopic compositions

from Playgrounds 4 and 5 dust wipes are similar to Broken Hill ore, and although there is minor scatter in the dust wipe sample data, the $^{206}Pb/^{207}Pb$ and $^{208}Pb/^{207}Pb$ values of all the dust wipe samples have no more than 1% relative difference (RPD) to published isotopic composition values of the Broken Hill ore (Chiaradia et al., 1997; Cooper et al., 1969; Gulson and Mizon 1979; Townsend et al., 1998). The lead isotopic data demonstrate that the Pb in dust at Playground 3 originates from the Broken Hill ore body. Although the Pb isotopic values from the remaining playgrounds are dominated by Broken Hill ore, it is evident that the dust contains Pb from other sources. These might include other natural sources such as dust and soil not from the ore body and industrial sources such as paint and petrol (Gulson et al., 1996).

4. Discussion

Elevated surface dust metal concentrations found in Broken Hill playgrounds, particularly with respect to Pb, demonstrate a
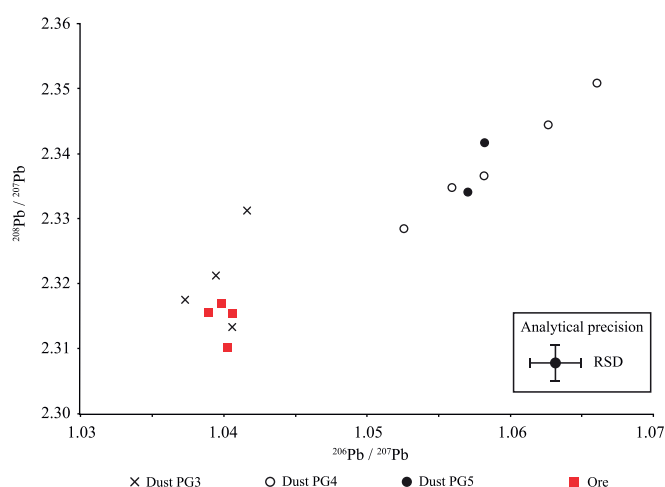
Fig. 4. Stable lead isotope ratios for playground dust Pb were similar to values published for Broken Hill ore body Pb (Chiaradia et al., 1997; Cooper et al., 1969; Gulson and Mizon, 1979; Townsend et al., 1998).

potential risk to the health of children living in the city. Data from the pre- and post-play hand wipes provide a direct measure of the dust metal exposure hazard available to children during the use of the play facilities. Although this study did not specifically measure blood Pb values and their isotopic composition in playground participants, the environmental data presented here are cause for concern, particularly with respect to the most metal-impacted playgrounds (Playgrounds 1–3). Blood Pb measured annually by NSW Health in Broken Hill children aged 1–4 years reveals the persistent risk of exposure in the community over the last 30 years, with 21% of children still having a blood Pb lead level above 10 $\mu g/dL$ in 2012 (Lesjak et al., 2013). Susceptibility to environmental metal exposure is greatest in children under three years of age who are more prone to hand to mouth behaviours, which are known to result in the ingestion of contaminated dusts (Simon et al., 2007).

Playground 3 not only had the highest concentrations of metals in soils, the wipe samples had the highest loadings of metal-rich dust consistently on surfaces and on post-play wipes (see Supplementary Image 1). The proximity of this playground to the Perilya Southern operations facility (~ 400 m) is unlikely to be coincidental as it lies within the downwind direction of the city's prevailing winds. Playground 6 in Broken Hill North, furthest from the ore body, had post-play dust Pb levels of 300 $\mu g/m^2$ on Day 4 of sampling. Prevailing winds on Day 4 were from the northwest (Bureau of Meteorology, 2014a), which indicate that even when the winds are not flowing across current mining operations and transporting contaminated dusts, elevated metals can still be found on playgrounds. Given the 130-year history of ore processing and extraction at Broken Hill, it is very likely that the contamination identified is sourced from historic metal deposition that is re-entrained and then re-deposited on surfaces. By contrast, on Day 2, dust Pb loadings at Playground 6 reached $> 400 \mu g/m^2$ when the wind flow at the time of sampling was 31 km/h from the west-south-west (Bureau of Meteorology, 2014a). The airflow patterns at this time would have been moving approximately across the ore body and the current mining operations, and would have had the capacity to transport contemporary emissions across the urban environment. Playground 5 surface dust levels returned elevated Pb concentrations (Table 1), which were inconsistent with the lower post-play wipe results (Fig. 3). This suggests the surface samples contained an additional source of Pb that is not attributable to daily dust depositions.

The Pb isotopic compositions $^{206}Pb/^{207}Pb$, $^{208}Pb/^{207}Pb$ from the hand-wipes at Playground 3 show that the dust is indistinguishable from the Broken Hill ore body. During September 2013 the nearest Pb-in-air monitoring site (Licence Point 12, LP12, Fig. 1) to Playground 3 returned an average value of 0.248 $\mu g/m^3$ (Perilya Broken Hill Ltd., 2013). Monthly dust deposition Pb values were elevated during September 2013 with the dust deposition licence point closest to Playground 3 (LP6, Fig. 1; Perilya Broken Hill Ltd., 2013) returning a Pb dust value of 7,000 $\mu g/m^2$/month. Licence point 3, proximal to the CBH Resources lease and the centre of the town (Fig. 1), returned a Pb dust value of 12,000 $\mu g/m^2$/month in September 2013 (Perilya Broken Hill Ltd., 2013). Although the EPA licence sets no specific limit for Pb dust deposition, its measurement is required as part of the facility licence environmental monitoring programme (Environmental Protection Authority, 2012). Lead dust loadings at monitoring site LP3 exceed the Australian Standard value for outdoor Pb dust of 8,000 $\mu g/m^2$ frequently (Standards Australia, 1998). The industry licence monitoring data show clearly that there is significant contemporary deposition of Pb rich dust, which is contributing to exposures in playgrounds and elsewhere in the city. Although the data presented herein show elevated As and Cd dust values, the existing licence arrangements do not require their measurement. The data show a strong statistical relationship between surface and post-play hand wipes for all metals, suggesting that they have a common source. Consequently, As and Cd should be monitored along with Pb. It would also be prudent to include trigger values for these contaminants, which could mirror those used for environmental monitoring of the Mount Isa Mines operations in north-west Queensland (Taylor et al., 2014a).

Elevated Pb in Broken Hill playgrounds may be compared with other locations reported in the literature that are frequented by children. Mean surface dust Pb loadings at Playground 3, the most heavily impacted site sampled in Broken Hill (27,500 $\mu g/m^2$), are almost four times higher than the highest mean surface loadings measured at Foreshore Park Playground (6,960 $\mu g/m^2$) in the smelting city of Port Pirie, South Australia (Taylor et al., 2013). Post-play hand wipe mean Pb loadings at Playground 3 (32,700 $\mu g/m^2$) were 1.8 times higher than those recorded at Memorial Park (18,500 $\mu g/m^2$), Port Pirie's most impacted playground in terms of post-play Pb hand wipe values (Taylor et al., 2013). The range of soil Pb concentrations across all Broken Hill (24–3,340 mg/kg) is also within the range reported by Glorennec et al. (2012) for playgrounds across France (2–3,400 mg/kg) and is similar to Port Pirie playground soil Pb values 22–2,600 mg/kg (Taylor et al., 2013). In New Orleans, USA, Viverette et al. (1996) reported on elevated soil and dust Pb in day care centres, the most impacted returning a median soil Pb concentration of 498 mg/kg (range 287–1,880 mg/kg). Playground 3 at Broken Hill returned a median soil Pb concentration of 2,540 mg/kg (range 1,390–3,340 mg/kg), which is more than five times the most impacted New Orleans day care centre.

Given the potential serious risk to children's health identified in the present study, it would be prudent to consider mitigation strategies. Mielke et al. (2011) demonstrated that soil remediation using geotextile and clean topsoil can reduce concentrations of Pb in soil significantly. Mielke et al. (2011) reported a decrease in median soil Pb from 558 mg/kg (range of 14–3,690 mg/kg) and not dissimilar to Broken Hill playgrounds soil Pb levels (Supplementary Table S2) to 4.1 mg/kg (range 2.2–26.1 mg/kg) using these methods. However, the contemporary data suggest strongly that subsequent recontamination due to ongoing emission, deposition and remobilisation of metal-rich dust sourced from mines in Broken Hill may render this kind of intervention ineffective. Taylor et al.'s (2013) research at Port Pirie prompted a frequent and widespread cleaning programme for the city's playgrounds (Port Pirie Regional Council, 2013),

but an evaluation of its effectiveness is still in review. Surface dust data from Broken Hill playgrounds showed that significant recontamination of playground surfaces occurred within 24 h of sampling. Despite the fact that sampling for the present study was carried out at a particularly windy time of year (Bureau of Meteorology, 2014b), a seasonal increase in hazard severity still presents a potential risk of harm. Notwithstanding the outcome of the evaluation of the Port Pirie cleaning regime, washing is unlikely to offer a long-term solution to the problem of daily dust contamination in the city of Broken Hill. The ongoing mine emissions and associated deposition of contaminants will also be affecting neighbouring residences, schools and kindergartens simultaneously, and needs to be addressed. Therefore, a more a sustainable and effective mitigation strategy in the longer term is required. Any such strategy will need to identify and then mitigate all source(s) of contamination and should include enclosure and containment of remaining surface ore processing operations.

5. Conclusions

Elevated As, Cd and Pb mining-related dust deposition continues to contaminate surfaces and contribute to blood Pb exposure risks in the city of Broken Hill.

Acknowledgements

Appendix A. Supplementary Information

Supplementary data associated with this article can be found in the online version at http://dx.doi.org/10.1016/j.envres.2014.08.036.

References

American Society for Testing and Materials. 2003. Standard practice for collection of settled dust samples using wipe sampling methods for subsequent lead determination. Available: ⟨http://www.astm.org/Standards/E1728.htm⟩ (accessed 02.12.13).

Bureau of Meteorology. 2014a. Broken Hill, N.S.W. September 2013 daily weather observations. Available: ⟨http://www.bom.gov.au/climate/dwo/201309/html/IDCJDW2020.201309.shtml⟩ (accessed 18.04.14).

Bureau of Meteorology. 2014b. Climate statistics for Australian locations: Broken Hill (Patton St). Available: ⟨http://www.bom.gov.au/climate/averages/tables/cw_047007.shtml⟩ (accessed 04.03.14).

California Environmental Protection Agency (CEPA). 2005. Use of Californian human health screening levels (CHHSLs) in evaluation of contaminated properties. Available: ⟨oehha.ca.gov/risk/pdf/screenreport010405.pdf⟩ (accessed 18.04.14).

Canadian Conference of Medical Education (CCME). 2013. Soil quality guidelines for the protection of environmental & human health. Available: ⟨http://st-ts.ccme.ca/⟩ (accessed 18.04.14.).

CBH Resources Ltd. 2014. Environmental monitoring. Available: ⟨http://www.cbhresources.com.au/operations/rasp-mine/sustainablity/environment/environmental-monitoring/⟩ (accessed 30.05.14).

Chiaradia, M., Chenhall, B.E., Depers, A.M., Gulson, B.L., Jones, B.G., 1997. Identification of historical lead sources in roof dusts and recent lake sediments from an industrialized area: indications from lead isotopes. Sci. Total Environ. 205, 107–128.

Cooper, J.A., Reynolds, P.H., Richards, J.R., 1969. Double-spike calibration of the Broken Hill standard lead. Earth Planet. Sci. Lett. 6, 467–478.

DuBois, D., DuBois, F., 1916. A formula to estimate the approximate surface area if height and weight be known. Arch. Intern. Med. 17, 869–871.

Environmental Protection Authority. 2012. Environmental protection licence no. 2688: Perilya Broken Hill ltd – version date: 20 June 2012. Griffith, NSW. (accessed 30.09.13).

Evans, A., 2012. Method NT2.49: Determination of acid extractable elements in soils, sediments, sludges and solid waste. National Measurement Institute (Inorganics Section).

Evans, A., 2013. Method NT2.52: Determination of trace elements in filters. National Measurement Institute (Inorganics Section).

Glorennec, P., Lucas, J.P., Mandin, C., Le Bot, B., 2012. French children's exposure to metals via ingestion of indoor dust, outdoor playground dust and soil: contamination data. Environ. Int. 45, 129–134.

Government of Western Australia. 2007. Response of the Western Australian Government to the Western Australian Legislative Assembly Education and Health Standing Committee in relation to the cause and extent of lead pollution in the Esperance area. Department of Health, Government of Western Australia, Western Australia. Available: http://www.public.health.wa.gov.au/cproot/1946/2/Esperance%20enquiry%20response.pdf (accessed 23.09.14).

Gulson, B., Davis, J.J., Mizon, K.J., Korsch, M.J., Bawden-Smith, J., 1995. Sources of lead in soil and dust and the use of dust fallout as a sampling medium. Sci. Total Environ. 166, 245–262.

Gulson, B.L., Mizon, K.J., 1979. Lead isotopes as a tool for gossan assessment in base metal exploration. J. Geochem. Explor. 11, 299–320.

Gulson, B.L., Davis, J.J., Mizon, K.J., Korsch, M.J., Law, A.J., Howarth, D., 1994. Lead bioavailability in the environment of children: blood lead levels in children can be elevated in a mining community. Arch. Environ. Health 49, 326–331.

Gulson, B.L., Mizon, K.J., Korsch, M.J., Howarth, D., 1996. Non-orebody sources are significant contributors to blood lead of some children with low to moderate lead exposure in a major lead mining community. Sci. Total. Environ. 181, 223–230.

Kranz, B.D., Simon, D.L., Leonardi, B.G., 2004. The behavior and routes of lead exposure in pregrasping infants. J. Expo. Anal. Environ. Epidemiol. 14, 300–311.

Lesjak M., Gough N., Belshaw D., Tall J., Jones T. 2013. Lead Health Report – children less than 5 years old in Broken Hill. Broken Hill: Population Health Unit, Western NSW & Far West Local Health District. Available: ⟨http://www.wnswlhd.health.nsw.gov.au/UserFiles/files/FarWest/ANNUAL%20LEAD%20REPORT%202012%20Final.pdf⟩ (accessed 30.05.14).

Lowry R. 2014. VassarStats: website for statistical computation. Available: ⟨http://vassarstats.net⟩ (accessed 18.05.13).

Mackay, A.K., Taylor, M.P., Munksgaard, N.C., Hudson-Edwards, K.A., Burn-Nunes, L., 2013. Identification of environmental lead sources and pathways in a mining and smelting town: Mount Isa, Australia. Environ. Pollut. 180, 304–311.

Mielke, H.W., Covington, T.P., Mielke Jr., P.W., Wolman, F.J., Powell, E.T., Gonzales, C. R., 2011. Soil intervention as a strategy for lead exposure prevention: the New Orleans lead-safe childcare playground project. Environ. Pollut. 159, 2071–2077.

National Environmental Protection Council. 2013. National Environmental Protection Measure (NEPM). In: Schedule B1: Guideline on investigation levels for soil and groundwater. Available: ⟨http://www.comlaw.gov.au/Details/F2013C00288/Html/Volume_2⟩ (accessed 19.10.13).

National Pollutant Inventory (NPI). 2014a. 2012-2013 report for CBH Resources-Rasp Mine-Broken Hill, NSW. Available: ⟨http://www.npi.gov.au/npidata/action/load/browse-search/criteria/year/2013/browse-type/Company/reg-business-name/BROKEN%2BHILL%2BOPERATIONS%2BPTY%2BLTD⟩ (accessed 30.05.14).

National Pollutant Inventory (NPI). 2014b. 2012-2013 report for Perilya limited, Perilya Broken Hill Operations-Broken Hill, NSW. Available: ⟨http://www.npi.gov.au/npidata/action/load/emission-by-individual-facility-result/criteria/state/NSW/year/2013/jurisdiction-facility/125⟩ (accessed 30.05.14).

National Toxicology Program (NTP). 2012. National toxicology monograph and health effects of low-level lead. U.S. Department of Health and Human Services. Available: ⟨http://ntp.niehs.nih.gov/?objectid=4F04B8EA-B187-9EF2-9F9413C68E76458E⟩ (accessed 18.12.13).

Needleman, H., 2004. Lead poisoning. Annu. Rev. Med. 55, 209–222.

Norwegian Pollution Control Authority (NPCA). 2009. Soil contamination in day-care centers and playgrounds. Available: ⟨www.miljodirektoratet.no/old/klif/publikasjoner/2550/ta2550.pdf⟩ (accessed 18.04.14).

Perilya Broken Hill Ltd. 2013. Pollution report – EPA licence 2688 (southern operations). Available: ⟨www.perilya.com.au/articles/september-2013-report-2/September_2013_Report2.pdf⟩ (accessed 12.03.14).

Perilya Broken Hill Ltd. 2014. Monthly reports – environmental reporting. Available: ⟨http://www.perilya.com.au/health–safety–environment/environment/enviro-reports⟩ (accessed 30.05.14).

Port Pirie Regional Council. 2013. Port Pirie Playground Cleaning Schedule. Available: ⟨http://www.pirie.sa.gov.au/webdata/resources/files/PlaygroundScedule_graph-May2013%20%28Large%29.jpg⟩ (accessed 17.12.13).

Simon, D.L., Maynard, E.J., Thomas, K.D., 2007. Living in a sea of lead-changes in blood- and hand-lead of infants living near a smelter. J. Expo. Sci. Environ. Epidemiol. 17, 248–259.

Solomon, R.J., 1988. The richest lode: Broken Hill 1883–1988. Hale & Iremonger, Sydney, NSW.

Soto-Jiménez, M.F., Flegal, A.R., 2011. Childhood lead poisoning from the smelter in Torreón, Mexico. Environ. Res. 111, 590–596.

Standards Australia. 1998. AS 4361.2-1998 Guide to lead paint management-residential and commercial buildings. Available: ⟨http://infostore.saiglobal.com/store2/Details.aspx?ProductID=313655⟩ (accessed 20.12.13).

Standards Australia. 2000. AS 4874-2000 Guide to the investigation of potentially contaminated soil and deposited dust as a source of lead available to humans. Available: ⟨http://infostore.saiglobal.com/store/details.aspx?ProductID=318623⟩ (accessed 02.12.13).

TA Luft. 2002. Technical instructions of air quality control, first general administration regulation pertaining the federal Immission Control Act. Available: ⟨http://www.bmu.de/files/pdfs/allgemein/application/pdf/taluft_engl.pdf⟩ (accessed 19.10.13).

Taylor, M.P., Hudson-Edwards, K.A., 2008. The dispersal and storage of sediment-associated metals in an arid river system: the Leichhardt River, Mount Isa, Queensland, Australia. Environ. Pollut. 152, 193–204.

Taylor, M.P., Mackay, A.K., Hudson-Edwards, K.A., Holz, E., 2010. Soil Cd, Cu, Pb and Zn contaminants around Mount Isa city, Queensland, Australia: potential sources and risks to human health. Appl. Geochem. 25, 841–855.

Taylor, M.P., Winder, C., Lanphear, B.P., 2012. Eliminating childhood lead toxicity in Australia–a little is still too much. Med. J. Aust. 197, 493.

Taylor, M.P., Camenzuli, D., Kristensen, L.J., Forbes, M., Zahran, S., 2013. Environmental lead exposure risks associated with children's outdoor playgrounds. Environ. Pollut. 178, 447–454.

Taylor, M.P., Davies, P.J., Csavina, J., Kristensen, L.J., 2014a. Licenced to pollute but not to poison: the ineffectiveness of regulatory authorities at protecting public health from atmospheric arsenic, lead and other contaminants resulting from mining and smelting operations. Aeolian Res. 14, 35–52.

Taylor, M.P., Winder, C., Lanphear, B.P., 2014b. Australia's leading public health body delays action on the revision of the public health goal for blood lead exposures. Environ. Int. 70, 113–117.

Townsend, A.T., Yu, Z., McGoldrick, P., Hutton J., A., 1998. Precise lead isotope ratios in Australian galena samples by high resolution inductively coupled plasma mass spectrometry. J. Anal. Atom. Spectrom. 13, 809–813.

United States Environmental Protection Agency (EPA). 2013. Regional screening levels. Available: ⟨http://www.epa.gov/region9/superfund/prg/⟩ (accessed 18.04.14).

Viverette, L., Mielke, H.W., Brisco, M., Dixon, A., Schaefer, J., Peierre, K., 1996. Environmental health in minority and other undeserved populations: benign methods for identifying lead hazards at day care centres of New Orleans. Environ. Geochem. Health 18, 41–45.

Woodward, O.H., 1965. A review of the Broken Hill lead-silver-zinc industry, second ed. NSW:West Publishing Corporation Pty. Ltd., Sydney.

Article Two

The Conversation

Toxic playgrounds: Broken Hill kids exposed to poisonous dust

_____

Taylor, M.P., Kristensen, L.J., **Rouillon, M.,** Mould, S.A

October 16, 2014 6.29am AEDT

Figure A.1: Children are particularly susceptible to the toxic effects of lead because their brains and bodies are still developing.

In the shadows of Broken Hill's rich mining history lies a legacy of contamination and regulatory failure that will likely outlive any benefits locals derive from mining. One in five children aged under five in Broken Hill have blood lead levels above the current national goal of ten micrograms per decilitre (µg/dL). And the trend is headed in the wrong direction. Our research, published today in the journal Environmental Research, shows children are exposed to contaminants in play areas. Metal-rich dust accumulates continually on play surfaces and is readily picked up on the hands of children as they play. When they touch their mouth, they ingest the metal particles. To pre-empt claims children are ingesting historical sources of lead, such as leaded gasoline and paint residue, we used lead isotopic analysis to show the most likely source of contamination is from the lead ore body that is still being mined.

Lead and human health

Lead is a neurotoxin, a poison that acts on the nervous system; children are particularly susceptible because their brains and bodies are still developing. Elevated blood lead is linked to permanent cognitive impairment measured in decreased IQ and has also been linked to a

greater likelihood to commit crime later in life. Although the current (under review) national goal for blood lead is 10 µg/dL, there is overwhelming evidence showing that damage occurs at levels below 5 µg/dL. Following significant and successful efforts by Broken Hill's Lead Health Program, childhood blood levels declined significantly from their peak in the early 1990s. But recent improvements in screening participation have revealed that the problem is now worse than previously thought. The proportion of children aged 12 months to five years with a blood lead level above 10 µg/dL has risen from 12.6 % in 2010 to 21 % in 2012. It is unfortunate for the children of Broken Hill that the successful Lead Health Program no longer exists in its own right and is only a poorly funded component of the Broken Hill Child and Family Health Centre.

Contaminated playgrounds

We measured the amount of metal-rich dust that could be picked up on the hands of children at public playgrounds in Broken Hill. We found that, on average, the amount of lead on hands after ten minutes play was 72 times the amount on hands before contact with play equipment. Although there is no Australian standard specifically for lead on hands, the Western Australian government set a goal in 2007, for the clean-up standards in Esperance, that outdoor surfaces accessible to children should not exceed 400 µg/m^2.

Our study found that, after playing at one particular playground, a child's hand could have the equivalent loading of 60,900 µg/m^2 – more than 150 times the goal set in WA and significantly higher than levels recorded in the smelter city of Port Pirie. As well as playgrounds, dust falling across most of the city and any outdoor surfaces is contributing to the harmful metal residues already present in the soil contaminated from more 130 years of mining activity.
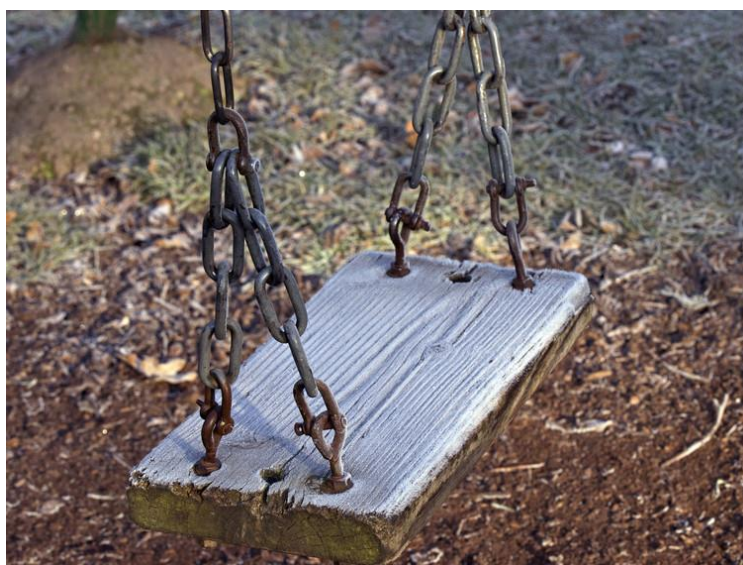
Figure A.2: Surfaces are being re-contaminated on a daily basis.

Lead in soils

Soils in playgrounds also had elevated lead. The National Environmental Protection Measure (2013) sets a soil lead standard of 600 mg/kg for recreational spaces. Three of the six playgrounds we tested exceeded this standard and four exceeded the lower residential standard of 300 mg/kg, which may be a more appropriate standard as it also applies to daycare centres. Of the other metals we analysed (arsenic, cadmium, silver and zinc), no soil samples exceeded the relevant Australian guidelines. However, it is worth noting that Australian standards for soil metal are more liberal than our international counterparts. California, Canada, and the United States Environmental Protection Agency set soil lead guidelines at 80 mg/kg, 140 mg/kg and 400 mg/kg respectively. Norwegian soil guidelines specifically limit soil used in children's playgrounds to 60 mg/kg. Only one playground in Broken Hill had soil below this level.

Lead dust from mining

Our data, combined with data collected by mining companies as part of their environmental monitoring, show that surfaces in Broken Hill are re-contaminated daily. And they indicate that contemporary mining activities are the most likely consistent source of airborne lead and other metal-rich particles. Although the bulk of mining today occurs underground, ore is processed at the surface and can generate large amounts of dust. It is unlikely to be a coincidence that the most impacted playground we measured was located at Zinc Lakes, less than 400 metres from an active ore processing facility.

Figure A.3: Ore processing as seen from Zinc Lakes playground.

Importantly, arsenic, cadmium, lead, silver, and zinc levels on hand wipes each correlated significantly with the amounts of the same metals deposited on wiped surfaces for each day, demonstrating a common source for the contamination of hands and dust-collecting surfaces.

What can be done?

The high likelihood of recontamination from ongoing lead deposition makes it unlikely that common approaches to containing lead and other soil metal contamination, including topsoil replacement and remediation techniques, would be effective in Broken Hill. Broken Hill is not alone with this problem either; similar work in the smelting towns of Port Pirie in South Australia and Mount Isa in Queensland has shown that environmental contamination is persistent and pervasive and that effective regulatory controls are often lacking. Some of early responses to the problem have been positive, with the mining company Perilya putting notifications on their Zinc Lakes playground that users should wash their hands after play. The Council is also following suit with similar signage on their playgrounds.

Figure A.4: The new signage at Zinc Lakes urges children to wash their hands after play.

In Broken Hill, there is currently no independent monitoring of air pollution. The monitoring that does take place is being carried out by the companies doing the polluting and is restricted, in the main, to their lease or adjacent areas and not in the larger residential environment. This monitoring does not include measurement or regulation of arsenic or cadmium, which are also known to cause significant detrimental health outcomes. The approaches used to measure air

pollution from mining activities in Australia rely on data averaged yearly as a benchmark. As a result, short-term spikes in emissions are not accounted for, potentially downplaying the risks. The Environmental Protection Authority (EPA) has an important role to play in setting effective limits for pollution and in the monitoring and enforcement of those limits for the benefit of communities in vulnerable locations. Recently, questions were raised about the NSW EPA's willingness – or ability – to fulfil this role. We need to explore more flexible monitoring programs, and to regulate and better manage the contamination risk in places such as Broken Hill. This is particularly important for communities that are already acknowledged as being significantly disadvantaged. People should not continue to suffer from the lingering impacts of industrial activity in their environments. Residents of mining and smelting towns should be able to live, work and play in the knowledge that their environments are clean and safe, and that effective pollution regulation will keep them that way. To lower exposures permanently and reduce the cycle of contamination, the New South Wales government needs to make a significant financial commitment to start a new Lead-Free Children's Health Program. While any such program needs to be independent, it will have to engage with and involve the whole community, the city's mining companies and government at all levels.

Update 13 February 2015: The New South Wales Government today announced a five-year $13 million program to address the issue of lead contamination and elevated blood lead levels among children in Broken Hill.

Paper Seven

Publication

Evaluating the efficacy of playground washing to reduce environmental metal exposures

Abstract:

Washing and wet mopping is often advocated as a remedial treatment to limit exposure to lead dust. Here, surface and pre- and post-play wipes were measured to ascertain dust metal exposures (arsenic, cadmium, copper, lead and zinc) following play routines at four playgrounds in the smelter city of Port Pirie, South Australia, which are washed regularly. Although post-play hand wipe metals were 55.9 % (95 % CI: −0.78, −0.34) lower on wash days, loadings increased ∼5.1 % (95 % CI: 1.2, 11.7) per hour after washing. Despite washing, post-play hand lead exceeded a conservative value of 800 μg/m^2 within 24 h or sooner, with loadings increasing in proximity to the smelter. Post-play lead loadings were always >1000 μg/m^2 at the playground closest to smelter. Playground washing results in short-lived exposure reduction and effective treatment requires elimination of smelter emissions.

Keywords: Lead, Children, Contamination, Dust, Metals, Smelter

ELSEVIER

CrossMark

Evaluating the efficacy of playground washing to reduce environmental metal exposures

Mark Patrick Taylor [a, *], Sammy Zahran [b], Louise Kristensen [a], Marek Rouillon [a]

[a] Department of Environmental Sciences, Faculty of Science and Engineering, Macquarie University, Sydney, NSW 2109, Australia
[b] Department of Economics, Center for Disaster and Risk Analysis, Colorado State University, C-312A Clark Building, Fort Collins, CO 80523-1771, USA

ABSTRACT

Washing and wet mopping is often advocated as a remedial treatment to limit exposure to lead dust. Here, surface and pre- and post-play wipes were measured to ascertain dust metal exposures (arsenic, cadmium, copper, lead and zinc) following play routines at four playgrounds in the smelter city of Port Pirie, South Australia, which are washed regularly. Although post-play hand wipe metals were 55.9% (95% CI: -0.78, -0.34) lower on wash days, loadings increased ~5.1% (95% CI: 1.2, 11.7) per hour after washing. Despite washing, post-play hand lead exceeded a conservative value of 800 $\mu g/m^2$ within 24 h or sooner, with loadings increasing in proximity to the smelter. Post-play lead loadings were always >1000 $\mu g/m^2$ at the playground closest to smelter. Playground washing results in short-lived exposure reduction and effective treatment requires elimination of smelter emissions.

© 2015 Elsevier Ltd. All rights reserved.

1. Introduction

The problem of childhood lead exposure remains a persistent problem in Australia's primary smelting and mining cities of Broken Hill, Mount Isa and Port Pirie, with the latest figures showing that 21%, 4.8% and 22.7%, respectively, of children under 5 years of age having a blood lead level above 10 $\mu g/dL$, the current (under review) Australian goal (Taylor et al., 2014b). However, the extent of exposures amongst the wider Australian population is unknown because of a lack of available population data. Nevertheless, estimates derived from USA exposure data have indicated that ~100,000 children <5 years of age may have exposures above 5 $\mu g/dL$ (Taylor et al., 2012, 2014c), which corresponds to the most recent study on Australian urban children that reported 7.5% (8/107) of the cohort had a blood lead >10 $\mu g/dL$ (Gulson et al., 2008).

Where exposures are well documented and the sources known, interventions, screening and advice programs are usually provided. One such case is in the city of Port Pirie in South Australia, where lead smelting has been ongoing since 1889. The effects of the smelter operations has resulted in widespread contamination of the natural and urban environment, which has been associated

with persistent, but declining blood lead exposures in children over the last two decades (Maynard et al., 2006; Simon et al., 2007; Taylor, 2012; Taylor et al., 2013). Strategic interventions, lead awareness programs in the city of Port Pirie (Maynard et al., 2006; Thumbs Up for Low Levels 2015), and emission reduction efforts from the city's smelter site (Environment Protection Authority South Australia (EPASA) 2009) have contributed to the fall in blood lead levels. However, the most recent annual data show that exposures have stabilised or even by some measures increased (Taylor et al., 2014c). For example, the geometric blood lead mean for all children under 5 years of age increased from 4.5 $\mu g/dL$ in 2012 to 5.0 $\mu g/dL$ in 2013. The primary source of the exposures is caused by the ongoing and contemporaneous lead-in-air emissions from the smelter (Simon et al., 2007; Taylor, 2012; Taylor et al., 2014a), which result in elevated concentrations of contaminated metal rich dust being deposited on surfaces (van Alphen, 1999; Taylor et al., 2013, 2014a; Csavina et al., 2014). In addition, there is a substantial reservoir of lead-contaminated soil from accumulated emissions in Port Pirie that has the potential for re-suspension (SA Health, 2013).

The spatial extent of metal- and metalloid-rich dust (hereafter referred to as metals), including lead, was detailed in a study of playgrounds across the city of Port Pirie in 2011 (Taylor et al., 2013). This study showed that atmospheric emissions from the

* Corresponding author.
E-mail address: mark.taylor@mq.edu.au (M.P. Taylor).

smelter were related directly to surface dust and hand metal exposures following the use of playground equipment (Taylor et al., 2013). Following this study, the Port Pirie Council and the smelter company, Nyrstar Port Pirie Limited Pty Ltd, agreed to a joint program of playground washing. Before these results were published, the playground washing intervention program was limited only to the Foreshore Playground (also known as Flinders View), which was washed twice a week on Monday and Friday mornings, with no other playgrounds washed regularly (D. Farquhar, Port Pirie Council, personal communication, 7th July 2011). Given the elevated metal loadings identified across the studied playgrounds (Taylor et al., 2013), we released the environmental data to SA Health and the Port Pirie Council ahead of publication to assist with their management of the problem. The authorities responded on August 1st, 2012 by increasing the frequency of playground cleaning to 22 washes per week across a range of different playgrounds in the city. The program was revised to include 9 playgrounds and 1 kindergarten (Supplementary Fig. S1). Following the online publication of the research on May 1st 2013 (Taylor et al., 2013), the Council and Nyrstar issued a further revision to the cleaning program on May 7th 2013. The new program increased the total number of playground wash events across the city to 49 per week covering 9 playgrounds (a total of 31 washes) and 9 child care centres, primary schools and kindergartens (a total of 18 washes) (Supplementary Fig. S2). Although the specifics of the washing techniques used on the play equipment are not provided in the cleaning schedules (Supplementary Figs. S1, S2), washing was observed at the Sports Park playground and involved scrubbing and hosing down of equipment. However, the effectiveness of the intervention strategy has not been evaluated but it warrants assessment given that other similarly impacted locations such as Broken Hill are considering equivalent regimes in response metal-rich dust contamination problems (Taylor et al., 2014b).

Intervention programs in lead contaminated environments typically involve advice to wet wipe and mop in order to reduce the hazard associated with the build-up of lead dusts (and other metals) in domestic environments (e.g. Living Safely with Lead, 2014; New South Wales Government 2014; Thumbs Up for Low Levels 2015). However, a Cochrane review of household interventions for preventing domestic lead exposure in children, including the removal of dust, demonstrated such approaches were not effective in reducing blood lead levels in children (Yeoh et al., 2012).

Lead in dust on surfaces in home environments at levels much lower than the typical intervention levels pose a measurable risk factor for elevated blood lead levels in children (Dixon et al., 2009). Data modelling predicted floor dust lead at concentrations as low as 12 $\mu g/ft^2$ (129 $\mu g/m^2$) would result in 4.6% of children living in USA homes constructed before 1978 (the era when the use of lead in paint was prevalent) to have a blood lead $\geq$ 10 $\mu g/dL$, with 27% to have a blood lead $\geq$ 5 $\mu g/dL$ (geometric mean 3.9 $\mu g/dL$) (Dixon et al., 2009). Given that the US Centers for Disease Control and Prevention have moved to using $\geq$5 $\mu g/dL$ as the reference level for children's blood lead and Australia appears to be moving to the same value for investigating environmental sources of exposure (NHMRC, 2014a,b), it is imperative that effective and evidence-based abatement and risk reduction strategies are promulgated (Taylor et al., 2014c).

Therefore, the purpose of this study was to evaluate the efficacy of the Port Pirie playground cleaning regime to reduce environmental metal exposure risks to children. Such information is useful for other similarly impacted locations where substantial regulatory effort and cost is invested in reducing potential exposures from contemporary metal-rich dust depositions.

2. Methods and approach

2.1. Field sampling

Field sampling was carried out in accordance with established methods (Taylor et al., 2013). The four Port Pirie playgrounds sampled in the previous study, Foreshore playground, Memorial Park playground, Sports Park playground and Woodward Park playground were sampled again each morning for a 5-day period between 20th July and 24th July 2013 (Fig. 1). The distances of the playgrounds from the smelter are: Foreshore Playground (1.0 km); Memorial Park Playground (1.2 km); Sports Park Playground (2.4 km); Woodward Park Playground (3.0 km) (Fig. 1). Images of each of the playgrounds showing the playground equipment and surrounds are provided in Fig. S2a–d of the Supplementary in Taylor et al. (2013).

Given that we wanted to evaluate the efficacy of washing as a remedial treatment, playgrounds that were subject to a morning wash according to the published schedule (Supplementary Fig. S2), were re-sampled in the afternoon approximately 6 h after the initial morning sample. These data were also used to investigate the dimension of washing for reducing playground surface contamination (Table 1).

Two playground surface dust wipe samples were also collected following the methods described in ASTM E1728-10 (ASTM, 2010) at each playground at the time of hand wipe sampling (n = 58). The playground surface wipe sampling approach detailed in ASTM (2010) is, for all intents and purposes, identical to that detailed in Australia's guide to lead paint management, AS 4361.2–1998 (Standards Australia, 1998). The areas wiped were measured to enable surface wipe metal values to be transformed to $\mu g/m^2$. As in the previous study, sites were selected to be close to, but away from the playgrounds, and unlikely to be interfered with during normal play routines or affected by the washing routines undertaken by Council or Nyrstar. The same researcher (L. Kristensen, as per Taylor et al., 2013) undertook the 20 min of child simulated play on the facilities from which we were able to obtain 29 paired samples of pre- and post-play hand wipes over the five-day study period. Hand contact was limited to the equipment and deliberately excluded contact with the ground surface around the playgrounds. The anterior (palmar) hand surface area of the play participant was calculated using the DuBois and DuBois (1916) method and metal concentrations transformed to $\mu g/m^2$ for pre- and post-play wipes.

2.2. Laboratory analyses

All wipe samples were tested for arsenic, cadmium, copper, lead and zinc at the National Measurement Institute, Sydney. Samples were digested in sterile polypropylene tubes using a mixture of 3 mL concentrated nitric acid and 1 mL hydrochloric acid (analytical reagent grade) on a digestion block at 110 °C for 90 min. A further 10 mL of Milli-Q was added to the samples prior to an additional 30 min digestion at 110 °C (Evans, 2013). Element concentrations were determined using a Varian Vista Pro ICP-OES and PerkinElmer Elan DRC II ICP-MS. Reagent blanks, dust wipe blanks, matrix spiking and reference materials AGAL-10 (Hawkesbury River Sediment) and AGAL-12 (Biosoil) were analysed concurrently for quality assurance. Reagent blanks were all below laboratory limit of reporting (LOR) as were the wipe blanks for arsenic (0.2 $\mu g/wipe$) and cadmium (0.05 $\mu g/wipe$). The wipe blanks returned an average copper concentration of 0.67 $\mu g/wipe$, lead concentration of 0.03 $\mu g/wipe$ and zinc concentration of 20.85 $\mu g/wipe$. Field blanks collected at each playground were below LOR for arsenic and cadmium and with average values of 0.84 $\mu g/wipe$ for copper, 25.44 $\mu g/wipe$ for zinc and 0.11 $\mu g/wipe$ for lead (0.07 $\mu g/wipe$ for Memorial Park, Sports Park and Woodward Park and 0.23 $\mu g/wipe$

Fig. 1. Site location map — the four playgrounds sampled and the Nyrstar Port Pirie Smelter, in Port Pirie, South Australia.

for Foreshore Playground). Recovery rates for matrix spikes and certified materials were 96—102% and 92—98% for arsenic, 97—100% and 81—95% for cadmium, 96—101% and 88—89% for copper, 95—101% and 94—98% for lead and 95—103% and 87—88% for zinc.

3. Results and discussion

3.1. Playground surface dust wipe results

The surface dust metal data derived from this study shows that

in nearly all cases the metals were markedly lower than those reported previously (Taylor et al., 2013). These differences are highlighted by examining the results from the two playgrounds closest to the smelter, Foreshore and Memorial Park. At Foreshore playground, mean playground surface metal loadings were reported previously as follows (values to 3 significant figures): arsenic — 112, cadmium — 23.6 and lead — 5060 $\mu g/m^2$ (Taylor et al., 2013). These previous values compare to the lower mean values reported in the current study (Supplementary Table S3) as follows: arsenic — 30.8, cadmium — 4.30 and lead — 850 $\mu g/m^2$. At Memorial Park, the mean

Table 1
Surface and play sample wipe times. Playgrounds washed (✓) according to the published schedule (Supplementary Figure S2).

	Saturday 20th July 2013		Sunday 21st July 2013		Monday 22nd July 2013		Tuesday 23rd July 2013		Wednesday 24th July 2013
Rainfall[a]	9.2 mm		5.2 mm		1.2 mm		0.8 mm		0.1 mm
Foreshore playground	✓ (1030)		✓ (1030)	(1530)	✓ (1130)	(1630)	✓ (1040)	(1620)	✓ (1110)
Memorial Park playground	✓ (1000)		✓ (1000)	(1500)	✓ (1030)	(1600)	✓ (1010)	(1545)	✓ (1035)
Sports Park playground	(0900)		(0900)		✓ (0905)	(1500)	(0900)		✓ (0930)
Woodward Park playground	(0930)		(0930)		✓ (1000)	(1500)	✓ (0930)	(1500)	✓ (1000)

[a] Total rainfall over previous 24 h measured at 9 am. Rainfall data is from Bureau of Meteorology, Port Pirie Aerodrome station, which is 7 km south of the city (Bureau of Meteorology (2014a)).

playground surface metal values reported previously were: arsenic − 91.8, cadmium − 25.0; lead − 6960 µg/m^2 (Taylor et al. (2013). The playground surface mean metal values recorded in this study were: arsenic − 18.8, cadmium − 3.50; lead − 2380 µg/m^2.

The differences in playground surface metals between the two studies may be attributable to rainfall that occurred during the July 2013 sampling campaign. No rain was recorded shortly before or during the sampling that took place in 2011 (Taylor et al., 2013). Average wind direction in Port Pirie during the months of June and July were from a north to north-east direction (Bureau of Meteorology (BoM) 2014b), indicating no variance in wind direction between the 2011 and 2013 sampling periods. In terms of atmospheric lead emissions, the Environment Protection Authority South Australia data shows that from ~ mid 2013, atmospheric emissions of lead were actually rising (Taylor and Isley, 2014; EPASA, 2014). Therefore, in the absence of rainfall, these emissions should have been associated with dust deposition levels on playground surfaces that were at least equivalent if not higher than that measured in the 2011 data (Taylor et al., 2013). Notwithstanding the differences between the two studies, this study shows clearly that mean playground surface dust metal loadings were in most cases, considerably in excess of international standards (annual average values, TA Luft, 2002) for arsenic − 4 µg/m^2/day; cadmium − 2 µg/m^2/day and lead − 100 µg/m^2/day. Although surface dust metal deposition is not regulated within the existing licence arrangements at Port Pirie, the TA Luft (2002) dust deposition standards are used in the Mount Isa Mines, Queensland Environmental Authority to regulate mining and smelting operations (Taylor et al., 2014). Consequently, these values are considered reasonable acceptable benchmarks to compare the results reported herein.

3.2. Hand wipe results

Overall, the values derived from the hand wipe assessments in this study (Supplementary Table S4) reflect the playground surface dust metals in that they are lower than those reported previously from the 2011 study (Taylor et al., 2013). Notable exceptions to this are cadmium post-play hand wipe loadings, which were elevated at Woodward Park playground compared to 2011 wipe data: Woodward Park 2013 cadmium mean 21.9 ± 15.9 µg/m^2 versus 2011 cadmium mean: 14.9 ± 16.1 µg/m^2. Nevertheless, it is notable that the overall mean dust metal loadings for arsenic, cadmium and lead are lower than what they were in 2011. These lower dust metal loadings are likely to have been influenced by rainfall that occurred during the sample period. The lower values at Foreshore may also have been influenced by the addition of a shade cloth over the playground area following publication of the 2011 data. Notwithstanding these lower levels, the data show the mean values on hands following play at all sites remain considerably elevated with respect to international values (TA Luft, 2002). As shown in Table 2 below, average post-play hand wipes exceed the 400 µg/m^2 of lead

on surfaces as applied by the Government of Western Australia (2011) as part of the lead-spill clean up in the town of Esperance (Gulson et al., 2009). These post-play levels demonstrate the persistence of environmental contamination despite the fact that all of the playgrounds were washed on at least two occasions during the sampling campaign (Supplementary Figure S2).

3.3. Playground surface and hand wipe dust metal modelling results and analysis

To understand the efficacy of playground cleaning as a suitable remedy for reducing exposure risks, particularly with respect to time-incremental accumulation of metal-rich dust, we applied a suite of statistical analyses and modelling techniques to the data.

Table 2 details paired t-tests comparing the mean metal loading of pre-versus post-play hand wipes across all sampled playgrounds. This shows that post-play hand wipes had significantly higher levels of arsenic (3.21 µg/m^2 vs 32.4 µg/m^2), cadmium (4.73 µg/m^2 vs 15.0 µg/m^2), copper (91.5 µg/m^2 vs 192 µg/m^2), lead (279 µg/m^2 vs 2090 µg/m^2), and zinc (2780 µg/m^2 vs 6160 µg/m^2), with all values at $p < 0.0001$. With respect to lead and arsenic, even with the increased playground washing regime, post-play levels were ~7 and 10 times higher than pre-play levels, respectively.

Fig. 2 depicts the mean pre- versus post-play hand wipe lead loadings (µg/m^2) across each playground. The height of each bar corresponds to the average lead loading over sample days at each playground, with the range markers depicting the 95% confidence intervals around the mean values. With the exception of the Woodward playground, hand wipe lead loadings increased significantly (where $p < 0.01$) after the timed 20 min play events. For example, at the Foreshore playground, average post-play hand wipe lead loadings are 4410 µg/m^2 (95% CI: 3633, 5186), compared to the pre-play average of 568 µg/m^2 (95% CI: 173, 962), representing more than a seven-fold increase in lead exposure. It is worth noting that Foreshore playground was the last playground sampled each day and that the pre-play wipes contain measurable lead loadings, despite hands having being wiped after play at the previous site. This indicates that the dust metals are pervasive and are being transferred readily between playgrounds to hands from the interior of vehicles, clothing and other surfaces despite efforts to limit any such contact during the sampling process.

As indicated in earlier studies (van Alphen, 1999; Maynard et al., 2006; Simon et al., 2007; Taylor et al., 2013), the data confirm the notion that residing in Port Pirie is akin to "*living in a sea of lead*" (Simon et al., 2007), *inter alia* other metal contaminants, from which there is virtually no escape. Indeed, washing playgrounds only deals with a very limited geographical area of exposure and the data show quite clearly that contamination not only blankets the city daily, it is pervasive and persistent (Taylor, 2011; Taylor et al., 2014a,c). In short the contamination does not 'go away', and even for vigilant persons, let alone young children, or their mothers vested with the responsibility of stopping innate hand-mouth behaviours. Thus, it is clear exposure cannot be avoided.

The effects of the new and extended 2013 Port Pirie playground washing regime (Supplementary Figure S2) was modelled (Table 3). In modelling the effect of washing, we also treated Woodward and Sport Park playgrounds as having been washed as a result of the prevailing 24-h rainfall of 9.2 mm (Table 1). Specifically, the purpose of the modelling was to evaluate the City's remedial response to metal exposure risks in public spaces frequented by children.

Evaluation of environmental health remedial treatments designed to protect children should be a requirement before they are promulgated as a solution in mining and smelting towns. Indeed, education remedies are often promoted as being an

Table 2
Paired t-tests comparing the mean metal loading of pre-versus post-play hand wipes at all playground.

Metal	Pre-play (µg/m^2)	Post-play (µg/m^2)	Difference (µg/m^2)	t	p
Arsenic	3.21 (0.66)	32.40 (5.17)	29.20	5.68	<0.0001
Cadmium	4.73 (1.20)	14.97 (1.97)	10.24	4.69	<0.0001
Copper	91.50 (5.91)	191.90 (20.77)	100.40	4.73	<0.0001
Lead	279.01 (58.87)	2088.46 (333.75)	1809.44	5.90	<0.0001
Zinc	2782.13 (168.14)	6158.81 (575.96)	3376.13	5.72	<0.0001

Note: Standard errors in parentheses.
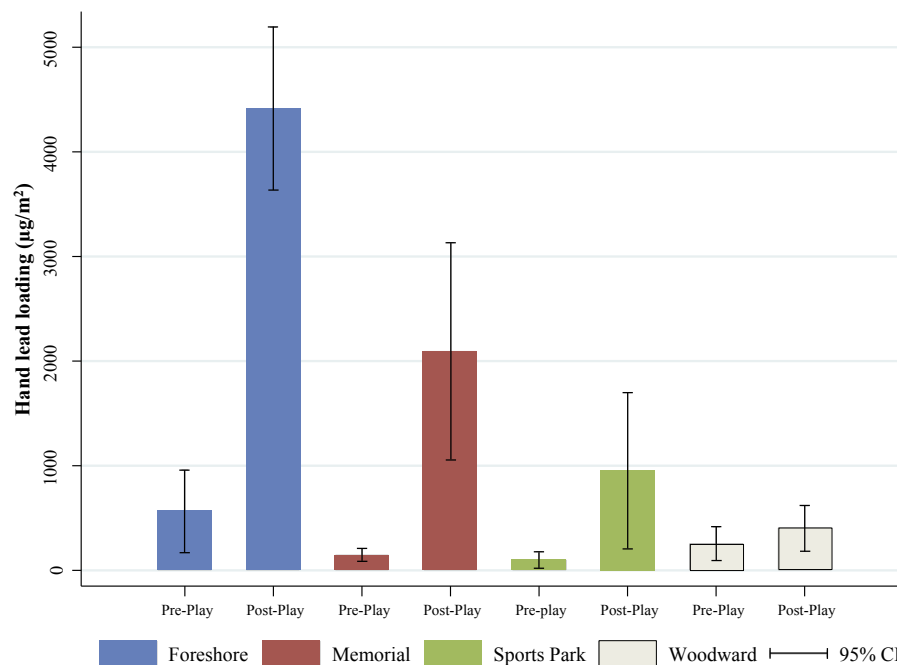
Fig. 2. Pre- versus post-play hand wipe lead loadings (µg/m²) by playground.

Table 3
Regression coefficients estimating the effect of playground wash on metal exposure risk (µg/m²) from timed play.

	Post-play (*ln*)
Playground wash	−0.559*** (0.114)
Pre-play wipes (*ln*)	0.008 (0.012)
Surface wipes (*ln*)	0.015 (0.010)
Reference = Arsenic	
Cadmium	−0.632*** (0.177)
Copper	1.901*** (0.191)
Lead	3.932*** (0.199)
Zinc	5.349*** (0.217)
Reference = Woodward Park	
Foreshore	1.446*** (0.152)
Memorial Park	0.579*** (0.151)
Sport Park	0.442*** (0.178)
Weekend	−0.256** (0.113)
Constant	2.877*** (0.170)
Observations	145
F-Test	187.61
R²	0.934

Note: Standard errors in parentheses ***p < 0.01, **p < 0.05, *p < 0.1. *ln* −data was normalised using natural log transformation (*ln*).

$$\ln\left(y_{ij}\right) = \alpha + \beta_1 W_j + \beta_2 \ln(P_{ij}) + \beta_3 \ln(S_j) + \gamma_1 M_{ij} + \gamma_2 G_j + \gamma_3 D_{ij} + \varepsilon_{ij} \tag{1}$$

where, α is our model constant (representing the natural log of the average post-play hand wipe metal loadings in our reference grouping), W_j is our wash indicator = 1 if the experiment occurred on a day where playground j underwent a wash, P_{ij} is the pre-play hand wipe metal loadings of subject i in the playground j, S_j is the mean metal dust loadings on surfaces of playground j, M_{ij} represents a set of dummy variables corresponding to metal type (with arsenic as our reference metal), G_j is a set of dummy variables corresponding to each playground (with Woodward Park as our reference playground), D_{ij} is an indicator variable = 1 if the playground experiment occurred on a weekend day, and ε_{ij} is the random disturbance term of the model.

The objective of equation (1) is to estimate the parameter β_1, corresponding to the impact of a playground wash, controlling for pre-play wipe metal loadings, levels of metal accumulation on playground surfaces, and fixed effects for metal type, playground location, and whether the play experiment occurred on a weekend day. If washing a playground reduces the risk of metal exposure, then β_1 ought to be negative and statistically significant. Our dependent variable − post-play hand wipe metal loadings − was normalized by natural log transformation. Because our dependent variable is natural logged, the coefficient corresponding to playground wash in Table 3 is interpretable in percentage terms. As shown in Table 3, we find that post-play hand wipe metal loadings were 55.9% (95% CI: −0.78, −0.34) lower on wash-days as compared to non-wash days, demonstrating the effect of washing a playground in lower exposure risk (Table 3).

Despite the clear reductions in metal loading due to washing (natural or as part of the cleaning regime), the salient question is whether washing should be promulgated as an effective strategy to counteract metal-rich dust hazards. To elucidate this pivotal question, Fig. 3 graphs the effect of a playground wash on lead exposure risk at each playground. Predicted values (and intervals of

acceptable response (Mount Isa − Living with Lead Alliance (2014), NSW Government (2014), Port Pirie − Thumbs Up for Low Levels (2015), Trail, Canada − Trail Area Health and Environment Program (2014)) as a way of mitigating unsafe exposures. However, their efficacy is unproven (Yeoh et al., 2012). Physical intervention measures in New Orleans child care centres involving covering contaminated soil with geotex fabric and overlaying it with clean soil have been shown to be affordable and highly effective (Mielke et al., 2011).

To assess whether washing a playground reduces the metal risk exposure, post-play hand wipe metal loadings were analysed (y) using a semi-log least squares regression procedure. Letting y_{ij} to denote the post-play hand wipe metal loadings of subject i in playground j, our regression model is:

Fig. 3. Effect of playground washing on hand lead exposure risk ($\mu g/m^2$). Note: point estimates and intervals of confidence derived with delta-method standard errors, and by fixing covariates at sample means (Supplementary Table S4).

confidence) are derived from the regression equation (1) for Table 3. Pre-play and playground surface wipe variables are fixed at their sample means. Post-play hand wipe lead levels on wash days are manifestly lower than non-wash days. At Woodward Park, for instance, post-play lead exposure is 42.8% lower on wash days versus non-wash days (502 versus 877 $\mu g/m^2$). While washing a playground clearly suppresses the quantity of lead on hand wipes after timed play, the salient issue is whether observed reductions are sufficient to protect children from potential exposures. Across all metals examined (Supplementary Table S4), post-play hand wipe values remain high relative to international and national dust-metal loading values (based on annual average values). Although the detailed results focus on lead deposition, the washing effect is reflected similarly in all the metals analysed in this study. This is not surprising given that metal emission and deposition are correlated strongly (van Alphen, 1999; Taylor et al., 2013).

Next, we addressed the question of how long the observed reduction in metal exposure risk lasts following a playground wash. To pursue this question, we estimate the following:

$$\ln\left(y_{ij}\right) = \alpha + \beta_1 \sqrt{W_j} + \beta_2 \ln\left(P_{ij}\right) + \beta_3 \ln\left(S_j\right) + \gamma_1 M_{ij} + \gamma_2 G_j + \gamma_3 D_{ij} + \varepsilon_{ij} \tag{2}$$

where the meaning of all terms carry from equation (1), with the exception of W_j, that now denotes the elapsed time (in hours) from the last playground wash. Elapsed time is measured in square root hours to capture the diminishing returns to metal exposure risk in time. By squaring the observed coefficient ($b = 0.226$) with respect to elapsed time reported in Table 4, we find that post-play hand wipe metal loadings increase ~5.1% (95% CI: 1.2, 11.7) for every hour from the last playground wash. This shows clearly that the benefit of a playground wash in terms of minimizing risk of metal exposure is short-lived.

In Fig. 4, we depict the predicted post-play hand wipe lead loadings at hours of elapsed time since the last playground wash. Predicted values are derived from the regression equation in

Table 4. Again, other covariates are fixed to their sample means. To be conservative, we graph the lower bound estimate of the 95% confidence interval for each playground. Results show that the average time it takes for post-play hand wipes to exceed 800 $\mu g/m^2$ after a playground wash is ~24 h at Woodward, ~9 h at Sports Park, and ~5 h at Memorial after playground washing. At Foreshore, post-play lead loadings are always >1000 $\mu g/m^2$ on hands regardless of when the playground is washed. A lead dust value of 800 $\mu g/m^2$ is a conservative estimate of risk, constituting twice the value used by the Western Australian Government (Government of Western Australia (2011)) for surfaces accessible to children during the Esperance lead-spill clean-up (see also Gulson et al., 2009). To stay under a conservative threshold of 800 $\mu g/m^2$, our results indicate that Woodward Park must be washed daily, Sports Park twice daily, and Memorial Park three times a day.

Table 4
Regression coefficients estimating hourly change in metal exposure risk from timed play following a playground wash.

	Post-play (ln)
Hours$^{0.5}$	0.226*** (0.033)
Pre-play wipes (ln)	0.012 (0.012)
Surface wipes (ln)	0.016 (0.010)
Reference = Arsenic	
Cadmium	−0.639*** (0.183)
Copper	1.873*** (0.197)
Lead	3.900*** (0.206)
Zinc	5.307*** (0.224)
Reference = Woodward Park	
Foreshore	1.258*** (0.157)
Memorial Park	0.479*** (0.157)
Sport Park	0.283*** (0.192)
Weekend	−0.215*** (0.117)
Constant	2.177*** (0.191)
Observations	145
F-Test	175.31
R-squared	0.930

Standard errors in parentheses *** p<0.01, ** p<0.05, * p<0.1.
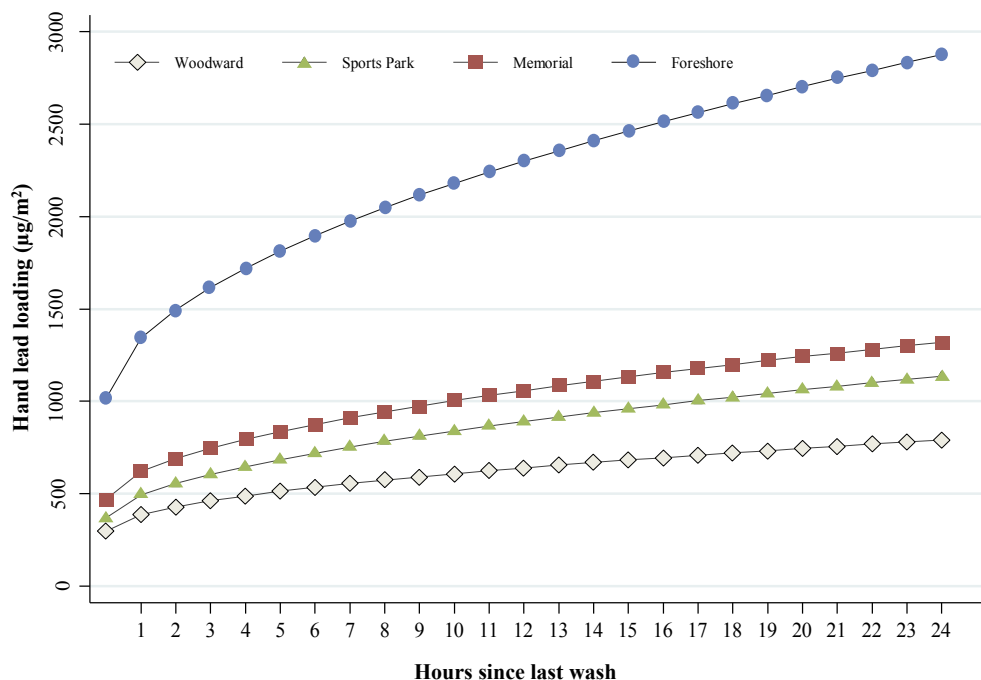
Fig. 4. Predicted hourly lead exposure risk ($\mu g/m^2$) from timed play following aplayground wash. Note: we graph the lower bound estimate of the 95 % interval ofconfidence derived with delta-method standard errors.

4. Conclusions

The results from this study are clear. Although washing reduces metal loading on playgrounds and hands after play, it does not resolve the problem of contemporary emissions and their deposition and accumulation on playground surfaces. Until the smelter reduces its emissions to the atmosphere, which is purported to occur following the completion of the $514 million smelter transformation project (COOE Pty Ltd, 2013; Government of South Australia (2014)) washing of playgrounds can provide only limited protection from toxic dust deposition exposures. Other locations experiencing ongoing atmospheric emissions and subsequent depositions are likely to face similar limitations from washing regimes that are designed to limit the hazard from metal environmental exposures.

Acknowledgements

Appendix A. Supplementary data

Supplementary data related to this article can be found at http://dx.doi.org/10.1016/j.envpol.2015.02.029.

References

American Society for Testing and Materials (ASTM), 2010. ASTM E1728-10-Standard practice for collection of settled dust samples using wipe sampling methods for subsequent lead determination. ASTM International, West Conshohocken, PA (accessed 03.12.14.). http://www.astm.org/Standards/E1728.htm.

Bureau of Meteorology, 2014a. Daily rainfall, Port Pirie Aerodrome (accessed 12.12.14.). http://www.bom.gov.au/jsp/ncc/cdio/weatherData/av?p_nccObsCode=136&p_display_type=dailyDataFile&p_startYear=2013&p_c=-89400807&p_stn_num=021118.

Bureau of Meteorology, 2014b. Rose wind direction versus Wind speed in km/h (01 Jan 1957 to 30 Sep 2010) (accessed 12.12.14.). http://www.bom.gov.au/clim_data/cdio/tables/pdf/windrose/IDCJCM0021.021043.9amJul.pdf.

COOE Pty Ltd., 2013. Nyrstar Port Pirie Smelter Transformation Proposal – Public Environmental Report. August 2013 (accessed 12.12.14.). https://www.sa.gov.au/__data/assets/pdf_file/0006/8619/Port_Pirie_PER_Part_1.pdf.

Csavina, J., Taylor, M.P., Félix, O., Rine, K.P., Sáez, A.E., Betterton, E.A., 2014. Size-resolved aerosol contaminants associated with copper and lead smelting emissions: Implications for emissions management and human health. Science of the Total Environment 493, 750–756.

Dixon, S.L., Gaitens, J.M., Jacobs, D.E., Strauss, W., Nagaraja, J., Pivetz, T., Wilson, J.W., Ashley, P.J., 2009. Exposure of U.S. children to residential dust lead, 1999-2004: II. The contribution of lead-contaminated dust to children's blood lead levels. Environ. Health Perspect 117, 468–474.

DuBois, D., DuBois, E.F., 1916. A formula to estimate the approximate surface area if height and weight be known. Arch. Intern. Med 17, 869–871.

EPASA (Environment Protection Authority South Australia), 2009. Environment Protection Authority Annual Report 1 July 2008–31 July 2009 (accessed 12.12.14.). http://www.epa.sa.gov.au/xstd_files/Corporate/Report/annualreport0809.pdf.

EPASA (Environment Protection Authority South Australia), 2014. Air quality Reports & summaries: monthly summaries (accessed 12.12.14.). http://www.epa.sa.gov.au/xstd_files/Air/Report/aq_monthly_aug2014.pdf.

Evans, A., 2013. Method NT2.52: Determination of trace elements in filters. National Measurement Institute (Inorganics Section).

Farquhar, D., 7th July 2011. Port Pirie Council, personal communication.

Government of South Australia, 2014. SA government guarantee secures Port Pirie's long-term future. Department of State Development (accessed 12.12.14.). http://www.minerals.dmitre.sa.gov.au/press_and_events/news_releases/sa_government_guarantee_secures_port_piries_long-term_future?SQ_DESIGN_NAME=printer_friendly.

Government of Western Australia, 2011. Lead Cleanup and Recovery Plan. An Overview of the Sampling and Cleaning Process (accessed 12.12.14.). http://www.oncue.org.au/docs/ECRP_cleanup_overview.pdf.

Gulson, B., Mizon, K., Taylor, A., Korsch, M., Stauber, J., Michael Davis, J., Louie, H., Wu, M., Antin, L., 2008. Longitudinal monitoring of selected elements in blood of healthy young children. J. Trace. Elem. Med. Biol. 22, 206–214.

Gulson, B., Korsch, M., Matisons, M., Douglas, C., Gillam, L, McLaughlin, V., 2009. Windblown Lead Carbonate as the Main Source of Lead in Blood of Children from a Seaside Community: An Example of Local Birds as "Canaries in the Mine". Environ. Health Perspect 117 (1), 148–154.

Living Safely with Lead, 2014. Living with Lead Alliance – Mount Isa QLD (accessed 12.12.14.). http://www.livingwithlead.com.au.

Maynard, E., Franks, L.J., Malcolm, M.S., 2006. Port Pirie Lead Implementation Program: Future Focus and Directions. South Australian Department of Health, Adelaide, South Australia (accessed 12.12.14.). http://www.health.sa.gov.au/pehs/PDF-files/ptpirie-future-focus-06.pdf.

Mielke, H.W., Corvington, T.P., Mielke Jr., P.W., Wolman, F.J., Powell, E.T.,

Gonzales, C.R., 2011. Soil intervention as a strategy for lead exposure prevention: The New Orleans lead-safe childcare playground project. Env. Pollut. 159 (8-9), 2071–2077.

NHMRC (National Health and Medical Research Council), 2014a. Draft paper on the health effects of lead released for consultation. Media releases (accessed 12.12.14.). https://www.nhmrc.gov.au/media/releases/2014/draft-paper-health-effects-lead-released-consultation.

NHMRC (National Health and Medical Research Council), 2014b. Review of lead exposure and health effects in Australia (accessed 12.12.14). https://www.nhmrc.gov.au/your-health/review-lead-exposure-and-health-effects-australia.

NSW Government, 2014. Lead – It's in our hands. Far West Local Health District (accessed 12.12.14). http://www.leadnsw.com.au.

SA Health, 2013. Port Pirie Soil Lead Concentrations Report. Government of South Australia (accessed 02.02.13.). http://www.sahealth.sa.gov.au/wps/wcm/connect/fe9ace8040cc6bd396eeb66c5432000f/2013+Port+Pirie+Soil+Lead+Concentrations+Report+(web).pdf?MOD=AJPERES&CACHEID=fe9ace8040cc6bd396eeb66c5432000f.

Simon, D.L., Maynard, E.J., Thomas, K.D., 2007. Living in a sea of lead- changes in blood- and hand-lead of infants living near a smelter. J. Expo. Sci. Environ. Epidemiol 17, 248–259.

Standards Australia, 1998. AS 4361.2-1998 Guide to lead paint management - Residential and commercial buildings (accessed 12.12.14.). infostore.saiglobal.com/store/PreviewDoc.aspx?saleItemID=380951.

Taylor, M.P., 2011. Report for the Environment Protection Authority, South Australia: Examination of the relationship between Nyrstar Port Pirie Pty Ltd smelter, airborne lead emissions and environmental health impacts, p. 66. Expert Witness report for a criminal prosecution case.

Taylor, M.P., 2012. Lead Poisoning of Port Pirie Children: a Long History of Looking the Other Way. The Conversation, 19 July (accessed 12.12.14.). http://theconversation.edu.au/leadpoisoning-of-port-pirie-children-a-long-history-of-looking-the-other-way-8296.

Taylor, M.P., Winder, C., Lanphear, B.P., 2012. Eliminating Childhood Lead Toxicity in Australia: A call to lower the intervention level. Med. J. Aust. 197 (9), 493.

Taylor, M.P., Camenzuli, D., Kristensen, L.J., Forbes, M., Zahran, S., 2013. Environmental lead exposure risks associated with children's outdoor playgrounds. Environ. Pollut.178 447–454.

Taylor, M.P., Isley, C., 2014. Measuring, monitoring and reporting but not intervening: Air Quality in Australian Mining and Smelting Areas. Air Qual. Clim. Change 48 (2), 35–42.

Taylor, M.P., Davies, P.J., Kristensen, L.J., Csavina, J., 2014a. Licensed to pollute but not to poison: the ineffectiveness of regulatory authorities at protecting public health from atmospheric arsenic, lead and other contaminants resulting from mining and smelting operations. Aeolian Res. 14, 35–52.

Taylor, M.P., Mould, S., Kristensen, L.J., Rouillon, M., 2014b. Environmental arsenic, cadmium and lead dust emissions from metal mine operations: implications for environmental management, monitoring and human health. Environ. Res. 135, 296–303.

Taylor, M.P., Winder, C., Lanphear, B.P., 2014c. Australia's leading public health body delays action on the revision of the public health goal for blood lead exposures. Environ. Int 70, 113–117.

TA Luft, (Technical Instructions on Air Quality Control), 2002. First General Administration Regulation Pertaining the Federal Emission Control Act (accessed 17.08.14.). www.bmu.de/files/pdfs/allgemein/application/pdf/taluft_engl.pdf.

Thumbs Up for Low Levels, 2015. Targeted Lead Abatement Program (accessed 02.02.15). http://www.tlap.com.au/.

Trail Area Health & Environment Program – Canada, 2014. Family Health Fact Sheet (accessed 12.12.14.). http://www.thep.ca/pages/familyhealth.

van Alphen, M.A., 1999. Atmospheric heavy metal deposition plumes adjacent to a primary lead-zinc smelt. Sci. Total Environ 236, 119–134.

Yeoh, B., Woolfenden, S., Lanphear, B., Ridley, G.F., Livingstone, N., 2012. Household interventions for preventing domestic lead exposure in children (Review). http://dx.doi.org/10.1002/14651858.CD006047.pub3. Cochrane Database of Systematic Reviews. Issue 4. Art. No.: CD006047 (accessed 12.12.14.). http://onlinelibrary.wiley.com/doi/10.1002/14651858.CD006047.pub3/abstract.

Paper Eight

Publication

Evaluation and assessment of the efficacy of an abatement strategy in a former lead smelter community, Boolaroo, Australia

Abstract:

This study examines the recent soil Lead Abatement Strategy (LAS) in Boolaroo, New South Wales, Australia, that was designed to "achieve a reduction in human exposure to lead dust contamination in surface soils". The abatement programme addressed legacy contamination of residential areas following closure of lead smelting operations in 2003 at the Pasminco Cockle Creek Smelter (PCCS). The principal objective of the LAS was to "cap and cover" lead-contaminated soils within the urban environment surrounding the PCCS. Soil lead concentrations of 2500-5000 mg/kg were scheduled for removal and replacement, while concentrations between 1500 and 2500 mg/kg were replaced only under limited circumstances. To date, there has been no industry, government or independent assessment of the clean-up programme that involved >2000 homes in the township of Boolaroo. Thus, by measuring post-abatement soil lead concentrations in Boolaroo, this study addresses this knowledge gap and evaluates the effectiveness of the LAS for reducing the potential for lead exposure. Soil lead concentrations above the Australian residential soil health investigation level value for residential soils (300 mg/kg) were identified at all but one of the residential properties examined (n = 19). Vacuum dust samples (n = 17) from the same homes had a mean lead concentration of 495 mg/kg (median 380 mg/kg). Bio-accessibility testing revealed that lead in household vacuum dust was readily accessible (% bio-accessible) (mean = 92 %, median = 90 %), demonstrating that the risk of exposure via this pathway remains. Assessment of a limited number of properties (n = 8) where pre-abatement soil lead levels were available for comparison showed they were not statistically different to post-abatement. Although the LAS did not include treatment of non-residential properties, sampling of community areas including public sports fields, playgrounds and schools (n = 32) was undertaken to determine the contamination legacy in these areas. Elevated mean soil lead concentrations were found across public lands: sports fields = 5130 mg/kg (median = 1275 mg/kg), playgrounds and schools = 812 mg/kg (median = 920 mg/kg) and open space = 778 mg/kg (median = 620 mg/kg). Overall, the study results show that the LAS programme that was

dominated by a "cap and cover" approach to address widespread lead contamination was inadequate for mitigating current and future risk of lead exposures.

Paper Eight of this thesis has been removed due to copyright reasons

Appendix B

Reference in paper	Reference in thesis	Caption
Table S1	Table B1	Radiation dose rates (µSv/h) for handheld XRF models A, B, C and D when measuring polyethylene at 0° to the horizontal plane. Data shown to two significant figures.
Table S2	Table B2	Radiation dose rates (µSv/h) for handheld XRF models A, B, C and D when measuring polyethylene at 45° to the horizontal plane. Data shown to two significant figures.
Table S3	Table B3	Radiation dose rates (µSv/h) for handheld XRF models A, B and C when measuring loose quartz sand at 0° to the horizontal plane. Model D's tripod could not fit around the loose quartz sand container and subsequently was not measured. Shaded measurements use 0.10 µSv/h as a conservative approach to instrument detection limits. Data shown to two significant figures.
Table S4	Table B4	Radiation dose rates (µSv/h) for handheld XRF models A, B and C when measuring loose quartz sand at 45° to the horizontal plane. Model D's tripod could not fit around the loose quartz sand container and was subsequently not measured. Shaded measurements use 0.10 µSv/h as a conservative approach to instrument detection limits. Data shown to two significant figures.
Table S5	Table B5	Radiation dose rates (µSv/h) for handheld XRF models A, B and C when measuring loose quartz sand at 45° to the horizontal plane. Model D's tripod could not fit around the loose quartz sand container and was subsequently not measured. Shaded measurements use 0.10 µSv/h as a conservative approach to instrument detection limits. Data shown to two significant figures.
Table S6	Table B6	Radiation dose rates (µSv/h) for handheld XRF models A, B, C and D when measuring quartz sandstone at 45° to the horizontal plane. Shaded measurements use 0.10 µSv/h as a conservative approach to instrument detection limits. Data shown to two significant figures.
Table S7	Table B7	Radiation dose rates (µSv/h) for handheld XRF models A, B, C and D when measuring steel at 0° to the horizontal plane. Shaded measurements use 0.10 µSv/h as a conservative approach to instrument detection limits. Data shown to two significant figures.
Table S8	Table B8	Radiation dose rates (µSv/h) for handheld XRF models A, B, C and D when measuring steel at 45° to the horizontal plane. Shaded measurements use 0.10 µSv/h as a conservative approach to instrument detection limits. Data shown to two significant figures.
Table S9	Table B9	Radiation dose rates (µSv/h) for handheld XRF models A, B, C and D when measuring all four materials at 90° to the horizontal plane. Shaded measurements use 0.10 µSv/h as a conservative approach to instrument detection limits. Data shown to two significant figures.

Reference in paper	Reference in thesis	Caption

Table B1: Radiation dose rates (μSv/h) for handheld XRF models A, B, C and D when measuring polyethylene at 0° to the horizontal plane. Data shown to two significant figures.

i) Model A - 50 kV

Degrees	10 cm	20 cm	30 cm	40 cm
0°	310	120	53	33
30°	280	100	47	27
60°	200	76	36	22
90°	120	50	23	15
120°	84	34	18	10
150°	58	27	14	8.8
180°	56	27	14	8.2
210°	58	26	13	8.7
240°	88	34	16	10
270°	130	49	25	15
300°	210	74	32	20
330°	270	97	46	27

ii) Model B - 40 kV

Degrees	10 cm	20 cm	30 cm	40 cm
0°	280	88	42	24
30°	200	68	35	17
60°	130	46	21	12
90°	76	25	12	7.4
120°	55	18	8.6	5.6
150°	36	13	6.8	3.9
180°	25	9.1	4.5	3.0
210°	42	14	7.3	3.9
240°	56	19	9.2	5.6
270°	88	30	14	8.6
300°	140	46	23	13
330°	230	74	33	20

iii) Model C - 50 kV

Degrees	10 cm	20 cm	30 cm	40 cm
0°	180	83	38	22
30°	150	70	35	20
60°	130	58	28	15
90°	100	42	22	12
120°	83	41	18	12
150°	57	28	15	7.7
180°	58	27	15	9.1
210°	56	30	16	9.6
240°	68	38	19	11
270°	110	50	23	13
300°	130	56	27	16
330°	180	81	37	22

iv) Model D - 40 kV

Degrees	10 cm	20 cm	30 cm	40 cm
0°	170	36	17	6.3
30°	180	32	11	6.1
60°	150	30	11	5.2
90°	64	19	7.8	3.8
120°	140	31	13	6.5
150°	180	36	13	7.1
180°	190	42	16	8.2
210°	140	31	13	6.4
240°	120	31	12	6.2
270°	120	32	14	7.0
300°	170	40	16	7.3
330°	190	38	14	7.8

Table B2: Radiation dose rates (μSv/h) for handheld XRF models A, B, C and D when measuring polyethylene at 45° to the horizontal plane. Data shown to two significant figures.

i) Model A - 50 kV

Degrees	10 cm	20 cm	30 cm	40 cm
0°	260	95	45	26
30°	230	86	42	24
60°	170	70	34	20
90°	86	40	22	13
120°	47	22	12	8.3
150°	31	15	8.3	5.4
180°	25	13	7.4	4.4
210°	28	14	8.6	5.0
240°	43	21	12	7.2
270°	82	42	23	13
300°	150	67	32	19
330°	210	85	43	24

ii) Model B - 40 kV

Degrees	10 cm	20 cm	30 cm	40 cm
0°	290	75	38	22
30°	250	62	34	20
60°	210	58	32	19
90°	160	51	30	19
120°	110	43	25	17
150°	85	29	26	11
180°	22	10	5.7	3.8
210°	56	21	15	9.3
240°	94	40	18	16
270°	150	50	31	19
300°	240	59	36	19
330°	250	63	34	20

iii) Model C - 50 kV

Degrees	10 cm	20 cm	30 cm	40 cm
0°	75	31	18	9.9
30°	60	30	17	9.6
60°	53	25	15	8.7
90°	25	12	6.9	4.0
120°	18	8.4	5.4	3.1
150°	16	8.1	5.0	2.8
180°	20	7.4	4.6	3.1
210°	23	9.5	4.7	2.8
240°	11	7.0	4.0	2.4
270°	23	9.1	5.6	3.3
300°	40	20	10	6.0
330°	43	23	13	7.1

iv) Model D - 40 kV

Degrees	10 cm	20 cm	30 cm	40 cm
0°	190	43	23	13
30°	180	49	24	14
60°	70	27	16	10
90°	23	7.5	3.5	2.1
120°	130	41	23	14
150°	150	52	27	16
180°	190	47	22	14
210°	160	47	25	14
240°	82	34	17	11
270°	49	17	8.1	4.8
300°	67	28	12	8.6
330°	110	41	16	12

Table B3: Radiation dose rates (μSv/h) for handheld XRF models A, B and C when measuring loose quartz sand at 0° to the horizontal plane. Model D's tripod could not fit around the loose quartz sand container and subsequently was not measured. Shaded measurements use 0.10 μSv/h as a conservative approach to instrument detection limits. Data shown to two significant figures.

i) Model A - 50 kV

Degrees	10 cm	20 cm	30 cm	40 cm
0°	2.5	0.68	0.20	0.13
30°	1.9	0.44	0.12	0.11
60°	0.80	0.25	0.16	0.11
90°	0.47	0.14	0.10	0.10
120°	0.18	0.15	0.21	0.11
150°	0.12	0.10	0.10	0.10
180°	0.10	0.10	0.10	0.10
210°	0.14	0.10	0.10	0.10
240°	0.15	0.13	0.10	0.10
270°	0.50	0.20	0.13	0.10
300°	1.3	0.39	0.10	0.10
330°	2.4	0.51	0.23	0.11

ii) Model B - 40 kV

Degrees	10 cm	20 cm	30 cm	40 cm
0°	7.6	1.8	0.47	0.12
30°	2.0	0.50	0.20	0.11
60°	5.1	1.3	0.39	0.21
90°	6.1	2.5	1.3	0.23
120°	1.8	0.79	0.36	0.21
150°	0.35	0.21	0.20	0.11
180°	0.20	0.11	0.10	0.10
210°	0.16	0.14	0.13	0.14
240°	0.85	0.35	0.25	0.19
270°	3.9	1.0	0.32	0.12
300°	6.1	1.5	0.33	0.17
330°	4.5	0.80	0.13	0.10

iii) Model C - 50 kV

Degrees	10 cm	20 cm	30 cm	40 cm
0°	5.6	0.95	0.75	0.70
30°	8.1	2.0	0.50	0.20
60°	11	3.0	0.85	0.60
90°	1.7	0.80	0.44	0.24
120°	1.4	0.60	0.20	0.17
150°	0.95	0.28	0.20	0.10
180°	1.3	0.80	0.22	0.14
210°	2.2	0.92	0.28	0.15
240°	1.4	0.23	0.13	0.13
270°	1.4	0.49	0.16	0.11
300°	9.7	1.9	0.22	0.20
330°	8.1	2.0	0.48	0.21

iv) Model D - 40 kV

Degrees	10 cm	20 cm	30 cm	40 cm
0°	-	-	-	-
30°	-	-	-	-
60°	-	-	-	-
90°	-	-	-	-
120°	-	-	-	-
150°	-	-	-	-
180°	-	No	Data	-
210°	-	-	-	-
240°	-	-	-	-
270°	-	-	-	-
300°	-	-	-	-
330°	-	-	-	-

Table B4: Radiation dose rates (μSv/h) for handheld XRF models A, B and C when measuring loose quartz sand at 45° to the horizontal plane. Model D's tripod could not fit around the loose quartz sand container and was subsequently not measured. Shaded measurements use 0.10 μSv/h as a conservative approach to instrument detection limits. Data shown to two significant figures.

i) Model A - 50 kV

Degrees	10 cm	20 cm	30 cm	40 cm
0°	3.9	1.7	1.3	0.35
30°	2.6	1.5	0.82	0.37
60°	1.5	1.2	0.60	0.25
90°	0.60	0.35	0.20	0.13
120°	0.20	0.24	0.14	0.11
150°	0.16	0.15	0.10	0.10
180°	0.11	0.10	0.10	0.10
210°	0.13	0.13	0.17	0.11
240°	0.21	0.16	0.13	0.11
270°	0.75	0.60	0.20	0.18
300°	1.8	0.81	0.60	0.18
330°	3.0	1.3	0.80	0.30

ii) Model B - 40 kV

Degrees	10 cm	20 cm	30 cm	40 cm
0°	7.8	2.0	1.3	0.90
30°	4.8	1.2	0.65	0.41
60°	7.0	2.8	1.4	0.95
90°	6.3	2.4	1.2	0.88
120°	2.7	1.1	0.55	0.45
150°	0.73	0.19	0.20	0.21
180°	0.15	0.10	0.10	0.12
210°	0.28	0.22	0.23	0.22
240°	1.3	2.3	1.3	1.1
270°	7.0	4.2	2.3	1.5
300°	9.4	3.6	2.1	1.2
330°	4.5	1.3	0.90	0.40

iii) Model C - 50 kV

Degrees	10 cm	20 cm	30 cm	40 cm
0°	10	4.5	2.6	1.4
30°	12	4.2	1.5	1.1
60°	15	5.2	2.6	1.6
90°	5.7	2.0	1.0	0.74
120°	1.7	0.80	0.60	0.30
150°	1.0	0.28	0.20	0.13
180°	0.85	0.20	0.14	0.10
210°	0.76	0.32	0.17	0.16
240°	1.9	1.0	0.23	0.20
270°	4.2	1.7	0.90	0.70
300°	13	3.7	1.6	0.90
330°	11	4.0	1.9	1.2

iv) Model D - 40 kV

Degrees	10 cm	20 cm	30 cm	40 cm
0°	-	-	-	-
30°	-	-	-	-
60°	-	-	-	-
90°	-	-	-	-
120°	-	-	-	-
150°	-	-	-	-
180°	-	No	Data	-
210°	-	-	-	-
240°	-	-	-	-
270°	-	-	-	-
300°	-	-	-	-
330°	-	-	-	-

Table B5: Radiation dose rates (µSv/h) for handheld XRF models A, B, C and D when measuring quartz sandstone at 0° to the horizontal plane. Shaded measurements use 0.10 µSv/h as a conservative approach to instrument detection limits. Data shown to two significant figures.

i) Model A – 50 kV

Degrees	10 cm	20 cm	30 cm	40 cm
0°	4.8	1.5	0.49	0.50
30°	5.1	1.1	0.42	0.21
60°	2.5	0.60	0.35	0.25
90°	0.62	0.40	0.25	0.17
120°	0.56	0.25	0.16	0.11
150°	0.40	0.20	0.15	0.10
180°	0.36	0.15	0.14	0.12
210°	0.30	0.20	0.12	0.17
240°	0.36	0.21	0.20	0.15
270°	0.55	0.40	0.26	0.17
300°	1.1	0.62	0.28	0.27
330°	3.3	1.2	0.42	0.28

ii) Model B – 40 kV

Degrees	10 cm	20 cm	30 cm	40 cm
0°	2.1	0.74	0.41	0.24
30°	2.3	0.79	0.32	0.23
60°	1.5	0.67	0.42	0.31
90°	0.87	0.52	0.20	0.20
120°	0.55	0.34	0.21	0.17
150°	0.21	0.16	0.11	0.12
180°	0.12	0.14	0.11	0.10
210°	0.14	0.14	0.13	0.10
240°	0.48	0.25	0.12	0.14
270°	1.1	0.45	0.32	0.22
300°	1.8	0.66	0.35	0.29
330°	1.7	0.66	0.28	0.30

iii) Model C – 50 kV

Degrees	10 cm	20 cm	30 cm	40 cm
0°	2.5	0.90	0.50	0.18
30°	2.2	0.90	0.34	0.20
60°	1.5	0.46	0.40	0.20
90°	1.2	0.55	0.25	0.15
120°	1.3	0.68	0.38	0.18
150°	0.67	0.28	0.20	0.15
180°	0.60	0.48	0.38	0.20
210°	0.30	0.25	0.20	0.10
240°	0.59	0.33	0.18	0.13
270°	0.85	0.37	0.22	0.13
300°	1.2	0.66	0.32	0.16
330°	1.5	0.75	0.30	0.15

iv) Model D – 40 kV

Degrees	10 cm	20 cm	30 cm	40 cm
0°	3.9	0.54	0.20	0.12
30°	3.8	0.84	0.24	0.17
60°	3.4	0.70	0.23	0.18
90°	0.60	0.28	0.17	0.14
120°	1.4	0.31	0.18	0.10
150°	2.5	0.45	0.22	0.18
180°	2.0	0.38	0.29	0.15
210°	2.0	0.60	0.20	0.11
240°	1.3	0.48	0.13	0.10
270°	0.45	0.28	0.12	0.10
300°	1.6	0.22	0.10	0.10
330°	2.2	0.42	0.19	0.14

Table B6: Radiation dose rates (µSv/h) for handheld XRF models A, B, C and D when measuring quartz sandstone at 45° to the horizontal plane. Shaded measurements use 0.10 µSv/h as a conservative approach to instrument detection limits. Data shown to two significant figures.

i) Model A - 50 kV

Degrees	10 cm	20 cm	30 cm	40 cm
0°	5.4	1.8	0.75	0.61
30°	3.4	1.3	0.67	0.46
60°	1.4	0.76	0.50	0.37
90°	0.55	0.43	0.27	0.28
120°	0.34	0.25	0.20	0.20
150°	0.27	0.27	0.23	0.19
180°	0.19	0.18	0.20	0.14
210°	0.20	0.24	0.18	0.13
240°	0.36	0.25	0.17	0.15
270°	0.81	0.60	0.33	0.27
300°	2.4	0.91	0.56	0.32
330°	4.3	1.5	0.80	0.49

ii) Model B - 40 kV

Degrees	10 cm	20 cm	30 cm	40 cm
0°	13	4.2	2.3	1.1
30°	5.5	1.6	0.89	0.66
60°	8.9	2.3	1.4	0.87
90°	6.0	2.7	1.8	0.97
120°	2.8	1.2	0.61	0.52
150°	0.56	0.20	0.10	0.16
180°	0.15	0.17	0.10	0.10
210°	0.46	0.35	0.17	0.17
240°	2.7	1.5	1.3	0.73
270°	8.8	3.3	2.4	1.6
300°	13	3.8	2.6	1.5
330°	5.3	2.1	1.2	0.61

iii) Model C - 50 kV

Degrees	10 cm	20 cm	30 cm	40 cm
0°	17	6.0	2.8	1.8
30°	22	8.0	2.9	1.8
60°	26	12	4.8	2.0
90°	6.0	2.9	1.8	1.0
120°	5.3	2.7	1.0	0.48
150°	3.0	0.65	0.36	0.19
180°	1.2	0.55	0.26	0.14
210°	2.6	1.1	0.13	0.17
240°	4.0	1.5	0.62	0.22
270°	7.6	2.7	1.4	0.71
300°	24	7.7	2.9	1.2
330°	18	7.1	2.6	1.5

iv) Model D - 40 kV

Degrees	10 cm	20 cm	30 cm	40 cm
0°	7.4	2.0	1.1	0.61
30°	1.9	1.0	0.66	0.55
60°	1.0	0.17	0.16	0.10
90°	0.24	0.16	0.10	0.10
120°	0.70	0.14	0.15	0.10
150°	6.8	2.3	1.1	0.51
180°	5.8	2.6	1.3	0.76
210°	3.1	0.90	0.50	0.22
240°	2.4	0.70	0.46	0.18
270°	0.15	0.11	0.10	0.10
300°	0.80	0.25	0.16	0.10
330°	4.6	1.8	0.80	0.42

Table B7: Radiation dose rates (μSv/h) for handheld XRF models A, B, C and D when measuring steel at 0° to the horizontal plane. Shaded measurements use 0.10 μSv/h as a conservative approach to instrument detection limits. Data shown to two significant figures.

i) Model A – 50 kV

Degrees	10 cm	20 cm	30 cm	40 cm
0°	0.18	0.24	0.24	0.16
30°	0.25	0.33	0.15	0.22
60°	0.12	0.16	0.17	0.14
90°	0.14	0.10	0.10	0.10
120°	0.12	0.10	0.10	0.10
150°	0.10	0.11	0.10	0.10
180°	0.10	0.10	0.11	0.10
210°	0.12	0.12	0.10	0.10
240°	0.10	0.11	0.10	0.10
270°	0.12	0.10	0.10	0.10
300°	0.10	0.10	0.13	0.11
330°	0.13	0.11	0.15	0.14

ii) Model B – 40 kV

Degrees	10 cm	20 cm	30 cm	40 cm
0°	1.3	0.41	0.10	0.12
30°	0.74	0.15	0.11	0.10
60°	0.88	0.22	0.17	0.13
90°	0.55	0.19	0.14	0.10
120°	0.30	0.12	0.12	0.10
150°	0.10	0.10	0.11	0.10
180°	0.10	0.10	0.11	0.10
210°	0.12	0.12	0.10	0.10
240°	0.25	0.12	0.13	0.10
270°	0.60	0.17	0.13	0.13
300°	0.97	0.34	0.13	0.11
330°	0.72	0.26	0.17	0.11

iii) Model C - 50 kV

Degrees	10 cm	20 cm	30 cm	40 cm
0°	0.35	0.10	0.10	0.10
30°	1.1	0.23	0.13	0.10
60°	2.0	0.28	0.16	0.10
90°	0.24	0.25	0.10	0.10
120°	0.25	0.11	0.10	0.10
150°	0.61	0.18	0.10	0.10
180°	1.1	0.48	0.24	0.12
210°	0.23	0.15	0.10	0.10
240°	0.34	0.11	0.10	0.10
270°	0.18	0.10	0.10	0.10
300°	1.7	0.38	0.15	0.16
330°	1.1	0.13	0.10	0.10

iv) Model D – 40 kV

Degrees	10 cm	20 cm	30 cm	40 cm
0°	3.2	0.98	0.71	0.32
30°	2.5	0.52	0.35	0.21
60°	0.98	0.23	0.16	0.10
90°	0.34	0.15	0.10	0.10
120°	0.85	0.26	0.15	0.10
150°	1.9	0.45	0.29	0.15
180°	2.5	0.62	0.30	0.16
210°	1.4	0.59	0.22	0.10
240°	0.52	0.30	0.14	0.10
270°	0.22	0.12	0.10	0.10
300°	0.35	0.16	0.10	0.10
330°	1.9	0.90	0.62	0.30

Table B8: Radiation dose rates (μSv/h) for handheld XRF models A, B, C and D when measuring steel at 45° to the horizontal plane. Shaded measurements use 0.10 μSv/h as a conservative approach to instrument detection limits. Data shown to two significant figures.

i) Model A – 50 kV

Degrees	10 cm	20 cm	30 cm	40 cm
0°	0.16	0.12	0.10	0.10
30°	0.13	0.11	0.10	0.10
60°	0.18	0.12	0.10	0.10
90°	0.10	0.10	0.10	0.10
120°	0.10	0.10	0.10	0.10
150°	0.10	0.10	0.10	0.10
180°	0.11	0.10	0.10	0.10
210°	0.10	0.10	0.10	0.10
240°	0.12	0.12	0.10	0.10
270°	0.15	0.12	0.10	0.10
300°	0.15	0.10	0.10	0.10
330°	0.18	0.13	0.10	0.10

ii) Model B – 40 kV

Degrees	10 cm	20 cm	30 cm	40 cm
0°	1.9	0.82	0.27	0.21
30°	0.81	0.33	0.17	0.14
60°	1.2	0.43	0.25	0.10
90°	0.82	0.34	0.27	0.14
120°	0.42	0.20	0.16	0.14
150°	0.17	0.12	0.11	0.10
180°	0.15	0.12	0.10	0.10
210°	0.10	0.12	0.12	0.10
240°	0.31	0.25	0.23	0.15
270°	1.0	0.62	0.37	0.35
300°	2.0	0.83	0.62	0.27
330°	0.89	0.33	0.20	0.15

iii) Model C – 50 kV

Degrees	10 cm	20 cm	30 cm	40 cm
0°	0.90	0.32	0.14	0.10
30°	2.50	0.80	0.12	0.10
60°	2.55	1.10	0.30	0.15
90°	0.32	0.21	0.17	0.11
120°	0.34	0.15	0.11	0.10
150°	0.71	0.17	0.10	0.10
180°	0.17	0.20	0.10	0.10
210°	0.20	0.10	0.10	0.10
240°	0.20	0.12	0.13	0.11
270°	1.90	0.50	0.20	0.12
300°	1.90	0.34	0.17	0.10
330°	0.65	0.60	0.16	0.10

iv) Model D – 40 kV

Degrees	10 cm	20 cm	30 cm	40 cm
0°	1.7	0.70	0.33	0.10
30°	0.65	0.15	0.10	0.10
60°	0.24	0.11	0.10	0.10
90°	0.30	0.15	0.11	0.10
120°	0.36	0.10	0.10	0.10
150°	1.3	0.30	0.20	0.10
180°	1.7	0.70	0.16	0.10
210°	0.90	0.39	0.15	0.10
240°	0.16	0.12	0.10	0.10
270°	0.13	0.10	0.10	0.10
300°	0.16	0.10	0.10	0.10
330°	0.84	0.16	0.10	0.10

Table B9: Radiation dose rates (μSv/h) for handheld XRF models A, B, C and D when measuring all four materials at 90° to the horizontal plane. Shaded measurements use 0.10 μSv/h as a conservative approach to instrument detection limits. Data shown to two significant figures.

i) Model A - 50 kV

Materials	5 cm	10 cm	20 cm
Steel	0.10	0.10	0.10
Quartz Sandstone	0.14	0.18	0.17
Loose Quartz Sand	0.10	0.13	0.17
Polyethylene	1.5	3.8	4.2

ii) Model B - 40 kV

Materials	5 cm	10 cm	20 cm
Steel	0.10	0.10	0.10
Quartz Sandstone	0.14	0.10	0.10
Loose Quartz Sand	0.10	0.10	0.13
Polyethylene	1.5	0.77	1.7

iii) Model C - 50 kV

Materials	5 cm	10 cm	20 cm
Steel	0.10	0.10	0.10
Quartz Sandstone	0.45	0.18	0.11
Loose Quartz Sand	0.22	0.19	0.17
Polyethylene	8.1	3.0	2.2

iv) Model D - 40 kV

Materials	5 cm	10 cm	20 cm
Steel	0.12	0.10	0.10
Quartz Sandstone	0.10	0.10	0.10
Loose Quartz Sand	-	-	-
Polyethylene	0.85	0.55	0.28

Appendix C

Reference in paper	Reference in thesis	Caption
Supplementary Table A	Table C1	Ten certified and reference materials used in this study. Values in bold represent certified values while non-bold values are reference values. Informational values were not considered in this study and are represented by n/a. SiO_2 estimates displayed as wt%, while all other values displayed as mg/kg.
Supplementary Table B	Table C2	Comparison of pXRF and ICP-AES measurements, recoveries and RP of six reference materials. Reference, ICP-AES and pXRF values are in mg/kg. Recoveries and RP are rounded to 1 decimal place.
Supplementary Table C	Table C3	Comparison of pXRF, ICP-AES and ICP-MS measurements, recoveries and RP of five contaminated soil samples and three reference materials. Iron was not measured by ICP-MS and subsequently was absent from this three technique comparison. Reference, ICP-AES, ICP-MS and pXRF values are in mg/kg. Recoveries and RP are rounded to 1 decimal place.
Supplementary Table D	Table C4	Mean pXRF measurements and recoveries of ten soil CRMs. Comparison of measurements using the manufacturers' factory settings and against a matrix matched calibration. Recoveries are calculated as ((pXRF value / reference value) x 100). Reference and pXRF values are in mg/kg.
Supplementary Figure A	Figure C1	Comparison of data quality for Mn pre- and post-calibration. The regression relationship (solid red line), ideal 100% recovery (dashed black line) and slope, intercept and r^2 are shown in each plot. Individual recoveries plotted against elemental concentrations for both calibration strategies are in the lower plot.
Supplementary Figure B	Figure C2	Comparison of data quality for Cr pre- and post-calibration. The regression relationship (solid red line), ideal 100% recovery (dashed black line) and slope, intercept and goodness of fit (r^2) are shown in each plot. Individual recoveries plotted against elemental concentrations for both calibration strategies are in the lower plot.
Supplementary Table E	Table C5	Recoveries, RP and RSD of ten soil CRMs using a matrix matched calibration. Data was categorised by element. Reference and pXRF values are shown in mg/kg. Recoveries, RP and standard deviation are rounded to 1 decimal place, whereas RSD is rounded to two decimal places.
Supplementary Table F	Table C6	Elemental summary on the performance of the pXRF in the measurement of 10 soil and sediment CRMs.
Supplementary Table G	Table C7	Parallel measurements by pXRF and ICP-AES of 75 contaminated soil samples. Tables are displayed per element, all pXRF and values are rounded to whole numbers, measurement values for cadmium are rounded to one decimal place. All recoveries are displayed to one decimal place.
Supplementary Table H	Table C8	Elemental summary on the performance of the pXRF in the measurement of 75 contaminated soil samples when compared against ICP-AES.

Table C1: Ten certified and reference materials used in this study. Values in bold represent certified values while non-bold values are reference values. Informational values were not considered in this study and are represented by n/a. SiO_2 estimates displayed as wt%, while all other values displayed as mg/kg.

		SiO₂	Ti	Cr	Mn	Fe	Ni	Cu	Zn	As	Sr	Cd	Pb
Sediment	**NRC BCSS-1** Marine sediment	64.1 ± 0.61	4400 ± 143	123 ± 14	229 ± 15	32873 ± 997	55.3 ± 3.6	18.5 ± 2.7	119 ± 12	11.1 ± 1.4	n/a	0.25 ± 0.04	22.7 ± 3.4
	NRC MESS-2 Marine sediment	56.3 ± 0.61	n/a	106 ± 8.0	365 ± 21	43503 ± 2168	49.3 ± 1.8	39.3 ± 2.0	172 ± 16	20.7 ± 0.8	125 ± 10	0.24 ± 0.01	21.9 ± 1.2
	NIST 1944 New York/New Jersey waterway sediment	53.3 ± 0.58	4300 ± 300	**266 ± 24**	**505 ± 25**	**35300 ± 1600**	**76.1 ± 5.6**	380 ± 40	**656 ± 75**	**18.9 ± 2.8**	n/a	**8.8 ± 1.4**	**330 ± 48**
	RM 8704 Buffalo river sediment	61.3 ± 0.62	4570 ± 200	121.9 ± 3.8	544 ± 21	39700 ± 1000	42.9 ± 3.7	n/a	408 ± 15	n/a	n/a	2.94 ± 0.29	150 ± 17
	NRC PACS-2 Marine sediment	55.7 ± 0.59	**4430 ± 320**	**90.7 ± 4.6**	**440 ± 19**	**40900 ± 600**	**39.5 ± 2.3**	**310 ± 12**	364 ± 23	**26.2 ± 1.5**	**276 ± 30**	**2.11 ± 0.15**	**183 ± 8**
Soil	**NIST 2586** Trace elements in soil containing lead from paint (nominal 500 mg/kg lead)	60.5 ± 0.59	6050 ± 660	**301 ± 45**	1000 ± 18	52610 ± 890	n/a	n/a	352 ± 16	**8.7 ± 1.5**	84.1 ± 8.0	**2.71 ± 0.54**	**432 ± 17**
	NIST 2587 Trace elements in soil (contains lead from paint)	70.3 ± 0.61	3920 ± 650	**92 ± 11**	651 ± 23	28130 ± 250	n/a	n/a	335.8 ± 7.6	**13.7 ± 2.3**	126 ± 19	**1.92 ± 0.23**	**3242 ± 57**
	NIST 2709a San Joaquin soil	58.8 ± 0.60	**3360 ± 70**	**130 ± 9.0**	**529 ± 18**	**33600 ± 700**	85 ± 2.0	33.9 ± 0.5	103 ± 4.0	10.5 ± 0.3	239 ± 6.0	**0.37 ± 0.00**	**17.3 ± 0.1**
	NIST 2710a Montana I soil	57.4 ± 0.59	**3110 ± 70**	23 ± 6.0	**2140 ± 60**	43200 ± 800	8.0 ± 1.0	**3420 ± 50**	**4180 ± 150**	1540 ± 100	255 ± 7.0	**12.3 ± 0.3**	**5520 ± 30**
	NIST 2711a Montana II soil	59.5 ± 0.60	**3170 ± 80**	**52.3 ± 2.9**	675 ± 18	28200 ± 400	**21.7 ± 0.7**	**140 ± 2**	414 ± 11	107 ± 5	242 ± 10	**54.1 ± 0.5**	**1400 ± 10**

Table C2: Comparison of pXRF and ICP-AES measurements, recoveries and RP of six reference materials. Reference, ICP-AES and pXRF values are in mg/kg. Recoveries and RP are rounded to 1 decimal place.

Element	Reference material	pXRF value	ICP-AES value	Reference value	pXRF recovery (%)	ICP-AES recovery (%)	pXRF RP (%)	ICP-AES RP (%)
	NIST 1944	4254	4100	4300	98.9	95.4	1.1	4.7
	NIST 2586	6204	5300	6050	102.6	87.6	2.6	12.4
	NIST 2587	4074	3600	4027	101.2	89.4	1.2	10.6
	NIST 2587_DUP	4074	3600	4027	101.2	89.4	1.2	10.6
Ti	NIST 2709a	3565	2900	3360	106.1	86.3	6.1	13.7
	NIST 2709a_DUP	3565	3000	3360	106.1	89.3	6.1	10.7
	RM 8704	4581	3800	4570	100.2	83.2	0.2	16.9
	NRC PACS-2	4329	3700	4430	97.7	83.5	2.3	16.5
	Mean				**101.7**	**88.0**	**2.6**	**12.0**
	NIST 1944	312	217	266	117.3	81.6	17.3	18.4
	NIST 2586	263	264	301	87.4	87.7	12.6	12.3
	NIST 2587	92	79	92	100.0	85.9	0.0	14.1
	NIST 2587_DUP	92	80	92	100.0	87.0	0.0	13.0
Cr	NIST 2709a	129	100	130	99.2	76.9	0.8	23.1
	NIST 2709a_DUP	129	96	130	99.2	73.8	0.8	26.2
	RM 8704	128	108	121.9	105.0	88.6	5.0	11.4
	NRC PACS-2	84	75	90.7	92.8	82.7	7.2	17.3
	Mean				**100.1**	**83.0**	**5.5**	**17.0**
	NIST 1944	477	504	505	94.5	99.8	5.5	0.2
	NIST 2586	990	944	1000	99.0	94.4	1.0	5.6
	NIST 2587	658	627	651	101.1	96.3	1.1	3.7
	NIST 2587_DUP	658	614	651	101.1	94.3	1.1	5.7
Mn	NIST 2709a	557	486	529	105.3	91.9	5.3	8.1
	NIST 2709a_DUP	557	491	529	105.3	92.8	5.3	7.2
	RM 8704	585	560	544	107.5	102.9	7.5	2.9
	NRC PACS-2	438	398	440	99.5	90.5	0.5	9.5
	Mean				**101.7**	**95.4**	**3.4**	**5.4**
	NIST 1944	36999	34400	35300	104.8	97.5	4.8	2.5
	NIST 2586	49080	47200	51610	95.1	91.5	4.9	8.5
	NIST 2587	28610	26500	28130	101.7	94.2	1.7	5.8
	NIST 2587_DUP	28610	26200	28130	101.7	93.1	1.7	6.9
Fe	NIST 2709a	32577	31300	33600	97.0	93.2	3.0	6.8
	NIST 2709a_DUP	32577	31200	33600	97.0	92.9	3.0	7.1
	RM 8704	39136	38700	39700	98.6	97.5	1.4	2.5
	NRC PACS-2	39333	38000	40900	96.2	92.9	3.8	7.1
	Mean				**99.0**	**94.1**	**3.1**	**5.9**
	NIST 1944	78	71	76.1	102.5	93.3	2.5	6.7
	NIST 2709a	70	73	85	82.4	85.9	17.6	14.1
Ni	NIST 2709a_DUP	70	73	85	82.4	85.9	17.6	14.1
	RM 8704	39	43	42.9	90.9	100.2	9.1	0.2
	NRC PACS-2	32	38	39.5	81.0	96.2	19.0	3.8
	Mean				**87.8**	**92.3**	**13.2**	**7.8**
	NIST 1944	387	339	380	101.8	89.2	1.8	10.8
	NIST 2709a	40	31	33.9	116.5	91.4	16.5	8.6
Cu	NIST 2709a_DUP	40	30	33.9	116.5	88.5	16.5	11.5
	NRC PACS-2	271	284	310	87.4	91.6	12.6	8.4
	Mean				**105.6**	**90.2**	**11.9**	**9.8**
	NIST 1944	679	619	656	103.5	94.4	3.5	5.6
	NIST 2586	327	358	352	92.9	101.7	7.1	1.7
	NIST 2587	341	358	335.8	101.5	106.6	1.5	6.6
	NIST 2587_DUP	341	342	335.8	101.5	101.8	1.5	1.8
Zn	NIST 2709a	111	100	103	107.4	97.1	7.4	2.9
	NIST 2709a_DUP	111	100	103	107.4	97.1	7.4	2.9
	RM 8704	373	419	408	91.4	102.7	8.6	2.7
	NRC PACS-2	343	342	364	94.2	94.0	5.8	6.0
	Mean				**100.0**	**99.4**	**5.4**	**3.8**

As	NIST 1944	28	18	18.9	149.2	95.2	49.2	4.8
	NIST 2586	8	9	8.7	92.0	103.4	8.0	3.4
	NIST 2587	<LOD	17	13.7	-	124.1	-	24.1
	NIST 2587_DUP	<LOD	14	13.7	-	102.2	-	2.2
	NIST 2709a	11	11	10.5	106.3	104.8	6.3	4.8
	NIST 2709a_DUP	11	10	10.5	106.3	95.2	6.3	4.8
	NRC PACS-2	24	22	26.2	91.5	84.0	8.5	16.0
				Mean	**109.1**	**101.3**	**15.7**	**8.6**
Sr	NIST 2586	78	87	84.1	92.2	103.4	7.8	3.4
	NIST 2587	126	130	126	100.1	103.2	0.1	3.2
	NIST 2587_DUP	126	131	126	100.1	104.0	0.1	4.0
	NIST 2709a	233	239	239	97.5	100.0	2.5	0.0
	NIST 2709a_DUP	233	237	239	97.5	99.2	2.5	0.8
	NRC PACS-2	282	269	276	102.1	97.5	2.1	2.5
				Mean	**98.2**	**101.2**	**2.5**	**2.3**
Cd	NIST 1944	8.8	7.8	8.8	100.0	88.6	0.0	11.4
	NIST 2586	2.7	2.6	2.7	100.0	96.3	0.0	3.7
	NIST 2587	<LOD	1.9	1.92	-	99.0	-	1.0
	NIST 2587_DUP	<LOD	1.7	1.92	-	88.5	-	11.5
	NIST 2709a	<LOD	<0.5	0.371	-	-	-	-
	NIST 2709a_DUP	<LOD	<0.5	0.371	-	-	-	-
	RM 8704	3.6	2.9	2.94	120.7	98.6	20.7	1.4
	NRC PACS-2	<LOD	2.1	2.11	-	99.5	-	0.5
				Mean	**106.9**	**95.1**	**6.9**	**4.9**
Pb	NIST 1944	348	310	330	105.5	93.9	5.5	6.1
	NIST 2586	415	420	432	96.1	97.2	3.9	2.8
	NIST 2587	3239	3180	3242	99.9	98.1	0.1	1.9
	NIST 2587_DUP	3239	3100	3242	99.9	95.6	0.1	4.4
	NIST 2709a	17	15	17.3	96.0	86.7	4.0	13.3
	NIST 2709a_DUP	17	16	17.3	96.0	92.5	4.0	7.5
	RM 8704	142	154	150	94.7	102.7	5.3	2.7
	NRC PACS-2	173	172	183	94.3	94.0	5.7	6.0
				Mean	**97.8**	**95.1**	**3.6**	**5.6**

Table C3: Comparison of pXRF, ICP-AES and ICP-MS measurements, recoveries and RP of five contaminated soil samples and three reference materials. Iron was not measured by ICP-MS and subsequently was absent from this three technique comparison. Reference, ICP-AES, ICP-MS and pXRF values are in mg/kg. Recoveries and RP are rounded to 1 decimal place.

Element	Sample name/ reference	pXRF value	ICP-AES value	ICP-MS value	Reference value	pXRF recovery (%)	ICP-AES recovery (%)	ICP-MS recovery (%)	pXRF RP (%)	ICP-AES RP (%)	ICP-MS RP (%)
	MR_7	2442	1900	2103	-	-	-	-	-	-	-
	MR_9	2699	2300	2714	-	-	-	-	-	-	-
	MR_15	2779	2400	2711	-	-	-	-	-	-	-
	MR_21	3790	3600	4418	-	-	-	-	-	-	-
Ti	MR_26	3144	2000	2311	-	-	-	-	-	-	-
	NIST 2586	6204	5300	4940	6050	102.5	87.6	81.7	2.5	12.4	18.3
	NIST 2587	4074	3600	4336	4027	101.2	89.4	107.7	1.2	10.6	7.7
	NIST 2587_DUP	4074	3600	4125	4027	101.2	89.4	102.4	1.2	10.6	2.4
	NIST 2709a	3565	2900	3206	3360	106.1	86.3	95.4	6.1	13.7	4.6
	Mean					**102.7**	**88.2**	**96.8**	**2.7**	**11.8**	**8.3**

Element	Sample name/ reference	pXRF value	ICP-AES value	ICP-MS value	Reference value	pXRF recovery (%)	ICP-AES recovery (%)	ICP-MS recovery (%)	pXRF RP (%)	ICP-AES RP (%)	ICP-MS RP (%)
	MR_7	43	22	22	-	-	-	-	-	-	-
	MR_9	67	40	32	-	-	-	-	-	-	-
	MR_15	42	28	26	-	-	-	-	-	-	-
	MR_21	42	27	33	-	-	-	-	-	-	-
Cr	MR_26	49	20	24	-	-	-	-	-	-	-
	NIST 2586	263	264	224	301	87.4	87.7	74.5	12.6	12.3	25.5
	NIST 2587	92	79	91	92	100.0	85.9	99.4	0.0	14.1	0.6
	NIST 2587_DUP	92	80	88	92	100.0	87.0	96.0	0.0	13.0	4.0
	NIST 2709a	129	100	105	130	99.2	76.9	80.4	0.8	23.1	19.6
	Mean					**96.7**	**84.4**	**87.6**	**3.3**	**15.6**	**12.4**

Element	Sample name/ reference	pXRF value	ICP-AES value	ICP-MS value	Reference value	pXRF recovery (%)	ICP-AES recovery (%)	ICP-MS recovery (%)	pXRF RP (%)	ICP-AES RP (%)	ICP-MS RP (%)
	MR_7	204	182	203	-	-	-	-	-	-	-
	MR_9	250	226	270	-	-	-	-	-	-	-
	MR_15	316	303	348	-	-	-	-	-	-	-
	MR_21	2701	2750	3241	-	-	-	-	-	-	-
Mn	MR_26	583	434	501	-	-	-	-	-	-	-
	NIST 2586	990	944	883	1000	99.0	94.4	88.3	1.0	5.6	11.7
	NIST 2587	658	627	726	651	101.1	96.3	111.6	1.1	3.7	11.6
	NIST 2587_DUP	658	614	665	651	101.1	94.3	102.1	1.1	5.7	2.1
	NIST 2709a	557	486	540	529	105.3	91.9	102.0	5.3	8.1	2.0
	Mean					**101.6**	**94.2**	**101.0**	**2.1**	**5.8**	**6.8**

Element	Sample name/ reference	pXRF value	ICP-AES value	ICP-MS value	Reference value	pXRF recovery (%)	ICP-AES recovery (%)	ICP-MS recovery (%)	pXRF RP (%)	ICP-AES RP (%)	ICP-MS RP (%)
	MR_7	<LOD	6	11	-	-	-	-	-	-	-
	MR_9	<LOD	11	15	-	-	-	-	-	-	-
	MR_15	<LOD	10	12	-	-	-	-	-	-	-
	MR_21	<LOD	10	13	-	-	-	-	-	-	-
Ni	MR_26	<LOD	10	14	-	-	-	-	-	-	-
	NIST 2586	75	73	66	-	-	-	-	-	-	-
	NIST 2587	36	35	40	-	-	-	-	-	-	-
	NIST 2587_DUP	36	36	42	-	-	-	-	-	-	-
	NIST 2709a	70	73	79	85	82.4	85.9	92.7	17.6	14.1	7.3

Element	Sample name/ reference	pXRF value	ICP-AES value	ICP-MS value	Reference value	pXRF recovery (%)	ICP-AES recovery (%)	ICP-MS recovery (%)	pXRF RP (%)	ICP-AES RP (%)	ICP-MS RP (%)
	MR_7	53	38	36	-	-	-	-	-	-	-
	MR_9	44	28	32	-	-	-	-	-	-	-
	MR_15	65	56	61	-	-	-	-	-	-	-
	MR_21	41	26	32	-	-	-	-	-	-	-
Cu	MR_26	320	309	327	-	-	-	-	-	-	-
	NIST 2586	76	73	64	-	-	-	-	-	-	-
	NIST 2587	165	156	174	-	-	-	-	-	-	-
	NIST 2587_DUP	165	151	165	-	-	-	-	-	-	-
	NIST 2709a	39.5	31	33	33.9	116.5	91.4	96.3	16.5	8.6	3.7

Element	Sample name/ reference	pXRF value	ICP-AES value	ICP-MS value	Reference value	pXRF recovery (%)	ICP-AES recovery (%)	ICP-MS recovery (%)	pXRF RP (%)	ICP-AES RP (%)	ICP-MS RP (%)
	MR_7	492	555	522	-	-	-	-	-	-	-
	MR_9	127	122	132	-	-	-	-	-	-	-
	MR_15	836	990	952	-	-	-	-	-	-	-
	MR_21	882	928	927	-	-	-	-	-	-	-
Zn	MR_26	1669	1825	1737	-	-	-	-	-	-	-
	NIST 2586	327	358	294	352	92.9	101.7	83.6	7.1	1.7	16.4
	NIST 2587	341	358	385	335.8	101.5	106.6	114.5	1.5	6.6	14.5
	NIST 2587_DUP	341	342	348	335.8	101.5	101.8	103.8	1.5	1.8	3.8
	NIST 2709a	111	100	120	103	107.4	97.1	116.8	7.4	2.9	16.8
					Mean	**100.8**	**101.8**	**104.7**	**4.4**	**3.3**	**12.9**

Element	Sample name/ reference	pXRF value	ICP-AES value	ICP-MS value	Reference value	pXRF recovery (%)	ICP-AES recovery (%)	ICP-MS recovery (%)	pXRF RP (%)	ICP-AES RP (%)	ICP-MS RP (%)
	MR_7	<LOD	<5	4	-	-	-	-	-	-	-
	MR_9	17	18	21	-	-	-	-	-	-	-
	MR_15	20	19	22	-	-	-	-	-	-	-
	MR_21	14	11	15	-	-	-	-	-	-	-
As	MR_26	27	32	38	-	-	-	-	-	-	-
	NIST 2586	8	9	8	8.7	92.0	103.4	92.4	8.0	3.4	7.6
	NIST 2587	<LOD	17	17	13.7	-	124.1	120.6	-	24.1	20.6
	NIST 2587_DUP	<LOD	14	15	13.7	-	102.2	108.7	-	2.2	8.7
	NIST 2709a	11	11	10	10.5	106.3	104.8	95.5	6.3	4.8	4.5
					Mean	**99.1**	**108.6**	**104.3**	**7.2**	**8.6**	**10.4**

Element	Sample name/ reference	pXRF value	ICP-AES value	ICP-MS value	Reference value	pXRF recovery (%)	ICP-AES recovery (%)	ICP-MS recovery (%)	pXRF RP (%)	ICP-AES RP (%)	ICP-MS RP (%)
	MR_7	50	52	53	-	-	-	-	-	-	-
	MR_9	73	75	82	-	-	-	-	-	-	-
	MR_15	47	46	50	-	-	-	-	-	-	-
	MR_21	94	103	108	-	-	-	-	-	-	-
Sr	MR_26	66	73	78	-	-	-	-	-	-	-
	NIST 2586	78	87	73	84.1	92.2	103.4	87.3	7.8	3.4	12.7
	NIST 2587	126	130	137	126	100.1	103.2	108.4	0.1	3.2	8.4
	NIST 2587_DUP	126	131	129	126	100.1	104.0	102.3	0.1	4.0	2.3
	NIST 2709a	233	239	237	239	97.5	100.0	99.4	2.5	0.0	0.6
					Mean	**97.5**	**102.6**	**99.3**	**2.6**	**2.6**	**6.0**

Element	Sample name/ reference	pXRF value	ICP-AES value	ICP-MS value	Reference value	pXRF recovery (%)	ICP-AES recovery (%)	ICP-MS recovery (%)	pXRF RP (%)	ICP-AES RP (%)	ICP-MS RP (%)
	MR_7	<LOD	0.5	0.6	-	-	-	-	-	-	-
	MR_9	<LOD	<0.5	0.3	-	-	-	-	-	-	-
	MR_15	6.3	7.4	8.2	-	-	-	-	-	-	-
	MR_21	3.2	4.0	4.0	-	-	-	-	-	-	-
Cd	MR_26	10.2	10.0	10.2	-	-	-	-	-	-	-
	NIST 2586	2.7	2.6	2.0	2.7	100.0	96.3	73.2	0.0	3.7	26.8
	NIST 2587	<LOD	1.9	2.0	1.92	-	99.0	105.1	-	1.0	5.1
	NIST 2587_DUP	<LOD	1.7	2.3	1.92	-	88.5	120.1	-	11.5	20.1
	NIST 2709a	<LOD	<0.5	0.4	0.371	-	-	117.9	-	-	17.9
					Mean	**100.0**	**94.6**	**104.1**	**0.0**	**5.4**	**17.5**

Element	Sample name/ reference	pXRF value	ICP-AES value	ICP-MS value	Reference value	pXRF recovery (%)	ICP-AES recovery (%)	ICP-MS recovery (%)	pXRF RP (%)	ICP-AES RP (%)	ICP-MS RP (%)
	MR_7	1351	1325	1403	-	-	-	-	-	-	-
	MR_9	90	88	98	-	-	-	-	-	-	-
	MR_15	488	480	537	-	-	-	-	-	-	-
	MR_21	651	663	723	-	-	-	-	-	-	-
Pb	MR_26	1419	1425	1489	-	-	-	-	-	-	-
	NIST 2586	415	420	361	432	96.1	97.2	83.5	3.9	2.8	16.5
	NIST 2587	3239	3180	3577	3242	99.9	98.1	110.3	0.1	1.9	10.3
	NIST 2587_DUP	3239	3100	3299	3242	99.9	95.6	101.8	0.1	4.4	1.8
	NIST 2709a	17	15	19	17.3	96.0	86.7	110.8	4.0	13.3	10.8
					Mean	98.0	94.4	101.6	2.0	5.6	9.8

Table C4: Mean pXRF measurements and recoveries of ten soil CRMs. Comparison of measurements using the manufacturers' factory settings and against a matrix matched calibration. Recoveries are calculated as ((pXRF value / reference value) × 100). Reference and pXRF values are in mg/kg.

Element	Reference material	Factory settings	Reference value	Recovery (%)	Soil matrix calibration	Reference value	Recovery (%)
Ti	NIST 1944	4163	4300	96.8	4254	4300	98.9
	NIST 2586	6296	6050	104.1	6204	6050	102.6
	NIST 2587	4055	3920	103.4	4074	3920	103.9
	NIST 2709a	3591	3360	106.9	3565	3360	106.1
	NIST 2710a	3412	3110	109.7	3416	3110	109.8
	NIST 2711a	3141	3170	99.1	3159	3170	99.7
	RM 8704	4659	4570	102.0	4581	4570	100.2
	NRC PACS-2	4262	4430	96.2	4329	4430	97.7
	NRC BCSS-1	4147	4400	94.3	4225	4400	96.0
			Mean	**101.1**		**Mean**	**101.4**
Cr	NIST 1944	238	266	89.5	312	266	117.3
	NIST 2586	198	301	65.8	263	301	87.4
	NIST 2587	63	92	68.6	92	92	100.0
	NIST 2709a	91	130	70.3	129	130	99.2
	NIST 2710a	8.0	23	30.4	21	23	91.3
	NIST 2711a	39	52.3	73.7	63	52.3	120.5
	RM 8704	90	121.9	73.8	128	121.9	105.0
	NRC PACS-2	56	90.7	61.7	84	90.7	92.6
	NRC MESS-2	78	106	73.6	113	106	106.6
	NRC BCSS-1	82	123	66.7	120	123	97.6
			Mean	**67.4**		**Mean**	**101.7**
Mn	NIST 1944	482	505	95.5	477	505	94.5
	NIST 2586	990	1000	99.0	990	1000	99.0
	NIST 2587	653	651	100.3	658	651	101.1
	NIST 2709a	558	529	105.4	557	529	105.3
	NIST 2710a	2253	2140	105.3	2303	2140	107.6
	NIST 2711a	664	675	98.4	677	675	100.3
	RM 8704	588	544	108.1	585	544	107.54
	NRC PACS-2	429	440	97.5	438	440	99.6
	NRC MESS-2	371	365	101.6	364	365	99.7
	NRC BCSS-1	246	229	107.4	236	229	103.0
			Mean	**101.9**		**Mean**	**101.8**
Fe	NIST 1944	36057	35300	102.1	36999	35300	104.8
	NIST 2586	51622	51610	100.0	49080	51610	95.1
	NIST 2587	26000	28130	92.4	28610	28130	101.7
	NIST 2709a	30994	33600	92.2	32577	33600	97.0
	NIST 2710a	49392	43200	114.3	48495	43200	112.2
	NIST 2711a	25475	28200	90.3	27830	28200	98.7
	RM 8704	39245	39700	98.9	39136	39700	98.6
	NRC PACS-2	39401	40900	96.3	39334	40900	96.2
	NRC MESS-2	41101	43503	94.5	40999	43503	94.2
	NRC BCSS-1	30494	32873	92.8	31911	32873	97.1
			Mean	**97.4**		**Mean**	**99.6**
Ni	NIST 1944	121	76.1	159.0	78	76.1	102.5
	NIST 2709a	115	85	135.3	70	85	82.4
	NIST 2710a	54	8.0	675	27	8.0	337.5
	NIST 2711a	51	21.7	234.1	21	21.7	96.8
	RM 8704	68	42.9	158.5	39	42.9	90.9
	NRC PACS-2	60	39.5	151.9	32	39.5	81.0
	NRC MESS-2	76	49.3	154.2	43	49.3	87.2
	NRC BCSS-1	82	55.3	148.3	47	55.3	85.0
			Mean	**227**		**Mean**	**120.4**

Cu	NIST 1944	426	380	112.1	387	380	101.8
	NIST 2709a	14	33.9	42.3	40	33.9	116.5
	NIST 2710a	3515	3420	102.8	3341	3420	97.7
	NIST 2711a	115	140	81.9	129	140	92.1
	NRC PACS-2	267	310	86.1	271	310	87.4
	NRC MESS-2	13	39.3	33.1	37.4	39.3	95.2
	NRC BCSS-1	<LOD	18.5		30	18.5	162.2
			Mean	**76.4**		**Mean**	**107.6**
Zn	NIST 1944	706	656	107.6	679	656	103.5
	NIST 2586	317	352	90.1	327	352	92.9
	NIST 2587	332	335.8	98.9	341	335.8	101.6
	NIST 2709a	89	103	86.4	111	103	107.4
	NIST 2710a	4325	4180	103.5	4237	4180	101.4
	NIST 2711a	385	414	92.9	391	414	94.4
	RM 8704	360	408	88.2	373	408	91.4
	NRC PACS-2	327	364	89.8	343	364	94.2
	NRC MESS-2	140	172	81.4	160	172	92.9
	NRC BCSS-1	102	119	85.7	126	119	105.6
			Mean	**92.5**		**Mean**	**98.5**
As	NIST 1944	31	18.9	161.9	28	18.9	149.2
	NIST 2586	8	8.7	92.0	8	8.7	92.0
	NIST 2709a	12	10.5	111.4	11	10.5	106.3
	NIST 2710a	1624	1540	105.5	1592	1540	103.4
	NIST 2711a	95	107	88.8	98	107	91.2
	NRC PACS-2	24	26.2	92.4	24	26.2	91.6
	NRC MESS-2	23	20.7	109.7	22	20.7	107.3
	NRC BCSS-1	11	11.1	96.4	12	11.1	106.3
			Mean	**107.0**		**Mean**	**106.2**
Sr	NIST 2586	84	84.1	100.2	78	84.1	92.2
	NIST 2587	135	126	107.3	126	126	100.1
	NIST 2709a	251	239	105.1	233	239	97.5
	NIST 2710a	268	255	105.1	253	255	99.2
	NIST 2711a	245	242	101.2	224	242	92.6
	NRC PACS-2	305	276	110.5	282	276	102.2
	NRC MESS-2	143	125	114.1	133	125	106.4
			Mean	**106.2**		**Mean**	**98.6**
Cd	NIST 1944	13	8.8	146.6	8.8	8.8	100.0
	NIST 2586	4.4	2.71	162.4	2.7	2.71	100.0
	NIST 2587	3.4	1.92	177.1	<LOD	1.92	
	NIST 2710a	16	12.3	128.5	11	12.3	89.4
	NIST 2711a	78	54.1	144.5	57	54.1	104.8
	RM 8704	4.6	2.94	156.5	3.6	2.94	120.8
			Mean	**152.6**		**Mean**	**103.0**
Pb	NIST 1944	349	330	105.8	348	330	105.5
	NIST 2586	422	432	97.7	415	432	96.1
	NIST 2587	3305	3242	101.9	3239	3242	99.9
	NIST 2709a	13	17.3	72.6	17	17.3	96.0
	NIST 2710a	5549	5520	100.5	5514	5520	99.9
	NIST 2711a	1432	1400	102.3	1385	1400	98.9
	RM 8704	137	150	91.4	142	150	94.7
	NRC PACS-2	173	183	94.4	173	183	94.3
	NRC MESS-2	17	21.9	76.7	22	21.9	99.1
	NRC BCSS-1	18	22.7	81.1	24	22.7	107.1
			Mean	**92.4**		**Mean**	**99.1**
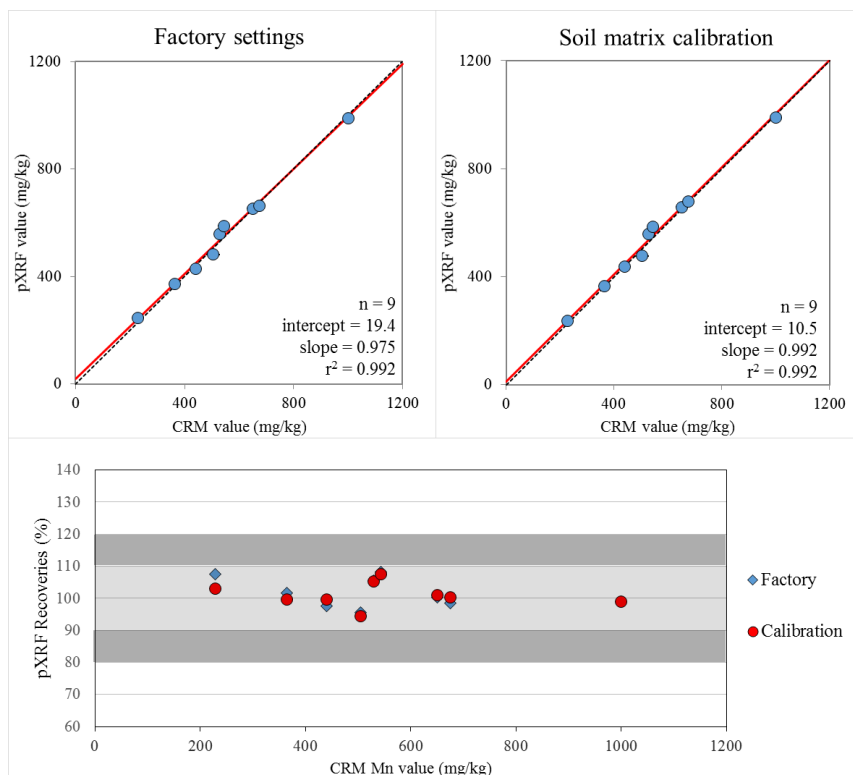
Figure C1: Comparison of data quality for Mn pre- and post-calibration. The regression relationship (solid red line), ideal 100% recovery (dashed black line) and slope, intercept and r^2 are shown in each plot. Individual recoveries plotted against elemental concentrations for both calibration strategies are in the lower plot.
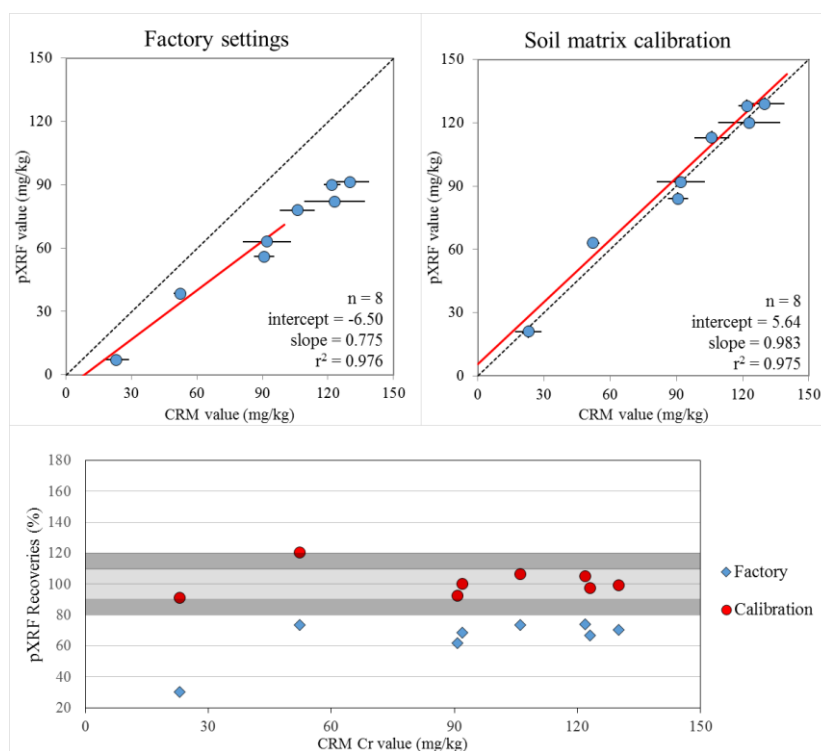
Figure C2: Comparison of data quality for Cr pre- and post-calibration. The regression relationship (solid red line), ideal 100% recovery (dashed black line) and slope, intercept and goodness of fit (r^2) are shown in each plot. Individual recoveries plotted against elemental concentrations for both calibration strategies are in the lower plot.

Table C5: Recoveries, RP and RSD of ten soil CRMs using a matrix matched calibration. Data was categorised by element. Reference and pXRF values are shown in mg/kg. Recoveries, RP and standard deviation are rounded to 1 decimal place, whereas RSD is rounded to two decimal places.

	Titanium							
Reference material	Measurement number	pXRF value	Reference material	Measurement number	pXRF value	Reference material	Measurement number	pXRF value
	#1	4276		#1	6208		#1	4063
	#2	4262		#2	6199		#2	4059
	#3	4271		#3	6244		#3	4064
	#4	4220		#4	6133		#4	4085
	#5	4242		#5	6237		#5	4101
NIST 1944	**Mean**	**4254**	NIST 2586	**Mean**	**6204**	NIST 2587	**Mean**	**4074**
	Reference value	4300		Reference value	6050		Reference value	4027
	Recovery	98.9		Recovery	102.6		Recovery	101.2
	RP	1.1		RP	2.6		RP	1.2
	Std Dev	23.1		Std Dev	44.1		Std Dev	18.0
	RSD	0.54		RSD	0.71		RSD	0.44
	#1	6208		#1	3430		#1	3159
	#2	6199		#2	3442		#2	3161
	#3	6244		#3	3387		#3	3169
	#4	6133		#4	3409		#4	3163
	#5	6237		#5	3414		#5	3141
NIST 2709a	**Mean**	**6204**	NIST 2710a	**Mean**	**3416**	NIST 2711a	**Mean**	**3159**
	Reference value	6050		Reference value	3110		Reference value	3170
	Recovery	102.6		Recovery	109.8		Recovery	99.7
	RP	2.6		RP	9.8		RP	0.3
	Std Dev	44.1		Std Dev	21.0		Std Dev	10.5
	RSD	0.71		RSD	0.61		RSD	0.33
	#1	4584		#1	4332		#1	4215
	#2	4616		#2	4282		#2	4187
	#3	4578		#3	4295		#3	4236
	#4	4560		#4	4394		#4	4245
	#5	4565		#5	4340		#5	4242
RM 8704	**Mean**	**4581**	NRC PACS-2	**Mean**	**4329**	NRC BCSS-1	**Mean**	**4225**
	Reference value	4570		Reference value	4430		Reference value	4400
	Recovery	100.2		Recovery	97.7		Recovery	96.0
	RP	0.2		RP	2.3		RP	4.0
	Std Dev	22.0		Std Dev	43.9		Std Dev	24.3
	RSD	0.48		RSD	1.01		RSD	0.57

Chromium								
Reference material	Measurement number	pXRF value	Reference material	Measurement number	pXRF value	Reference material	Measurement number	pXRF value
NIST 1944	#1	314	NIST 2586	#1	265	NIST 2587	#1	94
	#2	316		#2	266		#2	92
	#3	307		#3	261		#3	89
	#4	312		#4	261		#4	93
	#5	310		#5	264		#5	92
	Mean	**312**		**Mean**	**263**		**Mean**	**92**
	Reference value	266		Reference value	301		Reference value	92
	Recovery	117.3		Recovery	87.4		Recovery	100.0
	RP	17.3		RP	12.6		RP	0.0
	Std Dev	3.5		Std Dev	2.3		Std Dev	1.9
	RSD	1.12		RSD	0.88		RSD	2.03
NIST 2709a	#1	131	NIST 2710a	#1	24	NIST 2711a	#1	66
	#2	128		#2	19		#2	63
	#3	129		#3	20		#3	63
	#4	126		#4	20		#4	60
	#5	129		#5	22		#5	61
	Mean	**129**		**Mean**	**21**		**Mean**	**63**
	Reference value	130		Reference value	23		Reference value	52.3
	Recovery	99.2		Recovery	91.3		Recovery	120.5
	RP	0.8		RP	8.7		RP	20.5
	Std Dev	1.8		Std Dev	2.0		Std Dev	2.3
	RSD	1.41		RSD	9.52		RSD	3.65
RM 8704	#1	127	NRC PACS-2	#1	83	NRC MESS-2	#1	113
	#2	129		#2	81		#2	112
	#3	133		#3	91		#3	109
	#4	123		#4	85		#4	117
	#5	128		#5	81		#5	114
	Mean	**128**		**Mean**	**84**		**Mean**	**113**
	Reference value	121.9		Reference value	90.7		Reference value	106
	Recovery	105.0		Recovery	92.6		Recovery	106.6
	RP	5.0		RP	7.4		RP	6.6
	Std Dev	3.6		Std Dev	4.2		Std Dev	2.9
	RSD	2.82		RSD	4.94		RSD	2.58
NRC BCSS-1	#1	120						
	#2	120						
	#3	118						
	#4	122						
	#5	121						
	Mean	**120**						
	Reference value	123						
	Recovery	97.6						
	RP	2.4						
	Std Dev	1.5						
	RSD	1.24						

Manganese								
Reference material	**Measurement number**	**pXRF value**	**Reference material**	**Measurement number**	**pXRF value**	**Reference material**	**Measurement number**	**pXRF value**
NIST 1944	#1	470	NIST 2586	#1	982	NIST 2587	#1	659
	#2	477		#2	995		#2	659
	#3	478		#3	993		#3	653
	#4	481		#4	989		#4	653
	#5	479		#5	991		#5	668
	Mean	**477**		**Mean**	**990**		**Mean**	**658**
	Reference value	505		Reference value	1000		Reference value	651
	Recovery	94.5		Recovery	99.0		Recovery	101.1
	RP	5.5		RP	1.0		RP	1.1
	Std Dev	4.2		Std Dev	5.0		Std Dev	6.2
	RSD	0.88		RSD	0.51		RSD	0.93
NIST 2709a	#1	560	NIST 2710a	#1	2285	NIST 2711a	#1	674
	#2	560		#2	2307		#2	683
	#3	555		#3	2309		#3	677
	#4	552		#4	2317		#4	670
	#5	558		#5	2296		#5	678
	Mean	**557**		**Mean**	**2303**		**Mean**	**677**
	Reference value	529		Reference value	2140		Reference value	675
	Recovery	105.3		Recovery	107.6		Recovery	100.3
	RP	5.3		RP	7.6		RP	0.3
	Std Dev	3.5		Std Dev	12.5		Std Dev	4.8
	RSD	0.62		RSD	0.54		RSD	0.71
RM 8704	#1	589	NRC PACS-2	#1	437	NRC MESS-2	#1	363
	#2	581		#2	433		#2	369
	#3	583		#3	431		#3	361
	#4	590		#4	447		#4	363
	#5	586		#5	442		#5	365
	Mean	**585**		**Mean**	**438**		**Mean**	**364**
	Reference value	544		Reference value	440		Reference value	365
	Recovery	107.5		Recovery	99.6		Recovery	99.7
	RP	7.5		RP	0.4		RP	0.3
	Std Dev	3.8		Std Dev	6.6		Std Dev	3.0
	RSD	0.66		RSD	1.50		RSD	0.83
NRC BCSS-1	#1	235						
	#2	236						
	#3	238						
	#4	237						
	#5	233						
	Mean	**236**						
	Reference value	229						
	Recovery	103.1						
	RP	3.1						
	Std Dev	1.92						
	RSD	0.82						

					Iron			
Reference material	**Measurement number**	**pXRF value**	**Reference material**	**Measurement number**	**pXRF value**	**Reference material**	**Measurement number**	**pXRF value**
NIST 1944	#1	37029	NIST 2586	#1	48980	NIST 2587	#1	28588
	#2	36980		#2	49245		#2	28588
	#3	36938		#3	48950		#3	28638
	#4	37148		#4	49009		#4	28604
	#5	36901		#5	49218		#5	28632
	Mean	**36999**		**Mean**	**49080**		**Mean**	**28610**
	Reference value	35300		Reference value	51610		Reference value	28130
	Recovery	104.8		Recovery	95.1		Recovery	101.7
	RP	4.8		RP	4.9		RP	1.7
	Std Dev	95.9		Std Dev	139.8		Std Dev	23.8
	RSD	0.26		RSD	0.28		RSD	0.08
NIST 2709a	#1	32638	NIST 2710a	#1	48494	NIST 2711a	#1	27865
	#2	32464		#2	48312		#2	27838
	#3	32587		#3	48678		#3	27759
	#4	32635		#4	48466		#4	27892
	#5	32560		#5	48524		#5	27797
	Mean	**32577**		**Mean**	**48495**		**Mean**	**27830**
	Reference value	33600		Reference value	43200		Reference value	28200
	Recovery	97.0		Recovery	112.3		Recovery	98.7
	RP	3.0		RP	12.3		RP	1.3
	Std Dev	71.1		Std Dev	131.0		Std Dev	53.1
	RSD	0.22		RSD	0.27		RSD	0.19
RM 8704	#1	39160	NRC PACS-2	#1	39333	NRC MESS-2	#1	41023
	#2	39187		#2	39259		#2	40946
	#3	38976		#3	39365		#3	41001
	#4	39132		#4	39335		#4	40941
	#5	39227		#5	39376		#5	41087
	Mean	**39136**		**Mean**	**39334**		**Mean**	**40999**
	Reference value	39700		Reference value	40900		Reference value	43503
	Recovery	98.6		Recovery	96.2		Recovery	94.2
	RP	1.4		RP	3.8		RP	5.8
	Std Dev	96.3		Std Dev	45.7		Std Dev	60.2
	RSD	0.25		RSD	0.12		RSD	0.15
NRC BCSS-1	#1	31973						
	#2	32016						
	#3	31952						
	#4	31808						
	#5	31805						
	Mean	**31911**						
	Reference value	32873						
	Recovery	97.1						
	RP	2.9						
	Std Dev	98.0						
	RSD	0.31						

Nickel								
Reference material	**Measurement number**	**pXRF value**	**Reference material**	**Measurement number**	**pXRF value**	**Reference material**	**Measurement number**	**pXRF value**
NIST 1944	#1	76	NIST 2709a	#1	68	NIST 2710a	#1	25
	#2	79		#2	68		#2	31
	#3	77		#3	69		#3	27
	#4	79		#4	76		#4	29
	#5	80		#5	70		#5	21
	Mean	**78**		**Mean**	**70**		**Mean**	**27**
	Reference value	76.1		Reference value	85		Reference value	8
	Recovery	102.5		Recovery	82.4		Recovery	337.5
	RP	2.5		RP	17.6		RP	227.5
	Std Dev	1.6		Std Dev	3.4		Std Dev	3.9
	RSD	2.11		RSD	4.78		RSD	14.25
NIST 2711a	#1	20	RM 8704	#1	44	NRC PACS-2	#1	30
	#2	18		#2	35		#2	35
	#3	27		#3	34		#3	29
	#4	22		#4	40		#4	31
	#5	16		#5	40		#5	35
	Mean	**21**		**Mean**	**39**		**Mean**	**32**
	Reference value	21.7		Reference value	42.9		Reference value	39.5
	Recovery	96.8		Recovery	90.9		Recovery	81.0
	RP	3.2		RP	9.1		RP	19.0
	Std Dev	4.2		Std Dev	4.1		Std Dev	2.8
	RSD	20.09		RSD	10.51		RSD	8.84
NRC MESS-2	#1	41	NRC BCSS-1	#1	46			
	#2	47		#2	52			
	#3	43		#3	46			
	#4	40		#4	46			
	#5	46		#5	45			
	Mean	**43**		**Mean**	**47**			
	Reference value	49.3		Reference value	55.3			
	Recovery	87.2		Recovery	85.0			
	RP	12.8		RP	15.0			
	Std Dev	3.1		Std Dev	2.8			
	RSD	7.09		RSD	6.02			

Copper								
Reference material	**Measurement number**	**pXRF value**	**Reference material**	**Measurement number**	**pXRF value**	**Reference material**	**Measurement number**	**pXRF value**
	#1	386		#1	39.2		#1	3349
	#2	382		#2	39.8		#2	3331
	#3	387		#3	38.3		#3	3354
	#4	392		#4	41.6		#4	3341
	#5	387		#5	38.5		#5	3331
NIST 1944	**Mean**	**387**	NIST 2709a	**Mean**	**39.5**	NIST 2710a	**Mean**	**3341**
	Reference value	380		Reference value	33.9		Reference value	3420
	Recovery	101.8		Recovery	116.5		Recovery	97.7
	RP	1.8		RP	16.5		RP	2.3
	Std Dev	3.6		Std Dev	1.3		Std Dev	10.4
	RSD	0.92		RSD	3.36		RSD	0.31
	#1	129		#1	274		#1	35.2
	#2	132		#2	272		#2	36.8
	#3	126		#3	270		#3	38.5
	#4	130		#4	268		#4	38.4
	#5	127		#5	270		#5	37.9
NIST 2711a	**Mean**	**129**	NRC PACS-2	**Mean**	**271**	NRC MESS-2	**Mean**	**37.4**
	Reference value	140		Reference value	310		Reference value	39.3
	Recovery	92.1		Recovery	87.4		Recovery	95.2
	RP	7.9		RP	12.6		RP	4.8
	Std Dev	2.4		Std Dev	2.3		Std Dev	1.4
	RSD	1.85		RSD	0.84		RSD	3.70
	#1	32.6						
	#2	28.8						
	#3	30.8						
	#4	27.8						
	#5	29.8						
NRC MESS-2	**Mean**	**30**						
	Reference value	18.5						
	Recovery	162.4						
	RP	62.4						
	Std Dev	1.9						
	RSD	6.17						

Zinc								
Reference material	**Measurement number**	**pXRF value**	**Reference material**	**Measurement number**	**pXRF value**	**Reference material**	**Measurement number**	**pXRF value**
NIST 1944	#1	677	NIST 2586	#1	326	NIST 2587	#1	344
	#2	675		#2	327		#2	339
	#3	675		#3	323		#3	341
	#4	684		#4	327		#4	338
	#5	682		#5	329		#5	343
	Mean	**679**		**Mean**	**327**		**Mean**	**341**
	Reference value	656		Reference value	352		Reference value	335.8
	Recovery	103.5		Recovery	92.9		Recovery	101.6
	RP	3.5		RP	7.1		RP	1.6
	Std Dev	4.2		Std Dev	2.2		Std Dev	2.6
	RSD	0.61		RSD	0.67		RSD	0.75
NIST 2709a	#1	110.3	NIST 2710a	#1	4241	NIST 2711a	#1	393
	#2	109.8		#2	4227		#2	393
	#3	112.3		#3	4243		#3	390
	#4	110.1		#4	4236		#4	393
	#5	110.4		#5	4237		#5	388
	Mean	**110.6**		**Mean**	**4237**		**Mean**	**391**
	Reference value	103		Reference value	4180		Reference value	414
	Recovery	107.4		Recovery	101.4		Recovery	94.4
	RP	7.4		RP	1.4		RP	5.6
	Std Dev	1.0		Std Dev	6.2		Std Dev	2.3
	RSD	0.89		RSD	0.15		RSD	0.59
RM 8704	#1	372	NRC PACS-2	#1	345	NRC MESS-2	#1	158
	#2	375		#2	341		#2	160.5
	#3	369		#3	344		#3	157.2
	#4	372		#4	338		#4	161.7
	#5	375		#5	346		#5	161.2
	Mean	**373**		**Mean**	**343**		**Mean**	**159.7**
	Reference value	408		Reference value	364		Reference value	172
	Recovery	91.4		Recovery	94.2		Recovery	92.9
	RP	8.6		RP	5.8		RP	7.1
	Std Dev	2.5		Std Dev	3.3		Std Dev	2.0
	RSD	0.67		RSD	0.95		RSD	1.25
NRC BCSS-1	#1	128.3						
	#2	125.2						
	#3	127.1						
	#4	122.8						
	#5	124.8						
	Mean	**125.6**						
	Reference value	119						
	Recovery	105.6						
	RP	5.6						
	Std Dev	2.1						
	RSD	1.70						

Arsenic								
Reference material	**Measurement number**	**pXRF value**	**Reference material**	**Measurement number**	**pXRF value**	**Reference material**	**Measurement number**	**pXRF value**
	#1	30.3		#1	7		#1	<LOD
	#2	27.6		#2	<LOD		#2	<LOD
	#3	28.2		#3	12		#3	<LOD
	#4	25.9		#4	7		#4	<LOD
	#5	28.9		#5	8		#5	<LOD
NIST 1944	**Mean**	**28.2**	NIST 2586	**Mean**	**8**	NIST 2587	**Mean**	**<LOD**
	Reference value	18.9		Reference value	8.7		Reference value	13.7
	Recovery	149.2		Recovery	92.0		Recovery	n/a
	RP	49.2		RP	8.0		RP	n/a
	Std Dev	1.6		Std Dev	2.4		Std Dev	n/a
	RSD	5.76		RSD	29.8		RSD	n/a
	#1	12.4		#1	1595		#1	96
	#2	10.1		#2	1582		#2	95
	#3	11.1		#3	1580		#3	96
	#4	10.8		#4	1608		#4	103
	#5	11.4		#5	1596		#5	98
NIST 2709a	**Mean**	**11.16**	NIST 2710a	**Mean**	**1592**	NIST 2711a	**Mean**	**97.6**
	Reference value	10.5		Reference value	1540		Reference value	107
	Recovery	106.3		Recovery	103.4		Recovery	91.2
	RP	6.33		RP	3.4		RP	8.8
	Std Dev	0.8		Std Dev	11.5		Std Dev	3.2
	RSD	7.57		RSD	0.72		RSD	3.29
	#1	23.2		#1	23		#1	11.8
	#2	20.7		#2	23.1		#2	11.9
	#3	26.6		#3	21.8		#3	10.7
	#4	23.7		#4	21.5		#4	12.5
	#5	25.7		#5	21.5		#5	12.1
NRC PACS-2	**Mean**	**24**	NRC MESS-2	**Mean**	**22.2**	NRC BCSS-1	**Mean**	**11.8**
	Reference value	26.2		Reference value	20.7		Reference value	11.1
	Recovery	91.6		Recovery	107.3		Recovery	106.3
	RP	8.4		RP	7.3		RP	6.3
	Std Dev	2.3		Std Dev	0.8		Std Dev	0.7
	RSD	9.61		RSD	3.62		RSD	5.68

				Strontium				
Reference material	**Measurement number**	**pXRF value**	**Reference material**	**Measurement number**	**pXRF value**	**Reference material**	**Measurement number**	**pXRF value**
NIST 2586	#1	76.9	NIST 2587	#1	125.8	NIST 2709a	#1	232
	#2	77.4		#2	126.1		#2	235
	#3	76.1		#3	125.8		#3	231
	#4	78.8		#4	126.7		#4	231
	#5	78.6		#5	126.2		#5	235
	Mean	**77.5**		**Mean**	**126.1**		**Mean**	**233**
	Reference value	84.1		Reference value	126		Reference value	239
	Recovery	92.2		Recovery	100.1		Recovery	97.5
	RP	7.8		RP	0.1		RP	2.5
	Std Dev	1.1		Std Dev	0.4		Std Dev	2.1
	RSD	1.47		RSD	0.29		RSD	0.88
NIST 2710a	#1	250	NIST 2711a	#1	225	NRC PACS-2	#1	281
	#2	256		#2	225		#2	282
	#3	252		#3	221		#3	279
	#4	254		#4	228		#4	286
	#5	253		#5	222		#5	281
	Mean	**253**		**Mean**	**224**		**Mean**	**282**
	Reference value	255		Reference value	242		Reference value	276
	Recovery	99.2		Recovery	92.6		Recovery	102.2
	RP	0.8		RP	7.4		RP	2.2
	Std Dev	2.2		Std Dev	2.8		Std Dev	2.6
	RSD	0.88		RSD	1.24		RSD	0.92
NRC MESS-2	#1	133						
	#2	131.9						
	#3	131.4						
	#4	132.8						
	#5	136.2						
	Mean	**133**						
	Reference value	125						
	Recovery	106.44						
	RP	6.4						
	Std Dev	1.9						
	RSD	1.41						

	Cadmium							
Reference material	**Measurement number**	**pXRF value**	**Reference material**	**Measurement number**	**pXRF value**	**Reference material**	**Measurement number**	**pXRF value**
NIST 1944	#1	9.1	NIST 2586	#1	<LOD	NIST 2710a	#1	10.5
	#2	7.9		#2	<LOD		#2	10.4
	#3	9.1		#3	2.7		#3	10.9
	#4	9.3		#4	2.7		#4	11.8
	#5	8.6		#5	2.7		#5	11.4
	Mean	**8.8**		**Mean**	**2.7**		**Mean**	**11**
	Reference value	8.8		Reference value	2.71		Reference value	12.3
	Recovery	100.0		Recovery	99.6		Recovery	89.4
	RP	0.0		RP	0.0		RP	10.6
	Std Dev	0.6		Std Dev	0.0		Std Dev	0.6
	RSD	6.43		RSD	0.00		RSD	5.42
NIST 2711a	#1	56.6	NIST 2711a	#1	<LOD			
	#2	57.3		#2	<LOD			
	#3	55.4		#3	4.3			
	#4	56.8		#4	<LOD			
	#5	57.5		#5	2.8			
	Mean	**56.7**		**Mean**	3.55			
	Reference value	54.1		Reference value	2.94			
	Recovery	104.8		Recovery	120.8			
	RP	4.8		RP	20.8			
	Std Dev	0.8		Std Dev	1.1			
	RSD	1.45		RSD	29.88			

				Lead				
Reference material	**Measurement number**	**pXRF value**	**Reference material**	**Measurement number**	**pXRF value**	**Reference material**	**Measurement number**	**pXRF value**
	#1	348		#1	418		#1	3244
	#2	348		#2	415		#2	3230
	#3	348		#3	414		#3	3253
	#4	349		#4	413		#4	3233
	#5	345		#5	414		#5	3236
NIST 1944	**Mean**	**348**	NIST 2586	**Mean**	**415**	NIST 2587	**Mean**	**3239**
	Reference value	330		Reference value	432		Reference value	3242
	Recovery	105.5		Recovery	96.1		Recovery	99.9
	RP	5.5		RP	3.9		RP	0.1
	Std Dev	1.5		Std Dev	1.9		Std Dev	9.3
	RSD	0.44		RSD	0.46		RSD	0.29
	#1	17.7		#1	5511		#1	1388
	#2	15.4		#2	5501		#2	1388
	#3	17.2		#3	5546		#3	1377
	#4	16.3		#4	5517		#4	1389
	#5	16.7		#5	5493		#5	1385
NIST 2709a	**Mean**	**16.6**	NIST 2710a	**Mean**	**5514**	NIST 2711a	**Mean**	**1385**
	Reference value	17.3		Reference value	5520		Reference value	1400
	Recovery	96.0		Recovery	99.9		Recovery	98.9
	RP	4.0		RP	0.1		RP	1.1
	Std Dev	0.9		Std Dev	20.3		Std Dev	4.9
	RSD	5.30		RSD	0.37		RSD	0.36
	#1	142.5		#1	170.7		#1	23.2
	#2	140.7		#2	171.4		#2	20.3
	#3	141		#3	174		#3	22.3
	#4	144.3		#4	172.7		#4	20.3
	#5	142		#5	174.3		#5	22.1
RM 8704	**Mean**	**142.1**	NRC PACS-2	**Mean**	**172.6**	NRC MESS-2	**Mean**	**21.7**
	Reference value	150		Reference value	183		Reference value	21.9
	Recovery	94.7		Recovery	94.3		Recovery	99.1
	RP	5.3		RP	5.7		RP	0.9
	Std Dev	1.4		Std Dev	1.6		Std Dev	1.3
	RSD	1.01		RSD	0.91		RSD	5.95
	#1	23.4						
	#2	24.9						
	#3	23.6						
	#4	24.4						
	#5	25.3						
NRC BCSS-1	**Mean**	**24.3**						
	Reference value	22.7						
	Recovery	107.1						
	RP	7.1						
	Std Dev	0.8						
	RSD	3.36						

Table C6: Elemental summary on the performance of the pXRF in the measurement of 10 soil and sediment CRMs.

Ti	The detection limit was not calculated for Ti as even the lowest reference value (3110 mg/kg) did not approach the manufacturers detection limit of <10 mg/kg (Table 2). All but one CRM had reference values provided for Ti, ranging from 3110–6050 mg/kg. Both the slope (0.889) and goodness of fit (0.970) were close to their target of 1 suggesting the calibrated pXRF performed well for the measurement of Ti (Figure 2, Table 3). The intercept (514) remained high as no CRMs closer to the detection limit were available to refine the lower end of the regression (Figure 2). Individual CRM recoveries ranged from 96.0-110% with a mean absolute RP and RSD of 3.1% and 0.58% respectively (Table 2). The measurement of Ti produced definitive data for contaminated soils within the concentration range of 3110–6050 mg/kg.
Cr	The detection limit for Cr was 7.7 mg/kg which corresponds with the manufacturer's proposed detection limit of <10 mg/kg. The concentration ranges between 23–301 mg/kg, with eight of the ten reference values <150 mg/kg (Figure 2). The removal of two higher CRM values of 266 mg/kg (NIST 1944) and 301 mg/kg (NIST 2586) formed an untrimmed (Figure 2) and trimmed dataset (Figure 3). Both untrimmed and trimmed plots had similar slopes (1.023 and 0.983) and intercepts (2.68 and 5.64 respectively) yet the exclusion of the two higher CRM values in the trimmed plot resulted in a slight increase of r^2 (0.946 to 0.975) (Table 3). Both datasets produced comparable data quality to the CRM values as the mean RP is lower for the trimmed (6.4%) dataset than untrimmed (8.1%) (Table 2), most likely due to the focus on lower concentrations when developing the soil matrix calibration. Mean RSD was 3.0 and 3.5% for untrimmed and trimmed datasets respectively with the most imprecise CRM (NIST 2710a) measurements of 24, 19, 20, 20, and 22 mg/kg (target 23 mg/kg) resulted in a RSD of 9.5% (Supplementary Table E). This measurement variation is exacerbated at lower concentrations as RSD is a proportional function of variation. Definitive data was achieved for Cr during the measurements of the ten soil CRMs up to 301 mg/kg.
Mn	The concentration range of Mn for ten CRMs was 229–2140 mg/kg with a detection limit of 9.1 mg/kg, comparable to the manufacturer's suggested detection limit of <10 mg/kg (Table 2). The highest CRM value of 2140 mg/kg (NIST 2710a) was excluded to produce two datasets for Mn, one untrimmed and one trimmed for data <1200 mg/kg (Figure 3). Both untrimmed and trimmed datasets had excellent r^2 values of 0.998 and 0.992 respectively as seen in Table 3. Individual recoveries from the ten CRMs ranged from 94.5–108% with a mean absolute RP of 3.2 and 2.7% for untrimmed and trimmed datasets respectively (Table 2). The regression slope improved from 1.033 in the untrimmed plot (Figure 2) to 0.992 in the trimmed plot (Figure 3) due to the exclusion of NIST 2710a (108% recovery). The two best CRM recoveries for Mn were during the measurement of NIST 2711a (measured 677 mg/kg, target 665 mg/kg, 100.3% recovery) and NRC MESS-2 (measured 364 mg/kg, target 365 mg/kg, 99.7% recovery) (Supplementary Table E). Mean RSD values were low at only 0.80 and 0.87% (Table 3) for untrimmed and trimmed datasets, however may increase as concentrations approach typical detection limits, given the lowest CRM concentration was 229 mg/kg. The pXRF instrument performed exceptionally well in the measurement of Mn and produced definitive data (Table 3) within the concentration range of the CRMs.
Fe	The detection limit was not calculated for Fe as no CRM values were close to the suggested manufacturers detection limit of <10 mg/kg (Table 2). Typical background Fe concentrations in soils can range from 0.2–55 wt% (Bodek et al. 1988) and would rarely approach the manufacturers detection limit of <10 mg/kg in environmental investigations. The concentration range of ten CRMs for Fe was 2.8–5.2 wt%. The regression slope was close to the desired 1 at 1.019 with a good fit of 0.906 (Figure 2, Table 3). The NIST 2710a CRM had the worst individual recovery of 112% for Fe (measured 4.84 wt%, target 4.32 wt%), while the rest of the CRM recoveries ranged from 94.2–105% (Supplementary Table D). The mean CRM recovery of 99.6% demonstrates the pXRF instrument marginally underestimates Fe concentrations, even when using soil mode. Precision was excellent during the measurement of Fe, mean RSD was 0.2% with exceptional repeat measurement of NIST 2587 measuring 2.9 wt% all five times (RSD 0.08%) (Supplementary Table E). The pXRF produced definitive data for Fe within the concentration range of the ten CRMs.
Ni	Eight of the ten CRMs had reference values for Ni, with a concentration range of 8–85 mg/kg (Table 3). The detection limit achieved was 10.1 mg/kg (Table 2), just slightly above the manufacturer's suggested detection limit of <10 mg/kg. The poorest measurement of Ni had a recovery of 338% (NIST 2710a, measured 27 mg/kg, target 8.0 mg/kg), and was excluded in the trimmed plot as the certified value was below the calculated detection limit of 10.1 mg/kg (Figure 3). The removal of NIST 2710a increased the r^2 value from 0.866 to 0.937, increased the slope from 0.739 to 0.856 and decreased the intercept value from 8.29 to 0.90 (Figures 2 and 3, Table 3). Individual recoveries ranged from 81.0–102%, while mean RSD was 8.2% (Supplementary Table D). Excellent measurement repeatability (RSD 2.1%) was observed for NIST 1944 (measured 76, 77, 79, 79, 80 mg/kg, target 76.1 mg/kg), while poorer repeatability (RSD 20.1%) was observed for NIST 2711a (measured 16, 18, 20, 22, 27 mg/kg, target 21.7 mg/kg) as variation in lower CRM values exacerbate the RSD (Supplementary Table E). Despite having a higher RSD and stronger rotational bias than most other elements, Ni was reasonably well determined by pXRF and meets the requirements for definitive data quality for the trimmed dataset.
Cu	Six of the seven soil CRMs for Cu had reference values ranging from 18.5–380 mg/kg, with a maximum value of 3420 mg/kg (NIST 2710a) that was removed in a trimmed plot (Figure 3). The detection limit for Cu was 4.0 mg/kg, well beneath the <10 mg/kg suggested by the manufacturer (Table 2). The r^2 value for the untrimmed dataset was 0.999 (Figure 2), a result of the clustering of six <500 mg/kg CRMs and the high value of 3420 mg/kg. Both untrimmed and trimmed datasets had similar intercepts (4.93 and 9.61) and RSD values (2.4 and 2.6% respectively). Excellent CRM recovery and precision can be seen in the repeated measurements of NIST 2710a (measured 3331, 3341, 3341, 3349 and 3354 mg/kg, target 3420 mg/kg, recovery

	97.7%) (Supplementary Table E). Both datasets for Cu produced quantitative screening quality data in the measurement of seven CRMs between 18.5–3420 mg/kg.
Zn	The detection limit of Zn was 5.1 mg/kg, very close to the manufacturers detection limit of <5 mg/kg (Table 2). The majority of CRM values ranged from 103–656 mg/kg in a trimmed plot (Figure 3), with a maximum value of 4180 mg/kg included in an untrimmed plot (Figure 2). Similar to Cu, the high value of 4180 mg/kg (NIST 2710a) and the clustering of the other nine CRM values generated a high r^2 value of 0.999, which is misleading over the entire concentration range (Figure 4). The trimmed <1000 mg/kg dataset had superb fit and slope values of 0.927 and 0.988 respectively (Figure 3, Table 3). Individual recoveries for all ten CRMs ranged from 91.4% to 107% with the excellent individual recoveries by NIST 2710a (measured 4237 mg/kg, target 4180 mg/kg, 101.4% recovery) and NIST 2587 (measured 341 mg/kg, target 336 mg/kg, 101.6% recovery) (Supplementary Table E). Mean RSD for both untrimmed and trimmed datasets were low at 2.4 and 2.6% respectively, with excellent repeat measurements of 675, 675, 677, 682 and 684 mg/kg on NIST 1944 (RSD 0.61%) and 338, 339, 341, 343 and 344 mg/kg on NIST 2587 (RSD 0.75%) (Supplementary Table E). The pXRF measurement of Zn produced definitive and quantitative screening data quality (Table 2) over the concentration ranges for both trimmed and untrimmed plots, respectively (Table 3).
As	The concentration range of As for eight CRMs was 8.7–1540 mg/kg with a detection limit of 3.4 mg/kg, similar to the manufacturer's suggested detection limit of <5 mg/kg (Table 2). The highest CRM value of 1540 mg/kg (NIST 2710a) was excluded to produce two datasets for As, one untrimmed (Figure 2) and one trimmed for <120 mg/kg (Figure 3). Similar to Cu and Zn, the maximum value of 1540 mg/kg (NIST 2710a) clustered the lower CRM values and created a high r^2 value of 0.999 for the untrimmed plot which is misleading over that concentration range (Figure 2, Table 3). The mean RSD for As was 7.3% for the trimmed and 8.1% for trimmed datasets (Table 3). The poorest repeat measurements occurred towards detection limits for NIST 2586 (measured <LOD, 7, 7, 8 and 12 mg/kg, target 8.7 mg/kg) and resulted in a high RSD of 30% (Supplementary Table E). Arsenic was well determined by the pXRF instrument, producing definitive quality data for both datasets within the concentration range of the CRMs.
Sr	The detection limit for Sr was 2.7 mg/kg, well below the manufacturers' suggested detection limit of <5 mg/kg (Table 2). Seven CRMs had reference values for Sr ranged from 84.1–276 mg/kg (Table 2). The pXRF measured Sr exceptionally well, individual recoveries ranged from 92.2– 106.4% (Supplementary Table D) with a mean absolute RP of 3.8% (Table 2). The untrimmed plot demonstrated superb fit (0.987) and slope rotation (0.983) for the seven CRMs. Excellent individual recoveries and precision were observed in the repeated measurement of NIST 2587 (measured 126, 126, 126, 126 and 127 mg/kg, target 126 mg/kg) and NIST 2710a (measured 250, 252, 253, 254, 256 mg/kg, target 255 mg/kg) (Supplementary Table E). The mean RSD was 0.86% (Table 2), and satisfied the criteria for definitive data quality within the concentration range of the CRMs.
Cd	The detection limit for Cd was 2.2 mg/kg, well beneath the manufacturer's suggested detection limit of <10 mg/kg (Table 2). Ten CRMs provided reference values for Cd from 0.24–54.1 mg/kg however half were below the detection limit of 2.2 mg/kg and subsequently were not detected, and limited the evaluation to five CRMs (Tables 2). Hence, the concentration range of Cd for the detectable CRMs was 2.71–54.1 mg/kg (Figure 2) and up to 12.3 mg/kg for the trimmed dataset after the exclusion of NIST 2711a (Figure 3). The untrimmed plot shown in Figure 4 shows excellent fit (0.999), slope (1.070) and intercept (-1.35) values, yet the high fit value was again influenced by the high flier NIST 2711a, and was removed in the trimmed plot (Figure 3). Individual CRM recoveries ranged from 89.4% (NIST 2710a) to 121% (RM 8704) with a mean absolute RP of 7.2 and 7.8% for untrimmed and trimmed datasets respectively. Cadmium had the highest imprecision amongst all elements for the <20 mg/kg trimmed dataset at 10%, which is usually exacerbated at lower concentrations. Despite the slighter higher imprecision, Cd satisfied the definitive data quality criteria within the concentration range of 2.71–54.1 mg/kg.
Pb	The concentration range of Pb for ten CRMs was 17.3–5520 mg/kg with a detection limit of 3.0 mg/kg, within the manufacturers' suggested detection limit of <5 mg/kg (Table 2). The high CRM values of 1400 mg/kg (NIST 2711a), 3242 mg/kg (NIST 2587) and 5520 mg/kg (NIST 2710a) were excluded to create an untrimmed (Figure 2) and trimmed dataset with CRM values <500 mg/kg (Figure 3) to better assess data quality at lower Pb concentrations. The pXRF performed extremely well in the measurement of Pb in both datasets with excellent CRM recoveries ranging between 94.3–107% (Supplementary Table D) with a mean absolute RP of 3.4% for untrimmed and 4.6% for trimmed datasets (Table 2). The regression plots for both untrimmed and trimmed datasets were excellent as the r^2 (0.999 and 0.996) and slope values (0.995 and 0.958 respectively) were very close to the target of 1 (Figure 2 and 3, Table 3). Examples of excellent CRM recovery were observed for NIST 2587 (measured 3239 mg/kg, target 3242 mg/kg, 99.9% recovery), NIST 2710a (measured 5513 mg/kg, target 5520 mg/kg, 99.9% recovery) and NRC MESS-2 (measured 21.7 mg/kg, target 21.9 mg/kg, 99.1% recovery) (Supplementary Table D). The mean RSD for Pb was low at 1.8% and 2.5% for untrimmed and trimmed datasets demonstrating superb precision by the instrument (Table 2). The pXRF instrument performed exceptionally well in the measurement of Pb CRMs and generated definitive data quality (Table 3) within the concentration range of the CRMs.

Table C7: Parallel measurements by pXRF and ICP-AES of 75 contaminated soil samples. Tables are displayed per element, all pXRF and values are rounded to whole numbers, measurement values for cadmium are rounded to one decimal place. All recoveries are displayed to one decimal place.

Titanium

Sample name	pXRF value	ICP-AES value	Recovery (%)	Sample name	pXRF value	ICP-AES value	Recovery (%)	Sample name	pXRF value	ICP-AES value	Recovery (%)
MR_1	3769	2400	157.0	MR_26	3144	2000	157.2	MR_51	4769	3700	128.9
MR_2	3135	2300	136.3	MR_27	4618	3900	118.4	MR_52	4297	3600	119.4
MR_3	3170	2800	113.2	MR_28	4485	3400	131.9	MR_53	4037	2400	168.2
MR_4	1419	1200	118.3	MR_29	5352	4100	130.5	MR_54	4649	2700	172.2
MR_5	4340	3400	127.7	MR_30	1866	1400	133.3	MR_55	3537	2600	136.0
MR_6	3097	2400	129.0	MR_31	6836	6000	113.9	MR_56	3586	2400	149.4
MR_7	2442	1900	128.5	MR_32	1779	1300	136.8	MR_57	3997	3000	133.2
MR_8	2081	1700	122.4	MR_33	5878	5000	117.6	MR_58	3090	1600	193.2
MR_9	2699	2300	117.3	MR_34	6986	6000	116.4	MR_59	3510	2200	159.5
MR_10	3115	2400	129.8	MR_35	1779	1300	136.8	MR_60	3097	2500	123.9
MR_11	3135	2400	130.6	MR_36	3143	2400	3143	MR_61	2967	2200	134.9
MR_12	1419	1300	109.2	MR_37	3633	2500	3633	MR_62	3526	2700	130.6
MR_13	2455	2200	111.6	MR_38	3808	3100	3808	MR_63	3504	2800	125.1
MR_14	2105	1700	123.8	MR_39	2742	2200	124.6	MR_64	3519	2500	140.7
MR_15	2779	2400	115.8	MR_40	4781	3300	144.9	MR_65	2183	1700	128.4
MR_16	1992	1700	117.2	MR_41	3038	2300	132.1	MR_66	3007	1900	158.3
MR_17	3395	3000	113.2	MR_42	4917	4100	119.9	MR_67	3276	2100	156.0
MR_18	3395	3000	113.2	MR_43	3598	2800	128.5	MR_68	3226	2700	119.5
MR_19	5515	5300	104.1	MR_44	3325	2600	127.9	MR_69	1304	900	144.9
MR_20	4840	4800	100.8	MR_45	3015	2400	125.6	MR_70	2065	1700	121.5
MR_21	3790	3600	105.3	MR_46	2632	2200	119.6	MR_71	2391	1600	149.4
MR_22	4037	3800	106.2	MR_47	3603	2800	128.7	MR_72	2222	1400	158.7
MR_23	5119	5200	98.4	MR_48	3401	2400	141.7	MR_73	1343	800	167.9
MR_24	5119	5500	93.1	MR_49	3419	2900	117.9	MR_74	1898	1400	135.5
MR_25	5945	5100	116.6	MR_50	8474	7100	119.4	MR_75	3141	2400	130.9

Chromium

Sample name	pXRF value	ICP-AES value	Recovery (%)	Sample name	pXRF value	ICP-AES value	Recovery (%)	Sample name	pXRF value	ICP-AES value	Recovery (%)
MR_1	85	56	151.4	MR_26	49	20	244.0	MR_51	82	56	146.4
MR_2	62	38	163.8	MR_27	52	32	162.5	MR_52	67	47	143.4
MR_3	59	28	210.2	MR_28	44	36	122.2	MR_53	82	49	166.9
MR_4	46	26	177.3	MR_29	55	43	127.0	MR_54	98	52	187.7
MR_5	87	63	138.7	MR_30	36	9	397.8	MR_55	73	45	163.1
MR_6	55	34	160.3	MR_31	55	45	122.2	MR_56	77	45	170.2
MR_7	43	22	196.4	MR_32	38	14	271.4	MR_57	107	75	142.1
MR_8	44	24	181.3	MR_33	64	48	133.3	MR_58	62	28	220.3
MR_9	67	40	167.3	MR_34	47	45	104.4	MR_59	136	76	178.9
MR_10	61	35	174.9	MR_35	38	14	271.4	MR_60	52	39	133.9
MR_11	62	38	163.8	MR_36	62	43	145.3	MR_61	59	26	228.7
MR_12	46	27	170.7	MR_37	82	54	152.2	MR_62	95	70	135.1
MR_13	49	35	140.6	MR_38	70	49	143.7	MR_63	57	37	153.9
MR_14	44	33	133.3	MR_39	74	53	140.0	MR_64	82	60	136.3
MR_15	42	28	148.3	MR_40	148	109	135.6	MR_65	44	19	231.6
MR_16	44	24	183.4	MR_41	78	43	180.3	MR_66	57	21	269.5
MR_17	67	48	139.2	MR_42	84	66	127.3	MR_67	63	39	160.6
MR_18	67	49	136.3	MR_43	63	40	158.4	MR_68	73	45	163.0
MR_19	<LOD	40	-	MR_44	75	57	130.8	MR_69	50	25	200.0
MR_20	17	31	55.5	MR_45	62	42	146.7	MR_70	54	29	186.0
MR_21	42	27	157.0	MR_46	59	40	146.5	MR_71	76	54	140.4
MR_22	26	34	75.3	MR_47	55	27	204.7	MR_72	61	30	203.0
MR_23	<LOD	27	-	MR_48	85	57	148.4	MR_73	44	15	295.7
MR_24	<LOD	29	-	MR_49	82	79	103.8	MR_74	79	47	168.3
MR_25	65	53	123.0	MR_50	101	81	124.2	MR_75	65	38	170.0

<p style="text-align:center">Manganese</p>

Sample name	pXRF value	ICP-AES value	Recovery (%)	Sample name	pXRF value	ICP-AES value	Recovery (%)	Sample name	pXRF value	ICP-AES value	Recovery (%)
MR_1	233	205	113.5	MR_26	583	434	134.4	MR_51	242	213	113.6
MR_2	199	178	111.9	MR_27	653	585	111.6	MR_52	390	326	119.5
MR_3	266	220	121.1	MR_28	536	497	107.8	MR_53	277	204	136.0
MR_4	182	173	105.4	MR_29	542	494	109.6	MR_54	306	219	139.5
MR_5	264	239	110.6	MR_30	308	257	119.8	MR_55	216	185	116.8
MR_6	321	283	113.4	MR_31	1074	969	110.8	MR_56	231	184	125.4
MR_7	204	182	112.1	MR_32	333	287	116.0	MR_57	398	319	124.8
MR_8	274	256	107.0	MR_33	871	774	112.5	MR_58	102	85	120.4
MR_9	250	226	110.6	MR_34	696	645	107.9	MR_59	211	182	115.7
MR_10	143	132	108.3	MR_35	333	291	114.4	MR_60	730	608	120.0
MR_11	199	179	111.3	MR_36	223	191	116.5	MR_61	175	156	112.4
MR_12	182	183	99.7	MR_37	532	423	125.8	MR_62	419	360	116.5
MR_13	287	275	104.4	MR_38	362	328	110.3	MR_63	359	309	116.2
MR_14	568	603	94.2	MR_39	276	253	109.2	MR_64	398	335	118.7
MR_15	316	303	104.4	MR_40	323	278	116.0	MR_65	144	137	105.0
MR_16	218	221	98.6	MR_41	70	71	98.0	MR_66	83	73	113.0
MR_17	353	331	106.7	MR_42	237	209	113.4	MR_67	217	184	117.9
MR_18	353	336	105.1	MR_43	1140	899	126.8	MR_68	258	224	115.2
MR_19	19690	20100	98.0	MR_44	416	338	123.2	MR_69	58	58	100.7
MR_20	4632	4820	96.1	MR_45	435	375	116.1	MR_70	215	192	111.8
MR_21	2701	2750	98.2	MR_46	338	285	118.5	MR_71	241	228	105.8
MR_22	5240	5520	94.9	MR_47	104	92	113.3	MR_72	265	199	133.2
MR_23	7489	7180	104.3	MR_48	318	292	109.0	MR_73	115	87	132.2
MR_24	7489	7350	101.9	MR_49	281	274	102.7	MR_74	49	53	92.5
MR_25	881	806	109.3	MR_50	343	299	114.7	MR_75	279	246	113.3

<p style="text-align:center">Iron</p>

Sample name	pXRF value	ICP-AES value	Recovery (%)	Sample name	pXRF value	ICP-AES value	Recovery (%)	Sample name	pXRF value	ICP-AES value	Recovery (%)
MR_1	29908	26700	112.0	MR_26	31229	26700	117.0	MR_51	25014	23500	106.4
MR_2	18710	14700	127.3	MR_27	34713	33100	104.9	MR_52	24973	23100	108.1
MR_3	17857	12700	140.6	MR_28	63044	52900	119.2	MR_53	21544	15900	135.5
MR_4	13132	8200	160.1	MR_29	66009	55500	118.9	MR_54	20402	14700	138.8
MR_5	22850	20100	113.7	MR_30	16990	13400	126.8	MR_55	18934	15100	125.4
MR_6	17499	13800	126.8	MR_31	52221	48300	108.1	MR_56	20231	16300	124.1
MR_7	16392	12200	134.4	MR_32	22083	19500	113.2	MR_57	21556	18900	114.1
MR_8	11311	5800	195.0	MR_33	46660	44700	104.4	MR_58	11795	5800	203.4
MR_9	15789	11700	134.9	MR_34	55050	50400	109.2	MR_59	18398	14700	125.2
MR_10	14736	9900	148.8	MR_35	22083	19500	113.2	MR_60	19633	17500	112.2
MR_11	18710	14600	128.1	MR_36	19157	15400	124.4	MR_61	13641	9300	146.7
MR_12	13132	8500	154.5	MR_37	25374	22300	113.8	MR_62	20186	18000	112.1
MR_13	16401	12600	130.2	MR_38	21348	19100	111.8	MR_63	20556	18600	110.5
MR_14	26846	25300	106.1	MR_39	19572	17300	113.1	MR_64	19768	16500	119.8
MR_15	20350	16900	120.4	MR_40	16050	12100	132.6	MR_65	14025	9700	144.6
MR_16	15198	11200	135.7	MR_41	11062	5700	194.1	MR_66	12381	6800	182.1
MR_17	20047	17600	113.9	MR_42	30046	29700	101.2	MR_67	15021	10700	140.4
MR_18	20047	17600	113.9	MR_43	20584	17300	119.0	MR_68	19372	16800	115.3
MR_19	63752	52300	121.9	MR_44	18510	14300	129.4	MR_69	10586	4500	235.2
MR_20	45379	44200	102.7	MR_45	21500	19400	110.8	MR_70	15661	11900	131.6
MR_21	30598	33000	92.7	MR_46	19272	16100	119.7	MR_71	16140	12700	127.1
MR_22	32197	32400	99.4	MR_47	14660	9600	152.7	MR_72	15714	9800	160.3
MR_23	50453	46200	109.2	MR_48	21732	18600	116.8	MR_73	10980	4200	261.4
MR_24	50453	48300	104.5	MR_49	21959	20300	108.2	MR_74	11677	5700	204.9
MR_25	57315	51800	110.6	MR_50	36619	37000	99.0	MR_75	18552	14800	125.4

Nickel

Sample name	pXRF value	ICP-AES value	Recovery (%)	Sample name	pXRF value	ICP-AES value	Recovery (%)	Sample name	pXRF value	ICP-AES value	Recovery (%)
MR_1	30	32	94.4	MR_26	<LOD	10	-	MR_51	13	19	67.4
MR_2	<LOD	15	-	MR_27	13	17	74.1	MR_52	<LOD	15	-
MR_3	<LOD	11	-	MR_28	29	17	172.9	MR_53	17	16	105.0
MR_4	<LOD	9	-	MR_29	36	21	169.5	MR_54	11	12	93.8
MR_5	<LOD	19	-	MR_30	<LOD	6	-	MR_55	<LOD	12	-
MR_6	<LOD	11	-	MR_31	29	26	111.5	MR_56	14	20	70.0
MR_7	<LOD	6	-	MR_32	<LOD	8	-	MR_57	<LOD	16	-
MR_8	<LOD	7	-	MR_33	24	29	82.8	MR_58	<LOD	5	-
MR_9	<LOD	11	-	MR_34	29	26	111.5	MR_59	9	15	62.2
MR_10	<LOD	11	-	MR_35	<LOD	8	-	MR_60	<LOD	14	-
MR_11	<LOD	13	-	MR_36	<LOD	13	-	MR_61	<LOD	8	-
MR_12	<LOD	12	-	MR_37	23	27	86.7	MR_62	12	18	68.1
MR_13	<LOD	12	-	MR_38	10	24	40.3	MR_63	<LOD	11	-
MR_14	10	18	55.6	MR_39	13	23	54.8	MR_64	9	18	51.4
MR_15	<LOD	10	-	MR_40	21	26	79.2	MR_65	<LOD	9	-
MR_16	<LOD	11	-	MR_41	<LOD	7	-	MR_66	<LOD	6	-
MR_17	11	18	58.3	MR_42	9	16	53.1	MR_67	<LOD	12	-
MR_18	<LOD	19	-	MR_43	9	19	47.4	MR_68	<LOD	18	-
MR_19	41	22	187.3	MR_44	<LOD	9	-	MR_69	<LOD	4	-
MR_20	18	19	94.7	MR_45	<LOD	17	-	MR_70	<LOD	10	-
MR_21	<LOD	10	-	MR_46	<LOD	11	-	MR_71	11	24	46.9
MR_22	14	12	112.5	MR_47	<LOD	8	-	MR_72	<LOD	15	-
MR_23	21	13	160.0	MR_48	18	25	72.8	MR_73	<LOD	5	-
MR_24	21	15	138.7	MR_49	32	46	69.1	MR_74	<LOD	6	-
MR_25	31	30	104.7	MR_50	26	30	85.3	MR_75	12	20	60.0

Copper

Sample name	pXRF value	ICP-AES value	Recovery (%)	Sample name	pXRF value	ICP-AES value	Recovery (%)	Sample name	pXRF value	ICP-AES value	Recovery (%)
MR_1	161	153	105.0	MR_26	320	309	103.5	MR_51	64	51	125.1
MR_2	90	75	119.5	MR_27	422	465	90.7	MR_52	49	39	125.6
MR_3	105	92	114.3	MR_28	322	327	98.5	MR_53	138	113	121.8
MR_4	152	155	97.9	MR_29	266	267	99.7	MR_54	81	62	130.6
MR_5	208	209	99.7	MR_30	47	31	151.6	MR_55	77	61	125.6
MR_6	63	47	134.5	MR_31	131	136	96.3	MR_56	95	79	120.8
MR_7	53	38	139.5	MR_32	68	59	115.8	MR_57	113	108	104.8
MR_8	60	43	138.4	MR_33	342	378	90.5	MR_58	54	28	191.7
MR_9	44	28	157.1	MR_34	224	232	96.6	MR_59	79	59	133.1
MR_10	77	59	130.5	MR_35	68	58	117.8	MR_60	69	58	118.6
MR_11	90	74	121.1	MR_36	83	70	118.6	MR_61	59	42	140.0
MR_12	152	159	95.5	MR_37	163	158	103.3	MR_62	141	143	98.5
MR_13	81	67	120.6	MR_38	130	116	112.2	MR_63	50	33	152.3
MR_14	100	100	99.6	MR_39	494	560	88.2	MR_64	102	89	114.8
MR_15	65	56	116.8	MR_40	317	377	84.0	MR_65	53	34	155.8
MR_16	60	47	126.8	MR_41	51	34	149.0	MR_66	63	41	153.8
MR_17	89	81	109.9	MR_42	54	47	114.9	MR_67	96	85	112.5
MR_18	89	80	111.3	MR_43	64	47	135.4	MR_68	61	51	119.8
MR_19	127	126	100.5	MR_44	84	68	122.9	MR_69	61	41	149.6
MR_20	89	79	112.4	MR_45	354	380	93.1	MR_70	58	41	140.9
MR_21	41	26	156.9	MR_46	356	357	99.6	MR_71	85	73	116.4
MR_22	48	36	134.4	MR_47	64	40	159.5	MR_72	104	81	128.9
MR_23	127	111	114.6	MR_48	149	139	106.9	MR_73	44	19	231.9
MR_24	127	114	111.6	MR_49	44	25	174.7	MR_74	38	15	253.7
MR_25	687	764	89.9	MR_50	57	52	109.2	MR_75	77	63	122.2

Zinc

Sample name	pXRF value	ICP-AES value	Recovery (%)	Sample name	pXRF value	ICP-AES value	Recovery (%)	Sample name	pXRF value	ICP-AES value	Recovery (%)
MR_1	2710	2890	93.8	MR_26	1669	1825	91.5	MR_51	258	272	95.0
MR_2	740	795	93.1	MR_27	720	813	88.6	MR_52	157	155	101.2
MR_3	2230	2220	100.4	MR_28	3969	4070	97.5	MR_53	1087	1050	103.5
MR_4	225	238	94.5	MR_29	3788	3920	96.6	MR_54	1421	1390	102.2
MR_5	660	742	88.9	MR_30	183	174	105.3	MR_55	741	803	92.2
MR_6	253	271	93.4	MR_31	2945	3330	88.4	MR_56	764	827	92.4
MR_7	492	555	88.6	MR_32	145	144	100.5	MR_57	941	1020	92.2
MR_8	336	368	91.3	MR_33	661	761	86.9	MR_58	224	224	99.8
MR_9	127	122	103.7	MR_34	1945	2130	91.3	MR_59	228	233	97.8
MR_10	758	832	91.1	MR_35	145	144	100.5	MR_60	278	304	91.4
MR_11	740	813	91.0	MR_36	797	877	90.9	MR_61	181	185	98.0
MR_12	225	248	90.7	MR_37	1001	1070	93.5	MR_62	715	823	86.9
MR_13	522	591	88.4	MR_38	757	854	88.7	MR_63	102	92	111.2
MR_14	1670	2070	80.7	MR_39	886	1040	85.2	MR_64	529	555	95.2
MR_15	836	990	84.4	MR_40	1482	1650	89.8	MR_65	184	186	98.9
MR_16	515	597	86.2	MR_41	269	298	90.3	MR_66	363	388	93.5
MR_17	859	1030	83.4	MR_42	182	186	97.8	MR_67	557	622	89.5
MR_18	859	1020	84.2	MR_43	384	406	94.5	MR_68	238	258	92.3
MR_19	7342	6680	109.9	MR_44	471	488	96.6	MR_69	132	124	106.4
MR_20	4170	4230	98.6	MR_45	614	690	88.9	MR_70	186	191	97.5
MR_21	882	928	95.0	MR_46	337	353	95.5	MR_71	896	940	95.3
MR_22	1605	1745	92.0	MR_47	988	1060	93.2	MR_72	283	269	105.1
MR_23	7100	6300	112.7	MR_48	1046	1130	92.6	MR_73	112	84	133.6
MR_24	7100	6410	110.8	MR_49	102	91	112.1	MR_74	105	86	121.8
MR_25	2147	2370	90.6	MR_50	285	305	93.4	MR_75	415	432	96.1

Arsenic

Sample name	pXRF value	ICP-AES value	Recovery (%)	Sample name	pXRF value	ICP-AES value	Recovery (%)	Sample name	pXRF value	ICP-AES value	Recovery (%)
MR_1	26	15	170.7	MR_26	27	32	84.4	MR_51	17	14	120.3
MR_2	<LOD	6	-	MR_27	19	22	87.3	MR_52	11	8	136.8
MR_3	<LOD	<5	-	MR_28	142	134	106.1	MR_53	45	7	645.7
MR_4	<LOD	<5	-	MR_29	121	112	108.0	MR_54	35	5	708.0
MR_5	24	27	88.1	MR_30	5	6	85.0	MR_55	<LOD	<5	-
MR_6	<LOD	<5	-	MR_31	29	32	90.6	MR_56	16	10	164.0
MR_7	<LOD	<5	-	MR_32	7	6	120.0	MR_57	60	56	107.9
MR_8	<LOD	<5	-	MR_33	20	19	105.3	MR_58	<LOD	<5	-
MR_9	17	18	96.1	MR_34	46	46	100.0	MR_59	34	31	110.1
MR_10	<LOD	8	-	MR_35	7	8	90.0	MR_60	11	7	150.0
MR_11	<LOD	9	-	MR_36	<LOD	5	-	MR_61	4	<5	-
MR_12	<LOD	<5	-	MR_37	<LOD	<5	-	MR_62	<LOD	5	-
MR_13	9	8	106.3	MR_38	10	7	146.4	MR_63	8	6	139.7
MR_14	28	32	87.5	MR_39	<LOD	5	-	MR_64	<LOD	<5	-
MR_15	20	19	103.2	MR_40	20	20	98.0	MR_65	<LOD	<5	-
MR_16	9	10	87.6	MR_41	<LOD	<5	-	MR_66	7	<5	-
MR_17	10	19	54.7	MR_42	23	19	122.7	MR_67	9	6	149.7
MR_18	10	11	94.5	MR_43	11	9	122.7	MR_68	7	<5	-
MR_19	144	46	313.9	MR_44	12	7	176.2	MR_69	9	9	99.3
MR_20	52	39	134.4	MR_45	10	5	200.0	MR_70	9	<5	-
MR_21	14	11	129.1	MR_46	11	5	220.0	MR_71	12	12	101.7
MR_22	22	17	130.6	MR_47	<LOD	6	-	MR_72	7	7	104.9
MR_23	109	74	146.8	MR_48	24	14	168.6	MR_73	<LOD	5	-
MR_24	109	79	137.5	MR_49	3	<5	-	MR_74	4	<5	-
MR_25	49	53	91.7	MR_50	9	7	130.9	MR_75	<LOD	5	-

<div align="center">Strontium</div>

Sample name	pXRF value	ICP-AES value	Recovery (%)	Sample name	pXRF value	ICP-AES value	Recovery (%)	Sample name	pXRF value	ICP-AES value	Recovery (%)
MR_1	244	253	96.4	MR_26	66	73	90.8	MR_51	103	110	93.3
MR_2	139	140	99.0	MR_27	68	74	92.1	MR_52	120	118	102.0
MR_3	80	77	104.1	MR_28	69	69	99.9	MR_53	99	100	98.9
MR_4	50	49	101.4	MR_29	68	70	96.7	MR_54	113	113	100.4
MR_5	99	102	97.5	MR_30	73	81	90.0	MR_55	95	96	98.6
MR_6	63	65	96.6	MR_31	77	86	89.3	MR_56	127	132	96.5
MR_7	50	52	95.6	MR_32	66	73	90.1	MR_57	108	112	96.4
MR_8	84	83	101.2	MR_33	77	85	90.1	MR_58	26	30	85.7
MR_9	73	75	97.6	MR_34	77	85	90.9	MR_59	74	81	91.9
MR_10	79	77	102.1	MR_35	66	74	88.9	MR_60	120	123	97.7
MR_11	139	141	98.3	MR_36	92	95	96.7	MR_61	73	80	91.7
MR_12	50	51	97.4	MR_37	104	107	97.3	MR_62	71	77	92.3
MR_13	120	119	100.6	MR_38	110	116	95.2	MR_63	83	88	93.9
MR_14	97	105	91.9	MR_39	100	109	91.6	MR_64	98	98	99.6
MR_15	47	46	102.7	MR_40	119	125	95.4	MR_65	66	69	95.7
MR_16	61	64	95.4	MR_41	59	63	93.6	MR_66	46	48	96.2
MR_17	150	152	99.0	MR_42	83	88	93.9	MR_67	97	101	95.7
MR_18	150	152	99.0	MR_43	97	96	101.5	MR_68	115	116	99.1
MR_19	125	134	93.4	MR_44	125	119	105.4	MR_69	28	29	97.4
MR_20	106	119	89.0	MR_45	127	134	95.1	MR_70	241	256	94.1
MR_21	94	103	91.0	MR_46	118	117	101.1	MR_71	184	192	95.8
MR_22	75	83	90.3	MR_47	35	37	94.1	MR_72	161	153	105.2
MR_23	117	120	97.4	MR_48	145	148	98.2	MR_73	30	28	105.7
MR_24	117	123	95.0	MR_49	93	108	85.9	MR_74	38	37	102.9
MR_25	75	84	88.8	MR_50	147	160	91.6	MR_75	145	144	100.9

<div align="center">Cadmium</div>

Sample name	pXRF value	ICP-AES value	Recovery (%)	Sample name	pXRF value	ICP-AES value	Recovery (%)	Sample name	pXRF value	ICP-AES value	Recovery (%)
MR_1	11.1	10.7	103.9	MR_26	10.2	10.0	102.0	MR_51	<LOD	<0.5	-
MR_2	<LOD	1.0	-	MR_27	7.9	7.6	104.5	MR_52	<LOD	<0.5	-
MR_3	<LOD	1.0	-	MR_28	24.3	22.5	108.2	MR_53	<LOD	1.4	-
MR_4	<LOD	0.7	-	MR_29	30.5	28.8	105.8	MR_54	<LOD	0.9	-
MR_5	<LOD	2.3	-	MR_30	<LOD	0.9	-	MR_55	<LOD	0.8	-
MR_6	<LOD	<0.5	-	MR_31	17.1	16.5	103.6	MR_56	<LOD	1.0	-
MR_7	<LOD	0.5	-	MR_32	<LOD	1.3	-	MR_57	3.2	3.2	99.2
MR_8	<LOD	0.6	-	MR_33	8.4	8.6	97.7	MR_58	<LOD	0.5	-
MR_9	<LOD	<0.5	-	MR_34	12.4	12.0	103.3	MR_59	<LOD	<0.5	-
MR_10	<LOD	0.7	-	MR_35	<LOD	1.4	-	MR_60	<LOD	0.7	-
MR_11	<LOD	1.1	-	MR_36	<LOD	1.0	-	MR_61	<LOD	<0.5	-
MR_12	<LOD	0.7	-	MR_37	2.9	2.5	114.0	MR_62	<LOD	1.6	-
MR_13	10.0	9.8	102.4	MR_38	<LOD	1.3	-	MR_63	<LOD	<0.5	-
MR_14	11.2	11.6	96.9	MR_39	<LOD	2.8	-	MR_64	<LOD	0.9	-
MR_15	6.3	7.4	85.1	MR_40	<LOD	3.4	-	MR_65	<LOD	<0.5	-
MR_16	6.1	7.0	87.1	MR_41	<LOD	0.6	-	MR_66	<LOD	0.6	-
MR_17	6.2	7.0	89.1	MR_42	<LOD	<0.5	-	MR_67	<LOD	1.1	-
MR_18	6.2	7.2	86.7	MR_43	<LOD	0.6	-	MR_68	<LOD	0.9	-
MR_19	22.0	21.4	103.0	MR_44	<LOD	0.6	-	MR_69	<LOD	<0.5	-
MR_20	13.8	13.3	103.5	MR_45	<LOD	0.7	-	MR_70	<LOD	<0.5	-
MR_21	3.2	4.0	80.6	MR_46	<LOD	0.6	-	MR_71	<LOD	0.8	-
MR_22	6.1	6.0	101.7	MR_47	<LOD	0.8	-	MR_72	<LOD	<0.5	-
MR_23	29.5	25.3	116.8	MR_48	<LOD	1.6	-	MR_73	<LOD	<0.5	-
MR_24	29.5	26.0	113.6	MR_49	<LOD	<0.5	-	MR_74	<LOD	<0.5	-
MR_25	19.0	17.7	107.6	MR_50	<LOD	<0.5	-	MR_75	<LOD	0.8	-

Lead

Sample name	pXRF value	ICP-AES value	Recovery (%)	Sample name	pXRF value	ICP-AES value	Recovery (%)	Sample name	pXRF value	ICP-AES value	Recovery (%)
MR_1	4337	4170	104.0	MR_26	1419	1425	99.6	MR_51	186	186	99.9
MR_2	3006	2860	105.1	MR_27	603	598	100.9	MR_52	134	134	100.0
MR_3	6492	5970	108.7	MR_28	8619	8260	104.3	MR_53	3838	3510	109.3
MR_4	251	244	102.7	MR_29	6976	6810	102.4	MR_54	3307	3040	108.8
MR_5	1374	1350	101.8	MR_30	70	71	98.0	MR_55	1921	1855	103.6
MR_6	406	396	102.5	MR_31	1695	1700	99.7	MR_56	1535	1500	102.3
MR_7	1351	1325	102.0	MR_32	89	88	101.4	MR_57	1103	1100	100.3
MR_8	546	533	102.4	MR_33	390	400	97.5	MR_58	1104	1030	107.2
MR_9	90	88	102.7	MR_34	1625	1620	100.3	MR_59	98	99	99.2
MR_10	1709	1640	104.2	MR_35	89	87	102.5	MR_60	95	93	102.6
MR_11	3006	2880	104.4	MR_36	1071	1025	104.5	MR_61	79	78	101.8
MR_12	251	252	99.4	MR_37	860	827	103.9	MR_62	780	798	97.7
MR_13	747	723	103.3	MR_38	820	813	100.8	MR_63	28	26	106.4
MR_14	913	934	97.7	MR_39	1674	1745	95.9	MR_64	931	899	103.6
MR_15	488	480	101.7	MR_40	1224	1265	96.8	MR_65	568	564	100.7
MR_16	410	407	100.7	MR_41	313	315	99.4	MR_66	322	309	104.3
MR_17	545	569	95.9	MR_42	72	72	100.2	MR_67	372	369	100.8
MR_18	545	569	95.9	MR_43	151	143	105.5	MR_68	212	217	97.7
MR_19	9528	8960	106.3	MR_44	1399	1300	107.6	MR_69	173	168	103.2
MR_20	2537	2430	104.4	MR_45	1120	1145	97.8	MR_70	89	87	102.8
MR_21	651	663	98.2	MR_46	927	909	102.0	MR_71	465	485	96.0
MR_22	1124	1115	100.8	MR_47	3233	3050	106.0	MR_72	75	70	107.5
MR_23	3358	3000	111.9	MR_48	1424	1370	103.9	MR_73	76	65	116.4
MR_24	3358	3060	109.7	MR_49	25	24	103.8	MR_74	168	159	105.3
MR_25	2243	2260	99.3	MR_50	284	295	96.2	MR_75	1606	1620	99.1

Table C8: Elemental summary on the performance of the pXRF in the measurement of 75 contaminated soil samples when compared against ICP-AES.

Ti	The parallel measurement of Ti demonstrated significant underestimation by ICP-AES when compared to pXRF. The mean recovery and absolute RP of six CRMs by ICP-AES measurements were 88.0% and 12.0% when compared to 101.7% and 2.6% for the pXRF (Table 4). Almost every sample (73/75) was above the 100% recovery line for Ti in Figure 4, suggesting the four acid digestion was too weak to fully extract Ti from within the silicate matrix of these samples. Mean RSD for ICP-AES measurements was 2.7%, slightly higher than the RSD achieved by pXRF of 0.57%. The excellent CRM regression (Figure 2) and mean recovery (Table 4) achieved by pXRF and the poor CRM recoveries by ICP-AES demonstrate that Ti was more accurately determined by pXRF than ICP-AES.
Cr	Similarly to Ti, Cr was significantly underestimated by ICP-AES when compared to pXRF measurements. The mean recovery and absolute RP of six CRMs by ICP-AES measurements was 83.0% and 17.0% when compared to 100.1% and 5.5% for the pXRF (Table 4). All but two samples were above the 100% recovery line in Figure 4 suggesting the four acid digestion method was inadequate to fully extract Cr from the samples. Mean RSD values were similar between the two methods at 3.6% (pXRF) and 2.5% (ICP-AES). The definitive CRM regression (Figure 2) and mean CRM recoveries (Table 4) achieved by pXRF combined with the poor CRM recoveries by ICP-AES demonstrate that Cr was more accurately determined by pXRF than ICP-AES.
Mn	The Mn concentration range of 75 contaminated soil samples was 49–19700 mg/kg (Supplementary Table G). Regression plots were split into untrimmed and trimmed plots to focus on Mn concentrations <1200 mg/kg in Figures 4 and 5 respectively. Goodness of fit values were excellent for both untrimmed (0.999) and trimmed (0.990) datasets, while the slope value of 0.984 increased to 1.154 after the exclusion of data points >1200 mg/kg (Figure 5). The mean CRM recovery achieved by pXRF was 101.7%, compared to 95.4% by ICP-AES. The slight underestimation of Mn by ICP-AES at lower concentrations explains the increased slope value in Figure 5. Relative proximity away from 100% recovery was also slightly better by pXRF at 3.4% compared to ICP-AES at 5.4% (Table 4). Mean RSD values were comparable between the two techniques at 1.1% (pXRF) and 1.8% (ICP-AES). The parallel measurement of the six CRMs and the strong regression relationship show that pXRF was equivalent to, if not slightly better, than ICP-AES in the measurement of Mn in contaminated soils.
Fe	The Fe concentration range of 75 contaminated soil samples was 1.06-6.60 wt% (Supplementary Table G). The pXRF measured each of the six CRMs more accurately than the ICP-AES with individual recoveries ranging from 95.1-104.8% for pXRF compared to 91.5-97.5% for ICP-AES (Supplementary Table B). Mean CRM recoveries were 99.0 and 94.1% for pXRF and ICP-AES respectively, while the mean RP demonstrates the mean deviation away from the 100% target was just 3.1% for pXRF and 5.9% for ICP-AES measurements (Table 4). The regression fit and slope were ideal at 0.987 and 1.030, however the high intercept value of 0.31 wt% shifted the regression away from the ideal 100% recovery line (Figure 4). The relationship between pXRF and ICP-AES measurements of Fe appeared to be nonlinear as pXRF recoveries (using ICP-AES as a reference) increased as concentrations approached 0 and 6 wt% (Figure 4). This may suggest the pXRF required an additional calibration for Fe concentrations <2 wt% as the CRM range used for calibration was between 2.8-5.2 wt% (Table 2). Measurement repeatability was excellent for both techniques; mean RSD was 0.2% for pXRF and 1.2% for ICP-AES. The superior CRM recoveries achieved by the pXRF and parallel measurements of 75 soil samples demonstrates pXRF was equivalent to, if not better than, ICP-AES in the measurement of Fe in contaminated soils within the concentration range of the CRMs.
Ni	Twenty seven of 75 contaminated soil samples had detectable concentrations of Ni (detection limit of 10.1 mg/kg) ranging from 10.5-41.2 mg/kg (Supplementary Table G). Nickel displayed the poorest relationship between pXRF and ICP-AES values with a reduced goodness of fit and slope value of 0.515 and 0.759 respectively (Figure 4). Both measurement techniques performed rather poorly in the measurement of six CRMs. The mean deviation away from reference values of CRMs (RP) was 13.2% for pXRF and 7.8% for ICP-AES measurements, while mean recoveries were 87.8% and 92.3% respectively (Table 4). Mean RSD was lower for the ICP-AES at 6.0%, when compared to 13% for pXRF measurements. The poor regression relationship between the two measurement techniques, combined with relatively poor CRM recoveries by both pXRF and ICP-AES reveal that Ni was not well determined by the pXRF. The regression against ICP-AES values and CRM recoveries by pXRF would ultimately improve with the selection of a pXRF with a Rh or Ag X-ray tube.
Cu	The Cu concentration range for 75 contaminated soil samples was 38.1-687 mg/kg (Supplementary Table G). The majority of samples had Cu concentrations <200 mg/kg and subsequently were separated into untrimmed (Figure 4) and <200 mg/kg trimmed datasets (Figure 5). Agreement between the two measurement techniques was great with r^2 values of 0.998 and 0.987 for untrimmed and trimmed datasets respectively (Figures 4 and 5). Slope and intercept values were similar between both untrimmed (0.869 and 22.5) and trimmed datasets (0.881 and 21.3) and were indicative of a consistent regression relationship throughout the concentration range (Figures 4 and 5). Individual sample recoveries (using ICP-AES as a reference) increased as concentrations approached instrument detection limits (Figure 5), which are enhanced as recoveries are proportional functions of deviation away from a given reference value. Mean CRM recoveries of 105.6% for pXRF and 90.2% for ICP-AES demonstrate opposing rotational bias by the two techniques yet ICP-AES had a slightly lower RP at 9.8% compared to 11.9% by pXRF (Table 4). Mean RSD values were similar for pXRF (2.6% RSD) and ICP-AES (2.0%). The parallel measurement of six CRMs and the great relationship between pXRF and ICP-AES values demonstrated pXRF was a suitable alternative to ICP-AES the measurement of Cu in contaminated soils.

|	
Zn	The Zn concentration range for 75 contaminated soil samples was 102-7342 mg/kg (Supplementary Table G). Similarly to Cu, the majority of samples had Zn concentrations <1200 mg/kg and consequently were separated into untrimmed (Figure 4) and trimmed datasets (Figure 5). Exceptional agreement was apparent between the two techniques with a high r^2 value of 0.995 for both datasets, and slope values of 1.068 for untrimmed and 0.891 for trimmed datasets (Figures 4 and 5). Mean CRM recoveries of six CRM were similar for both pXRF at 100% and ICP-AES at 99.4%, while ICP-AES had a slightly lower mean RP of 3.8% when compared to 5.4% by pXRF (Table 4). Measurement repeatability by pXRF was marginally better at 0.6% RSD when compared to ICP-AES at 1.5%. The dual measurements of six CRMs and the excellent regression relationship demonstrated that pXRF was comparable to ICP-AES in the measurement of Zn in contaminated soils.
As	Forty eight of the 75 contaminated soil samples had detectable concentrations of As (detection limit of 3.4 mg/kg) ranging from 5.1-142 mg/kg (Supplementary Table G). Three outliers were excluded from the As regression for unusually high recoveries of 314%, 645% and 708% when using the ICP-AES values as a reference. After this exclusion, the dataset was split into untrimmed (Figure 4) and trimmed datasets to focus on As concentrations <70 mg/kg (Figure 5). Agreement between the two measurement techniques was excellent with r^2 values of 0.977 and 0.948 for untrimmed and trimmed datasets respectively (Figures 4 and 5). The slope values improved from 1.157 to 1.006 when focusing on the lower concentration values. Parallel measurements of the six CRMs revealed poorer recoveries by pXRF than ICP-AES. Mean recoveries were 109.5% and 101.3% and mean RP was 15.6% for 8.6% for pXRF and ICP-AES measurements respectively (Table 4). Mean RSD between the two techniques were typically higher than other elements at 13% and 16% for pXRF and ICP-AES. The dual measurements of six CRMs showed that pXRF returned poorer recoveries than ICP-AES achieved. The low CRM concentrations of 8.7-26.2 mg/kg contribute to the high recoveries and RP as both are proportional functions of deviation away from a given reference value.
Sr	The pXRF concentration range of 75 contaminated soil samples for Sr was 25.7-244 mg/kg (Supplementary Table G). Exceptional agreement between pXRF and ICP-AES values was evident through the high r^2 value of 0.994, slope value of 0.975 and intercept value of -1.31 (Figure 4). Mean CRM recoveries of 98.2 and 101.2% for pXRF and ICP-AES measurements were excellent with similarly low RP values of 2.5 and 2.3%, respectively (Table 4). The mean RSD for pXRF (1.5%) and ICP-AES (1.3%) were low indicating exceptional measurement repeatability by both techniques. The parallel measurement of six CRMs and the strong regression relationship in Figure 5 show that pXRF was a suitable alternative to ICP-AES in the measurement of Sr in contaminated soils.
Cd	Twenty three of the 75 contaminated samples had detectable concentrations of Cd (detection limit of 2.2 mg/kg) ranging from 2.9-30.5 mg/kg (Supplementary Table G). Both untrimmed and trimmed datasets had high r^2 values of 0.996 and 0.996, with slope values near 1 at 1.146 and 1.101 respectively (Figures 4 and 5), demonstrating excellent agreement between pXRF and ICP-AES measurements. The mean recoveries of six CRM measurements were 106.9% and 95.1% for pXRF and ICP-AES respectively (Table 4). Mean RSD values were comparable for pXRF (7.3%) and ICP-AES (7.4%) for the untrimmed dataset, while similar values were evident for the trimmed dataset (7.8% and 8.2%). The great regression relationship and the similar recoveries of six CRMs demonstrate that pXRF was comparable to ICP-AES in the measurement of Cd in contaminated soils.
Pb	The pXRF concentration range of Pb for 75 contaminated soil samples was 24.9–9530 mg/kg. Excellent goodness of fit (0.999 and 0.999) and slope values (1.059 and 1.014) were achieved between the two methods for the untrimmed and trimmed datasets (Figures 4 and 5, Table 4). Mean CRM recoveries achieved by pXRF was 97.8%, while ICP-AES achieved a slightly lower mean of 95.1% (Table 4). The mean absolute RP achieved by pXRF was 3.6% away from the target value of 100% recovery while ICP-AES achieved 5.6% (Table 4). Mean RSD between the two techniques were great for both untrimmed and trimmed datasets for pXRF (0.7% and 1.0%) and ICP-AES (2.0% and 2.4%). The parallel measurement of six CRMs by both techniques, and the excellent regression relationship in both datasets show that pXRF was equivalent to, if not slightly better, than ICP-AES in the measurement of Pb in contaminated soils.

Appendix D

Reference in paper	Reference in thesis	Caption
Supplementary Figure 1	Figure D1	Pilot study used to determine the ideal minimum number of samples required to determine a site mean. The small 400 m^2 site was divided into one hundred 2×2 m squares and measured in the centre of each square using in-situ pXRF. The estimated mean using all 100 measurements is plotted as the vertical black line at 2910 mg/kg. The grey band around this site mean is the 95 % confidence interval of the 100 data point mean. The coloured bands represent randomly selected samples from the 100 available, and their respective 95 % confidence interval bands. Thirty samples was identified as a robust minimum to adequately represent the site mean as per William Gosset who stated: *"with samples of 30 ... the mean value approaches the real value comparatively rapidly"* (Student 1908).
Supplementary Figure 2	Figure D2	Balanced experiment design for estimation of uncertainty using duplicate sampling and analysis at 10-15 % of sample targets at each site (adapted from Ramsey et al. 1992).
Supplementary Table 1	Table D1	Subset of samples used for pXRF data correction for each of the five metal-contaminated sites. Pre- and post-correction pXRF data is displayed alongside the estimated moisture content at the time of pXRF analysis and ICP-MS analysis of the same sample. Geochemical data and estimated moisture content are displayed up to 3 and 2 significant figures, respectively.
Supplementary Figure 3	Figure D3	Log linear regression of 20 second pXRF measurements (a) before and (b) after data correction for all five metal-contaminated sites. (c) Impact of sample preparation at the highly heterogeneous Site 1 where multiple matrices were present. pXRF data was corrected using a small subset (5-10 % of samples) of ICP-MS measurements sampled directly after *in-situ* pXRF measurements. Where a systematic relationship existed between pXRF and ICP-MS, the gradient and intercept of the relationship was used to correct pXRF at each site individually. This data correction was successful at four of the five sites where one matrix dominated the site, however multiple matrices (soil and glassy black slag pieces) were present at Site 1, which resulted in poorer relationship between the two techniques. To minimise the physical matrix effects between the two matrices, light sample preparation was conducted on the Site 1 samples, which consisted of drying and lightly crushing the soil with a mortar and pestle. Sample preparation improved both the accuracy and precision of pXRF measurements, when compared to commercial ICP-MS data. This figure demonstrates that where a systematic relationship cannot be attained using *in-situ* pXRF and ICP-MS, light sample preparation can be used to achieve a stronger relationship between the two techniques, and can be used to correct the rest of the pXRF dataset.
Supplementary Figure 4	Figure D4	a) Estimated total costs for the characterisation of metal-contaminated sites at the minimum sampling resolution for ICP–MS and *in-situ* pXRF. Cost assumptions include: labour call out rate = $150/hour, *in-situ* pXRF measurement = 20 secs, pXRF ownership cost = $83/assessment, time between samples = 45 secs, commercial laboratory eight element analysis = $22.60/sample. The cost of duplicate sampling to establish measurement uncertainty was not included given that this would vary according to the number of duplicate samples being taken. Circles in a) are estimated costs from the five-metal contaminated sites in this study, while diamonds are projected costs for sites larger than 3 ha. Soil Zn concentrations at Site 4 are shown for b) ICP–MS and c) pXRF Phase 1 measurement approaches, while d) real-time pXRF data enabled judgemental sampling directly after systematic sampling.
Supplementary Figure 5	Figure D5	Point by point graphs of the impact of sample preparation on 20 second *in-situ* pXRF measurements at highly heterogeneous Site 1. Relative proximity (RP) gives an indication of pXRF inaccuracy when compared to a reference value (ICP-AES data) and is calculated by RP = (absolute (100 - recovery value).
Supplementary Table 2	Table D2	Estimation of measurement uncertainty and variance using duplicate sampling and repeat analyses for Mn, Zn and Pb concentrations at Sites 1-5 using *ex-situ* ICP-MS and *in-situ* pXRF measurement approaches. In-situ pXRF Mn, Zn and Pb concentrations were not corrected at Site 1, and were not corrected for Mn concentrations at Site 5, due to non-systematic relationships between pXRF and ICP-MS data. Variance components $s_{geochem}$, s_{samp}, s_{anal} and s_{meas} represent geochemical, sampling, analysis and measurement standard deviations, respectively. The expanded relative uncertainties (95 % CI) for sampling, analysis and measurements were U_{samp}, U_{anal} and U_{meas} respectively. RANOVA could not estimate $s_{geochem}$ in a few cases where variance by sampling was too great (i.e. Site 1) and are represented by n/a. Values displayed to 3 significant figures.

20 × 20 m area of Pilot Study site.

Note: Grey vertical band represents 95 % confidence interval of site mean using 100 samples. Coloured bars represent 95 % confidence interval of site mean using 50 (red), 40 (orange), 30 (yellow), 25 (blue), 20 (light green) and 15 (dark green), randomly selected samples.

Figure D1: Pilot study used to determine the ideal minimum number of samples required to determine a site mean. The small 400 m² site was divided into one hundred 2×2 m squares and measured in the centre of each square using in-situ pXRF. The estimated mean using all 100 measurements is plotted as the vertical black line at 2910 mg/kg. The grey band around this site mean is the 95 % confidence interval of the 100 data point mean. The coloured bands represent randomly selected samples from the 100 available, and their respective 95 % confidence interval bands. Thirty samples was identified as a robust minimum to adequately represent the site mean as per William Gosset who stated: *"with samples of 30 ... the mean value approaches the real value comparatively rapidly"* (Student 1908).

Figure D2: Balanced experiment design for estimation of uncertainty using duplicate sampling and analysis at 10-15 % of sample targets at each site (adapted from Ramsey et al. 1992)

Table D1: Subset of samples used for pXRF data correction for each of the five metal-contaminated sites. Pre- and post-correction pXRF data is displayed alongside the estimated moisture content at the time of pXRF analysis and ICP-MS analysis of the same sample. Geochemical data and estimated moisture content are displayed up to 3 and 2 significant figures, respectively.

Site Number	Sample Code	Uncorrected *in-situ* pXRF			Corrected *in-situ* pXRF			Commercial ICP-MS			Estimated moisture content (%)
		Mn	**Zn**	**Pb**	**Mn**	**Zn**	**Pb**	**Mn**	**Zn**	**Pb**	
	Bell_8	664	2180	435	6500	20300	1260	4100	11200	1110	54
	Bell_9	5300	10100	1520	21400	50300	5720	22200	51600	5630	23
1	Bell_11	2240	5880	953	11500	26400	2450	8250	20800	2070	40
	Bell_13	794	3570	690	3140	9060	1620	5190	13000	1700	36
	Bell_18	8280	13400	2360	10400	24400	2770	13200	33800	3300	27
	MPS_6	30	83	17	67	148	48	71	171	23	69
	MPS_9	181	416	190	145	340	173	149	256	173	17
2	MPS_12	99	656	444	103	478	357	95	509	347	47
	MPS_20	29	325	148	67	287	142	71	355	174	35
	MPS_23	30	248	123	67	243	125	45	205	127	55
	Mary_2	228	486	466	171	476	425	199	539	643	5.4
	Mary_8	1030	697	430	486	575	373	479	549	345	65
3	Mary_13	84	487	465	115	476	423	97	443	480	39
	Mary_17	209	878	792	164	661	891	174	638	824	36
	Mary_22	458	1240	1010	261	829	1200	275	849	1240	44
	LAMB_6	796	498	305	371	481	388	347	431	325	44
	LAMB_9	766	515	330	363	500	421	381	464	337	36
	LAMB_10	788	472	216	369	452	269	266	299	199	17
4	LAMB_26	557	428	200	305	402	248	414	404	291	46
	LAMB_32	724	459	296	351	437	376	526	622	551	36
	LAMB_33	240	341	123	216	304	146	228	352	190	53
	LAMB_43	1400	744	498	539	759	645	497	780	644	2.5
	LAMB_45	315	118	64	237	52	66	92	36	24	1.1
	QEP_2	860	237	143	165	166	143	124	143	87	4.4
	QEP_9	913	944	254	348	513	313	404	501	308	3.7
5	QEP_24	847	1220	296	579	978	535	624	960	531	6.8
	QEP_36	857	555	455	448	570	457	323	616	450	2.2
	QEP_47	820	405	166	264	211	206	327	218	278	0.8

Figure D3: Log linear regression of 20 second pXRF measurements (a) before and (b) after data correction for all five metal-contaminated sites. (c) Impact of sample preparation at the highly heterogeneous Site 1 where multiple matrices were present. pXRF data was corrected using a small subset (5-10 % of samples) of ICP-MS measurements sampled directly after *in-situ* pXRF measurements. Where a systematic relationship existed between pXRF and ICP-MS, the gradient and intercept of the relationship was used to correct pXRF at each site individually. This data correction was successful at four of the five sites where one matrix dominated the site, however multiple matrices (soil and glassy black slag pieces) were present at Site 1, which resulted in poorer relationship between the two techniques. To minimise the physical matrix effects between the two matrices, light sample preparation was conducted on the Site 1 samples, which consisted of drying and lightly crushing the soil with a mortar and pestle. Sample preparation improved both the accuracy and precision of pXRF measurements, when compared to commercial ICP-MS data. This figure demonstrates that where a systematic relationship cannot be attained using *in-situ* pXRF and ICP-MS, light sample preparation can be used to achieve a stronger relationship between the two techniques, and can be used to correct the rest of the pXRF dataset.

Figure D4: a) Estimated total costs for the characterisation of metal-contaminated sites at the minimum sampling resolution for ICP–MS and *in-situ* pXRF. Cost assumptions include: labour call out rate = $150/hour, *in-situ* pXRF measurement = 20 secs, pXRF ownership cost = $83/assessment, time between samples = 45 secs, commercial laboratory eight element analysis = $22.60/sample. The cost of duplicate sampling to establish measurement uncertainty was not included given that this would vary according to the number of duplicate samples being taken. Circles in a) are estimated costs from the five-metal contaminated sites in this study, while diamonds are projected costs for sites larger than 3 ha. Soil Zn concentrations at Site 4 are shown for b) ICP–MS and c) pXRF Phase 1 measurement approaches, while d) real-time pXRF data enabled judgemental sampling directly after systematic sampling.

Figure D5: Point by point graphs of the impact of sample preparation on 20 second *in-situ* pXRF measurements at highly heterogeneous Site 1. Relative proximity (RP) gives an indication of pXRF inaccuracy when compared to a reference value (ICP-AES data) and is calculated by RP = (absolute (100 - recovery value).

Table D2: Estimation of measurement uncertainty and variance using duplicate sampling and repeat analyses for Mn, Zn and Pb concentrations at Sites 1-5 using *ex-situ* ICP-MS and *in-situ* pXRF measurement approaches. In-situ pXRF Mn, Zn and Pb concentrations were not corrected at Site 1, and were not corrected for Mn concentrations at Site 5, due to non-systematic relationships between pXRF and ICP-MS data. Variance components $s_{geochem}$, s_{samp}, s_{anal} and s_{meas} represent geochemical, sampling, analysis and measurement standard deviations, respectively. The expanded relative uncertainties (95 % CI) for sampling, analysis and measurements were U_{samp}, U_{anal} and U_{meas} respectively. RANOVA could not estimate $s_{geochem}$ in a few cases where variance by sampling was too great (i.e. Site 1) and are represented by n/a. Values displayed to 3 significant figures.

Site 1 - Mn

ICP-MS (n=3)

Target	S1A1	S1A2	S2A1	S2A2
B2	2700	2390	8020	9000
B5	5480	5030	510	510
B6	2260	2070	590	523

Mean	3260 mg/kg
SD	3610 mg/kg
$s_{geochem}$	n/a
s_{samp}	3600 mg/kg
s_{anal}	267 mg/kg
s_{meas}	3610 mg/kg
U_{samp}	221 %
U_{anal}	16.4 %
U_{meas}	222 %

In-situ pXRF (n=5)

Target	S1A1	S1A2	S2A1	S2A2
B8	293	271	800	610
B9	34400	34300	2040	2000
B11	7040	7160	510	354
B13	1540	1870	2250	2270
B18	2520	3410	1980	1850

Mean	3020 mg/kg
SD	3750 mg/kg
$s_{geochem}$	n/a
s_{samp}	3740 mg/kg
s_{anal}	126 mg/kg
s_{meas}	3750 mg/kg
U_{samp}	248 %
U_{anal}	8.37 %
U_{meas}	249 %

Site 1 - Zn

ICP-MS (n=3)

Target	S1A1	S1A2	S2A1	S2A2
B2	7524	7089	23500	25800
B5	12900	12200	1150	1110
B6	6506	6770	1720	1280

Mean	8967 mg/kg
SD	9959 mg/kg
$s_{geochem}$	968 mg/kg
s_{samp}	9903 mg/kg
s_{anal}	420 mg/kg
s_{meas}	9912 mg/kg
U_{samp}	221 %
U_{anal}	9.40 %
U_{meas}	221 %

In-situ pXRF (n=5)

Target	S1A1	S1A2	S2A1	S2A2
B8	1620	1570	2330	2070
B9	43000	42900	5690	5580
B11	12800	12900	2280	1970
B13	3880	4630	4870	4920
B18	5000	7860	4780	4650

Mean	6340 mg/kg
SD	6080 mg/kg
$s_{geochem}$	877 mg/kg
s_{samp}	6010 mg/kg
s_{anal}	177 mg/kg
s_{meas}	6010 mg/kg
U_{samp}	190 %
U_{anal}	5.57 %
U_{meas}	190 %

Site 1 - Pb

ICP-MS (n=3)

Target	S1A1	S1A2	S2A1	S2A2
B2	920	817	2170	2550
B5	1370	1390	265	245
B6	866	876	328	316

Mean	1010 mg/kg
SD	900 mg/kg
$s_{geochem}$	n/a
s_{samp}	899 mg/kg
s_{anal}	48.8 mg/kg
s_{meas}	900 mg/kg
U_{samp}	178 %
U_{anal}	9.68 %
U_{meas}	178 %

In-situ pXRF (n=5)

Target	S1A1	S1A2	S2A1	S2A2
B8	391	384	395	359
B9	4750	4840	1140	1150
B11	2380	2410	301	297
B13	1040	1100	1090	1110
B18	769	1270	1070	1040

Mean	1220 mg/kg
SD	1160 mg/kg
$s_{geochem}$	n/a
s_{samp}	1160 mg/kg
s_{anal}	32.6 mg/kg
s_{meas}	1160 mg/kg
U_{samp}	190 %
U_{anal}	5.36 %
U_{meas}	190 %

Site 2 - Mn

ICP-MS (n=3)

Target	S1A1	S1A2	S2A1	S2A2
P2	84.5	102	82.9	80.1
P6	34.7	38.3	38.4	36.0
P9	81.8	75.1	74.2	73.8

Mean	66.8 mg/kg
SD	30.5 mg/kg
$s_{geochem}$	29.8 mg/kg
s_{samp}	5.14 mg/kg
s_{anal}	3.82 mg/kg
s_{meas}	6.40 mg/kg
U_{samp}	15.4 %
U_{anal}	11.4 %
U_{meas}	19.2 %

In-situ pXRF (n=5)

Target	S1A1	S1A2	S2A1	S2A2
P6	69.6	67.8	127	130
P9	74.3	77.1	72.9	70.6
P12	97.0	97.0	115	99.8
P20	85.0	82.7	85.9	88.2
P23	109	100	65.0	LOD

Mean	90.0 mg/kg
SD	16.1 mg/kg
$s_{geochem}$	13.4 mg/kg
s_{samp}	8.69 mg/kg
s_{anal}	2.27 mg/kg
s_{meas}	8.99 mg/kg
U_{samp}	19.3 %
U_{anal}	5.05 %
U_{meas}	20.0 %

Site 2 - Zn

ICP-MS (n=3)

Target	S1A1	S1A2	S2A1	S2A2
P2	183	204	198	185
P6	131	125	128	122
P9	596	491	520	523

Mean	284 mg/kg
SD	247 mg/kg
$s_{geochem}$	247 mg/kg
s_{samp}	3.26 mg/kg
s_{anal}	11.9 mg/kg
s_{meas}	12.3 mg/kg
U_{samp}	2.30 %
U_{anal}	8.38 %
U_{meas}	8.70 %

In-situ pXRF (n=5)

Target	S1A1	S1A2	S2A1	S2A2
P6	168	168	205	205
P9	217	223	263	242
P12	337	339	476	453
P20	341	341	260	265
P23	300	278	286	286

Mean	283 mg/kg
SD	98.2 mg/kg
$s_{geochem}$	83.7 mg/kg
s_{samp}	51.0 mg/kg
s_{anal}	5.77 mg/kg
s_{meas}	51.3 mg/kg
U_{samp}	36.1 %
U_{anal}	4.10 %
U_{meas}	36.3 %

Site 2 - Pb

ICP-MS (n=3)

Target	S1A1	S1A2	S2A1	S2A2
P2	134	163	70.2	67.8
P6	30.1	30.5	34.8	33.1
P9	257	213.9	286	290

Mean	134 mg/kg
SD	136 mg/kg
$s_{geochem}$	127 mg/kg
s_{samp}	43.6 mg/kg
s_{anal}	8.79 mg/kg
s_{meas}	44.5 mg/kg
U_{samp}	65.0 %
U_{anal}	13.1 %
U_{meas}	66.3 %

In-situ pXRF (n=5)

Target	S1A1	S1A2	S2A1	S2A2
P6	27.9	27.8	37.6	37.0
P9	57.4	52.6	72.9	72.1
P12	121	124	274	236
P20	203	205	180	179
P23	344	341	169	172

Mean	147 mg/kg
SD	120 mg/kg
$s_{geochem}$	93.3 mg/kg
s_{samp}	74.9 mg/kg
s_{anal}	2.11 mg/kg
s_{meas}	75.0 mg/kg
U_{samp}	102 %
U_{anal}	2.90 %
U_{meas}	102 %

Site 3 - Mn

ICP-MS (n=3)

Target	S1A1	S1A2	S2A1	S2A2
M2	217	196	189	207
M3	112	115	141	115
M18	216	223	241	231

Mean	183 mg/kg
SD	64.2 mg/kg
$s_{geochem}$	62.3 mg/kg
s_{samp}	5.95 mg/kg
s_{anal}	13.0 mg/kg
s_{meas}	14.3 mg/kg
U_{samp}	6.50 %
U_{anal}	14.1 %
U_{meas}	15.5 %

In-situ pXRF (n=5)

Target	S1A1	S1A2	S2A1	S2A2
M2	134	142	182	207
M8	167	166	105	112
M13	90.6	98.6	128	128
M17	131	147	135	141
M22	223	271	156	212

Mean	152 mg/kg
SD	50.8 mg/kg
$s_{geochem}$	31.5 mg/kg
s_{samp}	37.8 mg/kg
s_{anal}	12.8 mg/kg
s_{meas}	39.9 mg/kg
U_{samp}	49.6 %
U_{anal}	16.7 %
U_{meas}	52.3 %

Site 3 - Zn

ICP-MS (n=3)

Target	S1A1	S1A2	S2A1	S2A2
M2	465	458	393	428
M3	426	466	372	414
M18	770	763	839	820

Mean	551 mg/kg
SD	245 mg/kg
$s_{geochem}$	240 mg/kg
s_{samp}	41.5 mg/kg
s_{anal}	23.2 mg/kg
s_{meas}	47.6 mg/kg
U_{samp}	15.1 %
U_{anal}	8.40 %
U_{meas}	17.3 %

In-situ pXRF (n=5)

Target	S1A1	S1A2	S2A1	S2A2
M2	337	336	430	447
M8	477	473	425	432
M13	462	475	461	435
M17	511	518	498	488
M22	889	792	706	838

Mean	480 mg/kg
SD	96.1 mg/kg
$s_{geochem}$	82.6 mg/kg
s_{samp}	47.0 mg/kg
s_{anal}	14.6 mg/kg
s_{meas}	49.2 mg/kg
U_{samp}	19.6 %
U_{anal}	6.10 %
U_{meas}	20.5 %

Site 3 - Pb

ICP-MS (n=3)

Target	S1A1	S1A2	S2A1	S2A2
M2	229	257	249	275
M3	390	448	315	353
M18	661	642	611	568

Mean	417 mg/kg
SD	216 mg/kg
$s_{geochem}$	209 mg/kg
s_{samp}	44.9 mg/kg
s_{anal}	29.9 mg/kg
s_{meas}	54.0 mg/kg
U_{samp}	21.6 %
U_{anal}	14.4 %
U_{meas}	25.9 %

In-situ pXRF (n=5)

Target	S1A1	S1A2	S2A1	S2A2
M2	LOD	LOD	111	126
M8	344	317	118	106
M13	291	337	478	382
M17	242	219	598	724
M22	1200	1360	1160	1110

Mean	562 mg/kg
SD	524 mg/kg
$s_{geochem}$	479 mg/kg
s_{samp}	202 mg/kg
s_{anal}	62.4 mg/kg
s_{meas}	212 mg/kg
U_{samp}	72.1 %
U_{anal}	22.2 %
U_{meas}	75.4 %

Site 4 - Mn

ICP-MS (n=5)

Target	S1A1	S1A2	S2A1	S2A2
L6	327	376	265	255
L19	288	337	350	362
L25	143	143	236	275
L27	249	282	380	364
L32	164	170	124	115

Mean	260 mg/kg
SD	108 mg/kg
$s_{geochem}$	82.1 mg/kg
s_{samp}	66.8 mg/kg
s_{anal}	22.5 mg/kg
s_{meas}	70.5 mg/kg
U_{samp}	51.4 %
U_{anal}	17.3 %
U_{meas}	54.2 %

In-situ pXRF (n=7)

Target	S1A1	S1A2	S2A1	S2A2
L6	286	292	325	303
L9	559	569	566	520
L10	556	517	434	405
L26	983	955	497	555
L32	1010	1050	767	774
L33	334	347	232	235
L43	587	529	895	901

Mean	571 mg/kg
SD	294 mg/kg
$s_{geochem}$	231 mg/kg
s_{samp}	180 mg/kg
s_{anal}	25.4 mg/kg
s_{meas}	182 mg/kg
U_{samp}	63.0 %
U_{anal}	8.90 %
U_{meas}	63.6 %

Site 4 - Zn

ICP-MS (n=5)

Target	S1A1	S1A2	S2A1	S2A2
L6	442	477	290	292
L19	456	437	496	488
L25	227	226	354	372
L27	331	365	421	394
L32	205	219	133	123

Mean	337 mg/kg
SD	142 mg/kg
$s_{geochem}$	111 mg/kg
s_{samp}	86.7 mg/kg
s_{anal}	16.4 mg/kg
s_{meas}	88.2 mg/kg
U_{samp}	51.4 %
U_{anal}	9.70 %
U_{meas}	52.3 %

In-situ pXRF (n=7)

Target	S1A1	S1A2	S2A1	S2A2
L6	253	295	369	362
L9	849	761	623	564
L10	527	390	659	556
L26	1210	1220	738	810
L32	1010	1050	954	832
L33	318	326	328	328
L43	406	340	683	677

Mean	623 mg/kg
SD	338 mg/kg
$s_{geochem}$	288 mg/kg
s_{samp}	168 mg/kg
s_{anal}	52.1 mg/kg
s_{meas}	176 mg/kg
U_{samp}	53.8 %
U_{anal}	16.8 %
U_{meas}	56.4 %

Site 5 – Mn

ICP-MS (n=6)

Target	S1A1	S1A2	S2A1	S2A2
Q2	217	246	241	241
Q3	270	271	301	339
Q15	317	317	188	178
Q29	265	216	282	263
Q32	278	269	281	291
Q38	421	374	287	278

Mean	274 mg/kg
SD	60.6 mg/kg
$s_{geochem}$	n/a
s_{samp}	58.0 mg/kg
s_{anal}	17.7 mg/kg
s_{meas}	60.6 mg/kg
U_{samp}	42.3 %
U_{anal}	13.0 %
U_{meas}	44.3 %

In-situ pXRF (n=7)

Target	S1A1	S1A2	S2A1	S2A2
Q2	775	593	647	622
Q9	155	150	280	289
Q17	994	1060	1640	1980
Q18	1110	1200	868	884
Q24	1110	1120	1690	1170
Q36	1070	973	1040	919
Q47	618	712	1190	1150

Mean	958 mg/kg
SD	432 mg/kg
$s_{geochem}$	336 mg/kg
s_{samp}	260 mg/kg
s_{anal}	76.2 mg/kg
s_{meas}	271 mg/kg
U_{samp}	54.3 %
U_{anal}	15.9 %
U_{meas}	56.6 %

Site 5 - Zn

ICP-MS (n=6)

Target	S1A1	S1A2	S2A1	S2A2
Q2	296	315	347	347
Q3	386	396	499	538
Q15	486	456	258	257
Q29	344	304	399	361
Q32	470	269	252	262
Q38	702	711	396	417

Mean	386 mg/kg
SD	129 mg/kg
$s_{geochem}$	n/a
s_{samp}	127 mg/kg
s_{anal}	21.3 mg/kg
s_{meas}	129 mg/kg
U_{samp}	65.9 %
U_{anal}	11.1 %
U_{meas}	66.8 %

In-situ pXRF (n=7)

Target	S1A1	S1A2	S2A1	S2A2
Q2	239	435	359	356
Q9	133	126	226	216
Q17	133	169	352	377
Q18	527	545	670	663
Q24	325	326	661	640
Q36	228	190	182	183
Q47	854	888	1050	919

Mean	401 mg/kg
SD	259 mg/kg
$s_{geochem}$	230 mg/kg
s_{samp}	118 mg/kg
s_{anal}	20.4 mg/kg
s_{meas}	120 mg/kg
U_{samp}	59.0 %
U_{anal}	10.2 %
U_{meas}	59.8 %

Site 5 - Pb

ICP-MS (n=6)

Target	S1A1	S1A2	S2A1	S2A2
Q2	256	266	202	222
Q3	203	193	207	236
Q15	407	387	208	218
Q29	236	206	292	234
Q32	192	182	136	146
Q38	384	430	396	397

Mean	253 mg/kg
SD	85.5 mg/kg
$s_{geochem}$	75.6 mg/kg
s_{samp}	36.0 mg/kg
s_{anal}	17.4 mg/kg
s_{meas}	40.0 mg/kg
U_{samp}	28.4 %
U_{anal}	13.7 %
U_{meas}	31.6 %

In-situ pXRF (n=7)

Target	S1A1	S1A2	S2A1	S2A2
Q2	199	160	205	199
Q9	29.2	23.4	64.1	58.4
Q17	109	98.0	365	477
Q18	468	459	530	541
Q24	390	379	1150	1330
Q36	180	176	198	180
Q47	301	356	600	618

Mean	334 mg/kg
SD	282 mg/kg
$s_{geochem}$	224 mg/kg
s_{samp}	170 mg/kg
s_{anal}	17.5 mg/kg
s_{meas}	171 mg/kg
U_{samp}	102 %
U_{anal}	10.5 %
U_{meas}	103 %

Appendix E

Reference in paper	Reference in thesis	Caption
Supplementary Figure 1	Figure E1	VegeSafe soil sampling instructions for the collection of garden soil samples.
Supplementary Figure 2	Figure E2	VegeSafe consent form to be completed before samples are screened.
Supplementary Figure 3	Figure E3	Comparison of pXRF soil metal concentration data to a) certified reference materials for Pb and ICP-AES laboratory data for b) Pb, c) Mn, d) Cu, e) Zn and f) As. Regression relationship (solid red line) and 100% recovery (dashed black line) are shown in each plot.
Supplementary Figure 4	Figure E4	Soil manganese concentrations in front yard (n=92), drip line (n=97), back yard (n=80) and vegetable gardens (n=141) areas in private residences of Sydney, Australia.
Supplementary Figure 5	Figure E5	Soil copper concentrations in front yard (n=92), drip line (n=97), back yard (n=80) and vegetable gardens (n=141) areas in private residences of Sydney, Australia.
Supplementary Figure 6	Figure E6	Soil zinc concentrations in front yard (n=92), drip line (n=97), back yard (n=80) and vegetable gardens (n=141) areas in private residences of Sydney, Australia.
Supplementary Figure 7	Figure E7	Soil arsenic concentrations in front yard (n=92), drip line (n=91), back yard (n=79) and vegetable gardens (n=140) areas in private residences of Sydney, Australia.
Supplementary Figure 8	Figure E8	Example of VegeSafe soil screening report.
	Excerpt E1	Submitted Letter to the editor in August issue of *Chemistry in Australia.*

VegeSafe - We love your dirt!

**Sample locations at your property:**

We would like you to take 5 samples from 3 sites (i.e. a total of 5 soil samples) from your garden area. Collect the soils when dry if you can. This will help us speed up the analysis on the day.

Site 1: Identify 3 places for soil sampling either where you already have vegetable beds or where you plan to start your veggie patch.

Site 2: Identify another sample site such as your front or rear garden or if you don't have a these as unpaved areas, a site on or adjacent to the roadside verge.

Site 3: Identify a sample site below the drip line of your gutter, close to your house.

How to sample and store your soil sample:
- At each site, use the trowel or scoop to take soil from the top 2 cm of the sampled area, i.e. the surface soil. If there is grass or other vegetation cover, you will need to remove it and take the soil from underneath.

- Collect about a cricket ball size amount of soil (more is better than less) from an area of ~ 30 x 30 cm, or up to a 1 m^2 if required.

- Put the soil sample in a **ziplock bag** and seal it. Don't worry about grass or sticks or rocks—we will remove these when we prepare the soil for testing.

- Label the ziplock bags with a permanent marker and include the site location and brief description, date the sample was collected, the address and the postcode. Then put the bagged sample inside another ziplock bag – this protects the label and helps protect against leakage if the inner bags splits.

- Labeling – make sure the label makes sense to you so you can explain it to us when we receive your sample e.g. veggie patch sample 1; veggie patch sample 2, front yard soil; dripline soil north side of house, etc. Below is an example of a labeled bag.

https://research.science.mq.edu.au/vegesafe/index.html

Updated August 21st 2015

Figure E1: VegeSafe soil sampling instructions for the collection of garden soil samples.

MACQUARIE University

VegeSafe Consent Form

VegeSafe web page:
http://research.science.mq.edu.au/vegesafe/

or our Facebook page:
facebook.com/pages/VegeSafe/571316076267515

Thank you very much for participating in the VegeSafe soil testing program provided by Environmental Science Staff at Macquarie University.

As part of your participation in this program, we would like to be able to use the results to produce a map showing the information. The map data will be de-identified to the extent that the locations will only be accurate to within 25 m and no address or other information will be included that can be used to specifically identify the precise locations of the soil samples. We may also use the same results, with your permission, in future publications, again with the aforementioned limitations. Therefore, in signing this form you acknowledge consent for these purposes.

We have run our project past the National Health and Medical Research Council Ethics and they have informed us as follows:

"*As collection of the soil samples and proposed analysis do not relate specifically to human health, medicine or human research, the National Statement on Ethical Conduct in Human Research does not apply.*" (NHMRC Ethics, June 2013).

We will provide you with a summary of the results and some links to documentation to provide guidance on soils and potential lead and other metal exposure.

Donations - We Need Your Support

VegeSafe currently operates as a Community Service and runs on the good will of staff and students. However, tax deductible donations to support our program can be made via the following link: MQ.edu.au/supporting or by sending in with the sample parcel. If your donation is specifically for our program please don't forget to register that fact when giving your support.

Name: _____ Email address: _____

Address of soil samples: _____

Primary construction material of property: _____
(e.g. double brick, timber, fibro, etc.)

Any exterior walls of the property painted?:
_____

Sample code (A, B, C, D, E)	Sample description (e.g. Veggie patch 1)

Approximate age of property: _____ years

Signature_____

Date: _____

Updated August 21st 2015

Figure E2: VegeSafe consent form to be completed before samples are screened.
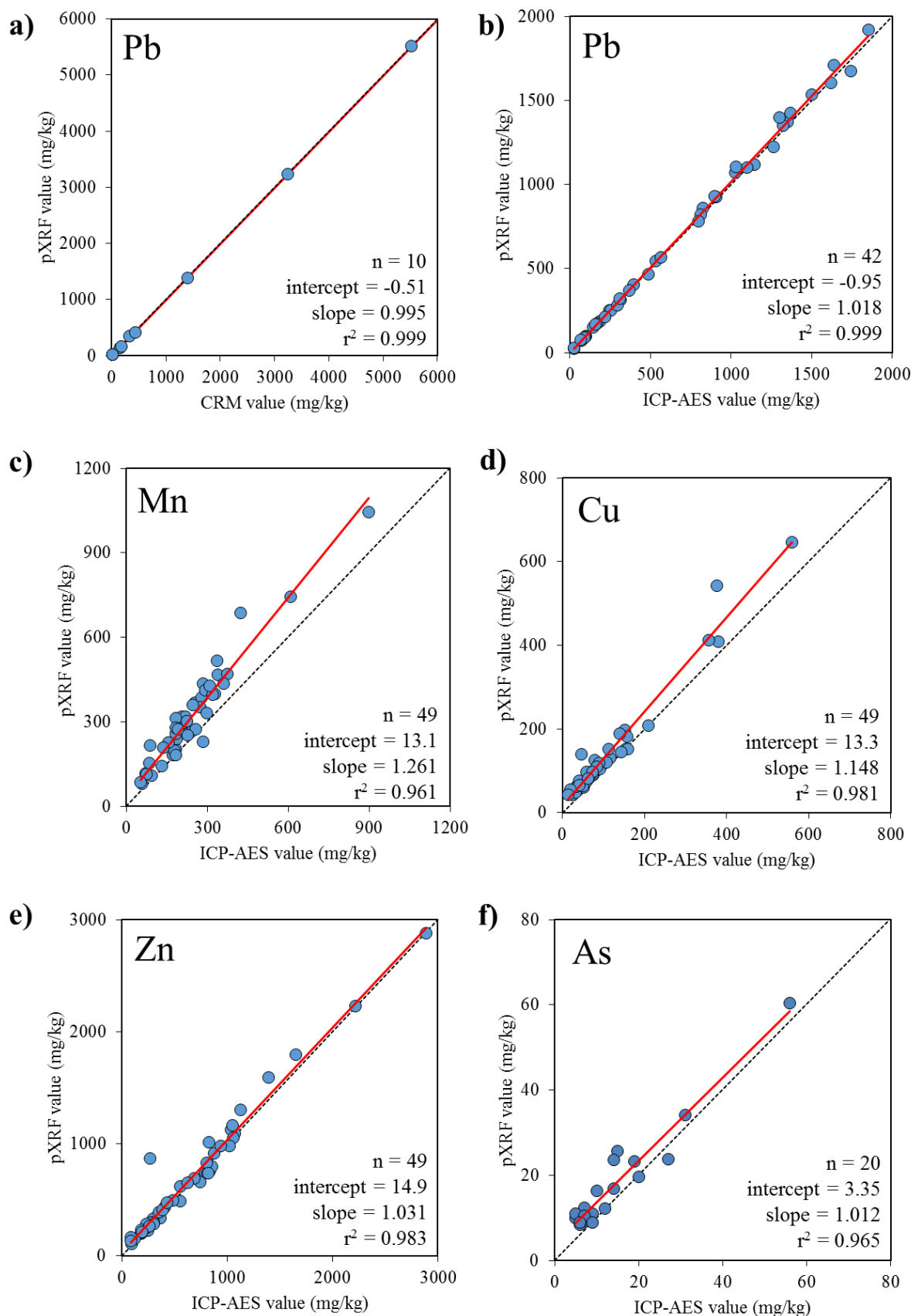
Figure E3: Comparison of pXRF soil metal concentration data to a) certified reference materials for Pb and ICP-AES laboratory data for b) Pb, c) Mn, d) Cu, e) Zn and f) As. Regression relationship (solid red line) and 100% recovery (dashed black line) are shown in each plot.
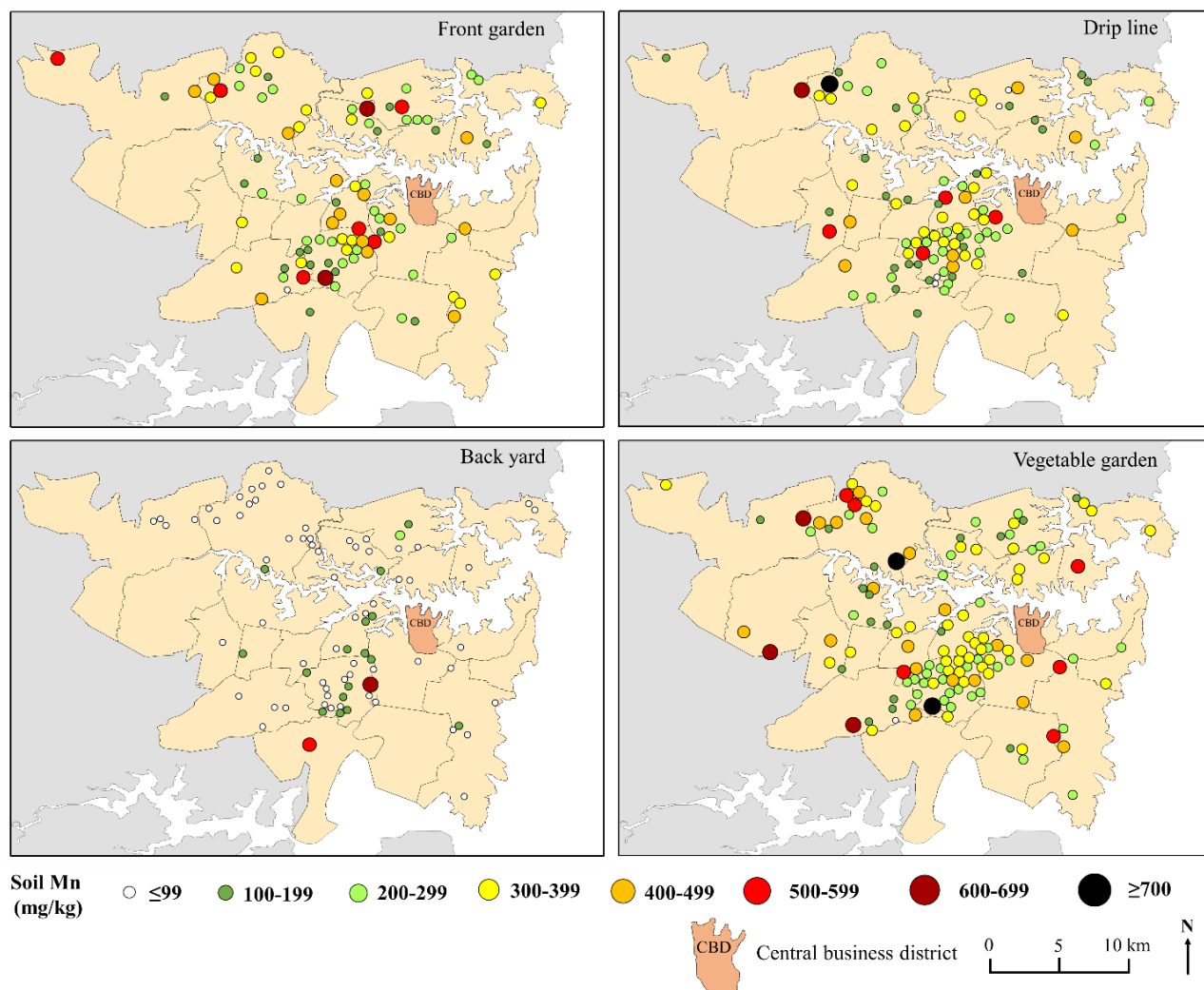
Figure E4: Soil manganese concentrations in front yard (n=92), drip line (n=97), back yard (n=80) and vegetable gardens (n=141) areas in private residences of Sydney, Australia.
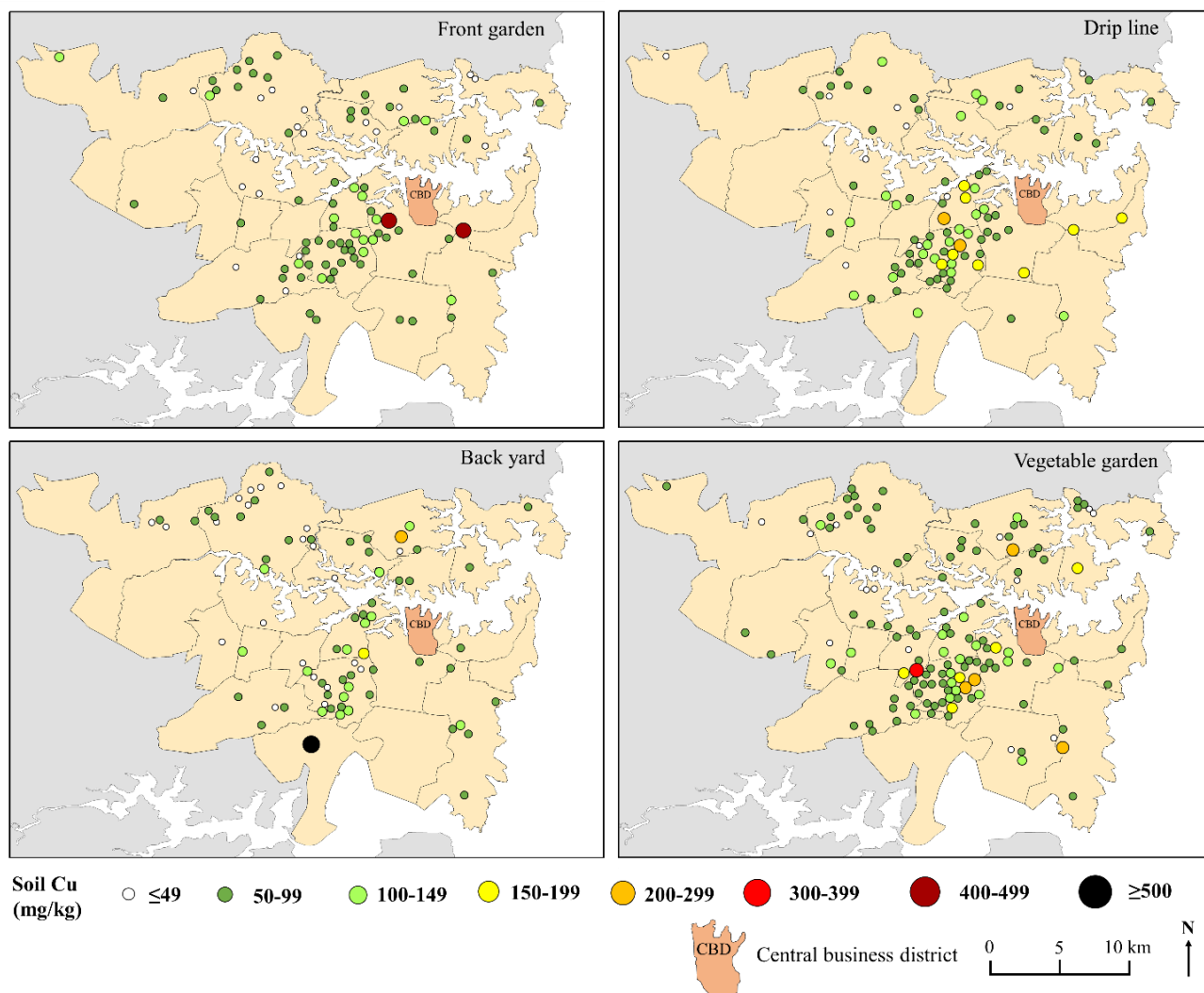
Figure E5: Soil copper concentrations in front yard (n=92), drip line (n=97), back yard (n=80) and vegetable gardens (n=141) areas in private residences of Sydney, Australia.
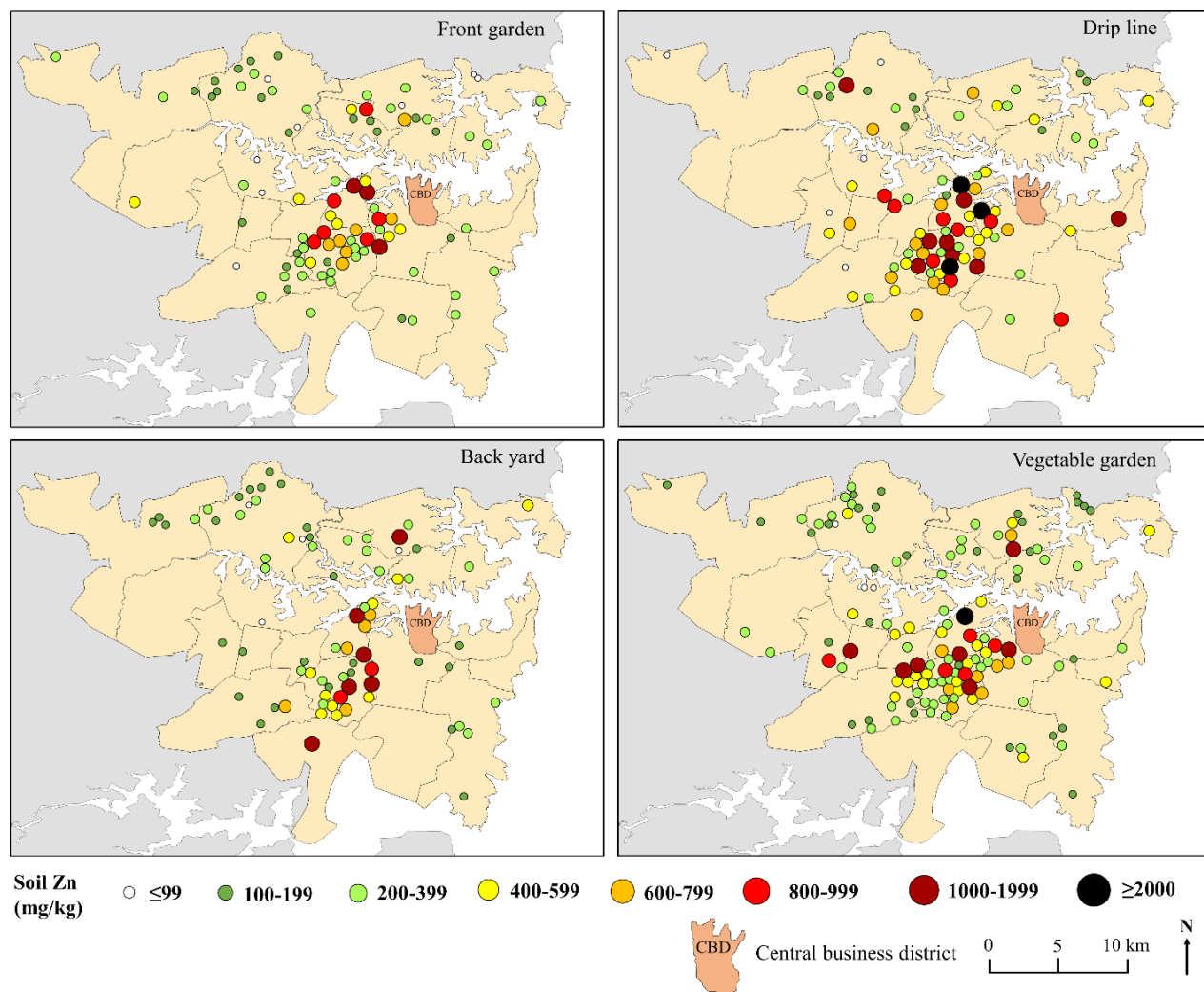
Figure E6: Soil zinc concentrations in front yard (n=92), drip line (n=97), back yard (n=80) and vegetable gardens (n=141) areas in private residences of Sydney, Australia.

Figure E7: Soil arsenic concentrations in front yard (n=92), drip line (n=91), back yard (n=79) and vegetable gardens (n=140) areas in private residences of Sydney, Australia.
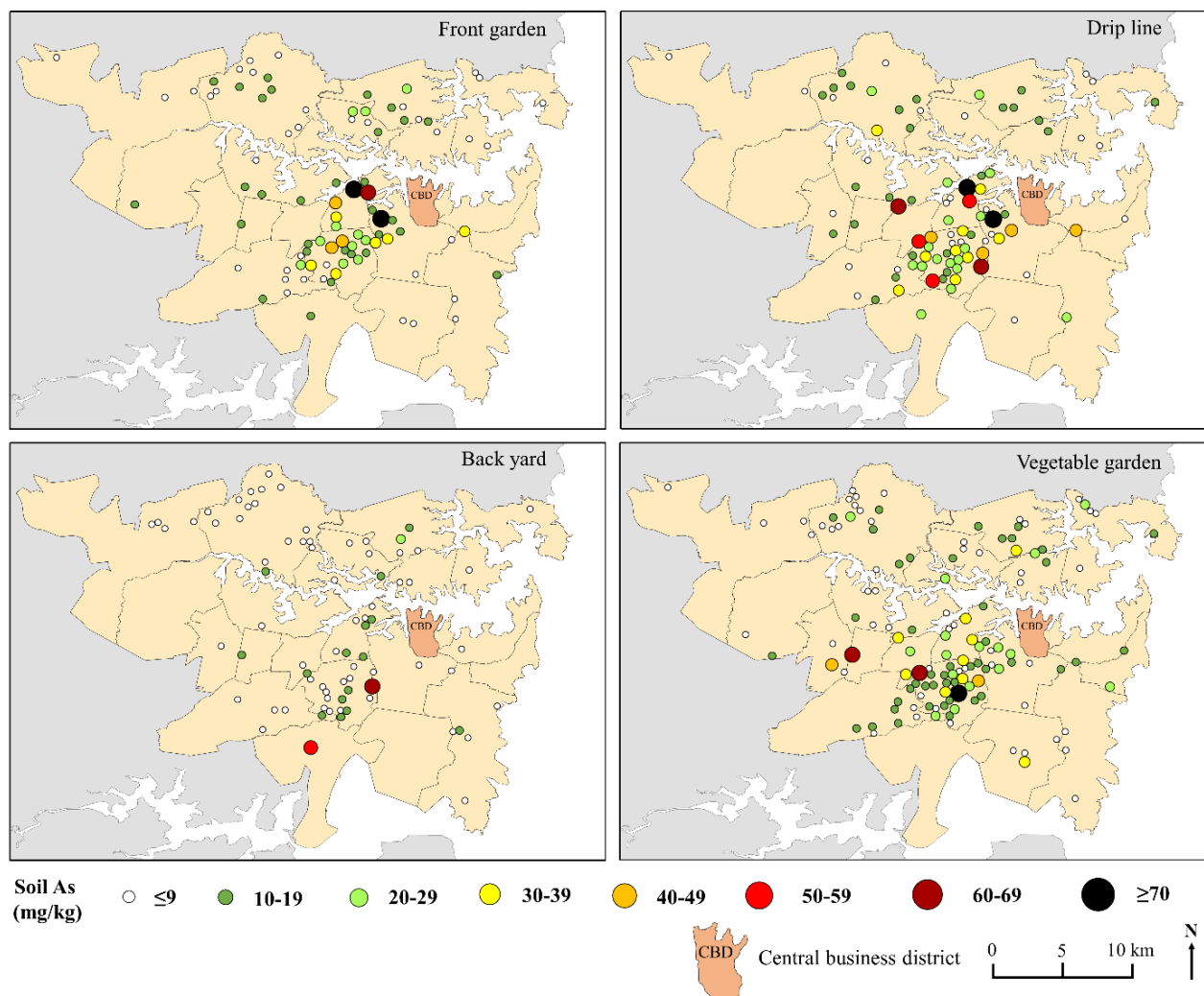
MACQUARIE UNIVERSITY

VegeSafe, Environmental Science, Macquarie University

Dear VegeSafe participant:

Below are the total metal concentrations results from the X-ray fluorescence analysis of your soils. The analysis of your soil is subject to various limitations including moisture content of the soil, its grain size and organic content. In a standard laboratory test additional and more intensive preparation of your soil samples would occur allowing greater reliability of the results. Therefore, we advise you that the analyses provided below are subject to these technical limitations and should be taken as a guide to the metal content of your soil. If you require more detailed analyses we recommend that you submit your samples to a laboratory accredited by NATA, which is the National Association of Testing Authorities – http://www.nata.asn.au/facilities-and-labs. We have made a short guide of how to deal with soil that may be contaminated with elevated lead or other metals – this can be found at the following website: http://research.science.mq.edu.au/vegesafe/advice-on-soil/.

Sample ID	Soil Location	As (mg/kg)	Cd (mg/kg)	Cr (mg/kg)	Cu (mg/kg)	Mn (mg/kg)	Pb (mg/kg)	Ni (mg/kg)	Zn (mg/kg)
A	Veggie patch 1	0	0	0	17	119	69.7	0	87
B	Veggie patch 2	0	0	30	42	141	225	0	315
C	Rear yard	12	0	21	46	189	245	0	341
D	Under eave / deck	29	0	45	136	161	609	19	718
E	Front verge (Chandos Street)	12	0	27	86	215	267	13	428

As – arsenic; Cd – cadmium; Cr – chromium; Cu – copper; Mn – manganese; Pb – lead; Ni – nickel; Zn - zinc

Element (mg/kg)	Australia NEPC[1] (2013)			California CEPA[2] (2005)	Canada CCME[3] (2013)	Norway NPCA[4] (2009)	United States EPA[5] (2013)
	Residential A	Residential B	Recreational C				
Arsenic	100	500	300	0.07	12	12	0.61
Cadmium	20	150	90	1.7	10	12.2	7
Chromium VI	100	500	300	17	0.4	75	0.29
Copper	6,000	30,000	17,000	3,000	63	150	310
Lead	300	1,200	600	80*	140	90	400
Manganese	3,800	14,000	19,000	-	-	-	180
Nickel	400	1,200	1,200	1,600	50	90	150
Zinc	7,400	60,00	30,000	23,00	200	300	2,300

The complete version of these guidelines along with links to the guidelines is available at http://research.science.mq.edu.au/vegesafe/advice-on-soil/. Residential A = with garden/accessible soil; Residential B = with minimal access to soil; Recreational C = public open space

Further information: Contact Professor Mark P. Taylor (mark.taylor@mq.edu.au), A/Professor Damian Gore (damian.gore@mq.edu.au) or Marek Rouillon (marek.rouillon@mq.edu.au)

Disclaimer All analyses or recommendations contained in this document are made in good faith and on the basis of information, national and international standards, measurements or guidelines supplied to or obtained by Macquarie University at the date of preparation of this document. You are strongly encouraged to seek independent medical advice or obtain independent testing of the soil in your property prior to taking any action based on this report. Macquarie University, its officers, employees and contractors are not liable for any loss (including legal costs and expenses), injury or damage including economic loss and consequential loss or liability incurred or suffered by you or your successors in title or any other party acting or purporting to act in reliance on the contents of this report.

Figure E8: Example of VegeSafe soil screening report.

Excerpt E1: Submitted Letter to the editor in August issue of *Chemistry in Australia.*

The work done by the Macquarie University team on lead concentrations in Sydney backyards (*Chem Aust* June 2017) is an admirable example of chemistry being applied for the public good. However, it seems Mark Taylor's team might be mis-applying the soil Health Investigation Levels (HILs) set out in the *National Environment Protection (Assessment of site contamination) Measure* 1999 ("the NEPM"), which sets the standards for conducting contaminated site investigations in Australia (it was updated in 2013). They write of the "300 mg/kg Australian health guideline" for lead in soil. The value of 300 mg/kg is the HIL applicable for low density housing and other sensitive sites (*e.g.* primary schools, childcare centres). However, the NEPM explicitly states: "*Investigation and screening levels are not clean-up or response levels nor are they desirable soil quality criteria*".

The HILs were set on the basis of a number of assumptions about human exposures and the characteristics of the contaminant in solution. These include: home grown fruit and vegetables represent less than 10% of the total amount consumed; the lead in soil is only 50% bioavailable, and; a blood lead concentration of 10 mg/dL is the target that should not be exceeded. The NHMRC has more recently revised this last value to 5mg/dL. These are among the range of factors to be considered if lead (or other contaminant) concentrations exceed the relevant HIL.

The NEPM provides additional guidance about how the HIL values should be applied. It suggests that where a HIL is exceeded, the 95% upper confidence limit of the mean concentration, the standard deviation of results, and the maximum concentration also be considered. Under some circumstances, it may be acceptable to allow soil with individual sample concentrations up to 250% of the HIL to remain on site. Therefore, in the data provided by Taylor's team, many of the soil samples taken in backyards and vegetable gardens, and with lead concentrations greater than 300 mg/kg, might be acceptable for on-site use.

The article is right to point out that that airborne lead and lead-based paint on the site can contribute to elevated lead concentrations in soil. However, caution also needs to be exercised in importing "clean garden soil" into garden beds. Occasionally, these soils from garden suppliers have a proportion of sewage treatment plant sludge incorporated in the mix, and elevated concentrations of metals can be present.

Paul Moritz FRACI
Contaminated sites auditor (Vic and NSW)

Appendix F

Reference in paper	Reference in thesis	Caption
Supplementary Data 1	Table F1	Soil metal(loid) concentrations (pXRF derived) for public (Zone A SB; A – sampling zone number, B – sample site) and private (PRSXY; X – property code, Y – sample number on property) samples. All concentrations mg/kg except where * denotes wt%.
Supplementary Data 2	Table F2	Soil PAH concentrations for the Newcastle city. All concentrations in mg/kg.
Supplementary Data 3	Table F3	Supplementary Data 3. Lead isotope compositions for soils, slag and galena. Standard deviations determined from repeat analysis (10 analyses) of one sample. Soil samples: public (Zone A SB; A – sampling zone number, B – sample site), private (PRSXY; X – property code, Y – sample number on property) and depth (SDPX X-Y cm; where X is the depth profile number and X-Y is the depth).
Supplementary Data 4	Table F4	Relative abundances of phases were estimated from XRD patterns using the relative intensity ratio (RIR) method.

Table F1: Soil metal(loid) concentrations (pXRF derived) for public (Zone A SB; A – sampling zone number, B – sample site) and private (PRSXY; X – property code, Y – sample number on property) samples. All concentrations mg/kg except where * denotes wt%.

Sample	x co-ordinate	y co-ordinate	Ti	Cr	Mn	Fe*	Zn	As	Cd	Pb
Zone 1 S1	151.754117	-32.921500	4,770	130	1,120	3.51	520	41	<LOD	300
Zone 1 S2	151.757272	-32.917458	10,100	110	1,200	3.88	990	41	<LOD	590
Zone 1 S3	151.755289	-32.918547	3,750	77	820	2.58	800	18	<LOD	280
Zone 1 S4	151.752281	-32.918856	1,930	54	560	2.07	600	17	<LOD	250
Zone 1 S5	151.749133	-32.918808	4,710	120	1,470	3.53	2,010	56	<LOD	1,820
Zone 1 S6	151.745742	-32.914514	4,650	97	3,190	4.15	2,230	60	<LOD	1,310
Zone 1 S7	151.743853	-32.912803	5,130	190	2,110	5.97	1,990	69	<LOD	1,550
Zone 1 S8	151.746250	-32.911394	6,300	190	1,270	5.17	510	37	<LOD	340
Zone 1 S9	151.750283	-32.914881	4,750	170	2,090	5.30	2,660	180	<LOD	4,650
Zone 1 S10	151.753450	-32.916361	4,850	170	1,830	4.27	1,410	25	<LOD	500
Zone 1 S11	151.754900	-32.914300	3,670	59	500	2.20	270	9	<LOD	62
Zone 1 S12	151.753094	-32.910250	4,650	160	3,880	5.69	1,690	83	3	1,650
Zone 1 S13	151.759181	-32.909817	3,660	94	720	2.25	520	19	<LOD	160
Zone 1 S14	151.759392	-32.906031	7,030	260	3,580	10.30	9,470	87	10	1,120
Zone 1 S15	151.756672	-32.904525	5,480	180	1,450	5.22	2,010	55	6	730
Zone 1 S16	151.754450	-32.904392	2,800	90	1,600	3.18	630	17	<LOD	230
Zone 1 S17	151.755342	-32.907642	3,770	57	610	2.51	140	9	<LOD	35
Zone 1 S18	151.750922	-32.907825	3,940	110	1,120	3.39	2,000	130	<LOD	740
Zone 1 S19	151.750175	-32.904172	2,700	75	1,670	2.43	470	15	<LOD	150
Zone 1 S20	151.753067	-32.898278	5,500	210	4,490	14.17	5,090	130	16	2,060
Zone 1 S21	151.748775	-32.895000	3,810	230	3,410	9.71	1,910	35	4	590
Zone 1 S22	151.747103	-32.899675	5,160	200	2,450	9.51	1,230	50	<LOD	790
Zone 1 S23	151.745039	-32.903125	5,640	160	1,200	3.99	400	14	<LOD	240
Zone 1 S24	151.742175	-32.900814	3,900	140	1,040	3.30	1,070	25	<LOD	450
Zone 1 S25	151.744000	-32.896467	4,120	100	2,210	4.85	1,470	34	<LOD	640
Zone 1 S26	151.738069	-32.890289	3,520	92	1,040	3.39	680	12	<LOD	210
Zone 1 S27	151.734183	-32.891683	4,050	140	500	3.22	340	11	<LOD	110
Zone 1 S28	151.731650	-32.893592	6,150	220	1,240	4.08	610	23	<LOD	590
Zone 1 S29	151.727119	-32.889044	4,450	210	1,870	4.27	900	22	<LOD	450
Zone 2 S1	151.763972	-32.907889	6,290	160	1,810	4.80	690	24	<LOD	290
Zone 2 S2	151.765667	-32.908611	4,920	81	1,980	3.94	830	29	<LOD	410
Zone 2 S3	151.766972	-32.907528	4,950	120	1,760	3.57	1,500	14	<LOD	270
Zone 2 S4	151.768639	-32.907889	13,700	710	3,630	17.08	12,100	200	7	2,550
Zone 2 S5	151.762028	-32.910972	5,130	92	546	2.82	140	6	<LOD	33
Zone 2 S6	151.764389	-32.910306	5,110	140	2,600	4.86	1,870	45	4	1,240
Zone 2 S7	151.766500	-32.910806	5,660	140	2,580	4.92	1,860	51	<LOD	1,240
Zone 2 S8	151.768417	-32.909250	5,670	350	3,110	7.18	2,570	61	6	930
Zone 2 S9	151.769806	-32.910778	6,560	330	2,370	4.15	1,130	23	<LOD	280
Zone 2 S10	151.762306	-32.912917	4,300	60	650	2.65	200	14	<LOD	57
Zone 2 S11	151.765167	-32.912889	5,200	130	2,100	4.39	3,050	69	<LOD	1,300
Zone 2 S12	151.767861	-32.912028	3,670	83	1,500	3.09	790	44	<LOD	400
Zone 2 S13	151.765417	-32.914111	3,690	110	1,540	3.00	1,010	32	<LOD	500
Zone 2 S14	151.768333	-32.914083	4,810	180	1,240	5.08	1,950	76	5	930
Zone 2 S15	151.761278	-32.915472	14,800	690	3,250	7.00	4,690	73	<LOD	900
Zone 2 S16	151.764556	-32.916500	4,950	120	1,230	3.54	1,040	36	<LOD	630

Sample	x co-ordinate	y co-ordinate	Ti	Cr	Mn	Fe*	Zn	As	Cd	Pb
Zone 2 S17	151.765389	-32.919556	6,280	190	1,540	4.34	4,260	380	5	2,770
Zone 2 S18	151.766722	-32.918250	4,990	120	1,850	4.11	2,290	42	11	1,220
Zone 2 S19	151.766972	-32.917083	6,040	200	1,530	4.48	4,940	96	13	1,970
Zone 3 S1	151.760889	-32.923492	3,450	59	660	2.21	360	13	<LOD	190
Zone 3 S2	151.762344	-32.924817	4,310	69	1,260	3.69	640	74	<LOD	370
Zone 3 S3	151.765656	-32.925775	3,770	120	770	2.71	690	23	<LOD	220
Zone 3 S4	151.769256	-32.925933	5,110	88	840	3.58	390	44	<LOD	230
Zone 3 S5	151.771983	-32.926467	4,890	91	541	2.79	320	10	<LOD	230
Zone 3 S6	151.775775	-32.925344	3,030	38	790	1.70	240	10	<LOD	39
Zone 3 S7	151.780153	-32.925839	4,500	78	820	2.28	140	6	<LOD	45
Zone 3 S8	151.785872	-32.925525	4,490	88	300	2.03	96	6	<LOD	22
Zone 3 S9	151.789786	-32.924081	4,950	81	730	2.90	380	14	<LOD	150
Zone 3 S10	151.791397	-32.923228	5,740	92	580	2.80	180	9	<LOD	68
Zone 4 S1	151.787817	-32.926988	5,460	140	660	2.78	170	8	<LOD	27
Zone 4 S2	151.785853	-32.927366	4,160	72	360	2.22	250	19	<LOD	110
Zone 4 S3	151.783673	-32.928302	1,750	55	790	1.82	800	21	<LOD	270
Zone 4 S4	151.779448	-32.929244	4,810	68	370	2.03	290	23	<LOD	560
Zone 4 S5	151.782722	-32.932442	5,910	130	680	5.14	220	56	<LOD	50
Zone 4 S6	151.778754	-32.931607	5,240	87	100	4.09	1,220	63	<LOD	3,450
Zone 4 S7	151.775584	-32.930542	3,870	94	660	2.50	170	5	<LOD	23
Zone 4 S8	151.776879	-32.929139	4,280	76	560	2.55	230	6	<LOD	75
Zone 4 S9	151.773684	-32.928170	4,400	74	430	2.12	280	7	<LOD	120
Zone 4 S10	151.770599	-32.929525	3,550	71	1,010	2.17	650	39	<LOD	720
Zone 4 S11	151.770951	-32.932130	8,890	140	280	1.67	98	25	<LOD	41
Zone 4 S12	151.767797	-32.930565	1,920	41	730	1.36	630	13	<LOD	360
Zone 4 S13	151.765789	-32.928902	6,590	160	920	3.27	510	13	<LOD	200
Zone 4 S14	151.766179	-32.927340	4,570	80	950	2.26	230	6	<LOD	150
Zone 4 S15	151.765789	-32.928902	5,390	100	830	3.29	300	23	<LOD	330
Zone 4 S16	151.762763	-32.926629	4,470	91	780	3.62	1,880	22	<LOD	620
Zone 4 S17	151.764658	-32.927587	5,760	110	860	3.58	510	17	<LOD	470
Zone 4 S18	151.789719	-32.926185	6,470	84	560	2.76	230	14	<LOD	69
Zone 4 S19	151.789625	-32.927671	5,880	130	540	2.96	130	9	<LOD	20
Zone 4 S20	151.785676	-32.925958	5,000	98	230	2.45	130	10	<LOD	120
Zone 4 S21	151.783617	-32.930237	5,970	110	540	2.83	460	21	<LOD	450
Zone 4 S22	151.777405	-32.930160	3,810	63	550	2.31	220	11	<LOD	83
Zone 4 S23	151.789632	-32.926502	6,340	93	740	3.41	150	7	<LOD	14
Zone 4 S24	151.784438	-32.927336	5,270	110	920	3.63	1,370	38	3	1,250
Zone 4 S25	151.770352	-32.928371	1,670	52	350	1.59	180	11	<LOD	53
Zone 5 S1	151.755858	-32.926782	3,870	63	780	2.64	420	12	<LOD	210
Zone 5 S2	151.755046	-32.927209	3,970	78	970	2.56	400	11	<LOD	120
Zone 5 S3	151.758133	-32.928261	3,500	96	1,100	2.34	540	18	<LOD	410
Zone 5 S4	151.754604	-32.930872	4,660	77	1,110	2.84	430	17	<LOD	220
Zone 5 S5	151.750771	-32.930600	2,320	77	580	1.84	280	8	<LOD	120
Zone 5 S6	151.753740	-32.933156	4,620	73	1,220	2.81	470	14	<LOD	240
Zone 5 S7	151.750693	-32.934451	4,970	80	700	2.59	280	36	<LOD	220
Zone 5 S8	151.750418	-32.937009	3,890	77	600	2.83	730	22	<LOD	560
Zone 5 S9	151.753171	-32.936175	4,590	68	600	2.34	330	83	<LOD	260
Zone 5 S10	151.755987	-32.938211	3,770	65	870	2.55	240	11	<LOD	180

Sample	x co-ordinate	y co-ordinate	Ti	Cr	Mn	Fe*	Zn	As	Cd	Pb
Zone 5 S11	151.756269	-32.935044	3,440	74	980	2.07	680	13	<LOD	250
Zone 5 S12	151.758250	-32.936281	4,250	86	600	2.53	600	33	<LOD	310
Zone 5 S13	151.760791	-32.937766	4,240	83	180	2.21	270	18	<LOD	440
Zone 5 S14	151.763637	-32.938862	4,790	74	750	2.42	550	42	<LOD	460
Zone 5 S15	151.763484	-32.935614	4,270	79	1,400	3.13	860	34	<LOD	590
Zone 5 S16	151.767670	-32.934845	4,290	57	320	2.06	190	15	<LOD	150
Zone 5 S17	151.765772	-32.934974	2,550	55	540	1.96	230	10	<LOD	140
Zone 5 S18	151.763240	-32.933954	5,360	88	590	2.85	190	10	<LOD	46
Zone 5 S19	151.762349	-32.931880	5,110	75	560	2.58	130	14	<LOD	71
Zone 5 S20	151.758135	-32.932137	3,610	83	1,480	3.08	780	47	<LOD	400
PRS1A	151.755494	-32.931677	2,900	85	760	1.97	640	33	<LOD	780
PRS1B	151.755494	-32.931677	3,940	83	670	2.07	530	39	<LOD	1,460
PRS1C	151.755494	-32.931677	2,520	80	700	2.10	500	25	<LOD	330
PRS2A	151.765575	-32.935832	5,440	73	330	2.09	610	39	<LOD	900
PRS2B	151.765575	-32.935832	5,230	89	460	2.28	400	21	<LOD	510
PRS2C	151.765575	-32.935832	4,140	100	490	2.33	2,090	85	<LOD	2,210
PRS3A	151.753439	-32.910121	4,470	97	790	2.99	880	25	<LOD	840
PRS3B	151.753439	-32.910121	5,670	120	790	3.61	1,030	48	<LOD	1,550
PRS3C	151.753439	-32.910121	5,460	120	1,850	4.32	1,130	63	<LOD	1,740
PRS3D	151.753439	-32.910121	6,790	220	2,220	5.61	6,240	85	3	3,420
PRS4A	151.750841	-32.914811	5,510	110	1,710	4.17	1,630	55	<LOD	1,730
PRS4B	151.750841	-32.914811	6,260	180	1,540	5.56	3,190	280	6	8,280
PRS4C	151.750841	-32.914811	6,610	390	1,650	6.48	8,570	280	5	11,600
PRS5A	151.765773	-32.935121	6,440	96	760	3.02	780	32	<LOD	960
PRS5B	151.765773	-32.935121	5,850	130	790	2.99	1,010	40	<LOD	1,690
PRS5C	151.765773	-32.935121	6,250	140	960	3.64	4,040	56	<LOD	2,090
PRS6A	151.765488	-32.935929	5,920	84	460	2.36	1,030	55	<LOD	1,190
PRS6B	151.765488	-32.935929	4,670	69	400	2.13	550	40	<LOD	740
PRS7A	151.753251	-32.911086	6,330	96	1,350	3.36	1,200	85	<LOD	2,830
PRS7B	151.753251	-32.911086	6,710	200	1,790	5.41	3,210	240	6	5,450
PRS8A	151.735041	-32.891055	4,690	140	650	3.90	1,880	24	<LOD	1,440
PRS8B	151.735041	-32.891055	3,690	110	590	3.47	710	19	<LOD	430
PRS8C	151.735041	-32.891055	4,340	130	600	2.89	660	32	<LOD	1,060
PRS9A	151.733763	-32.891786	3,520	96	340	2.53	560	10	<LOD	110
PRS9B	151.733763	-32.891786	6,210	120	790	3.38	220	10	<LOD	42
PRS9C	151.733763	-32.891786	5,550	110	940	4.26	720	25	<LOD	180
PRS10A	151.747068	-32.899573	5,090	170	1,870	5.86	1,190	46	<LOD	1,170
PRS10B	151.747068	-32.899573	6,040	520	3,360	16.01	5,500	240	<LOD	7,640
PRS10C	151.747068	-32.899573	4,400	120	730	4.69	700	34	<LOD	530
PRS10D	151.747068	-32.899573	5,180	110	617	2.15	830	14	<LOD	510
PRS11A	151.747014	-32.899688	5,180	180	2,070	6.30	2,500	79	<LOD	2,340
PRS11B	151.747014	-32.899688	6,790	310	3,600	10.01	1,720	95	<LOD	2,520
PRS12A	151.765242	-32.917256	12,200	210	960	5.14	1,560	110	<LOD	1,370
PRS12B	151.765242	-32.917256	6,930	180	1,140	3.90	3,560	74	6	1,840
PRS13A	151.764114	-32.917046	2,920	140	740	2.35	1,380	34	<LOD	780
PRS13B	151.764114	-32.917046	4,260	170	970	3.56	3,210	62	9	1,240
PRS13C	151.764114	-32.917046	2,870	190	770	2.28	1,200	35	<LOD	610

Sample	x co-ordinate	y co-ordinate	Ti	Cr	Mn	Fe*	Zn	As	Cd	Pb
PRS13D	151.764114	-32.917046	4,940	140	1,410	4.19	1,360	18	<LOD	400
PRS14A	151.764141	-32.917121	5,550	270	1,280	3.75	2,290	50	5	2,120
PRS14B	151.764141	-32.917121	5,720	180	1,200	3.05	1,420	35	<LOD	1,590
PRS14C	151.764141	-32.917121	5,690	300	960	3.14	2,060	64	<LOD	1,420
PRS14D	151.764141	-32.917121	6,360	410	1,790	5.96	2,800	150	<LOD	4,570
PRS15A	151.756360	-32.931232	4,040	87	700	2.34	1,160	20	<LOD	920
PRS15B	151.756360	-32.931232	2,720	98	910	1.94	793	16	<LOD	360
PRS15C	151.756360	-32.931232	4,690	81	670	2.69	1,320	22	<LOD	1,110
PRS16A	151.754543	-32.930401	4,950	2,400	480	5.59	140	18	<LOD	120
PRS16B	151.754543	-32.930401	3,190	580	500	2.62	420	16	<LOD	210
PRS16C	151.754543	-32.930401	2,880	65	590	2.09	200	21	<LOD	190
PRS17A	151.735603	-32.913977	4,810	98	660	2.66	1,230	42	<LOD	880
PRS17B	151.735603	-32.913977	5,170	160	930	3.98	3,850	160	4	1,450
PRS18A	151.737504	-32.891153	3,190	76	560	2.95	880	12	<LOD	430
PRS18B	151.737504	-32.891153	3,940	100	470	3.30	2,930	12	<LOD	1,230
PRS19A	151.758141	-32.911858	5,740	460	1,840	4.95	3,700	80	4	2,350
PRS19B	151.758141	-32.911858	6,200	160	910	3.22	1,970	30	<LOD	1,810
PRS20A	151.725239	-32.897365	6,350	170	1,100	4.24	2,600	28	<LOD	1,930
PRS20B	151.725239	-32.897365	5,230	160	580	3.40	1,880	24	<LOD	1,020
PRS20C	151.725239	-32.897365	5,310	130	580	3.30	1,320	14	<LOD	830
PRS21A	151.747123	-32.940503	4,740	75	1,000	2.47	1,290	15	<LOD	980
PRS21B	151.747123	-32.940503	3,450	72	920	2.39	970	17	<LOD	1,180
PRS22A	151.711666	-32.926700	3,500	74	410	1.75	1,070	17	<LOD	1,360
PRS22B	151.711666	-32.926700	2,910	54	120	1.31	380	8	<LOD	150
PRS22C	151.711666	-32.926700	3,970	68	480	2.13	380	15	<LOD	170
PRS23A	151.784001	-32.903409	7,080	180	740	5.60	770	47	<LOD	790
PRS23B	151.784001	-32.903409	9,120	210	1,390	8.05	1,090	55	4	1,140
PRS23C	151.784001	-32.903409	6,650	170	1,130	5.23	830	38	<LOD	610
PRS23D	151.784001	-32.903409	5,060	110	990	3.73	820	24	<LOD	450
PRS23E	151.784001	-32.903409	7,320	330	2,130	14.78	3,840	130	4	3,420
Soil Depth Profile a (0 - 2 cm)	151.780194	-32.933708	6170	67	360	2.27	330	20	<LOD	160
Soil Depth Profile a (2 - 10 cm)	151.780194	-32.933708	6370	63	320	2.39	260	28	<LOD	150
Soil Depth Profile a (10 - 20 cm)	151.780194	-32.933708	6400	77	270	2.36	220	30	<LOD	150
Soil Depth Profile a (20 - 30 cm)	151.780194	-32.933708	8400	71	200	2.21	170	21	<LOD	150
Soil Depth Profile a (30 - 40 cm)	151.780194	-32.933708	1.18*	98	99	1.54	110	30	<LOD	88
Soil Depth Profile b (0 - 2 cm)	151.760230	-32.908183	6730	140	1400	4.69	1350	67	<LOD	600
Soil Depth Profile b (2 - 10 cm)	151.760230	-32.908183	6650	170	1500	5.01	1380	62	<LOD	640
Soil Depth Profile b (10 - 20 cm)	151.760230	-32.908183	7280	160	1100	4.62	1330	69	<LOD	390
Soil Depth Profile b (20 - 30 cm)	151.760230	-32.908183	8590	89	670	3.81	410	40	<LOD	150
Soil Depth Profile b (30 - 40 cm)	151.760230	-32.908183	9400	83	280	3.55	150	31	<LOD	66
Soil Depth Profile c (0 - 2 cm)	151.746483	-32.911400	3270	87	700	2.29	330	33	<LOD	250
Soil Depth Profile c (2 - 10 cm)	151.746483	-32.911400	2370	78	470	1.97	210	26	<LOD	110
Soil Depth Profile c (10 - 20 cm)	151.746483	-32.911400	3320	82	600	2.29	340	23	<LOD	210
Soil Depth Profile c (20 - 30 cm)	151.746483	-32.911400	8020	160	810	3.46	320	30	<LOD	200
Soil Depth Profile c (30 - 40 cm)	151.746483	-32.911400	6470	98	1400	3.79	470	32	<LOD	400
Soil Depth Profile d (0 - 2 cm)	151.758508	-32.932803	2640	67	790	1.96	270	29	<LOD	120
Soil Depth Profile d (2 - 10 cm)	151.758508	-32.932803	4270	89	750	2.59	370	36	<LOD	150
Soil Depth Profile d (10 - 20 cm)	151.758508	-32.932803	5460	78	450	2.94	240	85	<LOD	100

Sample	x co-ordinate	y co-ordinate	Ti	Cr	Mn	Fe*	Zn	As	Cd	Pb
Soil Depth Profile d (20 - 30 cm)	151.758508	-32.932803	5860	77	270	2.47	150	44	<LOD	91
Soil Depth Profile d (30 - 40 cm)	151.758508	-32.932803	6450	56	210	1.9	110	32	<LOD	59
Soil Depth Profile e (0 - 2 cm)	151.695386	-32.909801	3270	59	150	1.48	96	3	<LOD	41
Soil Depth Profile e (2 - 10 cm)	151.695386	-32.909801	3570	58	140	1.51	94	6	<LOD	39
Soil Depth Profile e (10 - 20 cm)	151.695386	-32.909801	3510	46	37	1.35	40	4	<LOD	17
Soil Depth Profile e (20 - 30 cm)	151.695386	-32.909801	4130	61	16	1.9	31	6	<LOD	14
Soil Depth Profile e (30 - 40 cm)	151.695386	-32.909801	5240	67	36	3.51	38	13	<LOD	15
Soil Depth Profile f (0 - 2 cm)	151.621760	-32.902235	2830	77	140	1.65	230	14	<LOD	150
Soil Depth Profile f (2 - 10 cm)	151.621760	-32.902235	3040	96	54	1.58	110	13	<LOD	88
Soil Depth Profile f (10 - 20 cm)	151.621760	-32.902235	3010	58	31	1.82	60	12	<LOD	35
Soil Depth Profile f (20 - 30 cm)	151.621760	-32.902235	3260	79	30	1.91	58	9	<LOD	29
Soil Depth Profile f (30 - 40 cm)	151.621760	-32.902235	3260	79	30	1.91	58	9	<LOD	29

Table F2: Soil PAH concentrations for the Newcastle city. All concentrations in mg/kg. PAH: 1 – Naphthalene, 2 – Acenaphthylene, 3 – Acenaphthene, 4 – Fluorene, 5- Phenanthrene, 6 – Anthracene, 7 – Fluoranthene, 8 – Pyrene, 9 - Benz(a)anthracene, 10 – Chrysene, 11 - Benzo(b)&(k)fluoranthene, 12 - Benzo(a)pyrene, 13 - Indeno(1,2,3-cd)pyrene, 14 - Dibenzo(a,h)anthracene, 15 - Benzo(g,h,i)perylene. Soil samples: public (Zone A SB; A – sampling zone number, B – sample site).

Sample	x co-ordinate	y co-ordinate	PAH 1	PAH 2	PAH 3	PAH 4	PAH 5	PAH 6	PAH 7	PAH 8	PAH 9	PAH 10	PAH 11	PAH 12	PAH 13	PAH 14	PAH 15	∑ PAH
Zone 5 S1	151.765942	-32.935172	<0.5	<0.5	<0.5	<0.5	0.8	<0.5	2.2	2.1	0.8	0.7	1.4	1.0	0.6	<0.5	0.8	10
Zone 5 S4	151.751481	-32.936583	<0.5	<0.5	<0.5	<0.5	4.4	1.5	10	9.6	3.5	3.5	6.9	5.2	2.9	0.6	3.4	52
Zone 5 S5	151.755347	-32.931136	<0.5	<0.5	<0.5	<0.5	1.7	0.6	4.6	4.5	1.5	1.5	3.1	2.2	1.4	<0.5	1.6	23
Zone 2 S1	151.765858	-32.91974	<0.5	<0.5	<0.5	<0.5	2.4	0.7	6.9	6.4	2.4	2.1	4.5	3.3	2.0	<0.5	2.4	33
Zone 2 S2	151.765405	-32.914048	<0.5	<0.5	<0.5	<0.5	1.5	<0.5	5.7	5.4	2.0	2.0	4.2	2.7	1.9	<0.5	2.2	28
Zone 2 S2**	151.765405	-32.914048	<0.5	<0.5	<0.5	<0.5	2.1	0.7	6.3	6.0	2.3	2.2	4.5	3.2	2.0	<0.5	2.4	32
Zone 2 S3	151.764169	-32.909803	<0.5	<0.5	<0.5	<0.5	<0.5	<0.5	1.7	1.6	0.6	0.6	1.5	1.0	0.7	<0.5	0.9	8.6
Zone 2 S4	151.766314	-32.910977	<0.5	0.9	<0.5	<0.5	3.8	1.4	10	10	4.0	3.8	7.3	5.4	3.1	0.7	3.5	54
Zone 1 S5	151.746816	-32.900268	<0.5	<0.5	<0.5	<0.5	1.5	<0.5	5.4	5.3	2.0	2.0	4.4	2.9	2.0	<0.5	2.5	28
Zone 1 S2	151.750378	-32.914897	<0.5	<0.5	<0.5	<0.5	1.6	0.7	5.7	5.6	1.8	2.0	4.3	2.8	1.8	<0.5	2.0	28
Zone 1 S4	151.752958	-32.910561	<0.5	<0.5	<0.5	<0.5	1.9	0.6	5.5	5.3	1.7	1.8	3.7	2.7	1.6	<0.5	2.0	27
Zone 1 S7	151.734307	-32.891691	<0.5	0.8	<0.5	<0.5	8.2	2.4	20	18	7.3	7.5	14	9.8	6.1	1.4	7.6	103

Sample marked with ** is a field duplicate.

Table F3: Lead isotope compositions for soils, slag and galena. Standard deviations determined from repeat analysis (10 analyses) of one sample. Soil samples: public (Zone A SB; A – sampling zone number, B – sample site), private (PRSXY; X – property code, Y – sample number on property) and depth (SDPX X-Y cm; where X is the depth profile number and X-Y is the depth).

Sample	x co-ordinate	y co-ordinate	$^{208}Pb/^{207}Pb$ +/- 0.004	$^{206}Pb/^{207}Pb$ +/- 0.004	$^{206}Pb/^{204}Pb$ +/- 0.091
PRS4C	151.747014	-32.899688	2.400	1.114	17.483
PRS11A	151.747014	-32.899688	2.365	1.092	16.863
PRS8C	151.735041	-32.891055	2.402	1.126	17.483
PRS20C	151.725239	-32.897365	2.352	1.079	16.474
Zone 1 S20	151.753067	-32.898278	2.411	1.131	17.483
Zone 1 S9	151.750283	-32.914881	2.374	1.091	16.892
Zone 2 S17	151.755342	-32.907642	2.345	1.068	16.584
Zone 2 S4	151.768639	-32.907889	2.361	1.085	16.807
Zone 2 S4*	151.768639	-32.907889	2.365	1.117	17.513
Zone 2 S17**	151.755342	-32.907642	2.355	1.071	16.474
Slag 1	***	***	2.319	1.044	16.077
Slag 2	***	***	2.543	1.318	21.097
SDP b 30-40 cm	151.759338	-32.906211	2.384	1.099	16.949
SDP c 30-40 cm	151.747180	-32.911957	2.370	1.093	16.835
SDP d 30-40 cm	151.758508	-32.932803	2.406	1.124	17.544
SDP e 20-30 cm	151.695323	-32.910189	2.489	1.198	18.727
Wallaroo Galena	***	***	2.640	1.477	24.727
Broken Hill Galena	***	***	2.319	1.044	16.155

*field duplicate
**laboratory duplicate
***GPS co-ordinates not applicable

Table F4: Relative abundances of phases were estimated from XRD patterns using the relative intensity ratio (RIR) method.

Group	Phase	Chemical composition	PRS3B	PRS3D	PRS4C	PRS7A	Zone 1 S7	Zone 1 S9	Zone 2 S1	Zone 2 S4	Zone 2 S15
Silicates	Clinopyroxene	$(Ca,Mg,Fe,Al)_2Si_2O_6$		*	***		***	**			*
	Olivine	$(Ca,Fe,Mg)_2SiO_4$		*	*		*	***			
	Zircon	$ZrSiO_4$	*	tr	*	*	*		*	*	*
	Vesuvianite	$Ca_{10}(Mg,Fe)_2Al_4(SiO_4)_5(Si_2O_7)_2(OH,F)_4$					**				
	Melilite	$Ca_2(Mg,Fe,Zn)Si_2O_7$					*			tr	*
	Amorphous glass (slag)	Si-Ca-Fe		***	***	***	**	***		***	*
	Quartz	SiO_2	tr						*		*
Oxides	Hematite	Fe_2O_3	*	***	**	***	**	**	*	**	tr
	Spinel series	$(Fe,Zn,Mg)(Fe,Al,Cr)_2O_4$	*	*	*	*	tr	*	*	**	*
	Goethite	$FeOOH$							tr	tr	
	Wuestite	FeO								tr	
	Rutile	TiO_2	**	tr	tr		*	tr	*	tr	*
	Ilmenite	$FeTiO_3$	tr						***		tr
	Corundum	Al_2O_3	*								

*** abundant, ** common, * minor, tr trace
PRS3B – x co-ordinate: 151.754543; y co-ordinate: -32.930401
PRS3D – x co-ordinate: 151.747068; y co-ordinate: -32.899573
PRS4C – x co-ordinate: 151.750841; y co-ordinate: -32.914811
PRS7A – x co-ordinate: 151.753439; y co-ordinate: -32.910121
Zone 1 S7 – x co-ordinate: 151.743853; y co-ordinate: -32.912803
Zone 1 S9 – x co-ordinate: 151.750283; y co-ordinate: -32.914881
Zone 2 S1 – x co-ordinate: 151.761278; y co-ordinate: -32.915472
Zone 2 S4 – x co-ordinate: 151.768639; y co-ordinate: -32.907889
Zone 2 S15 – x co-ordinate: 151.761278; y co-ordinate: -32.91547

References

Gulson, B., Mizon, K., Taylor, A., Korsch, M., Stauber, J., Davis, J.M., Louie, H., Wu, M., Swan, H. 2006. Changes in manganese and lead in the environment and young children associated with the introduction of methylcyclopentadienyl manganese tricarbonyl in gasoline - preliminary results. Environmental Research 100, 100-114.

Kristensen, L.J. Taylor, M.P. 2016. Unravelling a 'miner's myth' that environmental contamination in mining towns is naturally occurring. Environmental Geochemistry and Health 38 (4), 1015-1027.

Morrison, A. L., Gulson, B. L. 2007. Preliminary findings of chemistry and bio-accessibility in base metal smelter slags. Science of the Total Environment 382, 30–42.

National Environmental Protection Measure (NEPM), 2013. Schedule B1: Guideline on Investigation for Soil and Groundwater, p. 57. <http://www.scew.gov.au/system/files/resources/93ae0e77-e697-e494-656f-afaaf9fb4277/files/schedule-b1-guideline-investigation-levels-soil-and-groundwater-sep10.pdf> (accessed 29 January 2017).